AD-A168 715 PROCEEDINGS OF WEST COAST REGIONAL COASTAL DESIGN 1/5
CONFERENCE HELD ON 7-8 NOVEMBER 1985 AT OAKLAND
CALIFORNIA(U) CORPS OF ENGINEERS SAN FRANCISCO CALIF
UNCLASSIFIED SOUTH PACIFIC DIV APR 86 F/G 13/2 NL

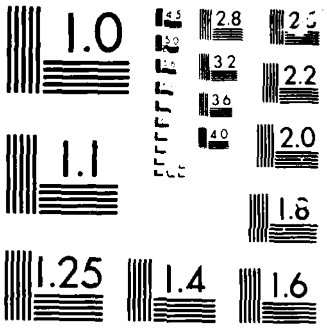
1.0
2.8
2.5
3.2
2.2
3.6
4.0
2.0
1.1
1.8
1.25
1.4
1.6

②

AD-A168 715

PROCEEDINGS

WEST COAST REGIONAL COASTAL DESIGN CONFERENCE

DTIC
S ELECTE D
JUN 1 0 1986
D

Proceedings of a Specialty Conference sponsored by:

- US Army Corps of Engineers
  - South Pacific Division
  - North Pacific Division
  - Waterways Experiment Station
- American Society of Civil Engineers
  - Waterway, Port, Coastal and Ocean Division
- American Shore and Beach Preservation Association

DTIC FILE COPY

7-8 November 1985
Oakland, California

86 6 10 150

Unclassified
SECURITY CLASSIFICATION OF THIS PAGE

AD-A168 715

REPORT DOCUMENTATION PAGE

Form Approved
OMB No 0704 0188
Exp Date Jun 30, 1986

1a REPORT SECURITY CLASSIFICATION Unclassified	1b RESTRICTIVE MARKINGS
2a SECURITY CLASSIFICATION AUTHORITY	3 DISTRIBUTION/AVAILABILITY OF REPORT Approved for public release; distribution unlimited
2b DECLASSIFICATION/DOWNGRADING SCHEDULE	
4 PERFORMING ORGANIZATION REPORT NUMBER(S)	5 MONITORING ORGANIZATION REPORT NUMBER(S)
6a NAME OF PERFORMING ORGANIZATION See reverse. 6b OFFICE SYMBOL (If applicable)	7a NAME OF MONITORING ORGANIZATION
6c ADDRESS (City, State, and ZIP Code) See reverse.	7b ADDRESS (City, State, and ZIP Code)
8a NAME OF FUNDING/SPONSORING ORGANIZATION USAEWES Coastal Engineering Research Center 8b OFFICE SYMBOL (If applicable) WESCV-I	9 PROCUREMENT INSTRUMENT IDENTIFICATION NUMBER
8c ADDRESS (City, State, and ZIP Code) PO Box 631 Vicksburg, MS 39180-0631	10 SOURCE OF FUNDING NUMBERS PROGRAM ELEMENT NO | PROJECT NO | TASK NO | WORK UNIT ACCESSION NO

11 TITLE (Include Security Classification)

PROCEEDINGS: WEST COAST REGIONAL COASTAL DESIGN CONFERENCE

12 PERSONAL AUTHOR(S)

13a TYPE OF REPORT Final report	13b TIME COVERED FROM 1985 TO 1986	14 DATE OF REPORT (Year, Month, Day) April 1986	15 PAGE COUNT 443

16 SUPPLEMENTARY NOTATION

Available from National Technical Information Service, 5285 Port Royal Road, Springfield, VA 22161.

17 COSATI CODES			18 SUBJECT TERMS (Continue on reverse if necessary and identify by block number)
FIELD	GROUP	SUB-GROUP	

19 ABSTRACT (Continue on reverse if necessary and identify by block number)

These Proceedings provide a record of the papers presented at the West Coast Regional Coastal Design Conference conducted on 7-8 November 1985 in Oakland, California. The Conference was divided into four sessions on the following topics: Harbors, Sedimentation and Material Disposal, Structures and Materials, and Coastal Processes. Each session was followed by a panel discussion which has been summarized and is included in these Proceedings.

The Conference was cosponsored by the US Army Corps of Engineers, American Society of Civil Engineers, and the American Shore and Beach Preservation Association.

20 DISTRIBUTION/AVAILABILITY OF ABSTRACT ☒ UNCLASSIFIED/UNLIMITED ☐ SAME AS RPT ☐ DTIC USERS	21 ABSTRACT SECURITY CLASSIFICATION Unclassified
22a NAME OF RESPONSIBLE INDIVIDUAL	22b TELEPHONE (Include Area Code) | 22c OFFICE SYMBOL

DD FORM 1473, 84 MAR

83 APR edition may be used until exhausted
All other editions are obsolete

SECURITY CLASSIFICATION OF THIS PAGE
Unclassified

6a. NAME OF PERFORMING ORGANIZATION (Continued).

US Army Corps of Engineers
    South Pacific Division (SPD)
    North Pacific Division (NPD)
    Waterways Experiment Station (WES)

American Society of Civil Engineers (ASCE)
    Waterway, Port, Coastal and Ocean Division

American Shore and Beach Preservation Association (ASBPA)

6c. ADDRESS (Continued).

SPD
630 Sansome Street, Room 1216
San Francisco, CA 94105-1905

NPD
PO Box 2870
Portland, OR 97208-2870

WES
PO Box 631
Vicksburg, MS 39180-0631

ASCE
United Engineering Center
345 East 47th Street
New York, NY 10017-2398

ASBPA
412 O'Brien Hall
University of California
Berkeley, CA 94720

DISCLAIMER

Technical papers in this publication are being published as submitted to the Coastal Engineering Research Center of the US Army Engineer Waterways Experiment Station (WES). Only the front matter and discussion sections have been edited by WES. Respective authors are entirely responsible for the content and presentation of the technical papers herein.

Accesion For

NTIS CRA&I ☒
DTIC TAB ☐
Unannounced ☐
Justification ....

By ....
Distribution /

Availability Codes

Dist	Avail and / or Special
A-1	

QUALITY INSPECTED 3

PREFACE

On 7-8 November 1985, the West Coast Regional Coastal Design Conference was held in Oakland, California. The conference was cosponsored by the US Army Engineer Division, South Pacific (SPD); the US Army Engineer Division, North Pacific (NPD); the Coastal Engineering Research Center of the US Army Engineer Waterways Experiment Station (WES); the Waterway, Port, Coastal and Ocean Division of the American Society of Civil Engineers; and the American Shore and Beach Preservation Association.

Acknowledgments are extended to the following: Messrs. Richard J. Dibuono and Hugh Converse, SPD, and Mr. John Oliver, NPD, who coordinated the conference; Messrs. Mark Dettle and William J. Brick, US Army Engineer District, San Francisco, who coordinated on-site logistics; Mr. Daniel Muslin, US Army Engineer District, Los Angeles, for publicity and registration; and Mrs. Shirley A. J. Hanshaw and Mr. Andre Z. Szuwalski, WES, for editing the front matter and discussion sections and for compiling the proceedings.

At the time of publication of these proceedings, COL Allen F. Grum, USA, was Director of WES, and Dr. Robert W. Whalin was Technical Director.

CONTENTS

Page

PREFACE 1

HARBORS

Rodney J. Sobey
University of California, Berkeley
"Exact and Approximate Solutions for Breakwater Gap Diffraction" 6

Gary B. Griggs
University of California, Santa Cruz
"Beach Compartments, Littoral Drift, and Harbor Dredging" 18

Larry S. Slotta, Roger S. Mustain, and Carlos R. Cobos
Slotta Engineering Associates
Corvallis, Oregon
"Shoaling of Port of Astoria, Oregon, by Sediment from Mt. St. Helens Eruption" 30

J. Michael Hemsley, C. Linwood Vincent, and Paul May
US Army Corps of Engineers, Waterways Experiment Station
Vicksburg, Mississippi
"Coastal Field Data Collection Program" 40

John M. Nichol
Moffatt & Nichol
Long Beach, California
"Observations in Small Boat Harbors: Harbor Design Concepts" 54

Carl Huval
US Army Corps of Engineers, Waterways Experiment Station
Vicksburg, Mississippi
"The WES Ship/Tow Simulator for Navigation Engineering" 65

Roderick A. Chisholm II
US Army Corps of Engineers, San Francisco District
"Navigation Simulation Applications" 66

David J. Illias and Kenneth Johnson
US Army Corps of Engineers, Portland District
"Rogue River Entrance" 73

Sung B. Yoon and Philip L-F. Liu
Cornell University, Ithaca, New York
"Interactions Between Water Waves and Currents in Shallow Water" 84

Carl D. Stormer
US Army Corps of Engineers, Alaska District, Anchorage
"The Alaska Coastal Data Collection Program: Past, Present, and Future" 94

Summary of Panel Discussion: HARBORS 105

SEDIMENTATION AND MATERIAL DISPOSAL

Page

James R. Reese
US Army Corps of Engineers, Portland District
"Generic Ocean Disposal Studies for the Oregon Coast".............. 108

Stephan A. Chesser
US Army Corps of Engineers, Portland District
"Monitoring Sediment Transport at Ocean Disposal Sites"............ 118

N. Timothy Hall and Richard C. Harding
Earth Sciences Associates
Palo Alto, California
John M. Musser, Jr.
Geo-Recon International
Seattle, Washington
"Geologic and Seismic Investigations of Dredge Disposal Sites off the Oregon Coast"...................................... 130

Robert H. Osborne
University of Southern California, Los Angeles
Peter A. Almendinger, Paul D. Hecht, and Anthony Price
US Army Corps of Engineers, South Pacific Division, San Francisco and Los Angeles Districts
"Littoral Segments: Dana Point to Mexico"......................... 141

Michael J. Trawle and B. H. Johnson
US Army Corps of Engineers, Waterways Experiment Station
Vicksburg, Mississippi
"Numerical Modeling of the Physical Fate of Dredged Material Dumped at Open Water Sites: San Francisco Bay and Puget Sound"......... 153

Larry S. Slotta
Slotta Engineering Associates
Corvallis, Oregon
"Dredge Cutterhead Flow Processes"................................ 165

Craig H. Everts
Moffatt & Nichol
Long Beach, California
Greg Hartman
Ogden Beeman and Associates
Portland, Oregon
Stephan A. Chesser
US Army Corps of Engineers, Portland District
"Sedimentation Rates and Channel Deepening, Mouth of Columbia River"... 180

Douglas J. Diemer
US Army Corps of Engineers, Los Angeles District
"Oceanside Experimental Sand Bypass".............................. 193

Summary of Panel Discussion: SEDIMENTATION AND MATERIAL DISPOSAL........ 218

STRUCTURES AND MATERIALS

Page

Senaka Ratnayake
University of Washington, Seattle
"Numerical Modeling of Floating Breakwater Behavior"................ 221

George G. England
US Army Corps of Engineers, Seattle District
"Testing and Analysis of ~~a~~ Floating Breakwater"................. 233

J. Michel Benoit
Morrison-Knudsen Engineers
San Francisco, California
"Construction Optimization Through Shipyard Fabrication"........... 250

Harold Davis and John B. Rutherford
Rutherford and Chekene
San Francisco, California
"Specifying Materials for Coastal Concrete Structures"............. 265

Richard Gutschow
US Army Corps of Engineers, Los Angeles District
"The Use of Steel Fiber Reinforced Concrete for Casting of Large Dolosse"... 277

Thomas R. Kendall, Gary L. Howell, and Thomas A. Denes
US Army Corps of Engineers, San Francisco District and Waterways Experiment Station
"Prototype Measurement of the Structural Response of Dolos Armor Units"... 288

Robert O. Van Atta
Portland State University, Portland, Oregon
"Degradation of Rock Used in Erosion Control"...................... 300

Lester E. Fultz
Neskowin, Oregon
Erosion Control on a Portion of the Siletz River Sandspit"......... 312

Wayne O. MacDonell and Bo M. Jensen
Earl and Wright Consulting Engineers
San Francisco, California
Daniel E. Mohn
Golden Gate Bridge, Highway and Transportation District
San Rafael, California
"Golden Gate Bridge Pier Ship Collision Study"..................... 324

R. D. Scott and D. J. Turcke
Queen's University
Kingston, Ontario, Canada
W. F. Baird
W. F. Baird and Associates
Ottawa, Ontario, Canada
"The Analysis and Design of Concrete Armour Units"................. 339

Page

Eric Nelson
US Army Corps of Engineers, Seattle District
Laurie Broderick
US Army Corps of Engineers, Portland District
"Results from a Prototype Floating Breakwater Test Program"........ 343

Summary of Panel Discussion: STRUCTURES AND MATERIALS.................. 356

COASTAL PROCESSES

Jung-Tai Lin
United Industries Corporation
Bellevue, Washington
"Empirical Prediction of Wind-Generated Gravity Waves"............. 359

Omar H. Shemdin
Ocean Research and Engineering
La Canada, California
"Extending Wave Station Measurements to Intermediate Locations by Wave Transformation Models"................................... 371

Thomas J. Dolan
US Army Corps of Engineers, Los Angeles District
"Coast of California Storm and Tidal Waves Study: Preliminary Observations from the San Diego Region Directional Wave Data Network and Beach Profile Program"............................... 372

Howard H. Chang
San Diego State University, San Diego, California
"Flushing of Entrance Channel for Coastal Lagoons: Mathematical Simulation".. 389

Edward B. Thornton, A. J. Sklavidis, W. Lima Blanco, D. M. Burych, S. P. Tucker, and D. Puccini
Naval Postgraduate School, Monterey, California
"Coastal Erosion Along Southern Monterey Bay"..................... 390

Maurice L. Schwartz, James Mahala, and Hiram Bronson, III
Western Washington University, Bellingham, Washington
"Net Shore-Drift along the Pacific Coast of Washington State"...... 402

Thomas Terich and Terence Levenseller
Western Washington University, Bellingham, Washington
"The Severe Erosion of Cape Shoalwater, Washington"................ 411

Norman K. Skjelbreia and Eric E. Nelson
US Army Corps of Engineers, Seattle District
"Performance of Beach Nourishment Projects in Varying Wave Climates"... 429

Syd Willard
California Department of Parks and Recreation
Sacramento, California
"Coastal Erosion in the California State Park System"............. 430

Summary of Panel Discussion: COASTAL PROCESSES........................ 436

Exact and Approximate Solutions for Breakwater Gap Diffraction

Rodney J. Sobey,* M. ASCE

Abstract. Commonly available diffraction diagrams for a breakwater gap are approximate solutions. They involve either a far-field approximation to the exact solution or an approximation to gap diffraction by superposition of partial solutions for a semi-infinite breakwater. Recently completed exact solutions provide quantitative detail of the extent of previous approximations. Differences are most extreme for narrow gaps and angled incidence.

Introduction

For preliminary harbor design purposes, standard diffraction diagrams have considerable value and are used extensively, especially following their inclusion in the Shore Protection Manual (9). The dimensionless format popularized by Wiegel (12) for diffraction about a semi-infinite breakwater is especially useful, the diffraction diagrams superimposing contours of wave magnitude (diffraction coefficient K_d) and wave phase in intervals of 2π. These solutions are based on the analytical solution of the Helmholtz equation by Sommerfeld (11), as adapted to surface gravity waves by Penney and Price (8).

Available diffraction diagrams for wave diffraction through a breakwater gap are rather less satisfactory. Details of the complementary problem, diffraction about an island breakwater, are more available yet still incomplete. The analytical solutions for both of these problems are closely related; they have been presented by Morse and Rubenstein (7). Their presentation of results is extremely brief, however, and restricted to the far-field response at large distances from the gap. In addition, scales have been omitted and detail is insufficient to permit re-drawing of the results in the Wiegel format. Additional far-field solutions have been computed by Carr and Stelzreide (3). Polar diagrams of far-field response are presented for gaps of 0.5, 1, 2, and 3 wavelength and incident wave angles of 0° (15°) 90°. The scale of these diagrams is quite small and precision is lost in re-drawing these results in the Wiegel format. The Carr and Stelzreide results for a gap of one wavelength have been redrawn by J. W. Johnson (4) and have been included in every edition of the Shore Protection Manual, with the implicit authority of exact solutions. Only in the far-field can these diagrams be called exact, although even there some precision has certainly

---

*Associate Professor, Department of Civil Engineering, University of California, Berkeley, CA 94720.

been lost in transformation from the Carr and Stelzreide polar diagrams. Results are presented also for the near-field, where engineering interest is mostly focussed, but where the Carr and Stelzreide results are not valid. In addition, no phase information is included in either the Morse and Rubenstein or Carr and Stelzreide presentations.

Johnson also presented an approximation to breakwater gap diffraction at normal incidence by superposition of partial mirror-image Sommerfeld solutions for a semi-infinite breakwater. Again these diagrams have been reproduced in the Shore Protection Manual for gaps of 0.5, 1, 2.95, 3.82 and 5 wavelengths, although Johnson did not recommend this approach for gaps of less than three wavelengths. There are no diagrams for angled incidence.

Recent computations by Sobey and T.L. Johnson (10) have sought to fill the remaining gaps, providing exact solutions for a range of gap widths and incident directions. Although the exact solution of Morse and Rubenstein has been available since 1938, it has not been used in the construction of any of the standard diffraction patterns commonly in use. The reason is clear. The exact solution involves Mathieu and modified Mathieu functions, the computation of which is not trivial. All the breakwater gap diffraction patterns reproduced in the Shore Protection Manual are approximations.

The present paper will focus on the details of the approximations, the consequences of these approximations and differences between the exact and approximate solutions.

Mathematical Formulation

Wave diffraction in water of constant depth is a boundary value problem for which the field equation is the Laplace equation, the dependent variable being the velocity potential function $\varphi(x,y,z,t)$. The independent variables are horizontal position x and y, vertical position z (positive upwards from the M.W.L.) and time t. Solutions that are periodic in time but not in horizontal space, and satisfy the bottom boundary condition at $z = -h$ follow from separation of variables:

$$\varphi(x,y,z,t) = A\, F(x,y) \cosh k(h+z) \exp(-i\omega t) \tag{1}$$

k is the wave number and ω the angular wave frequency. Back substitution into the Laplace equation and using both the kinematic and dynamic free surface boundary conditions reduces the problem to the Helmholtz equation

$$\frac{\partial^2 F}{\partial x^2} + \frac{\partial^2 F}{\partial y^2} + k^2 F = 0 \tag{2}$$

and the dispersion relationship

$$\omega^2 = gk \tanh kh \tag{3}$$

It follows that the free surface is represented as

$$\eta(x,y,t) = \frac{i\omega A}{g} F(x,y) \cosh kh \exp(-i\omega t) \tag{4}$$

Other dependent variables (velocity, acceleration, pressure) are available from the velocity potential function.

It remains to determine the complex function $F(x,y)$, in terms of horizontal plan boundary conditions that are specific to a particular problem. The classical approach is to specify the solution as the linear superposition of an incident wave, a reflected wave from the breakwater and a scattered wave from the gap:

$$F = F_I + F_r + F_s \tag{5}$$

The incident wave at a large distance from the structure is periodic in space, represented as the plane progressive wave of unit amplitude

$$F_I(x,y) = \exp[ik(x \cos\theta_0 + y \sin\theta_0)] \tag{6}$$

where θ_0 is the angle of incidence to the positive x axis. This is the first boundary condition. The origin of coordinates is located at the center of the breakwater gap, with the breakwaters along the positive and negative x axes. The width of the breakwater gap is $B = 2\rho$. The second boundary condition is the requirement that there be no flow through the thin, rigid breakwater, represented as

$$\frac{\partial F}{\partial y} = 0 \text{ for } x \geq \rho,\ y = 0 \quad \text{and} \quad x \leq -\rho,\ y = 0 \tag{7}$$

Representing $F(x,y)$ at the breakwater as the sum of incident and reflected waves defines the reflected wave as

$$F_r(x,y) = \exp[ik(x \cos\theta_0 - y \sin\theta_0)] \tag{8}$$

Finally, the gap introduces a scattered wave $F_s(x,y)$ which must go asymptotically to zero at large radial distances from the gap. This is represented by the "Sommerfeld radiation condition," which for $F_s(r,\theta)$ in polar coordinates is

$$\lim_{r \to \infty} r^{1/2} \left(\frac{\partial F_s}{\partial r} - ikF_s \right) = 0 \tag{9}$$

This is satisfied if $F_s(r,\theta)$ has the asymptotic form

$$F_s \approx (kr)^{-1/2} \exp(ikr) \tag{10}$$

The second and third boundary conditions are most conveniently represented by a coordinate transformation to elliptical cylinder coordinates (7). The elliptical cylinder coordinates u and v are related to cartesian x and y as

$$x = \rho \cosh u \cos v, \quad y = \rho \sinh u \sin v \tag{11}$$

The u is a curvilinear radial coordinate and v a curvilinear azimuthal coordinate. This also involves a transformation of the Helmholtz equation, the solutions of which become Mathieu and modified Mathieu functions (5).

Analytical Solution of Morse and Rubenstein

The solution (10) proceeds by representing the incident wave, Equation 6, and the reflected wave, Equation 8, as series expansions in terms of Mathieu function products. Their sum becomes

$$F_i(u,v) + F_r(u,v) = 4 \sum \left[\frac{1}{p_{2n}} Ce_{2n}(u)\, ce_{2n}(v)\, ce_{2n}(\theta_o) \right.$$

$$\left. + \frac{i}{p_{2n+1}} Ce_{2n+1}(u)\, ce_{2n+1}(v)\, ce_{2n+1}(\theta_o) \right] \tag{12}$$

eliminating the odd Mathieu functions from the expansion. Similarly, the scattered wave may be represented as a series expansion of Mathieu function products that automatically satisfies the Sommerfeld radiation condition (5):

$$F_s(u,v) = \sum_{n=0}^{\infty} [C_{2n} Me_{2n}^{(1)}(u)\, ce_{2n}(v)\, ce_{2n}(\theta_o)$$

$$+ C_{2n+1} Me_{2n+1}^{(1)}(u)\, ce_{2n+1}(v)\, ce_{2n+1}(\theta_o)$$

$$+ S_{2n+2} Ne_{2n+2}^{(1)}(u)\, se_{2n+2}(v) se_{2n+2}(\theta_o)$$

$$+ S_{2n+1} Ne_{2n+1}^{(1)}(u)\, se_{2n+1}(v) se_{2n+1}(\theta_o)] \tag{13}$$

Requiring the scattered wave to independently satisfy the no flow boundary condition at the breakwaters (only a scattered wave penetrates beyond the gap) gives the coefficients S_{2n+2} and S_{2n+1} as zero. The odd Mathieu functions are again eliminated.

The coefficients C_{2n} and C_{2n+1} in Equation 13 are determined from compatibility of the incident, reflected and scattered waves on the negative v side of the gap at $u = 0$ with the scattered wave on the positive v side. For the scattered wave in front of the gap ($-\pi < v < 0$)

$$C_{2n} = \frac{-2\, Ce_{2n}(u=0)}{p_{2n}\, Me_{2n}^{(1)}(u=0)} \tag{14a}$$

$$C_{2n+1} = \frac{-2i\, Ce_{2n+1}(u=0)}{p_{2n+1}\, Me_{2n+1}^{(1)}(u=0)} \tag{14b}$$

Beyond the gap ($0 < v < \pi$), the only change is that the sign in both expressions becomes positive. Since the publication of the Morse and Rubenstein solution (and its repetition by Carr and Stelzreide) the alternative development of the Mathieu and modified Mathieu functions by McLachlan (5) has become the standard. The above detail differs substantially from Morse and Rubenstein (7), although in principle the results are equivalent.

Asymptotic Approximations

As the dimensionless elliptical cylinder coordinate u becomes large, there is an asymptotic transition from the elliptical cylinder coordinate system in the gap near-field to circular cylinder or polar coordinates in the far-field. Equation 11 approaches

$$x = \rho\, \tfrac{1}{2} \exp(u) \cos v, \quad y = \rho\, \tfrac{1}{2} \exp(u) \tag{15}$$

in which $\tfrac{1}{2}\rho \exp(u)$ is the effective radial coordinate. The error of this approximation has fallen to less than 1% at a dimensionless u of 2.5, corresponding to a radius of $5\,\rho$ from the center of the gap. At large radii, the Mathieu functions become sine and cosine functions and the modified Mathieu functions become Bessel functions of the first and second kind (5). Adopting these asymptotic forms, the scattered wave becomes

$$F_s(u,v) = \tfrac{1}{2} C_o'\, H_o^{(1)}(v_2) + \sum_{m=1}^{\infty} C_m'\, H_m^{(1)}(v_2) \cos mv \cos m\theta_o \tag{16}$$

where $H_m^{(1)}(v_2)$ is the Hankel function $J_m(v_2) + i\, Y_m(v_2)$, $v_2 = q^{1/2} \exp(u)$ and $q = (k\rho/2)^2$. The coefficients C_m' in the front of the gap ($-\pi < v < 0$) are

$$C_{2n}' = \frac{-2(-1)^n\, J_{2n}(q^{1/2})}{H_{2n}^{(1)}(q^{1/2})} \tag{17a}$$

$$C_{2n+1}' = \frac{-2i(-1)^n\, J_{2n+1}(q^{1/2})}{H_{2n+1}^{(1)}(q^{1/2})} \tag{17b}$$

Again the sign of both expressions becomes positive beyond the gap ($0 < v < \pi$). This might be called an intermediate-field solution.

The asymptotic solution presented by Morse and Rubenstein and adopted also by Carr and Stelzreide is a further approximation, adopting asymptotic forms of the Bessel functions (1). The Hankel functions in Equation 16 (but not Equation 17) approach

$$H_m^{(1)}(v_2) = (2/\pi v_2)^{1/2} \exp[-i(v_2 - m\pi/2 - \pi/4)] \tag{18}$$

This is an appropriate approximation for v_2 at least greater than the first zero of the corresponding Y_n Bessel function. For n from zero to five, these zeros increase from approximately 0.89 to 6.74. It follows that the Equation 18 approximation would be appropriate for v_2 at least greater than 7.5. This is the far-field solution.

Given access to modern digital computers however, there is little need to continue to utilize these asymptotic approximations, which are of course not valid in the near-field. The Sobey and Johnson (10) computations were based on the complete solution.

The Superposition Approximation

The Penney and Price (8) presentation of the Sommerfeld solution for diffraction about a semi-infinite breakwater included an approximate solution for diffraction through a breakwater gap, by superposition of partial Sommerfeld solutions for separate left and right semi-infinite breakwaters. This approximation was presented only for 90° incidence and was used by J. W. Johnson (2, 4) to predict diffraction patterns for normal incidence and gap widths ranging from 0.5 to 5.0 wavelengths. These diagrams, Johnson Figures 4 to 6, are reproduced in the Shore Protection Manual as Figures 2-42 to 2-52. Penney and Price argue that superposition provides a reasonable approximation for 90° incidence and gap widths greater than one wavelength.

Neither Penney and Price nor Johnson considered angled incidence but this generalization of the superposition approximation is relatively straightforward (10). For a thin, rigid, semi-infinite breakwater extending along the positive x axis from the origin of coordinates to positive infinity, the Sommerfeld diffraction solution is (11)

$$F(r,\theta) = \frac{1+i}{2}\left\{\int_{-\infty}^{\sigma} \exp(-i\frac{\pi}{2}u^2)du + \exp\int_{-\infty}^{\sigma'} \exp(-i\ \frac{\pi}{2})du\right\} \tag{19}$$

where $\sigma = 2(kr/\pi)^{1/2} \sin \frac{1}{2}(\theta - \theta_o)$ and $\sigma' = -2(kr/\pi)^{1/2} \sin \frac{1}{2}(\theta + \theta_o)$. This solution may be represented in terms of an incident wave

$$F_I(r,\theta) = \exp[-ikr \cos(\theta - \theta_o)] \tag{20}$$

for $\theta_o \leq \theta \leq 2\pi$ and a reflected wave from the breakwater

$$F_r(r,\theta) = \exp[-i\, kr \cos(\theta + \theta_0)] \qquad (21)$$

for $2\pi - \theta_0 \le \theta \le 2\pi$, both following geometric optics. The balance of the complete solution is the scattered wave

$$F_s(r,\theta) = F - F_I - F_r \qquad (22)$$

radiating from the breakwater tip in all directions.

The diffraction patterns for this scattered wave for incident waves at 45° and 135° are presented by Sobey and Johnson. The decay of the scattered wave along the breakwater for positive x and the wave radiation from the breakwater tip are the dominant features. The response patterns for negative x however determine the success of superposition solutions. Mod F at least would be required to decay quite rapidly away from the radial lines at $\theta = \theta_0$ and $\theta = 2\pi - \theta_0$ that define the extent of the geometric shadow zones for the incident and reflected waves respectively. Contours of mod F = 0.5 lie along these lines and magnitudes do decay moderately rapidly away to zero at $\theta = \pi$, the negative x axis. This negative x axis is a line of symmetry along which both $\partial F / \partial r$ and $\partial F / \partial \theta$ are zero. It represents a stagnation line in the flow field. This is conveniently consistent with the no flow boundary condition, $\partial F / \partial \theta = 0$, across the superposed left-hand breakwater, but it also imposes a stagnation condition across the gap. Superposition solutions are thus inappropriate in the near-field and are suspect in the far-field to the extent that the imposed stagnation condition across the gap impacts the transmission of wave energy.

For wide gaps (at least one wavelength) together with normal incidence, Sobey and Johnson confirm that superposition does provide a reasonable prediction of the far-field diffraction pattern. For angled incidence or narrow gaps (less than one wavelength) or both, superposition of Sommerfeld solutions is less satisfactory. Sobey and Johnson have specifically compared exact and superposition solutions for gaps of 0.2 and 2.0 wavelengths in terms of profiles along the line of breakwaters and along the incident wave direction from the center of the gap. The imposed stagnation condition across the gap suppresses the standing wave pattern. Away from the gap, the profiles along the line of breakwaters are in reasonable agreement for 90° incidence, and also at 60° incidence if the gap is wide. Otherwise the agreement is relatively poor. The same trends are evident in the profiles along the incident wave direction, except that angled incidence has little influence for wider gaps.

Figure 1 is the superposition approximation for a gap of one wavelength and an incident angle of 45°. These are conditions where superposition is expected to provide a reasonable prediction, as is confirmed by comparison with Figure 2, the exact solution. There are some differences in detail but not in the general trends. These results should also be compared with Figure 2-56b in the Shore Protection Manual, which is the far-field approximation to the exact solution. Again the general trends are in agreement. Detail is sparse near the gap, where the far-field approximation is anyway not appropriate. Note in particular the contour discontinuity to the left of the dominant direction. this is of course a spurious feature, included in the Carr and Stelzreide far-field polar diagram and hence in every contour redrawn by Johnson.

Given access to the exact analytical solution, the superposition approximation and its uncertainties are unnecessary for the breakwater gap problem. For situations where an exact analytical solution is not available, however, superposition does have some continuing application. Non-aligned breakwaters would be such a problem, providing the alignment is such that multiple reflections do not result. Sobey and Johnson include one such example. Incident waves are at 60° to the right hand breakwater. The included angle of the breakwater alignments is 120°, the gap is 1.845 wavelengths and projection of the left-hand breakwater intersects the tip of the right-hand breakwater. The same configuration has been predicted by Memos (6) by an alternative approximation involving the numerical evaluation of Fredholm integral equations of the first kind. Memos' Figure 2 excludes phase information but there was general agreement in the mod F contours.

Conclusions

Standard diffraction diagrams can be established to significantly extend the usefulness of the original Morse and Rubenstein computations which were restricted to the far field from the gap. Comparisons of the common superposition approximation with the complete analytical solution reveal that the usefulness of superposition is restricted to wide gaps and near-normal incidence. Superposition retains some relevance in the estimation of diffraction patterns about non-aligned breakwater in configurations where multiple reflections do not result.

References

1. Abramowitz, M. and Stegun, I. A., *Handbook of Mathematical Functions*, Dover, New York, N.Y., 1964.

2. Blue, R. L. and Johnson, J. W., "Diffraction of Water Waves Passing through a Breakwater Gap," *Transactions*, AGU, Vol. 30, 1949, pp. 705-718.

3. Carr, J. H. and Stelzreide, M. E., "Diffraction of Water Waves by Breakwaters," *Proceedings, Symposium on Gravity Waves*, NBS Circular 521, 1951, pp. 109-125.

4. Johnson, J. W., "Generalized Wave Diffraction Diagrams," *Proceedings, 2nd International Conference of Coastal Engineering*, Houston, 1952, pp. 6-23.

5. McLachlan, N. W., *Theory and Application of Mathieu Functions*, Clarendon Press, Oxford, 1947.

6. Memos, D. D., "Water Waves Diffracted by Two Breakwaters," *Journal of Hydraulic Research*, Vol. 18, 1980, pp. 343-357.

7. Morse, P. M. and Rubenstein, P. J., "The diffraction of waves by ribbons and by slits," *Physical Review*, Vol. 54, 1938, pp. 895-898.

8. Penney, W. G. and Price, A. T., "Part 1. The diffraction theory of sea waves and the shelter afforded by breakwaters," *Philosophical Transactions of the Royal Society*, London, Vol A244, 1952, pp. 236-253.

9. *Shore Protection Manual*, Department of the Army, Coastal Engineering Research Center, 4th Edition, Vicksburg, 1984.

10. Sobey, R.J. and Johnson, R.L., "Diffraction Patterns near a Narrow Breakwater Gap," Manuscript under review, 1985.

11. Sommerfeld, A., "Mathematische Theorie der Diffraction," *Mathematische Annalen*, Vol. 47, 1896, pp. 317-374.

12. Wiegel, R. L., "Diffraction of Waves by a Semi-infinite Breakwater," *Journal of Hydraulics Division*, ASCE, Vol. 88, 1962, pp. 27-44.

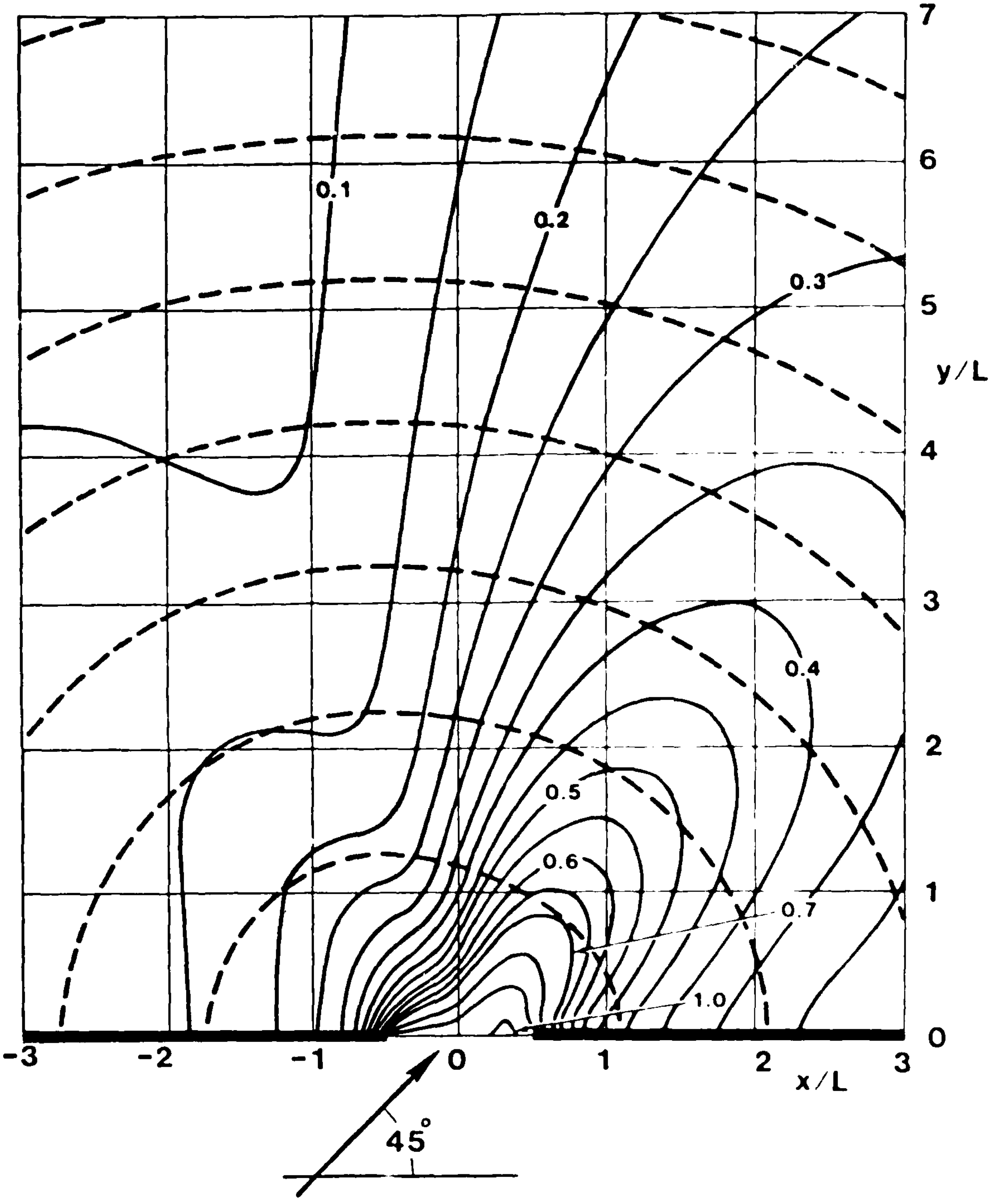

Figure 1. Superposition Approximation for Breakwater Gap, $B/L = 1.0, \theta_o = 45$

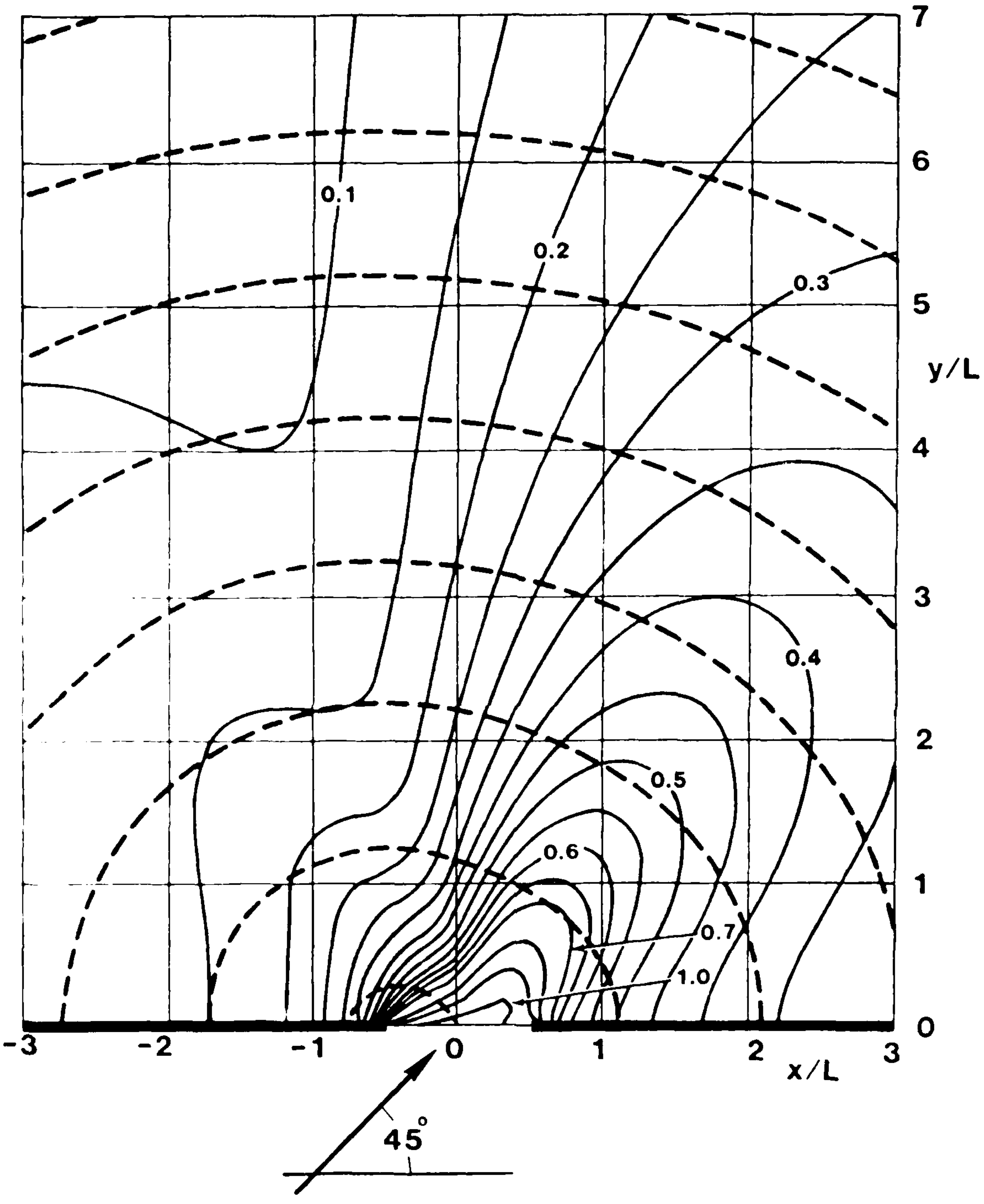

Figure 2. Exact Solution for Breakwater Gap, $B/L = 1.0, \theta = 45°$

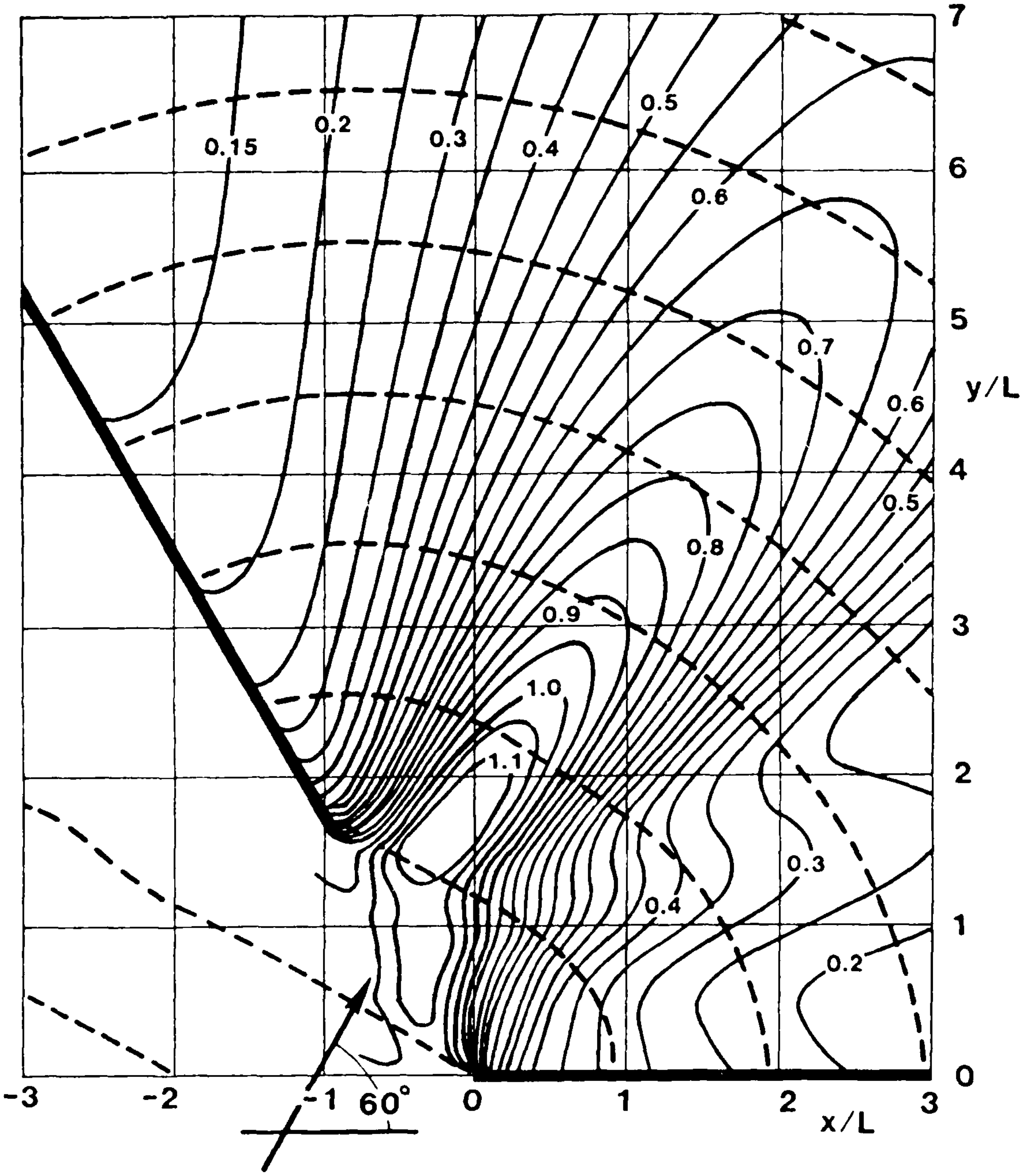

Figure 3. Superposition Approximation for Gap in Non-Aligned Breakwaters, $B/L = 1.845$, $\psi = 120$, $\theta_0 = 60°$

BEACH COMPARTMENTS, LITTORAL DRIFT AND HARBOR DREDGING

Gary B. Griggs*

ABSTRACT

Beach compartments or littoral cells form the framework for our understanding of the sources, transport, and sinks of sand in the nearshore zone. In general, along the California Coast, beach sand is derived from rivers or cliff erosion, moves alongshore under the influence of the prevailing wave conditions, and ultimately is lost either to a submarine canyon or dune field.

Marinas or harbors built either between or at the upcoast ends of beach compartments have been relatively maintenance free due to lack of significant littoral drift at these locations. On the other hand, those harbors built in the middle reaches or at the downcoast ends of littoral cells have had expensive annual dredging problems due to the interruption of large volumes of littoral drift. Although engineers have labored for years on various breakwater, jetty or entrance channel configurations, the actual design utilized is of secondary importance, with the critical factors being harbor location within a littoral cell and annual littoral drift volume.

INTRODUCTION

The movement of sand along the coastline under the influence of waves has been observed for many years. In addition, the actual impacts and costs of tampering with or obstructing the littoral drift process have been painfully obvious for over half a century. Construction of the Santa Barbara small craft harbor (initiated in 1927) and the consequent interruption of littoral drift was perhaps one of the first well studied examples along the California coast (see Wiegel, 1965) an still stands as a monument of sorts. Many of the immediate effects of breakwater construction at Santa Barbara including: upcoast accretion, costly annual harbor dredging, and increased downcoast erosion have been well documented at other California artificial harbor locations as well (for example, Norris, 1964, Griggs and Johnson, 1976, Adams, 1976, Lajoie et al., 1979). Annual dredging costs at some California harbors now exceed $1,000,000. On the other hand, there are other breakwaters and harbors which have had very little impact on the coastline and where no littoral drift obstruction and, therefore, dredging problems, have arisen.

The concept of littoral cells is now recognized as a key element in the littoral drift system, but was not well understood at the time many California harbors were built. Littoral drift has normally been seen as a factor which had to be dealt with after harbors were

---

* Professor, Earth Sciences Board, Applied Science Building, University of California, Santa Cruz, CA 95064

completed rather than a design parameter which would influence harbor siting. At some locations, littoral drift rates were seriously underestimated or inadequately understood prior to harbor construction. At the Ventura Marina, which became operational in 1963, the port district anticipated that littoral drift would accumulate against the north jetty and could be bypassed every 2 or 3 years (Adams, 1976). Annual dredging at an average rate of 144,000 m^3 (189,000 yds^3) had to be initiated soon after construction. Since 1978, average annual dredging has amounted to 440,000 m^3/year (575,000 yds^3) with 1983 costs reaching $1,425,000. These dredging costs have been paid by the federal government in the past. If and when a cost sharing policy is implemented, local port district costs will increase substantially.

Littoral Drift and Beach Compartments

Inman and Frautschy (1966) were the first to recognize the existence of littoral cells or beach compartments. These cells can be considered as distinct segments of the coastline and include three elements: 1) a source or sources of sediment, 2) littoral transport, and 3) a sink or depositional site for the sediment (Figure 1).

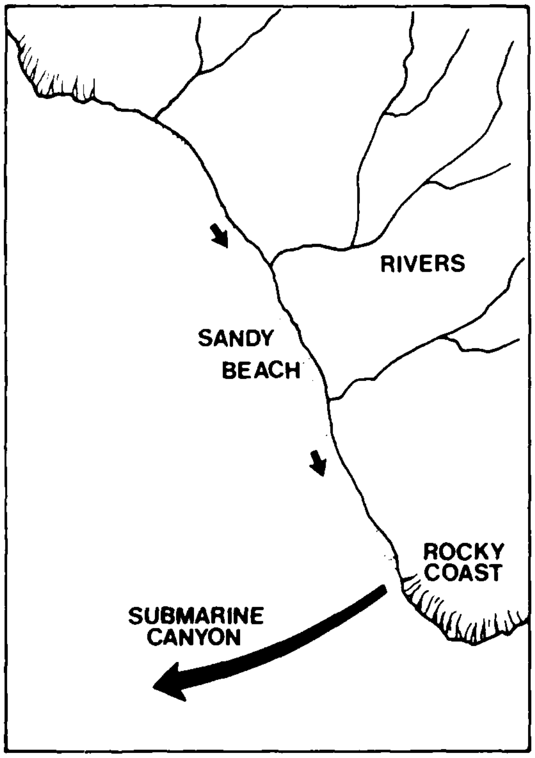

Figure 1. Littoral cell with sand supplied by rivers moved down coast by littoral drift and ultimately lost offshore into a submarine canyon.

Along the California coast, input from coastal streams and rivers is the dominant source of sediment, although cliff or bluff erosion, dredging of harbors, marinas, and embayments, and offshore sands of the inner shelf can be locally important as well. Littoral drift is predominantly from north to south or west to east along most of California's coast due to dominant wave approach from the northwest. Along the coast north of Cape Mendocino, littoral drift reversals are seasonally driven with no clear net drift. South of Cape Mendocino , local coastal segments may also have seasonal shifts in littoral drift or local reversals but display no annual net drift tendency (for summary diagrams, see Habel and Armstrong, 1978).

Sand can be lost from the littoral system through downslope transport into submarine canyons, through transport by wind onshore into dunes, and direct removal of sand through mining. Measurement in Scripps submarine canyon near La Jolla, for example, indicate as much as 150,000 m^3 (197,000 yds^3) of sand each year move down the canyon. This quantity is enough to form a beach 50 m wide, 2 meters deep, and 1500 m long. Similarly, sand mining in southern Monterey Bay removes an estimated 225,000 m^3 (300,000 yds^3) of sand from the littoral system annually (Combellick and Osborne, 1977).

The concept of littoral cells was originally developed for the southern California coastline from Pt. Conception to San Diego where littoral cells or compartments are well developed and quite distinct (Inman and Frautschy, 1966). There has been relatively little effort made to confirm whether or not such cells exist elsewhere, despite the importance of these compartments to coastal engineering, beach nourishment, cliff erosion, and dam and reservoir construction and maintenance in watersheds with high sediment yields. Habel and Armstrong (1978) did delineate a number of tentative littoral cells along the entire California coastline based on available literature. They felt that the littoral cells that they delineated could be used for general planning studies but should not be used to set coastal management criteria without more detailed studies.

The sediment traps which California's harbors have created and the annual volumes of sand dredged* (or lack of dredging), can give us important data regarding littoral drift and littoral cell boundary locations. In addition, planning and engineering efforts for any new small craft harbors must start by considering the littoral drift system within which they must operate.

HARBOR LOCATION AND DREDGING

Based on available maintenance dredging information for the past 4-6 years, it is clear that a number of California's coastal harbors are well located relative to littoral cell boundaries and near shore circulation and have avoided littoral drift problems. There are a number of others where dredging has become an increasingly expensive annual necessity. Several additional harbors or ports are more difficult to evaluate or fall into an intermediate maintenance category. In this paper the performance and dredging needs of individual harbors along three areas of the California coastline will be evaluated relative to their locations within littoral cells.

Monterey Bay

Littoral drift along the central California coast in the vicinity of Monterey Bay falls into two distinct littoral compartments, the Santa Cruz and southern Monterey Bay cells (Figure 2). Three harbors have been built in Monterey Bay, one which requires major annual dredging and two which are low maintenance.

An examination of beach and stream sand mineralogy (Yancey and Lee, 1972) and an evaluation of littoral drift directions and sand accumulation (Griggs and Johnson, 1976) indicates that the Santa Cruz small craft harbor is located in the middle of a littoral cell that extends at least 50 km (30 mi) upcoast and downcoast to Monterey Submarine Canyon.

---

* One difficulty with utilizing the data on annual dredging involves the lack of separation of reported yardage for "maintenance" dredging, in contrast to harbor deepening or beach nourishment dredging. Another limitation to the dredging data is that it represents a minimum value for littoral drift in that some sand bypasses harbor mouths and is not trapped.

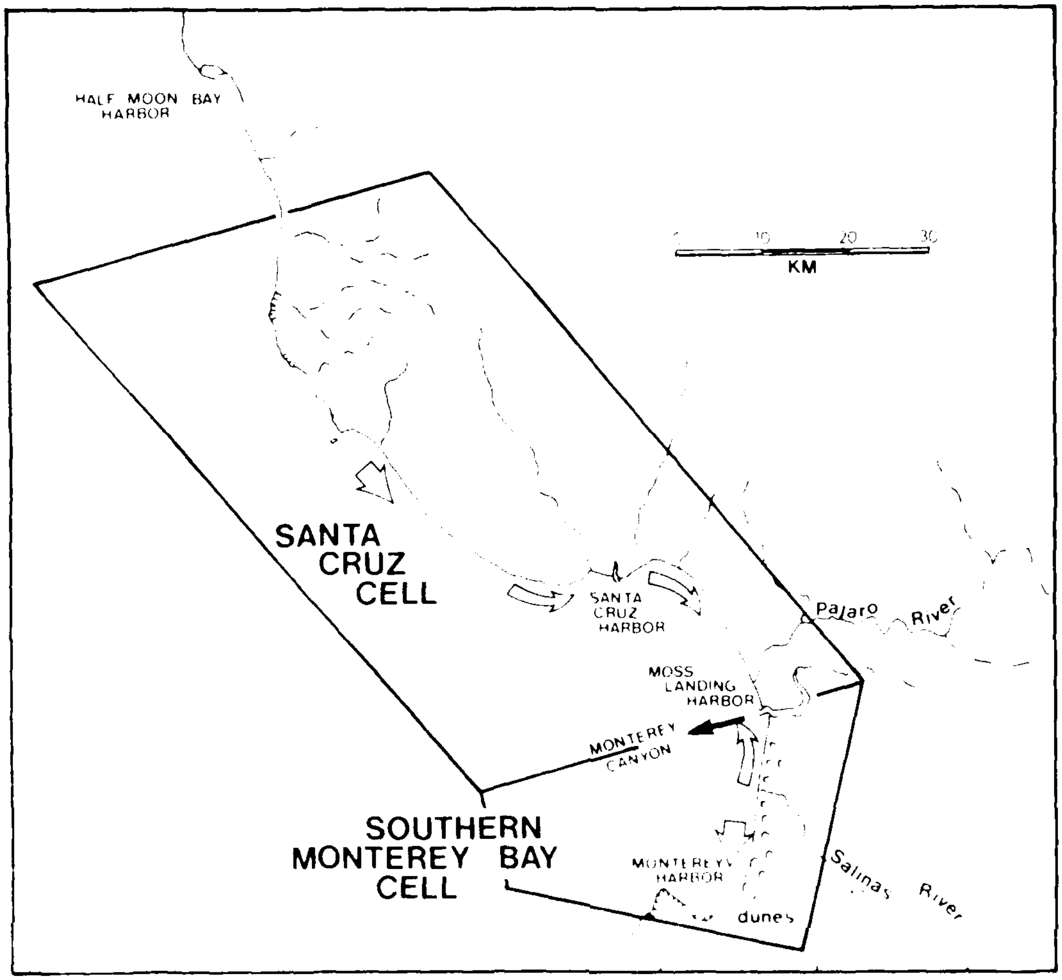
HALF MOON BAY HARBOR
0 10 20 30
KM
SANTA CRUZ CELL
SANTA CRUZ HARBOR
Pajaro River
MOSS LANDING HARBOR
MONTEREY CANYON
SOUTHERN MONTEREY BAY CELL
MONTEREY HARBOR
Salinas River
dunes

[illegible] Littoral cells, littoral drift directions, and harbor [illegible] Monterey Bay area.

Initial Corps of Engineers studies which preceded the construction of the Santa Cruz small craft harbor which was completed in 1963 indicated considerable uncertainty regarding rates of littoral drift. Estimates varied from 19,000 m^3 to 228,000 m^3/year (25,000-300,000 yds^3) in a downcoast direction (Griggs and Johnson, 1976). One important sediment source which was not evaluated at the time was the San Lorenzo River which empties into Monterey Bay less than a kilometer upstream from the harbor. Sediment discharge measurements and river channel surveys indicate the river may be contributing an average of 40,000-50,000 m^3 (50,000-65,000 yds^3) of sand per year to the beach, much of which eventually ends up in the harbor mouth. By 1965, two years after harbor construction, 456,000 m^3 (600,000 yds^3) of sand had accumulated against the west jetty. Dredging of the entrance channel has been required yearly since 1965 (Figure 3). Increased downcoast bluff erosion in the years immediately following jetty construction followed by the emplacement of costly rip-rap, and the loss of a public beach at the city of Capitola were also directly related to the interruption of littoral drift (Griggs and Johnson, 1976).

As the void upcoast from the west jetty has been progressively

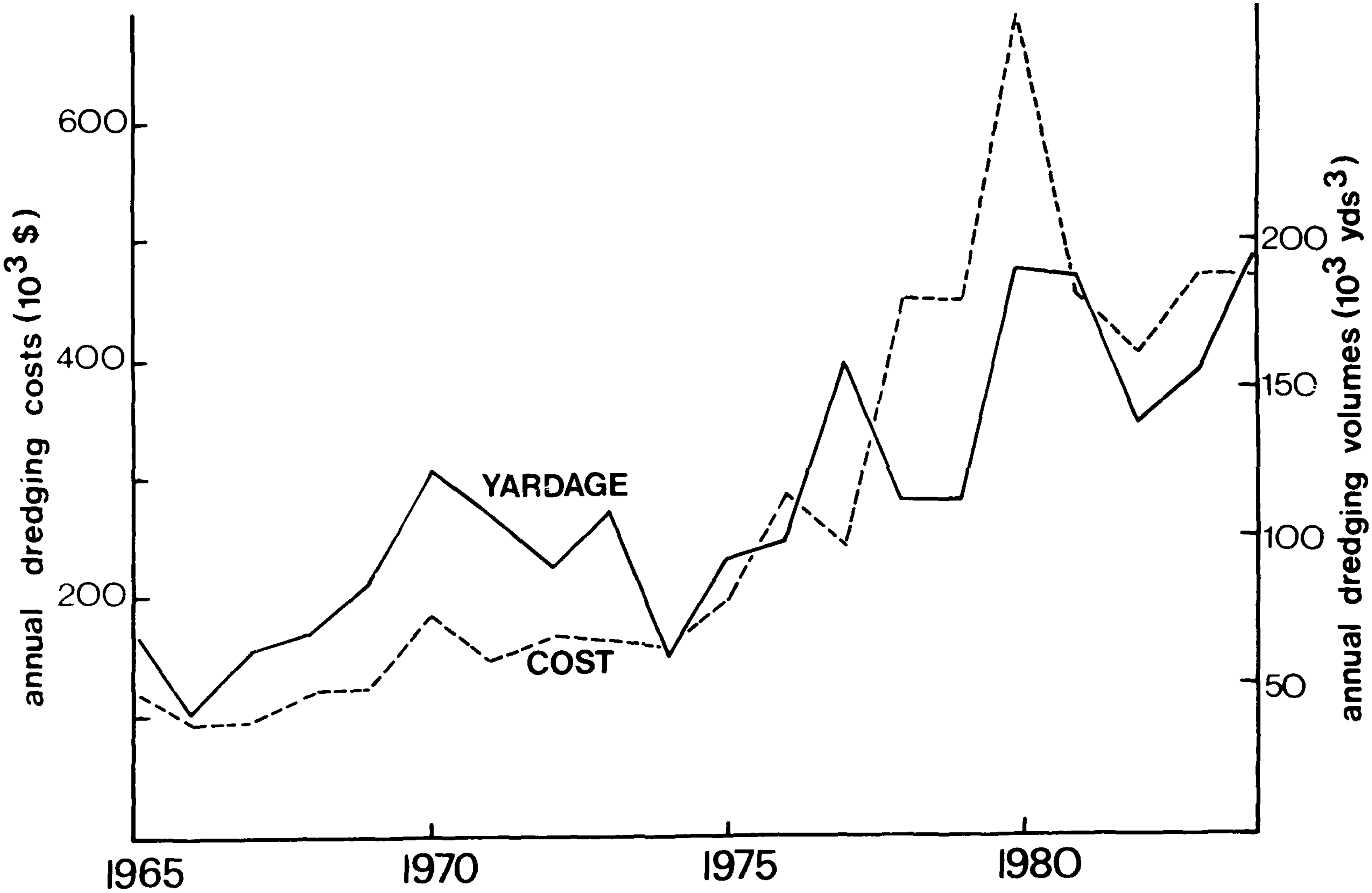

Figure 3. Annual dredge volumes and costs at Santa Cruz Harbor.

charged with sand, more sand has moved around the jetty, and greater volumes of sediment have had to be dredged from the entrance channel. Expectedly, costs have increased as well, in part due to phased dredging (Figure 3). Presently, about 120,000 to 145,000 m^3 (160,000-190,000 yds^3) of material is being dredged annually at a cost of about $450,000. Although many solutions have been proposed (Moffat and Nichols, 1978) and a jet pump system was tried for one brief period, annual dredging has up to the present been deemed the least expensive short term solution.

These annual dredging costs and volumes indicate the Santa Cruz Harbor is a high maintenance facility due to its location within the midst of a high littoral drift volume cell.

Moss Landing Harbor, in the center of the Monterey Bay coastline, has, in contrast, been a low maintenance harbor (Figure 2). Since 1971, the harbor has been dredged about every 3 or 4 years with average volumes of 16,600 m^3 (22,000 yds^3) accumulating yearly. The harbor lies at the seaward end of a large estuary, Elkhorn Slough. Tidal flow at the entrance assists in maintaining the harbor entrance. Of greatest significance, however, is the position of the harbor entrance, precisely at the head of Monterey Submarine Canyon, one of the world's largest and deepest submarine canyons (Figure 2). Littoral drift is dominantly downcoast to the north of the harbor mouth and also downcoast or seasonally variable south of the harbor. The two jetties at the harbor entrance direct littoral drift offshore into the head of the canyon such that the transport of littoral drift into the harbor is minimal. The canyon then serves as a boundary or node between two littoral cells, leading to a low maintenance harbor.

Monterey Harbor is also favorable sited relative to littoral drift, being at the end of a cell or compartment (Figure 2). The rocky Monterey peninsula which produces little sand due to very low erosion rates, occurs downcoast from the harbor. The configuration of southern Monterey Bay is in equilibrium with the dominant northwesterly waves, such that net littoral drift appears to be small with no dominant direction. Excess beach sand in the upcoast area was blown inland in the past and accumulated as an extensive dune field. Since the early 1900's however, the removal of some 225,000 m^3 (300,000 yds^3) of sand annually directly from the beaches by sand mining operators have produced a littoral drift deficit and the southern bay shoreline is now retreating. Approximately 750 m^3 of sand is removed annually from the harbor making it essentially a maintenance free harbor.

Santa Barbara Cell - Pt. Conception to Pt. Mugu

The Santa Barbara littoral cell extends from north of Pt. Conception downcoast to Hueneme and Mugu canyons (Figure 4). The Santa Maria and Santa Ynez Rivers are the major upcoast contributors to littoral drift in this cell. Existing data indicate that the Santa Maria River alone contributes an average of about 170,000 m^3 (222,000 yds^3) of sand and gravel annually to the coastline (Kroll, 1975).

Santa Barbara Harbor, like Santa Cruz, is located in the middle of a long, high drift rate, littoral cell (Figure 4). The harbor at Santa Barbara has existed for over 50 years and dredging has been carried out almost continually since construction. Following completion of the

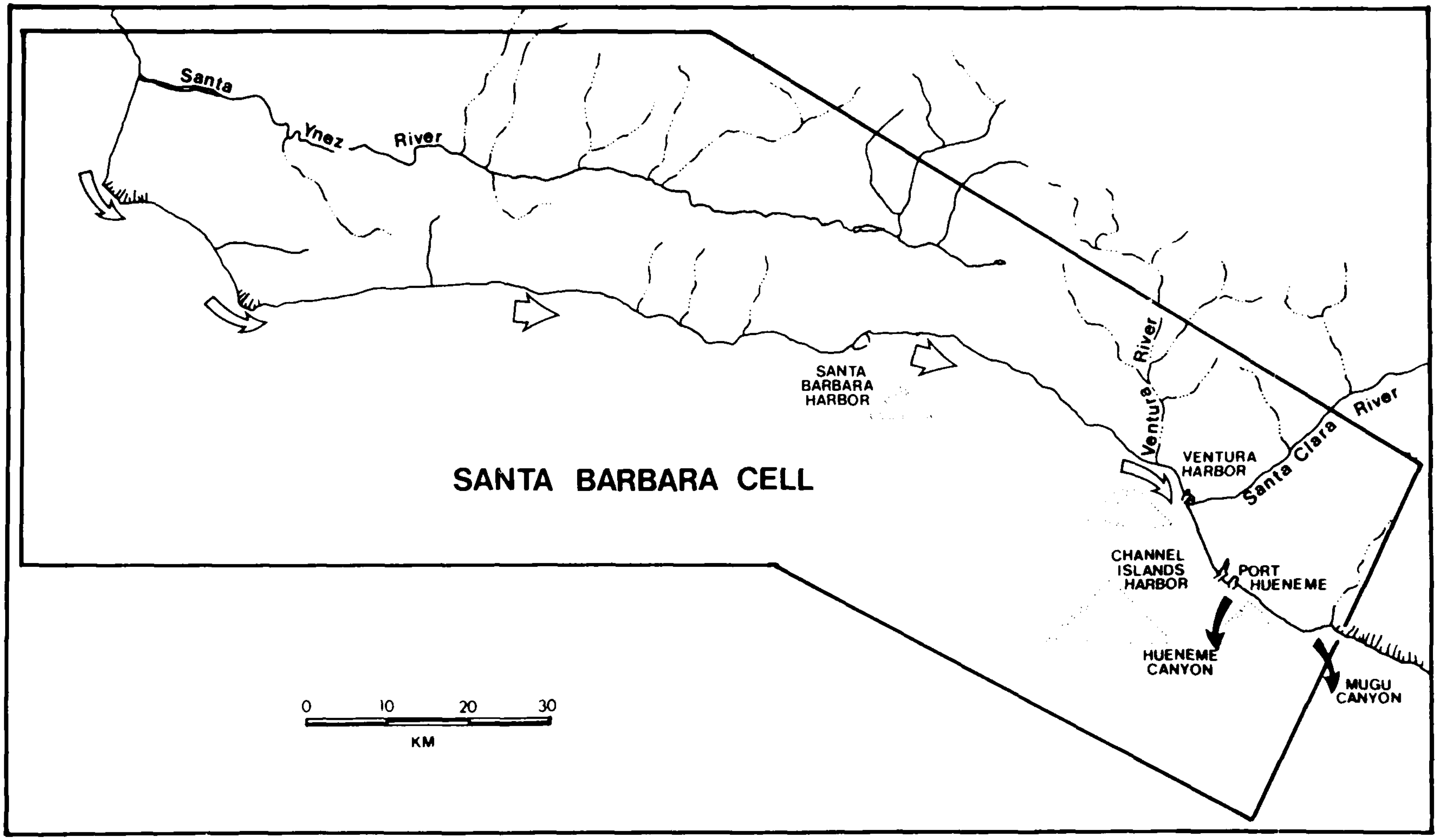
Santa
Ynez
River
SANTA
BARBARA
HARBOR
Ventura
River
VENTURA
HARBOR
Santa Clara
River
CHANNEL
ISLANDS
HARBOR
PORT
HUENEME
HUENEME
CANYON
MUGU
CANYON
SANTA BARBARA CELL
0
10
20
30
KM

Figure 4. Santa Barbara littoral cell showing major sediment sources (rivers), littoral drift, harbors, and sinks (canyons). The triangles next to each harbor are scaled according to average annual dredge volumes.

breakwater in 1930, littoral drift progressively filled a large embayment west of the breakwater. In succeeding years the sand traveled down the breakwater, swung around its tip and eventually began to fill the harbor entrance. The first dredging began in 1935. The harbor is now dredged almost continuously, with average annual yardage amounting to about 350,000 m^3 (450,000 yds^3) at a cost of about $750,000. One unanticipated impact of harbor construction was the loss of about 12 miles of downcoast beaches as sand was initially impounded by the breakwater. An erosion wave progressed downcoast which was initiated halfway through breakwater construction. Property damage exceeded one million dollars by 1934. As dredging began and the littoral system was replenished downcoast, the beaches began to reappear.

The Ventura and Channel Islands harbors were both constructed at the downcast end of this same Santa Barbara littoral cell (Figure 4). Ventura in 1963 and Channel Islands in 1960. The Ventura River discharges upcoast of the Ventura Harbor and the Santa Clara River discharges immediately downcoast. Both rivers are major sediment producers (average annual sand and gravel yields, Ventura River: 100,000 m^3 (131,000 yds^3) Santa Clara River: 550,000 m^3 (720,000 yds^3), Brownlie and Taylor, 1981), despite the fact that 66 percent of the Ventura River Basin and 37 percent of the Santa Clara River basin have now been blocked by dams.

Between 1978 and 1984, 4,145,000 m^3 (5,430,000 yds^3) of sediment were dredged from Ventura Harbor at a total cost of $6.9 million and returned to the littoral zone. Average annual dredging amounts to nearly 600,000 m^3 (785,000 yds^3). Ten kilometers downcoast the same sand is dredged again from the Channel Islands Harbor. Between 1977 and 1985 7,122,000 m^3 (9,330,000 yds^3) were dredged from the harbor at a total cost of over $14 million.

Port Hueneme Harbor was constructed in 1938-40 at the extreme downcoast end of the Santa Barbara littoral cell (Figure 4) two km south of Channel Islands Harbor. The head of Hueneme Submarine Canyon lies directly offshore from the harbor entrance. Records for the shoreline downcoast from Port Hueneme for the 82 years prior to harbor construction indicated a stable sandy shoreline. Evidently the sand bypassing both Point Hueneme and the head of the canyon was adequate to nourish the beaches (Johnson, 1975). The true end of the Santa Barbara Beach compartment actually lies about 11km further down the coast where the remaining beach sand moves off into Mugu Canyon (Figure 4).

After Port Hueneme Harbor jetties were constructed, accretion occurred upcoast, and recession of the shoreline took place up to 11 km downcoast. In order to protect this retreating coast, over 900 m of rip rap was emplaced south of the harbor, and considerable beach fill was added. In 1954 sand trapped against the upcoast jetty was dredged and deposited downcoast. The excavation of Channel Islands Harbor (1961-63) two km upcoast added about 5.3x10^6 m^3 (6.0 x 10^6 yds^3) of sediment to the beaches south of Port Hueneme. The detached breakwater constructed as part of the Channel Islands Harbor entrance protection also creates a sand trap. Every other year, 750,000 m^3 (982,000 yds^3) to as much as 1,900,000 m^3 (2,490,000 yds^3) are dredged from this trap area and delivered to the beaches south of Port Hueneme. Thus Port Hueneme has become a lower maintenance harbor than those upcoast due in part to its position at nearly the end of a littoral cell, but also because of the sand trap which has been built directly upcoast and the port's position near the head of Hueneme Canyon. A shipwreck near the west jetty apparently has tended to deflect some littoral drift into the Port Hueneme entrance channel. About 387,000 m^3 (507,000 yds^3) of material has beed dredged from the inner harbor within the past several years.

Most of the beach sand finally leaves this littoral cell via Hueneme Canyon a little over a kilometer downcoast from the Channel Islands Harbor. Some of this sand however, has already been dredged three or four times from three or four different harbors in its long and interrupted path through the Santa Barbara littoral cell.

Oceanside Cell - Newport to La Jolla

The stretch of coastline extending from Newport Bay to La Jolla contains three harbors; two of these are nearly maintenance free, while the third has moderately high annual dredging requirements. The differences are again due to harbor location within, in this case, the Oceanside cell (Figure 5).

The entrance to Newport Bay Harbor lies about 4.5 km downcoast from the head of Newport Submarine Canyon which marks the southern end of the San Pedro littoral cell (Figure 5). Much of the littoral drift moving downcast is lost to the canyon, some is blown inland as dunes, and some apparently continues past the canyon head. No sand has been removed from the harbor since 1981 when 62,000 m^3 were dredged.

Dana Point Harbor was built at the north end of the Oceanside littoral cell in 1970. Upcoast is a rocky stretch of shoreline which lies between the San Pedro and Oceanside cells (Figure 5), little net littoral drift is recognized along this rocky area. Downcoast from the harbor, San Juan Creek enters the ocean, sandy beaches again appear, and prevailing littoral drift is to the south, although reversals do occur. Dana Point Harbor has not required any dredging in the 15 years since its completion.

The Camp Del Mar Boat Basin - Oceanside Harbor is located immediately downcoast from the Santa Margarita River. It was built during World War Two and the jetties have been extended and modified four times since initial construction in 1942. This harbor is located in the middle of the Oceanside cell (Figure 5), and has long sandy beaches both upcoast and downcoast.

Beaches downcoast as far as Carlsbad have been eroding due to sand impoundment at the harbor, as well as a lack of major floods on the two major sediment sources, Santa Margarita and San Luis Rey Rivers, in recent years. The average annual sand and gravel yields from these two rivers under present conditions only amounts to about 39,000 m^3 (50,000 yds^3) (Brownlie and Taylor, 1981). Littoral drift is trapped by the breakwater and dredging has been carried out every 3 years. From 1978 to 1984, a total of 742,000 m^3 (972,000 yds^3) of sediment was removed from the harbor which gives an average annual accumulation rate of about 107,000 m^3 (140,000 yds^3).

Discussion and Conclusions

There are clear distinctions between most of California's harbors

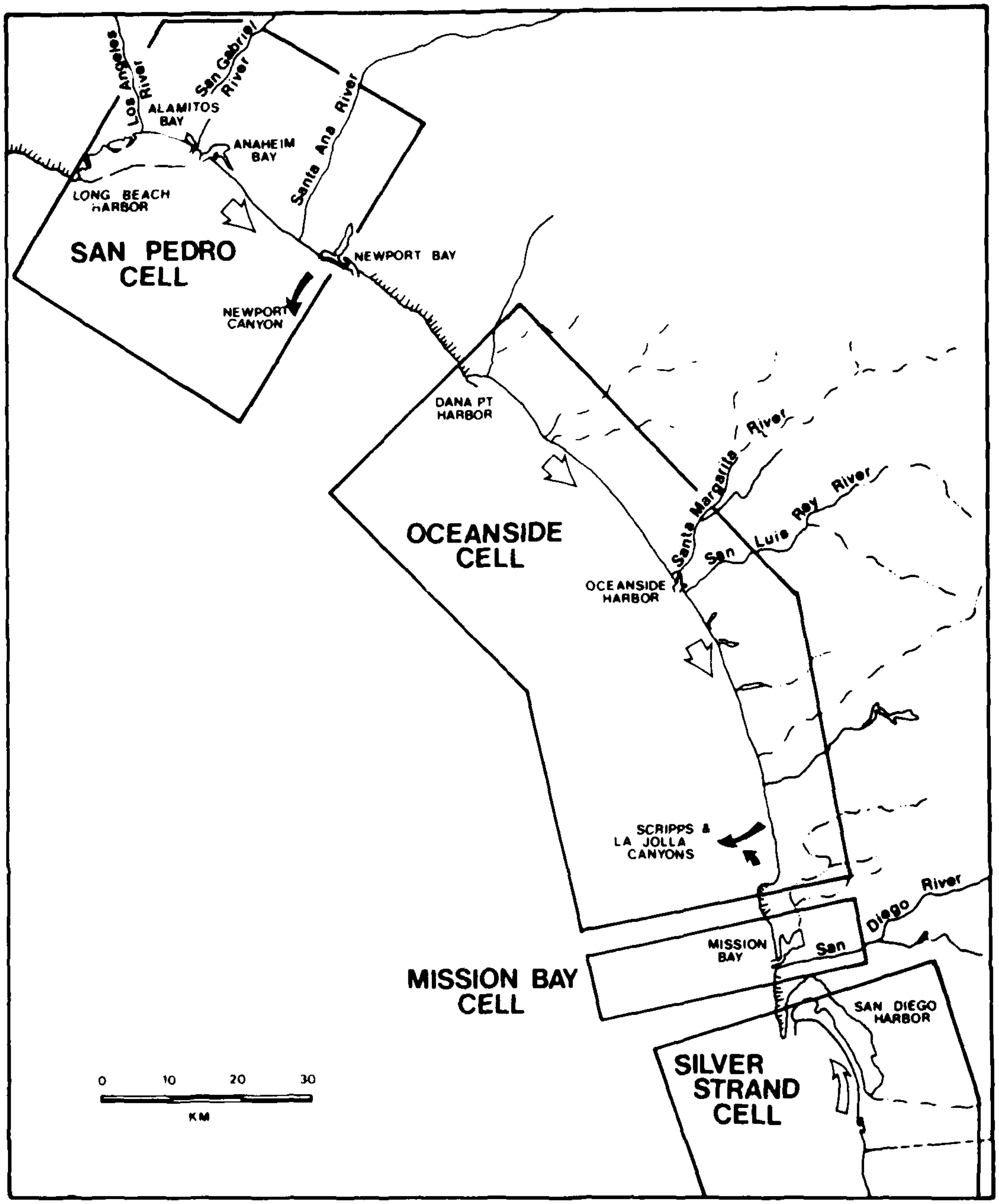
Los Angeles River
San Gabriel River
ALAMITOS BAY
ANAHEIM BAY
Santa Ana River
LONG BEACH HARBOR
SAN PEDRO CELL
NEWPORT BAY
NEWPORT CANYON
DANA PT HARBOR
Santa Margarita River
San Luis Rey River
OCEANSIDE CELL
OCEANSIDE HARBOR
SCRIPPS & LA JOLLA CANYONS
San Diego River
MISSION BAY
MISSION BAY CELL
SAN DIEGO HARBOR
SILVER STRAND CELL
0
10
20
30
KM

Figure 5. Littoral cells, littoral drift, harbors and submarine canyons of southern California.

and marinas in terms of the annual dredging required to maintain the entrance channels. Although engineers have labored for years on various breakwater, jetty and entrance channel configurations, for long term maintenance dredging considerations, the actual design utilized is of secondary importance. The critical factor is not harbor or entrance channel configuration, but location within a littoral cell. Of equal importance is the annual volume of littoral drift at that particular location in the littoral cell. Wherever marinas or small craft harbors have been built in the middle of or at the downcoast ends of littoral cells with large littoral drift rates (at Santa Cruz, Santa Barbara, Ventura or Channel Islands harbors, for example) maintenance dredging has become an expensive annual, biannual or year-round necessity. On the other hand, those harbors built in between or at the upcoast ends of littoral cells, or at locations where littoral drift rates are low, or tidal flow is channeled, have required little or infrequent dredging.

Several examples exist of repreated dredging of the same sand two or three times within a single cell. In the Santa Barbara cell, for example, the same sand is first removed from the Santa Barbara harbor, then Ventura, then Channel Islands and possibly even Port Hueneme, before it finally moves offshore into the head of Hueneme Submarine Canyon. At a dollar or two or more per cubic meter, and nearly two million cubic meters being moved yearly within this cell, this is a very expensive operation.

Once the littoral cell boundaries have been delineated, and one harbor has been built within the cell, the dredge volumes at that location can be used as minimum values expected for littoral drift further downcoast in the cell. Typically, however, additional creeks or rivers enter the system such that littoral drift volumes will increase. This is well exhibited by the statistics for the Santa Barbara cell. Average annual dredge volumes, and consequently costs, increase progressively through the cell. Although the Santa Barbara harbor had been dredging sand regularly at a rate of 225,000 - 300,000 m^3 (295,000 - 395,000 yds^3) year for 30 years prior to the construction of Ventura and Channel Islands harbors, the predictable downcoast maintenance dredging problems were not apparently major considerations in either case.

Although many of California's natural embayments or bays, which were later to become harbors had seasonal or permanent entrances maintained by tidal flow or river discharge, the common pattern with harbor development was to channelize the rivers and divert them from their estuaries. Examples include the Santa Clara River and Ventura harbor, Ballona Creek and Marina Del Rey, the Los Angeles River and Long Beach Harbor, the San Gabriel River and Alamitos Bay, the Santa Ana River and Newport Bay, and the San Diego River, and San Diego Bay - Mission bay. On the positive side this reduced sediment deposition from the rivers within the harbors, on the negative side, the ability of the river flow to maintain a natural entrance channel was eliminated.

There is also clear evidence that harbor construction has increased erosion rates downcoast. In the case of Santa Cruz, Santa Barbara, Port Hueneme, and Oceanside harbor's, this was a direct result of sand impoundment upcoast against a harbor's breakwater on jetty, followed by sand depletion and subsequent beach loss and erosion downcoast. Some of the erosion problems have persisted and other areas have returned to some semblance of equilibrium as dredging has replaced the sand. In the case of Santa Barbara, the sand is dredged daily such that the littoral drift is essentially continuous. With most of the other harbors, however, dredging is an annual or biannual project. Thus sand transport over the long term is essentially in balance, but through the course of a year or more, areas immediately downcoast will be deprived of sand seasonally and will only be nourished irregularly.

There are a number of successful harbors along California's 1750 km of coastline. Monterey, Moss Landing, Newport, and Dana Point are good examples of year round low maintenance harbors, due to their locations either between (at nodal points) or at the upcoast end of littoral cells.

REFERENCES

Adams, C.B., 1976. Case history of Ventura Marina, California. Shore and Beach, 44:2:32-35.

Brownlie, W.R. and Taylor, B.D., 1981. Sediment management for southern California Mountains, Coastal plain, and shoreline. Pt. C. Coastal sediment delivery by major rivers in southern California. Calif. Institute of Tech. Env. Quality Laboratory Report No. 17-C. 314 p.

Combellick, R.A. and Osborne, R.H., 1977. Sources and petrology of beach sand from southern Monterey Bay, California. Jour. Sed. Petrology 47: 891-907.

Griggs, G.B. and Johnson, R.E., 1976. The effect of the Santa Cruz small craft harbor on coastal processes in northern Monterey Bay, California. Environmental Geology 1:299-312.

Habel, J.S. and Armstrong, G.A., 1978. Assessment and atlas of shoreline erosion along the California Coast, State of California Dept. of Boating and Waterways, Sacramento, 277p.

Herron, W.J., 1983. The Influence of man upon the shoreline of southern California. Shore and Beach 51:3:17-27.

Inman, D.L. and Frautschy, J.D., 1966. Littoral processes and the development of shorelines. Proc. Coastal Engr. Specialty Conf. ASCE, p. 511-536.

Johnson, J.W., 1975. Littoral processes at some California shoreline harbors. Shore and Beach, 43:3:16-22.

Karp, L.B., 1976. Case history of Bodega harbor, California. Shore and Beach, 44:3:28-33.

LaJoie, K.R., Tinsley, J.C. and Weber, G.E., 1979. Accelerated coastal erosion rates in response to the construction of the Half Moon Bay breakwater, San Mateo County, In: Field trip guide-coastal tectonics and coastal geologic hazards in Santa Cruz and San Mateo County California. Cordilleran Section, Geol. Soc. Amer. 75th Annual Mtg.

LaJoie, K.R., Matthieson, S., 1985. San Mateo County, In: Living with the California Coast, G.B. Griggs and L.E. Savoy editors, Duke University Press, Durham, N.C., p. 140-177.

Moffat and Nichol Engineers, 1978. Santa Cruz Harbor shoaling study, Santa Cruz harbor, California. Long Beach, Calif.

Noble, R.N., 1971. Shoreline changes Humboldt Bay, California, Shore and Beach, 39:2:11-18.

Norris, R.M., 1964. Dams and Beach sand supply in southern California. In: Papers in Marine Geology, Shepard Commemorative Volume. Ed. R.L. Miller. MacMillan Co., New York, p. 154-171.

Wiegel, R.L., 1965. Oceanographical engineering. Prentice-Hall, London, 532p.

Yancey, T.E. and Lee, J.W. 1972. Major heavy mineral assemblages and heavy mineral provinces of the central California Coast Region. Geological Society of America Bulletin, 83:2099-2104.

SHOALING OF PORT OF ASTORIA, OREGON
BY SEDIMENT FROM MT. ST. HELENS ERUPTION

by Larry S. Slotta*, Roger S. Mustain and Carlos R. Cobos

INTRODUCTION

Sedimentation rates suddenly increased in the Lower Columbia River immediately following the May 18, 1980 eruption of Mt. St. Helens. The goal of this research conducted during 1981-1982 was to determine the origin of the sediment found in the Port of Astoria slips. Another significant concern was whether the severe sedimentation would prove to be a relatively short-term problem or could lead to chronic additional dredging.

Astoria is 78 miles (125 kilometers) from Mt. St. Helens by direct distance, as shown in Figure 1. The Port of Astoria is located at RM 13 (km 21) on the south bank of the Columbia River estuary (see figures 1 and 2). The Port of Astoria slip layout is shown in Figure 2. Both slips are open to the Columbia River at their north end.

PHYSICAL MODEL AND RESULTS

A small physical hydraulic model was used for preliminary investigation of the hydrodynamics and flushing in the Port area. Slips 1 and 2 as shown in Figure 2 were treated as a small embayments closed on the landward side, and open on the seaward side to the Columbia River. The tidal flow pattern was simulated by use of two pumping systems. One, representing the flow of the Columbia River, the second, representing the periodic tidal flow (incoming and outgoing). Injections of dye were made at frequent intervals along the length of each slip, in the river channel upstream to represent Columbia River suspended sediment, and just outside the mouth of each slip to represent the effect of disposing of dredge spoils at such locations. Time lapse cine photos were taken to document the dye movements associated with tidal exchanges.

The results from the model were highly illuminating and satisfactory. Details are given in Mustain (1982) and only summarized here. Figure 3 shows the results of the model run in which dye was released continuously in slip 2. Figure 4(a) illustrates the path of the dye on the ebb tide. On outgoing tides, the dye dispersed into slip 2 would flow into the Columbia River and proceed downstream. Figure 4(b) illustrates the changes in flow patterns which would occur during flood tide. As the flow in the Columbia River reversed, the dye would be carried upstream to and past the mouth of slip 1. A portion of

* President, Slotta Engineering Associates, Inc., P.O. Box 1376, Corvallis, Oregon 97339

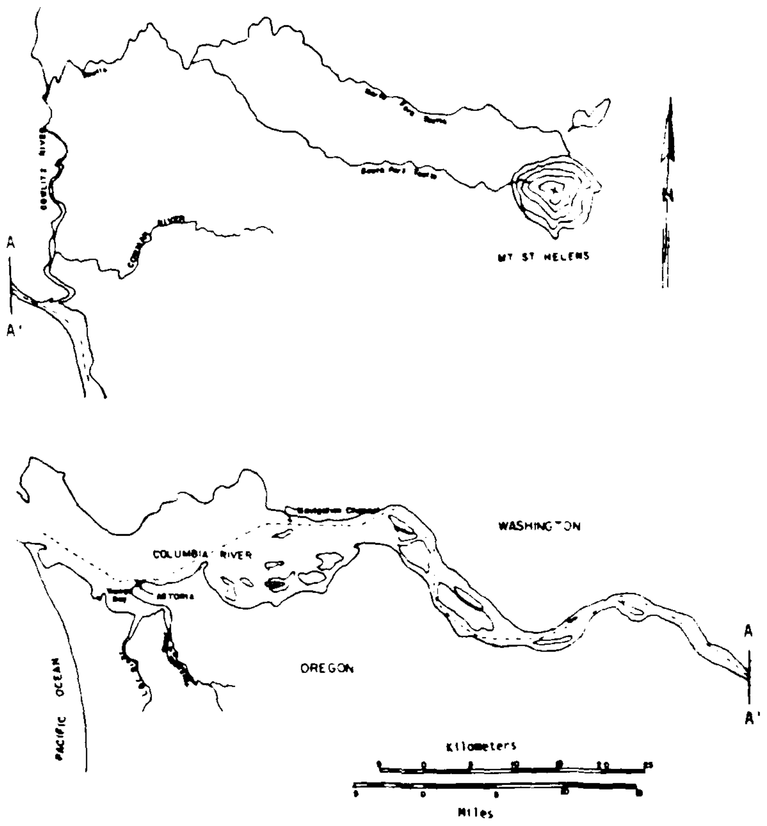
COWLITZ RIVER
COWLITZ RIVER
North Fork Toutle
South Fork Toutle
MT ST HELENS
N
A
A'
WASHINGTON
COLUMBIA RIVER
ASTORIA
OREGON
PACIFIC OCEAN
A
A'
Kilometers
Miles

FIGURE 1. MT. ST. HELENS, THE COLUMBIA RIVER ESTUARY AND ASTORIA

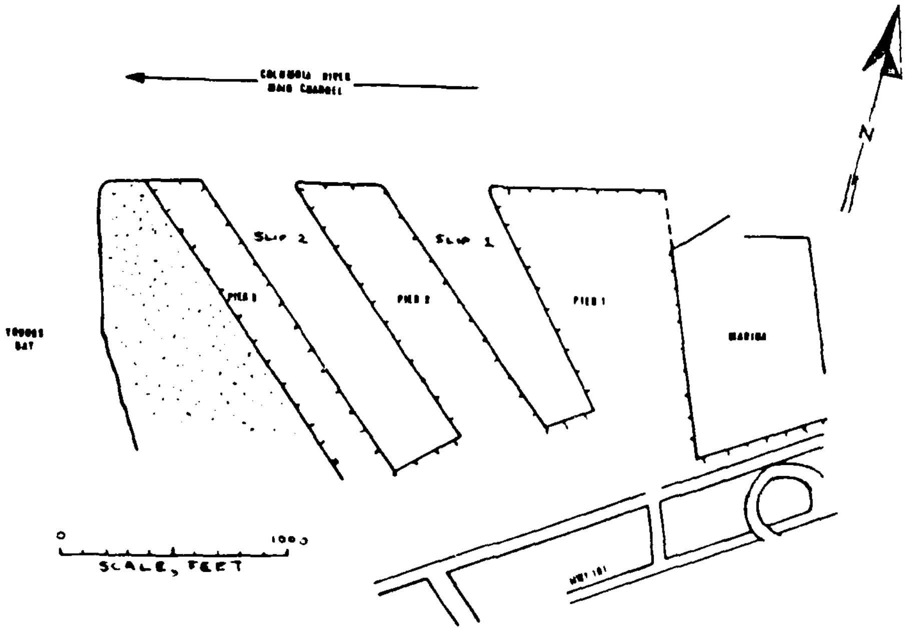
COLUMBIA RIVER
MAIN CHANNEL
N
SLIP 2
SLIP 1
PIER 3
PIER 2
PIER 1
YOUNGS BAY
MARINA
HWY 101
0
1000
SCALE, FEET

FIGURE 2. PORT OF ASTORIA PIER AND SLIP LAYOUT

FIGURE 3. DYE MOVEMENT IN PHYSICAL MODEL

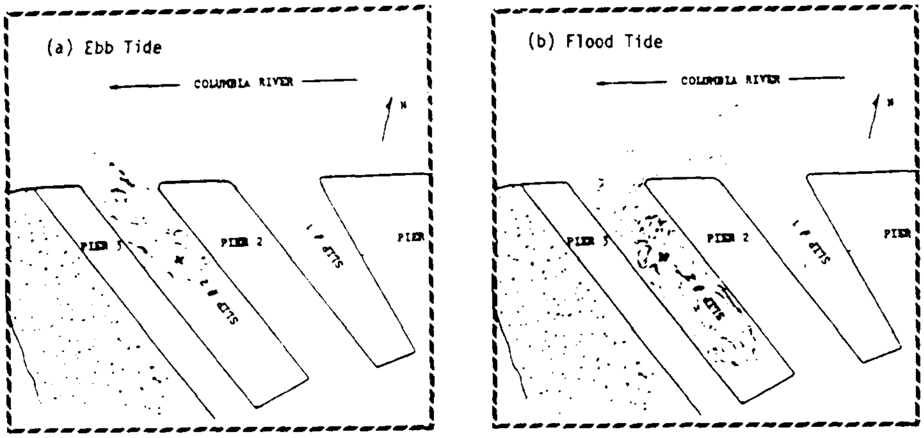

this dye would drift into slip 1 and remained there, even on the next ebb tide. The implication of this behavior for the Port of Astoria is that the generation of large volumes of suspended sediment in one slip (e.g. disposal of dredge spoils in slip 2) could result in increased sedimentation in the other slip.

NUMERICAL CIRCULATION MODEL AND RESULTS

McDougal's (1980) simple one-dimensional numerical model, used for the analysis of flushing in relatively narrow estuaries open to the tide at one end, was applied to examine the flushing and sedimentation of the Port of Astoria's slips. After making simplifying assumptions which are approximately met for the Port of Astoria, the only variables which vary over space are flow rates and concentrations of dissolved or suspended constituents. The slip was divided into several grid cells for analysis. Details of the applied model are given in Mustain (1982) and McDougal et. al. (1986).

Figure 4 illustrates the model results in which initial (normalized) concentrations (C) of 100 units and a tidal amplitude of 5.0 ft (1.72 m) were established in the landward (highest numbered) grid of the model. The higher tidal amplitudes resulted in greater predicted flushing rates since greater tidal amplitudes result in larger exchanges of water between adjacent cells in the model. A more subtle result was that, given the same tidal amplitude, the model with the greater number of cells predicts lower flushing rates, i.e. as the number of grids in the model increases, the volume exchanged between the grids decreases, which results in an apparently lower rate of hydraulic exchange.

FIGURE 4. RELATIVE CONCENTRATION VERSUS TIME

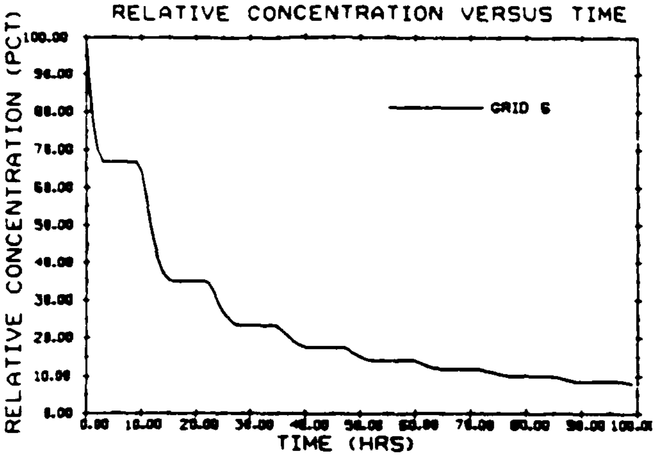

a = 5.0 ft

$C_{0,6} = 100$

S = 0

Figure 5 illustrates concentration versus time for grids located near the midpoint of the slip (grid 4) and at the mouth of the slip (grid 2) with tidal amplitude equal to 5.0 ft (1.72 m), initial concentration of 100 units in cell 6, and a six-cell model. The resultant concentrations on grids 2 and 4 begin at zero, rise to a peak, then decrease at a declining rate, which would eventually become asymptotic to C = 0. The concentration in the middle grid number 4, reaches its maximum in about half the time that a front grid number 2 would require. Also, the maximum concentration in grid 4 is about three times the maximum attained in grid 2.

FIGURE 5. CONCENTRATION VERSUS TIME

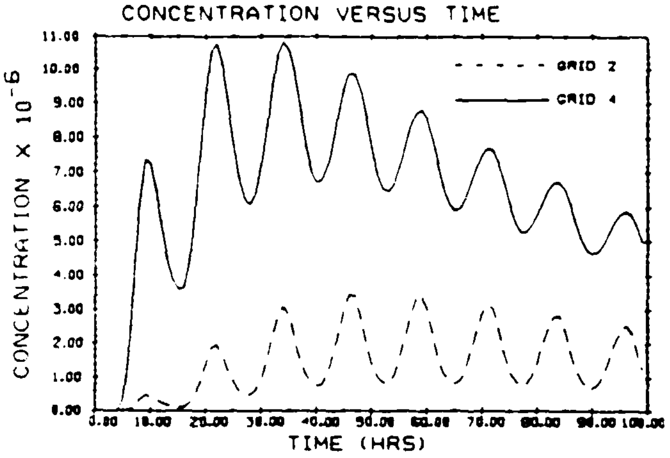

a = 5.0 ft

$C_{0,6} = 100$

S = 0

The model results give an indication of the hydraulic exchange which occurs between Slip 1 and the Columbia River. The predicted flushing rates ([illegible] percent over four days) indicate that the slip exchanges sufficient water to avoid stagnation. Another inference which may be drawn is that sufficient suspended-sediment-laden water from the river enters the slip to provide the source of the shoaling which occurs there. Further, the numerical circulation model's estimated residual circulation may be used as an initial estimate in planning field work. Finally, the numerical circulation model estimates the flow rates into and out of each cell over time. From these flow rates, the average velocity of the water flowing in the slip may be approximated, which will be important when considering the sedimentation within the slip.

FIELD RESEARCH AND RESULTS

The main objectives of the Port of Astoria field research program were to determine the magnitude of and mechanisms behind the siltation problems at the Port and, from the studies, to try to explain the sudden increase sedimentation in 1980-81. The harbor slips at the Port and at the adjacent small boat marina were studied in a field program consisted of six major physical interpretive efforts: a) examination of sedimentation buckets placed on the estuary bottom; b) examination of core samples of the estuary bottom; c) circulation studies using current meters and drogues; d) examination of water samples collected at various depths and locations; e) a side-scan sonar study; and f) a dye tracking study which incorporated aerial photographs.

Sea bed soil grain size analysis findings did not differ with those obtained by previous authors. Krone (1971) and Crane et al. (1981), dealing with pre- and post- eruption data, respectively, show almost no differences in grain size, uniformity coefficients, or mean diameters. This was expected since the currents, the flow regimes, and, in general, the estuary processes have not changed as a result of the eruption. Therefore, the particles of any determined size which settle in an area do so based on hydrodynamic conditions which vary similiarly over the seasons -- independent of volcanic releases.

The velocities within the slip were found to be extremely low -- usually under the threshold velocity of available current measuring instruments. However, current meter records showed that boat activities and ship propeller wakes induce relatively high velocities; high enough to resuspend the sediments on the bottom. The suspended sediment concentrations within the water column were surprisingly variable; more sampling would be required in order to describe their behavior for different tidal conditions.

INVESTIGATION OF SEDIMENT ORIGIN

Clay mineralogy, heavy minerals, and microprobe tests were made to investigate sediment origin. The three tests indicated that the Columbia River is the primary source that produces shoaling in the Astoria Harbor. In this study, the microprobe analysis provided the most definitive answer regarding the questions about the effects produced on the Port of Astoria by the Mt. St. Helens eruption. Since glass was found in some of the core samples taken in the Astoria slips and the glass was believed to be juvenile, five samples were selected for the microprobe test.

The microprobe test results were some what different than expected. The glasses found were of extrememly heterogenous composition and did not plot in the graphical field where most of the May 18, 1980 juvenile glass components plotted. However, the heterogenity observed is consistent with the nonjuvenile glass components from the May 18, 1980 eruption. Dr. Scheidegger, Oregon State University School of Oceanography, analyzed the samples and concluded that the ash in the samples came from the most voluminous phases of the May 18, 1980 Mt. St. Helens eruption.

Samples used for clay mineralogy tests were taken from within the slips and from Youngs Bay. The sample from Youngs ?BAy was taken far upstream, which reduces the possibility of diagenesis, a process which can occur in marine environments with high salt concentrations. The lack of kaolinite on the Youngs Bay sediment suggests that kaolinite had to be transported by the Columbia River, with the sediment's source probably being the Willamette river because Kaolinite is a common clay in Oregon's mid-valley soils. If this is true, it indicaes that the Columbia River is one of the sources of sediment into the Port of Astoria, although it does not disregard Youngs Bay as another source.

The microprobe results, together with the interpretation from the clay minerology tests, confirm that much of the sediment had the Columbia River as the primary source that produces shoaling in the Astoria Harbor. The microprobe analysis provided the most definitive answer regarding the questions about the effects produced on the Port of Astoria by the Mt. St. Helens eruption, indicating that part of the sediment sampled from the port slips contained non-juvenile glass from Mt. St. Helens. However, although the Columbia River is the main source of suspended sediment deposits in the port slips, it is possible under certain conditions for Youngs Bay sediments also to enter the Astoria Harbor.

SEDIMENT BUDGET FOR PORT OF ASTORIA

To compute the sediment budget at Astoria, information from the U.S. Geological Survey (USGS) was used to estimate the sediment load in the Columbia River in the pre- and post- eruption periods. Profiles from the depth soundings of the Port of Astoria were also used.

A sediment budget consists of making a mass balance of the sediment entering, leaving, and stored a defined area. For this case, the selected area is within slip 1. The amount of sediment trapped can be described as the rate of change in the volume with respect to time. The "mass in" is all the mass that comes from the source, in this case the Columbia River. The "mass out" is the dredged material and the resuspended sediment that is flushed out. It has been assumed here that the amount of material resuspended and flushed out is so small that it can be ignored.

Table 1 shows the computed annual volumes of sediment accumulated and the annual volumes of material dredged. The suspended sediment concentration in the Columbia River increased dramatically after May 1980. In fact the sediment load during June 1980 was almost 10 times higher than for June 1979. It is assumed that much of this sediment could settle temporarily in the upper part of the estuary and later be resuspended and carried downstream to within the reach of the turbidity maximum. Gelfenbaum (1981) mentioned that between Hammond and Astoria there is an area of relatively quiet water where sediment might be temporarily stored, which fits this hypothesis on sedimentation of the port slips.

TABLE 1 SEDIMENT BUDGET FOR SLIP 1.

YEAR	TOTAL IN TONS (cu.yards)	TOTAL OUT TONS (cu.yards)	NET SEDIMENT TONS (cu.yards)
1979	40 (20695)	66 (34274)	-26 (-13579)
1980	146 (76581)	124 (64716)	+22 (11865)
1981	132 (68888)	117 (61185)	+15 (7703)

Net sediment at the end of the period - Σ 11 tons (5989 cu. yards).
Negative quantities represent overdredging at the end of the period.

There was an obvious change in the magnitude of sediment being settled and being dredged over the years. The numbers imply that in 1979 dredging involved only approximately half as much volume as that during 1980. The bed level was below the minimum safe depth in 1979; in 1980 the relation is the opposite. Figure 7 shows the annual sediment budget for the 1979-1981 period.

During 1981, a decrease in the amount of sediment seems to have occured. If this is true, it implies a slow decrease on the sdimentation rate. Figure 8 shows a projection of the sediment budget. The discharges after 1981 were estimated using a table of random digits. The rate of sediment is assumed to decrease at a constant rate of 21 percent each year. Because of lack of analysis of pre-1979 dredging records, the values are only estimates.

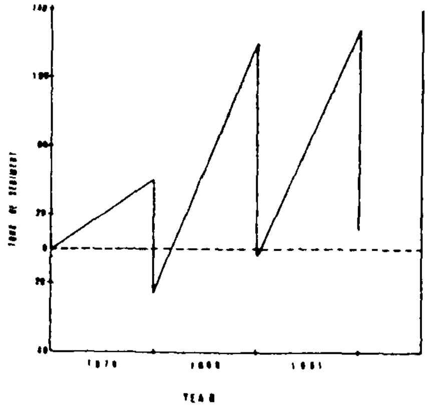

FIGURE 7. SEDIMENT BUDGET.

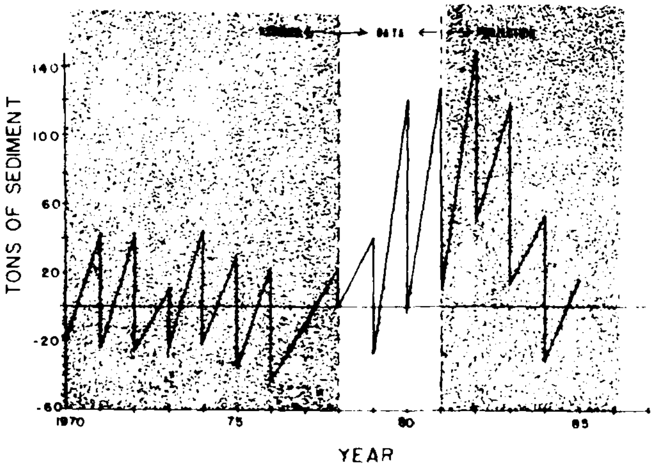

FIGURE 8. PROJECTION OF SEDIMENT BUDGET

GENERAL CONCLUSIONS

Field data collection, laboratory sample analyses, and various modeling techniques permitted determination of the shoaling mechanisms at the Port of Astoria. By inference, this provided insight to related shoaling problems at other lower Columbia River ports. Further research confirmed that some of the sediment was of recent Mt. St. Helens origin and allowed an assessment of the magnitude, the quickness of the impact at locations far downriver, and the likely duration of the impact.

The rate of sedimentation in the Port of Astoria was significantly affected by the eruption of Mt. St. Helens on May 18, 1980. The results from analysis of heavy minerals and clay minerology and, especially, from microprobe tests indicated that the sediment deposited at Astoria originated from the Mt. St. Helens eruption. Hence, the nearly-immediate impacts of the May 18th eruption extended throughout the runoff system and, presumably, reached the Pacific Ocean some 13 miles beyond Astoria.

A sudden increase in the Port of Astoria's sedimentation rate was noticed in 1980. The volume of sediment accumulated was 300 percent higher than that recorded for the previous year; in fact, the volume of accumulated suspended sediment trasported by the Columbia River during the first seven months of 1980 was one and a half times the total amount of the accumulated suspended sediment load for the entire previous year.

A decrease in the rate of sedimentation at Astoria has been noted from interpreting dredge records and data obtained after 1981. The Port of Astoria reported in 1984 less dredging requirements in each of the previous two years. It is anticipated this trend of higher-than-normal but slowly decreasing sedimentation will last for several years. Large quantities of sediment were added to storage in tributaries of the Columbia River by the Mt. St. Helens eruptions. This material will progressively move downstream in the river channels whenever it is disturbed, until it ultimately is either transported out of the Columbia River estuary into the ocean or settles in areas where it becomes protected against further resuspension and transport. Since the material found in 1981 in the slips contained silt and clay, which can be quite easily transported by water, it is moved downstream faster than coarser material. This probably means that the worst part of the sedimentation problem at the harbors in the lower Columbia River has already occurred.

ACKNOWLEDGEMENTS

The research upon which this report is based was financed in part by the U.S. Department of the Interior, Washington, D.C., under the Mt. St. Helens Research & Development Program. Work was carried out at the Water Resources Research Institute, located on the Oregon State University campus, Corvallis, OR and their extensive assistance is gratefully acknowledged. Jennifer Milbrat is thanked for her help in editing and typing this paper.

BIBLIOGRAPHY

Crane, Stephen, Larry S. Slotta and Chong Chu Teng, "Flow Lane Disposal Monitoring," Department of Civil Engineering, Oregon State University, Corvallis, August 1981.

Krone, Ray B., "Investigation of Causes of Shoaling in Slips One and Two, Port of Astoria," unpublished report to the Port of Astoria, Davis, California, 1971.

McDougal, William G., "1-Dimensional Marina Flushing Model," School of Engineering, Oregon State University, Corvallis, 1980.

McDougal, William G. and Larry S. Slotta, "Harbor and Marina Flushing: Water Quality," to be presented at the Ports '86 Specialty Conference, Oakland, CA, May 19-21, 1986.

Mustain, Roger S., "Circulation and Shoaling Study of the Port of Astoria," Engineering Report, Department of Civil Engineering, Oregon State University, Corvallis, 1982.

Slotta, Larry S., "Shoaling of Port of Astoria, Oregon, by Sediment from Mt. St. Helens Eruption," presented at American Geophysical Union Fall Meeting, December 3-7, 1984.

COASTAL FIELD DATA COLLECTION PROGRAM

By J. Michael Hemsley[1], M. ASCE,
C. Linwood Vincent[2], M. ASCE,
and Paul F. May[3]

INTRODUCTION

Funding for the CFDCP was first provided in FY 1976, initiating an ambitious program to collect data needed by the Corps of Engineers' coastal planners, engineers, and scientists. In 1982, the Coastal Engineering Research Center (CERC) of the U.S. Army Engineer Waterways Experiment Station (WES) was given the responsibility for managing the CFDCP. According to the provisions of Engineer Regulation (ER) 1110-2-1406, CERC's mission was to "...conceive, plan, and conduct a coastal data collection program on a nationwide basis to meet long-term Corps of Engineers (CE) needs." The necessity for these data was clearly delineated in the regulation as follows:

> Long-term statistical data on physical environmental parameters, such as the wave climate, the erosion and/or accretion rates along the shore, coastal currents, topographic changes, and the location and amount of sand resources, are needed for coastal navigation, hurricane, flood, and storm protection, and beach erosion control project planning, design, construction, operation, and maintenance.

To accomplish this mission, a data acquisition program composed of multiple tasks, each of which was designed to acquire certain generic types of data, was formulated. These tasks, discussed below, are contributing significantly to the Corps' mission in coastal planning, design, construction, operation, and maintenance.

---

[1] Research Hydraulic Engineer, U.S. Army Engineer Waterways Experiment Station, Coastal Engineering Research Center

[2] Research Physical Scientist, U.S. Army Engineer Waterways Experiment Station, Coastal Engineering Research Center

[3] Research Physical Scientist, U.S. Army Engineer Waterways Experiment Station, Coastal Engineering Research Center

FIELD WAVE GAGING PROGRAM (FWGP)

The need for characterizing the nearshore wave climate is much like the experience of conventional meteorological measurement programs. Along coastlines with high population densities, usage of the resource is intense. Ignorance of the processes at work carries a significant penalty. Past programs either have emphasized the collection of deepwater wave climatology or have been too regional or even site specific. With the Field Gaging Program (FWGP), the Corps intends to collect the long-term, nearshore wave data that are necessary for planning, design, construction, operation, and maintenance of coastal projects.

History and Objectives

In 1974, the American Society of Civil Engineers (ASCE) sponsored the Conference on Ocean Wave Measurement and Analysis. As a direct result of that conference, Scripps Institution of Oceanography installed a wave monitoring network for the State of California in 1975. The network began modestly, with only four stations operating by mid-1976, supported by the California Department of Boating and Waterways (Cal Boating) and the National Oceanographic and Atmospheric Administration (NOAA) Sea Grant Program. In 1978, the South Pacific Division (SPD) became involved and provided funding to begin the expansion of this network throughout California. The Coastal Data Information Program (CDIP) became a cooperative effort between the Corps and Cal Boating, with Scripps acting as a contractor for data collection, analysis, and reporting (Seymour, 1979).

Almost concurrently with the formation of the CDIP, the Corps established the nationwide CFDCP, one element of which was the FWGP. CDIP provided the starting point for the FWGP. The goals of the FWGP are to collect nearshore and relatively deepwater wave data to satisfy the immediate needs of the coastal planner, designer, and project operator; to support the Corps' effort to develop a wave hindcast/forecast model; and to provide a long-term data record for all of the nation's coastlines.

Gage Network

Eventually, the FWGP will acquire wave data along each of the nation's coasts. Primary data for the program will be collected at a number of deepwater or index sites. These stations will be operated continuously in order to provide reliable long-term statistical wave data for use in planning, design, operation, and maintenance of coastal engineering projects. They are located in water sufficiently deep to minimize bathymetric effects on the measured waves, often as deep as 200 m (650 ft).

Augmenting the index stations are nearshore gages located in areas generally representative of long stretches of coastline. These nearshore gages are, single pressure gages, or, more often, slope arrays. Data are to be collected from these stations for up to 5 years to provide the nearshore wave information so necessary to coastal projects and to assist in verification of the numerous wave propagation models. Site selection for slope arrays requires reasonably straight, parallel offshore contours.

To date, Datawell Waverider buoys have been used in all of the index station installations; the depth of these installations precludes the use of bottom-mounted sensors. The Waverider buoy is a proven instrument which uses a vertically stabilized accelerometer to sense the vertical component of the buoy's motion. Heave data from the buoy are transmitted up to 50 km (31 miles) to shore.

Nearshore wave measurements, in depths of up to 15 m (50 ft), are made using a bottom-mounted Kulite semiconductor strain gage pressure transducer mated to an underwater cable by a plastic underwater connector. The cable is used both to carry the signal ashore and to supply power to the sensor. Sufficient cable is stored in a service loop to allow the sensor housing to be brought to the surface for servicing, thereby increasing the system's reliability (Seymour, Sessions, and Castel, 1985.

An array of four pressure sensors has been developed by Scripps to obtain directional wave data. This array is 6 m (20 ft) square and uses a specially designed armored underwater cable for data and power transmission. This cable has effective abrasion resistance, waterblocking integrity, tensile strength, and resistance to cutting which greatly enhance the system's reliability. Details of the array are described by Seymour and Higgins (1978), and results of laboratory and field tests are discussed by Higgins, Seymour, and Pawka (1981) and a field test at Santa Cruz, CA, is described by Seymour, Domurat, and Pirie (1980).

Nearshore gages installed in support of specific projects supplement the data collected under the FWGP. On the Pacific coast, nine project-supported gages are operated through the FWGP network and data reported monthly. The program, therefore, provides an existing system through which project-specific data can be collected, analyzed, and reported. The system provides the considerable capacity and flexibility needed for coastal data collection and can accommodate any continuously reporting instrument. Tide, surge, current, wind, and wave data are being or have been collected on the system.

Related Data Collection Program

Alaska's coastal data needs are unique. The state has approximately 54,500 km (33,900 miles) of coastline with a climate varying from temperate to arctic. With communities heavily dependent on the sea scattered along the entire coast, Alaska needed a planned approach to its coastal data collection efforts. In 1982, a cooperative agreement was signed between the State of Alaska and the Corps of Engineers to collect coastal wind and wave data. The goals stated in that agreement were, briefly, to collect, analyze, report, and archive coastal data collected by either party; to develop a plan for the collection of coastal data; and to develop instruments, telemetry systems, and analysis procedures suited to the needs and environment of Alaska (Bales, 1984).

Data have been collected at Kodiak, Homer, Akutan, Nome, and Whittier. The Alaska Coastal Data Collection Program (ACDCP) has been supported by funds from the State Department of Transportation and Public Facilities (DOT/PF), the U.S. Army Engineer District, Alaska (NPA), and the FWGP. Short-term (2 to 3 years) data collection is planned to begin at 17 sites over the next 5 years if state funding continues.

Two types of stations have been developed: one for deep water and the other for nearshore measurements; both include a remote anemometer. For the deepwater sites, Waverider buoys are used. Nome is the only station currently in shallow-water operation. There the instrumentation consists of two P-U-V meters to provide directional wave data. Data from both station types are telemetered to a shore station and recorded on magnetic tape. Because data transmission over telephone lines is not reliable in Alaska, a meteor burst transmitter is used to send real-time data to the Corps office in Anchorage. The system uses meteor trails in the upper atmosphere as the medium from which the data are reflected. Meteor burst allows the data to be transmitted over great distances without the use of satellites or telephone lines and provides an inexpensive system check.

NPA publishes data reports periodically as data are processed. To date, three reports have been produced. As more stations become operational, the data reports will be published more frequently.

Another cooperative effort that receives some support from the FWGP involves a contract with the University of Florida to collect, analyze, and report wave and surge data from the Florida coast. The gaging effort is funded by the Corps through the Hurricane Surge Prototype Data Collection Work Unit and the FWGP, by the State of Florida, and by the U.S. Nuclear Regulatory Commission. Eight sites in Florida are operated by the University as the Florida Coastal Data Network (FCDN) using bottom-mounted single pressure transducers. Recently, three P-U-V in-situ recording meters were added to provide directional wave data.

The FCDN provides real-time data in support of the hurricane surge work unit. Data reports are produced monthly by the University of Florida for each of the sites operated under the contract. (Howell, 1980).

Deepwater wave data are also being collected by NOAA. Recently, in support of the Coast of California Storm and Tidal Wave Study, the capability to access the NOAA data for the Pacific was demonstrated. Consideration is being given to reporting these data in the monthly and annual reports prepared by Scripps.

Data Collection, Analysis, and Reporting

The data collection system developed by Scripps and used by the FWGP is based on burst rather than continuous sampling. While sampling frequency is field selectable, depending on the data to be collected, it is typically set at 1 Hz for ocean waves measured for the FWGP. Normally each instrument is interrogated once every 6 hr, although certain critical stations are called every 3 hr and the data transmitted to the National Weather Service (NWS).

Data analysis is composed of three phases. The first phase involves the receipt of the raw data from the shore stations and extensive data verification and editing in preparation for the second phase. An analysis phase performs the Fast Fourier Transform (FFT) operations on the edited time series. The final phase operates on the analyzed data to produce the end products, monthly and annual reports. Higgins, Seymour, and Pawka (1981) describe the analytical method for extracting wave directionality from the sea surface slope components measured by the array. The method developed by Longuet-Higgins, Cartwright, and Smith (1963) for use with a pitch-and-roll buoy is adapted for use with the array. An estimate of the longshore component of radiation stress S_{xy} can be extracted when surface elevation and components of sea surface slope are known at a point. The components of the slope are determined from differences between a pair of sensors.

The significant data collected under the FWGP are available to users in three forms: direct access via remote terminals, data archives at Scripps and WES, and monthly and annual reports. Data processed since the program's inception are directly available to any user with a computer terminal capable of remote telephone access of the data analysis computer at Scripps. A use-friendly program has been developed to call up tabular and plotted data. Edited raw data are archived on tape at both Scripps and WES and can be made available to users.

Monthly and annual reports produced by Scripps provide the widest dissemination of wave data collected within the FWGP. After the first month of operation of the original program in 1975, a report was issued showing spectra and other wave parameters for Imperial Beach, CA. Every month since, analyzed data have been provided through these reports to a large group of public and private users. These data are summarized in an annual report.

Future Effort

A nationwide network of index sites, including the Great Lakes and the Gulf of Alaska, is the goal of the FWGP. That goal will be pursued during the next few years if funding will allow.

WAVE INFORMATION STUDY (WIS)

Almost all coastal projects have a requirement for wave information, and frequently, it is critical to the determination of the type and cost of solution. Wave information most often must be provided for a 20- to 50-year design life. Short-term gaging, however accurate, does not meet this need because the climate is variable. When gage records are reviewed, it can be seen that there are relatively few years of observations, and often significant parts of the year can be missed because of gage failures. Equally important, unless the gage is in fairly deep water, the gage measurements can be highly site dependent.

The hindcast program uses state-of-the-art models to translate meteorological data and astronomical tide date into coastal wave and water level information. Benefits of this approach include:

(1) Generation of 20 years or more of data using consistent technology nationwide.

(2) Availability on a uniform geographical grid.

(3) Availability of directional spectral information.

(4) Absence of lost data.

(5) Application of system to other areas.

(6) Use of the system to model specific events.

(7) Use of data in an interactive data base.

(8) Use of the data to drive higher resolution wave models.

The trade-off is between lack of extreme wave data and sparsity of spatial coverage in gage data versus imperfections in the wave model. The wave model has been extensively compared to observations and performs as a quality, state-of-the-art model.

Past Efforts

In prior years the model system was developed and refined and hindcasts made in specific areas with different levels of density of information at 120-, 30-, and 10-nautical mile grids. Excepting hurricanes, the Atlantic and the large-scale Pacific have been finished for the 20 year period from 1956 through 1975. Major storms in the Atlantic have been analyzed back to 1900 to give a 75-year basis for extreme wave estimates. During 1985, the plan is to finish the Pacific with the exception of hurricanes, add hurricanes to the Atlantic, and finish the first level in the Gulf of Mexico. Additional work necessary in future years includes:

(1) Completion of Gulf of Mexico, including hurricanes.

(2) Addition of Pacific hurricanes.

(3) Addition of Great Lakes.

(4) Completion of water level data bases.

(5) Addition of more interactive programs to the Sea State Engineering and Analysis System (SEAS).

It should be noted that at each of the locations where data are saved, there will be over 58,000 sets of wave parameters available on an on-line data base for district office use. This data base, which has been designated the Sea State Engineering and Analysis System, is indeed the only way the information can be economically made available, because there is so much of it. CERC plans to add or interface other programs and models to SEAS to provide a basis for an integrated design system for applications that require wave and water level information. The purpose of SEAS is to provide the following:

(1) Rapid access data

  (a) Height, period, direction for sea and swell
    -Time series
    -Probability tables
    -Water levels

(2) Slower access data

  (a) Frequency spectra

  (b) Directional spectra

(3) Application programs

  (a) Statistics

  (b) Display

  (c) Engineering

Future Efforts

A state-of-the-art system for translating meteorological and tide data into coastal wave and water level information and disseminating the information through an interactive data base is in place. The system can be run in the long-term hindcast mode or can be used to study specific events. In principle, it can be applied to other areas of the world if the Army needs it.

Since the hindcast study began, the following events have occurred:

(1) The computers used have increased by a factor of about 30 in speed, and another factor of 10 can be expected in the next few years.

(2) Wave measurement systems have become more reliable and now can provide directional estimates.

Both of these provide unique opportunities for improvement of wave climate estimates. Although wave gages have improved and satellites are expected to become operational wave data collection platforms, it may be another 10 years before reasonably spaced spatial and temporal coverage is available and over a 5-year basis of information is gathered.

The increased speed of computers gives us the opportunity to increase the basic data base to 30 or even 40 years by the time gaging or satellites begin to provide climate information on a national basis at a lower cost compared to establishing the first hindcasts. This increased time base is particularly important to understand the effects of year to year variability in waves and water level climates. If significant advances are made in wave modeling, it will be possible to regenerate the climatology cost effectively because of the existing winds developed and the increase in speed of computers.

Even as more observations become available, it is unlikely that they will be available on the 10-mile spacing that the model can produce, even into the next century. One opportunity, however, is to incorporate the gage and satellite data directly into the wave model calculations, not simply to use them as verification. Then, the model system results can provide finer spatial scale information based upon a combination of both atmospheric and gage data. Models currently being tested at CERC will be able to refine coastal calculations down to a grid size of about 100 m or less for detailed site-specific studies.

Thus is can be seen that the future of WIS is to allow future improvement to the basic wave climate to a 30- to 40-year basis and to provide a framework for interpreting the field gage or satellite information into site specific wave statistics needed for design. Further, the model system allows the investigation of "what if" or hypothetical events. CERC sees WIS as providing the basis for the critical development of interactive design systems through interfacing advances in other coastal technological areas to this very basic data base. This systematic approach provides a rational framework for turning the numerous pieces of wave and water level data into information that can be used in design.

LITTORAL ENVIRONMENT OBSERVATION (LEO) PROGRAM

The Littoral Environment Observation (LEO) Program is a visual data collection program that has been ongoing under CERC's direction since 1968. The objective of the LEO Program is to establish an economical reservoir of repetitive and systematic observations of both the forces and response elements in the coastal zone at sites where no data exists or where funds are not available for sophisticated instrumentation. The data collected include wave height, period and direction, width of surf zone, wind speed and direction, longshore current and direction, and beach slope. Over its 15-year existence, data at over 200 sites have been collected.

A data base and a user-friendly retrieval system have been developed and are presently undergoing evaluation before they are made available to engineers at CE Districts. The data base and retrieval system is operational on Control Data Corporation's Cyber 865 Corps dedicated computer in Rockville, Maryland. The retrieval package consists of various statistical reports that summarize the data at a particular site. A user's manual is being developed and will be available to Corps engineers in Fiscal Year 1986.

Plans are under way to conduct a study in conjunction with an experiment scheduled for 1986 at CERC's Field Research Facility at Duck, North Carolina, to improve the methodology for visual coastal field data collection. Plans are also under way to develop a capability for downloading the LEO data from the main data base to a personal computer for local analysis.

In summary, the LEO Program has provided an economical data base of coastal information at sites where no other data exist.

THE COASTAL ENGINEERING INFORMATION MANAGEMENT SYSTEM INDEX SUBSYSTEM (CEIMS/IS)

Voluminous amounts of data and written reports exist for the United States and its territories. A need to make these valuable sources of information readily accessible to CE personnel presently exists, and will continue to increase in the future. A Corps-wide interactive Coastal Engineering Information Management System Index Subsystem (CIEMS/IS) has been developed to catalog the existence, location, and characteristics of coastal data and written documents containing information about specific coastal reaches. In order to adequately address all sources of coastal information, the CEIMS/IS is divided into two classes: coastal studies and technical journals. Coastal studies class references all data collection efforts, studies, and raw data sets; whereas the technical journals class provides a catalog for all written documents (published or unpublished). This user-friendly indexing subsystem, the first module of two to be implemented for CEIMS, points to the existence and location of coastal information for an area or data type. In addition, it provides a pathway to the second module, the Data Access Subsystem (DAS), which will be implemented in stages beginning in Fiscal Year 1986. The DAS module of CEIMS will allow access to a variety of coastal studies digital data residing on the Cybernet system and other computer storage facilities.

CEIMS/IS has been installed on the Control Data Corporation Cybernet Network System to provide availability to all Corps personnel. The host system exists on a Cyber 865 located in Rockville, Maryland, and uses BASIS, a relational data base software product. This software provides the backbone of the CEIMS/IS and is capable of running on a variety of machines. This host system may be accessed for data entry or retrieval using a dumb terminal, intelligent terminal, or personal computer (PC).

A PC-level capability has also been augmented into the system. This micro-software package provides an alternative to interactive data entry and retrieval on the main frame host system which results in a substantial user cost savings. Data may be transferred to and from the main frame host system via the PC. The PC capability allows a user to compile, retrieve, and manipulate data records at any location with a capability to connect to the host system when a communication line is available. The user can enter from the PC into the main frame host system through the communications software included in the PC package and query the main data set from the PC. Data records may be requested from the main frame system and downloaded to the PC-level work station where additional querying and sorting may be performed. Users may store on their PC's downloaded information retrieved from the main frame host system for manipulation at a later date.

The design of CEIMS/IS allows users to feed information directly into the system. This will allow a much more comprehensive and rapidly filled data base to be compiled. To ensure quality control, all data entered into the CEIMS/IS from either the PC or the main frame host-system level are verified by the system's administrator before final entry into the main data-base file.

CEIMS/IS has been well received to date. Requests for information concerning access to the data base have been filtering into CERC. A cooperative effort is presently under way between CERC and the Jacksonville District to enter information for the Coast of Florida Erosion and Storm Effects Study and the District is currently using the system. Inclusion of data and active participation from Florida state agencies and academic institutions is scheduled to begin this fiscal year. The Los Angeles District has also contributed data from the Coast of California Storm and Tidal Waves Study and is scheduled for user training in 1985.

Since the CEIMS/IS effort was begun in Fiscal Year 1984, design, development, and implementation of the Corps-wide interactive CEIMS/IS have been completed. The IS, the first of two CEIMS modules to be developed, points to the existence and/or location of coastal information for an area of interest or a specific data type. CEIMS/IS provides the Corps with a time-saving and efficient tool for cataloging and accessing sources of coastal information pertinent to their project interests.

FUTURE

In addition to the elements of the CFDCP discussed, it has been proposed that the program be expanded to include shore and beach information, measurement and documentation of episodic events, and increased support for the ACDCP.

Shore and Beach Information

This element of the program will incorporate LEO and renew the shoreline change map effort and profiles program. The objective is to quantify the long-term, seasonal, and storm-induced beach, dune, and nearshore profile changes. These data are essential to the determination of erosion and accretion rates. Preparation of shoreline change maps from historical information and the identification, interpretation, archiving, and reduction of profile data at District offices will provide the needed data.

Measurement and Documentation of Episodic Events

An existing research effort, Hurricane Surge Prototype Data Collection work unit, will become a part of the CFDCP and be expanded to include a wider variety of episodic events. The objective of this effort is to provide the quantity and quality of timely data required to more accurately document the characteristics and effects of events such as severe storms and tsunamis. Data collected will provide the information needed for verifying the numerous numerical models used to predict surges caused by severe events. The methodology developed under the work unit will benefit the expanded effort under CFDCP.

SUMMARY

The objective of the CFDCP is to systematically acquire and assemble the geophysical information required for cost-effective planning, design, construction, and maintenance of coastal projects, to archive the data in a computer-based information system, and to routinely and rapidly disseminate information to Corps planners, engineers, scientists, and managers. Work is under way to achieve that objective, but much is left to be done.

ACKNOWLEDGMENTS

The investigations described in this paper were undertaken by WES as a part of the Coastal Field Data Collection Program, Civil Works Program of the Corps of Engineers. Mr. John H. Lockhart, Jr., was technical monitor for this program which was managed by Mr. John Mikel, Operations and Readiness Division, Office, Chief of Engineers. The authors wish to acknowledge the Chief of Engineers, U.S. Army Corps of Engineers for permission to publish this paper.

REFERENCES

BALES, J. T., 1984 (Jun). "Alaska Coastal Data Collection Program, Proceedings of the 41st Meeting of the Coastal Engineering Research Board, Seattle, WA, Coastal Engineering Research Center, pp. 283-289.

Headquarters, Department of the Army. 1981 (Mar). "Monitoring Coastal Projects, Engineer Regulation 1110-2-8151, Washington, D.C.

Hemsley, J. M., Vincent, C. L., and May, P. F., 1985, "Coastal Field Data Collection Program", Proceedings of the Meeting of the Coastal Engineering Research Board, Vicksburg, MS, Coastal Engineering Research Center, In Press.

Higgins, A. L., Seymour, R. J., and Pawka, S. S. 1981. "A Compact Representation of Ocean Wave Directionality," Applied Ocean Research, Vol 75, No. 33, pp. 6778-6801.

Howell, G. L. 1980. "Florida Coastal Data Network," Proceedings of the 17th International Conference on Coastal Engineering, ASCE, Sydney, Australia, Vol 1, pp. 421-431.

Longuet-Higgins, M. S., Cartwright, D. E., and Smith N. D. 1963. "Observations of the Directional Spectrum of Sea Waves Using the Motions of a Floating Buoy," Ocean Waves Spectra, Proceedings of a Conference, pp. 111-136.

Seymour, R. J., 1979. "Measuring the Nearshore Wave Climate: California Experience," Marine Science, Vol 8, in Ocean Wave Climate, Marshall D. Earle and Alexander Malahoff, eds, Plenum Press, N. Y., pp. 317-327.

Seymour, R. J., Domurat, G. W., and Pirie, D. M. 1980. "A Sediment Trapping Experiment at Santa Cruz, CA.," Proceedings of the 17th International Conference on Coastal Engineering, ASCE, Sydney, Australia, Vol II. pp. 1416-1435.

Seymour, R. J., and Higgins, A. L. 1978. "Continuous Estimation of Longshore Sand Transport," Coastal Zone '78, ASCE, pp. 2308-2318.

Seymour, R. J., and Sessions, M. H., and Castel, D. 1985. "Automated Remote Recording and Analysis of Coastal Data," Journal of Waterways, Port, Coastal and Ocean Division, ASCE, NY, NY, pp. 388-400.

J. MICHAEL HEMSLEY

Mr. Hemsley is a research hydraulic engineer, U.S. Army Engineer Waterways Experiment Station, Coastal Engineering Research Center (CERC), Engineering Development Division, Prototype Measurement and Analysis Branch. He has been employed with CERC as either an Army officer or as a civilian for nine years since 1973. During his time at CERC, he has been principally involved with the development and conduct of monitoring/data collection efforts. He currently manages two national data collection programs, the Monitoring Completed Coastal Projects Program and the Field Wave Gaging Program.
Mr. Hemsley graduated from John Hopkins University with a B.E.S. degree in geophysical fluid mechanics and from George Washington University with an M.S. degree in harbor, coastal, and ocean engineering. He is a member of the American Society of Civil Engineers, American Shore and Beach Preservation Association, and Oceanic Society. Mr. Hemsley obtained his PE in the Commonwealths of Virginia and Pennsylvania.

PAUL F. MAY

Mr. May is a research physical scientist at the U.S. Army Engineer Waterways Experiment Station (WES), Coastal Engineering Research Center (CERC), Engineering Development Division, Coastal Structures and Evaluation Branch. He is the Principal Investigator on the Coastal Engineering Information Management System Program and is a technical advisor for the joint-agency (CERC/National Ocean Service (NOS)) Shoreline Movement Studies. Before joining the CERC staff, Mr. May worked as a researcher at the Department of Environmental Sciences, University of Virginia and as a geologic consultant with Coastal Research Associates. He received his degree in geology from Ball State University in Indiana and is registered as a professional geologist.

C. LINWOOD VINCENT

Dr. Vincent is a research physical scientist at the U.S. Army Engineer Waterways Experiment Station (WES), Coastal Engineering Research Center (CERC), Research Division, and he recently became technical manager of the Wave Information Study (WIS). Dr. Vincent joined the Wave Dynamics Division, WES, in 1974 and participated in the original development of WIS. He was Chief, Coastal Branch in the Wave Dynamics Division from 1975-1978. At Fort Belvoir, Virginia, he was Chief, Coastal Oceanography Branch, CERC, from 1978-1983 and was instrumental in the development of CERC's shallow-water spectral wave model capabilities. From 1983-1985, Dr. Vincent worked as a consultant with Offshore and Coastal Technologies, Inc. to develop a hurricane wave model used in reanalysis of the hurricane climatology in the Gulf of Mexico for several oil companies. Dr. Vincent is a member of Phi Beta Kappa and is a 1978 recipient of the U. S. Army Research and Development Award and the 1984 recipient of the A.S.C.E. Walter Huber Research Prize.

OBSERVATIONS IN SMALL BOAT HARBORS-
HARBOR DESIGN CONCEPTS

John M. Nichol*

Introduction

This paper addresses several subjects involved in small boat harbor design. It discusses general design issues and several regional approaches to solutions involving: (1) wave height limitation criteria; (2) entrance channel depth; and (3) recreational boat traffic including provisional considerations for interior channel width.

Wave Height Limitations Within Marina Basin

Several criteria exists as to suggested wave height limits within the marina basin. Included in these are: the Army Corps of Engineers SR-2(1) criteria; the work by Mercer et al.(2) suggesting consideration of other parameters, such as wave direction relative to boat alignment, wave period and frequency of occurrence; and the work by Rosen(3) suggesting the ultimate measure relating to resulting vessel motions. Other considerations could be regional such as the complaint at one marina that 1/2 ft, 8- to 10-second wave period agitation is not conducive to "candle-light dinners". Also the types and response of floating dock systems to wave environment conditions can also be a consideration.

It appears that the SR-2 wave height criteria should be tempered with judgment and the considerations of variables of relative wave direction and periods could be beneficial. Regional differences of threshold design criteria would be anticipated. A matrix of this type of format as suggested by Mercer et al.(2) is shown as Figure 1.

Although the definition of acceptable boat motions may be regional in nature, generally a recreational boat harbor on the open coast needs greater wave protection than a commercial or military harbor. In this respect, the concept that "small boats need small breakwaters" is entirely misleading.

Entrance Channel Design for Harbors on Open Coasts

Entrance channels should be relatively safe. If a harbor is intended to be safely navigated under all weather conditions, then it should also be safe during adverse weather. In Southern California, the Corps of Engineers criteria for entrance width requires a minimum of 300 feet for the first 1000 boats and 100 foot of added width for

---

*Moffatt & Nichol, Engineers, Long Beach, California.

SMALL CRAFT HARBOR

"Good" Wave Climate

	WAVE HEIGHT EXCEEDS		
	50 YEAR	1 YEAR	1 WEEK
HEAD SEA			
t ≥ 2 sec.	XX	XX	XX
2 < t > 6 sec.	XX		
t < 6 sec.	XX		
BEAM SEA			
t > 2 sec.	XX		
2 < t > 6 sec.	XX		
t < 6 sec.	XX		

EXCELLENT = 0.75 "good"

After MERCER, ISAACSON & MULCAHY

MODERATE = 1.25 "good"

Figure 1. Wave Height Criteria Matrix

each additional 1000 boats. It has generally proved adequate for initial design. The water depth in the entrance can affect wave breaking and safety navigation.

Harbor entrance depth determination may be approached by evaluating a range of depths, developing operational or closure criteria and comparing them with other harbor entrances in the vicinity. This approach is shown on Figures 2 through 4.

Boat Traffic

Because of the cost (both financial and ecological) involved in construction of new harbors, much emphasis is now being directed to increasing the number of boats within existing harbors. A major concern has arisen over the effects of increasing boat traffic on entrance navigation.

Congestion

Factors that must be considered to evaluate congestion include patterns of boat traffic generation and the apparent navigational interference between boats transiting a given water area. This second factor involves subjective considerations.

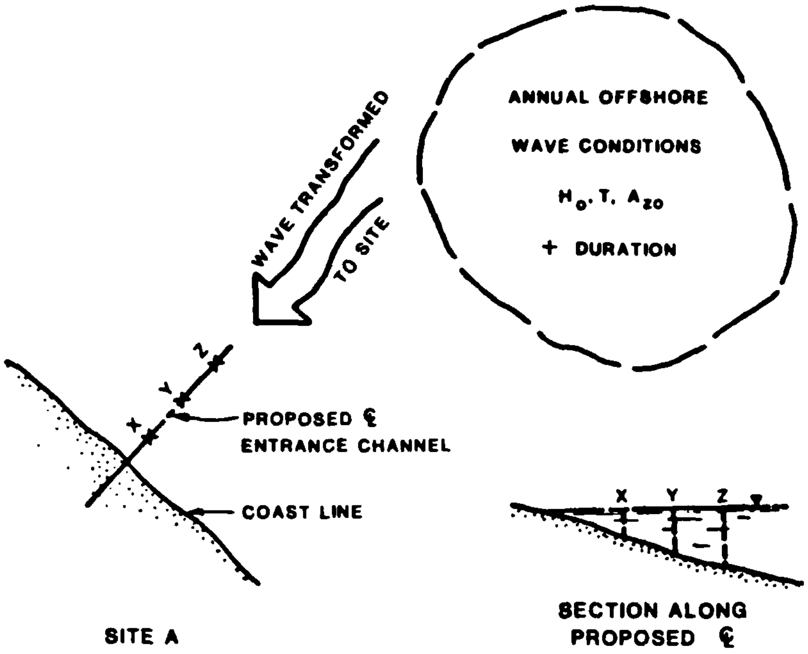
ANNUAL OFFSHORE
WAVE CONDITIONS
H₀, T, A₂₀
+ DURATION
WAVE TRANSFORMED
TO SITE
X
Y
Z
PROPOSED ℄
ENTRANCE CHANNEL
COAST LINE
SITE A
X
Y
Z
SECTION ALONG
PROPOSED ℄

Figure 2. Breaking Wave Climate Development-Parameters for Entrance Wave Climate

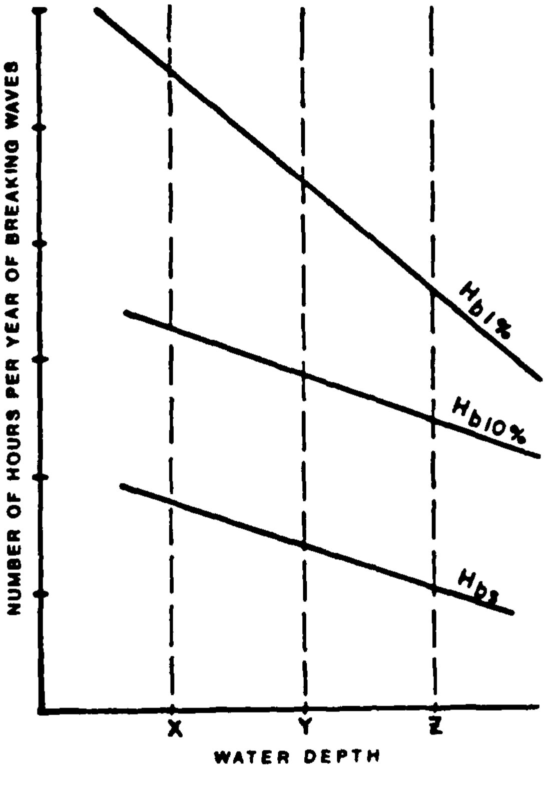

Figure 3. Estimate of Breaking Wave Conditions at Various Entrance Depths

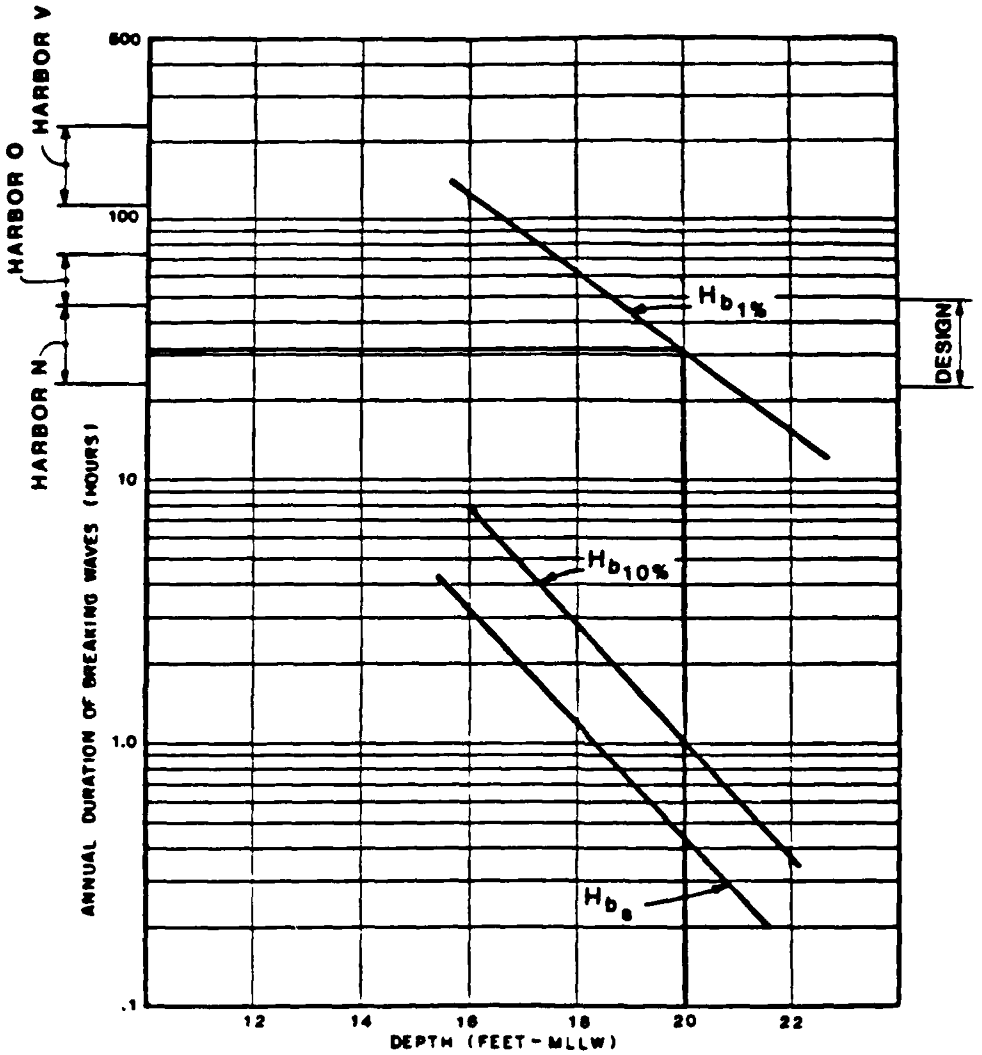

Figure 4. Entrance Depth Selection Using Comparative Harbors

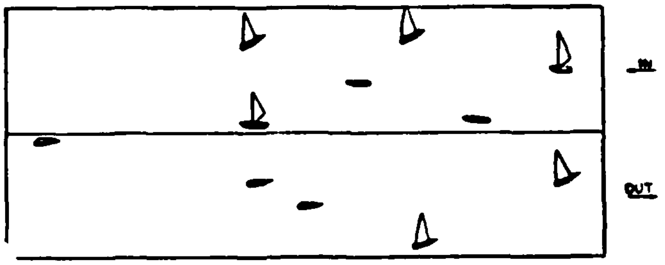

CONGESTION INDEX 11.52

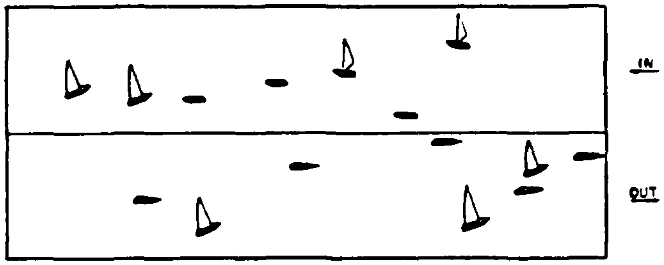

CONGESTION INDEX 20.04

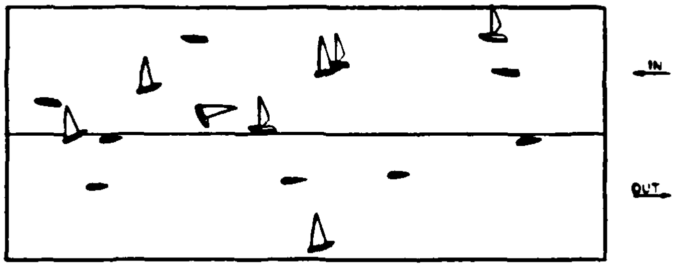

CONGESTION REPRESENTATION 25

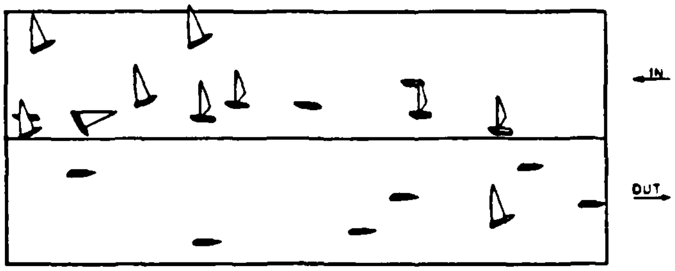

CONGESTION REPRESENTATION 35.5

Figure 5. Graphical Representation of Boating Densities for 1000-foot Channel Segment

Boat Traffic Generation

Data from Newport Harbor(4) in the mid 1960's provided a reasonable basis to define boat use patterns. Subsequent studies in Channel Island Harbor(5), confirmed these general patterns. Sunday is the most popular day. On busy summer Sundays, approximately 25% to 30% of the wet berthed sailboats and 15% to 25% of the wet berthed power boats can be in use. Outboard use is best determined by launch ramp counts. Pattern of use during day is a function of boat type. Channel Island data indicates that boats at residential docks may not be used as much as boats in public marinas.

Navigation Modeling

The problem of interference between tacking sailboats and parallel traveling boats has been analysed by Ely(6), which describes congestion in terms of an interference density index. Interpretation of index is subjective, but significant differences exists between levels at which congestion first becomes an initial concern and levels at which mitigation for congestion must be considered. Figure 5 illustrates representative boat traffic patterns at several levels of computed congestion indexes. Figure 6 represents a schematic of the relation of the apparent beginning of boater concern to navigation difficulties (C.I. 10 to 15) to those much higher levels of congestion indexes (C.I. 30 to 40) in which mitigation measures were actually undertaken(7,8).

Mitigation measures applied in Southern California marina entrances have involved traffic segregation and relocation of launch sites. The latter development has been particularly effective for catamaran sailboats.

As the navigation interference between tacking sailboats is reduced through mitigation, the concern becomes navigation interference due to parallel traveling traffic. Marina del Rey has in the past considered expansion which would enlarge their present 6000+ pleasure boat fleet. Analyses(7) have been made to assess the affect of the proposed expansions on entrance traffic. Here, the concern was the increase in the parallel traffic density. Field measurements of boat use patterns were made and a model using the "blockading" concept was developed by Gram(7). Figure 7 illustrates traffic conditions at computed congestion indexes for parallel moving boat traffic.

The parallel traffic congestion index in the Marina del Rey entrance channel at present was less than that experienced at Alamitos Bay. Boaters in Alamitos Bay consider traffic levels to be "comfortable"; therefore an increase of boat traffic in Marina del Rey to Alamitos Bay congestion index levels was suggested as acceptable.

The parallel congestion index can be used for estimating required channel width. Figure 8 shows the application of this technique for suggesting a 40-foot widening of an existing channel to accommodate anticipated future small boat traffic(9).

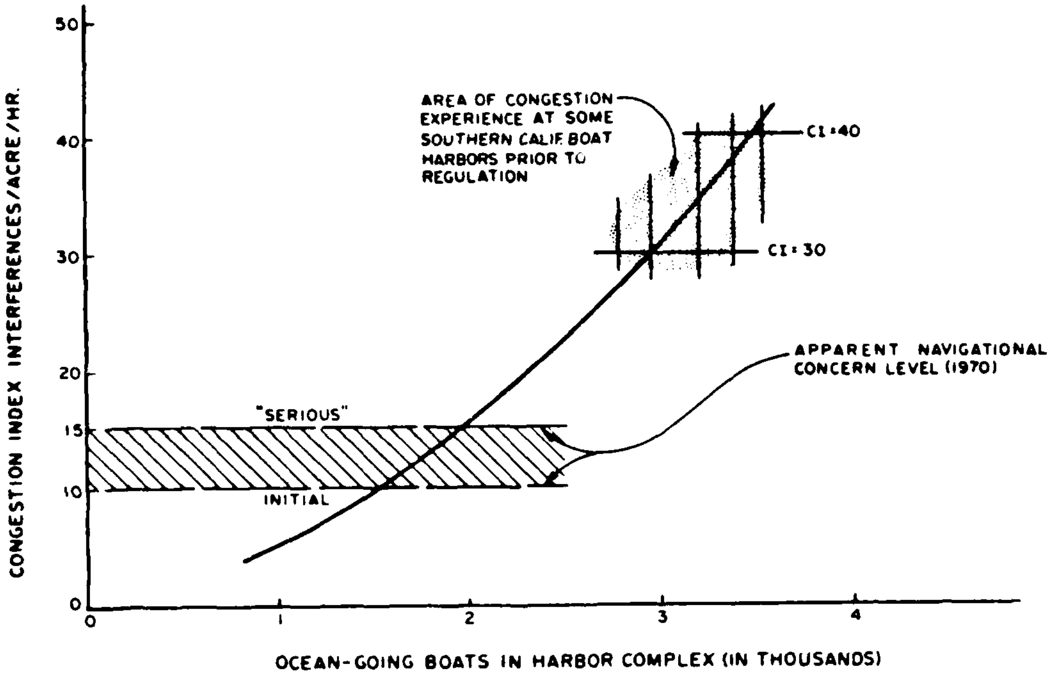

Figure 6. Channel Congestion Index

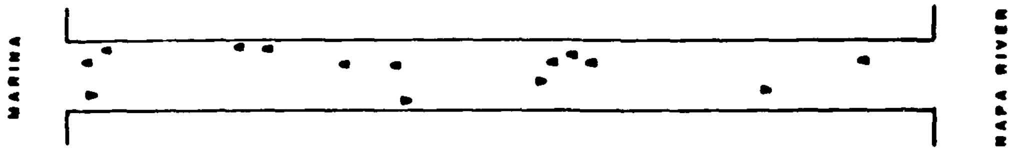
MARINA
NAPA RIVER

BOAT POPULATION = 1,500

C.I.-9

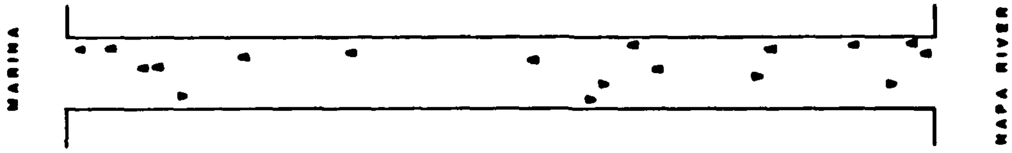
MARINA
NAPA RIVER

BOAT POPULATION = 2,000

C.I.-13

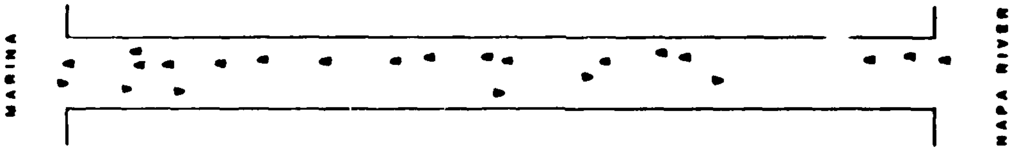
MARINA
NAPA RIVER

BOAT POPULATION = 2,500

C.I.-20

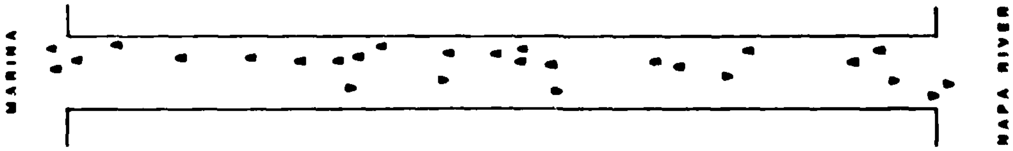
MARINA
NAPA RIVER

BOAT POPULATION = 3,000

C.I.-28

Figure 7. Simulated Peak Hour Traffic

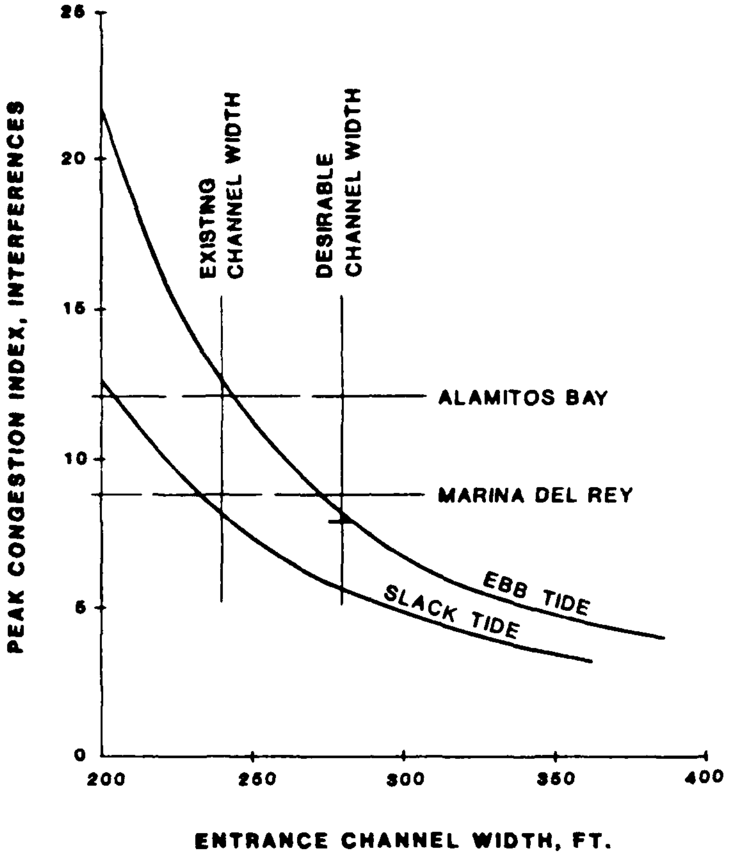

Figure 8. Effect of Channel Width on Congestion

In Southern California region, where boating use patterns are generally similar between harbors, a relationship between number of boats served and interior channel width can be developed. A suggested relationship is shown in Figures 8 and 9.

Conclusion

Several areas of small boat harbor design have been briefly addressed. Using data developed from presently operating harbors, some instances of provisional design criteria have been suggested. Hopefully, as more information is developed and analyzed, these provisional design concepts can be modified or verified to fit the regional needs of the design engineer.

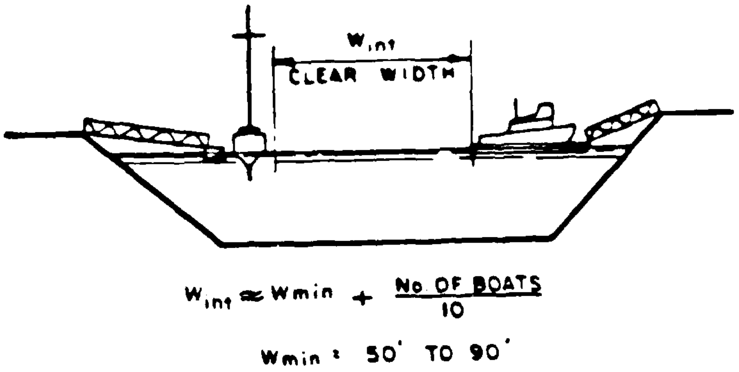
W int
CLEAR WIDTH
W int ≈ Wmin + No. OF BOATS / 10
Wmin = 50' TO 90'

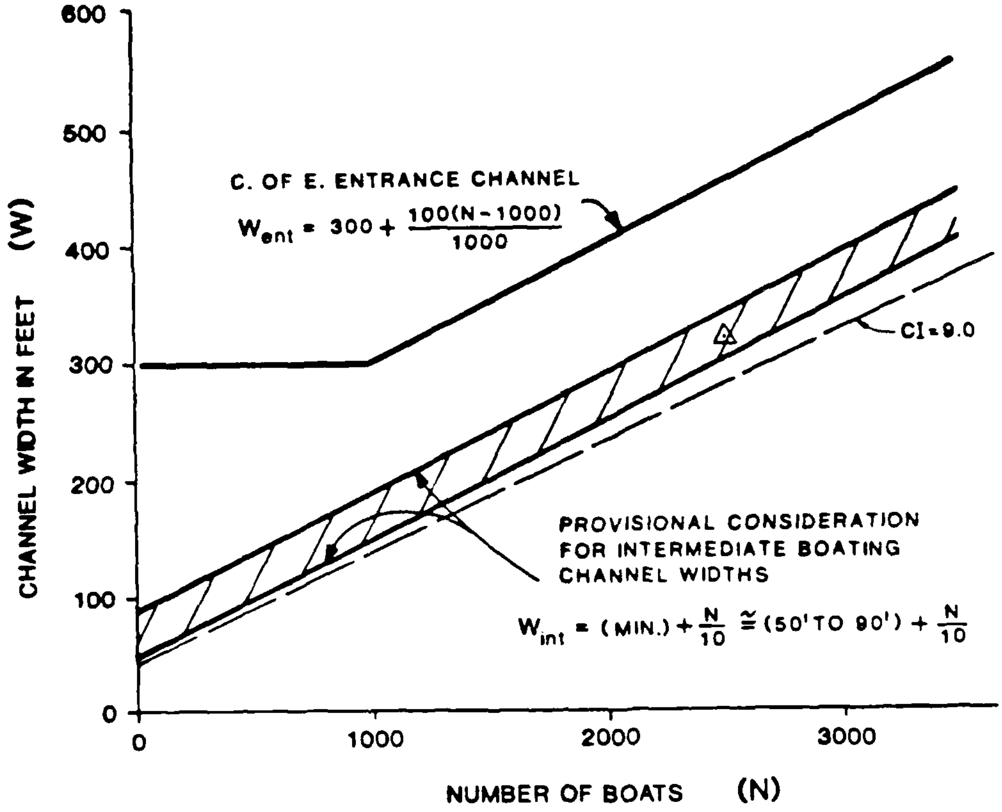

Figure 9. Pleasure Craft Channel Width Criteria

References

1. U.S. Army Corps of Engineers, "Small-Craft Harbors: Design, Construction, and Operation," Special Report No. 2 (SR-2), Coastal Engineering Research Center, December 1974.

2. Mercer, Isaacson & Mulcahy, "Wave Climate in Small Craft Harbors," Manuscript Report 1581, Canadian Dept. of Fisheries, N.W. Hydraulic Consultants Ltd., 1980.

3. Rosen, Dov Sergiu and Kit, Eliezer, "A Simultation Method for Small Craft Harbour Models," Proceedings, 19th Coastal Engineering Conference, ASCE, 1985.

4. Moffatt & Nichol, Engineers, "A Study of the Effects of Waterway Expansion Channel Islands Harbor," (Prepared for County of Ventura Department of Public Works) 1970.

5. Moffatt & Nichol, Engineers, "Channel Islands Congestion Study," (Prepared for Voss Co.), 1980.

6. Ely, Allen L. and Nichol, John M., "Congestion in Marina Entrance Channels Due to Sailboats," Journal of the Waterways, Harbors and Coastal Engineering Division, ASCE, November 1973.

7. Williams-Kuebelbeck, "Boat Traffic Conditions in Marina Del Rey," 1981 (Gram, A., "Appendix B: Boat Interference Theory").

8. Williams-Kuebelbeck, "Alamitos Bay Boat Traffic Study," (Prepared for City of Long Beach), December 1978.

9. Moffatt & Nichol, Engineers, "Boat Traffic Study - Cullinan Ranch," (Prepared for WR Williams), 1981.

THE WES SHIP/TOW SIMULATOR FOR NAVIGATION ENGINEERING

Carl Huval*

Paper unavailable at time of publication.

---

* US Army Corps of Engineers, Waterways Experiment Station.

NAVIGATION SIMULATION APPLICATIONS

Roderick A. Chisholm II*

ABSTRACT

The San Francisco District has completed one navigation simulation study for the John F. Baldwin Ship Channel, Phase II project (JFB) and is scheduling at least two more studies for projects at Oakland Harbor and Richmond Harbor. This paper presents the District's views on the application of navigation simulation studies in project planning. Using the JFB simulation as a base, the paper visits some major user questions concerning (1) the data input requirements of a simulation, (2) the usefulness of simulator results in project design, and (3) the effectiveness of the simulator as a planning tool. Also presented are the lessons learned by the District as applied to future requirements for navigation simulation studies.

Introduction

The primary mission of the San Francisco District, U. S. Army Corps of Engineers is the planning, engineering, construction and maintenance of navigation projects. As such, the District spends fully 3/4 of its resources on navigation efforts, mostly in San Francisco Bay. In 1984 the District completed an Interim Design Memorandum and Environmental Impact Statement for the John F. Baldwin Ship Channel Project (JFB) and is currently preparing Design Memorandums for deep-draft improvements at Oakland Inner Harbor, Oakland Outer Harbor, Richmond Harbor and Phase III of the JFB Project. Each of these projects is a major improvement project representing substantial investments by the Federal Government and the respective local sponsors. Recently navigation simulation studies have been included as a part of these investments.

As early as 1981, navigation simulation studies were investigated by the District for the JFB, Phase II project. At that time the District approached the National Maritime Research Center/CAORF to assist in developing a research plan for channel design in and around Richmond Harbor. CAORF

---

* Chief, Environmental Branch and Project Manager, John F. Baldwin Ship Channel Project, U.S. Army Corps of Engineers, 211 Main Street, San Francisco, CA 94105.

provided a proposal to test several routing and channel configuration options, but the proposal was tabled by the District while more traditional design studies were conducted. In 1983, navigation simulation requirements re-surfaced as the JFB project entered its reporting stage. Higher headquarters issued Corps-wide guidance that any investigations of deep draft navigation must include navigation simulations. In response to this guidance a navigation simulation study was included in the Baldwin Phase II project and was conducted by the Hydraulics Laboratory at the U. S. Army Waterways Experiment Station (WES) in Vicksburg, Mississippi.

The successful completion of the Baldwin simulation by WES encouraged the use of simulations in the District's other ongoing navigation studies. The Baldwin simulation provided the District with hands-on experience in the technology and with tangible project benefits in the end. This by-and-large has changed the District's opinion of simulations from mandate to witting tool. The Project Managers for the JFB, Oakland Harbor and Richmond Harbor projects have readily enfolded navigation simulation studies into their planning programs and, at present, their schedules show simulation studies occupying a large part of their FY 86 and FY 87 efforts.

Purpose

The purpose of this discussion of navigation simulation is to highlight the technology from a user's perspective. Like all computer assisted new technology there is a certain mystique surrounding its use. It is only after the technology is applied to an actual problem that its mysteries begin to clear and the technology can then be viewed in terms of technique. Although the San Francisco District's experience with navigation simulation is very limited, it is considered useful to at least present some observations of the experience, if for no other reason than to share information. If the discussion only stirs a greater consciousness of the navigation simulation applications, then the purpose has been served. However, if it stimulates a thought process which might strengthen the technology, then the purpose is fullfilled. Certainly the navigation simulation business is young enough to benefit from either result.

This discussion of the overall use of simulations in project planning relies on the District's experience with one navigation simulation, namely the Ship Simulation Study of J. F. Baldwin (Phase II) Navigation Channel, San Francisco Bay. The key topics are 1) data requirements, 2) use of results, and 3) planning uses. Wherever possible additional insight to the technology and lessons learned may be reflected upon in the topic discussion. The effort is to present a view of the application of the technology and not the technology itself.

Data Requirements

Basically, a navigation simulation is a computer reproduction of the interaction between a simulated prototype vessel and a simulated prototype environment. The heart of the simulator is a mathematical model that computes the response of a hydrodynamic model, representing a vessel, to vessel controls and external forces. The vessel's movement through a pre-defined study area is controlled by a pilot (man or computer) manipulating propulsion and rudder controls. A visual scene of this movement is usually provided by computer generated video imagery as well as a radar display. All data relating to the vessel's location and orientation in the study area and maneuvering details are recorded. Outputs are generally plots of the vessel's track through the study area and records of the magnitude and extent of maneuvering.

Since a simulation essentially models prototype conditions, a large amount of input data is required to build the models. The WES simulation used by the District for the JFB II project was no exception in this regard. Two different sets of input data were required. First was the ship data set which was developed by WES as a part of their contract scope. Second was the study area data set which was developed and furnished to WES by the District.

The JFB study area is located in central San Francisco Bay, south of the Richmond-San Rafael Bridge and west of the City of Richmond. The project in question consists of the 600-foot wide Southampton Shoal Channel, and a large irregular shaped maneuvering area in front of the Chevron Richmond Longwharf. The improvements under consideration were to deepen the channel and maneuvering area from its existing -35 feet MLLW to -45 feet MLLW. The fleet to be tested included 87,000 and 150,000 dwt tankers 763' and 915' in length respectively and 2 containerships of 638' and 810' lengths.

In the pre-simulation phase of the study, the District was tasked with setting up inbound trips by WES personnel on typical vessels to the study area. The purpose of these rides was to videotape the visual scene from the pilot's view and to record pilot maneuvering instructions. Arrangements for a ride on the typical tanker were relatively easy to secure. Chevron Shipping fully cooperated with the Corps in providing the necessary legal releases to allow Corps personnel and equipment on-board their ship. Additionally, the logistical arrangements for getting personnel and equipment on board were simplified by the fact that most tankers are at anchor in South San Francisco Bay prior to making their final in-bay destination. The easy tanker boarding situation is contrasted by the considerable logistical problems encountered in attempting to set up an inbound trip on a containership. Because containerships generally make a direct trip to Bay Area ports-of-call, boarding of a containership at San Francisco requires a boarding procedure while the ship is underway. An underway boarding is risky, even for experienced people such as pilots. Adding inexperienced people and equipment to an underway boarding was believed to be too risky and WES ultimately cancelled the containership ride. It is noted here that since the time of JFB simulation, WES has completed an in-bound ride on a containership for the Oakland Outer Harbor simulation, by boarding the ship while in port at Los Angeles.

While WES personnel were in San Francisco for their ship ride, the District provided them with a pre-requested information package on the study area. Included were large scale engineering drawings of the existing and proposed works annotated with distances and direction bearings, the location and type of aids to navigation, the position and size of major landmarks and pilot aids and finally photographs of the study area. WES also requested wind, tide and current data. Of particular importance was the current data and since the San Francisco Bay-Delta Hydraulic model could provide area specific current data, a special current study on the Bay Model was scoped as an alternative to providing standard current data from navigation charts.

As seen from the above, the data requirements for a simulation are relatively simple in nature. What can't be seen is the amount of time and resources involved in gathering the information. It is estimated that a total of two man-months of effort was required to provide the JFB study area information requested by WES for the simulation. This figure does not include the effort involved in the current study at the Bay Model which required an additional man-month of labor by their staff and $10,000 in operating costs. Having not been through a simulation before, the District found itself absorbing some unforeseen costs and schedule problems in the JFB simulation. These problems, however, are not occurring in the present Oakland or Richmond simulations.

Use of Result

In most cases one would think that the applications of simulator results would occur early in the planning process, in the design of project improvements. The typical situation would be where the engineer and simulator people work hand in glove testing and refining the layout of the project to come up with the most efficient and safe project. In the JFB project, this situation never really occurred because the project was basically the deepening of an existing project. The improvements would not change the channel width or alignment or maneuvering area configuration. Moreover, the project would not change the size of tanker using the project. The problem was that the depth of the channel was limiting its use by the existing fleet and the purpose of the improvements was to increase the efficiency of the project by reducing tidal delays and lightering operations. Therefore, the simulation could only be applied to assure the saftey margins of the proposed design.

Although the JFB simulator results were not used in the design of the project, the study proved to be surprisingly useful in another application. By the time WES had finished the final simulation report, the District had already released the Draft Design Memorandum and Environmental Impact Statement for review and was beginning the drive to win approval of the project. Key in this effort was a number of briefing and formal public presentations of the project. It was in this review process of the project that the simulator results had their greatest use and value to the District.

Without question, any project in San Francisco Bay that deals with oil tankers arouses public concern. The tanker collision and massive oil spill on the Bay in 1971 is the root of this concern. The District believed that this public concern should be addressed in the best possible manner and it was the simulator study that provided the most convincing evidence that the project was safe. WES simulator personnel was enlisted to present their study and its results at various review meetings being conducted by the District. The graphic, high tech nature of the study and WES's well organized professional presentations apparently left little doubt that the Corps had fully addressed the safety and navigation impacts of the improvements. The fact that the District received no comment concerning the safety of project after meeting with pilots, port captains and the general public and after review of the Draft EIS is credited to the use of navigation simulation study in the public involvement program.

Uses in Planning

The use of navigation simulations in project planning began in the late 1970's when the National Maritime Administration went on line with the Computer Aided Operations Research Facility (CAORF) located at Kings Point, New York. Since that time the Norfolk, Baltimore and Mobile Districts and the New England Division of the Corps have all sponsored simulation studies at CAORF. In the early 1980's the Waterways Experiment Station began to develop navigation simulation capabilities and have been strongly supported by the Office of the Chief of Engineers in conducting simulation studies for the Districts. The South Pacific Division has reviewed and evaluated the JFB simulation and is generally supportive of the San Francisco District's plans for additional simulation at Oakland and Richmond Harbors. These developments leave no doubt that navigation simulation studies will be a part of most navigation planning efforts by the Corps in the future.

The use of navigation simulations in project planning basically addresses the question of project risks. Changes needed to modify or improve a navigation system come with certain risks of damage to life, property or the environment. A navigation simulation is a tool with which one can analyze, predict, induce and, in fact, manage the risks of a project without ever leaving the drawing board and for a minimal investment in time and resources. The alternative approach to the problem of risk is to design the project with high confidence levels so risk is more or less eliminated. This approach has been the standard design method for many years and the simulator people believe that it is unnecessary and leads to over-designed expensive projects. They insist that with a simulator, a designer can make and test innumerable project designs with an eye on balancing risks against costs. What is more, this can be done with no investment in the construction of the project. The only question to worry about is how well can the simulator reproduce prototype conditions?

Aside from the design uses of simulators in planning, the San Francisco District found its JFB simulation study to be a powerful tool in bringing the project home to the public. The technology fits extremely well with today's love affair with computers, video gaming and the desire for choice. The fact that a simulation study allows a citizen to see the navigation effects of a project from his meeting hall chair or allows a pilot to see and feel a new situation from the bridge of a ship is a long way from communicating with a pointer and a slide of an engineering drawing. Simulation studies are high tech in a high tech society.

A final note on the application of simulation studies is that once a study has been conducted, the data can be used to provide quick answers to questions during and after construction. For example, in the JFB project a Value Engineering proposal was submitted after construction of the project was approved. At this time WES is using the base data from the original simulation study to evaluate and provide recommendations as to the feasibility of the V.E. proposal. According to the Value Engineering Officer, the use of the simulator is perfect for V.E. purposes because it provides a fast analysis for few dollars.

Summary

The purpose of this discussion is to reflect on the applications of navigation simulation from a user's perspective. Based on the San Francisco District's experience with one navigation simulation, the District is encouraged by the results of the study produced in the John F. Baldwin Ship Channel Project and it is looking forward to conducting more simulations of projects within San Francisco Bay. Although the District never got to fully use the simulation study in a design application for the Baldwin project, its design applications are readily apparent. The District did apply the simulator study in the public process of JFB project and discovered that it was very convincing in addressing the impacts of the project on navigation issues. The primary lesson learned by the District is that simulation studies require alot of data input prior to the start of simulation and that we must schedule additional time and money to conduct this work. The District recognizes that the value of simulation studies, in general, has not been fully demonstrated, but this will come with more experience.

References

1. Final Interim Design Memorandum No. 5 and Environmental Impact Statement, John F. Baldwin Ship Channel, Phase II, Richmond Harbor Approach; U.S. Army Corps of Engineers, San Francisco District; 1984

2. Technical Report HL-84-4; Ship Simulation Study of John F. Baldwin (Phase II) Navigation Channel, San Francisco Bay, California; U.S. Army Engineer Waterways Experiment Station, Hydraulics Laboratory; 1984

3. Proceeding Sixth CAORF Symposium, Harbor and Waterway Development, Computer Aided Operations Research Facility, U.S. Maritime Administration; 1985

ROGUE RIVER ENTRANCE

By David J. Illias* and Kenneth Johnson*

ABSTRACT

Technical studies of shoaling problems of the navigation project at the mouth of the Rogue River at Gold Beach, Oregon, were initiated in fiscal year (FY) 1978. The purpose of the studies was to determine if structural modifications or revised maintenance dredging practice would improve navigation conditions at the entrance and in the small boat basin access channel. Numerous plans were tested in a fixed-bed model at the U.S. Army Engineer Waterways Experiment Station (WES). Results of the studies did not identify a clearly superior engineering solution and because of the high cost of a movable-bed model, the conclusion was that prototype testing would be appropriate. Based on the effectiveness of the rock groins tested in the model, three experimental timber-pile groins were constructed to reduce upstream shoaling migration into the access channel. Construction was completed in the summer of 1984. A 5-year monitoring program consisting of aerial photography, gauge recordings, hydrographic surveys, and on-site inspections will evaluate the groin's effectiveness and be utilized to determine structural modifications for further improvements.

INTRODUCTION

The Rogue River entrance lies on the southern Oregon coast (see Figure 1), approximately 264 miles (425 km) south of the Columbia River and 319 miles (513 km) north of the entrance to San Francisco Bay (distances computed from difference in latitudes). The City of Gold Beach is located on the south side of the river estuary and the unincorporated town of Wedderburn is across on the north bank.

The original project improvements were authorized by the River and Harbor Act of 3 September 1954 (Senate Document No. 83, 83rd Congress, 2nd session). It provided for two jetties 700 feet (213 m) apart at the entrance; an entrance channel 13 feet (4 m) deep mean lower low water (MLLW) and 300 feet (91 m) wide, extending from the ocean to a point immediately downstream from the U.S. 101 highway bridge (river mile (RM) 0.9); and a turning basin 13 feet (4 m) deep MLLW, 500 feet (152 m) wide, and 650 feet (198 m) long between (RM) 0.5 and 0.65.

Preconstruction modifications included shifting the jetty alignment from a westerly to a southwesterly orientation to minimize flanking wave attack, and increasing the jetty spacing from 700 feet (213 m) to 1,000 feet (305 m), to pass a flood of 375,000 cubic feet per second (cfs) (10,613 cubic meters/s).

---

* Civil Engineer, U.S. Army Corps of Engineers, Portland District, P.O. Box 2946, Portland, Oregon 97208-2946, Civil Engineer.

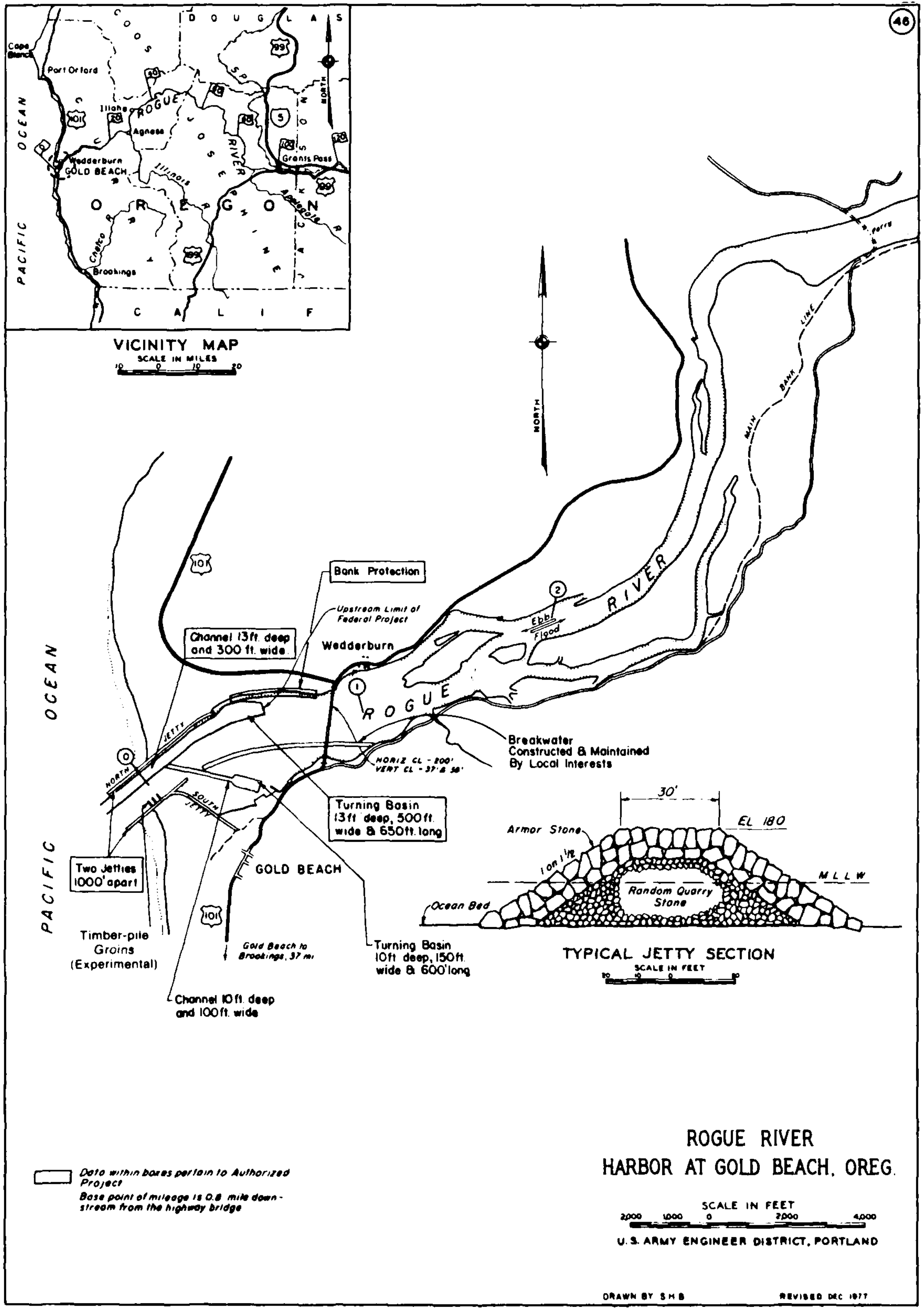
46
Cape Blanco
Port Orford
Illahe
Agness
Wedderburn
GOLD BEACH
Brookings
Grants Pass
COOS
DOUGLAS
CURRY
JOSEPHINE
ROGUE
RIVER
Illinois R.
Chetco R.
O R E G O N
C A L I F
PACIFIC
OCEAN
NORTH
VICINITY MAP
SCALE IN MILES
10 0 10 20
NORTH
Bank Protection
Upstream Limit of Federal Project
Channel 13 ft. deep and 300 ft. wide
Wedderburn
ROGUE
RIVER
Ebb
Flood
MAIN BANK LINE
Ferry
Breakwater Constructed & Maintained By Local Interests
HORIZ CL - 200' VERT CL - 37' & 38'
Turning Basin 13 ft. deep, 500 ft. wide & 650 ft. long
NORTH JETTY
SOUTH JETTY
GOLD BEACH
101
Two Jetties 1000' apart
Timber-pile Groins (Experimental)
Gold Beach to Brookings, 37 mi
Turning Basin 10 ft. deep, 150 ft. wide & 600' long
Channel 10 ft. deep and 100 ft. wide
PACIFIC
OCEAN
30'
EL 18.0
Armor Stone
1 on 1½
MLLW
Random Quarry Stone
Ocean Bed
TYPICAL JETTY SECTION
SCALE IN FEET
20 10 0 20
Data within boxes pertain to Authorized Project
Base point of mileage is 0.8 mile downstream from the highway bridge
ROGUE RIVER
HARBOR AT GOLD BEACH, OREG.
SCALE IN FEET
2,000 1,000 0 2,000 4,000
U.S. ARMY ENGINEER DISTRICT, PORTLAND
DRAWN BY S.H.B.
REVISED DEC 1977

Figure 1

Construction of the 3,400-foot-long (1,036 m) South Jetty was completed in October 1959 and the 3,300-foot-long (1,006 m) North Jetty was completed in September 1960. The entrance channel was completed in August 1961, and the inner channel and turning basin in October 1961.

In 1971 and 1972, the Port of Gold Beach constructed a breakwater to protect the small-boat basin on the south shore. Starting at approximately 1,000 feet (305 m) upstream of the highway bridge, the breakwater makes a long arc to the South Jetty with an opening provided for access. In 1972, the Corps of Engineers constructed a 10-foot (3 m) deep MLLW and 100-foot (30 m) wide access channel which extends 1,400 feet (427 m) from the entrance channel to a turning basin inside the breakwater. The turning basin is 10-feet (3 m) deep MLLW, 150-feet (46 m) wide, and 600-feet (183 m) long.

PHYSICAL ENVIRONMENT

The Rogue River rises on the western slopes of the Cascade Range, and flows south and west through the Coast Range. The drainage area of the basin is about 5,160 square miles (13,364 square kilometers). Annual precipitation in the basin varies from 20 inches (51 cm) to 120 inches (305 cm) maximum. About 70 percent of the precipitation occurs during the 5-month period November through March. The wettest months are December and January. Recorded flows vary from a minimum of 1,200 cfs (34 cubic meters/s) to a maximum of 500,000 cfs (14,150 cubic meters/s) at an average recurrence interval of 100 years (recorded in December 1964, largest on record).

Tides at the entrance have a mean range of 4.9 feet (1.5 m), a diurnal range of 6.7 feet (2.0 m), and an extreme range of about 11.0 feet (3.4 m). Tidal influence extends about 4 miles (6 km) upstream from the mouth. The tidal prism is about 1.59 x 10^8 cubic feet (4.5 x 10^6 cubic meters) for the mean range.

NAVIGATION PROBLEMS

Before project construction a sand spit about 1,800-feet (549 m) long extended northerly from the south bank. An entrance about 200-feet (61 m) wide at low water was located at the north end of the spit. The existing North and South Jetties were constructed on a southwesterly alignment through the spit.

The basic problem at the Rogue River entrance is that natural forces are attempting to reestablish the above pre-project conditions of sediment depositions between the jetties and in the estuary. These depositions have created channel shoaling that has restricted vessel traffic between the ocean and the small-boat basin, and has made maintenance dredging operations difficult and expensive.

Shoal Formations

Every year, uncontrolled shoal formations have developed near the ocean end of the North Jetty and along the South Jetty extending up and into the boat basin access channel. Reviewing the conditions throughout the year provide an understanding of how the shoals are formed.

In the winter and fall, storms can quickly fill in the entrance channel, making vessel passage over the bar difficult. On the opposite hand, during the same period, velocities from river flood flows tend to reopen the channel by scouring action. As the season moves into the summer and early fall, the low river flows and the northwest wave action will cause a shoal to develop that effectively blocks the north side of the entrance channel forcing vessels crossing the bar to follow an S-shaped route to stay in the deepest available water. Channel depths of only 1 to 3 feet (0.3 m to 1 m) MLLW have been recorded in the past.

The second shoal area is located along the South Jetty. It starts forming in the early spring slightly inland from the tip of the jetty. During the summer and fall the shoal migrates upstream along the jetty into the boat basin access channel, blocking access except during the higher tides. High river flows during the winter will move the shoal back out of the entrance. Then, in the spring, the cycle repeats itself. The shoal materials are finer toward the ocean, and the river deposit of coarse gravels and cobbles is found near the small-boat basin entrance.

Maintenance Dredging

The adverse weather conditions in the Pacific Northwest, the availability of dredging plant, and work priorities have all been limiting factors in the dredging of the Rogue River project. Based on the 1961-1983 dredging records, the average annual dredging volume is about 73,000 cubic yards (cy) (55,812 cubic meters) for the entrance channel, and about 46,000 cy (35,172 cubic meters) for the small-boat basin access channel. These amounts add up to a total annual project quantity of approximately 120,000 cy (91,752 cubic meters).

TECHNICAL CONSIDERATIONS

Riverine Sediments

The numerical model HEC-6, "Scour and Deposition in Rivers and Reservoirs," developed by the Corps of Engineers Hydrologic Engineering Center (HEC), was utilized to estimate the volume of riverine sediments in the lower 5 miles of the Rogue River. HEC-6 is a one-dimensional, movable bed simulation program designed to analyze scour and deposition by modeling the interaction between the water-sediment mixture, sediment material in the system, and the hydraulics of flow. (6)Results from the model study indicated that when flows were below 61,000 cfs (1,726 cubic meters/sec) deposition occurred between river miles (RM) 3 and 4. Flows above 90,000 cfs (2,547 cubic meters/sec) showed that more material flushed out of the river then into it. By the end of the winter simulation, about 170,000 cy (129,982 cubic meters) of bed material were transported out of the entrance. The conclusions drawn from the program are that most river sediment is carried out of the entrance into the ocean.

Littoral Environmental Observations

Littoral Environmental Observations (LEO) program data was collected for 44 months (from the fall of 1977 through September 1981) to develop estimates of the volume and direction of littoral transport. Hired and volunteer observers obtained measurements of breaker wave height and type, wind speed and direction, direction of wave approach and wave period, width of surf zone, and longshore current direction and rate. Procedures for data collection were in accordance with the Coastal Engineering Research Center's (CERC) publication, "Seaward Limit of Significant Sand Transport by Waves: An Annual Zonation for Seasonal Profiles" (CETA 81-2)(4). The data from the field observations was forwarded to CERC for compilation and analysis.

LEO program observations were made at a site approximately 1.6 miles (2.6 km) north of the entrance and at a second site approximately 0.9 mile (1.4 km) to the south.

Analysis of the data by CERC resulted in the following sediment transport rates during the following periods.

May - September (million cubic yards)		October - April (million cubic yards)	
0.5	(382,300 cubic meters) from the south	1.0	(764,600 cubic meters) from the south
0.25	(191,150 cubic meters) from the north	0.1	(76,460 cubic meters) from the north
0.75	(573,450 cubic meters) Total	1.1	(841,060 cubic meters) Total

The above results are only estimates that may have some inaccuracies because of the limitations of the field data collection methods. However, the calculations do clearly show the potential for large quantities of sediment moving past the Rogue River entrance.

After both jetties were completed, the area on the land side of both quickly filled. The deposition is estimated to be between 0.75 and 1 million cy (573,420 and 764,600 cubic meters) which appears to be consistent with the LEO results.

MODEL STUDIES

Numerous plans were tested in a Rogue River fixed-bed model at the U.S. Army Corps of Engineers Experiment Station (WES) between the periods May 1980-July 1981 and November 1982-February 1983. Test procedures and results are reported in WES Technical Report, HL-82-18, "Design for Flood Control, Wave Protection, and Prevention of Shoaling, Rogue River, Oregon," dated August 1982(1), and WES Technical Report, HL-82-18,

"Design for Flood Control, Wave Protection, and Prevention of Shoaling, Rogue River, Oregon: Appendix B: Results of Additional Tests; Hydraulic Model Investigation," dated June 1983(2).

The following objectives were outlined for the investigation(2):

a. Study shoaling, wave, current, and riverflow conditions in the Rogue River entrance for existing conditions and proposed improvements.

b. Develop remedial plans for the alleviation of undesirable conditions.

c. Determine if design modifications to the proposed plans could be made that would reduce construction costs significantly and protect against shoaling, wave, and floods.

The tests included two initial base tests for the existing conditions (with and without entrance shoals) and 61 variations of following basic plans:

a. Groins added normal to the existing South Jetty.

b. Extending the North Jetty.

c. Extending both jetties.

d. Constructing a new entrance into the small-boat basin.

e. Realignment of the jetties and narrowing the spacing.

The model was constructed by WES to an undistorted linear scale of 1:100. It included 6,700 feet (2,042 meters) of the lower river, the small-boat basin, and about 1.3 miles (2.1 km) of beach on the north and south sides of the entrance. The model was calibrated from prototype data obtained in 1978, and wave heights and characteristics in the model were developed from a 1977 wave-refraction analyses by WES and from material published by the National Marine Consultants, Surface Marine Observations and Fleet Numerical Weather Center.

A movable-bed model was not utilized because of the high cost (estimated to be $7 million) of such a model and the lack of historical data required for calibration.

Model Study Results

The rubblemound groin alternatives showed they were effective in preventing migration of the South Jetty shoal into the small-boat basin access channel. However, results indicated substantial increases in water surface elevations upstream during river flood flow conditions.

The jetty extension plans with the extensions oriented toward the west (45° to the existing alignment) were the most effective in preventing shoaling of the entrance from littoral material, although a shoal did form from riverine deposits in the entrance. The plan extending the North and South Jetties 1,760 feet (536 m) and 1,610 feet (491 m), respectively, was preferred because it required less jetty stone. The cost to construct this alternative was estimated to be $31,800,000 at 1984 price levels.

A total of 14 variations was tested with direct access from the small-boat basin to the ocean. The plan involving a 1,950-foot (594 m) extension of the existing South Jetty and a 3,200-foot (975 m) new South Jetty was the only one that showed substantial protection from littoral drift sediment. Since the new entrance would be separate from the river, the riverine sedimentation would not be a problem. The estimated cost for the construction of a new entrance would be $38,704,000 at 1984 price levels.

OTHER PLANS CONSIDERED

Intensive Maintenance Dredging

A program of intensive maintenance dredging was considered from May through September when project usage is the heaviest and weather is the most favorable.

The estimated volume of material that would have to be removed to provide project depths during this period is approximately 220,000 cy (168,212 cubic meters). Because the Rogue River entrance usually experiences the worst entrance conditions on the Oregon coast, a program of increased dredging would be dependent on good wind and wave conditions.

Relocating the Small-Boat Basin Access Channel

Constructing a new upstream access channel into the small-boat basin was an alternative to the present shoaling problems created by the South Jetty shoal. Although, after considering the added length of a new channel and increased costs for removing coarser upstream gravels, it was doubtful that it would be economical.

Sand Bypassing

The feasibility of a sand bypassing system at the Rogue River was reviewed by staff personnel at CERC and discussed with other districts with expertise in this area. The concensus was that a bypassing system would not be practical at this location because of the adverse weather near the end of the jetties, and that the South Jetty shoal would be too wide for a fixed pumping system.

TIMBER-PILE GROINS

Because the district's studies and WES model tests did not identify a clearly superior solution, and because of the high costs of a movable-bed model, it was concluded that a prototype test installation would be appropriate. Based on the effectiveness of the rock groins in the model study, a three timber-pile groin system (Figure 2) was selected for construction along the South Jetty to the slow movement of the south bank shoal. The groins were spaced at 400-foot (122 m) intervals and oriented perpendicular to the entrance channel at approximately RM 0. The contract for the groin construction was awarded by the Corps of Engineers for a bid amount of $379,700 in August 1983 and completed in August 1984.

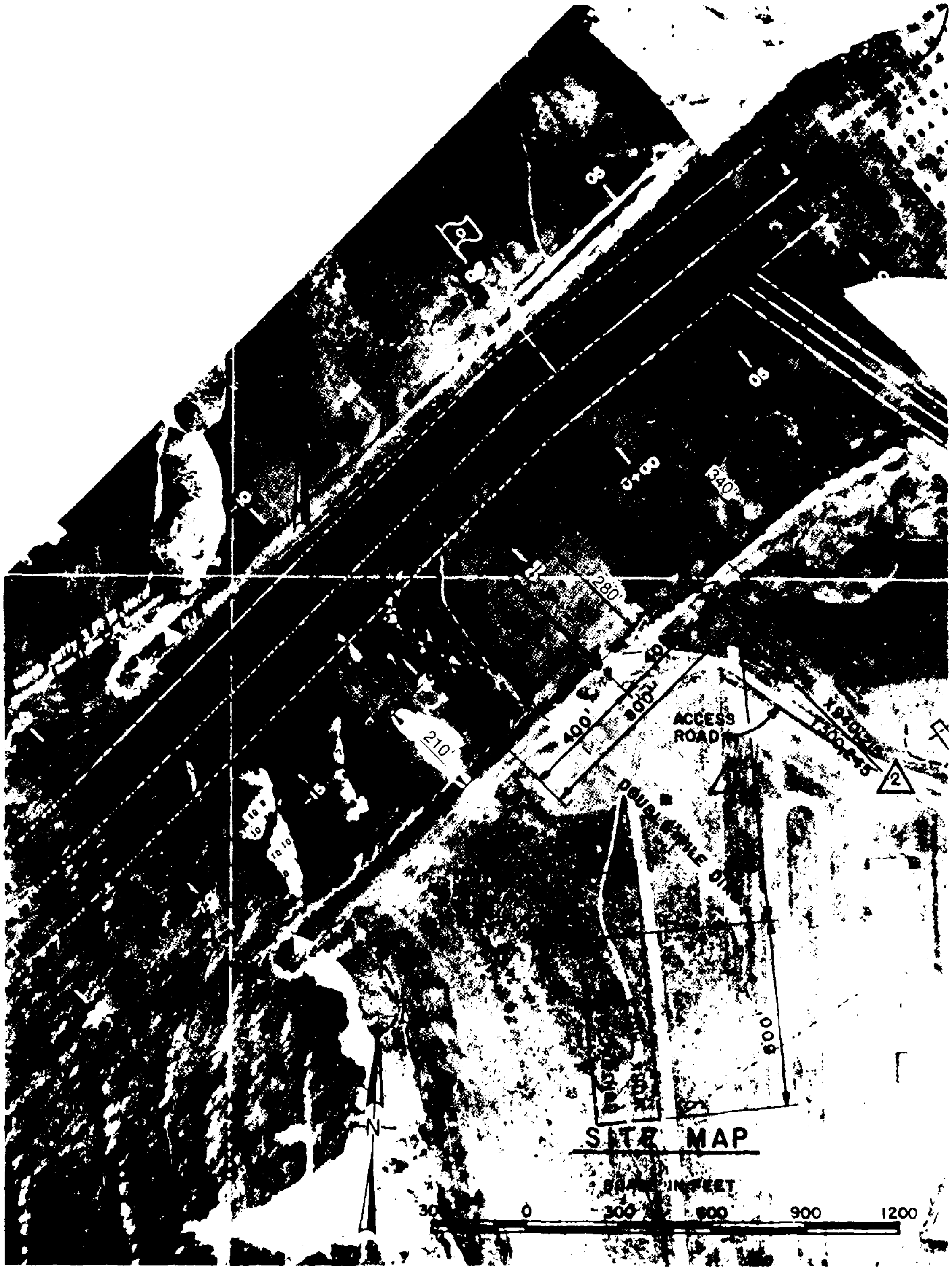
280'
340'
210'
400'
800'
ACCESS ROAD
DOUBLE-FILE DI
2
900
SITE MAP
SCALE IN FEET
300
0
300
600
900
1200
N

Figure 2

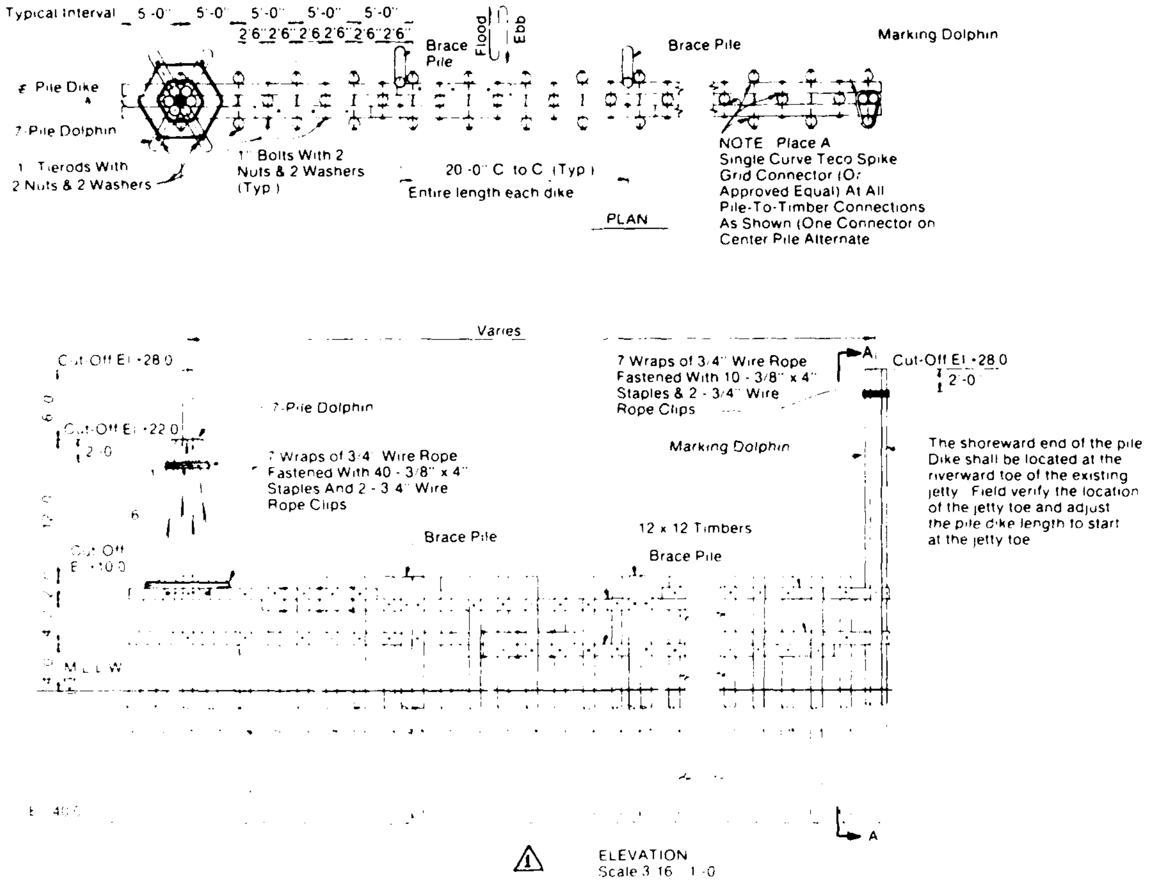

Typical Interval 5'-0" 5'-0" 5'-0" 5'-0" 5'-0"
2'6" 2'6" 2'6" 2'6" 2'6" 2'6"
Flood
Ebb
Brace Pile
Brace Pile
Marking Dolphin
℄ Pile Dike
7-Pile Dolphin
1" Tierods With 2 Nuts & 2 Washers
1" Bolts With 2 Nuts & 2 Washers (Typ.)
20'-0" C. to C. (Typ.)
Entire length each dike
PLAN
NOTE Place A Single Curve Teco Spike Grid Connector (Or Approved Equal) At All Pile-To-Timber Connections As Shown (One Connector on Center Pile Alternate
Varies
Cut-Off El. +28.0
Cut-Off El. +22.0
2'-0
7-Pile Dolphin
7 Wraps of 3/4" Wire Rope Fastened With 40 - 3/8" x 4" Staples And 2 - 3/4" Wire Rope Clips
7 Wraps of 3/4" Wire Rope Fastened With 10 - 3/8" x 4" Staples & 2 - 3/4" Wire Rope Clips
Cut-Off El. +28.0
2'-0
Marking Dolphin
The shoreward end of the pile Dike shall be located at the riverward toe of the existing jetty. Field verify the location of the jetty toe and adjust the pile dike length to start at the jetty toe
12 x 12 Timbers
Brace Pile
Brace Pile
Cut-Off El. +10.0
M.L.L.W.
A
A
ELEVATION
Scale 3/16" = 1'-0"

Figure 3

The concept of the pile groin system is that it would reduce wave energies sufficiently to slow or stop the upstream shoal migration; thus, reducing the dredging in the small-boat basin entrance and possibly improving entrance bar conditions. In addition, the timber piles would permit sediment transport oceanward during high river flows and outgoing tides, and should have less backwater effect than the relatively impermeable rock groins.

The Gold Beach pile structure (Figure 3) is similar in design to the Columbia River estuary pile dikes. Each structure consists of three rows of piling alternately spaced at 2.5 feet (0.8 m) centers connected with a double row of 12-inch x 12-inch (30 cm x 30 cm) timber spreaders. Batter piles at 20-foot (6 m) centers are attached to the upstream side of the structure. The design analysis for the pile dikes was based on an ASCE publication "Design of Columbia River Pile Dikes," dated July 26-30, 1971(3) and U.S. Army Coastal Engineering Research Center, Shore Protection Manual(5). The structure was designed for a river flow velocity of 15 ft/sec (4.6 m/sec), wave height of 12 feet (3.7 m), and wave period of 13 seconds.

PILE GROIN MONITORING

A 5-year monitoring program has been developed for the timber pile groin system to evaluate the effectiveness and determine structural modifications for further improvements. Included in the program are the following major features: (1) hydrographic surveys; (2) photographic coverage; (3) recording gauges; (4) on-site inspections; and (5) structural modification and maintenance.

The hydrographic surveys are being obtained periodically at the entrance channel, the small-boat basin access channel, and bank to bank in the vicinity of the groins. Photographic coverage to visually monitor the South Jetty shoal includes low level oblique aerial photos in color taken at low tides on a 2- to 4-week cycle, high level black and white aerials taken once a year during the peak shoal formation period, monthly ground level photos at set locations, and ground level video taken during severe storm conditions. Crest gauges (powdered cork pipes) were installed on each side of the entrance and a continuously recording gauge (tide gauge) for backwater data was installed on the north bank just upstream of the highway bridge. On-site inspections are made twice annually to survey changes to the shoaling in the area and to assess the structural condition of the groins.

CONCLUSIONS

With only about a year passing since completion of the timber groins, it is too early to draw any conclusions. Preliminary results indicate that some improvements may be taking place in both the entrance and access channels. The aerial and ground photographs show that the groins have been effective in stabilizing the south jetty shoal since they were completed.

In 1984, hydrographic surveys indicated that the entrance channel depths were maintained throughout the summer, and blockage by shoaling did not begin until late in the season. There was no entrance channel dredging performed in 1984. In 1985 the shoaling process started in the spring and 34,000 cubic yards (25,996 cubic meters) were removed from the entrance in late May and early July.

In the access channel 40,000 cubic yards (30,584 cubic meters) were dredged in 1984 and 50,000 cubic yards (38,230 cubic meters) in 1985, which still approximates the previous annual average of 46,000 cubic yards (35,172 cubic meters). However, this year almost all the material removed was located in the section of the channel that lies outside the boat basin. Boats were still able to obtain access through a deeper water route to the east. The channel through the gap in the breakwater and to the basin docks has remained open throughout the year.

In 1985 the river flows were below average and there were no significant flood events during the winter months which may have contributed to the shoaling problems both in the entrance and access channels.

As the data from the monitoring program is analyzed, structural modifications will be made to the groin system that may provide further improvements.

REFERENCES

1. Bottin, R. R. Jr., 1982, Design for Flood Control, Wave Protection, and Prevention of Shoaling, Rogue River, Oregon, Technical Report HL-82-18, U.S. Army Engineers Waterways Experiment Station, Vicksburg, MS.

2. Bottin, R. R. Jr., 1983, Design for Flood Control, Wave Protection, and Prevention of Shoaling, Rogue River, Oregon, Appendix B: Results of Additional Tests, Technical Report HL-82-18, U.S. Army Engineers Waterways Experiment Station, Vicksburg, MS.

3. Dodge, R. O., 1971, Design of Columbia River Pile Dikes, Joint ASCE-ASME Transportation Engineering Meeting, Meeting Reprint 1424.

4. Schneider, C., 1981, The Littoral Environment Observation (LEO) Data Collection Program, CETA-81-5, Coastal Engineering Research Center, Fort Belvoir, VA.

5. U.S. Army Coastal Engineering Research Center, Shore Protection Manual, Fourth Edition, 3 Vols., Washington, DC.

6. U.S. Army Hydrologic Engineering Center, 1977, HEC-6 Scour and Deposition in Rivers and Reservoirs, Users Manual, Davis, California.

Interactions between water waves and currents in shallow water

By Sung B. Yoon and Philip L-F. Liu
Joseph H. Defrees Hydraulics Laboratory, School of Civil
and Environmental Engineering, Cornell University

The interactions between water waves and currents in shallow water are invesitgated. Boussinesq equations are used to derive evolution equations for spectral wave components in a slowly varying two-dimensional domain. The magnitude of currents is assumed to be the same as that of the leading order wave field. The parabolic approximation is developed to calculate the refraction and diffraction of cnoidal waves over a vortex ring.

1. Introduction

Interactions of waves and currents can have a significant impact on shoreline stability. In design for shoreline protection measures or harbor facilities, it is an accepted practice to hindcast deep water waves and refract these waves into the shallow water region without considering the currents that waves may cross in reaching the coastal water. These currents could significantly change the wave height and direction of the wave propagation. These effects are particularly important near tidal inlets or projecting headlines where strong currents appear or large semipermanent eddies exist.

Peregrine (1976) and Peregrine and Jonsson (1983) have reviewed various theories for wave-current interactions. It appears that a bulk of research work has been developed for large scale currents where the length scale for current variation is much greater than the wavelength. There are very few theories discussing the moderate or small scale currents, especially in the shallow water. Mei and Lo (1984) studied the wave diffraction problem by a jet-like current in shallow water. Their theory is limited to linear waves.

In this paper, attempt is made to examine the nonlinear wave-current interactions in shallow water. Boussinesq equations are used to derive evolution equations for spectral wave components. The current intensity is assumed to be in the same order of magnitude as that of the waves. The length scale of the variation of the currents is the same as the wavelength. To facilitate numerical computations, the parabolic approximation model is developed. A numerical example is given for the refraction and diffraction of cnoidal waves over a vortex ring.

2. Boussinesq Equations

In the present study, the wave motion is assumed to be in the same order of magnitude as the leading order current velocity. Using ω as the characteristic frequency, a_0 as the characteristic wave amplitude and h_0 as the characteristic water depth, the following dimensionless variables can be introduced:

$$t = \omega t' \ , \ (x,y) = \frac{\omega}{\sqrt{gh_0}} (x',y'), \ z = \frac{z'}{h_0}$$

$$h = \frac{h'}{h_0} \ , \ \vec{u} = \vec{u}' \ / \ [\frac{a_0}{h_0} \sqrt{gh_0}], \ \zeta = \frac{\zeta'}{a_0} \tag{2.1}$$

where ζ is the free surface displacement and $\vec{u}$ denotes the depth - averaged horizontal velocity vector. The quantities with a prime represent dimensional quantities. The Boussinesq equations take the following dimensionless forms:

$$\frac{\partial \zeta}{\partial t} + \nabla \cdot [(h + \varepsilon\zeta) \vec{u}] = O(\varepsilon^2, \ \varepsilon\mu^2, \ \mu^4) \tag{2.2}$$

$$\frac{\partial \vec{u}}{\partial t} + \varepsilon\vec{u} \cdot \nabla\vec{u} + \nabla\zeta = \mu^2 \{ \frac{1}{2} h \frac{\partial}{\partial t} \nabla[\nabla \cdot (h\vec{u})] - \frac{1}{6} h^2 \frac{\partial}{\partial t}$$

$$\nabla(\nabla \cdot \vec{u}) \} + O(\varepsilon^2, \ \varepsilon\mu^2, \ \mu^4) \tag{2.3}$$

where

$$\mu^2 = \frac{\omega^2 h_0}{g} << 1 \ , \ \text{and} \ \varepsilon = \frac{a_0}{h_0} << 1 \tag{2.4}$$

are small parameters representing the relative importance of dispersion and nonlinearity, respectively and are assumed to be of the same order of magnitude.

Assuming that the free surface displacement and the velocity field can be written as Fourier series with the fundamental frequency ω; i.e.

$$\zeta(x,y,t) = \frac{1}{2} \sum_n \zeta_n(x,y) e^{int} \quad , \quad n = 0, \pm 1, \pm 2, \cdots \tag{2.5}$$

$$\vec{u} \ (x,y,t) = \frac{1}{2} \sum_n \vec{u}_n \ (x,y) e^{int} \quad , \quad n = 0, \pm 1, \pm 2 \cdots \tag{2.5b}$$

where $(\zeta_{-n}, \ \vec{u}_{-n})$ are the complex conjugates of $(\zeta_n, \ \vec{u}_n)$, the governing equations for each Fourier component become

$$-in\zeta_n + \nabla \cdot (h\vec{u}_n) + \frac{\varepsilon}{2} \sum_s \nabla \cdot (\zeta_s \vec{u}_{n-s}) = O(\varepsilon^2, \ \varepsilon\mu^2, \ \mu^4) \tag{2.6}$$

$$-in\vec{u}_n + \left(1 - \frac{\mu^2 n^2}{3} h\right) \nabla\zeta + \frac{\varepsilon}{4} \sum_s (\vec{u}_n \cdot \vec{u}_{n-s}) = O(\varepsilon^2,\ \varepsilon\mu^2,\ \mu^4) \qquad (2.7)$$

where $s = 0, \pm 1, \pm 2, \cdots$. For the steady current field ($n = 0$), (2.6) and (2.7) are reduced to

$$\nabla \cdot \left[\left(h + \frac{\varepsilon}{2} \zeta_0\right) \vec{u}_0\right] + \frac{\varepsilon}{2} \sum_{s\neq 0} \nabla \cdot (\zeta_s \vec{u}_{-s}) = O(\varepsilon^2,\ \varepsilon\mu^2,\ \mu^4) \qquad (2.8)$$

$$\nabla \zeta_0 + \frac{\varepsilon}{2} \vec{u}_0 \cdot \nabla \vec{u}_0 + \frac{\varepsilon}{2} \sum_{s\neq 0} \vec{u}_s \cdot \nabla \vec{u}_{-s} = O(\varepsilon^2,\ \varepsilon\mu^2,\ \mu^4) \qquad (2.9)$$

It is remarked here that the variation of water depth is small in a wave length; i.e. $O(|\nabla h|) \sim O(\varepsilon, \mu^2)$. The current field can be split into two parts:

$$\vec{u} = \vec{\bar{u}}_0 + \varepsilon \hat{\vec{u}}_0 \qquad (2.10a)$$

$$\zeta_0 = \bar{\zeta}_0 + \varepsilon \hat{\zeta}_0 \qquad (2.10b)$$

where $\vec{\bar{u}}_0$ and $\bar{\zeta}_0$ represent the ambient velocity vector and free surface displacement without the influence of waves, $\hat{\vec{u}}_0$ and $\hat{\zeta}_0$ correspond to the wave-induced current velocity and the mean free surface displacement. Substituting (2.10) into (2.8) and (2.9) yields

$$\nabla \cdot \left[\left(h + \frac{\varepsilon}{2} \bar{\zeta}_0\right) \vec{\bar{u}}_0\right] = 0 \qquad (2.11a)$$

$$\nabla \bar{\zeta}_0 + \frac{\varepsilon}{2} \vec{\bar{u}}_0 \cdot \nabla \vec{\bar{u}}_0 = 0 \qquad (2.11b)$$

and

$$\hat{\vec{u}}_0 = -\frac{1}{2h} \sum_{s\neq 0} \zeta_s \vec{u}_{-s} \qquad (2.12a)$$

$$\hat{\zeta}_0 = -\frac{1}{4} \sum_{s\neq 0} \vec{u}_s \cdot \vec{u}_{-s} \qquad (2.12b)$$

Equations (2.11) are the shallow-water equations for the ambient current field. Equations (2.12) calculate the wave-induced currents and mean free surface displacement, once ζ_s and $\vec{u}_s$ are found.

Using (2.11) and (2.12) in (2.8) and (2.9) and combining the resulting equations, we obtain

$$\nabla\cdot(G_n \nabla\zeta_n) + n^2\zeta_n + \varepsilon\{in\vec{\bar{u}}_0 \cdot \nabla\zeta_n + \frac{1}{2} \nabla\bar{\zeta}_0 \cdot \nabla\zeta_n + \frac{1}{2} \bar{\zeta}_0 \nabla^2\zeta_n$$

$$- \frac{ih}{n} \left(\frac{\partial V}{\partial x} + \frac{\partial U}{\partial y} \right) \frac{\partial^2 \zeta_n}{\partial x \partial y} + \frac{ih}{n} \left(\frac{\partial U}{\partial x} \frac{\partial^2 \zeta_n}{\partial y^2} + \frac{\partial V}{\partial y} \frac{\partial^2 \zeta_n}{\partial x^2} \right) \} = \varepsilon \sum_{\substack{s \neq 0 \\ n \neq s}} \{ \frac{(n^2 - s^2)}{2h}$$

$$\zeta_s \zeta_{n-s} - \frac{(n+s)}{2(n-s)} \nabla \zeta_s \cdot \nabla \zeta_{n-s} + \frac{h}{s(n-s)} [\frac{\partial^2 \zeta_s}{\partial x \partial y} \frac{\partial^2 \zeta_{n-s}}{\partial x \partial y} - \frac{1}{2} \frac{\partial^2 \zeta_s}{\partial x^2}$$

$$\frac{\partial^2 \zeta_{n-s}}{\partial y^2} - \frac{1}{2} \frac{\partial^2 \zeta_s}{\partial y^2} \frac{\partial^2 \zeta_{n-s}}{\partial x^2}] \} \tag{2.13}$$

where $\vec{u}_0 = (U,V)$, and $G_n = (h - \frac{\mu^2 n^2 h^2}{3})$. Equation (2.13) can be used to find ζ_n with appropriate boundary conditions. Once ζ_n $(n = 1, 2, \cdots)$ are obtained, the corresponding velocity field can be calculated by

$$\vec{u}_n = - \frac{i}{n} \nabla \zeta_n \tag{2.14}$$

If the ambient velocity field is absent, i.e. $\vec{u}_0 = \bar{\zeta}_0 = 0$, (2.13) reduces to the equation derived by Liu, Yoon and Kirby (1985).

3. Parabolic Approximation

Consider the cases where the dominating wave propagation is known to be in the x-direction. The free-surface displacement for the nth harmonic can be written as

$$\zeta_n = \Psi_n (x,y) e^{inx} \tag{3.1}$$

where $\Psi_n(x,y)$ represents the amplitude function. Substitution of (3.1) into (2.13) yields

$$\left(G_n + \frac{\varepsilon}{2} \bar{\zeta}_0 + \frac{i\varepsilon h}{n} \frac{\partial V}{\partial y} \right) \frac{\partial^2 \Psi_n}{\partial x^2} + \left(G_n + \frac{\varepsilon}{2} \bar{\zeta}_0 + \frac{i\varepsilon h}{n} \frac{\partial U}{\partial x} \right) \frac{\partial^2 \Psi_n}{\partial y^2}$$

$$- \frac{i\varepsilon h}{n} \left(\frac{\partial V}{\partial x} + \frac{\partial U}{\partial y} \right) \frac{\partial^2 \Psi_n}{\partial x \partial y} + \left(2inG_n + \frac{\partial G_n}{\partial x} + i\varepsilon n U + \frac{\varepsilon}{2} \frac{\partial \bar{\zeta}_0}{\partial x} + i\varepsilon n \bar{\zeta}_0 \right.$$

$$\left. - 2\varepsilon h \frac{\partial V}{\partial y} \right) \frac{\partial \Psi_n}{\partial x} + \left[\frac{\partial G_n}{\partial y} + i\varepsilon n V + \frac{\varepsilon}{2} \frac{\partial \bar{\zeta}_0}{\partial y} + \varepsilon h \left(\frac{\partial V}{\partial x} + \frac{\partial U}{\partial y} \right) \right] \frac{\partial \Psi_n}{\partial y}$$

$$+ \left(in \frac{\partial G_n}{\partial x} - n^2 G_n + n^2 - \varepsilon n^2 U + \frac{i\varepsilon n}{2} \frac{\partial \bar{\zeta}_0}{\partial x} - \frac{\varepsilon n^2}{2} \bar{\zeta}_0 - i\varepsilon n h \frac{\partial V}{\partial y} \right) \Psi_n$$

$$= \varepsilon \sum_{\substack{s \neq 0 \\ s \neq n}} \{ \frac{i}{2h} [n^2 - s^2 + hs(n+s)] \Psi_s \Psi_{n-s} - \frac{(n+s)}{2(n-s)} [\nabla \Psi_s \cdot \nabla \Psi_{n-s}$$

$$+ is\, \Psi_s \frac{\partial \Psi_{n-s}}{\partial x} + i(n-s)\, \Psi_{n-s} \frac{\partial \Psi_s}{\partial x}] + \frac{h}{s(n-s)} [\frac{\partial^2 \Psi_s}{\partial x \partial y} \frac{\partial^2 \Psi_{n-s}}{\partial x \partial y}$$

$$+ i(n-s) \frac{\partial^2 \Psi_s}{\partial x \partial y} \frac{\partial \Psi_{n-s}}{\partial y} + is \frac{\partial \Psi_s}{\partial y} \frac{\partial^2 \Psi_{n-s}}{\partial x \partial y} - s(n-s) \frac{\partial \Psi_s}{\partial y} \frac{\partial^2 \Psi_{n-s}}{\partial y^2}$$

$$- \frac{1}{2} \frac{\partial^2 \Psi_s}{\partial x^2} \frac{\partial^2 \Psi_{n-s}}{\partial y^2} - is \frac{\partial \Psi_s}{\partial x} \frac{\partial^2 \Psi_{n-s}}{\partial y^2} + \frac{s^2}{2} \Psi_s \frac{\partial^2 \Psi_s}{\partial y^2} - \frac{1}{2} \frac{\partial^2 \Psi_s}{\partial y^2} \frac{\partial^2 \Psi_{n-s}}{\partial x^2}$$

$$- i(n-s) \frac{\partial^2 \Psi_s}{\partial y^2} \frac{\partial \Psi_{n-s}}{\partial x} + \frac{(n-s)^2}{2} \frac{\partial^2 \Psi_s}{\partial y^2} \Psi_{n-s}]\} \qquad (3.2)$$

In principle (3.2) can be used to solve for Ψ_n as a system of nonlinear boundary-value problems.

The amplitude function Ψ_n is primarily a function of the water depth and the ambient current field due to refraction. Therefore, Ψ_n varies slowly in the direction of wave propagation at the same rate as that of *h* and $\vec{u}$ *in the x-direction. Thus*

$$\frac{\partial \Psi_n}{\partial x} \sim \left|\frac{\partial h}{\partial x}\right| \sim \left|\frac{\partial \vec{u}_0}{\partial x}\right| \sim O(\varepsilon, \mu^2)$$

$$\frac{\partial^2 \Psi_n}{\partial x^2} \sim O(\varepsilon^2, \varepsilon\mu^2, \mu^4) \qquad (3.3a)$$

However, if the diffraction effects are important or the variation of *current in y-direction is of* O(1) *the rate of change of* Ψ_n *in the* y-direction is significant; i.e.

$$\frac{\partial \Psi_n}{\partial y} \sim O(1) \qquad (3.3b)$$

Using (3.3), equation (3.2) may be simplified to be

$$2in\, G_n \frac{\partial \Psi_n}{\partial x} + [G_n + \varepsilon \frac{\bar{\zeta}_0}{2}] \frac{\partial^2 \Psi_n}{\partial y^2} + [\frac{\partial G_n}{\partial y} + \varepsilon\, (inV + \frac{1}{2} \frac{\partial \bar{\zeta}_0}{\partial y}$$

$$+ h \frac{\partial U}{\partial y})] \frac{\partial \Psi_n}{\partial y} + [in \frac{\partial G_n}{\partial x} - n^2 G_n + n^2 + \varepsilon\, (-n^2 U - \frac{n^2}{2} \bar{\zeta}_0$$

$$-inh \frac{\partial V}{\partial y})] \Psi_n = \varepsilon \sum_{\substack{s \neq 0 \\ s \neq n}} \{ \frac{1}{2h} [n^2 - s^2 + hs\, (n+s)] \Psi_s \Psi_{n-s} - [\frac{(n+s)}{2(n-s)}$$

$$+ h] \frac{\partial \Psi_s}{\partial y} \frac{\partial \Psi_{n-s}}{\partial y} + \frac{sh}{n-s} \Psi_s \frac{\partial^2 \Psi_{n-s}}{\partial y^2} \} \qquad (3.4)$$

When the ambient current vanishes, (3.4) reduces to the equations derived by Liu, Yoon, and Kirby (1985).

Eq. (3.4) is a set of nonlinear parabolic equations for Ψ_n. The Crank-Nicolson method can be used to rewrite the governing equations in a finite-differences form. The detailed numerical procedure is similar to that developed by Liu, Yoon, and Kirby (1985) and is not repeated here.

4. Numerical Examples

The propagation of cnoidal waves over a vortex ring is examined here. The current velocity satisfying the governing equations (2.11 a,b) can be written as

$$V_r = 0, \quad V_\theta = \begin{cases} c_3 \, (r/r_1)^n \quad , & r \leq r_1 \\ c_2 \exp \left[-\left(\frac{r_2 - r}{c_1}\right)^2 \right] \quad , & r > r_1 \end{cases} \qquad (4.1)$$

where V_r and V_θ are velocity components in the radial r and θ-direction, respectively, In (4.1), r_1, c_1, c_2 and c_3 are arbitrary constants which determine the shape of the velocity profile. The mean free surface displacement, $\bar{\zeta}_0$, can be obtained by integrating (2.11b). Thus

$$\bar{\zeta}_0 = \int_\infty^r \frac{V_\theta^2}{r} dr \qquad (4.2)$$

where $\bar{\zeta}_0 \to 0$ as $r \to \infty$. In numerical computations, the following data are used: c_1 = 131.8m, c_2 = 0.5m/s, c_3 = 0.433m/s, r_1 = 350m, r_2 = 400m, n = 2. The velocity profile and the free surface displacement are shown in Figure 1.

The incident waves are described as cnoidal waves with wave height H = 2m and wave period T = 19.43s. The water depth is h = 10m so that the wave length is 188.9/m. Rewritting the cnoidal waves solution in Fourier series and truncating the series up to the fifth harmonic, one can calculate the wave amplitudes for each harmonic as: A_1 = 0.7864m, A_2 = 0.37m, A_3 = 0.1382m, A_4 = 0.046m and A_5 = 0.0144m.

As the result of refraction and diffraction over the vortex ring, the contour lines for the absolute values of the free surface displacement are plotted in Figure 2. It is clear that waves converge along two lines creating relatively larger wave amplitudes. In the regions where the currents move in the direction opposite to the

the wavelength decreases and the amplitudes increase. On the other hand, in the region where waves move in the same direction as currents, wavelength is increased. These features are indicated in Figure 3 where the normalized free surface displacements are plotted along y = ± 400m.

Acknowledgement This research has been supported by New York Sea Grant Institute.

References

Liu, P. L-F., Yoon S.B. and Kirby, J.T. 1985. Nonlinear refraction-diffraction of waves in shallow water, J. Fluid Mech. Vol. 153, pp. 185-201.

Mei, C.C. and Lo, E., 1984. The effects of a jet-like current on gravity waves in shallow water, J. Physical Oceanography, Vol.14, pp. 471-477.

Peregrine, D.H. and Jonsson, I.G. 1983. Interaction of waves and currents, Misc. Rept. No. 83-6, U.S. Army Coastal Engineering Research Center 88p.

Peregrine, D.H. 1976. Interaction of water waves and currents. Advances in Applied Mechanics, Vol. 16, pp. 9-117.

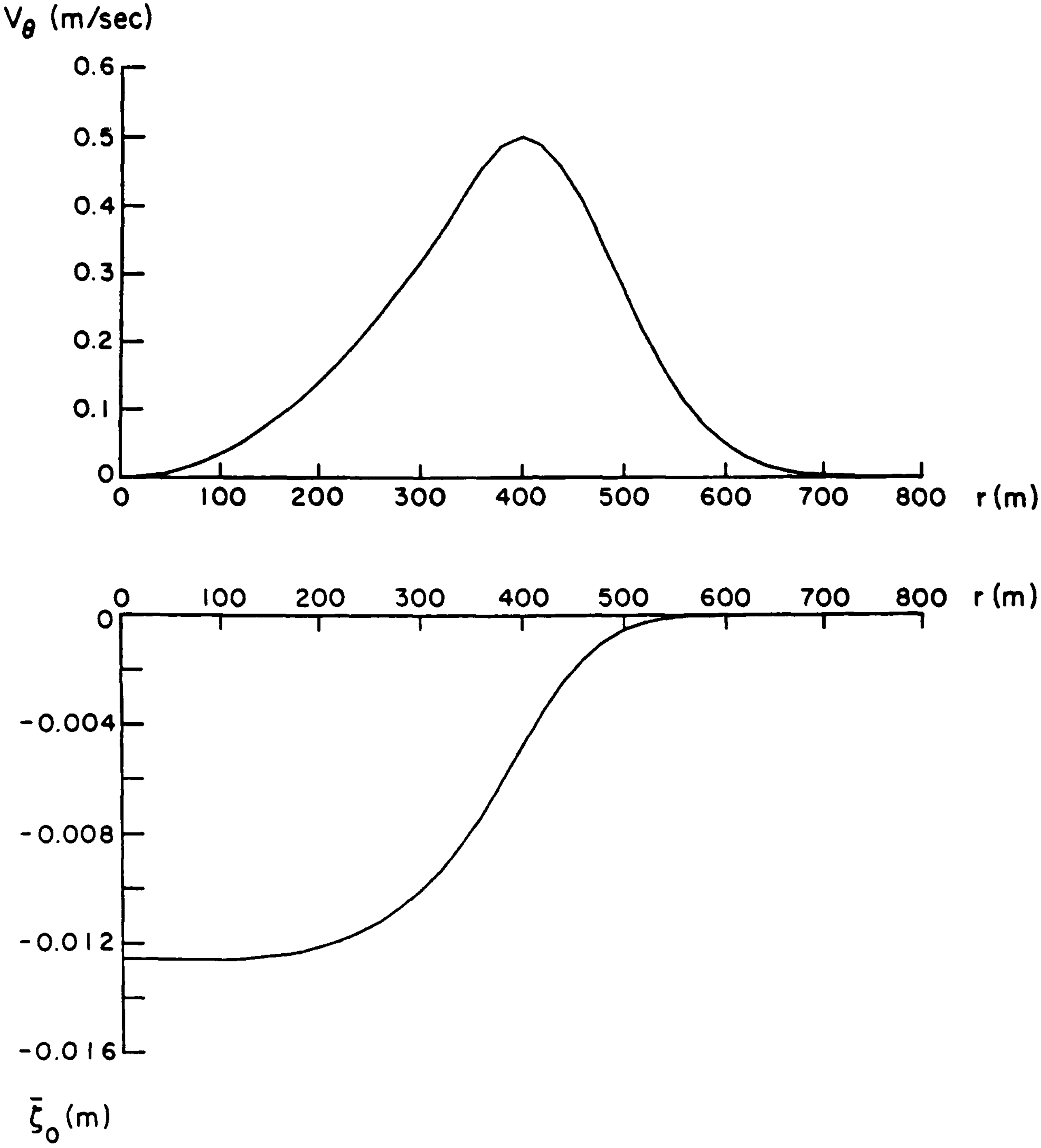

Figure 1. Current velocity distribution and mean free surface set-down.

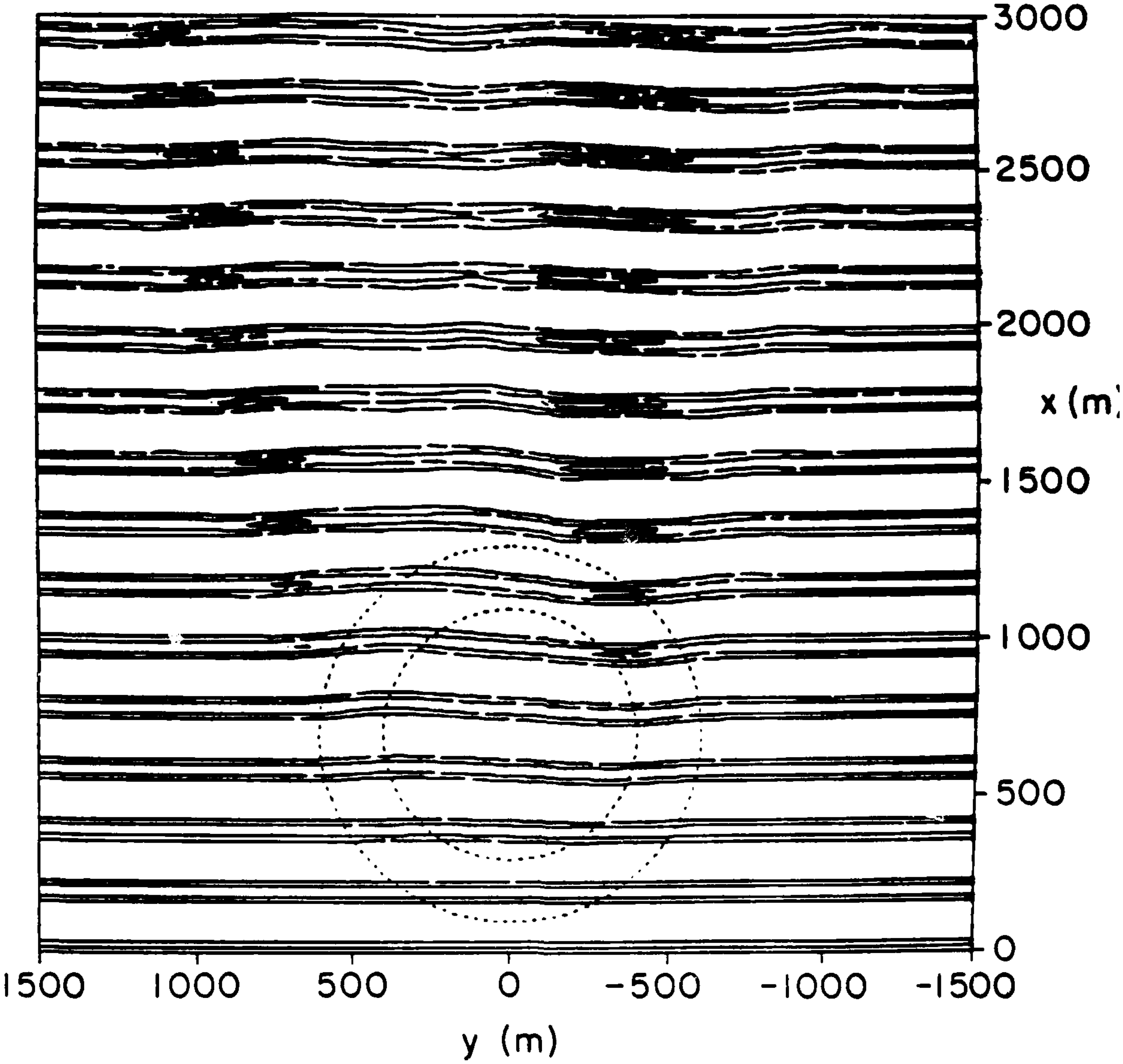

Figure 2. Contour lines of free surface displacement, ζ/H = 0.4, 0.8 and 1.2.

AD-A168 715 PROCEEDINGS OF WEST COAST REGIONAL COASTAL DESIGN 2/5
CONFERENCE HELD ON 7-8 NOVEMBER 1985 AT OAKLAND
CALIFORNIA(U) CORPS OF ENGINEERS SAN FRANCISCO CALIF
UNCLASSIFIED SOUTH PACIFIC DIV APR 86 F/G 13/2 NL

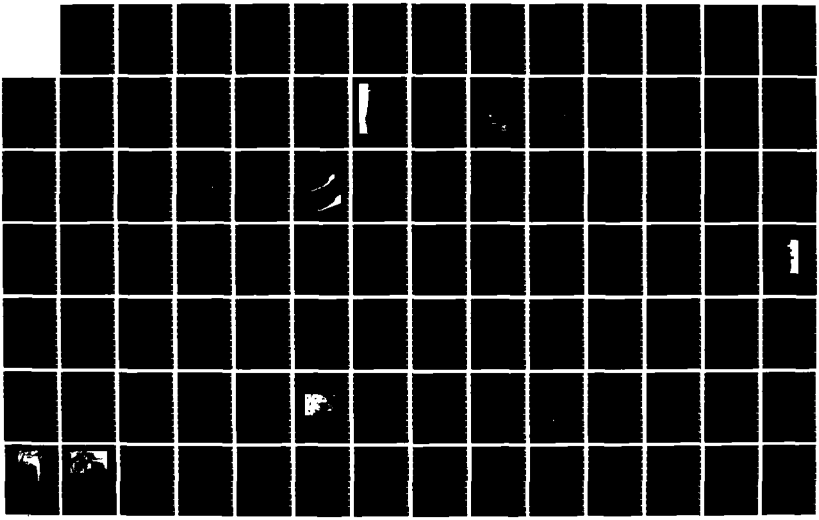

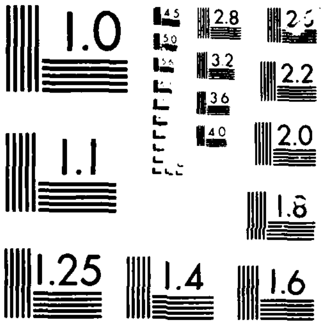
1.0
4.5
5.0
5.6
2.8
2.5
3.2
2.2
3.6
4.0
2.0
1.1
1.8
1.25
1.4
1.6

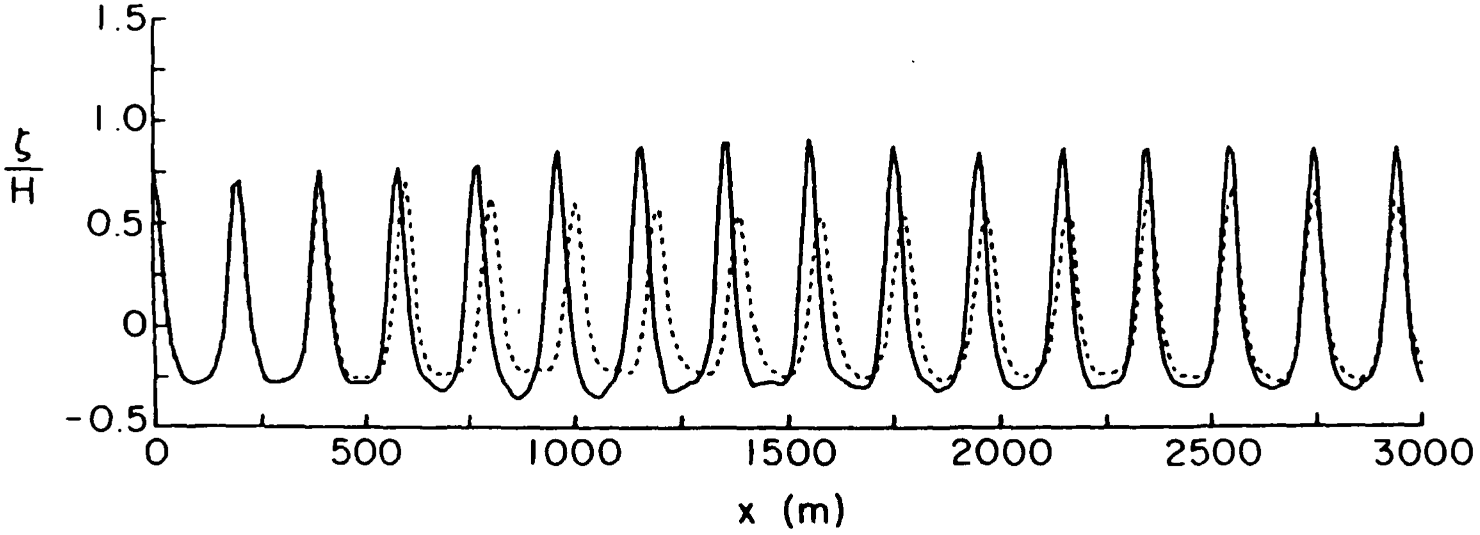

Figure 3. Normalized free surface displacement along y = ± 400m.

THE ALASKA COASTAL DATA COLLECTION PROGRAM

PAST, PRESENT, AND FUTURE

By Carl D. Stormer*

INTRODUCTION

A prime lifeline for many of Alaska's people has been and continues to be the sea. Traditionally, Alaska's coastal communities, which are scattered along its 33,900 miles of coastline, depended heavily on resources from the sea. Today, the dependence of Alaska's economy on the sea has grown to include an expanded fishing industry, exportation of Alaska's mineral, timber, and fish resources, importation of goods to Alaska's increasing population, and marine transportation systems to Alaska's remote coastal settlements. Engineers in Alaska must face challenges unlike those found elsewhere in the coastal United States to plan for and develop ports and harbors to meet Alaska's economic needs. A few of these challenges are arctic conditions, unusually high tides, and remote project locations. Perhaps the biggest challenge that engineers confront, however, is the lack of data necessary to economically complete navigation projects. For that reason, projects are more often overdesigned but occassionally underdesigned, resulting in economic losses.

WHERE HAVE WE BEEN?

The Alaska Coastal Data Collection Program (ACDCP) was conceived in 1981 and 1982 by the U.S. Army Engineer District, Alaska, and the State of Alaska Department of Transportation and Public Facilities (DOT/PF). It originated as a cooperative effort to collect coastal data in Alaska to provide the vital data necessary to respond effectively to Alaska's urgent port and harbor development needs.

---

*Chief, Hydraulics and Waterways Section, U.S. Army Engineer District, Alaska, P.O. Box 898, Anchorage, Alaska 99506-0898

The Alaska District and the State of Alaska DOT/PF have a long history of mutual cooperation as the two predominant government agencies in Alaska responsible for the development of coastal public works projects. The ACDCP is without question of mutual benefit to the Alaska District and the State of Alaska in their continued work on coastal projects. A third agency, the U.S. Army Corps of Engineers, Coastal Engineering Research Center (CERC), was designated as the appropriate organizational element within the Corps of Engineers (COE) to enter into the interagency agreement with the State of Alaska because of its Congressional authority to collect coastal data.

The State of Alaska DOT/PF and CERC entered into an interagency agreement on July 30, 1982, "...for the purpose of facilitating the systematic accumulation of coastal field measurements of wind, waves, and other data necessary for planning, design, construction, operation, and maintenance of port, harbor, and shore protection facilities in Alaska..."

Other interested agencies and individuals have provided valuable input to the ACDCP during its three-year history. Local communities have also provided a significant contribution to the overall success of the program. Without their valuable support, the ACDCP would not be where it is today.

Program Goals and Operations

The goals for the ACDCP, as stated in the Interagency Agreement, are:

1. Collection of field data for coastal engineering purposes by either partly or through their joint efforts in a standardized format compatible with the automatic data processing means available, and with the CERC data base that is included in the Design Wave Information Center.

2. Storage of field data collected for coastal engineering purposes by either party or joint efforts at a central location for ready retrieval as public information.

3. Establishment and maintenance of a statewide network of coastal field data collection sites at key locations for long term accumulation of data with regional applications.

4. Development of coastal field data collection instrumentation and telemetry suited to the Alaskan environment.

5. Development of coastal field data storage, retrieval, and analysis procedures and computer software suited to current circumstances and specific needs of developments along Alaska's coastline.

The overall direction of the ACDCP is monitored and directed through the Interagency Coastal Data Technical Committee. This Committee is made up of representatives from the Alaska District and the State of Alaska DOT/PF to provide the guidance for the program management and technical aspects of coastal data collection in Alaska. One co-chairperson from both the Alaska District and DOT/ PF is selected by the Committee to serve for at least one calendar year.

The Committee has the following general duties and responsibilities as defined in the original program plan:

1. To provide the overall guidance for the pursuit of the program goals.

2. To prepare a Program Plan to include the plan of proposed activities for the coming year and for the proposed activities 5 years into the future.

3. To annually prepare a summary report of the prior year's activities.

4. To establish a standardized format for recorded field data, data storage procedures, data retrieval procedures, and procedures for furnishing data to the public.

5. To plan and implement a program to develop instrumentation, telemetry, and data analysis software suited to current needs and circumstances in Alaska.

6. To coordinate the respective user agency requirements and the requirements for those agencies other than the Alaska District and DOT/PF.

The Committee meets twice a year to review progress of activities, confirm future plans, and hear input from interested parties not officially members of the Committee. All of the day-to-day activities are accomplished by the Alaska District who coordinate as necessary with the State of Alaska DOT/PF and others on program matters.

The ACDCP began its life slowly as those involved gained knowledge and experience in the field of coastal data collection in one of the most difficult areas to collect data in the world. The general strategy was to move forward carefully building a stock of data collection equipment and experience in the first few years. The initial site locations were selected to give maximum return for the data collected as soon as possible in addition to being located in a relatively accessible area with good support facilities. Where wind data was already good, a wave buoy installation could provide wave information to correlate both the wind and wave data. The first site selected was at Kodiak, Alaska (see Figure 1) where both the State DOT/PF and the Alaska District had strong interest and active projects. Other sites followed at Homer, Nome, Akutan, and Whittier, Alaska. The stock of equipment grew based on the general success of the Kodiak instrumentation. Due to the variety of site characteristics, the instrumentation was varied to include the waverider buoys for deep water large wave sites to wave spar buoys

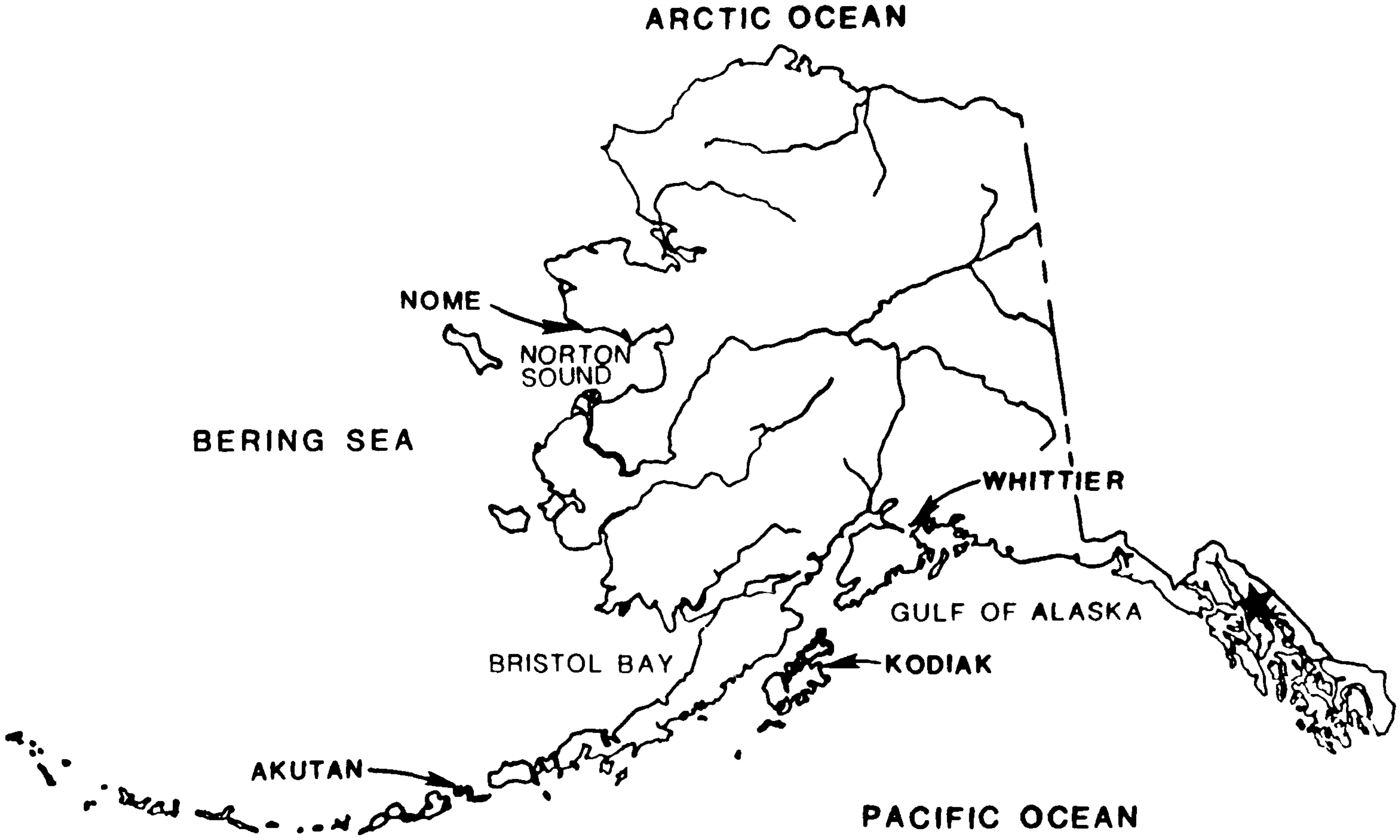
ARCTIC OCEAN
NOME
NORTON SOUND
BERING SEA
WHITTIER
GULF OF ALASKA
BRISTOL BAY
KODIAK
AKUTAN
PACIFIC OCEAN

Figure 1 - Alaska Coastal Data Collection Sites, 1985

for smaller wave and wave period sites and current-pressure sensor installations for nearshore directional wave data collection.

A long term goal identified in the original program document was to acquire regional data at selected sites throughout Alaska from Norton Sound in the northern part of the state to the Gulf Coast and inland passages of southeastern Alaska. These regional measurements would serve multiple applications including harbor and port engineering, beach protection, pilotage aid with real time information on waves and wind conditions, and regional or area wind data correlation with measured wave heights. Additionally, as new construction took place, it was planned data collection instrumentation could be "built in" to the project features. Thus, the capability to obtain long term site specific measurements would be provided to evaluate design methods and structure performance and maintenance needs.

The potential cost savings for coastal structures based on more accurate and reliable wind and wave data is very evident. Reductions in breakwater design wave heights of only one foot could result in a cost reduction of as much as $1 million. More accurate design data would at the same time greatly reduce the risk of expensive repairs. This is vitally important in Alaska with its extensive coastline and need for coastal and harbor facilities in very remote parts of the state.

The operational arrangements between the Alaska District and State of Alaska DOT/PF are detailed as follows:

1. Financial. An annual Joint Funding Agreement between the Alaska District and DOT/PF is the instrument to specify each agency's respective contributions.

2. Procurement and Equipment Ownership. The responsibility of procurement and ownership of equipment used for this program rests with the Alaska District. The Interagency Technical Committee reviews the selection of the types of equipment to be purchased. The equipment is procured with the intention that it be applied to the ACDCP.

3. Equipment Installation and Maintenance. The installation and maintenance of the equipment used to collect the coastal data are the responsibility of the Alaska District. The DOT/PF provides assistance within its capabilities when requested by the Alaska District.

4. Data Collection, Analysis, Storage, and Reporting. These operations and methods employed in the field and office are the responsibility of the Alaska District. The Interagency Technical Committee reviews the standards of accuracy required for coastal engineering purposed in Alaska and assures that the data collection program reflects the necessary accuracy. Data collected by agencies other than the Alaska District are reviewed for applicability and accuracy and incorporated into the data bank and reports directly or

by reference. Formats for reporting are determined by the Interagency Technical Committee.

5. Local Community Participation. Participation in the ACDCP by local communities is needed to efficiently carry out the program. Local communities are called upon to supply community facilities to house instrumentation equipment, to provide support services by the local harbormaster or city engineer to tend the equipment, to notify or assist the Alaska District in the event of equipment failures or problems, and generally to assure the security of the equipment.

Instrumentation Descriptions

The instrumentation is basically the same for sites located at Kodiak, Homer, and Akutan. The instrumentation at Kodiak was removed in October 1984, however, in anticipation of being relocated to Chignik, Alaska, which was subsequently dropped. The Kodiak and Homer sites have operated reasonably well. Akutan, being extremely remote with a very poor location for the shore base station, has proven to be essentially unsuccessful in data recovery.

Waverider buoys manufactured by Datawell of the Netherlands are the prime wave measurement instruments. These instruments continuously transmit wave height and period data ashore by VHF-FM radio broadcast. A receiver ashore transforms the signal to a form compatible with most recording devices. An anemometer of standard design used by the Alaska District is also installed at each site. It can be provided with a radio telemetry arrangement with a receiver at the same site as the buoy receiver or directly "hardwired" to the collection system. A microprocessor is programmed to manipulate the buoy and anemometer signals, recording both the digitized raw data and computed summaries at specified time intervals on magnetic tape. Because of the remoteness of the data collection system, a meteor burst communications transceiver is provided which automatically transmits summary data to Anchorage along with information about the status of various system components. It also allows review in Anchorage of conditions in the field as they occur. The National Weather Service has arranged to receive this same information and use it in weather reports. The summary information can be printed at each shore base station and used to provide real time wind and wave data to local interested parties. It has, for example, been used quite extensively by the commercial charter fishing fleet in Homer, Alaska. Local city officials assist by providing a location for the on site shore station, security for the equipment, data tape changes, and sending full tapes to the Alaska District in Anchorage for processing.

The summary data provided via the meteor burst communications system are used for scanning the data for interesting periods and for sorting the data for certain types of statistical analyses. The digital time series (raw data) recorded on magnetic tape are used for spectral analysis.

The wave data analysis computer programs now on line at the Alaska District produce useful output in a number of forms. When an adequate amount of data has been collected, at least 1 to 2 full years' worth, it will be used to determine design criteria in the form of energy spectra. These design spectra can then be used as input to numerical models that will predict wave refraction, shoaling, diffraction, and breaking at the project site.

The instrumentation currently located at Shotgun Cove near Whittier is specifically designed to measure waves from 0 to 4 feet with short periods, below the range of the waverider buoys. These instruments are staff gages made up from PVC pipe which is spirally wound with a resistance wire such that when it is immersed in seawater, the electrical resistance varies in direct proportion to the length of the exposed staff. The electronics are located in a sealed container attached to the bottom of the wave damping plate on the bottom of the buoy. Data is recorded on a 6-inch cartridge system integrally built into the electronics package. The system is completely self-contained, having no capability to transmit summary or status information back to the Alaska District in Anchorage. Recording capability and power supply limits the time between service to each buoy to approximately 4 to 6 months maximum.

The Alaska District has a reader/processor with appropriate software to do complete data analysis and graphics. The system is manufactured by Measurement Research Corporation, Gig Harbor, Washington. A remote anemometer is also located near the mouth of Shotgun Cove which transmits summary wind data directly to the Alaska District office through the meteor burst telemetry system. There were some initial development and start up problems which have been worked out. There is good confidence in the system reliability and capability.

Directional wave data collection has been less successful than either of the two systems described above. Instrumentation was placed approximately one-half mile off shore at about a 20-foot depth near Nome, Alaska, for the last 2 years. The basic wave information was obtained from a pressure gage and current meter type system. Initially, wave data was transmitted via cable to a surface buoy which in turn transmitted it to a shore station similar to the Homer, Akutan, and Kodiak systems. An anemometer was also part of the total system. The surface buoy was torn loose during a storm 2 weeks after the initial deployment the first summer. This past summer a similar directional pressure gage current meter system with self-recording capability from CERC were deployed and retrieved successfully. Data analysis is currently in progress at CERC.

Data Collection, Analysis, and Publication

The primary goal of the ACDCP is to provide user-oriented data for both regional and site-specific application. Data reports contain one-line listings of wind and wave data for each record over the period of record. Emphasis is placed on identifying individual events in some detail. Wind speed and wind direction information, as well as wave spectral data, are reported in 3-hour intervals. As data reports become more numerous, a yearly data report will be published in which reports will be summarized in the form of probability distribution tables of basic wind and wave parameters.

Wind data are analyzed in the field at the shore base station. At a standard wind station which includes a directional vane and anemometer, wind direction and wind speed are sampled once per second. The base station microprocessor computes the hourly average wind speed and direction, along with the maximum 10-second wind speed recorded in the hour, the standard deviations of wind speed and direction, and a printed status code indicating data collection or transmission errors. This hourly wind summary is recorded on the magnetic data tape and is also transmitted to Anchorage via the meteor burst communications system.

Wave data in the form of a wave height signal is continuously transmitted from the waverider (accelerometer) buoys to the shore base station. Data sampling characteristics may be varied over a broad range and are selected through a remote communications terminal at the shore station. Preliminary wave data analysis is performed on-site at the shore base station. A one-line summary of each record is transmitted to Anchorage via the meteor burst system. This includes information on the sampling characteristics, number of data samples, maximum and minimum wave amplitudes, significant wave height, zero-crossing period, and a status code to indicate data transmission errors. Spectral analysis of the wave records is performed by Alaska District using computer programs provided by CERC. The standard output format adopted for data reports includes a one-line summary for each spectral record, showing the significant wave height, total wave energy, and a normalized wave energy spectrum.

The final published data table consists of a summary of wind and wave data. This format includes basic wind and wave parameters used in most coastal engineering design formulae, such as average wind speeds and directions, and significant wave height and peak period.

WHERE ARE WE?

The ACDCP has arrived at a major crossroads in its life. The choice must be made whether to continue to develop the program strengthening its capabilities and reaching for the long term goals or maintain it as a strictly site specific short term data collection program. The program has done amazingly well for the amount of funds and level of effort that has been put forth. There have been some failures to be sure, but this experience has been valuable and forms the foundation on which a stronger more productive coastal data collection program will be built.

WHERE ARE WE GOING?

The primary and most important goal for the ACDCP in the next year, fiscal year 1986, is to renew the emphasis on the program and strengthen it administratively, financially, and operationally.

The coastline of Alaska is an important part of the total coastaline of the entire United States. As such, the national priority for coastal information needs to be emphasized and strengthened through further support and involvement to the ACDCP from the Coastal Field Data Collection Program administered by CERC. Happily, it can be said that there is excellent support presently from CERC and it appears the future continues to look promising. At the Alaska District, a higher priority is being established for support of the ACDCP and its continued development as a quality coastal data collection program. Additional time is anticipated to pursue the overall goals of the program. The District is the lead agency in this work with the other agencies looking to the Alaska District for guidance related to the program.

The Interagency Coastal Data Technical Committee has carried out its responsibilities well. The Committee must adjust to changing conditions, however, as the ACDCP develops. This means that as the nature of the program changes from primarily a site and project specific type of program, the Committee will be required to accept new members as additional sources of funding are developed and the direction expands to regional sites and existing data collection inputs by other agencies or organizations. Additionally, those involved in the program will need to support it by their positive commitment to it. The program needs to develop and sell itself to gain and retain the support it must receive to survive in a very cost conscious time where value for the dollar spent is looked at critically. The administration of the program must develop dynamically to meet the challenges of the future.

Recent funding for the ACDCP has relied heavily on sources through the State of Alaska DOT/PF. The individuals there share the concern and need for coastal data and a quality data collection program. Unfortunately, State of Alaska funding sources have been inconsistent and unsupported in the State budget due to declining oil revenue. Therefore, the need exists for the ACDCP to develop additional means for supplying the required funds by broadening the base of agencies supporting the program and finding new and imaginative ways to obtain funding. Direct project support, where it would apply, would be good for specific sites. Regional buoy locations could come from non-site specific State and Federal funds. Funding through Operations and Maintenance avenues as it relates to existing projects will be explored further. While not in the form of financial support, the data collected through State or Federal regulatory programs would be an asset to the program because it is data at little or no cost. This too is being pursued. Plant Replacement & Improvement Program (PRIP) funds, through the Corps of Engineers, have been used to acquire the wave staff gages, which have become part of the ACDCP equipment inventory. Continued support through this avenue will be helpful. ACDCP must review and strengthen its financial base to eliminate the painful budget fluctuations of the past, if it is to meet the demands of a quality data collection program in the future.

Operation and maintenance of the data collection instrumentation has been the emphasis of the ACDCP in the last few years. Much has been learned about what works and what doesn't in various situations in Alaska, especially the very remote ones. Shore base stations have proven to be high maintenance items, especially the magnetic tape recording equipment and reliable power sources. Improvements are presently under contract and with its completion the reliability and data retrieval percentage will improve substantially. Work will continue as funding permits to develop new and more reliable data collection equipment. Direct satellite communication from the buoy to Anchorage is seriously being considered for future remote locations.

As mentioned above, providing data in a useful form is the prime objective of the ACDCP. Efforts will be initiated to find unreported data sources and bring them into the system. Through the State of Alaska and Federal regulatory agencies, additional data either that is already being collected or from new near shore development could relatively easily be added. This area alone could expand the Alaska coastal data base considerably. The long term regional sites are necessary for broad based initial planning studies and for developing additional data points for the Pacific Ocean Wave Information Study currently being worked on by CERC. These sites will be developed as rapidly as funding or data sources become available.

Conclusions

The goals of the ACDCP as described earlier in this paper and the original program document will remain basically unchanged. Additional emphasis will be placed on establishing financial stability and making improvements to the existing systems and procedures. Developing the long term regional data collection sites in addition to the short term specific project sites is a particular goal where emphasis will be directed. Those things which can be done to improve the quality and quantity of coastal data available to engineers and designers working in Alaska will reap significant benefits to everyone.

REFERENCES

Interagency Technical Committee, Alaska Coastal Data Collection Program, "1983 Program Plan," Anchorage, Alaska, July 1982.

Smith, O.P., Kriehel, D.L., and Bales, J.T., "The Alaska Coastal Data Collection Program," The Third Symposium on Coastal and Ocean Management, June 1983.

Summary of Panel Discussion

HARBORS

Chairman: William J. Brick
Corps of Engineers, San Francisco District

Panelists: Charles Roberts, Port of Oakland, California
C. Eugene Chatham, US Army Corps of Engineers
Waterways Experiment Station (WES), Vicksburg, Mississippi
Richard E. Millard, Richard E. Millard and
Associates, Inc., Napa, California
Carl D. Stormer, US Army Corps of Engineers, Alaska
District, Anchorage

Based on what I saw and heard, I believe that the first session, Harbors, was quite successful. Most of the time the room was essentially full. Of the nine papers presented, two were theoretical, presenting mathematical derivations of solutions to problems: "Exact and Approximate Solutions for Breakwater Gap Diffraction" by Dr. Rodney Sobey and "Interaction Between Water Waves and Currents in Shallow Water" by Dr. Philip Liu.

Dr. Gary Griggs' presentation, entitled "Beach Compartments, Littoral Drift, and Harbor Dredging," related the success of, or problems associated with, several small-craft harbors along the California coast to their locations in littoral cells.

Mr. Michael Hemsley's presentation, "Coastal Field Data Collection Program," discussed the types of coastal data being collected by the US Army Corps of Engineers (Corps).

Two of the presentations dealt with navigation simulation. Mr. Carl Huval's discussion centered on the capabilities of WES' ship tow simulator and the uses to which it has been put. Mr. Roderick Chisholm's presentation centered on the user's points of view of the simulator. He indicated that the simulator is not a panacea, but its use should be considered in the planning process.

Mr. John Nichol's presentation, "Observations in Small-Boat Harbors: Harbor Design Concepts," summarized a number of design considerations ranging from entrance widths, depths, and configuration considerations to interior channel design. Mr. Nichol's talk was highlighted by a number of slides showing vessels trying to leave harbors at times when they shouldn't which kept the after lunch hour audience awake.

The remaining two presentations were application, or case study, oriented. Dr. Slotta's presentation, "Shoaling of the Port Astoria, Oregon, by Sediment from Mt. St. Helens Eruption," discussed studies conducted to identify the source and magnitude of material being deposited in the harbor. Mr. Illias' presentation, "Rogue River Entrance," discussed studies and construction undertaken to solve shoaling problems in the entrance channel generated by the construction of jetties at the mouth of the Rogue River.

Following the presentations, the panelists were given approximately 5 minutes each to present their thoughts on the presentations. Gene Chatham's comments were primarily based on his research oriented perception of the presentations. Also from the Corps, Carl Stormer gave comments from a District's perspective, applying some of what he heard in the presentations to his day-to-day activities at the District. The comments of Mr. Charles Roberts, of the Port of Oakland, were consistent with his role as the chief engineer of a major deepwater port. Lastly, Mr. Richard Millard's comments reflected his role as a consultant.

Many of the panelists' comments related to thoughts presented by Ogden Beeman in his theme address that morning concerning, primarily, the thought provoking area of cost sharing. Gary Griggs' presentation addressed the problems associated with several small-craft harbors along the California coast, and he suggested that more thought be given to littoral cell considerations when locating the harbors. Mr. Roberts pointed out that politics is quite often more of a driving force regarding the location of small-craft harbors than are engineering considerations. With cost sharing, however, Mr. Roberts pointed out that we, as engineers, will have to assume more responsibility in identifying and quantifying problems associated with the location of small-craft harbors now that the locals will be required to pay for mistakes which may be made in locating harbors (i.e. high maintenance dredging costs).

Mr. Roberts also pointed out that tonnage fees will be assessed in order to pay for harbor maintenance, as proposed in the Roe Bill (H.R. 6). As a result, users of the ports, such as Salinas Valley farmers who use the Port of Oakland to ship produce to the Orient, will find it difficult to accept that their shipping rates are being raised so that other harbors may be maintained.

Mr. Millard's thoughts were more general in nature. He felt that what we left the conference with, per se, was not all important. He suggested, however, that we catalog what we had heard, for future reference, and that our knowledge, based on meeting with and talking to other conference attendees, is as important, and perhaps as meaningful, as literature available in libraries. He emphasized that conference attendees should take this opportunity to get together and discuss their mutual problems and areas of interest.

Following the presentations by the panelists, there was limited open discussion among the audience and/or the panelists. A question arose concerning the amount of mathematics engineering students are receiving. Dr. Liu responded that he thought the mathematical background of engineering students, at least at his university, was sufficient. Dr. Liu also pointed out that most universities now require classes in computer programming.

During the open discussion period, cost sharing and the need to study in more detail project maintenance costs, with cost-sharing, were reiterated. The need for engineers to get more involved in politics and the decision making process was also reiterated.

Finally, there was considerable discussion throughout the day that this conference was worthwhile and that thought should be given to organizing similar conferences in the future. I wish to add that I have enjoyed meeting and working with the speakers and panelists of my session, and I hope that we contributed to the success of the conference.

William J. Brick
Chairman, Harbors Session

Generic Ocean Disposal Studies for the Oregon Coast

James R. Reese*

Abstract

The Marine Protection, Research and Sanctuaries Act of 1972 (MPRSA) was passed in recognition that the disposal of wastes into ocean waters could potentially result in adverse environmental impacts. Under Title I of the MPRSA, the U.S. Environmental Protection Agency (EPA) and the U.S. Army Corps of Engineers were assigned the basic responsibility for developing and implementing regulatory programs to ensure that ocean disposal would not "adversely affect human health, welfare, or amenities, or the marine environment, ecological systems, or economic potentialities." As required by MPRSA, ocean disposal of dredged material can occur only at a site that has been designated to receive dredged material. EPA developed ocean dumping criteria (40 CFR, Part 228) require that site designations be based on environmental studies of each site, and on historical knowledge of the impact of dredged material disposal on areas similar to such sites in physical, chemical, and biological characteristics. General criteria (40 CFR 228.5) and specific factors (40 CFR 228.6) must be considered prior to site designation. Portland District Corps of Engineers is presently evaluating eight interim ocean disposal sites for permanent designation to provide for continued maintenance of federal navigation projects along the Oregon coast. The evaluations are utilizing new procedures developed jointly by EPA and the Corps in 1985 in a workbook entitled "General Approach to Designation Studies for Ocean Dredged Material Disposal Sites." These procedures greatly reduced the costs of evaluating disposal sites while still providing for a thorough environmental evaluation of the site. This paper reports on the new procedures, information that was collected for the studies, results to date and management decisions necessary for final selection and evaluation of the eight disposal sites.

Introduction

The Corps of Engineers and EPA share statutory responsibilities for designating and managing ocean dredged material disposal sites (ODMDS). This responsibility was established in the Marine Protection, Research, and Sanctuaries Act of 1972 (P.L. 92-532, called the Ocean Dumping Act). Also under Section 103 of the above Act, the Corps is required to administer a permit program for authorizing the transport of dredged material in ocean waters for disposal at designated sites.

---

*Environmental Specialist, Portland District, Corps of Engineers, P.O. Box 2946, Portland, Oregon 97208-2946.

All existing ODMDS were designated as interim in the Code of Federal Regulations (40 CFR 228.12) and were required to have evaluation studies as described in 40 CFR 228.1-228.9 completed prior to final site designation. Because the Corps and EPA share the statutory responsibility for designating and managing ODMDS, they recognized the need for joint guidance on a technical approach. This would provide consistent site evaluations by the two agencies and lead to the designation of environmentally acceptable and operationally efficient disposal sites. A working group under the direction of the Assistant Secretary of the Army for Civil Works and the EPA Assistant Administrator for Water prepared a draft technical guidance workbook for site designation (USACE/EPA 1984). Portland District's Planning Division, at the request of the working group, used the book to prepare a pilot study at Yaquina Bay, Oregon. The "Yaquina Bay Interim Ocean Dredged Material Disposal Site Evaluation Study" (USACE 1985) has been widely accepted and is being used as a model for remaining site evaluations in Portland District. The report will also be included as an appendix to the final USACE/EPA workbook. A full discussion of the procedures used is given in "Implementation of EPA/Corps Site Evaluation Guidance" (Chesser and Reese 1984). The basic procedures followed are given in Figure 1.

Based on the success of the Yaquina Bay report and the reasonable cost of preparing the document, evaluation studies for eight interim ODMDS within Portland District boundaries were initiated. The sites are: Chetco River Entrance; Rogue River Entrance; Port Orford; Coquille River Entrance; Umpqua River Entrance; Siuslaw River Entrance; Depoe Bay; and Tillamook Bay Entrance. Figure 2 shows the general location of the sites. The two obvious omissions from this list are the sites at Coos Bay and the mouth of the Columbia River. Documentation on these sites is completed and they are awaiting final site designation by EPA.

Generic Ocean Disposal Site Studies

The similarity of all eight areas and the type of studies to be accomplished at each led to establishing the Generic Ocean Disposal Site Study (GODSS). An interdisciplinary team was formed, consisting of a study leader, physical oceanographer, geological oceanographer, marine ecologists, cultural resource specialist, recreation planner, wildlife biologist, and engineer. This team is examining all data and evaluating each site based on the procedure outlined in Figure 1. Phase I is completed and Phase II is being finalized at this time.

Factors that must be evaluated in the studies are listed in 40 CFR 228.5 and 228.6. The studies can consist of as little as a literature survey or, if there is no existing information, limited field studies as necessary. Table 1 shows an evaluation sheet being used for each of the eight study areas and progress to date. The left hand column of the table lists the 27 factors that must be considered prior to preparing an evaluation report. The factors are the various elements required by 40 CFR 228.5 and 228.6.

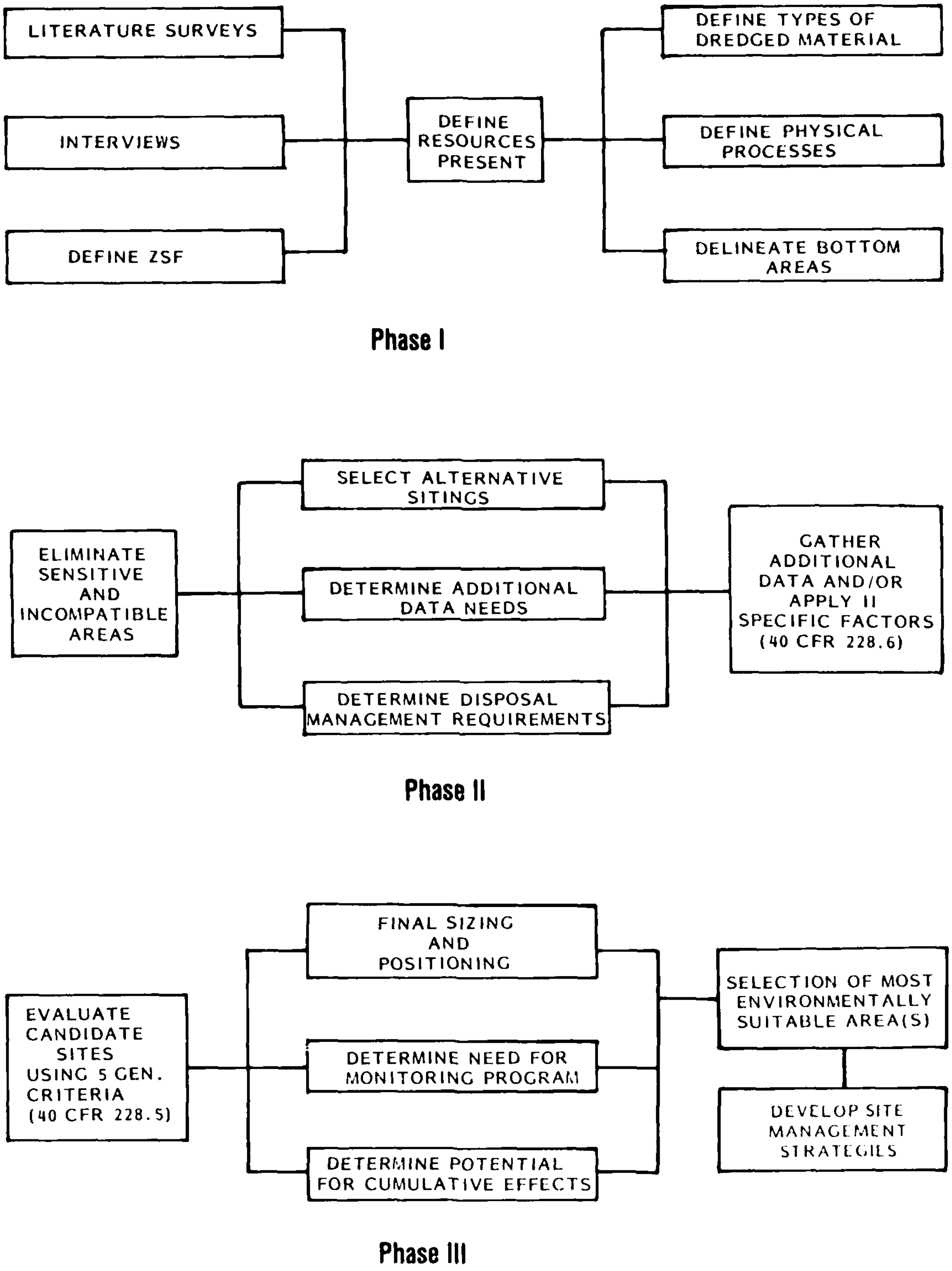
LITERATURE SURVEYS
INTERVIEWS
DEFINE ZSF
DEFINE RESOURCES PRESENT
DEFINE TYPES OF DREDGED MATERIAL
DEFINE PHYSICAL PROCESSES
DELINEATE BOTTOM AREAS
Phase I
ELIMINATE SENSITIVE AND INCOMPATIBLE AREAS
SELECT ALTERNATIVE SITINGS
DETERMINE ADDITIONAL DATA NEEDS
DETERMINE DISPOSAL MANAGEMENT REQUIREMENTS
GATHER ADDITIONAL DATA AND/OR APPLY 11 SPECIFIC FACTORS (40 CFR 228.6)
Phase II
EVALUATE CANDIDATE SITES USING 5 GEN. CRITERIA (40 CFR 228.5)
FINAL SIZING AND POSITIONING
DETERMINE NEED FOR MONITORING PROGRAM
DETERMINE POTENTIAL FOR CUMULATIVE EFFECTS
SELECTION OF MOST ENVIRONMENTALLY SUITABLE AREA(S)
DEVELOP SITE MANAGEMENT STRATEGIES
Phase III

Figure 1. Overall Process for Ocean Dredged Material Disposal Site Evaluations (USACE/EPA 1984)

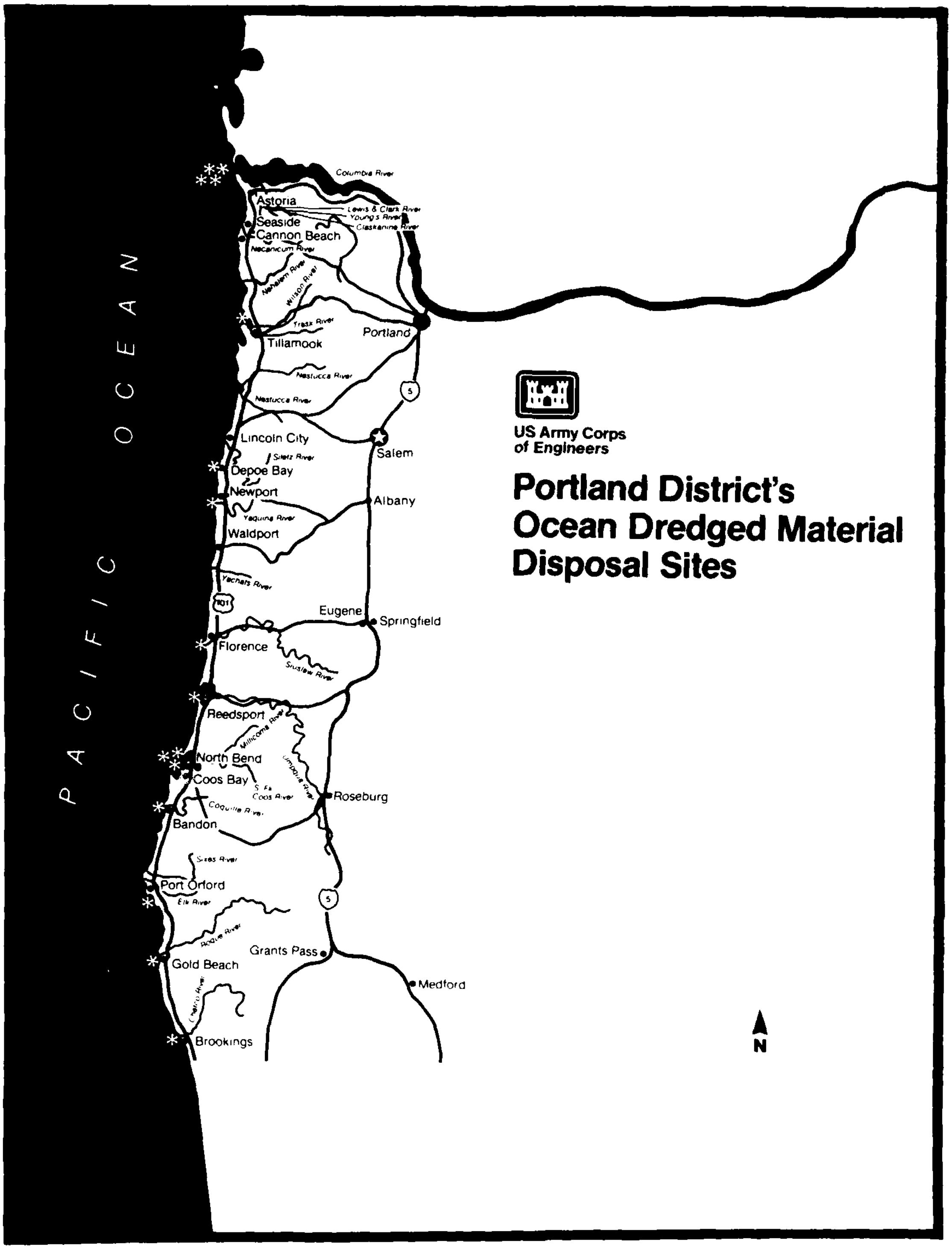
US Army Corps of Engineers
Portland District's Ocean Dredged Material Disposal Sites
PACIFIC OCEAN
Columbia River
Astoria
Lewis & Clark River
Youngs River
Clatskanine River
Seaside
Cannon Beach
Necanicum River
Nehalem River
Wilson River
Trask River
Tillamook
Portland
Nestucca River
Lincoln City
Salem
Siletz River
Depoe Bay
Newport
Albany
Yaquina River
Waldport
Yachats River
101
5
Eugene
Springfield
Florence
Siuslaw River
Reedsport
Millicoma River
North Bend
Coos Bay
Umpqua River
S. Fk. Coos River
Roseburg
Coquille River
Bandon
Sixes River
Port Orford
Elk River
Rogue River
Grants Pass
Medford
Gold Beach
Chetco River
Brookings
N

Figure 2. General Location of Portland District's Ocean Dredged Material Disposal Sites.

Study Schedules

Studies were initiated on 15 May 1984 and are scheduled to be completed by 30 March 1987. Table 2 shows the time frames and major elements necessary to complete the studies. The horizontal divisions on the table correspond to the Phases shown in Figure 1. The evaluation studies will be considered complete when a site has been determined to be in the best environmental and economic location and either a request for final site designation is made to EPA or the Corps utilizes its Section 103 authorities and designates the site.

Experience at Yaquina Bay, Oregon (USACE 1984) and Coos Bay, Oregon (Sollitt et al. 1984) and literature surveys conducted for each of the eight sites demonstrated a need for additional field data. Side-scan sonar, subbottom profiling and topographic considerations, benthic and fishery surveys, and physical oceanography (waves, currents, and sediment transport) were contracted to universities, Federal agencies, and private firms. An example of some results received to date and a typical sampling scheme are shown in Figure 3. Side-scan sonar, subbottom profiles and bathymetric surveys are completed. Current information and sediment transport analyses are being completed now at Oregon State University. Figure 3 also shows a typical benthic sampling scheme recently accomplished at the eight areas for two seasons, winter and summer. This was necessary because of near shore seasonal current reversals off the Oregon coast and to characterize the times of the year a hopper dredge could dispose of dredged material. The sample collection was done by the National Marine Fisheries Service, Hammond, Oregon, Laboratory. Benthic species abundance, composition, and diversity are being accomplished for each site. Otter trawls and underwater video recordings are also being analyzed to compliment box cores collected for the benthic work. Five replicate box cores were taken at each station so statistical comparisons can be made between the interim disposal site and surrounding areas. The remaining study elements listed in Table 1 are being accomplished in-house by literature review and interviews. When combined with new data collection efforts discussed above, there will be sufficient information to address requirements of 40 CFR 228.5 and 228.6.

Management Decisions

Each site will be evaluated by the interdisciplinary team for all action items listed in Table 1. Each discipline's information will be overlaid on a base map of the area under consideration and determinations made as to the most environmentally acceptable and operationally efficient disposal site. This decision will be made by using the above-mentioned overlay technique fully described by Pequegnat (1984). The best location at each site will be determined and then the final size and shape will be considered.

A centroid and radius will be recommended for the configuration of the disposal sites because of the concentric shape dredged material assumes after dumping and the availability of any compass reading to the dredge captain for steaming into seas.

TABLE 1

GENERIC OCEAN DISPOSAL SITE DESIGNATION SEQUENCE AND CHECK LIST

Factors Considered as per 40 CFR 228.5-228.6	**C Tillamook**	**A/D Depoe Bay**	**B Siuslaw**	**B Umpqua**	**B Coquille**	**A/D Port Orford**	**B Rogue River**	**B Chetco**
Topography	C	C	C	C	C	C	C	C
Phys/Chemical -	I	C	C	C	C	C	C	C
Sed. Compatibility	I	C	C	C	C	C	C	C
Past Disp. Influences	I	I	I	I	I	I	I	I
Resources of -	I	I	I	I	I	I	I	I
Limited District	I	I	I	I	I	I	I	I
Commer/Rec Fisheries	I	I	I	I	I	I	I	I
Breeding/Spawn areas	I	I	I	I	I	I	I	I
Nursery Areas	I	I	I	I	I	I	I	I
Feeding Areas	I	I	I	I	I	I	I	I
Migration Routes	I	I	I	I	I	I	I	I
Critical Habitats	C	C	C	C	C	C	C	C
Benthic Dist.	I	I	I	I	I	I	I	I
Marine Mammals	I	I	I	I	I	I	I	I
Mineral Deposits	I	I	I	I	I	I	I	I
Nav. Hazard	O	O	O	O	O	O	O	O
Other uses of Ocean -	O	O	O	O	O	O	O	O
Degraded Areas	O	O	O	O	O	O	O	O
Water Quality	C	C	C	C	C	C	C	C
Recreational Uses	I	I	I	I	I	I	I	I
Cultural/Historic Sites	I	I	I	I	I	I	I	I
Physical Oceanography	I*	I*	I*	I*	I*	I*	I*	I*
Sediment Transport	I*	I*	I*	I*	I*	I*	I*	I*
Potential for Monitoring	O	O	O	O	O	O	O	O
Shape/Size	O	O	O	O	O	O	O	O
Buffer Zone	O	O	O	O	O	O	O	O
Cumulative Effects	O	O	O	O	O	O	O	O

Potential designation action at each site
A = as is
B = consider move or change
C = more study
D = cancel site

Legend
I = In Progress
C = Compiled
O = Not Compiled

* Additional field studies may be required

TABLE 2

GENERIC OCEAN DISPOSAL SITE DESIGNATION SCHEDULE

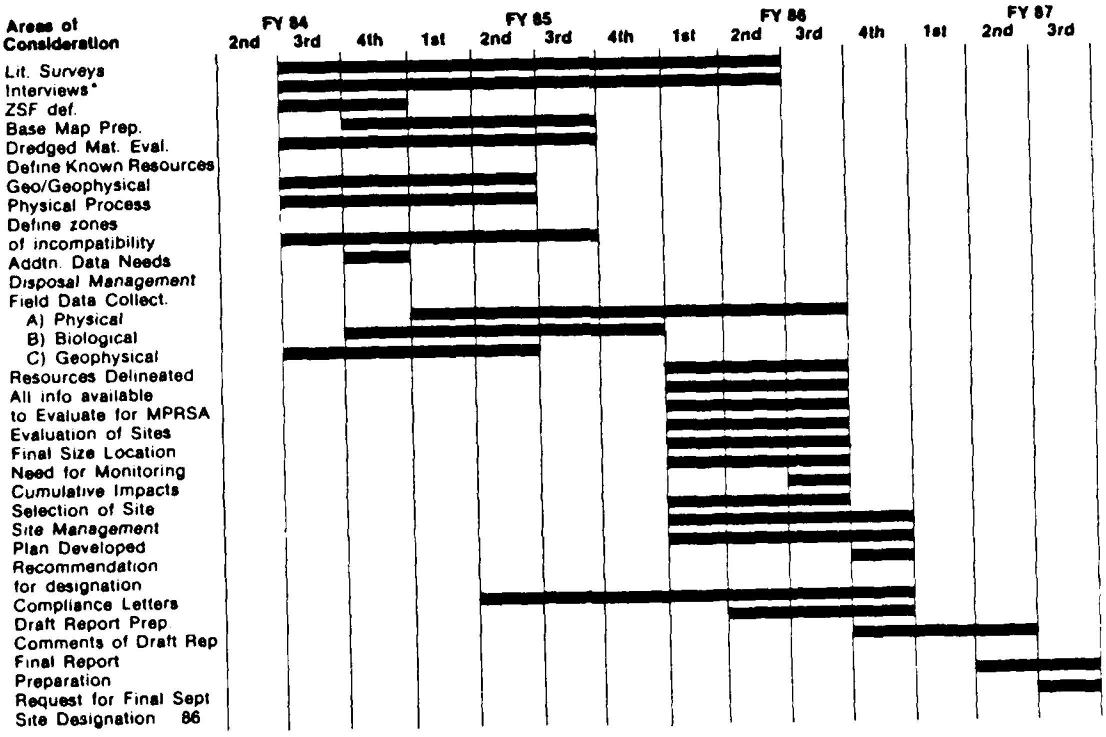

* Formal contracts with user groups still to be made

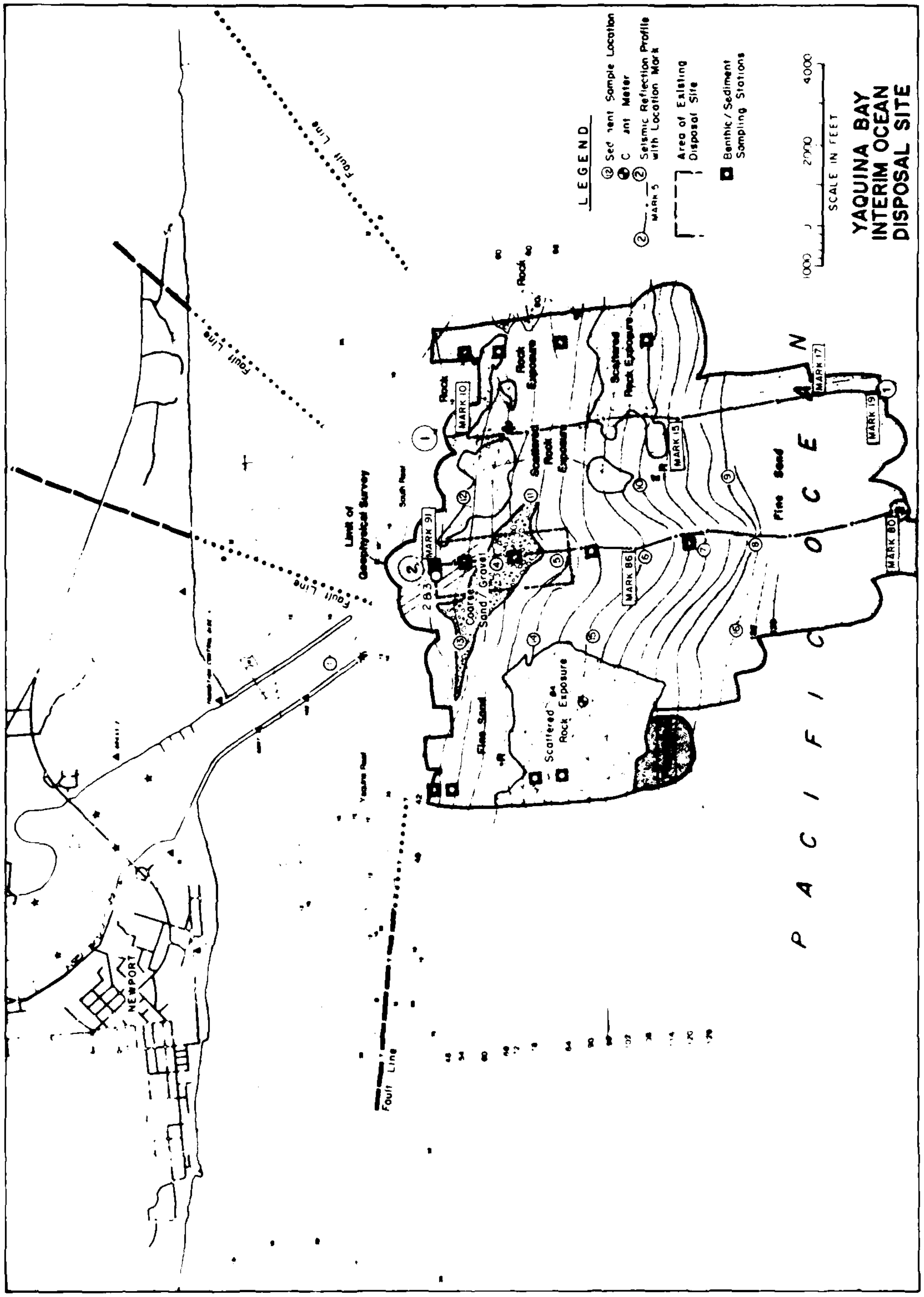
LEGEND
Sediment Sample Location
Current Meter
Seismic Reflection Profile with Location Mark
MARK 5
Area of Existing Disposal Site
Benthic / Sediment Sampling Stations
1000
2000
4000
SCALE IN FEET
YAQUINA BAY
INTERIM OCEAN
DISPOSAL SITE
PACIFIC OCEAN
NEWPORT
Fault Line
Fault Line
Fault Line
Fault Line
Limit of Geophysical Survey
South Reef
Yaquina Reef
MARK 10
MARK 15
MARK 17
MARK 19
MARK 80
MARK 86
MARK 91
Rock
Rock Exposure
Scattered Rock Exposure
Scattered Rock Exposure
Scattered Rock Exposure
Coarse Sand / Gravel
Fine Sand
Fine Sand

Figure 3. Example of Results of Topographic Studies and a Typical Sampling Scheme for Generic Ocean Disposal Site Studies.

Finally, a Site Management Plan will be prepared for the disposal site. This plan will include a monitoring plan, if needed, and any restrictions for the use of the area.

Coordination

Prior to the preparation of the draft report for each of the eight areas, the findings of the Corps will be presented to affected publics and interested resource agencies. This will be done in a series of workshops conducted in the vicinity of each disposal site. Recommendations and comments received at these workshops will be considered in the draft siting evaluation report.

One of the most useful tools developed by the team for evaluating the sites, a conflict matrix, is shown in Table 3. The matrix allows comments on the 27 areas of consideration to be evaluated and displayed. This demonstrates to the public and concerned agencies that these comments are being considered.

The report will be prepared in draft form and submitted for review to workshop participants and any other groups requesting it. The draft report will also be used to request compliance letters from the following agencies responsible for the listed laws:

o Endangered Species Act of 1973, as amended	U.S. Fish & Wildlife Service National Marine Fisheries Service
o National Historical Preservation Act of 1966, as amended	State Historic Preservation Officer
o Coastal Zone Management Act of 1972, as amended	Oregon Department of Land Conservation and Development

All comments and coordination letters received will be incorporated into the final evaluation report and used for the final designation of the interim sites.

Conclusions

Table 1 shows progress to date on each of the 27 areas of consideration that must be evaluated. Also shown is the potential designation action at each site. Studies to date are demonstrating that changes are needed in the location or size and shape of the majority of the sites. The offshore geology and sediment make-up are proving to be much more diverse than originally suspected. None of the anticipated changes are expected to substantially alter the day-to-day operations or economics of the federal project involved. They will make the site either more environmentally compatible or operationally efficient or both with the surrounding area. Upon completion of the designation process, all eight sites will have been evaluated and designated much more efficiently than was possible for previous designations, done prior to the joint EPA/Corps workbook. This is a result of building on findings from past studies and a recognition that existing information and expert knowledge can in some cases be used in place of long-term expensive field efforts to meet the letter and intent of federal regulations.

Table 3
Example of Conflict Matrix for Generic Ocean Disposal Studies

AREA OF CONSIDERATION	CONFLICT	POTENTIAL CONFLICT	NO CONFLICT	BENEFICIAL USE	COMMENTS	RELEVANT SPECIFIC FACTOR (FROM TABLE 1)	RELEVANT GENERAL CRITERIA (FROM TABLE [illegible])
1. Coastal Topography			X			1, 6, 8, 11	a
2. Physical Sediment Compatibility		X			Silty material incompatible, no conflict with sands, however	3, 4, 9	b, [illegible] d
3. Chemical Sediment Compatibility		X			Silty material incompatible, no conflict with sands, however	3, 4, 7, 9	a, b, [illegible] d
4. Influence of Past Disposal			X			5, 7, 9, 10	a, b, d
5. Living Resources of Limited Distribution		X			Site-specific benthic community descriptions needed.	2, 3, 6, 8, [illegible]	a, b, d
6. Commercial Fisheries		X			Substantial trawling and crabbing occur throughout; crabbing mostly in spring and summer	2, 8	a, b
7. Recreational Fisheries		X			Salmon trolling throughout during July-Sept. (seasons determined yearly).	2, 8	a, b
8. Breeding/Spawning Areas		X			Razor clam recruitment areas may exist	2, 8	a, b
9. Nursery Areas		X			Nurseries may occur throughout for Dungeness crab, squid, and flatfish	2, 8	a, b
10. Feeding Areas			X			2, 8	a, b
11. Migration Routes			X			2, 8	a, b
12. Critical Habitats of Threatened or Endangered Species			X			2, 8	a, b
13. Spatial Distribution of Benthos			X			2, 8, 10	a, b
14. Marine Mammals			X			2, 8	a, b
15. Mineral Deposits		X			Coincides with Black Sands mining area	1, 8	a, b, e
16. Navigation Hazard		X			Same as Area K. Also, dredges must bear N-NE from MCR, broadside to waves, to reach area.	1, 8	a, b, d
17. Other Uses of Ocean (cables, pipelines, etc.)		X			Same as Area K. However, collision potential exists with Black Sands mining operation, which includes anchored barge with submerged pipeline in immediate area.	8	a, b, d
18. Degraded Areas			X			4, 6, 7	a, b, d
19. Water Column Chem./Phys. Characteristics			X			4, 6, 9	a, b, d
20. Recreational Uses			X			2, 8, 11	a, b, [illegible] d
21. Cultural/Historical Sites		X			Entire area has higher probability of encountering shipwrecks than deeper areas. Site specific surveys needed.	11	b
22. Physical Oceanography (Waves, Circulation)		X			Potential shoreline/erosion effects of waves refracted by disposal mounds	[illegible], 3, 6, [illegible]	a, b, d
23. Direction of Transport & Potential for Resettlement				X	Assuming sand disposal, beach nourishment potential for Long Beach peninsula. Also, potential to fill excavation of Black Sands mining operation and return to bottom to natural condition.	[illegible], 3, 6, [illegible]	a, b, d
24. Monitoring			X			5	
25. [illegible]					Cannot evaluate; sites not yet specified	1, 4, 7	d
26. Site Buffer Zone			X		Area is 3 nmi from wheat ship wreck, no impact expected	2, 3, 4, 7, 11	b, d
27. Potential for Cumulative Effects			X			4, 7	[illegible], d

References

1. Chesser, S. A., and J. R. Reese. 1984. Implementation of EPA/Corps Site Evaluation Guidance. In: Dredging and Dredged Material Disposal, Vol. 2, pp. 964-972. Proceedings of the Conference Dredging '84. American Society of Civil Engineers.

2. Chesser, S. A. (In press). Monitoring Sediment Transport at Ocean Disposal Sites. Proceedings of the West Coast Regional Coastal Design Workshop 1985. American Society of Civil Engineers.

3. Pequegnat, W. E. 1984. Specifications of a Model Ocean Disposal Site for Dredged Material. In: Management of Bottom Sediments Containing Toxic Substances, pp. 167-183. Proceedings of the 8th US/Japan Experts Meeting. U.S. Army Corps of Engineers Water Resources Support Center.

4. Sollitt, C. K., D. R. Hancock and P. O. Nelson. 1984. Coos Bay Offshore Disposal Site Investigation Final Report Phases IV, V, July 1981-September 1983. U.S. Army Corps of Engineers, Portland District, Portland, Oregon, for Contract No. DACW57-79-C-0040, Oregon State University, Corvallis, Oregon.

5. U.S. Environmental Protection Agency and U.S. Army Corps of Engineers. 1984. General Approach to Designation Studies for Ocean Dredged Material Disposal Sites. U.S. Corps of Engineers Waterways Experiment Station, Vicksburg, Mississippi.

6. U.S. Army Corps of Engineers. 1985. Yaquina Bay Interim Ocean Dredged Material Disposal Site Evaluation Study. U.S. Army Corps of Engineers, Portland District, Portland, Oregon.

Monitoring Sediment Transport at Ocean Disposal Sites

Stephan A. Chesser*

Abstract

Portland District is evaluating eight interim ocean disposal sites for permanent designation. The objective is to provide for continued maintenance of federal navigation projects along the Oregon coast. An important aspect of the site evaluation process is determining whether or not the sites are operationally and environmentally appropriate. There is also a requirement for a long-term monitoring plan for off-site impacts from disposal. Portland District is acquiring baseline sediment and oceanographic data at these sites and attempting to evaluate new approaches in data acquisition and sediment transport monitoring.

Most of the ocean disposal sites in Oregon are in less than 100 feet of water within 1 mile of an estuary entrance. Ocean bottom and sub-bottom characteristics were mapped by geophysical methods within a 2 mile radius around the entrance. Basic wave and current records were acquired at the sites for typical winter and summer conditions. This data will be used to develop a model of bottom currents related to more easily obtainable wave, wind, and tide data. This will allow an approximation of bottom currents from such data. The importance of nearshore wave data has led the District to evaluate the use of land-based seismometry to record nearshore wave height and period. The District is also evaluating the use of natural sediment tracers for use in monitoring and model verification.

Introduction

Part of the Corps responsibility on the Oregon coast involves the structures and maintenance associated with 12 estuary entrances stretching 350 miles from Astoria to Brookings (Fig. 1). There are entrance jetties at 11 projects. There are 9 coastal entrances that require routine dredging with ocean disposal of material dredged from the entrance and upstream channel. Maintenance of safe navigation has required periodic dredging despite structural control by dikes and jetties. Dredging has historically been done by Corps hopper dredges working between April and October. Maintaining authorized channel depths requires balancing dredging requirements with constraints imposed by dredge availability at all projects, equipment capability and technology, severe weather and distance between dredging and disposal sites. Portland District has addressed the constraints of

*Oceanographer, Portland District, Corps of Engineers, PO Box 2946, Portland, Oregon, 97208-2946.

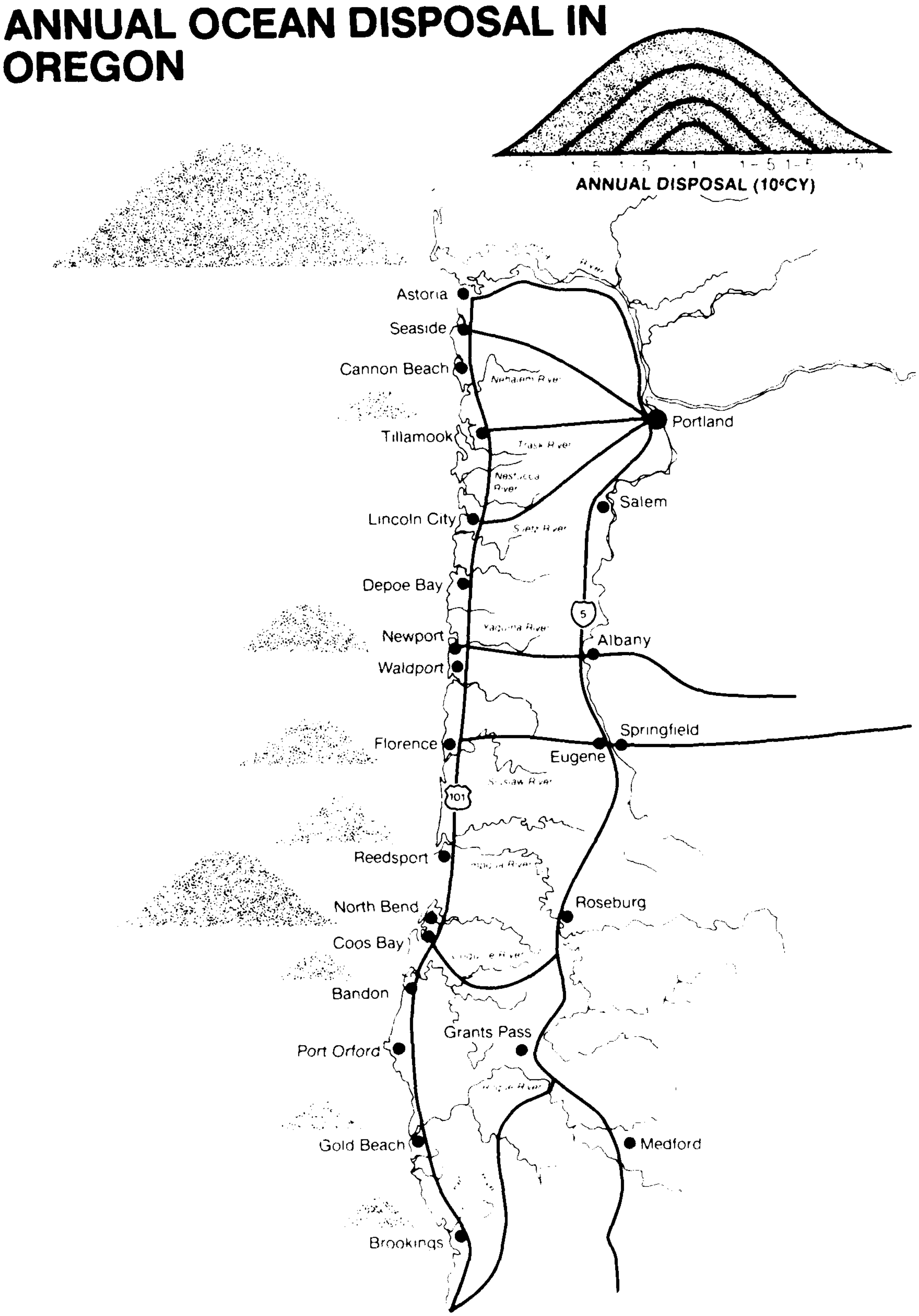
ANNUAL OCEAN DISPOSAL IN OREGON
ANNUAL DISPOSAL (10^{6}CY)
Astoria
Seaside
Cannon Beach
Nehalem River
Portland
Tillamook
Trask River
Nestucca River
Salem
Lincoln City
Siletz River
Depoe Bay
5
Yaquina River
Newport
Albany
Waldport
Springfield
Florence
Eugene
Siuslaw River
101
Reedsport
Umpqua River
Roseburg
North Bend
Coos Bay
Coquille River
Bandon
Grants Pass
Port Orford
Rogue River
Gold Beach
Medford
Brookings

Figure 1. Coastal Dredging in Oregon.

TABLE 1. PORTLAND DISTRICT OCEAN DISPOSAL SITES

Project	Sites	Depth Range (ft.)	Distance To Channel (ft.)	Area (ac.)	Grain Size Channel (mm)	Grain Size Ocean (mm)	1974 - 1985 Ocean Disposal Volumes Ave. (cu. yds. x 1000)	Min.	Max.
Columbia River	A	50-80	4,500	230	.18	.15	1,101.0	2.6	4,063.0
Columbia River	B	80-140	12,000	230			754.8	16.2	3,897.1
Columbia River	E	40-60	1,200	92			2,827.8	606.2	4,936.1
Columbia River	F	130-140	11,000	92			5.3	7.8	45.4
Columbia River	G	70-100	10,000	230			58.2	581.6	581.6
Columbia River	(All)						(4,747.1)	(1,214.4)	(13,523.2)
Tillamook Bay		60-120	5,000	116	.3	.2	3.9	39.4	39.4
Depoe Bay		80-90	5,500	28	.2	.16	427.5	81.1	670.7
Yaquina Bay		40-70	2,300	116	.22	.16	241.9	97.0	459.4
Siuslaw River		50-90	3,300	62	.2	.3	227.7	91.1	470.0
Umpqua River		60-110	3,000	116	.2	.3	227.7	91.1	470.0
Coos Bay	E	50-60	5,500	116	.3	.25	627.5	207.3	1,120.0
Coos Bay	F	60-70	6,000	116			502.9	104.7	1,161.8
Coos Bay	H	180-210	16,500	120			5.6	55.6	55.6
Coos Bay	(All)						(1,181.0)	(367.6)	(2,337.4)
Coquille River		40-90	3,500	116	.4		53.2	2.5	101.4
Port Orford		40-60	1,500	29			15.4	153.6	153.6
Rogue River		50-90	6,200	116	.5	.15	38.6	24.3	142.3
Chetco River		40-60	4,200	74	.7	.17	52.2	7.8	76.3
ALL							6,988.5	2,078.8	17,973.7

dredge availability, capability, and technology over the last decade. Study of the remaining factors of weather and siting will improve coastal operations.

Historically the entrance channel dredged material has been taken to ocean disposal sites. Most of the ocean disposal sites are in less than 100 feet of water within 1 mile of an estuary entrance. Waves and other forces cause extensive reworking of beach and nearshore sand which contributes to the channel shoaling at these projects. Each year 7-10 million cubic yards of material, mostly sand, are dredged to maintain authorized channel depths at these coastal projects (Table 1). In most cases this dredging is done by hopper dredge with disposal at a nearby ocean disposal site. The location of disposal sites is determined by a balance of efficient haul distance and environmental effects. One issue recognized early by Portland District was the advantage of keeping the dredged sand in the littoral system for beach nourishment (USACE, 1973). The dredged material and native sediment are very similar in most cases, being clean, fine grained sand. Disposal of dissimilar material such as organic mud has been tried and may be more frequent in the future. Where and how fast this finer material will be transported has to be determined before an acceptable ocean disposal site can be chosen. Recent changes in entrance structures and dredging technology may also affect location of disposal sites.

Site Evaluation

A discussion of the ocean disposal site evaluation process is presented elsewhere (Reese, in press). Basic to site evaluation is a knowledge of the biophysical setting and physical processes. Little specific data on biology, geology, sediment, waves and currents exists for the individual disposal sites. Previous studies suggested that a minimal field data acquisition program was necessary. Concurrent studies were begun to characterize the disposal sites and surrounding areas. Studies relating to sediment transport included a geologic/ geophysical survey of each site, wave and current monitoring, evaluation of a land-based seismic wave recorder, and evaluating the use of natural sediment tracers in dredged material.

In the summer of 1984 nine ocean disposal sites were surveyed by sidescan sonar and sub-bottom profiler within a 2-mile radius of the entrance channel (Earth Sciences Associates and GeoRecon, 1985). The coastline of Oregon consists of a series of resistant headlands with beaches of varying length between them and frequent occurences of offshore stacks and rocks. Only two of the nine projects studied do not have an adjacent rocky headland or nearshore rock reefs. Sub-bottom profiles reveal that the nearshore sediment layer is thin and discontinuous at Yaquina and from Coos Bay south. Figure 2 illustrates the geology and structure of the nearshore at Yaquina Bay, which is fairly typical of all the sites surveyed. Sediments sampled in and near all the disposal sites are similar, ranging from .12 to .25 mm mean diameter. This is commonly finer than the adjacent beach or river sand.

During 1985 six ocean disposal sites were monitored for waves and

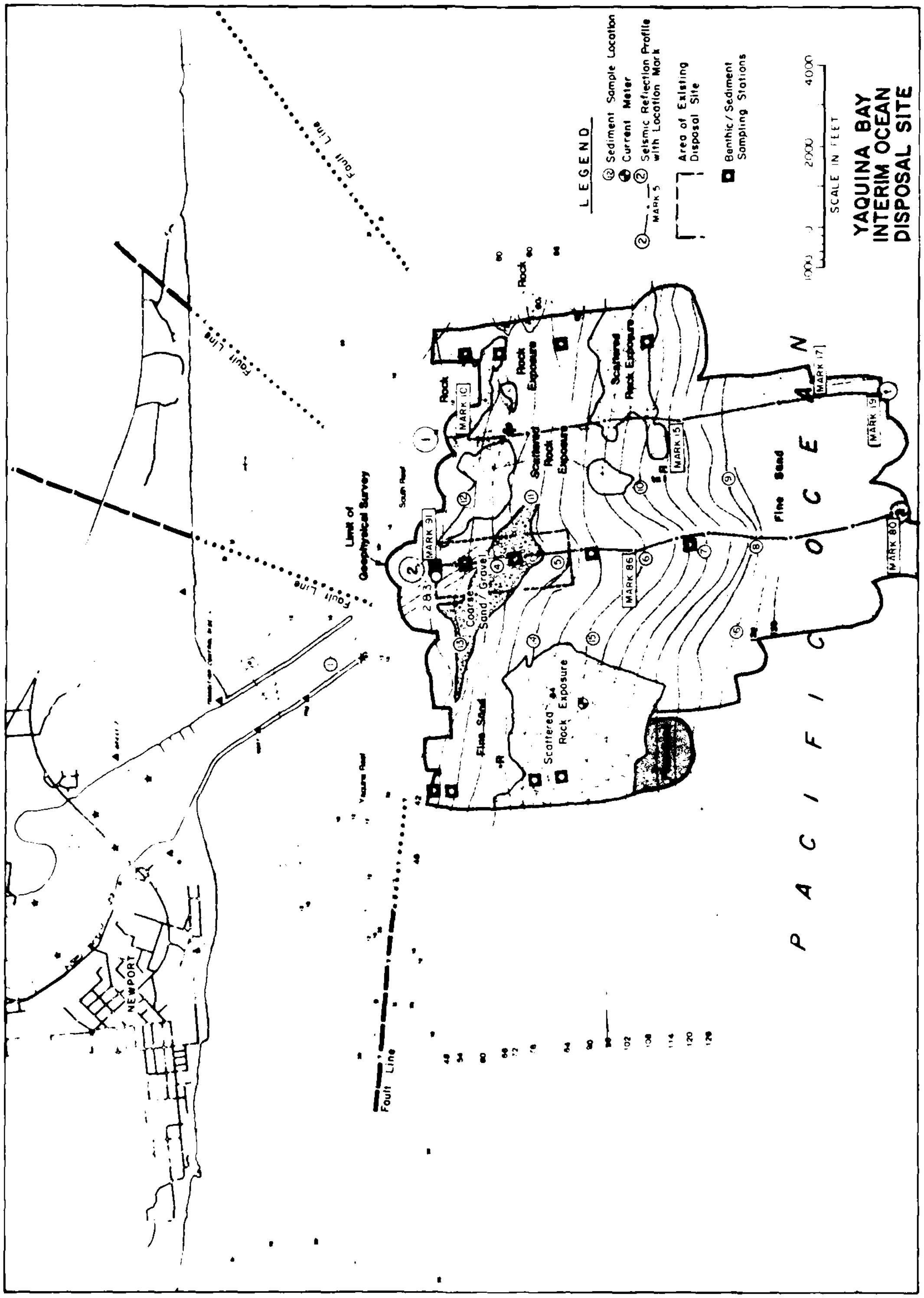
LEGEND
Sediment Sample Location
Current Meter
Seismic Reflection Profile with Location Mark
MARK 5
Area of Existing Disposal Site
Benthic / Sediment Sampling Stations
SCALE IN FEET
2000
4000
YAQUINA BAY
INTERIM OCEAN
DISPOSAL SITE
PACIFIC OCEAN
Fault Line
Fault Line
Fault Line
Fault Line
NEWPORT
Limit of Geophysical Survey
South Reef
Yaquina Reef
Rock
Rock
Rock Exposure
Scattered Rock Exposure
Scattered Rock Exposure
Scattered Rock Exposure
Coarse Sand / Gravel
Fine Sand
Fine Sand
MARK 91
MARK 86
MARK 80
MARK 15
MARK 17
MARK 19
MARK 1C

Figure 2. Nearshore Geology at Newport, Oregon (from Earth Sciences Associates/GeoRecon 1985).

bottom currents during a winter storm period and during a summer swell period. The instrumentation and techniques are described more fully in Hancock et al. (1984). The physical processes affecting sediment movement along the Oregon coast include regional currents, ocean waves, local winds, and tides. Our picture of the littoral system along the Oregon coast is seasonal, with regional currents and weather patterns driving the system. During the winter the waves are strongly from the southwest with winds from the south or southeast. This combines with the Davidson current flowing northward to produce a net northward transport. A transitional period occurs from March to May, with waves and wind coming more nearly out of the west. This results in no predominant transport direction. During the summer both waves and wind are strongly from the northwest and periodic upwelling events occur. Combined with the south flowing California current this produces net southward transport. Komar (1976) and others have desribed the seasonal change in beach and nearshore profiles. In Komar's model, the winter profile reflects offshore transport of material, while there is onshore transport in the summer. Figure 3 illustrates the general concept of the nearshore sediment transport system along the Oregon coast related to this seasonal picture. The two major features are the seasonal alongshore flow reversal and the onshore-offshore transport.

In the site evaluation process it was recognized that not enough data could be collected to adequately characterize the dynamic nearshore sediment transport processes. It was also recognized that the hydrodynamic models available were useless without adequate data to adjust the empirical constants. The approach decided upon was to attempt to use limited wave and current records to correlate with longer term records more readily available to develop a model of sand transport. Nearshore wave data is a critical need. In the Pacific Northwest the geography and climate present serious problems for conventional wave data collection. In 1971 Oregon State University developed a system using a land-based seismometer to record ocean wave generated microseisms. By calibrating the seismic signal with actual wave measurements, an estimate of nearshore wave height and period can be obtained. The usefulness and reliability of such data led OSU to install seismic wavemeters at Coast Guard station at Humboldt Bay, Chetco River, Coos Bay, Yaquina Bay, Columbia River, Grays Harbor and Quillayute. The fact that such a system was available at so many sites and the need for site specific wave data led the Portland District to have the Coastal Engineering Research Center (CERC) evaluate the wavemeter concept and correlate wavemeter records with other wave data. The first location evaluated was at Yaquina Bay. Detailed results of this study are being published by CERC (Thompson, et al., in press). In brief, the study found that the theory of microseism generation was valid and that seismic records correlated well with nearshore wave data. In fact, the wave height correlation was 98% and the wave period correlation was 77-80%. CERC suggested that further analysis of the OSU system could lead to improvements in the wave period correlation and method of data recording and analysis. Portland District is pursuing the suggested improvements at the Chetco wavemeter. Correlations will be made with nearshore wave data at Chetco and with wave data from the Scripps gage near Coquille. The previous study showed good correlation between Yaquina and Coquille for winter wave conditions despite the distance. CERC will analyze the

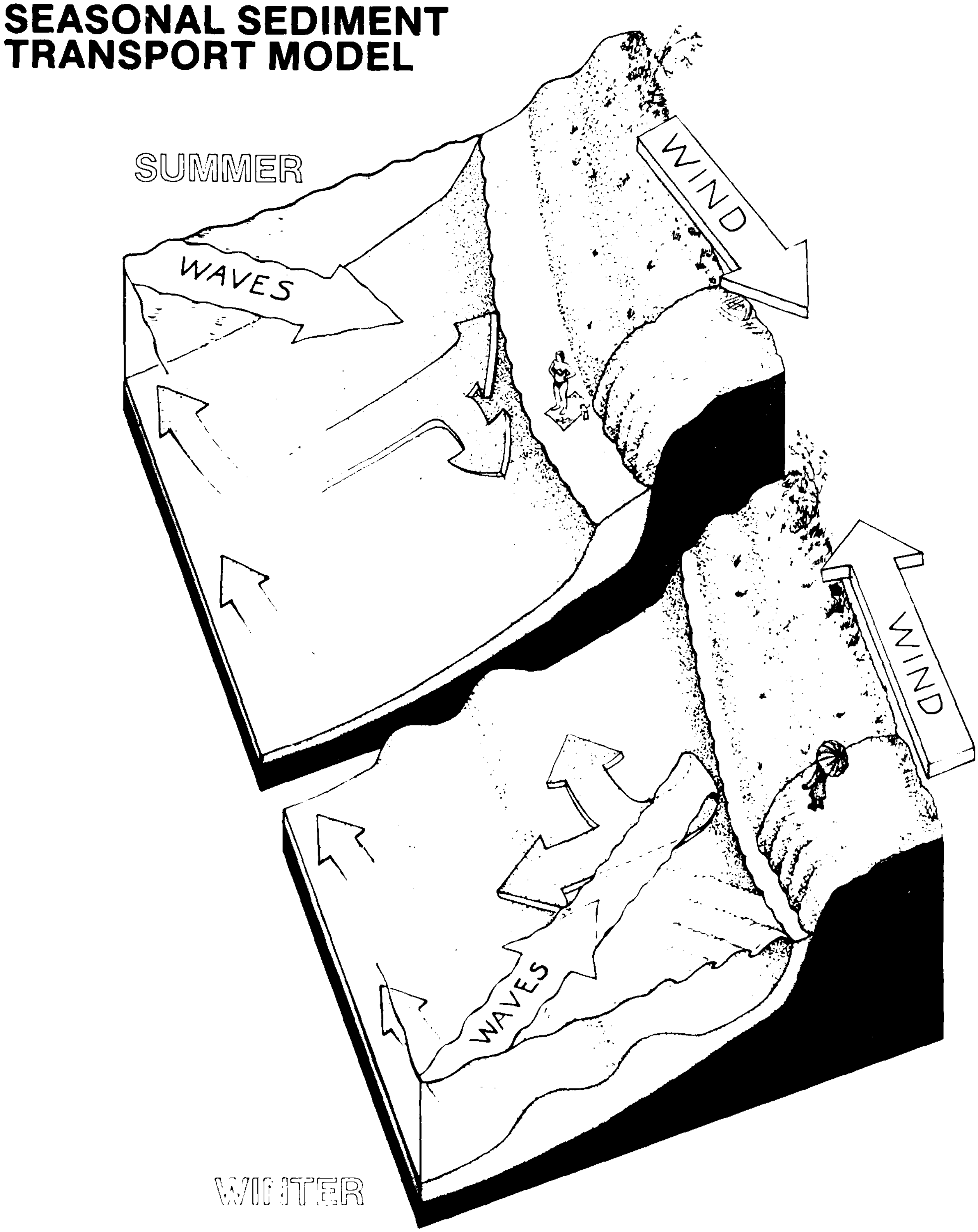
SEASONAL SEDIMENT TRANSPORT MODEL
SUMMER
WAVES
WIND
WIND
WAVES
WINTER

Figure 3. Seasonal Sediment Transport Along the Oregon Coast.

wavemeter data to both calibrate the Chetco site and implement the system improvements. While directional data is not obtained with this system, there are many applications for low cost, accurate, reliable real time nearshore wave climate data. Both the National Weather Service and the Coast Guard believe the system can provide badly needed, cost effective wave data.

Portland District is also investigating the feasibility of using natural sediment characteristics to trace the movement of dredged material at ocean disposal sites. Part of the site evaluation process requires addressing off-site impacts of dredged material. A long term monitoring plan is required where such movements may adversely affect adjacent resources such as commercial shellfish beds. Such long term monitoring is prohibitively difficult and expensive along the Oregon coast. Use of a sediment transport prediction technique may give an order of magnitude estimate of the rate and direction of movement. However, some verification of such prediction is desirable. Previous studies along the Oregon Coast have found a mineral distinction between estuarine river sands and adjacent beach or ocean sands. This technique was used to distinguish marine sand intrusion into estuaries (Kulm and Byrne, 1966), and was used in tracing movement of littoral sand in the ocean during the past 18,000 years (Scheidegger et al., 1971). Preliminary results at Coos Bay (Peterson, 1985) indicate this technique can discriminate shelf sands from estuarine river sands and beach sands. This suggests a way to trace the movement of dredged estuarine sand at ocean disposal sites.

Modelling Sediment Transport

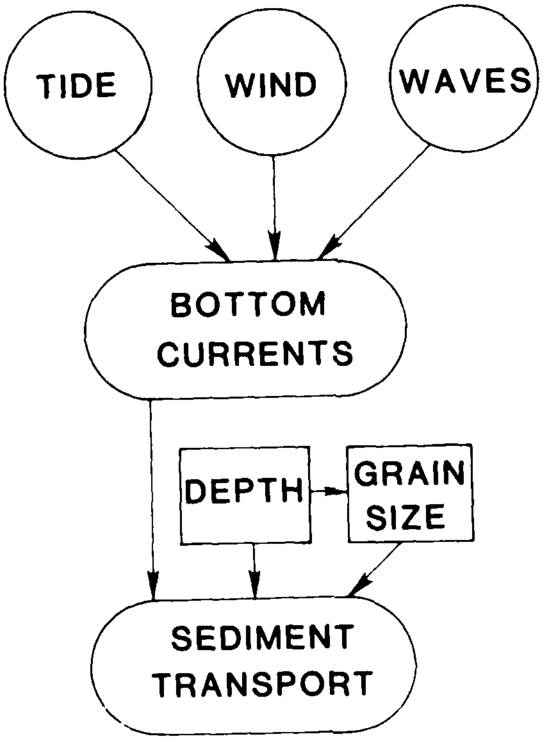

Figure 4. Sediment Transport Model

Figure 4 represents a simple process-response model for sediment transport at the ocean disposal sites being studied. The components of the bottom current responsible for eroding and transporting sediments are simplified into tidal, wind, and wave velocities. This was done previously in the Columbia River by Sternberg et al., 1977, who showed good correlations between the bottom current and recorded winds and tides. Sediment transport is shown to be related to currents, grain size and water depth. There are actually two models to define. The current model depends upon accurately correlating the observed current components with the forces assumed to be driving them. The other model for sediment transport must contain both alongshore and onshore-offshore components, each dependent upon grain size and water depth. Numerous hydrodynamic models are applicable if the time-varying nature of the velocity forces are incorporated.

It is recognized that a combination of wave-induced instantaneous velocities and directional mean bottom currents are important in the movement of sediment in the nearshore region. Seismic wavemeter records since 1971 at Newport show that significant wave height and period average 8 feet and 13 seconds in winter, with summer waves averaging 4 feet and 8 seconds (Creech, 1981). Bourke et al (1971) and others have shown that the depth of motion for fine sand by wave action is related to wave period and height. For average wave conditions the depth of motion can be over 50 feet in summer and over 120 feet in winter. Thus under typical wave conditions there can be frequent movement of bottom sands at each disposal site. Superimposed on this is whatever directional current component exists due to wave direction, tidal ebb and flood, upwelling or regional currents. The relative magnitude of the summer and winter transport may determine whether disposal material returns to the dredged channel. The effective depth of onshore transport in summer may determine whether dredged material remains in the littoral system for down drift beach nourishment. The effects of local factors such as bathymetry, winds and tidal flushing complicate this picture at specific sites. Bottom currents may vary from less than 1 to more than 50 cm/sec with 10-20 cm/sec average. In shallow water local wind generated currents may exceed 30 cm/sec. Tidal currents offshore may exceed 15 cm/sec (Sternberg et al., 1977).

Due to the variability of the factors affecting bottom currents, a short term current record is not adequate to directly characterize the annual mean bottom current and directional bias responsible for net sand transport. Previous studies suggest the possibility of using seasonal wave and current data to develop a correlation model. Such a model would compare observed currents with concurrent wind, wave, and tidal data. Lynch (1982), compared wave heights 300 miles offshore with wave induced currents near Coos Bay. Although direct correlation was poor, the resulting analysis suggests ways of improving the correlation if better wave data is available. Nelson et al., (1984), compared current meter records offshore of Coos Bay with wind and tidal current models. The current at one third water depth correlates best with a wind driven current. The current one meter above the bottom correlated best with a tidal driven current (Figure 5). The dependency of currents on depth and season was also shown.

CORRELATION OF CURRENTS AND TIDAL MODELS OFF COOS BAY

NEAR-BOTTOM CURRENTS

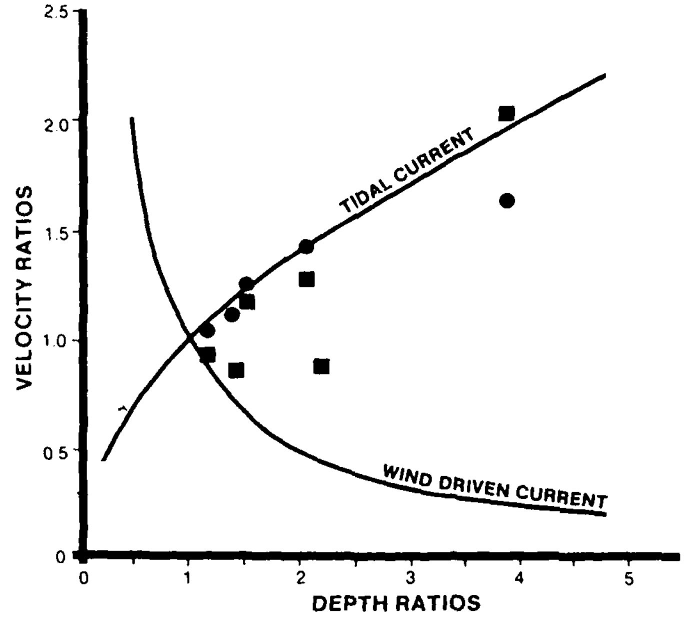

NEAR-SURFACE CURRENTS

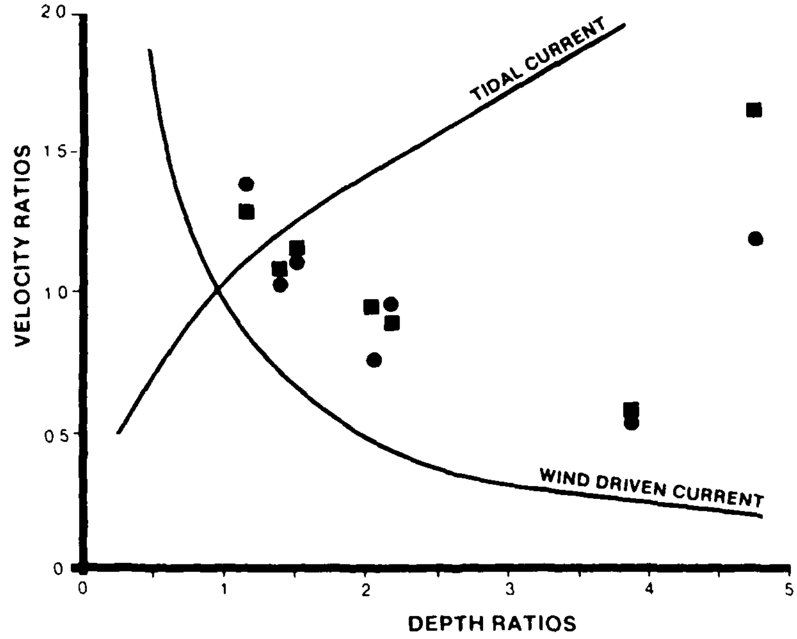

Figure 5. Comparison of Current Meter Records off Coos Bay with Wind and Tidal Current Models. (From Hancock et al. 1984)

One concern in a sediment transport model is to define the depth limit of significant onshore movement. Dredged sand placed deeper will presumably not be available for beach nourishment. Finer silt and clay material needs to be placed deep enough to assure offshore movement predominates. Various researchers have used wave parameters and grain size to define this depth. It is also likely that tidal influences near estuary entrances affect this depth. The seasonal variability of wave climate in the Pacific Northwest must also be taken into account. One approach is to relate depth and grain size to threshold velocity needed for transport. Sternberg, (1972), developed such a procedure to predict sand transport using mean velocity and grain size. This has been applied off the Columbia River (Sternberg et al., 1977). Hancock et al. (1984) used a similar approach off Coos Bay to show the probability of exceeding significant current values related to sand transport.

Conclusions

In many coastal engineering and planning applications a knowledge of sediment transport in the nearshore ocean is necessary. The difficulty and expense of acquiring data to support such understanding along the Oregon coast has led Portland District to attempt innovative approaches. Properly interpreted, a sidescan/seismic survey can be used to characterize relatively large areas of the nearshore region. For local wave climate, a seismic wavemeter was shown to correlate well with actual wave measurements nearby and provides a highly reliable system for real-time wave measurement. Local wave data and related wind and tidal data should theoretically yield an approximation of the forces driving sediment transport. Site specific information and future monitoring should allow this approximation to be progressively refined. This will improve our ability to predict sediment transport as it affects channel shoaling, beach erosion and benthic resources. Use of a natural mineral difference between estuarine river sand and offshore marine sand appears to be useful in monitoring movement of dredged material. This may provide needed verification of sediment transport predictions.

References

1. Bourke, R. H., B. Glenn, and B. W. Adams, 1971. The Nearshore Physical Oceanographic Environment of the Pacific Northwest Coast, Oregon State University, Department of Oceanography, reference 71-45, Corvallis, Oregon.

2. Creech, C., 1981. Nearshore Wave Climatology Yaquina Bay, Oregon. (1971-1980) Oregon State University, Pub. ORESU-T-81-002, Corvallis, Oregon.

3. Earth Sciences Associates and Geo Recon International, 1985. Geologic and Seismic Investigations of Oregon Offshore Dredge Disposal Sites. Report to Portland District, Corps of Engineers, Portland, Oregon, Contract DACW57-84-D-0043.

4. Hancock, D. R., P. O. Nelson, C. K. Sollitt, and K. J. Williamson, 1984. Coos Bay Offshore Disposal Site Investigation. Interim Report, Phase I to Portland District, Corps of Engineers, Portland, Oregon, Contract DACW57-79-C-0040.

5. Komar, P. D., 1976. Beach Processes and Sedimentation. Prentiss-Hall 429 p.

6. Kulm, L. D. and J. V. Byrne, 1966. Sedimentary Response to Hydrography in an Oregon Estuary. Mar. Geol., V. 4, pp. 85-118.

7. Lynch, C. 1982, Statistical Correlations Between Offshore Wave Heights and Nearshore Wave Induced Currents. MS Thesis, Oregon State University, Department of Civil Engineering, Corvallis, Oregon, 124 p.

8. Nelson, P. O., C. K. Sollitt, K. J. Williamson and D. R. Hancock, 1984. Coos Bay Offshore Disposal Site Investigation, Interim Report Phase II, III to Portland District, Corps of Engineers, Portland, Oregon, Contract DACW57-79-C-0040.

9. Peterson, C. D., 1985. Feasibility of Using a Natural Sand Tracer for Establishing Dispersal of Dredged Sand Disposed on the Ocean Shelf: Coos Bay, Oregon. Report to Portland District, Corps of Engineers, Portland, Oregon.

10. Reese, J. R., (in press). Generic Ocean Disposal Studies for the Oregon Coast. Proceedings of the West Coast Regional Coastal Design Workshop, USACE/ASCE.

11. Sheidegger, K. F., L. D. Kulm, and E. J. Runge, 1971. Sediment Sources and Dispersal Patterns of Oregon Continental Shelf Sands. Jour. Sed. Pet. V. 41, N. 4, pp. 1112-1120.

12. Sternberg, R. W., 1972. Predicting Initial Motion and Bedload Transport of Sediment Particles in the Shallow Marine Environment in Shelf Sediment Transport, Swift et al., eds. p. 61-82.

13. Sternberg, R. W., J. S. Creager, W. Glassley and J. Johnson, 1977. Aquatic Disposal Field Investigations Columbia River Disposal Sites, Oregon, Appendix A. DMRP Tech. Report D-77-30, USACE, Waterways Experiment Station, P.O. Box 631, Vicksburg, MS 39180.

14. Thompson, E. F., G. L. Howell, and J. M. McKee, (in press). Evaluation of Seismometer Wave Gage and Comparative Analysis with Wave Data at Yaquina and Coquille Bays, Oregon. Coastal Engineering Research Center Report to Portland District, Corps of Engineers, Portland, Oregon.

15. U.S. Army, Corps of Engineers, 1973. Study of Hopper Dredging Coastal Harbor Entrances and Columbia River Estuary Bars, States of Oregon and Washington. Report by Navigation Division, Portland District, Portland, Oregon, 317 p.

GEOLOGIC AND SEISMIC INVESTIGATIONS OF DREDGE DISPOSAL SITES OFF THE OREGON COAST

N. Timothy Hall,* Richard C. Harding* and John M. Musser, Jr.**

ABSTRACT

Ocean bottom conditions at ten sites off the Oregon coast including the mouth of the Columbia River were investigated by geologic and geophysical means in order to evaluate their suitability for disposal of dredged materials. The study consisted of two major parts: (1) a synthesis of existing geologic, seismic, and oceanographic data pertinent to the offshore study areas, and (2) a geophysical investigation of foundation conditions using sidescan sonar and subbottom acoustic reflection profiling to determine the nature, distribution, thickness, and structure of earth materials at and underlying each of the study areas. The geologic and geophysical data for each area were compiled on a bathymetric base map, each with several cross sections, and preferred sites for the disposal of dredged materials were outlined.

I INTRODUCTION

This paper presents the methodology and some typical results of geologic studies and offshore geophysical surveys of ten proposed or currently used dredged material disposal sites offshore of the Oregon Coast including the mouth of the Columbia River (Figure 1).

A. Purpose of the Investigation

This study was undertaken to provide geologic and geophysical information that will assist the U.S. Army Corps. of Engineers (COE) to evaluate existing and proposed offshore disposal sites and adjacent areas. The study consisted of two major parts: 1) a synthesis of existing geologic and oceanographic data pertinent to each offshore study area and; 2) a geophysical investigation of site foundation conditions using sidescan sonar and sub-bottom acoustic reflection profiling to determine the nature, distribution, thickness, and structure of the earth materials at and underlying each of the study areas. This investigation included no analysis of shoal area sediment or collection of site-specific data on hydrodynamic conditions.

B. General Site Selection Criteria

Based upon a previous COE investigation at Coos Bay, Oregon (Hancock and others, no date; Nelson and others, no date), general environmental guidelines for offshore disposal sites of dredged materials include:

1. Minimizing the physical and chemical differences between the shoal material and the natural in-situ material at the sea disposal site.

---

* Earth Sciences Associates, 701 Welch Road, Palo Alto, CA 94304.
** Geo Recon International, P.O. Box 55189, Seattle, WA 98155.

2. Avoiding impacts on unique and/or valued biological communities or other natural resources.

3. Minimizing the probability of onshore transport of dredged material after placement at the disposal site.

Depending upon the characteristics of the dredged material (texture, cohesiveness, volume, method of dispersal, etc.), nature of the disposal site (depth, bottom and adjacent shoreline topography, tectonic setting vis-a-vis earthquake potential for sediment mobilization, and foundation conditions such as bedrock and unconsolidated sediment characteristics and structure), and prevailing hydrodynamic conditions (magnitude and direction of currents throughout the water column at the time of dispersal and shear stresses at the sea bed throughout the year), the dredged material will remain essentially stationary or will be prone to redistribution. If the dredged material does not move, it may be important for site analysis to estimate the height and rate of growth of disposal mounds. On the other hand, if the dredged material is likely to be remobilized on the sea floor, it is important to predict in which direction(s) it will migrate and at what rates.

C. Scope of the Investigation

In order to provide a partial evaluation of the coastal Oregon and Columbia River mouth sites according to these three criteria, various geophysical and geological investigations to characterize the physical parameters and significant processes operating at each potential disposal site were undertaken. The investigation included the following tasks:

1. Locate, compile, and analyze existing geologic reports and maps and oceanographic studies that contain details of physical conditions within and/or adjacent to the Oregon offshore disposal study areas.

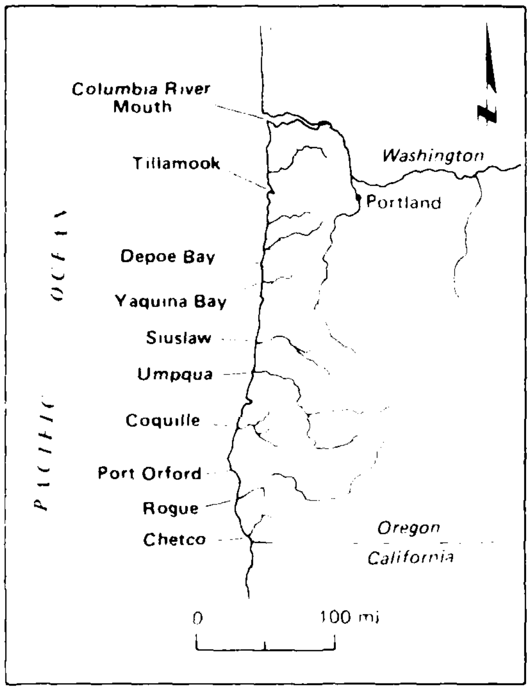
Columbia River Mouth
Tillamook
Washington
Portland
Depoe Bay
Yaquina Bay
Siuslaw
Umpqua
Coquille
Port Orford
Rogue
Chetco
Oregon
California
PACIFIC OCEAN
0
100 mi

Figure 1. Location Map of Oregon Offshore Disposal Sites

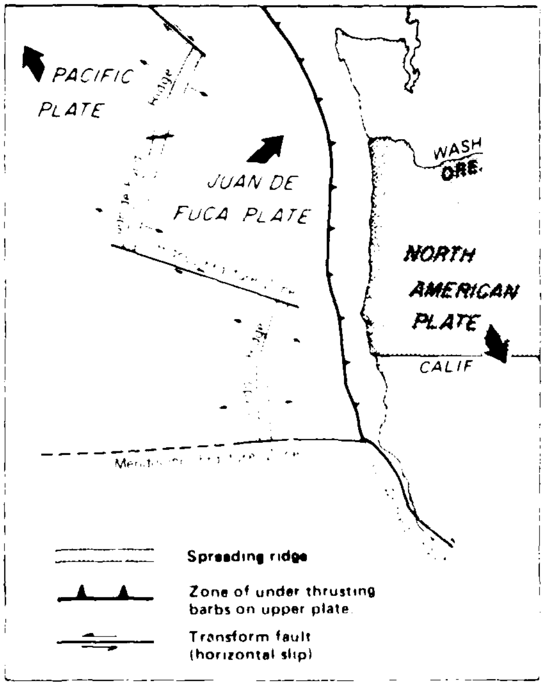
PACIFIC PLATE
JUAN DE FUCA PLATE
WASH
ORE.
NORTH AMERICAN PLATE
CALIF
Spreading ridge
Zone of under thrusting barbs on upper plate
Transform fault (horizontal slip)

Figure 2. Tectonic Setting of the Oregon Coast

2. Prepare preliminary base maps for each study area at a suitable scale indicating all known and/or projected and interpretive geologic information pertaining to ocean bottom and sub-bottom conditions that could possibly affect use of the areas for disposal of dredged materials.

3. Complete and interpret side-scan sonar and sub-bottom seismic reflection surveys for the ten study areas with identifications of all unconsolidated sediment and bedrock materials, sediment thicknesses, and other pertinent geologic conditions.

4. Summarize geologic and geophysical investigative results with a brief report which includes a detailed interpretive plan map and sections for each of the offshore disposal study areas.

Earth Sciences Associates compiled the geologic data and prepared the preliminary base maps, interpretive maps, and report. Geo Recon International, as subcontractor, conducted the offshore geophysical surveys and interpreted the results. The Portland District COE provided topographic base maps, bathymetric data for bottom contours, and survey vessels NORMAN BRAY and HICKSON.

II GEOLOGICAL INVESTIGATION

A. Tectonic Setting of the Oregon Continental Margin

The tectonic evolution of the Oregon coastline appears to be controlled at present by the underthrusting of the Juan de Fuca plate beneath the North American plate (Figure 2). The existence and recent activity of the Cascadian volcanoes provides the most visible evidence for ongoing convergence between the North American and Juan de Fuca plates (Drake, 1982). In addition, sub-bottom marine profiles and borehole data show evidence for crustal convergence in the form of anticlines and synclines near the outer continental shelf and upper continental slope (Byrne and others, 1966; Snavely and others, 1977; and Clarke and others, 1981) and for underthrusting beneath the same region (Snavely and others, 1980; Snavely, 1984).

However, two features typical of convergent plate margins, a well developed Benioff zone (a landward-dipping plane of earthquake hypocenters which marks the descending slab of lithosphere) and an oceanic trench, are absent along the Oregon coast. Coastal earthquakes related to subduction, like the 1964 Alaska event, typically occur when a segment of the overlying plate rebounds elastically after being deformed by an underthrusting oceanic plate. Perhaps because of its relative youth and high temperature, the Juan de Fuca slab produces few brittle failures and therefore generates few deep earthquakes (Atwater, 1970). The absence of a trench might be explained by rapid sedimentation, a slow rate of convergence, or both.

Oregon is not usually considered to be earthquake country. None of the mapped surface faults in the Coast Range are known to be active (Beaulieu and others, 1974). The portion of the circumpacific seismic belt that extends along the west coast of North America appears to bifurcate and pass on either side of Oregon (Barazangi and Dorman, 1969). The average seismic energy released in the Oregon Coast Ranges for the 100-year period from 1870 through 1970 is approximately equivalent to one magnitude 5.0 earthquake (Intensity V) per decade (Couch and Lowell, 1971). Thus, Oregon appears as a relatively quiet "island" within a very active seismic belt (Couch and Lowell, 1971).

Based upon the absence of known active faults onshore, the short length of the two offshore faults of presumed Holocene age mapped by Clarke and others, (1981), and the historical record, most workers have considered it very unlikely that coastal Oregon will be the site of magnitude 7 or greater earthquakes. However, recent work by Heaton and Kanamori (1984) demonstrates that the Juan de Fuca subduction zone shares many features with other subduction zones around the world that have experienced great (M8+) earthquakes. Further research is obviously required to clarify the seismogenic potential of the Oregon coast.

B. Geologic Setting of the Oregon Coast

Coastal Oregon lies within two physiographic provinces, the Klamath Mountains on the south and the Coast Ranges on the north. The Coast Ranges are further divided into northern and southern ranges along the Alsea River (Baldwin, 1964). The Klamath Mountains contain the oldest rocks in western Oregon and consist mostly of folded and faulted rocks of pre-Tertiary age which have been intruded by granitic and serpentinized ultrabasic rocks (Spigai, 1971). The oldest group of rocks, called the "subjacent" sequence by Irwin (1966), were intensely folded and thrust-faulted during the Late Jurassic Nevadan Orogeny. These rocks are unconformably overlain by the "superjacent" rocks of uppermost Late Jurassic or Early Cretaceous age (Irwin, 1966). Middle and Late Cretaceous formations, the latter at Cape Sebastian, cap the Mesozoic sequence of the Klamath Mountains in Oregon, with Cenozoic marine and alluvial formations forming the youngest overlying deposits (Spigai, 1971).

The southern Coast Ranges, which stretch northward from the middle fork of the Coquille River, consist mainly of Eocene sedimentary and volcanic rocks, with younger Mio-Pliocene and Quaternary formations found only near Coos Bay and Cape Blanco (Spigai, 1971). The two most widespread formations within the southern Coast Ranges are the Umpqua Formation (*Early to Middle Miocene*), which consists mainly of interbedded basalt and sandstones with minor siltstone and conglomerate, and the overlying Tyee Formation which is composed mainly of rhythmically bedded micaceous sandstones and siltstones (Spigai, 1971).

The central core of the northern Coast Ranges is made up of thick submarine lava flows, breccias, and tuffaceous sedimentary rock of the Siletz River Volcanics of Eocene age, overlain in the central part by the Tyee sandstone (Baldwin, 1964). The seaward side of the Coast Range contains younger and less continuous Oligo-Miocene formations, some in local embayments such as Yaquina Bay. The Oligo-Miocene rocks wrap around the north end of the range along the Columbia River. Marine Pliocene rock, unknown onshore, is present west of Newport, suggesting that the late Tertiary section may thicken under the continental shelf.

The primary sources of onshore geologic data are the State of Oregon bulletins on the environmental geology of the coastal counties and maps published by the U.S. Geological Survey. The map prepared for each disposal site study area shows the bedrock geology exposed in the adjacent cliffs, headlands and sea stacks. Mesozoic rocks of the Klamath Mountains have been so complexly folded and faulted that it was not possible to project onshore structural data (strikes and dips, faults, etc.) into the study areas located off the southern coast of Oregon. For the lesser deformed strata of Tertiary age in central and northern Oregon, some onshore data have been projected into the offshore disposal sites. All projected data must be considered highly speculative, however, because no onshore geologic mapping was undertaken for this investigation.

C. Submarine Geology of the Oregon Continental Shelf

1. The Continental Shelf Environment

In addition to the large-scale tectonic patterns of converging plates outlined above, glacio-eustatic sea level changes caused by Pleistocene climatic fluctuations have also had a major influence on the geology of Oregon's coastal margin. The Holocene rise in sea level of approximately 400 feet (120m) drowned the river mouths to form large coastal lakes and bays and produced a transgressive sand sheet that is exposed along much of Oregon's inner shelf. Stillstands during this most recent transgression produced submerged terraces or shorelines at various depths which are still exposed on the sea floor as relict features (Spigai, 1971).

Following the stabilization of sea level at approximately its present level for the last 3,000 years, the continental shelf off northern California, Oregon, and Washington developed three distinctive zones: (1) an inner shelf, (2) a central or mid shelf, and (3) an outer shelf. The continental shelf near the Columbia River has an inner shelf on which modern sand accumulates at depths of less than 130 to 200 feet (40-60 m), a mid shelf of 200 to 400 feet (60-120 m) depth on which modern mud—mostly silt--accumulates, and an outer shelf at depths greater than 400 feet (120 m) (Nittrouer and Sternberg, 1981). The inner shelf deposit is the landward and modern portion of the Holocene transgressive sand sheet which unconformably overlies consolidated bedrock (of Tertiary age and older) and which underlies the mid-shelf silt.

The supply of sand to the Oregon shelf comes from the erosion of the shoreline, primarily marine terrace deposits of Pleistocene age, and from rivers. The sand from fluvial sources is limited, however, because of trapping in estuaries (Kulm and others, 1975). The sand that does reach the coastline is subject to seasonal back-and-forth movements between the beach face in summer and offshore bars in winter (Fox and Davis, 1978). Near the Rogue River (and presumably along the entire Oregon coast), offshore sands are much finer-grained than adjacent beach sand. Apparently, the very fine sand and finer particles are removed from the high-energy beach environment and transported through the turbulent surf zone to the shelf (Kulm and others, 1975).

Finer-grained sediments (mud facies) occur largely on the mid shelf and in patches near rivers that have a high discharge. Very fine sand and finer materials are either held in suspension or are resuspended by wave-induced bottom stresses that stir the bottom to depths of at least 410 feet (125 m) and possibly 656 feet (200 m) in winter (Kulm and others, 1975). Wave stirring controls the landward extent of the mud facies, i.e., the mid shelf-inner shelf boundary, off the coast of Oregon.

2. Sediment Transport on the Oregon Shelf

On continental shelves, the most common causes for the initiation of sediment transport are waves and unidirectional bottom currents (Komar, 1976). Although basal shear stresses exerted by waves and currents often act together to affect sediment transport, the direction of transport is usually controlled by currents (Komar, 1976; Grant and Madsen, 1979). Along the Oregon coast the mean surface currents flow southward during the summer and northward during the winter in response to a sloping sea surface caused by offshore and onshore Ekman transport (Hickey, 1979). At the coast, Ekman dynamics cause offshore surface flow and onshore bottom flow (upwelling) during summer, and onshore surface flow and offshore bottom flow (downwelling) during winter. However, both local coastal topography and the submarine topography can significantly alter this general pattern for any given disposal site.

The depth to which significant amounts of sand can be carried offshore has not been established unequivocally. On the basis of heavy mineral distributions in the offshore sands of southern Oregon, Kulm and others (1968) suggest that modern beach sand is generally not transported to water depths greater than about 10 fathoms (18 m). These authors presume that sands lying between the 10-fathom contour and the shoreward edge of the central shelf mud facies at about 40 fathoms (73 m) are relict Holocene transgressive sands deposited during the last rise of sea level. Although these deeper sands may be reworked periodically by shelf bottom currents, they are presumed to be out of equilibrium with their present environment (Kulm and others, 1968). Spigai (1971) also concluded that 10 fathoms is the limiting depth for significant offshore transport of sand. From a detailed investigation of coastal sands north of San Francisco, Cherry (1965) extended this depth somewhat, and concluded that sand on the shelf at greater depths than 15 fathoms (27 m) is essentially stationary.

Other research suggests, however, that sands are currently being transported offshore to depths greater than 27 m. For example, Maloney (1965) traced the distribution of oxidized sand grains from the present Oregon shoreline to the seaward edge of the inner shelf. He interpreted this as evidence for cross-shelf transport of sand related to the present hydraulic regime. The work of Drake and Cacchione (1981) and Cacchione and others (1983) demonstrates that sands on the inner shelf are subject to movements to depths of at least 35 m and probably to 60-70 m. A mathematical analysis by Maloney (1965) indicates that the largest storm waves experienced along the Oregon coast can generate oscillating velocitites on the sea floor capable of eroding fine sand and unconsolidated silt to depths of 328 to 492 feet (100 to 150 m). Kulm and others (1975) report that very fine sand and finer sediment is either held in suspension off the Oregon coast or resuspended by wave-generated bottom currents which stir the shelf to depths of at least 410 feet (125 m) and possibly to 656 feet (200 m) by long-period winter waves.

Due to prevailing northwesterly winds, southerly longshore transport of sand occurs during the summer months, while during the winter, large storm waves approach the coast from the southwest and cause northerly transport. While all writers agree that the direction of longshore transport changes seasonally along the Oregon coast, there is no consensus as to whether there is a net annual northerly or southerly transport of sediment. For example, a final environmental impact statement for the Chetco, Coquille, and Rogue River estuaries prepared by the COE (U.S. Army Eng. Dist., Portland, 1975) reports a net southerly longshore transport on the basis of rapid accretion of sand on the north side of the north jetties. On the other hand, on the basis of heavy mineral studies, Scheidegger and others (1971) and Kulm and others (1968, 1975) have identified a northerly component of drift on the Oregon shelf and beaches and conclude that it is the predominant regional direction of transport. Kulm and others (1975) qualify this conclusion somewhat by reporting that during the last 3,000 years when sea level has been essentially stationary, there has been only a limited northward littoral transport of modern beach sand.

A review of the literature suggests that the following conclusions for sediment transport on the coast of Oregon can be drawn:

1. It appears likely that silt and clay are subject to transport along or across the entire Oregon continental shelf. Net transport of fine-grained sediments typically is to the north or northwest.

2. Large waves and strong currents experienced along the Oregon coast are capable of winnowing fine to very fine sand from the inner shelf and moving it about on the central shelf.

3. Unless mobilized by a seismic event, medium to coarse sands and gravel do not typically move beyond the inner shelf and may be stationary at water depths greater than about 15 fathoms (27 m).

4. Sands in the near shore environment move back and forth between the beach face in summer and offshore bars in the winter. The direction of net littoral transport, if indeed there is any, should be determined from observations at each specific site of interest.

III SUBMARINE GEOPHYSICAL INVESTIGATION

A. Geophysical Mapping of the Offshore Disposal Sites

Offshore mapping consisted of side scan sonar and seismic reflection surveys conducted to reveal the distribution of bedrock outcrops on the sea floor and the configuration of the bedrock-sediment interface along two or more traverses across each of the ten study areas. Survey operations were made from COE survey vessels which made traverses approximately 500 feet (150 m) apart across the study areas. The basic remote sensing tools included a fathometer, side-scan sonograph, and sub-bottom profilers ("Uniboom" and "Bubble Pulser" systems).

Both the side-scan and sub-bottom field data were recorded on paper recorders. In both cases, a sound velocity of 5,000 feet/second for water was assumed for distance and depth calculations. The raw side-scan field data was interpreted and four units, rock, scattered rock exposure, coarse sand/gravel, and sand/silt were plotted on the COE base maps. The sub-bottom data was interpreted and displayed as computer-drawn cross-sections. Two to three representative profiles from each area were selected for interpretation and their locations noted on the side-scan base maps.

B. Interpretation of Sonographs

The sidescan sonograph produces a recording of the sea floor very similar to that of side-looking radar (SLR) imagery, and in many ways similar to oblique areal photographs. The image recorded on a sonograph is a negative image, such that shadows are "white" and images from highly reflective materials are "dark." Sea floor outcrops are delineated in the sonograph with varying shades of dark to light images, coupled with "white" shadows. The material comprising the surface of the sea floor is quantitatively defined by sampling, then correlated with its tone and pattern on the sonograph. The difference in dark-light recording is a function of both the gain setting of the equipment at the time the records are made and the type of bottom material. The sea state and boat speed across the sea floor also play important roles in determining the limitations and qualifications of a sidescan survey. Thus interpretation of the sonographs is to a large extent dependent on the experience of the interpreter. The sonographs provide an instantaneous "snapshot" of the disposal study areas. Since the sea floor is a dynamic environment, what is found in the spring may differ dramatically from that found at the end of the summer.

C. Interpretation of Seismic Reflection Profiles

The sub-bottom records revealed the geometry of acoustic reflectors at and beneath the sea floor as well as the apparent dip of Tertiary strata at several sites. Strike and dip determinations via seismic reflection profiling are complicated by geometry. To determine the strike and dip of a structure requires detailed profiling to define the structure spatially. Without detailed profiling, the strike and dip of a structure is only an apparent determination, which is partially dependent on the direction of travel across the structure. Additional complications are presented by velocity changes of the overlying and underlying layers and the relationship of the receiver to the point of reflection on the dipping structure. The reflected returns must be migrated to place their points of origin in their true spacial positions, rather than directly beneath the points midway between the source and receiver. The migration involves both geometric and velocity transformations. In general, dips and strikes determined from reflection records, unless otherwise corrected, can be no more specific than, for example, a "westerly dip."

IV RESULTS OF THE INVESTIGATION

A. General Recommendations for the Oregon Disposal Sites

Based upon the general site selection criteria previously outlined and the known tectonic, geologic, and oceanographic conditions of the Oregon coast, the following general recommendations, from a geologic viewpoint, for locating and evaluating offshore disposal sites for dredged materials were made:

1. If possible, dredged material should be physically and chemically compatible with the unconsolidated sediment occurring naturally at the disposal site.

2. Dredged material should be placed so that it does not cover existing rocky outcrops on the sea bottom either at the time of placement or by subsequent lateral transport across the sea floor.

3. Dredged material should be placed in water deep enough so that it does not return to the near-shore environment and cause tubidity adjacent to beaches or contribute to undesirable shoaling in the dredged area and/or elsewhere along the adjacent coastline. Sediment as coarse as medium sand and coarser is probably stable in water depths greater than 90 feet (27 m). Without site-specific hydrodynamic data for each disposal site, however, it is not possible to predict with any certainty how fine sand and finer sediment will behave once it has reached the sea floor. In general, the deeper and more distant the disposal site is from the river mouth/harbor, the less likely it will be for dredged material to return to the shoal area.

4. If there is more than one site within a study area with essentially the same desirable characteristics for disposal of dredged material, it is recommended that preference be given to sites with at least 20 feet (6 m) thickness of naturally occurring sediment on the gentlest slopes available in the local area at or below the minimum recommended water depth. Since sediment in an inner shelf environment typically accumulates rather slowly, it is likely that 20 feet (6 m) of sediment will have experienced the spectrum of seismic events that typically strike the Oregon coastline. The chances of a future earthquake

triggering a failure of dredged material by submarine landsliding can be minimized by choosing horizontal to subhorizontal disposal sites underlain by unconsolidated sediment that has remained stable for a long period of time.

B. Example of a Site Map and Seismic Section

Depoe Bay is located on the north-central Oregon coast (Figure 1) and is surrounded by cliffs and headlands made of three bedrock formations of middle Miocene age (Snavely and others, 1976). The oldest is the Depoe Bay Basalt which consists of approximately 75 feet (25 m) of pillow breccia, pillow flows, extrusive breccia, lapilli tuff, and columnar-jointed subaerial flows (Schlicker and others, 1973). Next is the Sandstone of Whale Cove which consists of 200-300 (61-91 m) feet of massive sandstone and thin-bedded siltstone of marine origin. The youngest formation is the Cape Foulweather Basalt which unconformably overlies the sandstone of Whale Cove (Schlicker and others, 1973) and which consists of subaerial flows, extrusive breccia, tuff breccia, and subaqueous lapilli tuff. This latter formation forms the submarine rock outcrops along the eastern margin of the study area (Figure 3). These three formations have been moderately tilted to the west and cut by north-trending, high-angle faults with small apparent dip separations (Snavely and MacLeod, 1971; Snavely and others, 1976).

The sub-bottom records indicate that west of the submarine rock outcrops, stratified bedrock beneath the veneer of unconsolidated sand/silt also dips to the west (Figure 3). A line of anomalous topography in the submerged lava flows between Depoe Bay and Whale Cove might mark the trace of a fault along the eastern margin of the study area. Apart from the eastern margin of the study area, which is underlain by the Cape Foulweather Basalt, the rest of the area has a sand/silt bottom. This unconsolidated sediment is of Holocene age,has filled in irregularities in the underlying eroded bedrock surface, and varies in thickness from less than 10 to 35 feet (Figure 3).

The existing dredged material disposal area is reasonably well located as judged by the geologic criteria outlined above. The existing disposal site lies in water depths greater than 60 feet (18 m) and is everywhere more than 500 feet (150 m) away from submarine rock outcrops. Shifting the disposal site 500 to 1000 (150-300 m) feet to the west would bring it entirely into water depths greater than 90 feet (27 m).

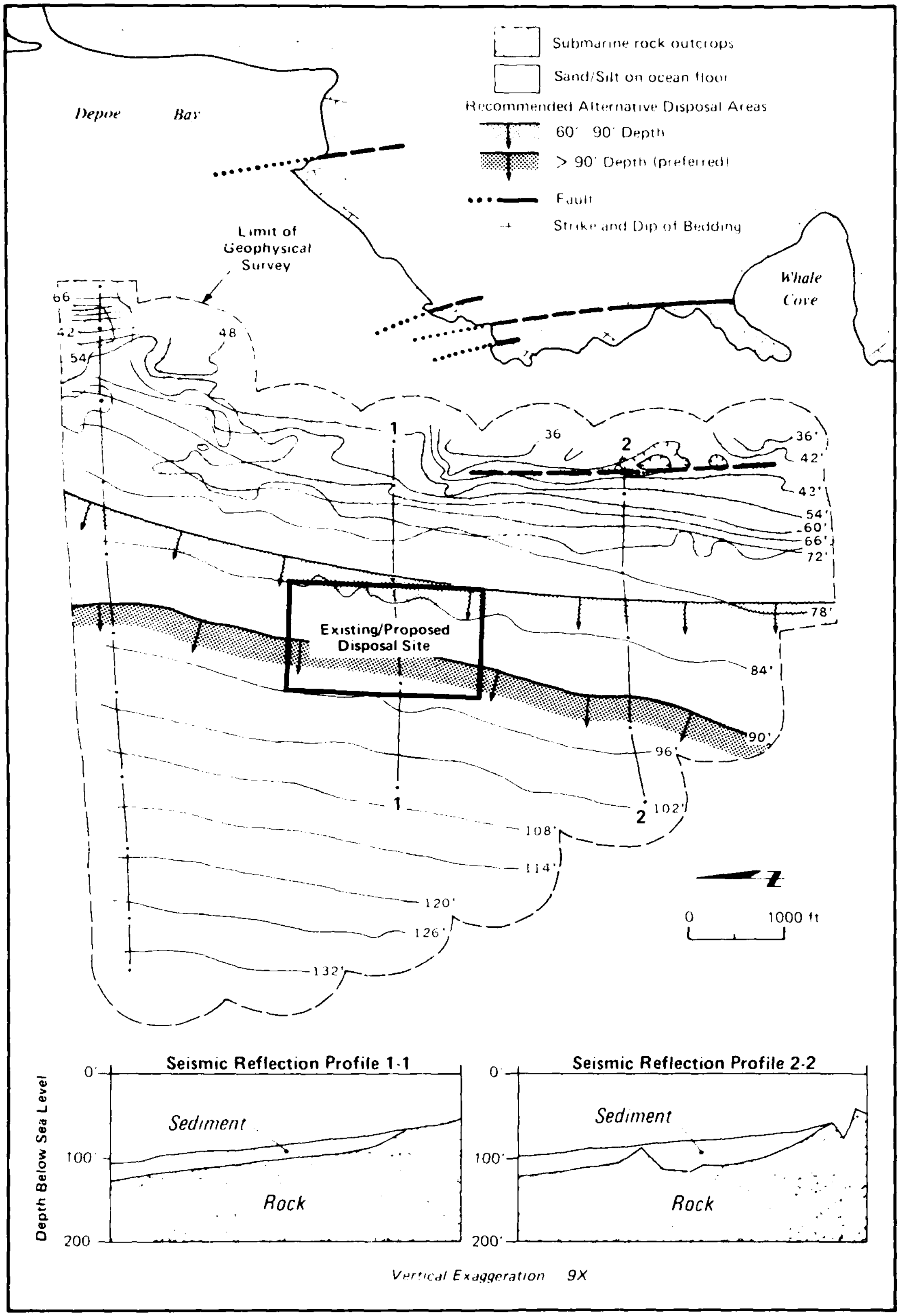
Submarine rock outcrops
Sand/Silt on ocean floor
Recommended Alternative Disposal Areas
60' 90' Depth
> 90' Depth (preferred)
Fault
Strike and Dip of Bedding
Depoe Bay
Whale Cove
Limit of Geophysical Survey
66
42
54
48
36
36'
42'
48'
54'
60'
66'
72'
78'
84'
90'
96'
102'
108'
114'
120'
126'
132'
1
1
2
2
Existing/Proposed Disposal Site
N
0
1000 ft
Seismic Reflection Profile 1-1
Seismic Reflection Profile 2-2
Depth Below Sea Level
0'
100'
200
0
100'
200'
Sediment
Rock
Sediment
Rock
Vertical Exaggeration 9X

Figure 3. Depoe Bay Disposal Site, Map and Profiles

V REFERENCES CITED

Atwater, T., 1970, Implications of the plate tectonics for the Cenozoic tectonic evolution of western North America: Geol. Soc. Am. Bull., v. 81, no. 12, p. 3513-3535

Baldwin, E. M., 1964, Geology of Oregon: Univ. of Oregon Coop. Book Store, Eugene, 165, p.

Barazangi, M., and Dorman, J., 1969, World seismicity maps compiled from ESSA, Coast and Geodetic Survey, Epicenter Data, 1961-1967: Seism. Soc. Am. Bull., v. 59, p. 369-380.

Beaulieu, J. D., Hughes, P. W., and Mathiot, K. R., 1974, Geologic hazards inventory of the Oregon coastal zone: Oregon Dept. Geol. and Min. Ind., Misc. Paper 17, 94 p.

Byrne, J. V., Fowler, G. A., and Maloney, N. J., 1966, Uplift of the continental margin and possible continental accretion off Oregon: Science, v. 154, no. 3757, p. 1654-1655.

Cacchione, D. A., Drake, D. E., Grant, W. D., Williams, A. J. III, and Tate, G. B., 1983, Variability of sea-floor roughness within the coastal oceanic dynamics experiment (CODE) region: Woods Hole Oceanog. Inst., Tech. Report WHOI 83-25, 50 p.

Cherry, J., 1965, Sand movement along a portion of the northern California coast: U.S. Army Corps of Engineers, Coastal Eng. Research Center Tech. Mem. 14, 125 p.

Clarke, S. H. Jr., Field, M. E., and Hirozawa, C. A., 1981, Reconnaissance geology and geologic hazards of offshore Coos Bay Basin, central Oregon continental margin: U.S. Geol. Survey, Open File Report 81-898, 84 p.

Couch, R. W., and Lowell, R. P., 1971, Earthquakes and seismic energy release in Oregon: Oregon Dept. Geol. and Min. Ind., Ore Bin, v. 33, no. 4, p. 61-84.

Drake, D. E., and Cacchione, D. A., 1981, Near-bottom currents and sediment transport on the continental shelf off the Russian River, California (abs.): Trans. Amer. Geophys. Union, 62 (45), p. 915.

Drake, E. T., 1982, Tectonic evolution of the Oregon continental margin: Oregon Dept. Geol. and Min. Ind., Oregon Geology, v. 44, no. 2, p. 15-21.

Fox, W. T., and Davis, R. A. Jr., 1978, Seasonal variation in beach erosion and sedimentation on the Oregon coast: Geol. Soc. Am. Bull., v. 89, p. 1541-1549.

Grant, W. D., and Madsen, O. S., 1979, Combined wave and current interaction with a rough bottom: Jour. Geophys. Res., v. 84, p. 1797-1808.

Hancock, D. R., Nelson, P. O., Sollitt, C. K., and Williamson, K. J., no date, Coos Bay offshore disposal site investigation, Interim Report, Phase I, February 1979-March 1980: Report to Portland Dist., Corps of Engineers, Contract No. DACW57-79-00040.

Heaton, T. H., and Kanamori, H., 1984, Seismic potential associated with subduction in the northwestern United States: Seis. Soc. America Bull., v.74, No. 3, p. 933-941.

Hickey, B. M., 1979, The California current system hypotheses and facts: Prog. Oceanog., v. 8., no. 4, p. 191-279.

Irwin, W. P., 1966, Geology of the Klamath Mountains Province, in Bailey, E. H., ed., Geology of northern California: Calif. Div. Mines and Geol. Bull. 190, p. 19-38.

Komar, P. D., 1976, The transport of cohesionless sediments on continental shelves: in Stanley, D. J., and Swift, D.J.P., eds., Marine sediment transport and environmental management: Wiley, New York, p. 107-125.

Kulm, L. D., Roush, R. C., Harlett, J. C., Neudeck, R. H., Chambers, D. M., and Runge, E. J., 1975, Oregon continental shelf sedimentation: interrelationships of facies distribution and sedimentary processes: Jour. Geology, v. 83, p. 145-175.

Kulm, L. D., Scheidegger, K. F., Byrne, J. V., and Spigai, J. J., 1968, A preliminary investigation of the heavy mineral suites of the coastal rivers and beaches of Oregon and northern California: Oregon Dept. Geol. and Min. Ind., Ore Bin, v. 30, no. 9, p. 165-181.

Maloney, N. J., 1965, Geology of the continental terrace off the central coast of Oregon: Unpub. Ph.D. thesis, Oregon State Univ., Corvallis, 233 p.

Nelson, P. O., Sollitt, C. K., Williamson, K. J., and Hancock, D. R., no date, Coos Bay offshore disposal site investigation, Interim Report, Phase II, III, April 1980-June 1981: Report to Portland Dist. Corps of Engineers, Contract No. DACW57-79-00040.

Nittrouer, C. A., and Sternberg, R. W., 1981, The formation of sedimentary strata in an allochthonous shelf environment: The Washington continental shelf: Marine Geol., v. 42, p. 201-232.

Scheidegger, K. F., Kulm, L. D., and Runge, E. J., 1971, Sediment sources and dispersal patterns of Oregon continental shelf sands: Jour. Sed. Petrol., v. 41, no. 4, p. 1112-1120.

Schlicker, H. G., Deacon, R. J.; Olcott, G. W., and Beaulieu, J. D., 1973, Environmental geology of Lincoln County, Oregon: Oregon Dept. Geol. and Min. Ind. Bull. 74, 164 p.

Snavely, P. D., Jr., 1984, Sixty million years of growth along the Oregon continental margin, in Clarke, S. H., ed., Highlights in marine research: U.S. Geol. Survey Circular 938, p. 9-18.

Snavely, P. D. Jr., and MacLeod, N. S., 1971, Visitor's guide to the geology of the coastal area near Beverly Beach State Park, Oregon: Oregon Dept. Geol. and Min. Ind., Ore Bin, v. 33, no. 5, p. 85-105.

Snavely, P. D. Jr., MacLeod, N. S., Wagner, H. C., and Rau, W. W., 1976, Geologic map of the Cape Foulweather and Euchre Mountain Quadrangles, Lincoln County, Oregon: U.S. Geol. Survey Misc. Inv. Series Map I-868.

Snavely, P. D. Jr., Pearl, J. E., and Lander, D. L., 1977, Interim report on petroleum resources potential and geologic hazards in the outer continental shelf - Oregon and Washington Tertiary province: U.S. Geol. Survey, Open-File Report 77-282, 68 p.

Snavely, P. D. Jr., Wagner, H. C., and Lander, D. L., 1980, Interpretation of the Cenozoic geologic history, central Oregon continental margin: Cross-section summary: Geol. Soc. Am. Bull., v. 91, no. 3, p. 143-146.

Spigai, J. J., 1971, Marine geology of the continental margin off southern Oregon: Unpub. Ph.D. thesis, Oregon State Univ., Corvallis, 214 p.

U.S. Army Corps of Engineers, 1975, Final environmental impact statement, Corps of Engineers activities in the Chetco, Coquille and Rogue River estuaries and Port Orford, Oregon: U.S. Army Eng. District, Portland, Oregon.

LITTORAL SEGMENTS: DANA POINT TO MEXICO

Robert H. Osborne[1], Peter A. Almendinger[2], Paul D. Hecht[2]
and Anthony Price[3]

ABSTRACT

The Oceanside, Mission Beach and Silver Strand littoral cells each may be subdivided into segments defined either by (1) distinctive mineralogic assemblages (petrofacies) due to natural or man-influenced processes (especially beach nourishment programs), or (2) by known natural of man-made barriers (jetties and breakwaters) to littoral sand transport. Modal analysis of the light- and heavy-mineral fractions of 23 sediment samples collected from February to June, 1984 permits the tentative identification of 14 such segments from Dana Point to the United States-Mexico border. The observed mineral suites reflect ultimate derivation from plutonic rocks of the southern California batholith and from the Catalina Schist terrane, which is supplied to the modern littoral zone by recycling from older sedimentary strata exposed along the coast.

INTRODUCTION

Major sedimentologic events in the nearshore zone are episodic, site-specific, and strongly related to meteorologic and topographic influences, substrate stability within a given area, and to a complex set of erosive agents, both natural and man-induced, that may act upon them. All of these factors are time-dependent, and are related through a poorly-known set of major and partial dependencies, interaction effects, lag times, feedback loops, etc. Unfortunately, the parameters necessary to quantitatively relate the principal variables and their interactions in a realistic, time-dependent predictor model are subject to substantive random effects, which considerably reduce the efficiency and accuracy of such models.

Such environmental complexities necessitate the partitioning of the shorezone into discrete segments, each of which may respond quantitatively to coastal energy fluxes in a sedimentologically distinct manner. As such, this report will better define sediment source areas and sand transport paths in the littoral zone from Dana Point to the United States-Mexico border by using mineralogic data to define littoral segments along this portion of the southern California coast (Fig. 1).

---

[1] Department of Geological Sciences
University of Southern California
Los Angeles, California 90089-0741

[2] SPD Laboratory
U.S. Army Corps of Engineers
P.O. Box 37
Sausalito, CA 94947

[3] Los Angeles District
U.S. Army Corps of Engineers
P.O. Box 2711
Los Angeles, CA 90053-2325

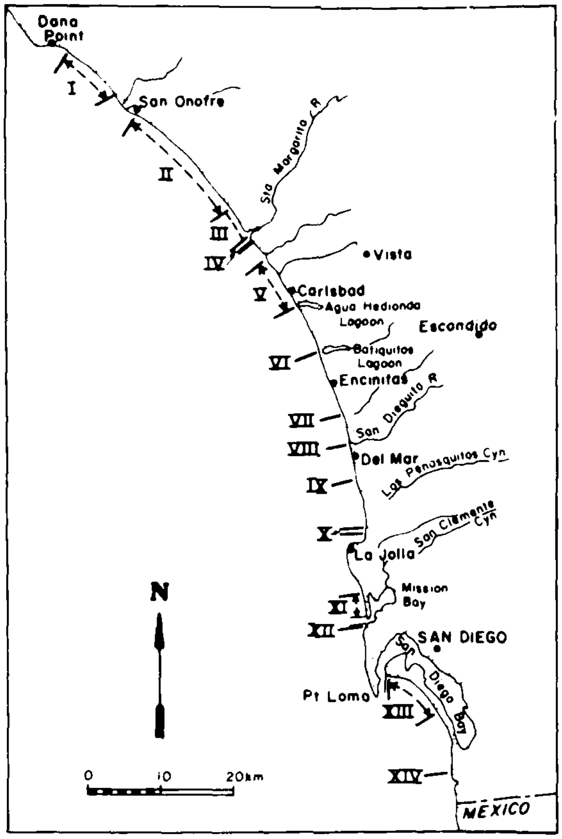
Dana Point
I
San Onofre
Sta Margarita R
II
III
IV
Vista
V
Carlsbad
Agua Hedionda Lagoon
Escondido
VI
Batiquitos Lagoon
Encinitas
San Dieguito R
VII
VIII
Del Mar
Los Penasquitos Cyn
IX
X
San Clemente Cyn
La Jolla
N
Mission Bay
XI
XII
SAN DIEGO
San Diego Bay
Pt Loma
XIII
XIV
0
10
20km
MEXICO

Fig. 1. Map showing location of littoral segments from Dana Point to the United States-Mexico border.

Principal Detrital Minerals Identified in Sample Set	Regional Sample Set (%)	Woodson Mountain Granodiorite (%)	Bonsall Tonalite (%)	San Marcos Gabbro (%)
Quartz	42	33 (30-40)	20-25	4 (0-10)
Potassium Feldspar	11	20 (10-30)	4-15	Tr
Plagioclase Feldspar	25	41 (30-55)	55-60	59 (47-66)
Biotite	1	5 (1-8)	5-15	3 (0-6)
Opaque Minerals	2	Tr	Tr	3
Pyroxene	Tr	Tr	Tr	8 (0-28)
Augite		Tr	Tr	7 (0-17)
Hornblende	13	1 (0-2)	10	
Garnet	Tr		Tr	13 (1-42)
Zircon	Tr			
Sphene	1			
Rutile	Tr			
Piedmontite	Tr			
Clinozoisite-Epidote	3			
Actinolite-Tremolite	Tr			
Glaucophane	Tr			
Glaucophane Schist	1			

Table 1. Modal mineralogic composition of sample set and principal source rocks.

Methods

The mineralogical data were divided into two sets. The first set reflected the total light and heavy mineral composition of each sample, and included quartz, potassium feldspar, plagioclase feldspar, and the total heavy mineral suite. The second set contained only the heavy mineral fraction of each sample, and included the following minerals: biotite, opaque minerals, pyroxene (other than augite), augite, hornblende, garnet, zircon, sphene, rutile, piedmontite, clinozoisite- epidote, actinolite-tremolite, glaucophane, and glaucophane schist (a rock fragment). Each of these data sets was recast to sum to 100 percent.

GENERAL SEDIMENTOLOGIC CONSIDERATIONS

Emery (1960) and Inman and Chamberlain (1960) identified a series of littoral cells along the southern California coast. These cells are based on the concept of longshore transport of dominantly fluvially-derived sediment, which is entrapped either by submarine canyon heads or by points of land which extend seaward from the general position of the coastline. Three major coastal divisions are present in this study area. The Oceanside Littoral Cell extends from Dana Point to Point La Jolla, which may be further subdivided by Carlsbad Submarine Canyon. The second division is the coastal lowland in the Pacific and Mission Beach area, which occurs on the former delta of the San Diego River. The jetties constructed at the mouth of Mission Bay have interrupted the transport of sand from Mission Beach to Ocean Beach (Kuhn and Shepard, 1984), therefore, Ocean Beach is treated as a pocket beach in the present study. The coastal segment from the entrance to San Diego Bay to the United States-Mexico border comprises the Silver Strand Littoral Cell. At present, the interpretation of petrologic trends is confounded by two major factors. Additional samples are needed adjacent to suspected point sources, namely stream mouths and beach nourishment projects, to document their importance and to determine the net transport direction associated with each such point source. Secondly, there is a paucity of information concerning potential lithologic trends present in the sedimentary strata in areas with contributing sea cliffs (Osborne and Pipkin, 1983).

SEDIMENT SOURCES

Inasmuch as all mineralogic materials in sediment and sedimentary strata are directly or indirectly derived from crystalline rocks of the earth's crust, it is necessary to consider (1) the ultimate crystalline source rocks and (2) the local fluvial and cliff sediment sources.

The Geologic Map of the Corona, Elsinore, and San Luis Rey Quadrangles, California (Larsen, 1948) shows that the basement complex consists of two principal units: (1) the Late Jurassic Santiago Peak Volcanics and (2) the mid-Cretaceous plutonic rocks assigned to the southern California batholith, which intrudes the

Santiago Peak Volcanics. The Santiago Peak Volcanics occur as an elongate belt of low-rank metamorphosed volcanic, volcaniclastic and sedimentary rocks that crop out from the southern edge of the Los Angeles basin southward into Mexico (Gray and others, 1971). Compositionally these rocks range from basalt to rhyolite, but are predominantly dacite and andesite. A number of low-rank metamorphosed, small gabbroic plutons, which were probably feeders for the volcanic strata, are included in the Santiago Peak Volcanics.

Plutonic rocks of the southern California batholith are generally quartz diorite and gabbro. The quartz diorite contains large phenocrysts of plagioclase and potassium feldspar, and hornblende and biotite are present in minor amounts. The gabbroic units are compositionally variable, but consist mostly of calcic feldspar and pyroxene, with minor amounts of quartz and biotite. Larsen (1948) named the principal units in the southern California batholith the Woodson Mountain Granodiorite, the Bonsall Tonalite, and the San Marcos Gabbro. Table 1 summarizes the modal mineralogic composition for the regional sample set and the principal source rocks. The compositional data for the Woodson Mountain Granodiorite, Bonsall Tonalite and San Marcos Gabbro are from Larsen (1948). It is clear from Table 1 that crystalline rocks in the southern California batholith are capable of producing the major mineral assemblages present in the sample set. Minor accessory minerals, such as zircon, sphene and rutile commonly are associated with acid plutonic rocks; piedmontite and clinozoisite-epidote are associated with mafic igneous rocks; and actinolite-tremolite is a high-rank metamorphic mineral and may be a constituent of some glaucophane schist.

The occurrence of glaucophane, glaucophane schist and actinolite-tremolite reflects ultimate derivation from the Mesozoic metamorphic age (110 m.y.b.p.) Catalina Schist terrane, which consists of a glaucophane-rich blueschist. Stuart (1979, p. 36) reports a diverse set of clast types, which occur in the San Onofre Breccia. These include clasts of (1) the blueschist facies, which is rich in glaucophane and contains quartz, albite and chlorite; (2) the glaucophanic greenschist facies, which is rich in epidote and contains albite; (3) the greenschist facies, which is rich in actinolite and contains epidote, albite and chlorite; (4) the quartz schist facies, which consists of foliated quartz with greenschist and abundant glaucophane; (5) the saussurite gabbro facies, which contains actinolite, zoisite, clinozoisite and albite; (6) the amphibolite facies which contains amphibole, zoisite and garnet; and (7) the serpentinite facies, which contains calcite, tremolite, chlorite and actinolite. Such terranes are exposed on Santa Catalina Island and the Palos Verdes Hills, and occur in the subsurface of the Los Angeles basin, but are not known to occur within the uplands associated with the southern California batholith. The San Onofre Breccia (Miocene) is the most extensive deposit containing Catalina Schist detritus (Stuart, 1979). Scattered exposures of this unit occur from Santa Cruz Island southeastward to the Laguna Beach-Oceanside area, and then again south of Tijuana. The San Onofre

Breccia is exposed as a strike ridge extending from San Onofre Mountain near Dana Point almost to Oceanside, and this exposure as well as younger sedimentary strata exposed along the coastal cliffs may have served as the local source for the glacophane, glaucophane schist and perhaps the actinolite-tremolite grains present in the sample set.

LITTORAL SEGMENTS: DANA POINT TO THE UNITED STATES-MEXICO BORDER

Given the occurrence of the Oceanside, Mission Beach and Silver Strand littoral divisions, each may be subdivided into segments defined either by (1) distinctive mineralogic assemblages due to natural or man-influenced processes (especially beach nourishment programs), or (2) by known natural or man-made barriers (jetties and breakwaters) to littoral sand transport. Fourteen littoral segments tentatively may be identified using these criteria. It must be stressed that the petrologic data base used to define these segments is marginal. Eight of the fourteen segments identified consist of only one sample, which is usually associated with an apparent point source - either the mouth of a river or estuary or the site of one or more beach nourishment programs. Additional sampling is required in the lower reaches (above the zone of tidal influence) of each such river to establish the river as the primary sand source - if, in fact, this presumed relationship is true. Furthermore, closely-spaced ($\cong$ 1 km) samples taken along the beach both upcoast and downcoast of such point sources would permit the determination of the net transport direction by means of the reduction of petrologically distinct light and heavy mineral assemblages in the direction of transport as well as the areal asymmetry (elongated in the net transport direction) of such petrofacies. The average mineralogy by segment is shown in Figure 2.

The reader is referred to the First Year-End Report for Task 1D, Sediment Sampling, CCSTWS for the location of range lines employed in this report.

Littoral Segment I. Stations DB-1805 through SC-1623

Segment I is backed by non-contributing cliffs. A slight downcoast decrease in quartz occurs with corresponding increases in plagioclase and potassium feldspar and a relatively consistent set of heavy minerals. The boundary between segments I and II occurs between stations SC-1623 and SO-1530. This area is backed by non-contributing cliffs, and includes the mouths of the San Mateo and San Onofre Rivers, which may serve as important sand contributors. Although there is a slight downcoast increase in plagioclase and total heavy minerals with a corresponding decrease in quartz and potassium feldspar, there is no substantive downcoast change in the total lithology. There is, however, a major decrease in hornblende and sphene, with associated increases in clinozoisite-epidote and composite grains. The enrichment of hornblende at SC-1623 may reflect upcoast transport from sediment input through the San Mateo River. There is a slight upcoast decrease in heavy minerals, which

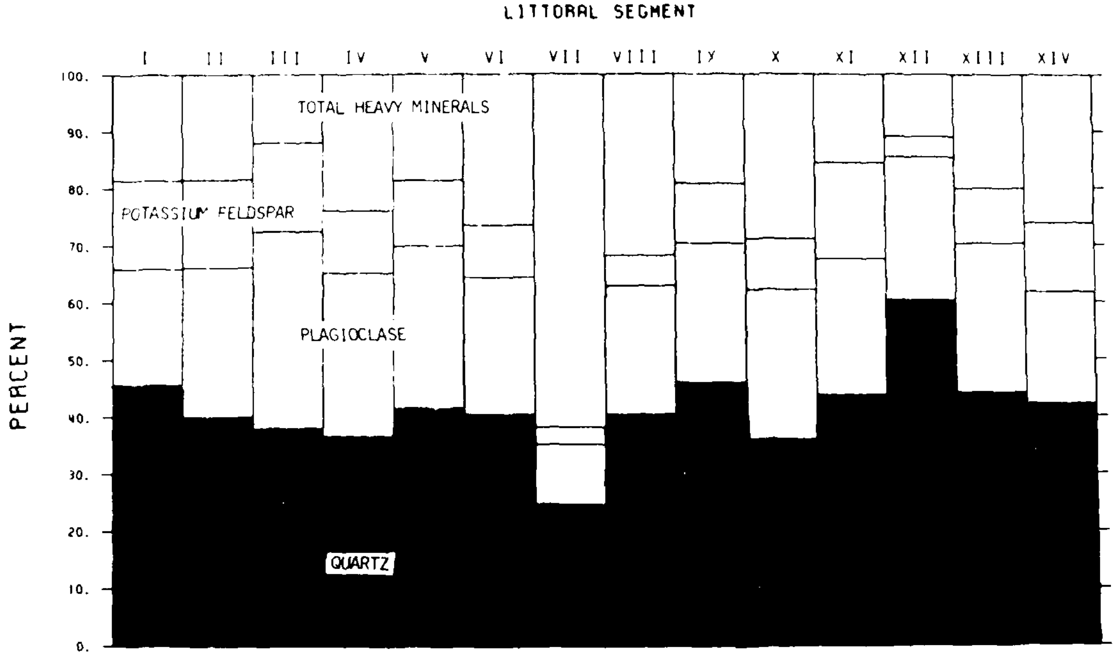

Fig. 2. Average mineral composition of sediment samples by segment from the end-of-winter regional data set.

may reflect net upcoast transport, but this argument cannot be substantiated with the available data.

Littoral Segment II. Stations SO-1530 through PN-1290

Segment II is backed by contributing cliffs. There is a downcoast decrease in total heavy minerals with associated slight increases in plagioclase and potassium feldspar. A notable decrease in opaque minerals occurs with corresponding increases in clinozoisite-epidote, glaucophane schist and hornblende. The occurrence of glaucophane schist is interesting, because it reflects the reworking of grains that were ultimately derived from the Catalina Schist terrane. In this area, the most likely local source for the grains of glaucophane schist is the San Onofre Breccia. The boundary between segments II and III occurs between stations PN-1290 and PN-1240, which includes contributing cliffs and Los Flores Creek. There is a downcoast decrease in quartz and total heavy minerals with an associated increase in plagioclase. There is an important downcoast increase in hornblende, and minor increases in biotite and perhaps glaucophane schist, with a corresponding decrease in clinozoisite-epidote. This change most likely reflects sediment input from Los Flores Creek.

Littoral Segment III. Station PN-1240

Segment III is backed by contributing cliffs, and occurs upcoast of the mouth of the Santa Margarita River. Inasmuch as this segment contains only one sample, no downcoast trends within this segment can be discerned. The boundary between segments III and IV occurs between stations PN-1240 and PN-1110, which is backed by contributing cliffs and contains the mouth of the Santa Margarita River. There is a marked downcoast increase in the volume of total heavy minerals between these two stations, with corresponding decreases in plagioclase and potassium feldspar. There is also a dramatic downcoast increase in hornblende and biotite, and a corresponding decrease in clinozoisite-epidote. These mineralogic trends most likely are associated with input from the Santa Margarita River, but additional samples are needed to demonstrate this relationship.

Littoral Segment IV. Station PN-1110

Segment IV occurs south of the mouth of the Santa Margarita River, and probably is bounded downcoast by the north jetty at the Camp Pendleton Boat Basin and Oceanside Harbor. There are no contributing cliffs in this area. As this segment contains only one sample, no trends within this coastal zone can be described. The boundary between segments IV and V occurs between stations PN-1110 and OS-1000. There are no contributing cliffs in this area, but the Santa Margarita River and beach nourishment programs are important local sand sources. A marked downcoast increase in hornblende and to a lesser degree biotite occurs, with corresponding decreases in clinozoisite-epidote and opaque minerals. There is a downcoast decrease in total heavy minerals with a corresponding increase in plagioclase.

Littoral Segment V. Stations OS-1000 through CB-820

Segment V is partially backed by contributing cliffs (south of CB-880 almost to CB-120), has been affected by beach nourishment programs (OS-1000 through at least OS-930), and includes a possible estuarine source through outflow from Buena Vista Lagoon (CB-880) and Aqua Hedionda Lagoon (CB-820). This segment also includes the head of Carlsbad Submarine Canyon, which may serve to divide the Oceanside Littoral Cell. A modest downcoast increase in quartz, potassium feldspar and total heavy minerals occurs from station OS-1000 to OS-930, and there is a minor increase in plagioclase and decrease in potassium feldspar from OS-930 to OS-820. The heavy mineral data display an increase in hornblende and clinozoisite-epidote and a marked decrease in biotite from OS-1000 to OS-930, and are rather consistent to CB-820. No major mineralogical changes coincide with the position of the head of the Carlsbad Submarine Canyon. The boundary between segments V and VI is between stations CB-820 and CB-720, which occurs immediately south of the mouth of Bataquitos Lagoon. This area is backed by contributing cliffs. There is a modest downcoast increase in the volume of total heavy minerals, with minor decreases in quartz and plagioclase. A marked downcoast increase in opaque minerals and a modest increase of clinozoisite-epidote occurs, and a major reduction in the volume of hornblende. It is suspected that these mineral assemblages are related to episodic flushing of Bataquitos Lagoon, but this relationship cannot be established with the available data.

Littoral Segment VI. Station CB-720

Segment VI consists only of station CB-720, and is likely to contain cliff-derived sediment as well as sediment periodically flushed from Bataquitos Lagoon. The boundary between segments VI and VII occurs between stations CB-720 and SD-630, which occurs at Cardiff State Beach immediately downcoast of the San Elijo River. There is a tremendous downcoast increase in the volume of total heavy minerals from CB-720 to SD-630 with associated decreases in quartz, plagioclase and potassium feldspar. Interestingly enough, there is a modest downcoast increase in clinozoisite-epidote, but all other heavy minerals remain in relatively constant proportions between these two stations.

Littoral Segment VII. Station SD-630

Segment VII consists only of station SD-630, and may receive sediment from contributing cliffs as well as the San Elijo River. Station SD-630 is located immediately south of the San Elijo Lagoon, and is characterized by an anomalously high value for total heavy minerals. This concentration of heavy minerals is most likely related to episodic flushing of the San Elijo Lagoon, and subsequent wave reworking in the swash zone. The boundary between stations VII and VIII occurs between stations SD-630 and DM-580, which is backed by contributing cliffs. There is a major downcoast decrease in total heavy mineral content, modest increases in quartz and potassium feldspar, and a minor increase in plagioclase. There is a small downcoast increase in the volume of total opaque minerals, but the proportions of the other heavy minerals remain relatively constant.

Littoral Segment VIII. Station DM-580

Station DM-580 is located immediately south of the mouth of the San Diequito River, and may receive fluvial sediment from this local source as well as from contributing cliffs. The boundary between segments VIII and IX occurs between sample stations DM-580 and TP-520, and this area may receive sediment from contributing cliffs and Soledad Creek. There is a downcoast decrease in the volume of total heavy minerals, with associated increases in quartz, plagioclase and potassium feldspar. A tremendous downcoast increase in the volume of glaucophane schist occurs at TP-520, with a corresponding decrease in opaque minerals, and a modest reduction is clinozoisite-epidote and garnet.

Littoral Segment IX. Station TP-520

Station TP-520 occurs near the mouth of Soledad Creek, and therefore may receive episodic fluvial as well as cliff-derived sediment. The sample from station TP-520 is highly enriched in glaucophane schist. The occurrence of glaucophane schist grains indicates that these particles were ultimately derived from the Catalina Schist terrane. Inasmuch as no crystalline Catalina Schist terrane is exposed in the study area, the presence of these grains implies that they have been reworked from older sedimentary strata such as the Miocene San Onofre Breccia or the Monterey Formation. Since the most extensive exposure of the San Onofre Breccia occurs between Dana Point (San Onofre Mountains) and Oceanside (Stuart, 1979), it is not clear why this highly enriched sediment occurs as far south as Torrey Pines. Sampling may have to be performed to determine if such material is being derived from strata exposed in the adjacent contributing cliffs. The boundary between IX and X occurs between stations TP-520 and LJ-460. There is a major downcoast increase in total heavy minerals, and an associated increase in quartz. There is a major downcoast reduction in glaucophane schist, with corresponding increases in clinozoisite-epidote, opaque minerals, and a minor increase in hypersthene.

Littoral Segment X. Stations LJ-460 through LJ-450

Stations LJ-460 and LJ-450 are located betwen Scripps and La Jolla Submarine Canyons, and are backed by contributing cliffs. There is a substantial downcoast decrease in total heavy minerals and a minor decrease in potassium feldspar from stations LJ-460 to LJ-450, with corresponding increases in quartz and plagioclase. Heavy minerals also show marked changes between these two stations. There is a substantial downcoast increase in hornblende, and modest increases in biotite and glaucophane schist. These changes are coupled with a notable downcoast decrease in clinozoisite-epidote, and moderate downcoast decreases in opaque minerals and zoisite. The observed variability in relatively closely-spaced samples may be related to the complex littoral wave and current system between the heads of Scripps and La Jolla Submarine Canyons (Shepard, 1950), or such trends may be partly inherited from cliff-derived sediment. The Oceanside Littoral Cell is terminated at the submarine canyon complex associated with Point La Jolla.

Littoral Segment XI. Stations MB-384 through MB-270

Stations MB-384 through MB-270 occur along a downcoast-directed spit which extends most of the way across the mouth of Mission Bay. The San Diego River enters Mission Bay, where it has deposited a considerable volume of sediment, and the coastal lowland occupied by Pacific and Mission Beaches occurs on older deltaic sediment deposited by the San Diego River. Such fluvial sediment extends almost to Crystal Pier at Pacific Beach, where the character of the sediment changes and extends downcoast as a spit. The sediment comprising Mission Beach presumably was derived by the reworking of older San Diego River alluvium combined with downcoast littoral drift. No beach nourishment programs have been performed between these two stations. From samples MB-384 through MB-310, there is a downcoast increase in the total heavy minerals and plagioclase, with associated decreases in quartz and potassium feldspar. From MB-310 to MB-270, there is a downcoast decrease in total heavy minerals and plagioclase, and a corresponding increase in quartz. From MB-384 to MB-340, there is a tremendous downcoast increase in biotite, with noteworthy decreases in hornblende and opaque minerals. From MB-340 to MB-310, there is a dramatic downcoast reduction in biotite, and appreciable increases in the amount of hornblende and opaque minerals. From MB-310 to MB-270, there is a downcoast increase in biotite, and a decrease in opaque minerals. The increases in the amount of biotite may be due to the acquisition of samples in areas characterized by low mechanical-energy during or before the sampling period. Littoral segment XI is bounded downcoast by the north jetty at the entrance to Mission Bay.

Littoral Segment XII. Station OB-230

Station OB-230 is located at Ocean Beach, which is a pocket beach extending from the south San Diego River jetty to Sunset Cliffs. Damming of the San Diego River considerably reduced the volume of sand received by Ocean Beach, and the three jetties constructed at the mouth of Mission Bay have terminated the sand supply received from Mission Beach. As a result, the cliffs at Ocean Beach have receded considerably, and sand obtained from north of the Mission Bay jetties was placed along Ocean Beach to reduce the rate of cliff erosion (Kuhn and Shepard, 1984). Fill placed in 1950 migrated upcoast to form a spit across the mouth of the San Diego River, and downcoast erosion was initiated. Additional fill dredged from Mission Bay was placed in 1955, and was contained by a groin at Cape May Avenue. Although the sample from OB-230 may be a combination of cliff-derived and beach fill, it most likely represents sand supplied by beach nourishment. As this segment is represented by only one sample, no trends within this pocket beach can be defined. However, when compared to MB-270, the sample from OB-230 is significantly enriched in quartz, moderately enriched in plagioclase, moderately reduced in potassium feldspar, and slightly reduced in total heavy minerals. The heavy mineral suites are similar; however, OB-230 is enriched in hornblende and depleted in total opaque minerals. Littoral Segment XII is bounded downcoast by Sunset Cliffs.

Littoral Segment XIII. Stations SS-160 through SS-90

Stations SS-160 through SS-90 occur within the Silver Strand Littoral Cell. This cell extends from Zuniga jetty, which forms the southern boundary of the entrance to San Diego Bay, to the border between the United States and Mexico. The principle natural sediment source for this cell is the Tijuana River, which was particularly important prior to damming. Beach nourishment programs have been performed at Imperial Beach and in the area adjacent to Hotel del Coronado (Kuhn and Shepard, 1984). The Silver Strand Littoral Cell consists of a long, upcoast-directed spit, which extends from the embayment associated with the Sweetwater and Tijuana Rivers. Inman (1976) has documented that the primary zone of net accretion is at and directly offshore of Zuniga Shoal by comparing isolines of sand accretion obtained from surveys carried out in 1923 and 1934. Unfortunately there is no petrographic data for stations SS-200 and SS-180, so it is not possible to determine whether or not the upcoast portion of this spit is compositionally similar to segment XIII. Although beach nourishment has occurred near Hotel del Coronado, the sand in the foreshore zone may be dominated by sand derived from the area of Imperial Beach, therefore meaningful compositional trends might be obtained by sampling the upcoast part of this spit. From SS-160 to SS-90, there is a slight downcoast decrease in total heavy minerals and potassium feldspar, with corresponding minor increases in quartz and plagioclase. There is a downcoast increase in hornblende, and an associated decrease in biotite between these two stations. The boundary between segments XIII and IV occurs between stations SS-90 and SS-35. There is a moderate downcoast increase in heavy minerals and a minor increase in potassium feldspar, which is associated with a reduction in the amount of plagioclase. More dramatic changes are recorded in the heavy mineral assemblages. Substantial downcoast increases occur in the volume of composite grains and total opaques, with an associated decrease in hornblende.

Littoral Segment XIV. Station SS-35

Station SS-35 is located about 1.25 miles north of the mouth of the Tijuana River, and sand obtained from this area most likely represents some mixture of sediment derived from the Tijuana River as well as by beach nourishment programs. There is a possibility that some sand may have been derived from the contributing cliffs south of the Tijuana River.

REFERENCES

Emery, K. O., 1960, The sea off southern California: A modern habitat of petroleum: New York, John Wiley and Sons, 366 p.

Gray, C. H., Jr., Kennedy, M. P., and Morton, P. K., 1971, Petroleum potential of southern coastal and mountain area, California: American Association of Petroleum Geologists, Memoir 15, p. 372-383.

Inman, D. L., 1976, Summary report of man's impact on the California coastal zone: Technical Report, State of California Department of Navigation and Ocean Development, 150 p.

Inman, D. L., and Chamberlain, T. K., 1960, Littoral sand budget along the southern California coast: Report of the Twenty-first International Geological Congress, Copenhagen, Volume of Abstracts, p. 245-246.

Kuhn, G. G., and Shepard, F. P., 1984, Sea cliffs, beaches and coastal valleys of San Diego County: Berkeley, University of California Press, 193 p.

Larsen, E. S., 1948, Batholith of Corona, Elsinore, and San Luis Rey quadrangles, southern California: Geological Society of America Memoir 29, 182 p.

Osborne, R. H., and Pipkin, B. W., 1983, Shorezone contribution of cliff-derived sediment, Dana Point to the United States-Mexico border, San Diego County, California: Technical Report, Los Angeles District, U.S. Army Corps of Engineers, 27 p.

Shepard, F. P., 1950, Longshore current observations in southern California: U.S. Army Corps of Engineers Beach Erosion Board Technical Mem. No. 13, 54 p.

Numerical Modeling of the Physical Fate of Dredged Material Dumped at Open Water Sites: San Francisco Bay and Puget Sound

M. J. Trawle* and B. H. Johnson*

Introduction

The short-term fate of dredged material dumped at any open water disposal site is a key factor in site management. There are two basic types of disposal sites that will be referred to in this paper as dispersive and nondispersive sites. If a site is designated as nondispersive, dumped material should deposit with the disposal site boundaries (Figure 1a). A nondispersive site has a finite site capacity and therefore a finite useful life. If a site is designated as dispersive, the opposite is true (Figure 1b). In fact, if dumped material tends to accumulate at a dispersive site, the loss of the site for dredged material disposal could be the eventual result. A truly dispersive site has unlimited capacity and therefore an unlimited life.

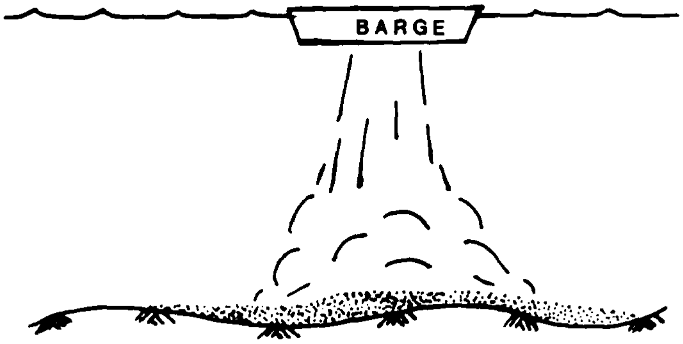

Figure 1a. Nondispersive site-accumulation of disposed material

---

* Research Hydraulic Engineer, Hydraulics Laboratory, USAE Waterways Experiment Station, Vicksburg, Miss.

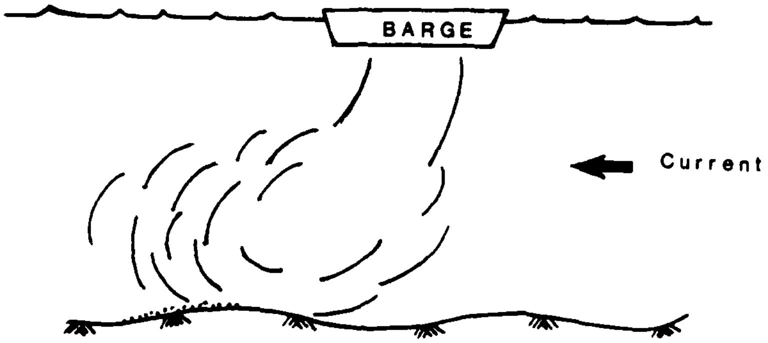

Figure 1b. Dispersive site - no accumulation of disposed material

Predictive techniques are needed to effectively design and manage both dispersive and nondispersive disposal sites. For nondispersive sites, reliable techniques are needed to estimate site capacity, i.e., to estimate at what point further dumping would cause deposition of dumped material outside the disposal site limits. Also, reliable techniques are needed to estimate what ambient conditions, such as tidal currents, cause initial deposition of dumped material outside disposal site limits. For dispersive sites, techniques are needed to evaluate the dispersive capability of the material currents at the site. In other words, techniques are needed to estimate the ability of the ambient current environment to remove dumped material from the site before material strikes the bottom and to resuspend and remove any material that does initially deposit within the site.

One such technique or tool for investigating the short-term fate of dumped material is the set of numerical dump models called DIFID (Disposal from Instantaneous Dump), DIFCD (Disposal from Continuous Discharge), and DIFHD (Disposal from Hopper Dredge). This paper describes the numerical model DIFID and discusses two recent applications of the model DIFID conducted by the Hydraulics Laboratory at the Waterways Experiment Station (WES). The applications consist of the Alcatraz disposal site in San Francisco Bay and a generic study applicable to Puget Sound.

The Numerical Model, DIFID

Description

The instantaneous dump model (DIFID) was developed by Brandsma and Divoky (1976) for the U.S. Army Engineers Waterways Experiment Station (WES) under the Dredged Material Research Program. Much of the basis for the model was provided by earlier model development by Koh and Chang (1973) for the barged disposal of wastes in the ocean. That work was conducted under funding by the Environmental Protection Agency (EPA) in Corvallis, Oregon. Modifications to the original model have been made by Johnson and Holiday (1978) and Johnson (in preparation).

The model requires that the dredged material be broken into various solid fractions with a settling velocity specified for each fraction. In many cases, a significant portion of the material falls as "clumps" that may have a settling velocity of perhaps 1 to 5 fps. This is especially true if the dredging is done by clamshell and can be true in the case of hydraulically dredged material if consolidation takes place in the hopper during transit to the disposal site. The specification of a "clump" fraction is rather subjective, so the inability to accurately characterize disposed material in some disposal operations prevents a quantitative interpretation of model results in those operations.

The behavior of the disposed material is assumed to be separated into three phases: convective descent, during which the dump cloud or discharge jet falls under the influence of gravity; dynamic collapse, occurring when the descending cloud either impacts the bottom or arrives at the level of neutral buoyancy at which descent is retarded and horizontal spreading dominates; and long-term passive dispersion, commencing when the material transport and spreading are determined more by ambient currents and turbulence than by the dynamics of the disposal operation. Figure 2 illustrates these phases.

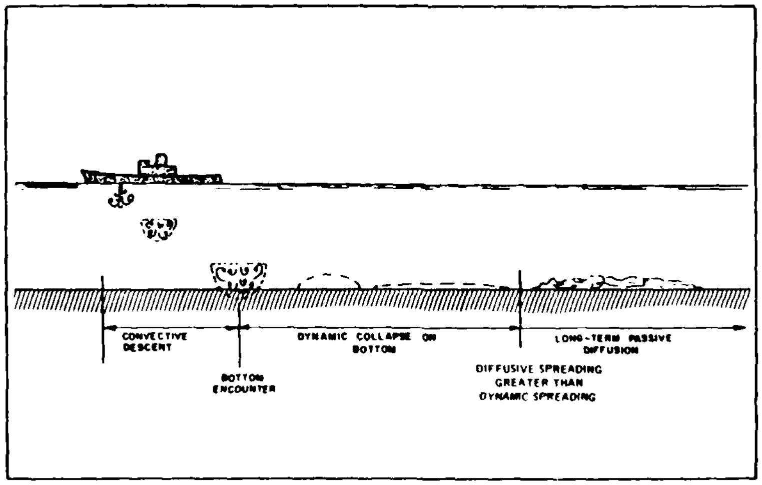
CONVECTIVE DESCENT
DYNAMIC COLLAPSE ON BOTTOM
LONG-TERM PASSIVE DIFFUSION
BOTTOM ENCOUNTER
DIFFUSIVE SPREADING GREATER THAN DYNAMIC SPREADING

Figure 2. Illustration of idealized bottom encounter after instantaneous dump of dredged material (from Brandsma and Divoky)

During convective descent, the dumped material cloud grows as a result of entrainment. Eventually, either the material reaches the bottom, or the density difference between the discharged material and the ambient fluid becomes small enough for a position of neutral buoyancy to be assumed. In either case, the vertical motion is arrested and a dynamic spreading or collapse in the horizontal direction occurs. The basic shape assumed for the collapsing cloud in he water column is an oblate spheroid. For the case of collapse on the bottom, the cloud takes the shape of a general ellipsoid and a frictional force between the bottom and the collapsing cloud is included. When the rate of horizontal spreading in the dynamic collapse phase becomes less than an estimated rate of spreading due to turbulent diffusion, the collapse phase is terminated and the long-term transport-diffusion begins. During collapse, solid particles can settle as a result of their fall velocity. As these particles leave the main body of material, they are stored in small clouds that are assumed to have a Gaussian distribution. The small clouds are then advected horizontally by the imposed current field. In addition, the clouds grow both horizontally and vertically as a result of turbulent diffusion. Since settling of the suspended solids occurs at each grid point, the amount of solid material deposited on the bottom and a corresponding thickness are determined. As previously noted, no subsequent erosion of material from the bottom is allowed.

Required Input Data

The required input data to DIFID can be grouped into (a) a description of the ambient environment at the disposal site, (b) characterization of the dredged material, (c) data describing the disposal operation, and (d) model coefficients.

The first task is that of constructing a horizontal grid over the disposal site. Ambient conditions on the grid can be represented by (a) a constant water depth and time invariant velocity, (b) a time varying depth-averaged flow field, or (c) a time varying three-dimensional flow field. In each case, a single water density profile at the deepest point on the grid must be prescribed.

The dredged material can be characterized by as many as 12 solid fractions, a fluid component, and a conservative chemical constituent. For each solid fraction, its concentration by volume, density, fall velocity, voids ratio, and an indicator as to whether or not the fraction is cohesive must be input. In addition, the bulk density and aggregate ratio of the dredged material must be prescribed.

Disposal operations data required include the position of the barge or hopper on the horizontal grid, the volume of material dumped, and the loaded and unloaded draft of the disposal vessel.

There are 14 model coefficients in DIFID. Default values are contained in the code that reflects the model developer's judgment. However, the user may input other values. Computer experimentation such as that presented by Johnson and Holliday (1978) has shown that results appear to be fairly insensitive to many of the coefficients. The most important coefficients are drag coefficients in the convective descent and collapse phases as well as coefficients governing the entrainment of ambient water into the dredged material cloud. The values selected for the entrainment and drag coefficients in this study were based upon experimental work done by JBF Scientific (1978).

Alcatraz Disposal Site Study

Background

The Alcatraz disposal site in San Francisco Bay, shown in Figure 3, is a dispersive site that is not intended to accumulate disposed material (Figure 1). The strong tidal currents at the site are expected to transport most of the disposed material from the bay toward the Golden Gate bridge and out to sea. The disposal site has been in use for about 90 years. For the last 10 years, it has been the only authorized open-water disposal site within the central San Francisco Bay. Historically, depths within the site have ranged from about 70 to greater than 120 ft mllw.

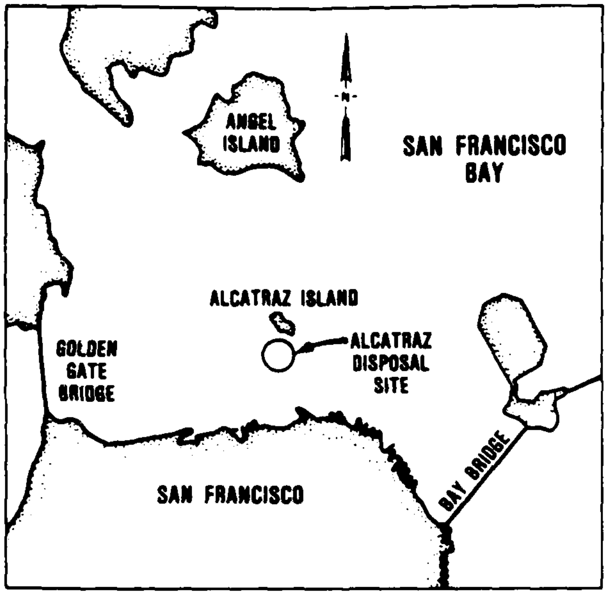

Figure 3. Location of Alcatraz disposal site

A recent hydrographic survey revealed a loss of depth at the site and raised questions as to the site's ability to disperse future new work and maintenance material dredged from bay navigation projects. The survey showed that a mound of material existed within the eastern half of the disposal site, resulting in a loss of depth to as little as 28 ft as shown in Figure 4. The loss of depth is a problem for two reasons. First, the site is located in the established shipping lane, thus requiring a depth of 40 ft. Second, since this is the only authorized central bay disposal site, abandonment of this site could mean that dredged material disposal would become much more expensive if an alternate site were selected and approved that was more distant from dredging sites.

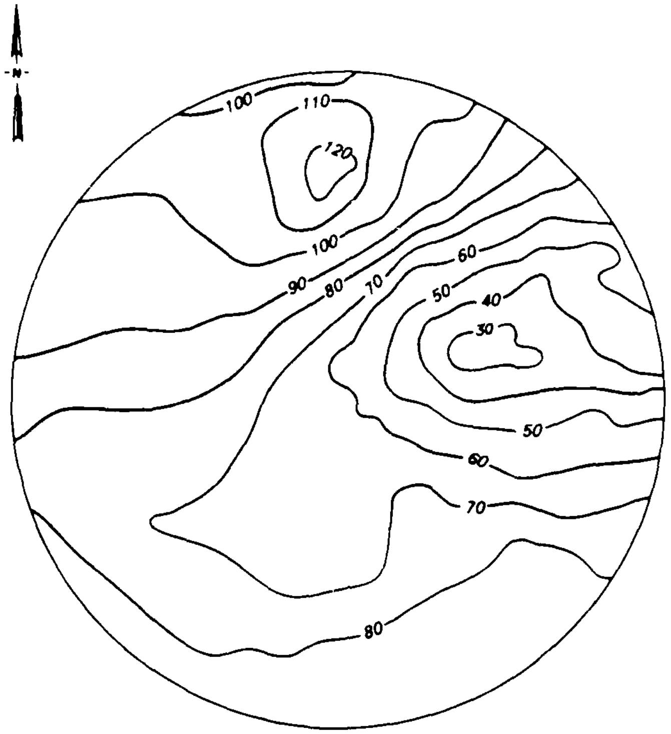

Figure 4. Alcatraz disposal site depth contours from 11 January 1984 survey

Objective

The objective of the Alcatraz site investigation described in the paper was to estimate (a) the percent of material dumped at the mound location during strength of ebb, which initially deposits within the disposal site limits, and (b) the percent of material dumped in the deeper northern zone of the site every 2 hours over a complete tidal cycle which initially deposits within the disposal site limits.

Approach

The approach was to simulate the dumping of dredged material using the computer model DIFID. The model predicted the portion of the dumped material that was transported from the disposal site by ambient currents before striking the bay bottom and the portion that was deposited within the disposal site for each of the conditions and material tested.

Test Conditions

Disposal site currents collected on the San Francisco Bay-Delta physical model for five different hydrodynamic conditions were used for the Alcatraz disposal simulations (Tetra Tech 1984). The five hydrodynamic conditions tested in the physical model were as follows:

Series	Tide Range	Delta Net Outflow, cfs
11	19-yr mean	4,400
12	19-yr mean	40,000
21	neap	4,400
22	neap	40,000
31	spring	4,400

The tidal currents used in DIFID were based on those obtained from the physical model tests, which did include the recent bathymetry at the Alcatraz site. At the mound location dump spot, which was conducted for all five conditions (Series 11, 12, 21, 22, and 31), the strength-of-ebb currents ranged from about 6 ft per sec for the Series 11 condition to about 7.5 ft per sec for the Series 31 condition. At the North Zone dump spot, which was conducted for the Series 11 condition only, currents ranged from a strength-of-ebb current of about 2.5 ft per sec to a strength-of-flood current of about 1.5 ft per sec.

The dump spots are shown in Figure 5. The mound location dumps occurred at strength of ebb only. The North Zone dump schedule, imposed on the tidal currents at the dump spot, is shown in Figure 6.

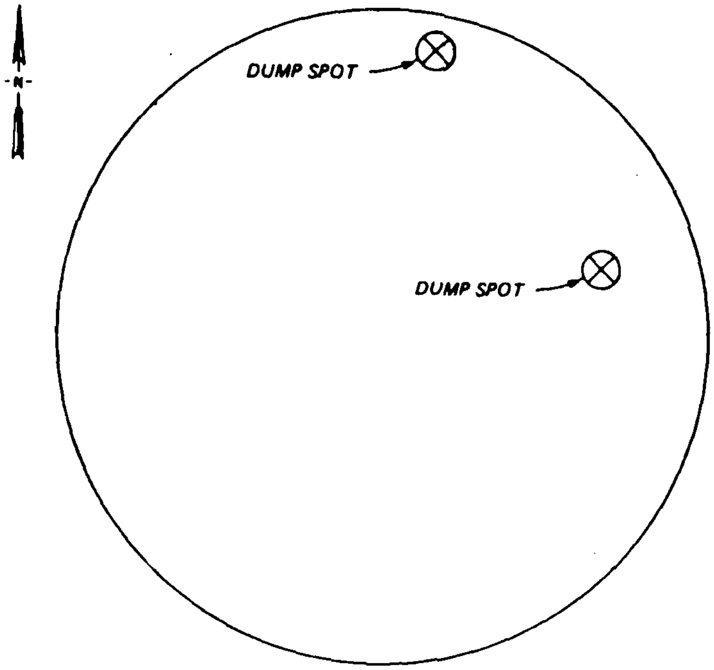

Figure 5. Dump locations

The material simulated in the mound location dumps consisted of 60 percent clay-silt and 40 percent fine sand. The bulk density of the barge slurry was 1.44 gm/cc, resulting in a moisture content of about 74 percent. The dump size was 1,000 cu yd. Testing included a slurry with no clumps to simulate barge material obtained from a hydraulic dredging operation and a slurry in which 30 percent of the clay-silt fraction was in the form of clumps or clods to simulate barge material from a clamshell or bucket dredging operation.

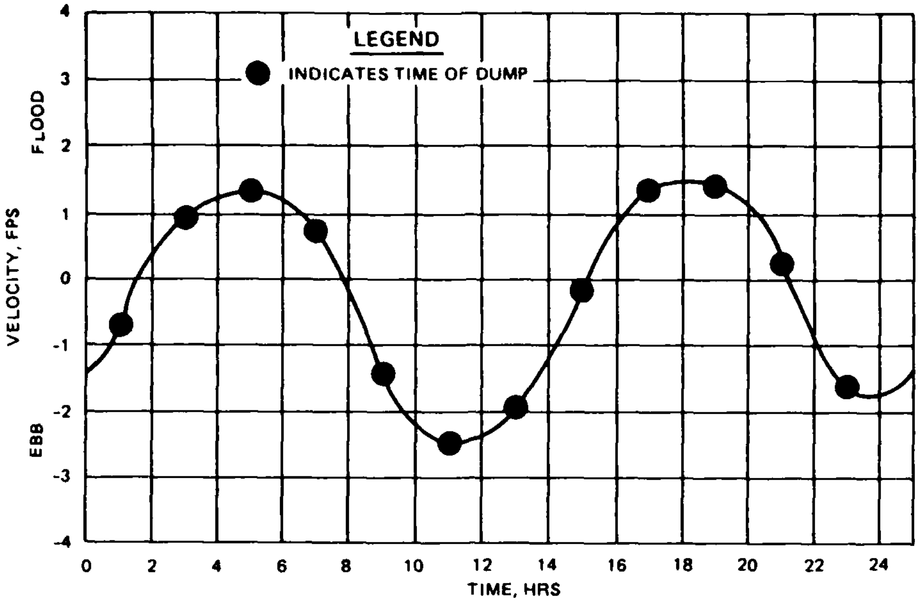

Figure 6. Dump schedule for North Zone dumps

Three materials were simulated in the North Zone dumps. The first material tested contained 60 percent clay-silt and 40 percent sand. The sand fraction was classified as one-third fine, one-third medium, and one-third coarse sand. The second material tested contained 80 percent clay-silt and 20 percent sand. The sand fraction was classified as one-half fine sand and one-half medium sand. The third material tested contained 95 percent clay-silt and 5 percent fine sand. The bulk density of the hopper dredged slurry was 1.35 gm/cc for all materials dumped at the North Zone location, corresponding to a moisture content of 79 percent. The dump size was 4,000 cu yd.

Results

For the dumps at the mound location, DIFID estimated the initial deposition of material within the disposal site and on the mound for the five conditions tested. The summary results are shown in Table 1.

For the dumps at the North Zone location, DIFID estimated the initial deposition of material within the disposal site. To evaluate model results, the Alcatraz disposal site was divided into four equally sized zones, referred to as the north, east, south, and west zones, as shown in Figure 7.

Table 1

Mound Location Dumps
Deposition of Each Fraction of Material in Percent
from a 1,000-Cubic Yard Maximum Ebb Dump

	Deposition					
Series	Site Sand	Mound Sand	Site Silt-Clay	Mound Silt-Clay	Site Clumps	Mound Clumps
			No Clumps			
11	24	17	15	12	NA	NA
12	29	19	15	12	NA	NA
21	27	17	13	12	NA	NA
22	29	18	15	12	NA	NA
31	20	12	7	5	NA	NA
			30 Percent Clumps			
11	25	17	10	7	100	100
12	29	19	12	8	100	100
21	23	17	11	7	100	100
22	29	18	11	7	100	100
31	18	12	9	5	99	87

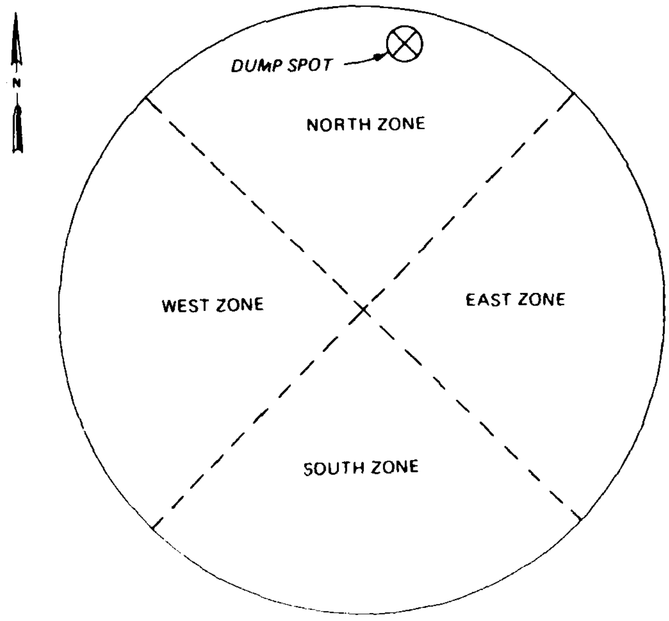

Figure 7. Zone designations for North Zone dumps

23. The summary results for each of the three materials tested are tabulated as follows:

Table 2

North Zone Dumps
Initial Deposition in Percent by Zone
over a Tidal Cycle

Zone	Clay-Silt	Fine Sand	Medium Sand	Coarse Sand	Total
			Material #1		
North	52	53	66	90	59
East	8	6	4	1	6
South	0	1	0	0	0
West	11	15	8	4	10
Site	71	75	78	95	76
			Material #2		
North	49	52	63	--	51
East	8	7	3	--	8
South	0	0	0	--	0
West	12	11	9	--	11
Site	68	70	75	--	70
			Material #3		
North	51	49	--	--	51
East	7	7	--	--	7
South	1	0	--	--	1
West	11	11	--	--	11
Site	70	67	--	--	70

Puget Sound Generic Study

Background

The Seattle District is assessing Puget Sound dredged disposal site alternatives for future dredged material derived from new work and maintenance dredging activities. The potential open water sites are located in water depths ranging from about 100 to 800 ft. Currents range from still water to as great as 2 knots. A key factor in the feasibility of each disposal site is the ability to place disposal material within the defined boundaries of each site without significant dispersal beyond these limits.

At this time, the study has not been completed and results have not been fully evaluated. Interim results will be discussed in this paper.

Objective

The objective of the investigation described in this paper is to predict the short-term fate of material representative of the type dredged in maintenance activities in the Puget Sound area and barge dumped in waters with depths of 100, 200, 400, 600, and 800 ft and ambient currents ranging from 0 to 2 knots (3.38 fps).

Approach

The approach being used is to simulate the barge disposal of dredged material with the numerical dump model DIFID. The model predicts the deposition pattern of disposed material for the various conditions being tested. A brief description of the model is given earlier in this paper.

Test conditions

To date a total of 30 dumps have been simulated using DIFID. Water depths ranged from 100 to 800 ft; the ambient currents ranged from 0.1 to 3.38 fps; and the barge bulk density varied from 1.35 to 1.48 gm/cc. The model grid represents a bottom area of 12,000 by 12,000 ft. Each grid cell represents an area 400 by 400 ft in size. The material simulated in the barge dump consisted of 25 percent fine to medium sand and 75 percent silts and clays. The typical barge bulk density ranged from 1.35 to 1.48 gm/cc, resulting in water content ranging from 79 to 71 percent of the total slurry, respectively. The characterization of the dredged material in DIFID included for each solid fraction its concentration by volume, density, fall velocity, voids ratio, as well as aggregate voids ratio and bulk density.

The duration of each test was 60 minutes after the barge dump. To be representative of a typical disposal barge in the Puget Sound area, the dump volume was 1,500 cu yd for all tests.

Discussion of interim results

Interim results to date indicate that material from dumps in the shallower depths (100 and 200 ft) is deposited within relatively small bottom areas, as long as the ambient current is less than about 1 fps. As the current magnitude exceeds 1 fps, the finer portion of the disposed material is transported further away from the dump spot before depositing, possibly outside of proposed disposal site limits.

For the deep water dumps (600 and 800 ft), material dumped into still water may deposit within an area approximately the size of a typical designated disposal site, but the imposition of an ambient current causes deposition of the finer portion of the material to occur at bottom locations far removed from the dump spot.

As noted earlier, the above results are preliminary. Additional testing is being conducted and analysis of model runs has not been completed.

Acknowledgments

The work described here was funded by the U.S. Army Engineer Districts, San Francisco and Seattle. Permission to publish this paper was granted by the Office, Chief of Engineers.

References

Brandsma, M. G., and Divoky, D. J. 1976. "Development of Models for Prediction of Short-Term Fate of Dredged Material Discharged in the Estuarine Environment," Contract Report D-76-5, US Army Engineer Waterways Experiment Station, Vicksburg, Miss.

JBF Scientific Corporation. 1978 (Sep). "Calibration of a Predictive Model for Instantaneously Discharged Dredged Material," R-804994, Wilmington, Mass.

Johnson, B. H., and Holliday, B. W. 1978. "Evaluation and Calibration of the Tetra Tech Dredged Material Disposal Models Based on Field Data," TR D-78-47, US Army Engineer Waterways Experiment Station, Vicksburg, Miss.

Johnson, B. H. _____. "User's Guide for Dredged Material Disposal Models for Computing the Short-Term Physical Fate at Open Water Sites," in preparation.

Koh, R.C.Y., and Chang, Y. C. 1973. "Mathematical Model for Barged Ocean Disposal of Waste," Environmental Protection Technology Series EPA 660/2-73-029. US Environmental Protection Agency, Washington, DC.

Tetra Tech. 1984 (Feb). "Report on the Study of Currents at the Alcatraz Disposal Site, San Francisco Bay-Delta Model," Draft Report, prepared for US Army Engineer District, San Francisco, Calif.

DREDGE CUTTERHEAD FLOW PROCESSES

Larry S. Slotta *

ABSTRACT -- Feasibility studies of new dredge intake and cutterhead shielding techniques were conducted to improve hydraulic cutterhead dredge performance. Simple modification of the suction mouth to the intake piping, and utilizing both internal as well as external dredge cutter shrouds, have been found to significantly improve the production of a cutter suction dredge model.

INTRODUCTION

In sustaining the nation's navigable waterways, the USACOE annually dredges over 400 million cubic yards in maintenance dredging operations and over 200 million cubic yards in new work dredging at a (1976) cost over $150 million. Much of this work is contracted out competitively to independent dredgers. Surprisingly, dredging work is difficult to obtain as the work is spread seasonally and spatially into small work packages. The result is that about half of the USA contractor-owned dredging fleet is idle at any given time. With a bleak economic outlook, the private dredging contractors are unmotivated to upgrade and modernize dredging equipment to operate more efficiently or to reduce environmental impacts caused during dredging operations in rivers and estuaries.

NSF-SBIR support was received for investigating the economic effect on dredging production of cutterhead dredges through simple design modifications such as adding on cutterhead shields, making minor changes to the cutterhead form, and properly placing the suction inlet relative to the cutterhead rotation. The ultimate goal was to provide the dredging industry with cutterhead and suction inlet design concepts that would increase the excavation and production efficiency of hydraulic cutterhead pipeline dredges, and accordingly reduce objectionable turbidity currents frequently created by dredges operating in waterways.

Computer model simulations were used to investigate the processes of soil movement and transport by a confused 3-D flow field affected by complex boundaries, rotating cutterblades, variable flow rates and positioning of the intake to the dredge pump. Rotational speed, haul velocity, depth of suction inlet, and cutterhead shielding techniques were verified and tested during hydraulic model simulations. Suction inlet types, internal cowls and external shields utilized in these feasibility studies are shown in Fig. 1.

* President, Slotta Engineering Associates, Inc., PO Box 1376,
Corvallis, Oregon 97339

For both computer model and hydraulic model simulations, a cylindrical shaped disc cutter was utilized as a basic model. Evaluations of the cylindrical cutter can easily be extended to basket type cutters. The characteristic feature of the cylindrical shaped disc cutter (Fig. 1H) is the potential optimal positioning of the suction mouth which extends into the interior of the cutter towards the rotating blades. High suction velocities to a reentrant suction mouth would reduce the recirculation of the soil cuttings within the cutterhead's crown. This suction mouth can be turned towards the direction of cut to improve the inflow to the pump intake.

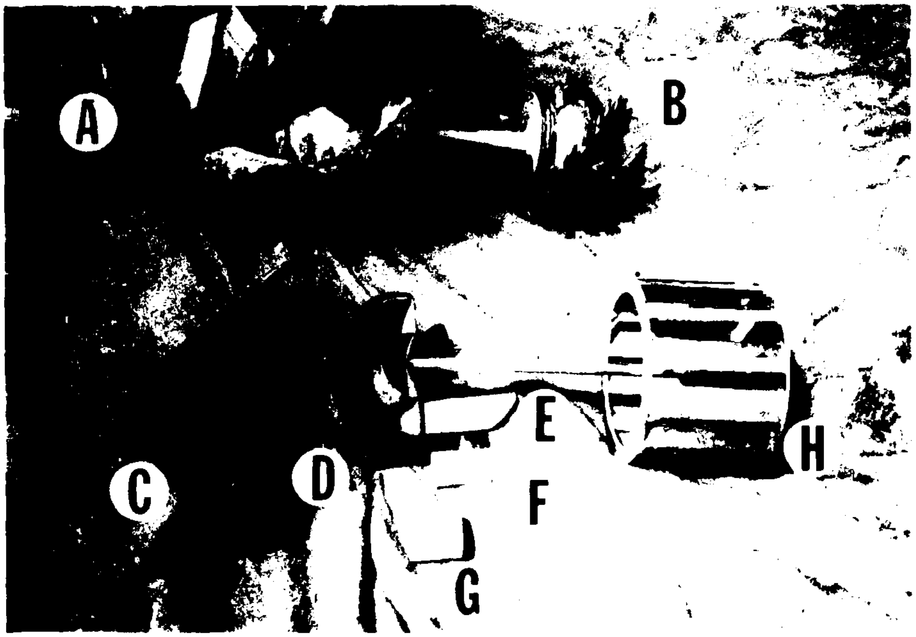

Figure 1. A: crown shaped cutter (1:6 scale, 19 inch diameter, 16 inch long; B: crown shaped cutter (1:12 scale, 9 inch diameter, 6 inch long); C: dog-eared cutter shroud; D: half cylinder inner core; E: 45° beveled suction mouth; F: long beveled suction mouth; G: small reentrant suction mouth; H: 12 bladed cylindrical cutterhead (1:12 scale, 9 inch diameter, 6 inch long).

COMPUTER CODES

Complex computer codes recently made available by CHAM Ltd. (Concentration, Heat and Momentum Limited, Bakery House 40 High Street, Wimbledon, London SW195AU ENGLAND) and CREARE R&D, Inc. (CREARE R&D, Inc., PO Box 71, Hanover, New Hampshire 03755), provide 3-D results of turbulent two-phase flows past moving boundaries. Sediment transport into the moving blades of rotating dredge cutterhead were simulated using both CHAM Ltd.'s PHOENICS and CREARE R&D Inc.'s FLUENT codes.

CHAM Ltd. developed a software package designed for the simulation of fluid-flow, heat-transfer, mass-transfer and chemical-reaction processes. It is called PHOENICS, which stands for Parabolic, Hyperbolic or Elliptic Numerical Integration Code Series. In the parabolic form, effects do not propagate upstream; in the elliptic form, effects do propagate upstream; and in the hyperbolic form effects propagate along "characteristics."

PHOENICS uses a finite difference numerical procedure to solve the fundamental equations governing fluid flow (the Navier-Stokes equations). Built into PHOENICS are the major laws of conservation: the mass of each present phase, the three components of momentum for each phase, the thermal-energy contents of each phase, the mass concentration of each chemical species, the energy and length scale of the turbulence and the fluxes of radiation. The equations include individual terms expressive of the processes of convection, diffusion, generation and destruction, and appropriate accounting of the interactions of turbulence with the laminar-flow phenomena.

With CHAM Ltd.'s PHOENICS code a cylindrical model was numerically created to represent a simplified dredge cutter having four blades or arms. Figs. 2 to 5 are representative of these PHOENICS graphics. Fig. 2 is a perspective view of a rotating four blade cutter with a velocity field located at one-tenth the cutter length. The outflow of water to the suction mouth located at the six o'clock backplate position is clearly represented. Fig. 3 shows an end view of the cutterhead, orthogonal to the drive axis and cutter blades. The rotational velocity field about the blades accelerating into the suction mouth illustrates some of the flow representations possible with PHOENICS graphics routine. Fig. 4 is a perspective composite of the previous information, including: cutterhead shape, blade position, velocity field near the backplate and the flow paths of particles released at "tenth" positions long the top of the cutterhead. Superposed on Fig. 5 are the flow trajectories of particles cut from the 12 o'clock position.

The PHOENICS code utilizes an Eulerian approach in which the fluid density in a cell of a computational grid is uniform and continuous. However, the density in an adjacent cell can be designated as having a different value, thus allowing for two-phase flow calculations.

The two-phase flow test representation used a submerged vertical suction pipe held above a sand bed. Fig. 6 shows the sediment velocity flow field on the right while sediment volume fractions are presented on the left. By examining the break in the sediment volume fractions one observes the zone of sediment pickup into the suction mouth. These results are being analyzed in reference to previous physical model data on the threshold pickup zone of sand taken into a suction intake. See Figs. 8a (Slotta, 1968) and 8b (Gladigau, 1975). The results show similarities to potential flow techniques and physical measurements reported by H. Salzmann (1977) and S. B. Brahme

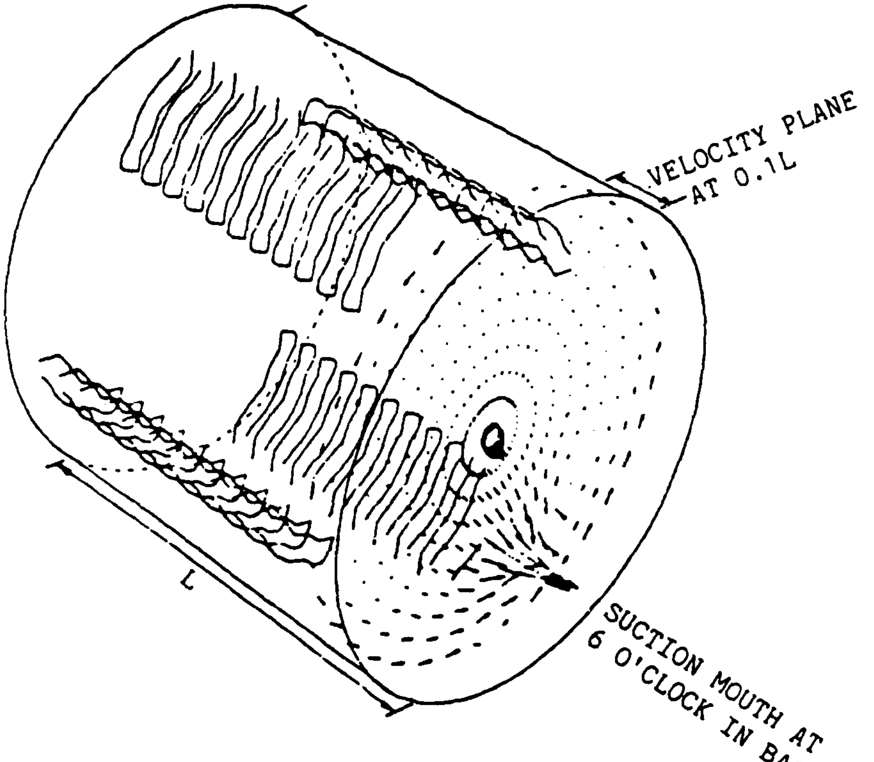
VELOCITY PLANE
AT 0.1L
L
SUCTION MOUTH AT
6 O'CLOCK IN BACKPLATE

Figure 2
Cylindrical dredge cutterhead flow simulations

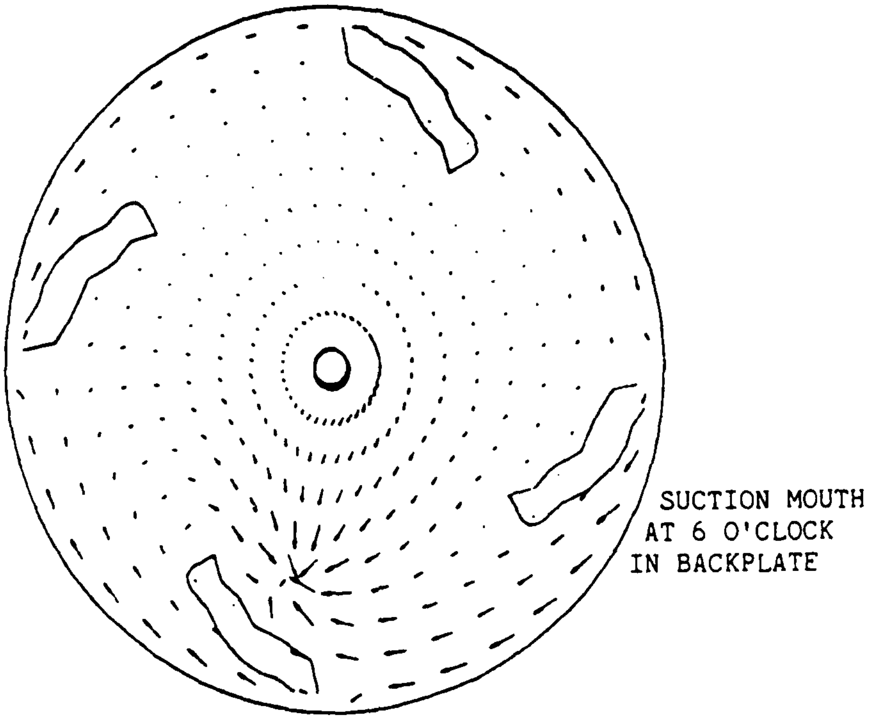
SUCTION MOUTH
AT 6 O'CLOCK
IN BACKPLATE

Figure 3
Cylindrical dredge cutterhead flow simulations

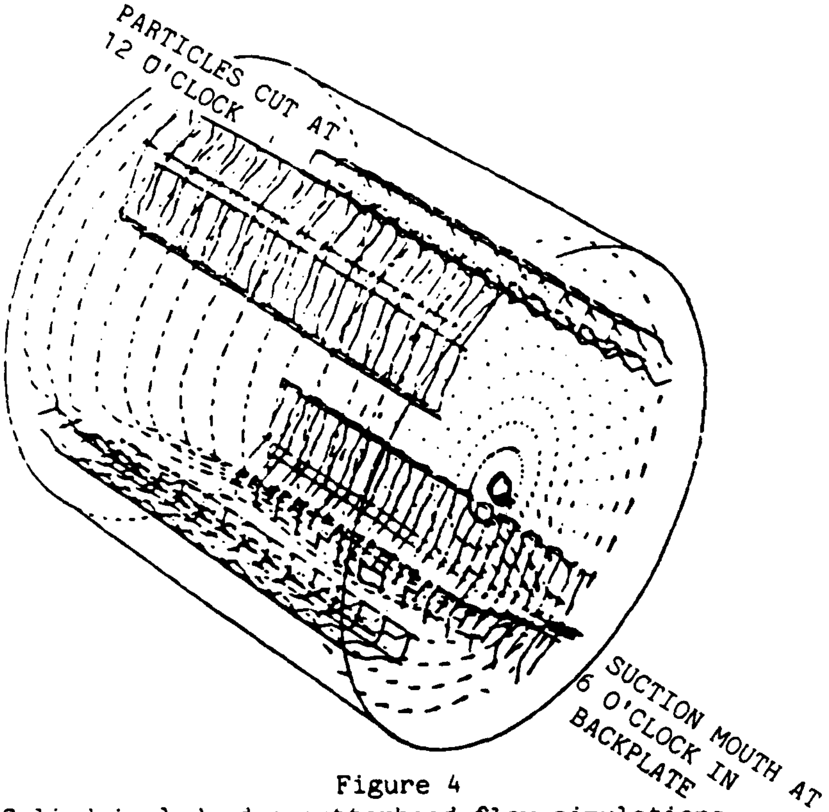
PARTICLES CUT AT 12 O'CLOCK
SUCTION MOUTH AT 6 O'CLOCK IN BACKPLATE

Figure 4
Cylindrical dredge cutterhead flow simulations

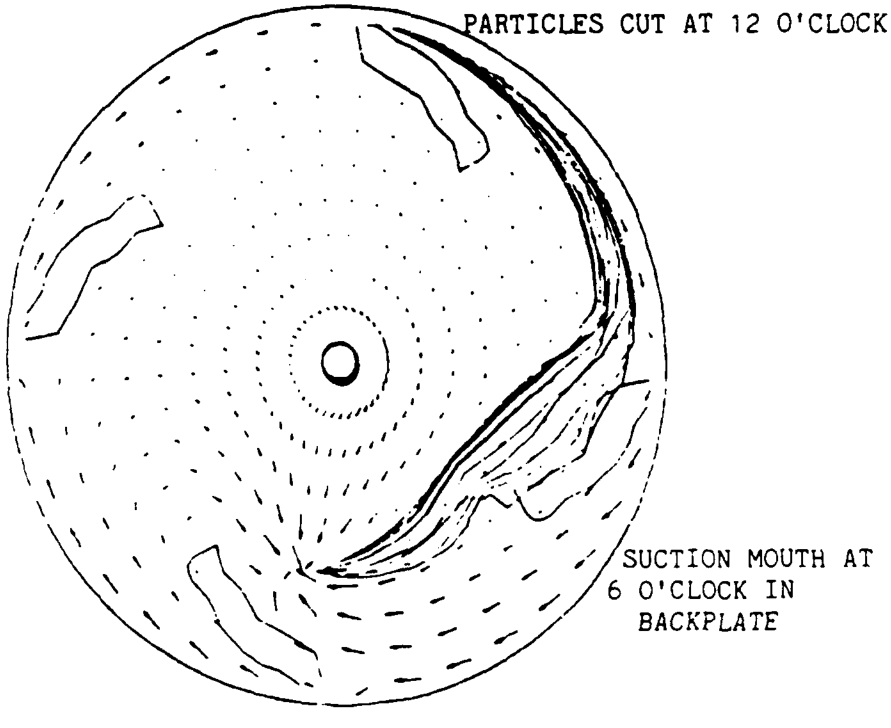
PARTICLES CUT AT 12 O'CLOCK
SUCTION MOUTH AT 6 O'CLOCK IN BACKPLATE

Figure 5
Cylindrical dredge cutterhead flow simulations

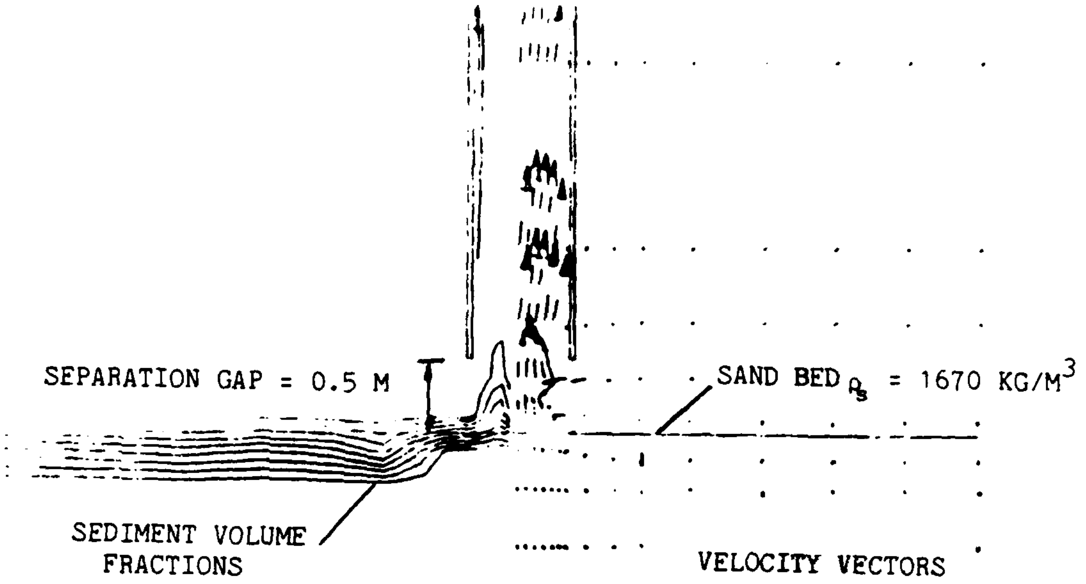
SEPARATION GAP = 0.5 M
SAND BED ρ_s = 1670 KG/M^3
SEDIMENT VOLUME FRACTIONS
VELOCITY VECTORS

Figure 6
Sediment pickup simulation

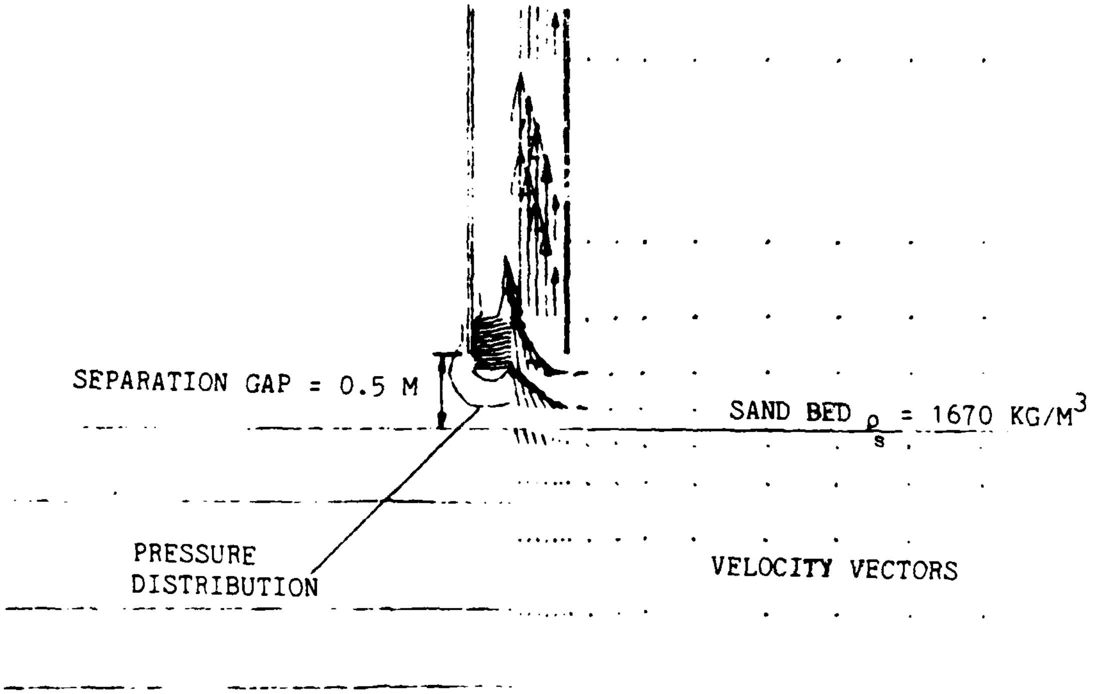
SEPARATION GAP = 0.5 M
SAND BED ρ_s = 1670 KG/M^3
PRESSURE DISTRIBUTION
VELOCITY VECTORS

Figure 7
Sediment pickup simulation

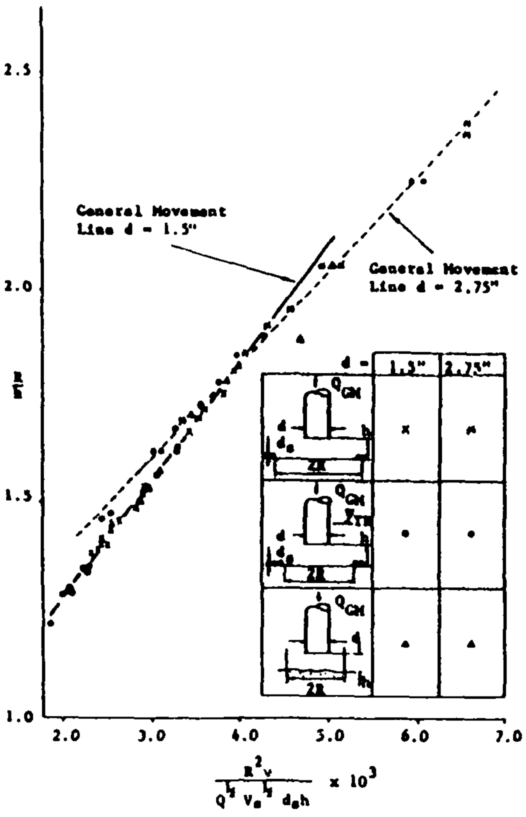

Figure 8a. Slotta's Relationship for General Movement (Slotta, 1968)

$$R/h = f\left(\frac{R^2\ \nu}{Q^{1/3}\ V_s^{1/3}\ d_s\ h}\right)$$

where R = radius of area of scour (L)
h = height of pipe above the bed (L)
f = functional relationship (-)
Q = flow rate (L^3/t)
V_s = sand settling velocity (L/t)
ν = fluid kinematic viscosity (μ/ρ) (L^2/t)
d_s = diameter of aggregate particles (L)

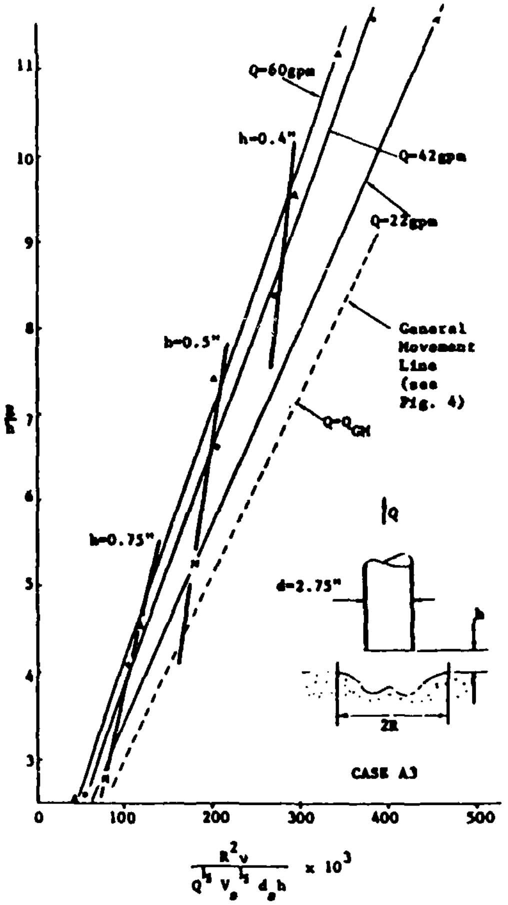

Figure 8b. Equilibrium Profile d = 2.75 inches (Gladigau, 1975)

(1983). In Fig. 7 the velocity and pressure field of flows up a 0.6 m (23.6 in) diameter intake tube with 0.03 m walls is represented. The flow is created by a negative pressure of one atmosphere within the intake pipe. For the sake of symmetry, water phase velocities are shown on the right while the pressure drops associated with the flow are shown on the left.

CHAM Ltd.'s staff believes PHOENICS can properly simulate sediment transport with the density continuum approach. A sand bed might appropriately be represented by a volume fraction in each grid cell of 0.6 solids and 0.4 fluid. Transient flow simulations using PHOENICS of the loosely packed soil revealed the bed to progressively settle with time under the action of gravity. In actuality, such a bed would remain rigid through granular interactions rather than collapse. As these computational studies are preliminary, plans have been made to continue to evaluate this code for properly representing the physics of sediment transport.

CREARE R&D, Inc. has developed a competitive user friendly, general purpose computer program for modeling fluid flow called FLUENT. FLUENT is made accessible to the user by means of an interactive menu driven interface for problem definition, computation, and powerful built-in graphics. FLUENT enables the fluids engineer to apply state-of-the-art computer simulation methods to analyze and solve practical design problems without costly, time-consuming programming.

FLUENT uses a finite difference numerical procedure to solve the fundamental equations governing fluid flow (the Navier-Stokes equations). Additional equations are solved for the conservation of the parameters of the k-e turbulence model, chemical species and enthalpy. Their numerical techniques involve the subdivision of the domain of interest into a finite number of control volumes or cells, the partial differential equations being discretioned over these cells to obtain sets of simultaneous algebraic relations. Presently FLUENT is programmed only for solving steady flow problems. The FLUENT code conveniently incorporates a Lagrangian method for utilizing marker particles of various grain sizes and densities. This is most useful for the portraying sediment transport through dredge cutters as shown in Figs. 9a to f. A present limitation of the FLUENT scheme is that particles can not be assembled as a bed but can only be introduced singly at a point or in a layer through a desired boundary.

FLUENT dredge cutterhead flow simulations are depicted in Figures 9a to f. By considering symmetry, only the left half of the cylindrical cutterhead was plotted and for clarity, the cutter blades were omitted. A range of soil particle diameters and densities were cut at different positions on the rotating cutterhead and their trajectories were plotted. The flow field vectors, as seen on a vertical plane below the axis of rotation, pass through a segmented gap in the backplate (Fig. 9a). Fig. 9b shows the trajectories of light particles (ρ = 1670 kg/m) released from the 12 o'clock position of the rotating cutterhead with a 45° angle; one particle is noted to enter the suction mouth. Fig. 9c represents the trajectories of a

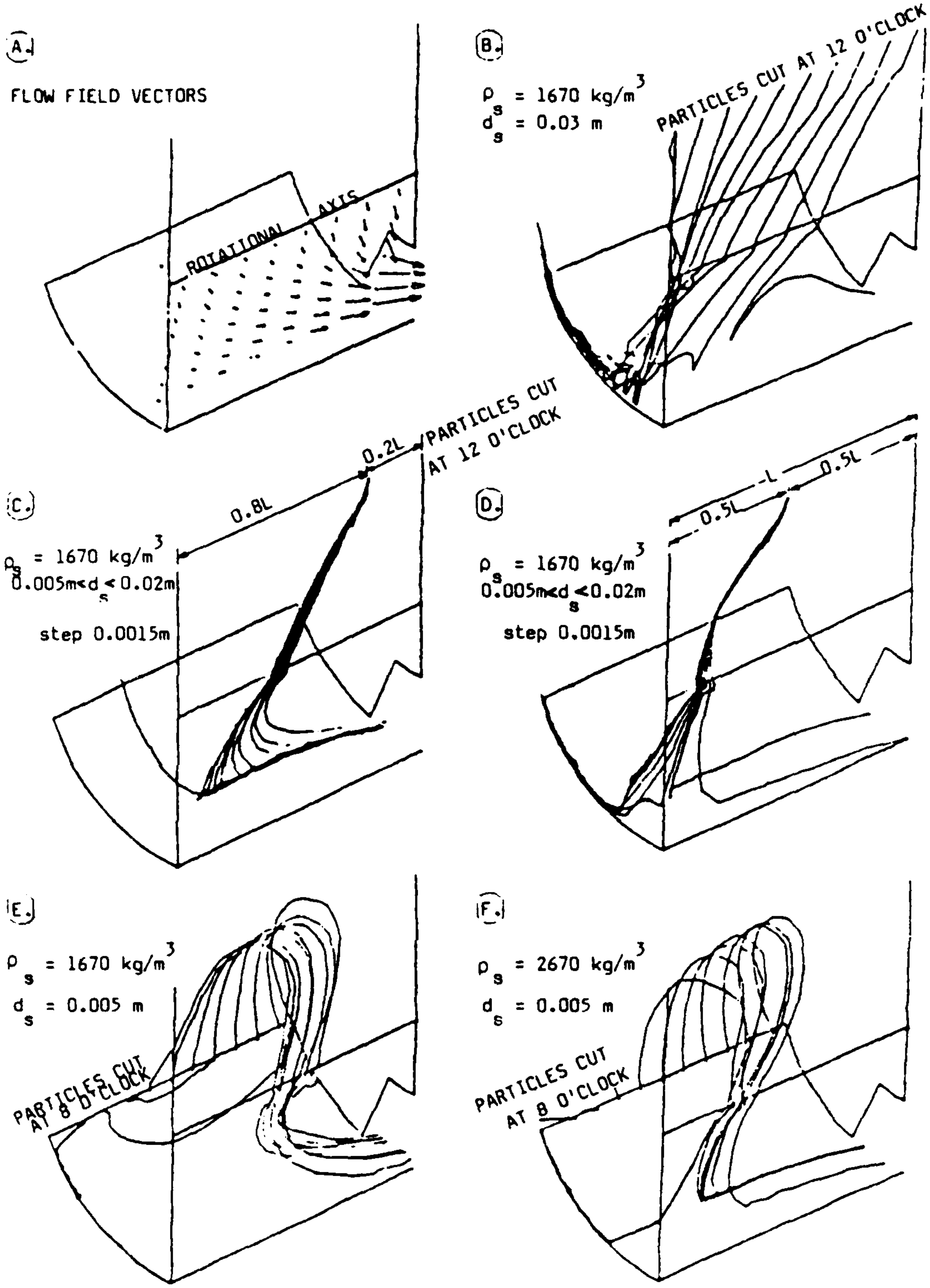
A.
FLOW FIELD VECTORS
ROTATIONAL AXIS
B.
ρ_s = 1670 kg/m^3
d_s = 0.03 m
PARTICLES CUT AT 12 O'CLOCK
C.
0.8L
0.2L
PARTICLES CUT AT 12 O'CLOCK
ρ_s = 1670 kg/m^3
0.005m<d_s<0.02m
step 0.0015m
D.
0.5L
L
0.5L
ρ_s = 1670 kg/m^3
0.005m<d_s<0.02m
step 0.0015m
E.
ρ_s = 1670 kg/m^3
d_s = 0.005 m
PARTICLES CUT AT 8 O'CLOCK
F.
ρ_s = 2670 kg/m^3
d_s = 0.005 m
PARTICLES CUT AT 8 O'CLOCK

Figure 9. Perspective view of cylindrical dredge cutterhead flow simulations, CREARE R&D, Inc.
Suction mouth at 6 o'clock in backplate.

range of particle diameters, having a constant (ρ = 1670 kg/m) density, which are released at the two-tenths length position at 12 o'clock; nearly all the grains escape. Fig. 9d represents similar conditions but the particle release point is midway along the cutter length; note only two particles escape while the others are trapped to recirculate about the crown of the cutter. Light (Fig. 9e) and heavy (ρ = 2670 kg/m)(Fig. 9f) particle trajectories are shown for release points near the 8 o'clock digging position. The light particles are nearly all drawn out the suction mouth whereas the heavy particles are not as successfully drawn into the intake.

In summary both the PHOENICS and FLUENT codes have exceptional 3-D graphics for representing hydraulic and hydrodynamic phenomena. The beginning availability of user friendly computer programs for solving complex three-dimensional flow fields involving gravity, viscosity, turbulence, and difficult boundary conditions of inflow and outflow is being witnessed. Problems, previously intractable by analytical or numerical techniques are now solvable. The results gained in these dredge studies cause one to remark that these hydrodynamic codes are at a stage corresponding to the state where finite element structural dynamics codes were ten years ago.

For cases involving dredge excavation technology, it would be preferable to have a user friendly hydrodynamic code which could represent a submerged static soil bed without collapsing as a function of time or being limited to having only a single layer of particles accessible for transport. Perhaps in the future, such user friendly hydrodynamic codes will be refined to properly represent sediment erosion and transport.

HYDRAULIC MODELS

A 1:12 hydraulic model test facility (Figs. 10 and 11) was utilized as a beginning step to validate the numerical models as well as to examine improved dredge cutter performance using simplex modification to the suction inlet. A nine-inch (0.23 m) diameter cylindrical shaped disc cutterhead model having a depth of six inches (0.15 m) was used to compare basic parameters including: angular rotational speed, haul velocity, ladder angle and the position of the suction inlet. The model cutterhead was mounted on an adjustable ladder connected to a frame holding a 1/8 hp gearmotor with a speed controller and a 18.3 m /hr or (0.18 cfs) pump. The rim of a 10 foot (3.04 m) by 3 foot (0.91 m) stock watering tank served as a track for four castor wheels under the carriage (Fig. 10).

Masonry sand with a mean grain size diameter of 0.5 mm (0.02 in) was hardpacked with the intent of representing hard digging of consolidated sediments and to insure reproducibility of results between runs. To consolidate the sand, a concrete-cement stinger or vibrator was first used for fluidizing the bed. Three 1.25 inch (0.03 m) perforated PVC pipe units were interconnected and placed at the bottom of the two foot (0.61 m) deep oval holding tank. Nylon netting was laid down over the pipe to prevent sand intake to the pipes. A consistently hard sand bed was prepared for each run by connecting the dredge pump intake to this network and running the pump for 20 minutes. Dense compaction of the sand was checked prior to excavation runs.

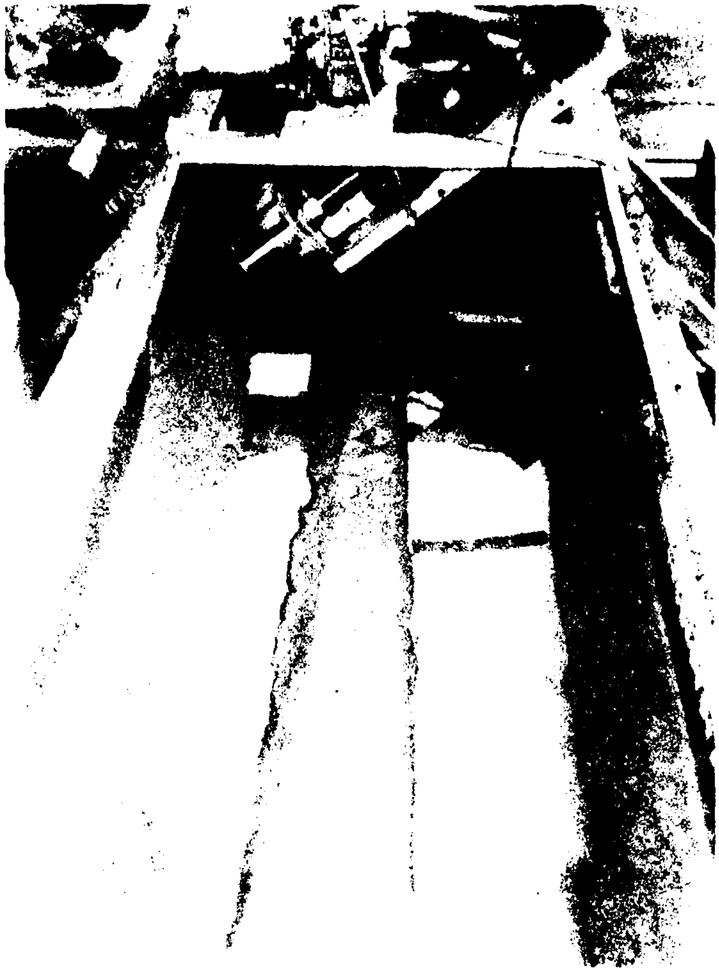

Figure 10. Three meter long cutterhead test dredge facility with water partially drained for viewing tracks of the dredge cuts.

The cutter production tests were run with haul velocities averaging 4.19 cm/sec (0.14 ft/sec) and average rotational speeds of 48 to 96 RPM. The average velocity in the 32 mm (1.25 in) suction mouth delivery line was 3.2 m/s (10.5 ft/s). The ladder inclination angle was set at 45° for all tests.

The hydraulic laboratory studies confirm that extending the intake pipe within the dredge cutter will significantly increase most hydraulic dredge's production. Tests compared: a) plain suction mouth, b) long extended mouth, c) 45° beveled mouth ("looking down"), d) 45° beveled mouth with an internal cowl and a dog-eared external shroud and e) 45° beveled mouth with a dog-eared external shroud (Fig. 11). Overcut and undercut mode results are plotted in Fig. 12. Cutter speeds are shown as a percentage of full speed of the drive. Accordingly, 100% corresponds to 160 RPM; 50%: 80 RPM; 40%: 64 RPM and 30%: 48 RPM.

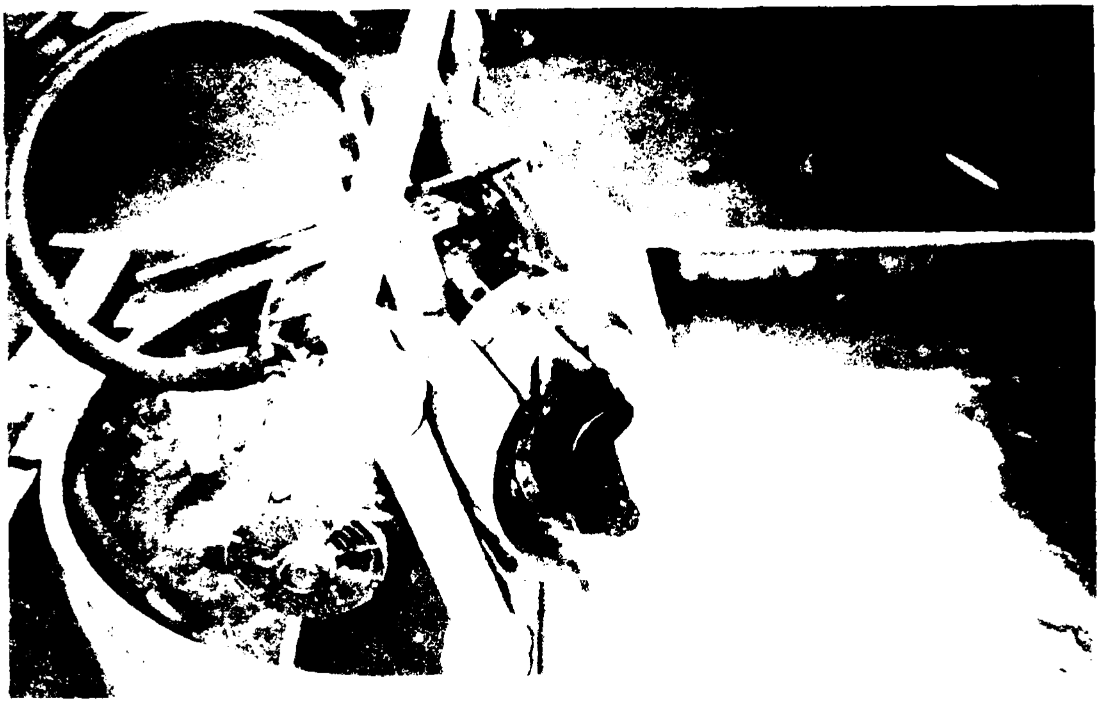

Figure 11. Cutterhead carriage tilted to allow examination of dog-eared cutterhead shroud, half cylinder internal cowl and extended 45° beveled suction inlet.

Hydraulic model summary results (Table 1) show that maximum production was observed in the undercut mode at 48 RPM and when the 45 beveled mouth and external shroud were used. The 45.5% solids by weight concentration corresponds to a 24% solids by volume discharge. This production is quite impressive when compared to that achieved by most operational dredges.

TABLE 1

SUCTION MOUTH INLET	MAXIMUM SEDIMENT PRODUCTION % SOLIDS BY WEIGHT	INCREASE IN PRODUCTION RELATIVE TO PLAIN SUCTION MOUTH (%)
OVERCUT---48 RPM(30%)		
PLAIN	11	0
LONG MOUTH	29	160
45° BEVELED MOUTH	36	225
BEVEL + SHROUD	36	225
BEVEL + SHROUD + COWL	41	227
UNDERCUT--48 RPM (30%)		
PLAIN	30	0
LONG MOUTH	30	0
45° BEVELED MOUTH	34.5	15
BEVEL + SHROUD	45.5	51.7*
BEVEL + SHROUD + COWL	41	36

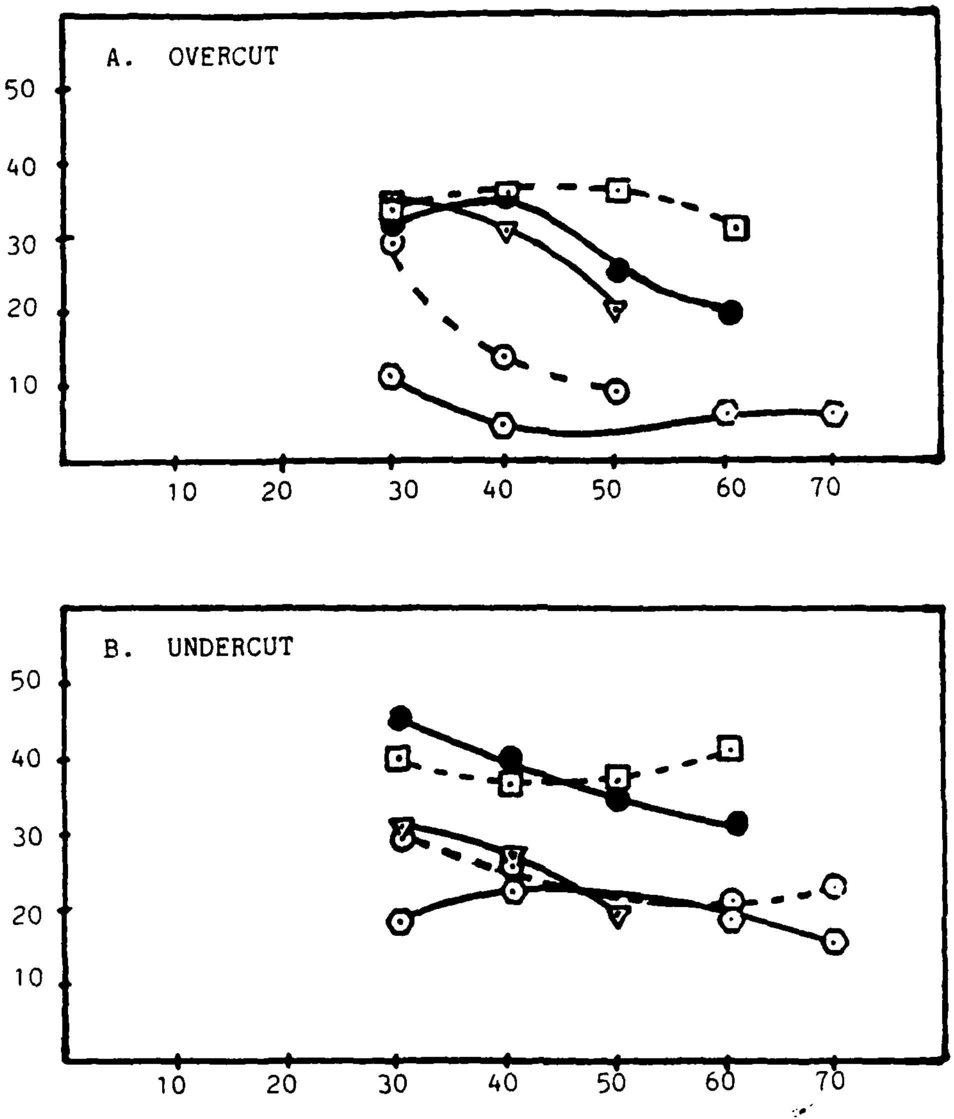

Figure 12. Plots of maximum production (% solids by weight) and cutter speed for different shroud, cowl, and intake conditions.

—○— PLAIN SUCTION MOUTH INTAKE

- -○- LONG MOUTH

—▽— 45° BEVELED MOUTH

- ⊡ - BEVEL, SHROUD, COWL

—●— BEVEL, SHROUD

CONCLUSIONS

This research involves both 3-D numerical analyses and hydraulic model studies of rotating machinery involved in submerged sediment excavation. These hydrodynamic codes were shown to have the promise of properly simulating complex, 3-D, rotating flows conveying water and sediments through dredge cutterheads. Hydraulic modeling showed that simple modifications to the suction intake and the addition of dog-eared external cutter shrouds and internal cowls gave marked increases of dredge production.

The results of more extensive confirming investigations could be used to encourage private contractors to easily and economically adapt their equipment to increase their dredging output, and in the course of operation, to reduce dredge-caused turbidity in the waterway being excavated.

These investigations, particularly advancing the use of numerical hydrodynamic flow simulations, could also assist the development of a broad-based methodology for more scientific studyies of drilling, tunneling and dredging equipment than what has been previously available.

ACKNOWLEDGEMENTS

The material herein was gained through work supported by the National Science Foundation under award number MEA-8360994. Any opinions, findings, and conclusions or recommendations expressed in this publication are those of the author and do not necessarily reflect the views of the National Science Foundation. NSF's support is gratefully acknowledged. Interest and communications on this project with Dr. John Weese, Director of NSF's Division of Mechanical Engineering and Applied Mechanics have been gratifying.

Dr. C. M. Aldham of CHAM, Ltd., Wimbledon, England is thanked for cooperative programming of PHOENICS hydrodynamic code results presented herein. Dr. Sengal of CHAM of North America, Huntsville, AL worked on two-phase flow representation using the PHOENICS code and his efforts are gratefully acknowledged. Ms. Barbara Hutchins of CREARE R&D, Inc. of Hanover, New Hampshire is thanked for programming the FLUENT code for particle size trajectories through a rotating dredge cutter.

SEA's staff are thanked for their help in seeing this work completed in a professional and timely manner: Ms. J. Milbrat did much to organize the report, Mr. T. Callahan in conducting the dredge head lab tests, Mrs. S. Shribbs did a most commendable job in typing the text of the paper.

Thanks are extended to ESCO Corporation, Riedel International, Inc., and DREDGEMASTERS International, Inc. for their continuing interest in dredging research.

APPENDIX 1. - REFERENCES

Brahme, S. B., "Environmental Aspects of Suction Cutterheads," Thesis, Texas A&M University, December 1983.

Gladigau, L. N., "An Appreciation of the Scale Effects of Solid/Liquid Flow in Dredging Studies," Thesis, University of Adelaide, February, 1975.

Salzmann, Helmut, "Fluid and Soil Mechanics Processes During Hydraulic Dredging," Franzius-Institut, Hannover, West Germany, February, 1977, (David R. Basco, Technical Editor, Translated by Gertrud M. Adam, Texas A&M University, College Station, Texas.).

Slotta, L. S., "Flow Visualization Techniques Used in Dredge Cutterhead Evaluation," Proceedings of WODCON '68 held in Rotterdam, Holland, published by World Dredging Conference, Palos Verdes Estates, California, 1968, pp. 56-77.

SEDIMENTATION RATES AND CHANNEL DEEPENING, MOUTH OF COLUMBIA RIVER

Craig H. Everts, M. ASCE[1]
Greg Hartman, M. ASCE[2]
Steve Chesser[3]

INTRODUCTION

An increase in the depth of the navigation channel through the bar at the mouth of Columbia River has been proposed. This paper discusses the results of a three-part investigation taken to forecast the rate of sedimentation that would exist if the channel was deepened from 55 to 63 ft and from 55 to 70 ft. An analysis of available bathymetric surveys and dredged volumes formed the basic data set used to establish past sedimentation rates. Causes of the sedimentation problem were evaluated based on independent variables thought to have a possible effect. Simple, mostly deterministic, hydraulic analyses were made to determine, semi-quantitatively, the effects future changes in those variables, including channel deepening, would have on sedimentation. A more detailed discussion of the investigation can be found in Ogden Beeman and Associates, and Moffatt & Nichol, Engineers (1985).

---

[1] Moffatt & Nichol, Engineers, 250 W. Wardlow Rd., Long Beach, CA 90807, (213) 426-9551

[2] Ogden Beeman and Assoc., 522 SW 5th Ave., Portland, OR 97204, (503) 223-8254

[3] Portland District, Corps of Engineers, P.O. Box 2946, Portland, OR 97208, (503) 221-6465

SEDIMENTATION HISTORY

Maintenance dredging is required throughout the navigable length of the Columbia River. The river mouth shoal (Fig. 1) requires the most extensive dredging. Two bars comprise that shoal. Sedimentation has been most prevalent on the Inner Bar. About four-fifths of the materials have accumulated on the south side of the channel and about one-fifth on the north side adjacent to and upstream of Disposal Area E (Fig. 1). Maintenance requirements at the Outer Bar have been negligable even though the navigation channel through the Outer Bar has been deepened almost 15 ft since 1955. At the Inner Bar sedimentation is near the edges of the channel; at the Outer Bar sedimentation is normal to and across the channel. Between 1978 and 1983 maintenance dredging averaged between 3×10^6 yd^3/yr and 3.5×10^6 yd^3/yr.

Prototype survey and dredging data from Portland District files were used to quantify past sedimentation rates where sedimentation is defined as the difference between the change in channel volume (surface to bottom) calculated using bathymetric survey data, and the volume of sediment dredged between two surveys. Two periods when major channel deepenings occurred, 1952-1961 and 1976-1981, were used to obtain sedimentation rates. The dredging rate for the period from 1945 to 1984 was evaluated with respect to its relationship to the sedimentation rate when new work is removed.

1. Sedimentation Rates. The average sedimentation rate and average channel depth are shown in Figure 2 for the period 1952-1961. Note the large increase in the sedimentation rate after the channel was deepened in 1956-1957. Most of the 60 percent increased rate of sedimentation occurred within 2 years after the 55-ft average depth was reached. Average depth is almost always greater than authorized depth because average depth is based on the entire channel reach through the bar. A similar increase was observed after other episodes of channel deepening.

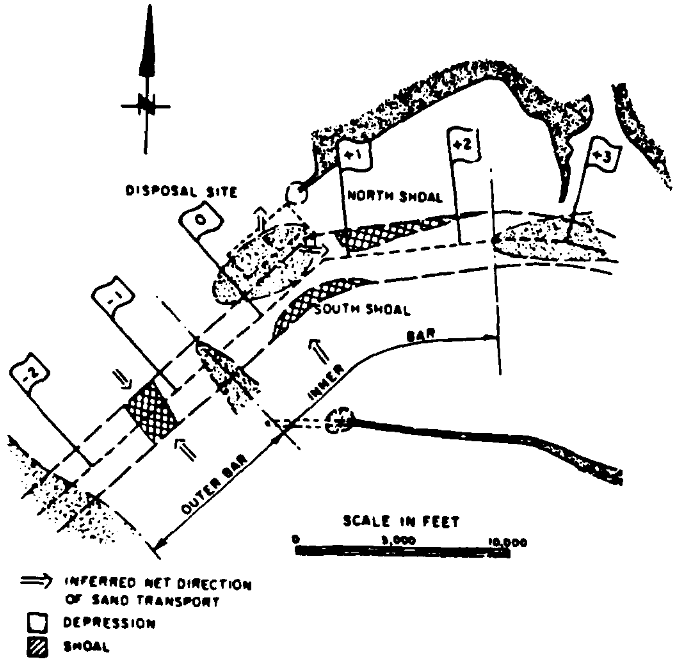
N
DISPOSAL SITE
0
-1
-2
+1
+2
+3
NORTH SHOAL
SOUTH SHOAL
INNER BAR
OUTER BAR
SCALE IN FEET
0
5,000
10,000
INFERRED NET DIRECTION OF SAND TRANSPORT
DEPRESSION
SHOAL

Figure 1. General morphology of the Inner and Outer Bars at the MCR.

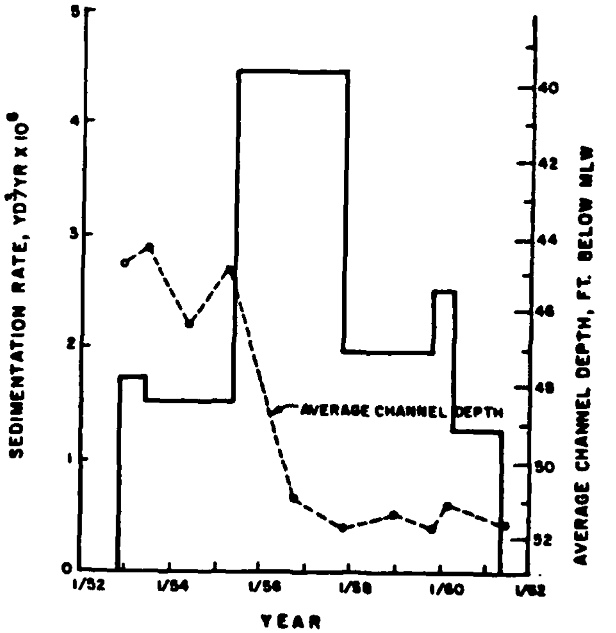

Figure 2. Sedimentation rate and average channel depth (channel water volume/channel plan area) for a 10-yr period. Since surveys indicated a volume decrease of 0.86x10^{6} yd^{3} between May 1953 and May 1955, while 3.89x10^{6} yd^{3} were dredged from the channel, the resulting sedimentation rate was 3.03x10^{6} yd^{3} in two years or 1.5x10^{6} yd^{3}/yr for that time period.

An historic bathymetric analysis shows the depression separating the Inner and Outer Bars deepened slightly but remained fixed in location between 1945 and 1984 (Fig. 3). Since the mid-1950's, however, the depression north of the channel has been deepening, expanding, and moving southward. This is the period after Disposal Area E was established (Fig. 1). Sediment disposed of within the depression at present does not remain there.

2. Bar Length. Bar length decreased by about 3000 feet between 1945 and 1984 (Fig. 3). A bathymetric analysis indicates a 25 ft/yr seaward shift in the center of mass of the Bar. Average channel depth (channel water volume/channel plan area) increased by about 7.5 ft in this period. A bar length decrease of 400 ft occurred per average depth increase of 1 ft, or about 75 ft/yr.

3. Channel Side Surfaces. After the channel was deepened, the undredged bottom adjacent to the channel deepened naturally because the dredged boundary could not stand vertically. Some or all of the material liberated as the side-surface depth increased was subsequently carried to and deposited in the newly-deepened channel.

Following channel deepening, two types of side-surface change were observed: (1) the slope of the side surface remains constant, but moves to a lower elevation, or (2) the side surface evolves to a steeper gradient and reaches a point of cross-section closure (or "pinch-out") some distance from the deepened channel boundary. Using bathymetric charts made from surveys taken at different times, it appears the near-constant type slope change was most common on the Inner Bar. Between 1935 and 1982 the region south and away from the channel experienced a gradual deepening while the sideslope remained constant at an average 0.008 (rise/run). This corresponds to a net sidewall volume readjustment (scour) of about 130 yd^3/ft (depth)-ft (channel length) for a 40-ft deep channel. This volume was depth-dependent and increased with depth. The time required for the side slopes to reach a stable or

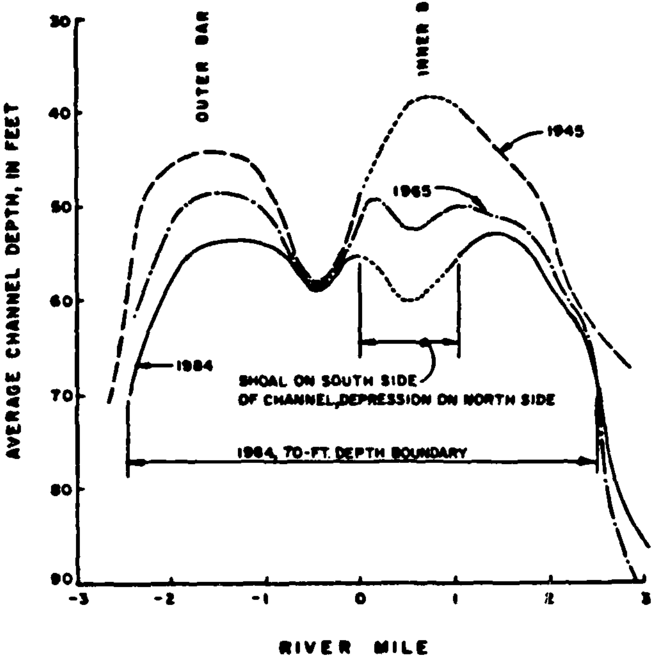

Figure 3. Profiles of the navigation channel in 1945, 1965 and 1984. Depth values are averages across the channel. Because of the three-dimensional nature of sedimentation on the bar, these profiles should be used only for general, qualitative purposes.

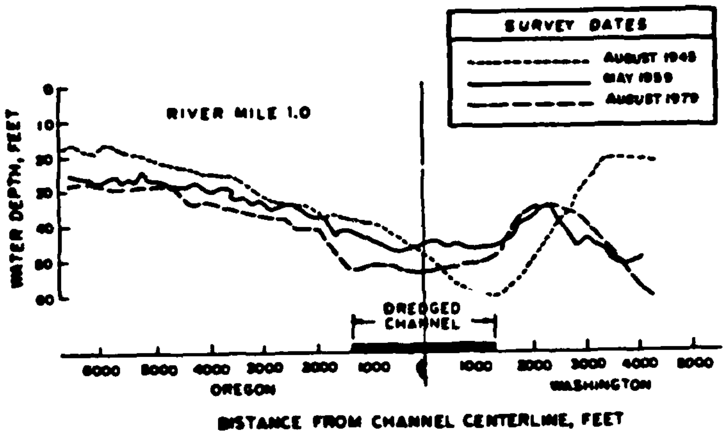

Figure 4. Changes in Inner Bar bathymetry adjacent to the navigation channel (side slopes) as the navigation channel was deepened. VERTICAL SCALE IS 70X HORIZONTAL SCALE.

equilibrium slope was 2 to 4 or more years when channel deepening was on the order of 5-ft. It would likely be greater if the depth increase was greater; perhaps 0.5 to 1 yr for each foot of depth increase.

4. Channel Orientation. From a sedimentation perspective, the ideal maintained channel is one that follows the maximum depth trace (thalweg) across a shoal area. Because of navigation practicability this is often not possible. Channel reorientation, however, should at least be considered when a deepening project is proposed, and/or when natural changes indicate the maintained channel is not positioned coincident with the natural deep trace. Both reasons apply to the Columbia River mouth at present. A recent (1965-1984) increase in depth north of and in the north one-half of the channel between River Mile (RM) 1.0 and RM -0.5 and in the south one-half the channel east of RM 2.0 (Fig. 1), indicate large savings could be achieved in the initial removal of sediment to deepen the channel below 55 ft if it were oriented to follow the thalweg.

Although strict adherence to the deep trace channel is not practical because of navigation considerations, some reorientation within navigation constraints might produce initial and future cost savings. The volume of sand that initially would require removal from within the present channel boundaries is 3 times as great at 63 ft and 2 times as great at 70 ft using present channel orientation as it would be if the deep trace channel were followed. Subsequent maintenance dredging rates would also probably decrease if the channel were oriented closer to the natural deep trace. Flow parallel to the axis of the channel will generally result in less sediment entering the channel than would occur when flow has a cross-channel component.

COMPONENTS OF THE SEDIMENT PROBLEM

Without an understanding of the causes of the sedimentation problem, estimates of sedimentation rates following channel deepening must rely soley on statistical extrapolations of past rates. Since great changes in the hydraulics and availability of sediment in the estuary and river system have occurred since surveys began, and will occur in the future, extrapolations without an understanding of causes is not recommended. Three casual components of the sedimentation rate were identified and investigated.

1. Outside Source Component. This is sedimentation that occurs more or less continuously because some or all of the sediment brought in from outside sources is deposited in the channel. Sand may reach the bar from upstream in the estuary and river, the ocean seaward of the bar, and beaches north and south of the river mouth.

The estuary and river will likely contribute less sand in the future as its channel is deepened because cross-section increases will reduce (slightly) flow velocities and the bed shear stress and, consequently, the rate at which sand is transported. A small present estuary contribution is indicated because Flavel Bar, located about 12-mi upstream (Fig. 5) at a salinity intrusion node, is a bottom flow convergence reach. Sand moving downstream in the navigation channel is preferentially trapped there. The channel further downstream, thus receives sand principally from sources below Flavel Bar in the ebb-dominated navigation channel. The North Channel (Fig. 5) is flood-dominated and there is not much liklihood that large quantities of sand reach Desdemona Bar and the mouth of the Columbia River from that source.

Disposal Area E (Fig. 1) is the site of an expanding depression and is quite likely also a present source of sand for the Inner Bar. Since at least 1958 (about the time Area E was established) the triangular area formed by the north side of the channel, the North Jetty, and Jetty A has been filling (there was a volume loss in this region between 1935 and 1958.

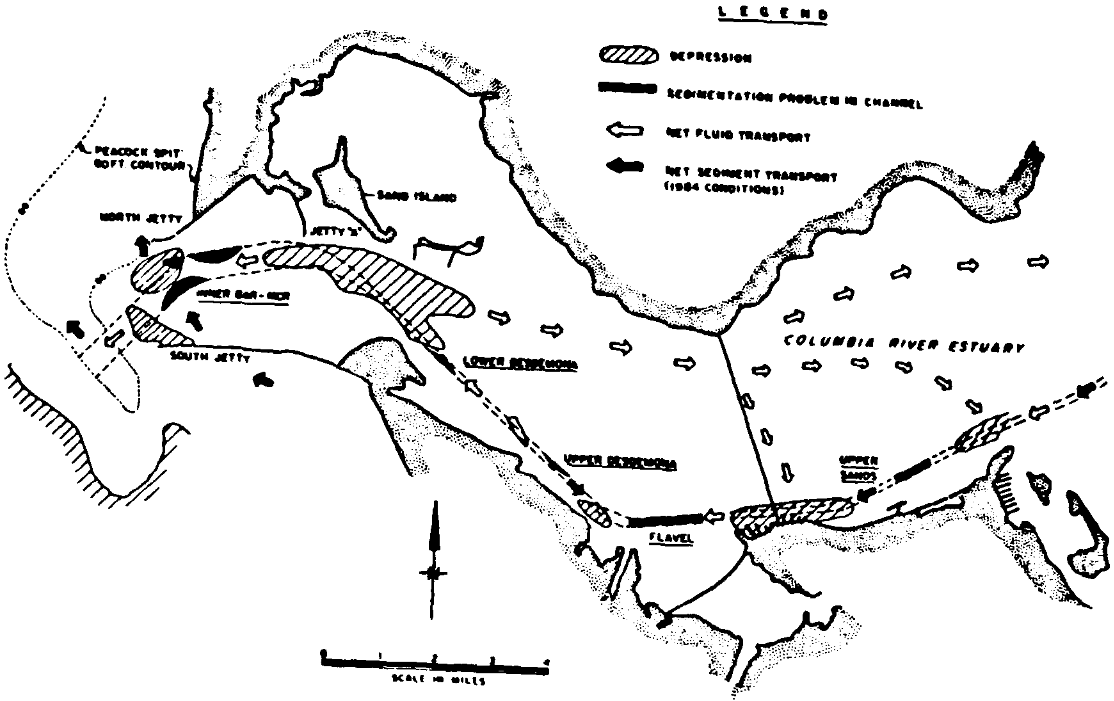
LEGEND
DEPRESSION
SEDIMENTATION PROBLEM IN CHANNEL
NET FLUID TRANSPORT
NET SEDIMENT TRANSPORT (1984 CONDITIONS)
PEACOCK SPIT 60FT CONTOUR
SAND ISLAND
NORTH JETTY
JETTY "A"
INNER BAR - NCR
SOUTH JETTY
LOWER DESDEMONA
COLUMBIA RIVER ESTUARY
UPPER DESDEMONA
UPPER SANDS
FLAVEL
0 1 2 3 4
SCALE IN MILES

Figure 5. Location and definition map, Lower Columbia River.

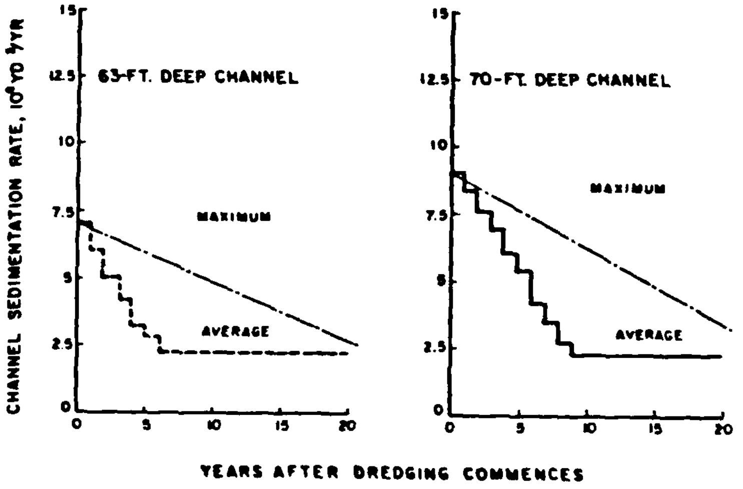

Figure 6. Estimates of the Channel Sedimentation rate for the 20 years following deepening to 63 ft and 70 ft. dashed line represents maximum error bound equal to extrapolated value.

The rate of sand transport landward from ocean sources is probably small. Like the river source, onshore sand transport not likely to increase as the channel is deepened. Wave, wind and tide-generated currents in the ocean will not be greatly affected by channel deepening.

Longshore sediment transport will also be little affected by channel deepening. Deepening could, however, have an effect on the rate at which littoral sand is deposited in the channel if less than the total volume reaching the bar at present is not deposited there. A longshore sediment transport analysis using the Energy Flux Factor Method indicates transport to the north is 3 times as great as transport to the south. Prototype sedimentation data from the channel, and an analysis of the elongated sand fillet that formed south of the south jetty after its construction, suggest 2×10^6 yd^3/yr (all the gross longshore sand transport) is presently deposited in the Inner Bar channel. Hydraulic analyses indicate deepening will not cause a large enough increase in tidal prism to offset the increase in cross-sectional area. Sediment scour will be reduced slightly and deposition slightly enhanced, but channel stability will not be significantly affected by the proposed deepening. All the sand transported to the Inner Bar from longshore sources will continue to be deposited there.

2. Regional Disequilibrium Component. This is channel sedimentation that occurs because a disequilibrium condition was previously imposed on the bar and nearby areas by human activities. Five human activities have influenced the movement and deposition of sand at the Bar. These are jetty construction, land reclamation in the estuary, the creation of reservoirs on the Columbia River and its tributaries, regulation of flow in the Columbia River, and channel deepening in the Columbia River. In all cases the present trend is toward less sand entering the estuary and less sand moving within the estuary. Sedimentation rates in the future resulting from this component will likely decline.

Changes in bathymetry following construction of the North and South Jetties (1885 to 1917) were enormous and continue to have a significant,

AD-A168 715 PROCEEDINGS OF WEST COAST REGIONAL COASTAL DESIGN 3/5
CONFERENCE HELD ON 7-8 NOVEMBER 1985 AT OAKLAND
CALIFORNIA(U) CORPS OF ENGINEERS SAN FRANCISCO CALIF
UNCLASSIFIED SOUTH PACIFIC DIV APR 86 F/G 13/2 NL

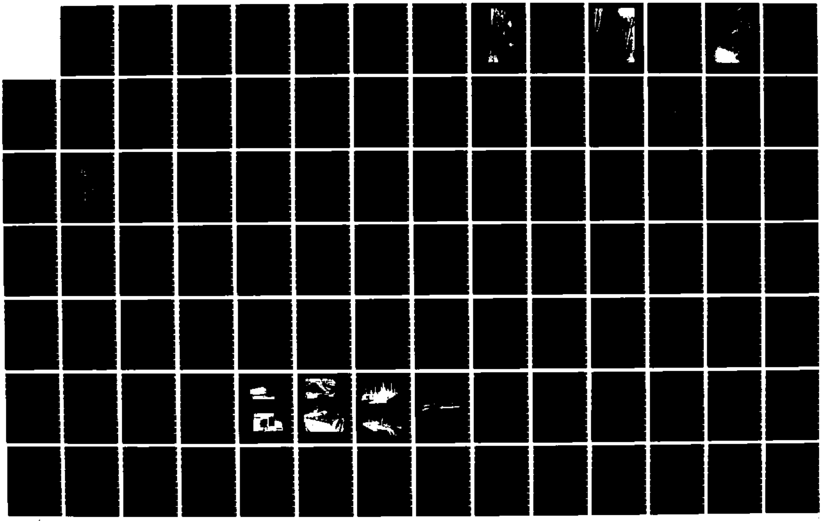

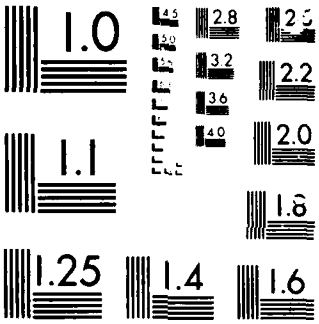
1.0
1.1
1.25
1.4
1.6
1.8
2.0
2.2
2.5
2.8
3.2
3.6
4.0
4.5
5.0

but secondary, effect on the Outer Bar. The jetties constricted flow at the mouth of the estuary compared to previous conditions. The mouth deepened dramatically, perhaps with a loss of sand for 10-20 years at a rate of 10 x 10^6 yd^3/yr. Coincident with the between-jetty scour, Peacock Spit (Fig. 5) formed with a hook-like shape to the south. It reached its zenith sometime before 1935. Since that time the spit has been retreating in a north and eastward direction. Between 1935 and 1958, for example, there was a large eastward and northward movement of all bathymetric contours down to the 60-ft depth. Thus, the channel between and landward of the jetties reached a near-equilibrium depth comparatively quickly after jetty construction, and Peacock Spit was formed as quickly by river and tide-transported sand eroded from that channel. But Peacock Spit has and is degrading at a comparatively slow rate (perhaps 0.1 x the rate at which it formed). The degradation is caused by shore-parallel coastal and ocean currents acting on the Outer Bar which is near the south extension of Peacock Spit. This is the present Outer Bar. The rate at which the south end of Peacock Spit will degrade and move into a deepened channel is about 0.5 x 10^6 yd^3/yr. This rate will remain constant and then decrease as the south end of the spit is removed above wave base. In about 6 years the degradation will be advanced and sedimentation in the channel will decrease.

In the century preceeding about 1930 approximately 24 percent of the intertidal area of the estuary was diked (20 percent) or filled (4 percent). This effectively reduced the tidal prism (to River Mile 50) by 10 to 15 percent. The result is a slight decrease in channel velocities and a slight decrease in the distance saline waters intrude in an upstream direction. This has not affected sediment discharge from the river to the estuary, but has decreased the rate at which sediments move and are deposited within the estuary. The magnitude of this past decrease in tidal prism is about three times the magnitude of the increase in tidal prism that would occur if the channel was deepened to 70 ft.

More than 50 dams have been constructed on the Columbia River and its tributaries since 1933. The rate of movement of sand to the river below the most downstream dam has consequently declined. With time, the rate sand is supplied from riverbed degradation below that dam will also decline as the river bed reaches an equilibrium hydraulic cross-section in the absence of upstream sand input. Flow regulation has also diminished the movement of sand in the river. Because bedload discharge is approximately equal to the square or cube of flow velocity, the decline in freshet flow has significantly reduced the volume of sand that moves. This situation will continue into the future.

3. Local Sediment Adjustment Component. Channel deepening, as previously noted, will not increase the quantity of sediments reaching the Bar from outside sources. It will, however, temporarily increase the rate at which sand enters the channel from the bar itself. The analysis of prototype data clearly indicates that after the channel was deepened, bottom surfaces away from the channel boundary adjusted downward (Fig. 4). The length of the Inner and Outer Bar system as measured along the channel is also decreasing (Fig. 3).

CHANNEL SEDIMENTATION ESTIMATES

Figure 6 shows sedimentation rate estimates for the deepened channels for each sedimentation component. Continuous sedimentation, probably at least 75 percent of which enters from the littoral system, will continue at about 2×10^6 yd^3/yr. The river and the ocean offshore of the Bar will likely not be a major source of sand at the Columbia River mouth in the future. Disposal Area E is assumed to be a source.

The effects of past human activity at MCR are assumed to be wholly related to the influence the jetties have had on sedimentation. Further changes in river regulation and estuary infilling will likely be small. Much of the sand now transported north across the channel at the Outer Bar will, upon channel deepening, be deposited in the channel. Post-deepening deposition will probably continue until the south extension of Peacock Spit is removed to wave base.

Sand deposited in the channel from side wall sources will decline to zero at an estimated rate of about 0.6 yr per foot of channel depth increase. Deepening only the outbound lane will result in a reduction in long-term dredging requirements at the Inner Bar because the volume eroded as a result of slope adjustments will be less on the north side of the channel. Adjustments south of the channel will be tempered by the existing inbound channel that will not be deepened. Combined axial bar length, which has been shortening at a rate of 75 ft/yr will likely continue into the future.

DISCUSSION AND SUMMARY

This paper presents a fundamental approach to obtain information that can be applied in planning, and some cases design efforts, to mitigate sedimentation problems in navigation channels. Past channel behavior is extrapolated to forecast future channel behavior when appropriate analyses of the causes of the behavior are made to account for changes in sediment supply, hydraulics, and bottom configuration.

Analyses of prototype data provide a useful first step in understanding and dealing with complex sedimentation problems. In some situations sophisticated models may not work because the physics of the prototype system is not known to the degree required to model it, and/or an adequate field data set is not available. Where models can be applied, the calibration of physical models or testing of numerical models requires an understanding of prototype behavior.

Prototype data analyses can be made and the results applied anywhere sufficient prototype data are available. The most beneficial approach would be to create a working, evolving, ever-improving data base to better understand and manage the sedimentation problem in the future. Based on continuing prototype data collection (for whatever reason, including payment purposes), and continuing analyses of those data, channel improvement and maintenance costs could be reduced by:

(a) better scheduling of dredges, including the use of advance maintenance dredging;

(b) improved knowledge of implications when establishing in-water disposal sites;

(c) better dredge cost projections, based on a knowledge of future trends in sedimentation;

(d) better understanding of the causes of sedimentation which can sometimes be rolled directly into improvements in the type and effectiveness of mitigation solutions, and

(e) improvements in the type, methods, location and frequency of prototype data collected.

ACKNOWLEDGMENTS

The cooperation of the Portland District, Corps of Engineers, in providing survey data and dredging records was most helpful. Moffatt and Nichol, Engineers supported the preparation of this paper.

REFERENCES

Ogden Beeman and Associates, and Moffatt & Nichol, Engineers, 9 May 1985, "Columbia River, Lower Estuary and MCR Shoaling Investigtion", Final Report, prepared for U.S. Army Corps of Engineers, Portland District, 193p.

OCEANSIDE EXPERIMENTAL SAND BYPASS

Mr. Douglas J. Diemer
Civil Engineer
Los Angeles District

ABSTRACT

Oceanside Harbor and the neighboring downcoast beaches have been the focus of controversy and of scientific study since the construction of the original harbor jetties in 1942. Shoaling of the harbor entrance channel and the erosion of Oceanside city beaches has been a continous problem. The Federal Government has assumed full responsibility for restoration of the Oceanside beach and maintenance of the harbor. The Corps of Engineers has conducted several studies of the harbor and beach and has tried periodic renourishment of Oceanside's beaches in an attempt to slow the effects of erosion. It has become clear that periodic nourishment is not effective and that alternative structural solutions do not have local support. Survey studies conducted by the Corps of Engineers in 1980 to investigate alternative harbor maintenance and beach erosion control alternatives led to the development of an experimental sand bypass system for Oceanside Harbor. The Oceanside Experimental Sand Bypass System is designed to reduce maintenance dredging costs in Oceanside Harbor and to provide the downcoast beaches with a continous source of beach sand.

INTRODUCTION

The City of Oceanside is located on the southern California coast about 30 miles north of the city of San Diego (Figure 1). The city was founded in the late nineteenth century as a coastal resort. During the early years of its development the city's beaches were typically wide and were capable of providing recreation for the many tourists who flocked there during the summer months (Figure 2).

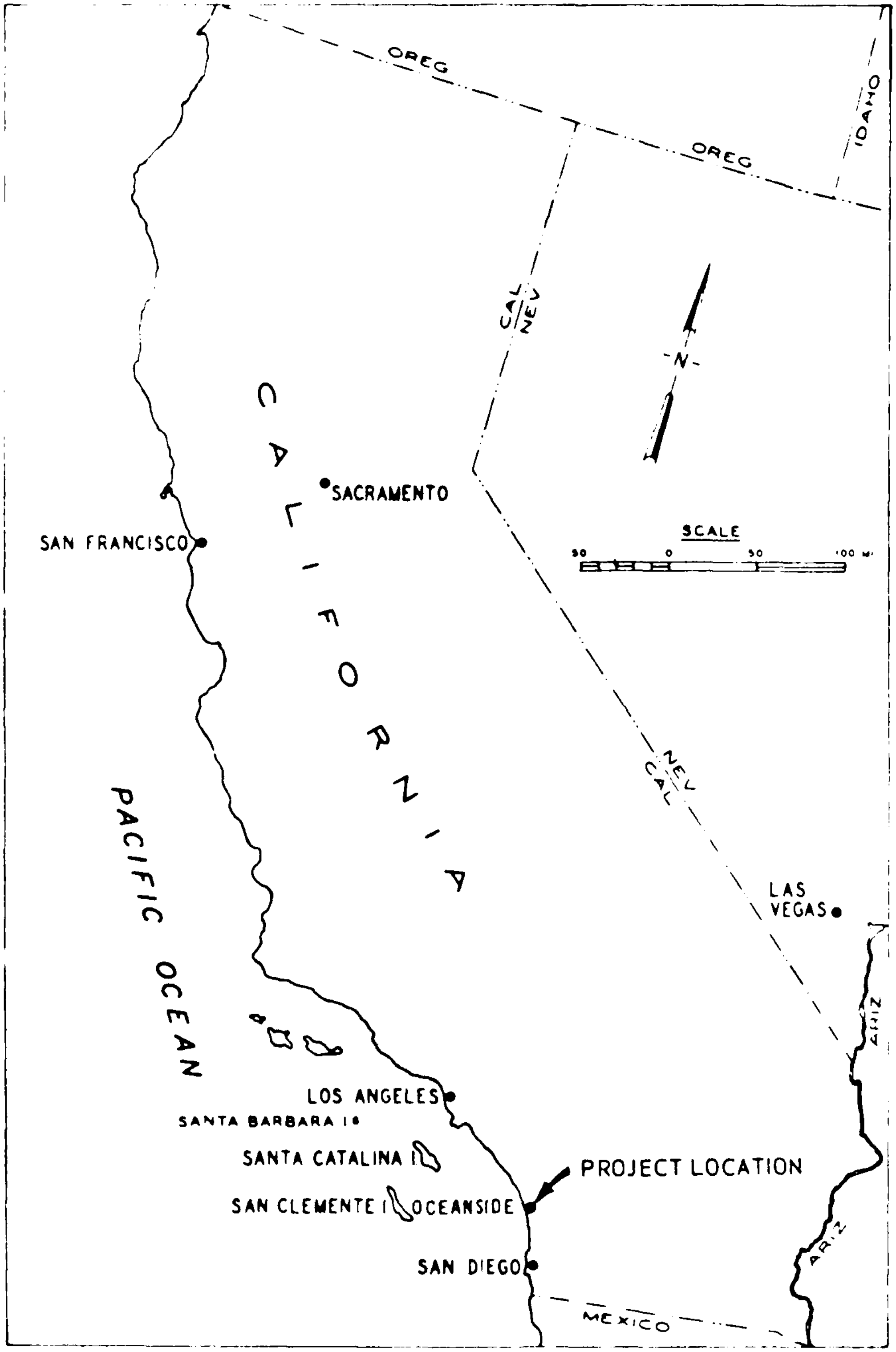
OREG
OREG
IDAHO
CAL NEV
N
CALIFORNIA
SACRAMENTO
SAN FRANCISCO
SCALE
50 0 50 100 MI
NEV CAL
LAS VEGAS
PACIFIC OCEAN
ARIZ
LOS ANGELES
SANTA BARBARA I
SANTA CATALINA I
PROJECT LOCATION
SAN CLEMENTE I
OCEANSIDE
SAN DIEGO
ARIZ
MEXICO

FIGURE 1 Project location

Figure 2

Since its early years the Oceanside beachfront has changed dramatically. Many man-induced changes have altered the natural physical processes which shape the coastline. The city of Oceanside has been faced with dealing with the effects of these changes for many years. The problem is beach erosion.

The first evidence of development which ultimately had an impact on the beaches of Oceanside occured in 1922, with the construction of Henshaw Reservoir on the San Luis Rey River. This structure reduced the sediment-carrying capacity of the river, thereby diminishing the natural supply of beach material for the Oceanside area. Construction of Vail Dam on the head-waters of the Santa Margarita River was completed in 1949. This construction undoubtedly had an effect on the supply of sand to the local beaches. Damming of the Santa Magarita and San Luis Rey rivers resulted in significant reductions of natural beach replenishment material for the Oceanside area.

In 1942, the United States Marine Corps constructed the Del Mar Boat Basin, just north of the city of Oceanside at the southern limit of Camp Pendelton (Figure 3). At the time of its construction, little was known about its eventual impact on local littoral processes. The original harbor construction consisted of two (2) converging jetties extending seaward to about the minus 20 foot depth; the [illegible] jetty was about

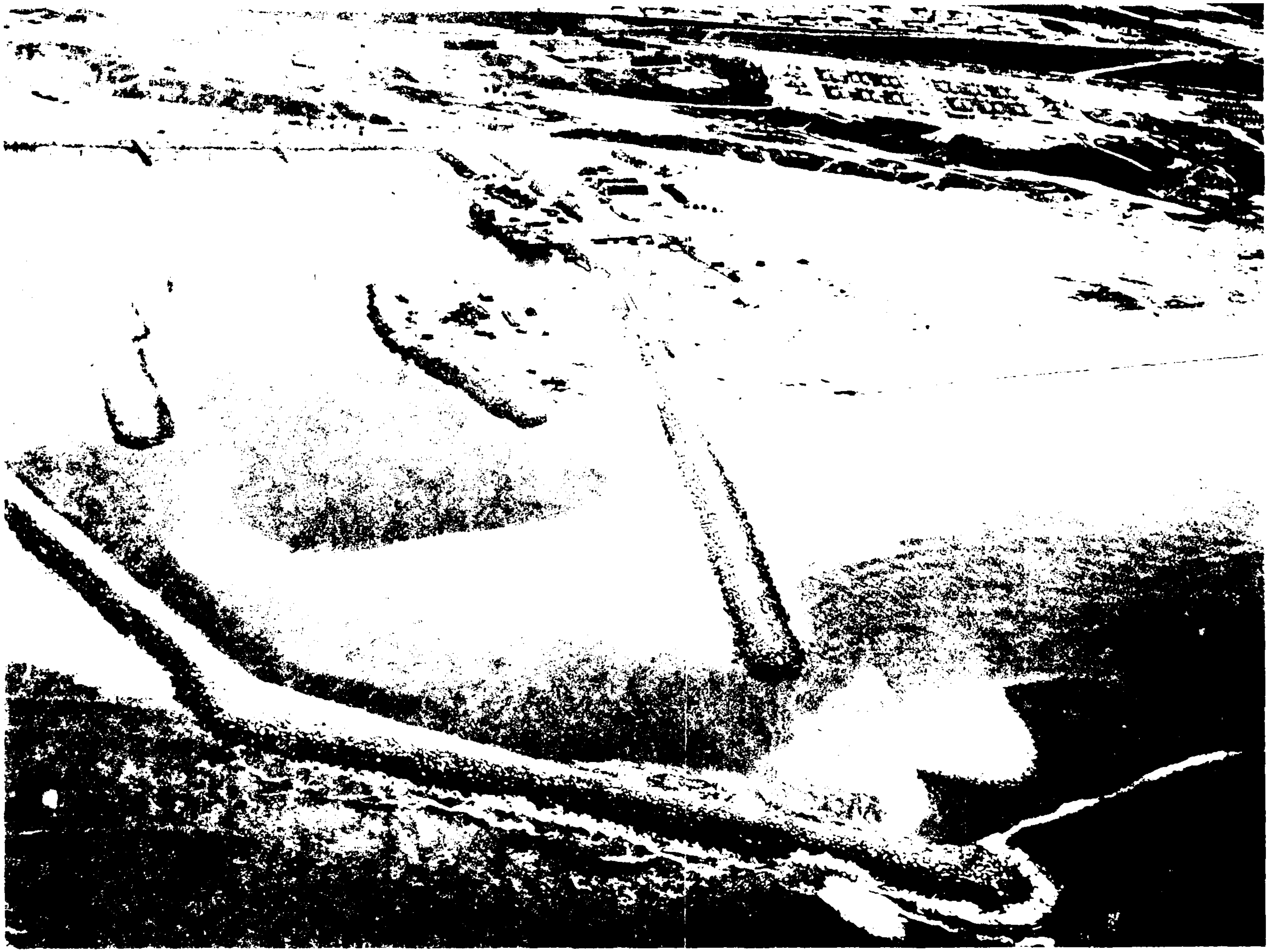

2100 feet long and the southern jetty 1300 feet in length.

During and immediatedly following construction of the harbor, effects in the area of the harbor entrance and on the local shoreline were recognized. By 1945 the entrance channel had shoaled from a constructed depth of 20 feet to only 14 feet and had decreased in width from 190 to 50 feet. The entrance channel was dredged that year with approximately 220,000 cubic yards of material being removed. Within eight (8) months of the dredging the harbor entrance was plugged again.

The downcoast shoreline was also immediatedly affected by the harbor construction. Erosion was evident during and after completion of the harbor (Figure 4).

It was clear that the construction of the Harbor jetties had caused the downcoast erosion of Oceanside's sandy beahes, beginning a history of studies on the harbor and local littoral processes, and a search for a solution to the problem.

LOCAL PHYSICAL PROCESSES

The Oceanside littoral cell extends from Dana Point on the north to Point La Jolla on the south. The littoral cell contains about 50 miles of mostly sandy beach, predominantly facing southwest (Figure 5).

Along most of the Oceanside littoral cell from Del Mar to San Onofre, the sea cliffs range in height from about 30 to 120

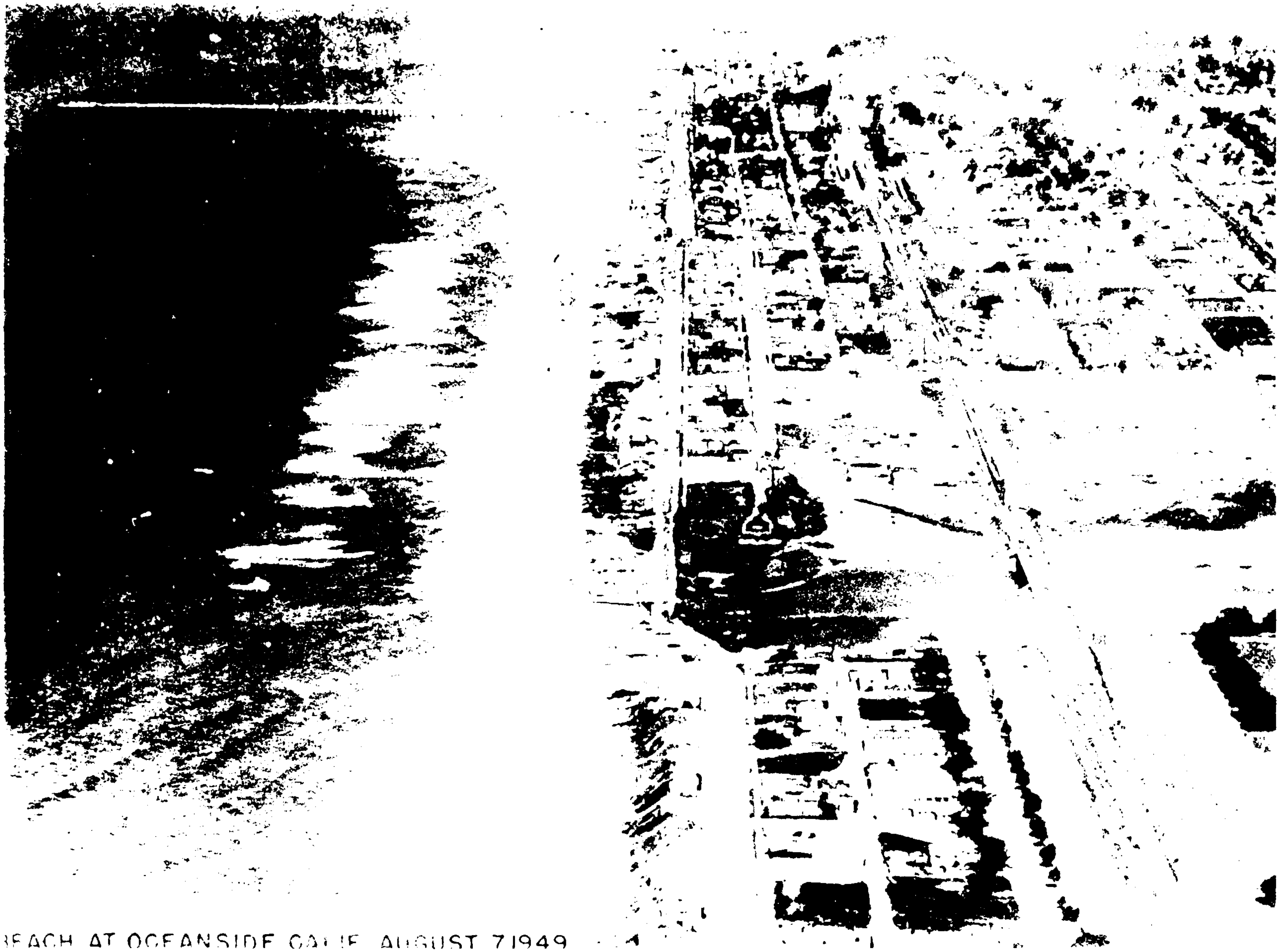

BEACH AT OCEANSIDE CALIF AUGUST 7 1949

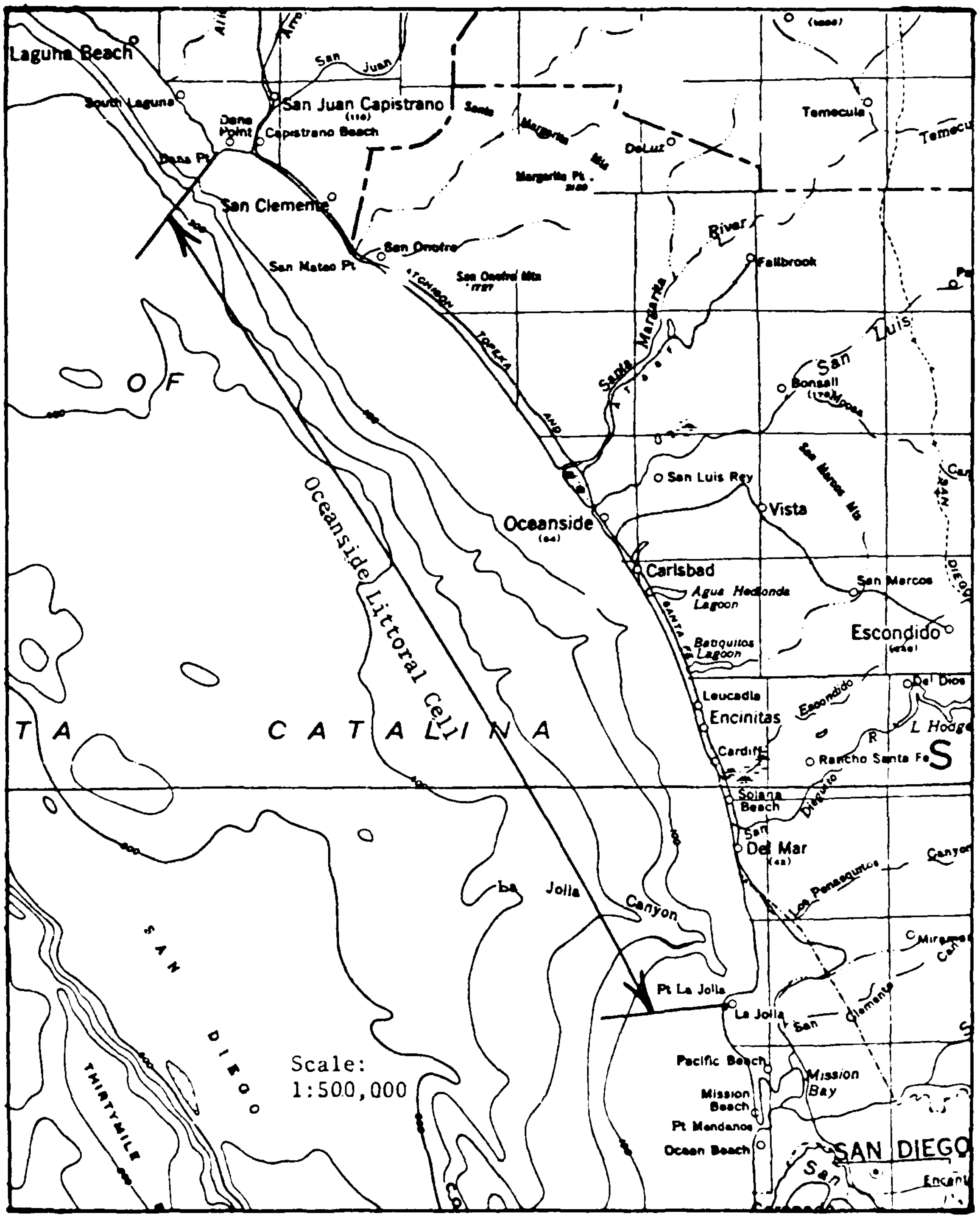
Laguna Beach
South Laguna
San Juan Capistrano
Dana Point
Capistrano Beach
Dana Pt
San Clemente
San Onofre
San Mateo Pt
San Onofre Mts
DeLuz
Temecula
Fallbrook
Santa Margarita
San Luis
Bonsall
San Marcos Mts
San Luis Rey
Vista
Oceanside
Carlsbad
Agua Hedionda Lagoon
Batiquitos Lagoon
San Marcos
Escondido
Leucadia
Encinitas
Cardiff
Rancho Santa Fe
Solana Beach
Del Mar
Los Penasquitos
La Jolla Canyon
Pt La Jolla
La Jolla
Pacific Beach
Mission Beach
Mission Bay
Pt Mendanos
Ocean Beach
SAN DIEGO
O F
T A
C A T A L I N A
SAN DIEGO
THIRTYMILE
Oceanside Littoral Cell
Scale:
1:500,000

FIGURE 5 Oceanside, California, Littoral Cell

feet. The sandy beaches are relatively wide during the summer, but retreat during storms, when waves break directly against the cliffs. The cliffs along this region of coastline are interrupted by eight partly filled estuaries at the mouths of mostly seasonal, winter streams. Usually these estuaries are seperated from the ocean by barrier sand-spits, formed by a predominant southern littoral drift.

Most of the moveable sediment within the cell comes from the streams and to a lesser extent from erosion of the sea cliffs. The beach sand moves up and downcoast during periods of heavy wave action, depending on the angle of wave approach. A dynamic equilibrium exists along much of the cell, with a surface layer of beach sand constantly moving either upcoast or downcoast.

At the southern end of the cell there is strong evidence of large sand losses to the La Jolla submarine canyon. Also, there is little evidence that sand migrates around the northern boundary of the cell at Dana Point. These observations, together with considerable data gathered in the past, supports the observation that net drift within the Oceanside littoral cell is to the south (Figure 6).

Coastal processes studies conducted in the Oceanside area in the past have shown the potential for longshore transport by sea and swell to be on the order of 640,000 cubic yards south and 540,000 cubic yards north, with a net annual transport of about 100,000 cubic yards to the south (Table 1).

The harbor at Oceanside is located approximately at the middle of the Oceanside littoral cell. The harbor can be considered a sediment "sink", as sand moving along the coast is

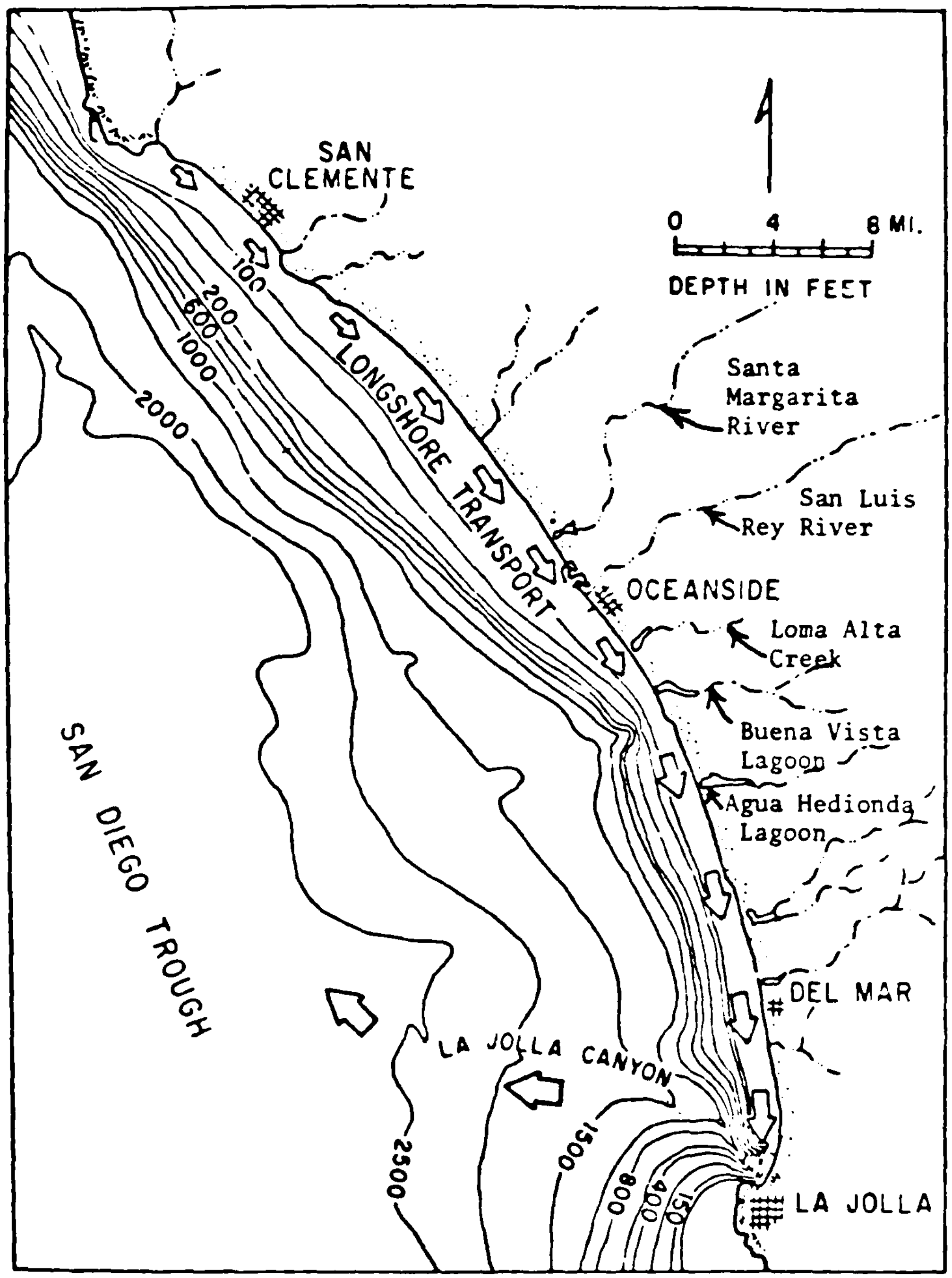
SAN CLEMENTE
0 4 8 MI.
DEPTH IN FEET
Santa Margarita River
San Luis Rey River
OCEANSIDE
Loma Alta Creek
Buena Vista Lagoon
Agua Hedionda Lagoon
DEL MAR
LA JOLLA
LONGSHORE TRANSPORT
SAN DIEGO TROUGH
LA JOLLA CANYON
100
200
600
1000
2000
2500
1500
800
400
150

FIGURE 6

Theoretical Oceanside California Littoral Cell, showing probable direction of net longshore transport (after Inman)

TABLE 1

Summary of
Potential Longshore Transport Computations

OCEANSIDE, CALIFORNIA

	Sea		Northern Swell		Southern Swell		Sum		Net		Gross
	+	-	+	-		-	+	-	+	-	
Month	North	South	North	South	North	South	North	South	North	South	Gross
Jan	35,501	25,281	1,741	9,148	0	0	37,242	34,429	2,813		71,671
Feb	26,188	25,188	3,544	8,759	0	0	29,732	33,947		4,215	63,679
Mar	9,788	63,737	5,977	8,080	0	0	15,765	71,817		56,052	87,582
Apr	2,993	61,542	1,735	6,896	0	0	4,728	68,438		63,710	73,166
May	88	90,521	180	8,265	61,979	0	62,247	98,786		36,539	161,033
Jun	34	99,024	0	9,852	36,889	0	36,923	108,876		71,953	145,799
Jul	9	57,129	0	7,804	112,906	0	112,915	64,933	47,982		177,848
Aug	0	42,133	8	6,105	84,664	0	84,672	48,238	36,434		132,910
Sep	63	33,445	375	3,472	89,151	0	89,589	36,917	52,672		126,506
Oct	1,307	27,342	43	2,970	35,147	0	36,497	30,312	6,185		66,809
Nov	10,389	16,595	1,127	6,541	0	0	11,516	23,136		11,620	34,652
Dec	17,244	15,418	1,546	7,841	0	0	18,790	23,259		4,469	42,049
Annual	103,604	557,355	16,276	85,733	420,736	0	540,616	643,088	146,086	248,558	1,183,704
Net		453,751		69,457	420,736			102,472		102,472	

trapped at the harbor jetties and entrance channel. The main northern breakwater traps sand moving to the south, piling sand on its north side until the shoreline realigns so that sand can move around the breakwater and into the harbor. South of the harbor sand moving northerly is trapped as it moves upcoast and into the harbor. Once in the harbor, this sand is lost to the littoral system, as the harbor is sheltered from wave action and littoral currents. This sand can only be returned to the system by means such as dredging. Dredging records indicate that approximately 360,000 cubic yards of material is lost to the harbor annually. On a regional scale the "sink" effects of the harbor are only slightly significant, but at Oceanside, just downcoast of the harbor, its effects are well recognized.

ALTERNATIVES SOLUTIONS AND DEVELOPMENT OF THE SAND BYPASS CONCEPT

The Oceanside Harbor complex today includes the Del Mar Boat basin and the Oceanside small craft harbor which was constructed in 1963. While the Del Mar basin is used exclusively for military puposes, the small craft harbor and downcoast beach are used primarily for recreation. Today the harbors are protected by a 4350 foot-long north jetty and a 1330 foot-long south jetty. Presently a 920 foot-long groin is located at the mouth of the San Luis Rey River, about 1/2 mile south of the harbor. A chronological summary of the harbor development is shown in Figure 7.

From 1962 to 1981 the Federal Government has dredged nearly 9 million cubic yards of sand from the Oceanside and Camp Pendelton harbors and placed the material on Oceanside's beaches.

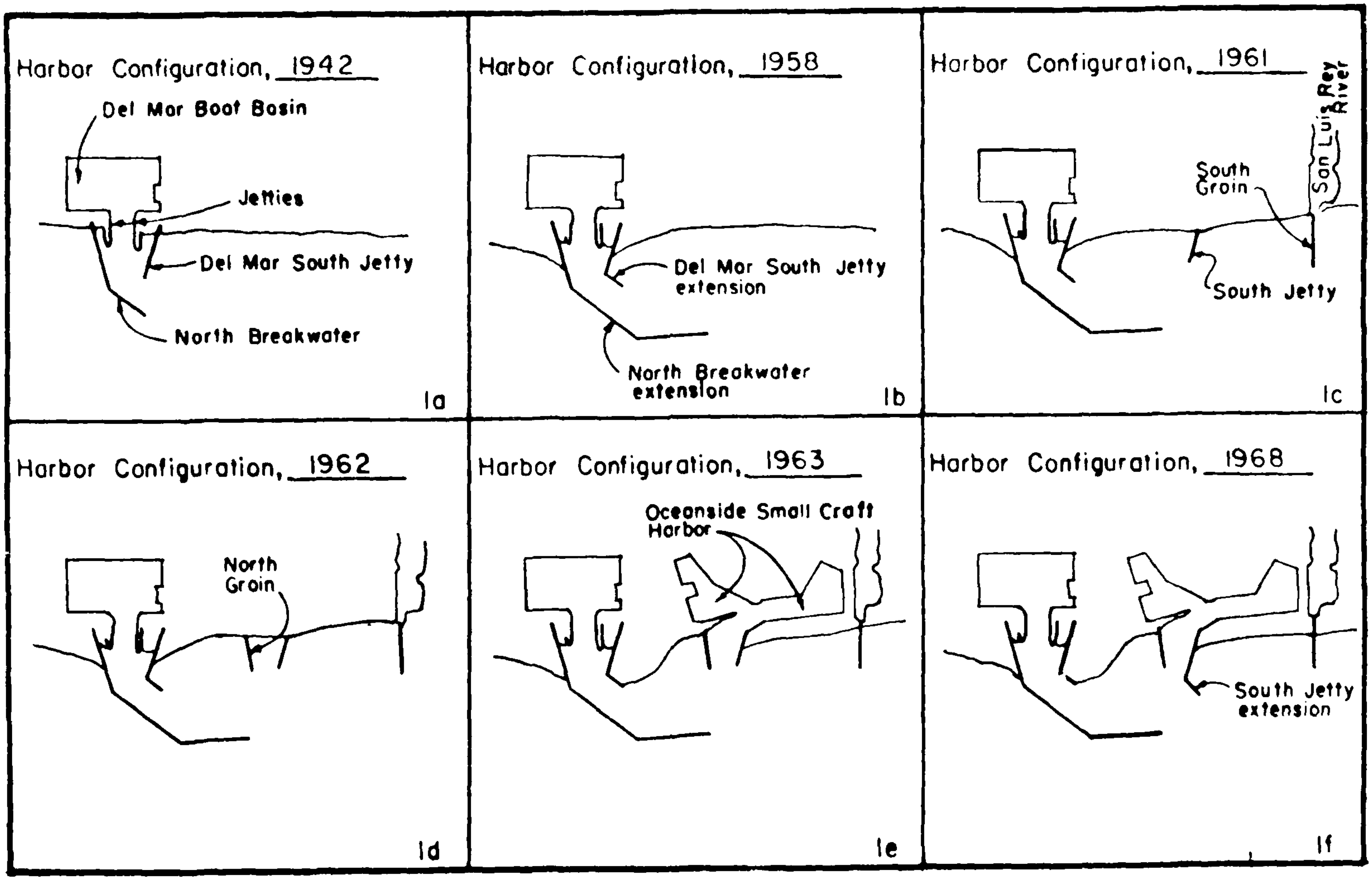
Harbor Configuration, 1942
Del Mar Boat Basin
Jetties
Del Mar South Jetty
North Breakwater
Ia
Harbor Configuration, 1958
Del Mar South Jetty extension
North Breakwater extension
Ib
Harbor Configuration, 1961
San Luis Rey River
South Groin
South Jetty
Ic
Harbor Configuration, 1962
North Groin
Id
Harbor Configuration, 1963
Oceanside Small Craft Harbor
Ie
Harbor Configuration, 1968
South Jetty extension
If

FIGURE 7 Changes in harbor configuration, 1942 - 1968

Despite this nourishment, the downcoast beaches have continued to erode. Further renourishment efforts were tried in 1982, with approximately 1 million cubic yards of sand from the San Luis Rey River being truck-hauled to Oceanside. This sand was lost along with most of the original existing beach, to the large storms of the winter of 1983.

In 1967, Congress authorized a review study of the beach erosion at Oceanside. Little progress was made toward an erosion solution during the 1970's. For the most part, this was due to a lack of information and of understanding of the problem.

In 1978, model studies of various proposed solutions were conducted at the Waterways Experiment Station (WES), in Vicksburg, Mississippi. The studies were conducted to gain a better understanding ot the effects of proposed structural, beach stabilization measures.

The model studies concluded that a proposed 5-groin plan was not effective in preventing erosion, but recommended a combination offshore submerged breakwater-groin system for controlling beach erosion. A survey report was prepared in 1980 which included the breakwater recommendation and proposals for other erosion solutions. Although the groin plan had local community support, the breakwater plan did not. Reaction to the offshore breakwater proposal was universally negative. Beachfront property owners, surfers, downcoast local and State agencies, were all opposed. The only erosion solution which received universal local support was a sand bypass system.

THE SAND BYPASS

The Sand Bypass System was originally conceived in the Corps' 1980 Survey Report on Beach Erosion Control. The proposed bypass consisted of a series of fixed jet pumps placed in the harbor entrance. By mechanically bypassing sand from in and around the haror, the natural littoral transport which was interrupted by the original construction of the harbor breakwaters, theoretically could be restored. The survey report acknowledged that a bypass system was the enviromentally preferred solution, but could not conclude that the proposed system would totally correct the erosion problem.

In 1982, as part of the Corps of Engineers' Operation and Maintenance Program for Oceanside Harbor, authorization was given to proceed with the design and construction of an experimental sand bypass system. This authorization came through the 1982 Energy and Water Development Appropriation Bill, whereby Congress appropriated $700,000 for the bypass design.

The first phase of the sand bypass system development consisted of data collection and analysis. As part of this study effort, local and technical committees assisted the Corps in developing and evaluation sand bypass concepts. The final recommendation comprised: 1) an array of fixed jet pumps on the south side of the channel entrance, at the south harbor jetty; 2) fluidizers that feed sand to jet pumps on the north side of north fillet, at the north end of the harbor. Discharge was to be at various points along the beach with the last point at Wisconsin Avenue, approximately 2 miles south of the harbor.

Subsequent studies included the development of the system hydraulics and drive components, and later the development of the final concept and design (Figure 8).

The basic components of the jet pump system are a clear water supply with intake pump, a clear water supply line, a jet pump, and the jet pump discharge line

The jet pump is a "Y"-shaped pipe that utilizes the basic principles of fluid dynamics to 'vacuum' sand from the ocean bottom. Supply water is forced through a nozzle where the large increase in velocity is compensated by a large decrease in pressure. Sand is vacuumed up through the jet, creating a crater in the sand deposit where the jet pump is positioned (Figure 9a).

Fluidizers will also be employed as part of the sand bypass system. This device will force sand into suspension, allowing more sand to be drawn toward the jet pump crater and thereby widening the effective area of the jet pump (Figure 9b).

A fluidizer is a manifold-type pipe with several perforations. Water is pumped through the pipe and flows out of the holes at high velocity. The high velocity of the water 'fluidizes' the sand, which then flows toward the jet pump.

The ultimate bypass system will have a bank of 10 jet pums on the south side of the harbor channel entrance. These pumps are intended to intercept sand moving into the harbor from the south. On the north side of the channel entrance, two jet pumps fed by three fluidizers will intercept sand moving around the harbor from the north. The north fillet system consists of a single jet pump that can be moved about by a hinge. This pump is intended to collect sand that would otherwise migrate around or through the north breakwater, into the harbor.

Fixed riser structures, or platorms, will be constructed on

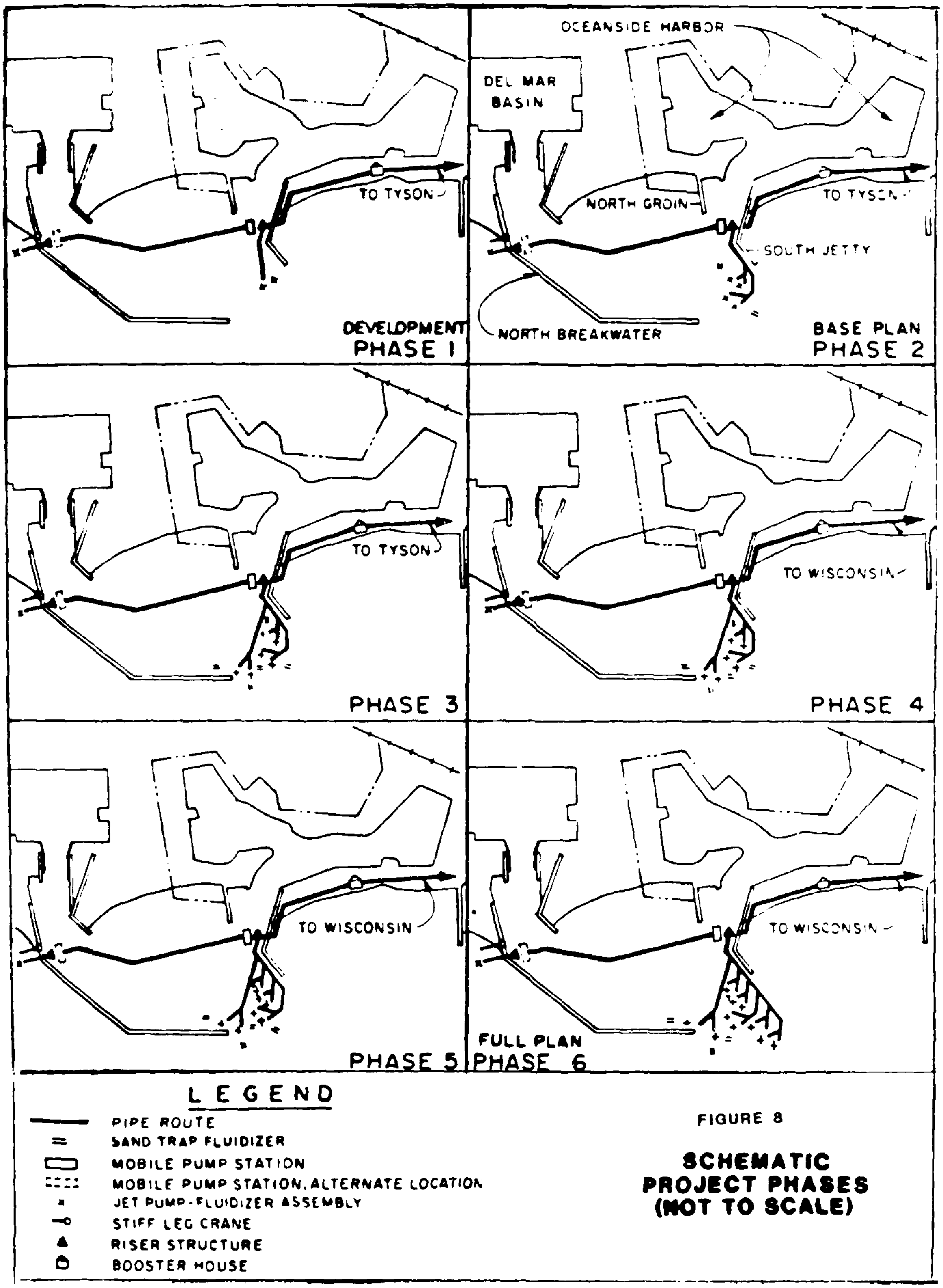
OCEANSIDE HARBOR
DEL MAR BASIN
TO TYSON
NORTH GROIN
SOUTH JETTY
NORTH BREAKWATER
DEVELOPMENT PHASE 1
BASE PLAN PHASE 2
PHASE 3
TO WISCONSIN
PHASE 4
PHASE 5
FULL PLAN PHASE 6
LEGEND
PIPE ROUTE
SAND TRAP FLUIDIZER
MOBILE PUMP STATION
MOBILE PUMP STATION, ALTERNATE LOCATION
JET PUMP-FLUIDIZER ASSEMBLY
STIFF LEG CRANE
RISER STRUCTURE
BOOSTER HOUSE

FIGURE 8

SCHEMATIC PROJECT PHASES (NOT TO SCALE)

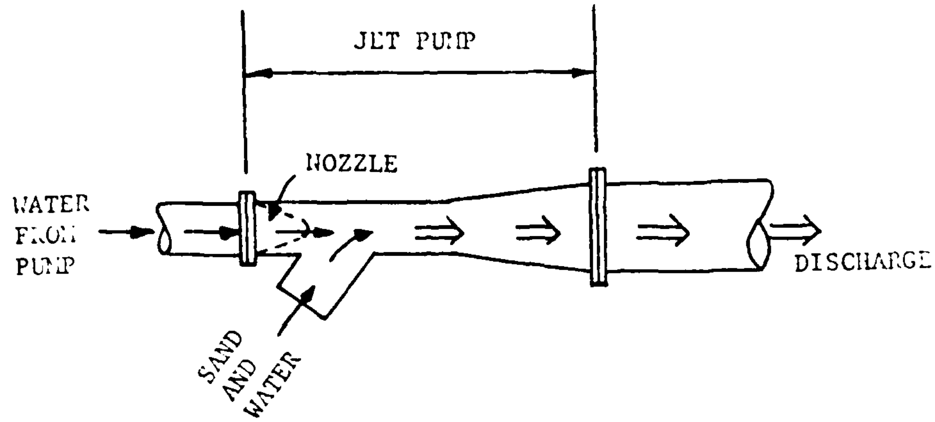
JET PUMP
NOZZLE
WATER FROM PUMP
DISCHARGE
SAND AND WATER

FIGURE 9a JET PUMP OPERATING PRINCIPLE

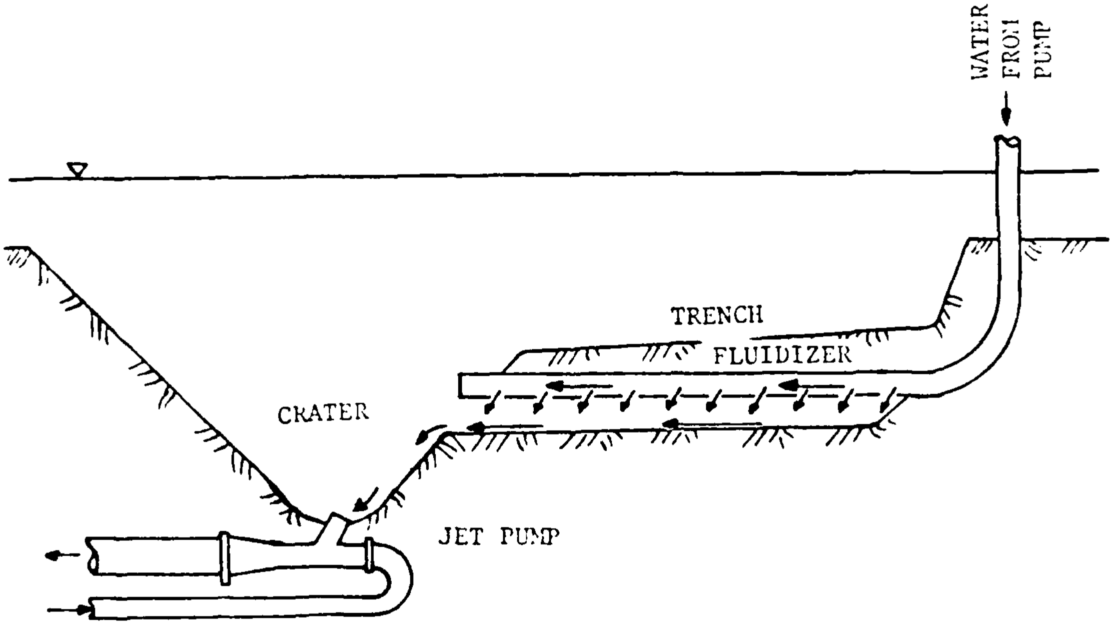
WATER FROM PUMP
TRENCH
FLUIDIZER
CRATER
JET PUMP

FIGURE 9b FLUIDIZER/JET PUMP COMBINATION

each of the jettys. The north fillet platform and equipment is represented in Figure 10. These platforms will be used to interface the subsea jet pumps and piping system to a mobil pumping platform. The mobil pumping platform is a barge with jack-up capability. The jack-up barge will be positioned at either the south or north jetty riser structure depending on the season.

Power to drive the pumps on the mobil barge will be supplied by diesel engines while an intermediate system booster pump, located near the south jetty, will be driven by an electric motor.

Other auxiliary equipment includes small cranes on the north fillet and barge to deploy and recover the jet pumps, piping and service equipment, a work boat for servicing, and a crew boat.

The installation of the beach discharge pipeline was completed in early 1985. When completed the jet pump system will be joined to the discharge pipeline to facilitate the discharge of sand removed from the harbor entrance and north fillet, to the beaches of Oceanside.

The north fillet system is intended to operate during the winter months when the littoral transport is to the south. The entrance channel system will work during the summer months when littoral transport is to the north. Only two jet pumps would operate at any one time in the entrance channel. Each of the 4-inch entrance channel pumps is capable of pumping 100 cubic yards per hour, while the 6-inch north fillet pump has a pumping capacity of 200 cubic yards per hour. The ultimate system is expected to bypass about 400,000 cubic yards of sand annually to the downdrift beach.

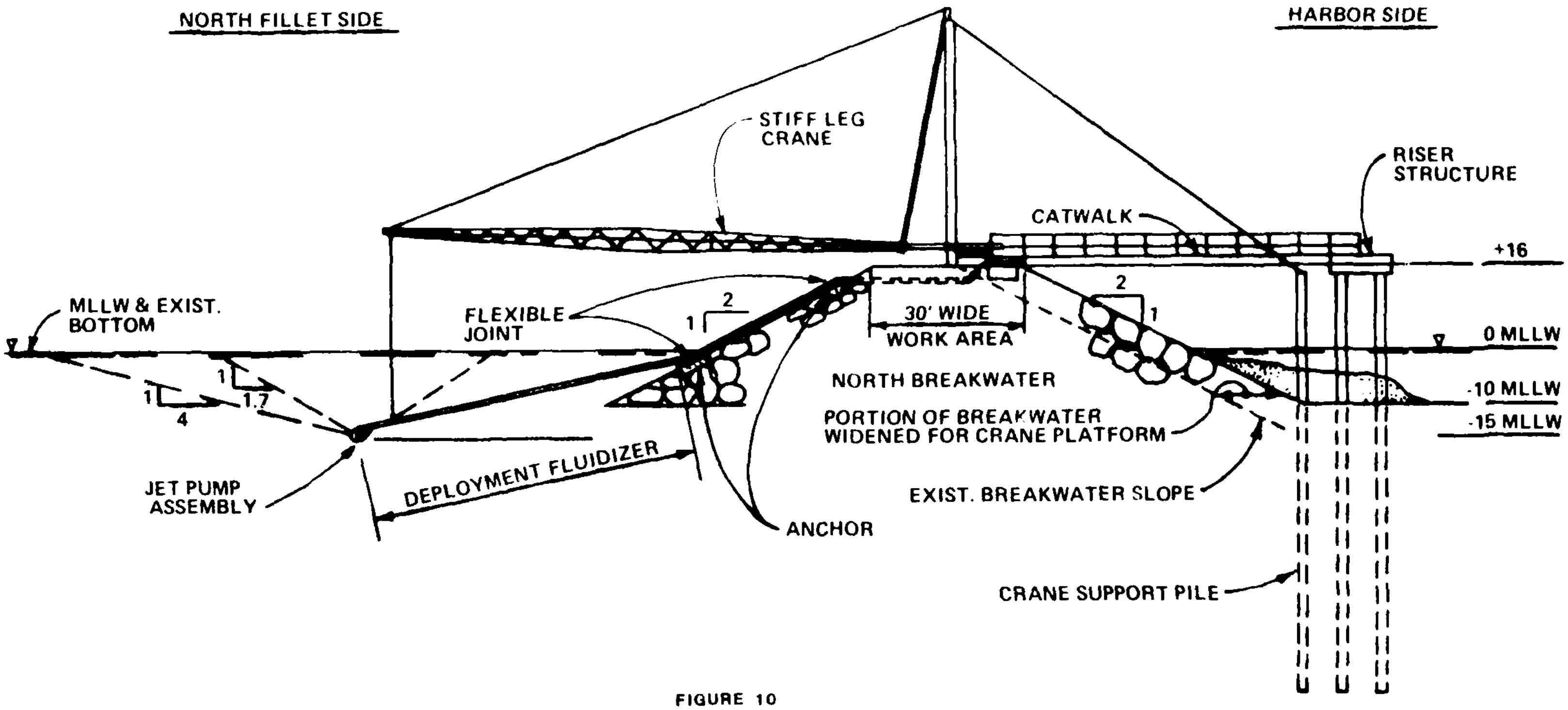
NORTH FILLET SIDE
HARBOR SIDE
STIFF LEG CRANE
RISER STRUCTURE
CATWALK
+16
0 MLLW
-10 MLLW
-15 MLLW
MLLW & EXIST. BOTTOM
FLEXIBLE JOINT
2
1
30' WIDE
WORK AREA
2
1
1
1.7
1
4
NORTH BREAKWATER
PORTION OF BREAKWATER WIDENED FOR CRANE PLATFORM
EXIST. BREAKWATER SLOPE
JET PUMP ASSEMBLY
DEPLOYMENT FLUIDIZER
ANCHOR
CRANE SUPPORT PILE

FIGURE 10

Sand bypassing on this scale has not been attempted on the West Coast and consequently, is considered to be an experiment. Because the exact littoral transport quantities and paths are not well documented, and because of the experimental nature of the system technology, the bypass system will be constructed in phases. Phasing will allow for construction of incremental portions, monitoring of that portion's operation, and for refinement and implementation of future stages based upon prior system performance and experience.

The first phase is known as the 'development plan.' It includes the construction of the north fillet jet pump system and the installation of two fixed jet pumps at the south jetty of the harbor entrance. Since the system is designed to have only two jet pumps operating at any given time, these two initial jet pumps will be capable of pumping the design capacity of the system, provided that sand is available in sufficient quantities and that clogging of the jet pumps does not become a problem. The development plan includes the construction of a booster pump on Harbor Beach. Sand slurry removed by the jet pumps will flow through the booster pump, downcoast through the discharge pipeline (14-inch HDPE) for about one mile, to its discharge location at Tyson street.

The initial development phase should be operational by summer of 1986. The Corps of Engineers intends to operate the system for about one year before evaluating and then possibly adding to the system. Future construction will depend on the success of the intial system performance. Refer to Figure 8.

If the development plan is successful and a need is demonstrated for the expansion of the system, two more jet pumps and two fluidizers will be constructed in the south entrance channel. If the fluidizers also prove successful, the north entrance channel system will be added. Following that, the remaining jet pumps will be constructed in the south entrance channel and the discharge pipeline will be extended to Wisconsin Street (about 2 miles south of the harbor).

MONITORING

The performance of the sand bypass system and its effects on the physical and biological enviroment will be monitored during its installation and during the 5-year experimental period.

Biological monitoring will include studies of the effects of the project on infauna, fish, plankton, grunion, and other marine habitats.

Performance monitoring will be accomplished by a computer-based Supervisory Control and Data Aquisition (SCADA)System. This system is an integrated hardware and software package that provides the capacity of both controlling and monitoring the sand bypass system. The SCADA system is designed to monitor, record, and process data for sand quantities pumped, fuel and electric consumption, operating time, and such processes as engine start/stop status, valve open/close status, and fluid temperatures and pressures.

A physical monitoring program has also been implemented. This monitoring includes semiannual beach profiles to a depth of minus 40 feet, harbor surveys, wave measurements, and sand sample analysis.

The inner harbor surveys are conducted using a conventional fathometer. Wave measurements are obtained using the existing SXY guage located off the end of Oceanside pier. Sand samples will be collected at predetermined locations by diving.

The beach profiles are obtained by a system that utilizes a lightweight towed sled with a high mast, carrying reflectors for a shore-based laser survey system. The sled is pulled along the rangelines by the Los Angeles District's Litter Amphibious Resupply Cargo (LARC) vessel (Figure 11). The survey system locates the sled's reflectors both horizontally and vertically, reads the data values, and stores the values immediatedly on a computer-readable data module.

The data obtained from the monitoring program will be used to gain an understanding of local littoral and harbor dynamics, and to recommend changes to the system operation.

A major benefit of the experimental sand bypass system will be the opportunity for scientists and engineers to learn more about the littoral processes at Oceanside and to develop new technologies for harbor maintenance and beach erosion control, By simulating the continuous flow of sand along the coast through the use of the bypass system, it is believed that the bypass will be more effective in stabilizing the beach than periodic dredging, which creates a 'bulge' of sand that is subject to accelerated erosion.

Dredging costs are also expected to be reduced once the bypass technology is developed and refined. Costly mobilization will be eliminated and through the use of energy efficient jet pumps, the bypass has the potential for significant savings over conventional dredging.

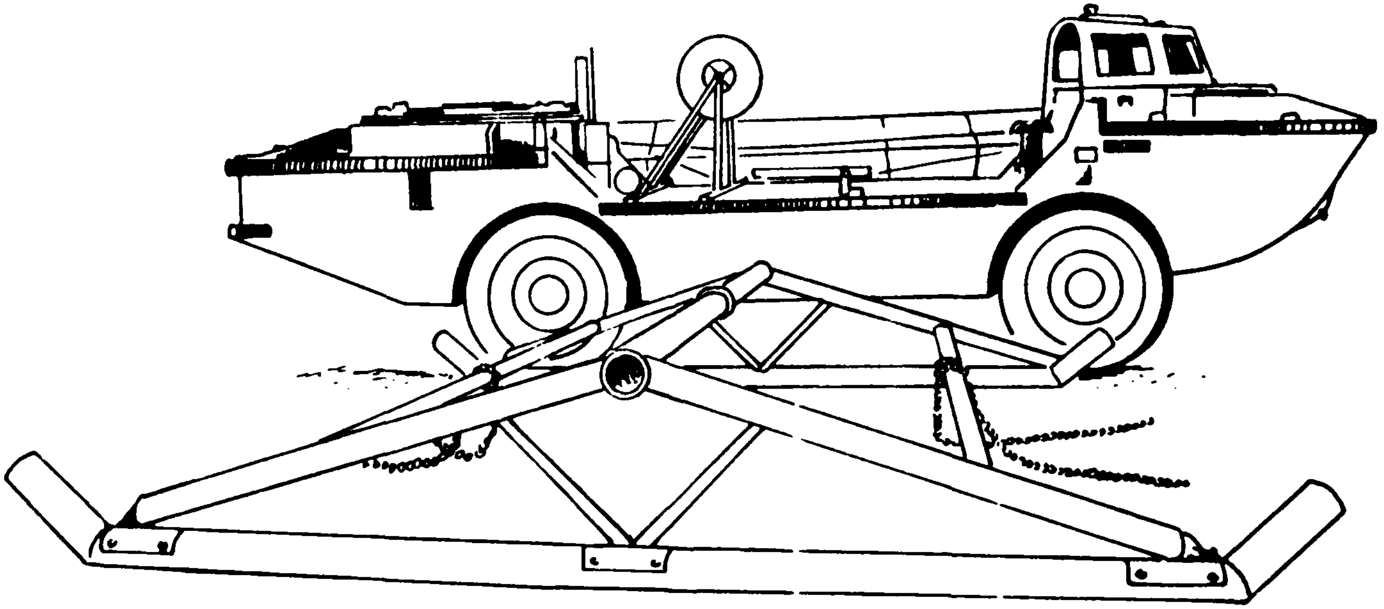

FIGURE 11

Survey sled with Amphibious vehicle LARK
(SURVEY SLED MAST NOT SHOWN)

The contract for the development phase of the bypass system has been awarded to Maecon Construction Company, Inc. of Irvine, California. The cost of the development plan construction was bid at $5.5 million.

Construction is expected to be completed by early summer, 1986, with system start-up to follow.

The sand bypass system is important to the Corps of Engineers as well as the local community of Oceanside. The successful operation of the system could result in a significant reduction in the erosion problems Oceanside has experienced. The Corps looks forward to advancing harbor dredging technology through the development of this system. This experimental system is consistent with the current government trend in identifying and developing reliable means of minimizing long-term government expense related to harbor maintenance.

Summary of Panel Discussion

SEDIMENTATION AND MATERIAL DISPOSAL

Chairman: Harold Herndon
US Army Corps of Engineers, Portland District

Panelists: Gregory L. Hartman, Ogden Beeman and Associates
Portland, Oregon
Ray Krone, University of California, Davis
Robert J. Hopman, US Army Corps of Engineers, North Pacific Division, Portland, Oregon
Charles Sollitt, Oregon State University
Corvallis, Oregon

The session on sedimentation and material disposal was comprised of several interesting papers. Dr. Osborne presented preliminary results of a study which addresses the potential use of sediment analysis (mineral content) as an indicator of source and transport direction. Dr. Slotta presented results of a study which examines modifications in the design of dredge cutterheads to increase productivity. Mr. Muslin presented a paper on the Oceanside Experimental Sand Bypassing Project which will test an alternative to the usual dredging techniques. If successful, the system could provide solutions to other persistent problem areas. Dr. Everts presented an excellent and extremely interesting paper on a study of sedimentation rates following channel deepening. The study, utilizing an existing data base, suggests that the sedimentation rate would not necessarily increase if the channel were deepened. That conclusion is contrary to widely held opinion, but Dr. Everts' analysis of historical bathymetric data makes a strong argument for the validity of his conclusions. Mr. Reese, Mr. Chesser, Dr. Hall, and Mr. Trawle all presented papers involving various aspects of inwater disposal of dredged material.

At first glance the subjects of the papers presented were somewhat disparate, but as Dr. Sollitt (a session panel member) noted, they all involved the movement of material by water and cited the inadequacy of available sediment transport models to answer the questions being posed. Mr. Beeman noted in his theme address that ships are increasing in size, demanding deeper and wider channels and more facilities, i.e. turning basins, anchorage areas, etc. As the requirement for dredging is increasing, available upland disposal areas are decreasing; and more and more inwater disposal of dredged material is necessary--in the ocean, in the estuaries, and upriver. The impact of such disposal is the cause of some concern to the resource agencies, and rightfully so. They want to know if the material will remain where it is placed, and, if not, what will be the fate of the sediment. We need a methodology to better define the transport of the material.

The following is an attempt to summarize the comments of the session's panel members whose participation in the conference added immeasurably to its success and is greatly appreciated by this writer. The comments relate generally to the session's topic and not to any specific presentation.

Mr. Robert Hopman: There is a need to reassess our thinking regarding dredged material. Clean sands, which constitute much of the dredging on the Pacific Coast, may be a resource to be utilized rather than something to be thrown away. Possible beneficial uses include beach nourishment, habitat creation, and river control structures. With the advent of local cost sharing for improvements, the US Army Corps of Engineers needs to reduce the time and costs of studies.

Dr. Charles Sollitt: The state of the art in sedimentation modeling is incapable of supplying the answers needed to successfully manage dredged material disposal. While there is no shortage of models, they often yield widely varying answers when applied to real world problems. There is a great need for increased funding for research in sediment transport modeling.

Mr. Greg Hartman: Engineers should not be afraid to adopt new and perhaps innovative approaches to problems. The paper presented by Dr. Everts demonstrates the successful application of a new approach. Reanalysis of old data resulted in conclusions which could have great impact on the feasibility of a proposed improvement. There may be a wealth of information filed away, unused, which could be extracted and given a fresh approach. There should be greater consideration and funding given to postconstruction monitoring programs. There could be much learned from the successes and failures of the past.

Dr. Ray Krone: There is a need to develop a management plan for material disposal. One needs to know the characteristics of the material:

(1) Is the material easily transportable?

(2) What is the transport capability of the receiving waters?

(3) Is the site designed to be a permanent storage area?

(4) Is it expected that the material will be dispersed away from the site?

If the site is a permanent storage area or the material is not easily transportable, an evaluation of the site capacity is required. Much greater use should be made of bathymetric surveys because those made over a period of time can be the source of much information.

Harold Herndon
Chairman, Sedimentation and
Material Disposal Session

NUMERICAL MODELING OF FLOATING BREAKWATER BEHAVIOR

Senaka Ratnayake*

ABSTRACT

A two stage micro computer numerical model was developed for the analysis of two important types of motions that are experienced by a typical floating structure. The first stage predicts what is commonly referred to as the "dynamic motion response" (also called the "wave frequency response"); the motion of the structure at frequencies identical to those of the incident wave field. Such an analysis is critical in the determination of structural design forces. The second stage, by using the results produced by the first stage, is used to predict the possible "drift motion" produced by the second order hydrodynamic forces produced by the combination of pairs of wave fronts in the incident wave field. Such motions are typically of very low frequency. If the natural frequency of the mooring system happens to be within the range of the frequencies of these "drift forces" (which is usually the case), the amplitude of oscillation can be large enough to cause excessive mooring forces. During all stages of the model, directionality of the sea was considered. Since the numerical model is stochastic in nature, most results are presented in their spectral form so that the end user can further manipulate them to obtain statistical quantities of interest. The predictions were later compared with prototype field data and the agreement was very satisfactory.

Introduction

The interest on the performance and analysis of floating breakwater behavior has been growing steadily during recent years. Considerable attention has been focused on the problem of obtaining structure and mooring design forces with inexpensive and efficient methods and the use of numerical models stands out among them due to their economical and less time consuming nature. Cost of physical model studies on the other hand can be prohibitive. Even during the unlikely circumstance where a physical model study is economically feasible there is no way to assure a

---

* Post Doctoral Research Associate, University of Washington Seattle

one to one correlation between model results, which most often are obtained under monochromatic and/or unidirectional wave conditions, and the prototype, which is almost always subject to random multi directional waves. Development of numerical prediction models has been slow since such a task requires extensive applications of hydrodynamic and structural analysis concepts as well as numerical techniques. Another obstacle has been the high computational cost which is a common feature in models of such nature. With the increasing availability of powerful and dedicated micro computers, that drawback has virtually disappeared.

Multi directional sea

The accuracy of almost all the theoretical prediction models depend heavily on the correct modeling of the sea state. In most practical situations, the sea surface elevation can be categorized as a stochastic process in time and space. The concept of wave energy spectrum can then be effectively used to describe the statistical properties of the sea. It is widely known that the wave directionality must not be ignored in a realistic description of the sea state and many authors have suggested possible spectral models (1), a discussion of which is beyond the scope of this paper. The importance of this lies in the fact that the stochastic properties of the hydrodynamic force field is directly dependent on the directional spread of wave energy.

Field monitoring program

In 1981 the U.S Army Coastal Engineering Research Center (CERC) through the Seattle District, Army Corps of Engineers contracted the University of Washington to conduct a prototype floating breakwater monitoring program aimed at learning more about the wave transmission characteristics, wave forces on floating structures, anchor cable behavior, structure response and inter module rubber connector behavior. A sketch of the field set up is shown in Figure 1. The site was located in the Puget Sound near West Point in Seattle and often experienced conditions currently considered suitable for the use of floating breakwaters. A linear array of spar buoys was used economically and successfully to collect directional wave data. A vast amount of data were gathered and some of the data were used to validate the numerical model discussed in this paper. A detailed description of the data acquisition effort can be found in reference (2).

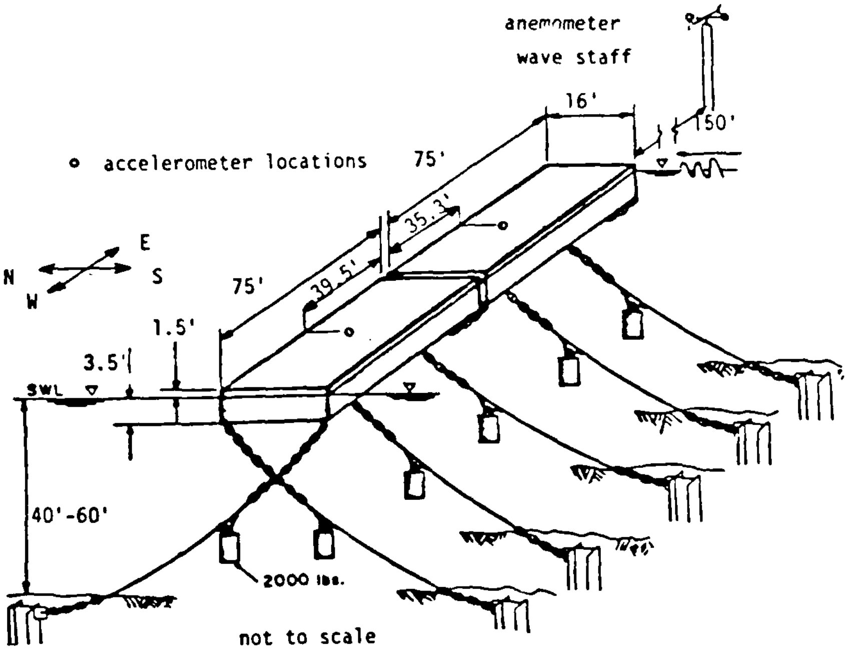
anemometer
wave staff
16'
50'
accelerometer locations
75'
35.3'
E
N
S
W
75'
39.5'
1.5'
3.5'
SWL
40'-60'
2000 lbs.
not to scale

Figure 1. Prototype floating breakwater

Numerical model

(a) Assumptions

The following assumptions were made in the development of the numerical model

1) The structure is long enough so that the end effects can be neglected.

2) The structure is large enough with respect to the incident wave heights to warrant the use of the potential flow solution to determine the hydrodynamics of the problem.

3) The sea state can be adequately described by the superposition of random wave fronts using the Small Amplitude Wave Theory.

(b) Theory

It has been shown by many authors (3) that the random sea caused by wind generated water waves can be effectively described by a (directional) wave spectrum whose ordinates are proportional to the wave energy density at each frequency and direction of concern. Given such a sea state, the major effort in a theoretical model attempting to predict the response of a floating structure is usually dedicated to the computation of the hydrodynamic force. In the numerical model presented, the following types of hydrodynamic forces are computed:

1) First order (linear) hydrodynamic force:

This is the hydrodynamic force that is proportional to the wave amplitude and the frequency of oscillation of the force is identical to that of the wave front under consideration. This also called the "wave frequency force" and the resulting motion the "wave frequency motion". The classical linear spectral techniques are used in order to obtain the spectra of the hydrodynamic force and other variables of interest.

2) Second order (nonlinear) hydrodynamic force:

The second order force, as its name implies, is proportional to the square of the wave amplitude and the computation is much more tedious and extremely time consuming when compared with the linear force. This is also simply called the "Drift force" in many literature even though many other phenomena (e.g. wind and currents) can cause similar forces. It can be mathematically shown (4) that the combination of a pair of incident wave fronts propagating in any two directions causes the generation of a mean drift force and one oscillating at the difference frequency of the two wave fronts as shown schematically in Figure 2. The surface wave shown in the

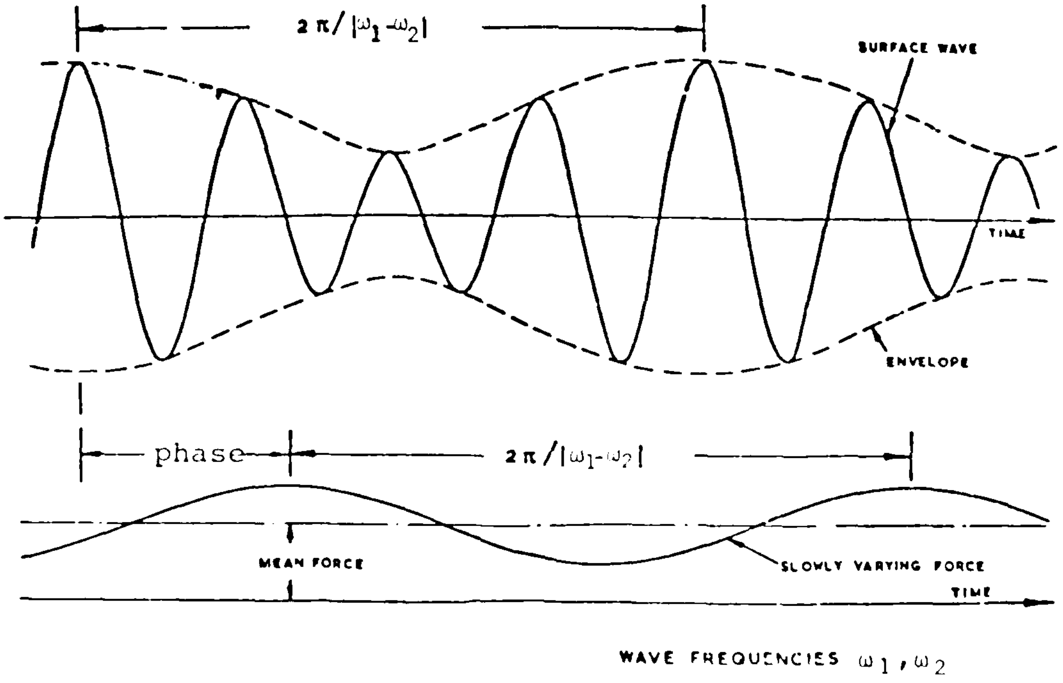
$2\pi/|\omega_1-\omega_2|$
SURFACE WAVE
TIME
ENVELOPE
phase
$2\pi/|\omega_1-\omega_2|$
MEAN FORCE
SLOWLY VARYING FORCE
TIME
WAVE FREQUENCIES ω_1, ω_2

Figure 2. Drift force generation by two linear wave fronts

figure is the sum of two general sinusoids. The slowly varying drift force at the difference frequency shown immediately below the surface wave is observed to be varying with the envelope. Therefore, all such possible combinations have to be considered when the computation is carried out for a random sea state requiring an enormous amount of computational time. The "transfer function" that defines the wave height to force relationship now becomes quadratic instead of being linear as before.

Once the hydrodynamic forces are computed, the "wave frequency" and "drift" motions can be obtained by applying the equation of motion after properly modeling the structural and mooring charateristics. The correct modeling of the mooring characteristics become important in the determination of the drift oscillation which occurs at the natural frequency of the mooring system. The computed wave frequency motion is then utilized to obtain internal structure forces (and moments) while the mooring forces are computed using the drift motion. Since the results are presented in their spectral form, the user is able to obtain many statistical quantities of interest (e.g. mean square value, probabilities of occurrence etc.) of the variables of interest. The mathematical expressions are complicated and therefore are left out in order to improve the readability of this paper, but can be found in reference (4).

Computer programs

The numerical model discussed in the previous section was fully implemented using a series of computer programs, developed in a 16 bit micro computer. The flow diagram depicting its major functions are shown in Figure 3. Although under normal circumstances 1 M Bytes of memory is likely to be adequate, the programs can be transferred to a mainframe computer if and when necessary. Use of standard FORTRAN-77 programming language is responsible for this portability.

Results and comparisons

In order to validate the numerical model, it was used to predict the motion of the West Point prototype floating breakwater and the results were compared with the field data. A summary of the sea state used in the comparison is given below:

Significant wave height = 1.8 ft (0.55 M)
Significant wave period = 2.4 s
Wind speed = 15 m.p.h (24 KMH)
Mean wind direction = 10 deg from the normal to the breakwater axis (approx.)

The above sea state is described by the wave spectrum shown

ANALYSIS FLOW DIAGRAM

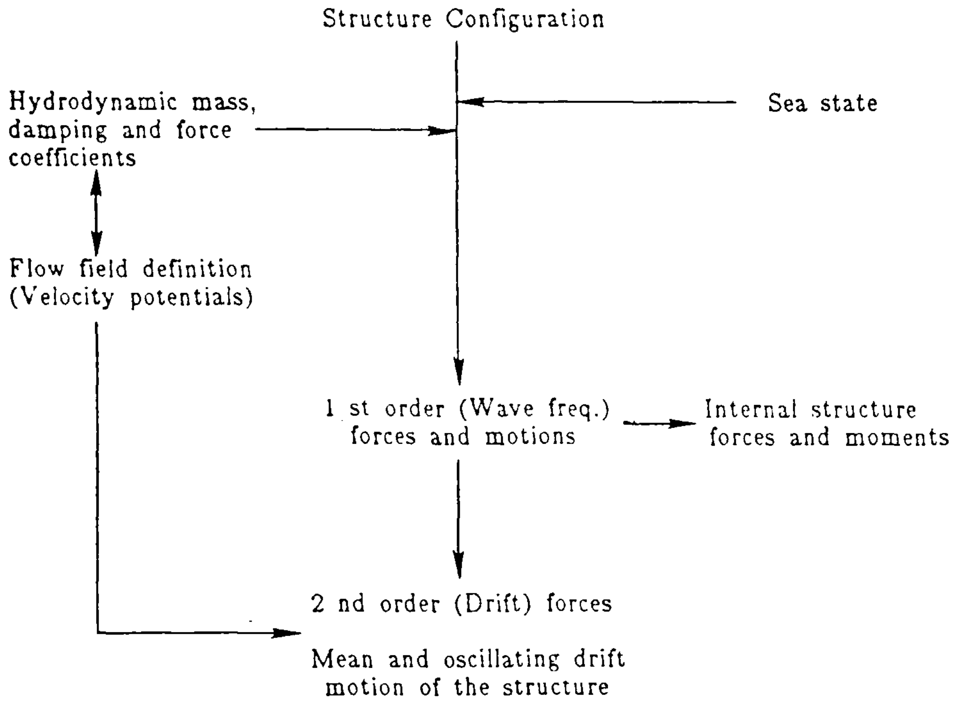
Structure Configuration
Hydrodynamic mass, damping and force coefficients
Sea state
Flow field definition (Velocity potentials)
1 st order (Wave freq.) forces and motions
Internal structure forces and moments
2 nd order (Drift) forces
Mean and oscillating drift motion of the structure

Figure 3. Program flow diagram for floating breakwater Analysis

in Figure 4. The predicted (wave frequency) hydrodynamic force spectrum at the mid point of the structure is shown in Figure 5. Figure 6 shows a typical sway acceleration timeseries measured off the accelerometer on the east pontoon. Its spectrum compared with that predicted by the numerical model is shown in Figure 7. The agreement is very close. Similar agreements were obtained in heave and roll directions. The resulting horizontal structural shear force and bending moment about the vertical axis at the mid point predicted by the model is shown in Figures 8 (a) and (b). The predicted sway drift force spectrum shown in Figure 9 exists at the low end of the frequency spectrum. Notice the difference in the orders of magnitude in the wave frequency and drift hydrodynamic forces. Also obvious is the non zero ordinate at zero frequency which indicates the existence of a mean drift force. A comparison between the measured and predicted drift oscillation can be found in Figure 10. The agreement is satisfactory although not exact. Several reasons can be attributed for this occurrence. Among them are:

1) The number of points in the field data timeseries were insufficient for spectrum computation at a frequency range as low as the one encountered. This resulted reduced frequency resolution in the spectrum and possibly "lost" spectral peaks.

2) Errors in the computation of hydrodynamic damping. The spectrum becomes increasingly "spread out" with higher damping.

3) Contribution by other phenomena not accounted for in the model

The following table summarizes the wave frequency and drift motions predicted by the model:

Table 1. Comparison of predicted wave frequency and drift motions

Type of motion	Mean disp.	Std. Dev.
Wave frq.	0.0	.082 FT (.025 M)
Drift	.224 FT (.068 M)	.565 FT (.172 M)

It is clear therefore that the drift forces, that are much smaller than the wave frequency forces, are capable of inducing a much larger motion than the latter depending on the mooring characteristics.

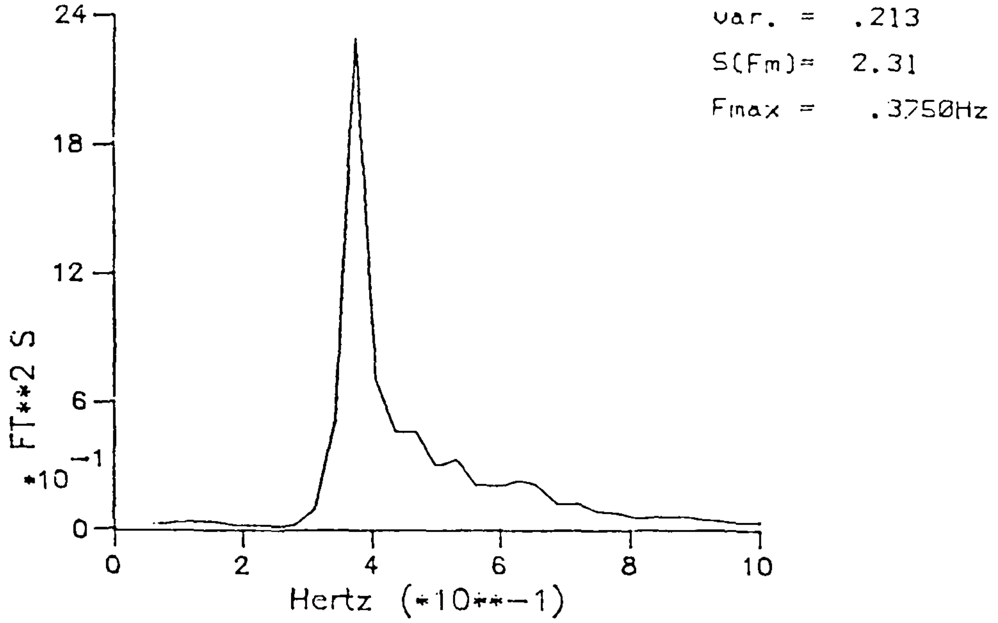

Figure 4. Measured incident wave energy spectrum

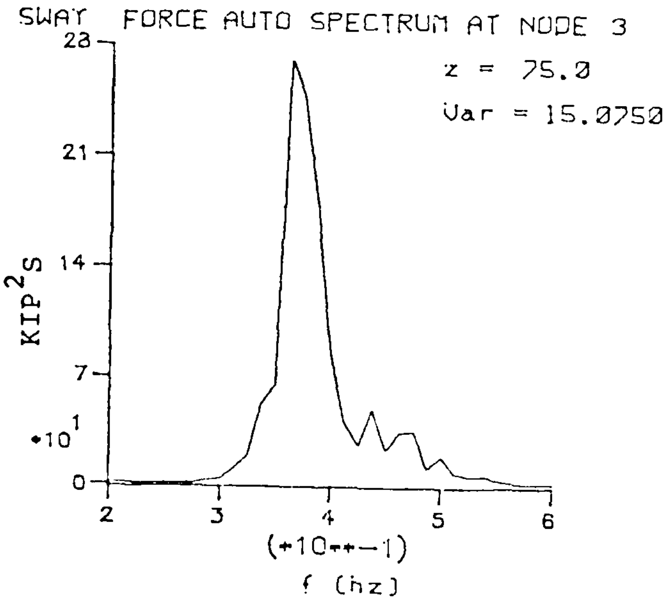

Figure 5. Predicted hydrodynamic sway force at mid point

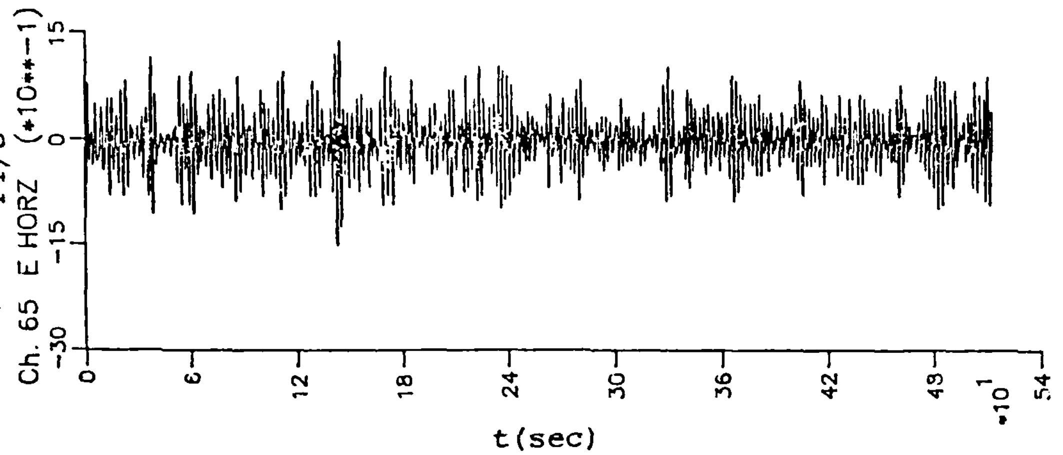

Figure 6. Measured sway acceleration at east pontoon

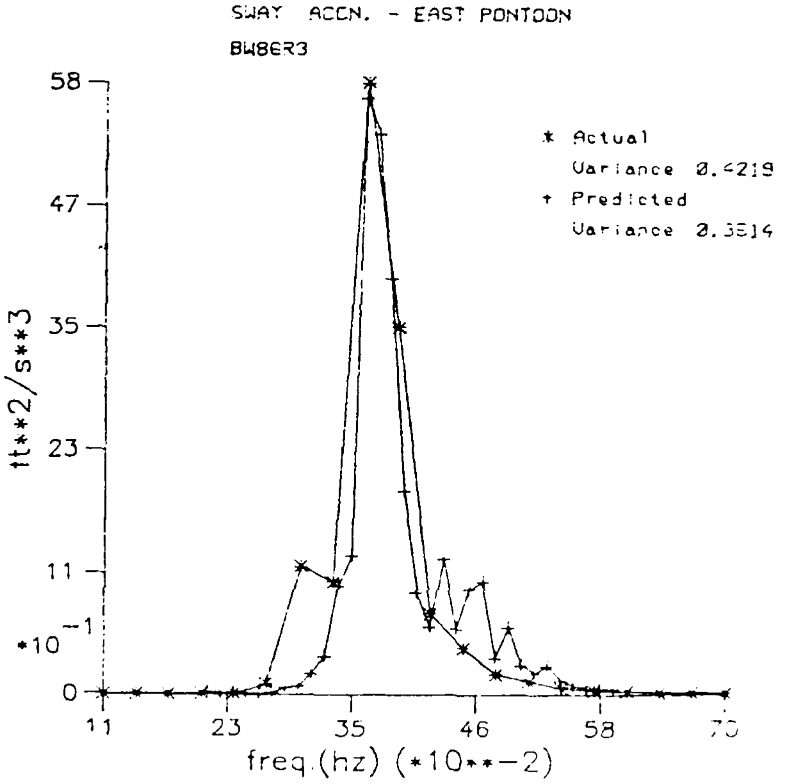

Figure 7. Predicted and measured sway acceleration

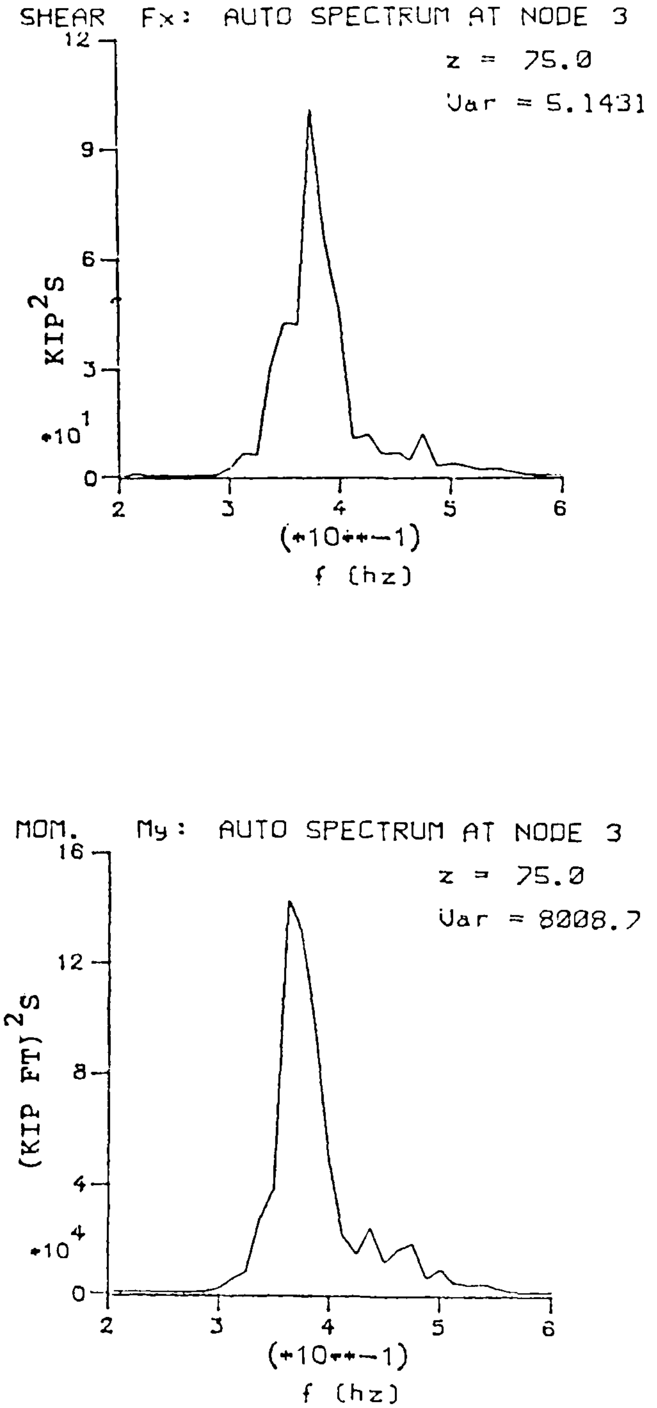

Figure 8. Predicted horizontal structural shear force and bending moment about vertical axis at mid point

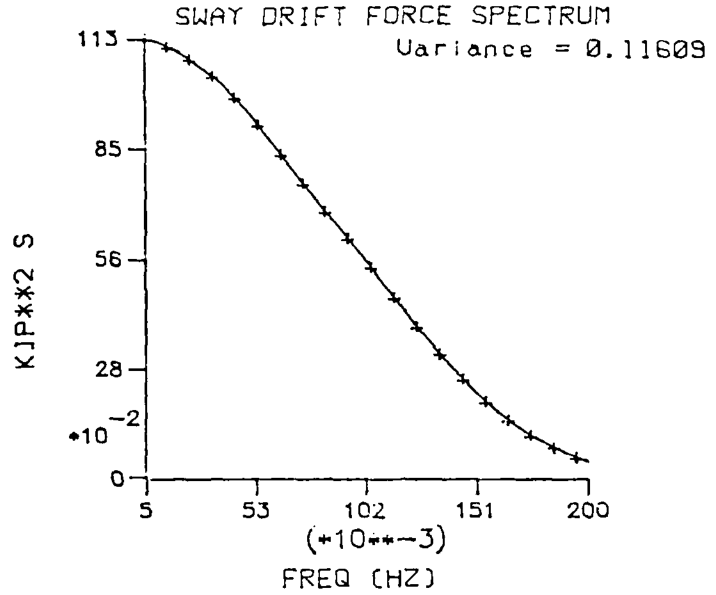

Figure 9. Predicted sway drift force spectrum

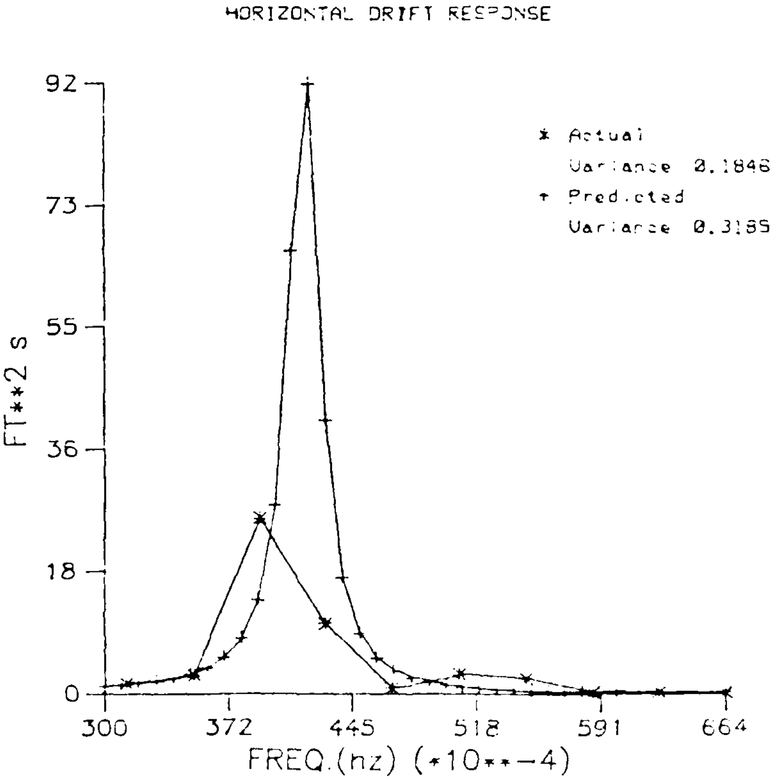

Figure 10. Predicted and measured sway drift motion response spectrum

Conclusions

Numerical modeling of floating breakwaters is a viable alternative to costly physical model studies. Under certain conditions the structure can undergo large amplitude drift oscillations which must not be neglected if mooring forces are of interest.

Acknowledgements

The field data used in the comparisons of this paper were obtained from the Floating Breakwater Monitoring Program sponsored by the U.S. Army Coastal Engineering Research Center through the Seattle District Army Corps of Engineers. Acknowledgement is also extended to Derald Christensen who played a major role in instrumentation and data acquisition.

APPENDIX I - REFERENCES

1. Kinsman, Blair: Wind Waves, Englewood Cliffs, New Jersey: Prentice Hall Inc., 1965

2. Christensen, D.R. and Ratnayake, S.: Installation, Operation and Maintenance Manual for Breakwater Data Acquisition and Analysis System, Technical Report 91, Water Resources Series, Department of Civil Engineering, University of Washington, Seattle, 1984.

3. Baggeroer, A.B.: "Recent Signal Processing Advances in Spectral Estimation and their Application to Offshore Structures", Proc. Second International Conference on the Behavior of Offshore Structures, London, England, 1979.

4. Ratnayake, S: Dynamic and Drift Response of Floating Structures in Multi directional Seas, Ph.D dissertation, University of Washington, Seattle, 1985.

TESTING AND ANALYSIS OF
A FLOATING BREAKWATER
BY GEORGE G. ENGLAND 1/

Introduction. Since the turn of the century there has been a slow increase in the use of floating breakwaters for protecting shorelines, structures, and moored vessels from damage by storm or ship created wave action. Increasing pressure for additional small craft facilities has put a premium on all protected inland waters, even those which are only moderately sheltered. Floating breakwaters, if placed in judiciously chosen locations, appear to provide an attractive solution, particularly in areas where deepwater or poor foundation conditions preclude the installation of conventional fixed breakwaters.

Attention in floating breakwaters is presently focused upon the following: (1) the use of model studies for determining the most efficient breakwater for a particular wave climate, (2) verification of methods for predicting forces expected to act on structures and anchor systems, (3) determining optimum construction materials and providing a low cost means of connecting and fendering individual breakwater modules, and (4) developing more recent comprehensive summaries of practical experience with floating breakwaters.

For these reasons, the U.S. Army Corps of Engineers initiated the "Floating Breakwater Test Program" to develop consistent design criteria for floating breakwater applications in semiprotected coastal waters, lakes, and reservoirs. One type of floating breakwater studied was the concrete box design shown in figure 1.

The major objective of this report is to compare assumptions and procedures used in designing the breakwater with results provided by actual field test data. This analysis includes comparisons of design and full-scale quantities such as moments, shears, and wave pressures, in the two 75-foot-long (23 M) rigidly connected modules.

The test site was selected on the basis of access, wave action, water depth, navigation environment, bottom characteristics, and adjacent shoreline features. Water depth at the concrete breakwater was

1/Supervisory Structural Engineer, U.S. Army Corps of Engineers, Seattle District, P.O. Box C-3755, Seattle, Washington 98124-2255.

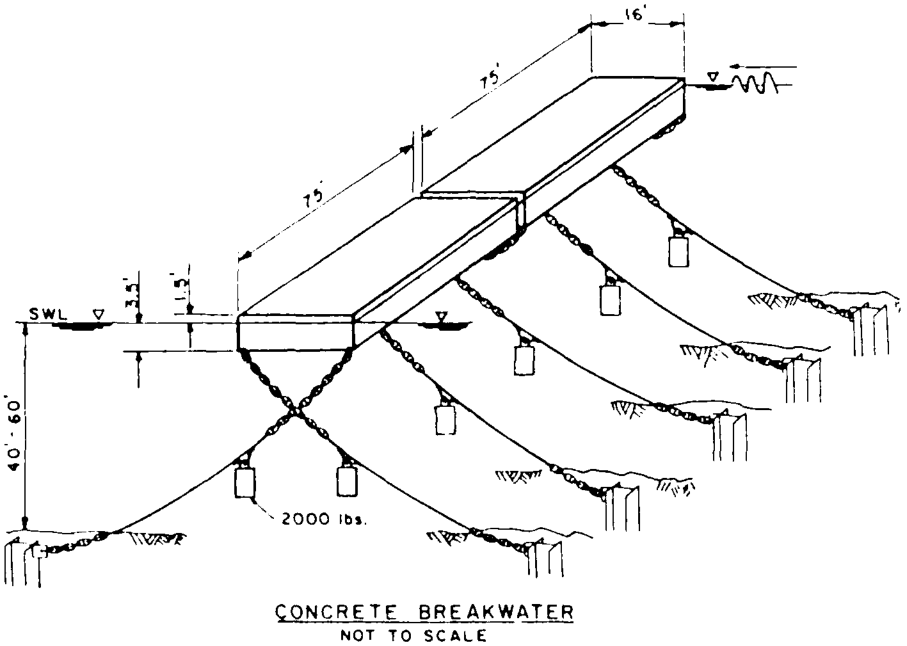

Figure 1: Isometric Drawing of Concrete Breakwater

approximately 50 (15.2 M) feet at mean lower water (MLLW).1/ Waterdepths on the north side of the breakwater were between 20 to 50 feet (6-15 M) MLLW, while depth on the south side increased with distance from the breakwater. The foundation consisted of sand and gravelly sand underlain by very dense glacial clay.

The maximum design wind speed of 47 miles per hour (m.p.h.) (75 kph) was based on wind speed data provided by wind velocity duration curves developed by the Corps of Engineers. Tides at the site are typical of the Pacific Coast of North America and are of the mixed type with two unequal highs and lows each day. Tidal range data for the site vicinity indicated the diurnal range was 11.32 feet (3.45 M). Based on the Corps of Engineers measured values, the average daily maximum speed was estimated to be 2.0 f.p.s. (.6 mps).

Design loading for the breakwater was of three types: wave, current, and sway2/ forces. Wave loads act in both the sway and heave directions while current and sway loads act in the sway direction only.

1/MMLW is the datum developed and used by the National Ocean Survey (NOS). It is based on the average of the daily lowest low tide for a 19-year period of record taken in the local vicinity. MLLW is always used for work in the tidal zone.

2/Sway forces are due to slight low frequency oscillations of the structure caused by the interaction of swell and wind wave loadings and anchor system flexibility.

The design or significant wave[1] height and period (6.0 feet (1.7 M) and 5.0 second) was calculated using the design wind speed and maximum effective fetch length (7). Short period wave forces were calculated using the Miche-Rundgren (6) method for nonbreaking waves on a vertical wall and design wave height and period, with allowance made for wave transmission. The design wave load in the sway direction was calculated to be 1,750 pounds per foot, (lb/ft) (25.5 KN/M) over a crest length of 128 feet (39.0 M).

The current drag force on the breakwater was calculated using a combination of wind generated and tidal currents and the hydraulic pressure drag formula. The estimated wind generated current was 2.0 f.p.s. (.61 M/S), giving a total current velocity was 4.0 f.p.s (1.22 M/S). A current drag load of 120 lb/ft (1.75 KN/M) was calculated using the total current velocity and a pressure drag coefficient $C_D = 2.0$.

To account for long period swells, the sway force was calculated as being equal to 5 percent of the structure weight. This 5 percent value was based on forces measured on the breakwater at Tenekee, Alaska, which suggested that only a small portion of the swell is ultimately transmitted to the breakwater. The sway load calculated was 180 lb/ft (2.6 KN/M), and combining with the wave load and current drag, provided a maximum loading in the sway direction.

Heave forces on the concrete breakwater were calculated using a design wave height of 8.2 feet (2.5 M) having a period of 4.6 seconds corresponding to the 1 percent significant wave.[2] The use of the 1 percent significant wave was based on the rigidly connected floats spanning between crests of two large waves. The heave loading of 486 pounds per square foot (p.s.f.) (23.3 KN/M2) in a triangular distribution was thought to be representative of the actual distribution of wave loads.

The concrete breakwater design was the result of combining previous field and design experience with recent detailed engineering effort. In order to provide an efficient wave attenuating structure, a width of 16 feet (4.9 M) and a depth of 5 feet (1.52 M), with 1.5 feet (0.5 M) of freeboard, was selected. The final design concept was the two post-tensioned concrete units. Each one was subdivided into compartments formed by cut styrofoam blocks, which also provide positive bouyancy in the event of hull leakage due to structural damage. The two units were post-tensioned together with Dywidag bars to form a rigid 150-foot-long (45.7 M) breakwater. The complete structure was held inplace by means of anchor cables.

---

[1] The significant wave is defined as the average height of the highest one third of waves. $H_s = H_{1/3}$

[2] The 1 percent significant wave is defined as the average height of the highest 1 percent of waves: $H_1 = 1.67\ H_s$

The two rigidly connected 75-foot (23 M) modules were analyzed for the maximum moments and shears using computer programs FLOATX and ICES STRUDL II (ICES) (1 and 2). Maximum moments, shears, and axial forces for design of interior and exterior top and bottom walls and slabs were calculated by modeling a 1-foot length of breakwater cross section. The anchor lines were modeled as elastic supports inputting three stiffness values of 8, 16, and 40 k/ft (116.7, 233.4, and 583.6 KN/M).

Dynamic analysis of the prototype breakwater was performed by a relatively new computer program "FLOATX" developed at the University of Washington (1). Dynamic frequency domain responses were calculated using the program generated design wave spectrum for periods of 2 to 6 seconds and wave time series. Response quantities are shown in table 1.

The design of the prototype breakwater, based on a static structural analysis, was calculated using ICES (Integrated Civil Engineer System) STRUDL II (Structural Design Language, Second Version). ICES is a large-scale computer program developed by the Civil Engineering Department at the Massachusetts Institute of Technology (2). Maximum response quantities, shown in table 1, were calculated by moving the design wave load in 1-foot (.30 M) increments along the length of the breakwater.

TABLE 1
MAXIMUM DESIGN RESPONSE QUANTITIES
Breakwater

	Sway Direction		Heave Direction	
Program	Moment ft-k (KN.M)	Shear K (KN)	Moment ft-k (KN.M)	Shear k (KN)
FLOATX	1140 (1546)	44 (196)	1646 (2232)	37 (164.6)
ICES	4363 (5916)	89 (396)	970 (1315)	37 (164.6)

Comparison of design responses shows differences in both sway and heave moments which are from variations in the methods of resolving the stiffness matrices, wave load modeling, hydrodynamic mass used for the dynamic case only, and the vertical component of the anchor stiffness. The heave shears are identical since the hydrodynamic mass has a larger effect in bending than shear. The sway shear varies due to different wave loading models used in the dynamic and static cases.

Instrumentation, Data Collection, and Reduction. A major feature of the prototype test program was the state-of-the-art field monitoring system capable of measuring the following quantities: anchor forces, incident and transmitted wave heights, dynamic pressures, concrete strains, accelerations, relative motions, wind speed and direction, water current velocity, air and water temperature, and flexible and rigid connection forces.

An RCA microprocessor based data acquisition system (DAS) capable of sampling 96 channels of data at a sampling rate of up to 4 hertz (Hz) was used for field monitoring. The system was designed to be operated manually or to sample automatically, at hourly intervals, certain key parameters such as wind speed and wave height. At the start of the program, monitoring was initiated when the average wind speed exceeded 15 m.p.h. (24 K/hr) for a 1-minute period, or if selected anchor force gages measured loads exceeding 2,000 pounds above the initial tension. If these preset levels were exceeded during the brief hourly sampling interval, the DAS was switched on taking 8-1/2-minute records during which time series of 2048 points per channel for 80 input channels was generated at a sampling rate of 4 Hz. Instrumentation details are discussed in further detail in reference 7.

It should be kept in mind that only a fraction of the total available data recorded has been analyzed. The major effort has been directed toward the analysis of wave pressures and concrete strains. Data was taken from five 8-1/2-minute records occurring at different times during the test, four containing storm data and the fifth record, a boat wake attenuation test. These five records provided for random and monochromatic wave loadings, of which the latter should develop the larger response quantities.

The internal force resultants of the breakwater were evaluated from the reading of four longitudinal strain gages located in the corners of the breakwater section or the four pairs of transverse strain gages located in the two walls and top and bottom slabs. Using elementary theory for flexure of prismatic beams, and a program to add concrete strains, the three forces and moments were calculated. Verification of the east moments and tension force were also made by adding the transverse gages.

The data presented is based on the summary statistics, which include minimum, maximum, mean and standard deviation values, as well as filtering at the Nyquist frequency, fast Fourier transforms (FFT's), and cross-spectral phase and coherency analysis (4).

Observation and Discussion. In comparing measured response parameters to those calculated by a model, the first step is verifying the model. A fundamental check is the verification of mode shapes and natural periods, so an independent study was done to verify the authenticity of the computer program FLOATX.

Using the same finite element model as input to the FLOATX program and knowing that sway, heave, and roll motions can be treated independently, the verification model was developed. Using bending, torsional, and buoyancy stiffness matrices with the consistent mass matrix and elastic springs for anchor stiffness, the equations of motion are:

$$[M]\{\ddot{X}\ (t)\} + [C]\{\dot{X}\ (t)\} + [K]\{X\ (t)\} = \{R(t)\}$$

where the matrix form can be written as:

$$\ddot{\underline{X}} + (2\ \lambda\ W)\ \dot{\underline{X}} + W^2\ \underline{X} = \underline{\phi}^T\ \underline{R}(t)$$

where W and ϕ^T are the eigenvalues and eigenvectors, respectively, and are found from the determinate of the mass and stiffness matrices. The global coordinate system was used in constructing the total stiffness matrix by the direct stiffness method.

Additionally, the elastic spring stiffnesses were merged into their appropriate locations within the total stiffness matrix and were of the form K = kip/ft. Static condensation was used to reduce out the rotational degrees of freedom since the float was considered torsionally very stiff.

The mass matrix was developed by using the consistent mass method, and rotational degrees of freedom were reduced out. A nondimensionalized scale of (M+Ma)/M was added to include effect of hydrodynamic mass. Hydrodynamic mass and damping coefficients were calculated from graphs by Vugts (8) which are based on two-dimensional theory and experiments for rectangular cross sections. The interpolated breadth to draft ratio (B/D) was used to determine the added mass Ma = $C\rho A$ and percent critical damping.

The resulting matrices were solved using a mathematical analysis program and the sway and heave mode shapes and natural periods when compared with mode shapes and natural periods calculated by FLOATX have identical mode shapes with minor variations in the natural periods. These differences are due to the method used for solving the eigenvalues and eigenvectors, to the values used for the added hydrodynamic mass and the degree of accuracy of the input values.

The original intent had been to add the longitudinal and transverse strains and to use the equations of bending of prismatic beams to determine the actual breakwater response parameters and compare them to the FLOATX program output. During the investigation it was found that two gages located near the point of maximum moments were giving bad data. As a result, with only two active gages, the heave moment can be calculated with certainty, although the sway moment can be estimated by assuming the axial force is zero.

It was assumed, based on a review of the literature (4 and 5), the data should follow a Rayleigh distribution. This Rayleigh distribution assumption was checked by looking at several time series for wave heights, strains, pressures, and accelerations. When examining the data it should be noted that the significant or 1 percent value must be based on the standard deviation of reliable data.

Since floating structures such as the breakwater are very dependent on the period of energy, the peak energy density, Tp, of the incident wave field was calculated and compared to the peak energy period of anchor forces, strains, pressures, and accelerations. The resulting comparison yielded favorable results. The range of peak periods, when compared to the natural periods output by FLOATX for heave, sway, and roll, shows the structural response is in between the first and third frequencies. For the most part, the breakwater is witnessing rigid body motion.

As discussed previously, the intent of this report is to compare the field measured breakwater responses with those predicted by FLOATX. The first step was the establishment of the computer program capable of adding or subtracting the measured concrete strains to obtain moments, shears, tensions, and torsion. The comparison of measured and predicted values was based on the following methods: (1) Use of the Rayleigh distribution with standard deviations of measured structural parameter time series; (2) establishment for each of the measured parameters, mean values depicting the "at rest" state of the breakwater, then subtracting these from the calculated maximum values; and (3) inputting the proper significant wave height and period into FLOATX and obtaining the predicted values. Items 1 and 3 have been previously discussed but 2 has not. The establishment of mean values for each structural parameter was done by determining the mean strain values for each gage during a period of calm seas and, at best, when slack tide occurred. Mean strain values where calculated by averaging the sum of the means from 13 time series records each containing 2,048 data points. The mean strain values, once established, were added or subtracted to calculate mean or "at rest" values of moments, shears, tensions, and torsions. These values, as well as the Rayleigh distribution and FLOATX results of a typical record, are shown in table 2.

Comparisons were made using five prototype breakwater time series records. The significant incident wave heights varied from 1.5 to 3.2 feet (.46-1.0 M) and periods from 2.5 to 3.3 seconds, attacking the breakwater from the north at 90 degrees to the longitudinal axis. Using summary statistics the standard deviation and maximum values for moments, shears, tensions, and torsions were determined.

As is the case with any comparative study between predicted and measured parameters, difficulty in obtaining good clear results is always present and caution should be used in trying to establish design criteria based upon such comparisons. For this reason, to add reliability and accuracy to the results and because only two of the four east longitudinal strain gages were functioning properly, three additional response parameters were calculated. Using the east transverse stain gages, these three responses were the east heave and sway verification moments and east verification tension. They were used to verify the results produced using the east longitudinal gages and their results are tabulated in table 2.

TABLE 2

Typical Structural Response Comparison

H_s=2.40 Feet (0.73 M)
T_s=2.50 Seconds

Structural Response	FLOATX Output Maximum		Rayleigh Distribution 40		Measured	
West Heave Moment (F-K) (KN.M)	328.5	(445.4)	98.0	(132.9)	68.2	(92.5)
West Sway Moment (F-K) (KN.M)	392.9	(532.8)	121.2	(164.3)	114.0	(154.6)
West Tension (K) (KN)	--		8.4	(37.4)	20.3	(90.3)
East Heave Moment (F-K) (KN.M)	432.0	(585.8)	100.4	(136.1)	106.8	(144.8)
East Heave Ver.[1] Moment (F-K) (KN.M)	432.0	(585.8)	118.0	(160)	130.4	(176.8)
East Sway Moment (F-K) (KN)	517.0	(701.0)	49.2	(66.7)	101.4	(137.5)
East Sway Ver.[1] Moment (F-K) (KN.M)	517.0	(701.0)	109.6	(148.6)	108.6	(147.3)
East Tension (K) (KN)	--		13.2	(58.7)	7.6	(33.8)
East Ver.[1] Tension (K) (KN)	--		14.0	(62.3)	40.8	(181.5)
East Heave Shear (K) (KN)	10.0	(44.5)	3.2	(14.2)	6.2	(27.6)
East Sway Shear (K) (KN)	11.6	(51.6)	2.4	(3.2)	10.2	(45.4)
East Torsion Moment (F-K) (KN.M)	1.9	(2.6)	10.8	(14.6)	43.7	(59.2)

[1] Ver. = Verification

The comparison between measured and Rayleigh distribution values was done as a check for added reliability of the results. Both methods are based on actual data. The measured values are calculated by using a mean value for a particular response parameter established from calm sea strain gage data when the structure was "at rest." This value was then subtracted from the maximum value of any of that parameter's time series. The Rayleigh distribution uses the standard deviation from the parameter's time series. This standard deviation gives the statistical dynamic response about the mean of a given time series.

A direct observable result of the difference in the two methods is that in several cases, both east heave moments and shears, the measured value exceeds the Rayleigh value. For a "true" Rayleigh distribution this would not be the case. An explanation for the measured being greater than the Rayleigh distribution is the difference in the parameters mean values. The measured parameters mean value, for all intents and purposes, shall be considered zero, but is not due to the instrumentation system, the stain gage output settings, the current velocity not being known at the time of reading, and summary statistics of the entire time series containing portions of monochomatic waves. For these reasons, the measured mean value is greater, or even less, than the mean of the generated time series used in the Rayleigh method. This difference creates an additional measured parameter response value. This additional value may be added to any parameter and is the reason for using a sway load equal to 5 percent of the breakwater's weight in the original design loadings discussed previously. In other words, the breakwater feels a base force caused by a storm which produces small but significant structural responses about which the dynamic response fluctuates because of wave loading.

Good comparison between the Rayleigh method and the measured values appears evident for moments and shears at both the east and west locations. The exceptions being west heave moment measured value and the east sway moment Rayleigh value. Experience and engineering judgment would reject the use of both values as being too low when compared to the overall results. There are also large differences observed between the Rayleigh and measured value at tension and torsion locations.

Except for the east torsion moment, none of the actual measured parameters exceeds the maximum value of those parameters given by FLOATX. In fact, most do not exceed the average value predicted by FLOATX, the exceptions being east heave and sway shears. By observation, the accuracy and reliability of the west heave moment and tension and east verification tension and torsion may be questioned and rejected as being too high or low based on sound engineering judgment. No direct comparison can be made between FLOATX and the measured value for east and west tensions since this parameter is not output by the model program.

Similar to the measured values, only one of the parameters based on the Rayleigh distribution exceeded the average or maximum values predicted by FLOATX. The one exception is the east torsion moment. By observation, the east sway moment, Rayleigh method can be discarded as too low. The Rayleigh distribution values appear to be in better agreement than the actual measured values because of the more realistic results for all the responses. This is due to the higher margin for error that may occur in the establishment of the mean values used in the measured response calculations previously discussed.

The general trend of the results in the comparisons are that the response parameter values observed were quite low during this storm. This, coupled with the fact that the peak frequency of these response parameters, definitely shows that the breakwater is witnessing only rigid body motion. The rigid body motion is in direct agreement with the results of work done by Miller (3) on the same prototype breakwater. Miller also stated the torsion response output by his model was in fact low. Table 2 shows this is indeed the case with the present FLOATX using the Rayleigh distribution east torsion result as a reasonable value. Using the measured and Rayleigh method, the maximum sway moment occurred at the west location, a direct violation of elementary beam bending, meaning there is some uncertainity in the measured values calculated.

A brief summary of the possible causes of errors is as follows: (1) the mean values for the strain gages used to establish the mean response parameter value may be in error due to the current velocity not being known and the summary statistics used contained portions of monochromatic waves, (2) the periodic loss of a properly functioning gage and the definite loss of two east longitudinal gages, (3) large random errors in all or some of the gages, which in some cases canceled each other, but in other cases were additive. The random errors were the result of very small measured strains and an inevitable high noise-to-signal ratio, (4) a possible error in the STRANAD program which can be discounted because of results obtained in other comparisons to be discussed later, and (5) periodic glitches caused by DAS (Christensen, 1984).

It should also be noted at this point that FLOATX does not account for the long period sway forces caused by drift, tidal, or current loadings. This lack of long period loading, which may in fact cause low frequency oscillations of the float and significant forces, under predicts sway moments. Second generation work currently being conducted by Ratnayake (1985) will account for these long period loadings.

In addition to this report is the cursory analysis of the effective crest lengths, those "seen" by the structure, for short crested, wind generated, or monochromatic waves. Even today the present practice is the use of long crested wave in design force predictions for the design of floating structures. It is assumed, as done by Seltzer (1979), that a crest exists as long as high correlation is maintained. Transducer time series were analyzed in conjunction with the auto-spectrum to determine, if possible, what crest lengths the breakwater was seeing.

Coherency and phase angle, were used to measure the crest length. Since in theory all pressure transducers being attacked at 90 degrees by the same wave crest will measure identical signals, i.e., all signals should be highly correlated with zero phase differences. For waves attacking at angles less than 90 degrees, it can be assumed that the coherency signal will drop off more rapidly as spacing distance increases. This is a highly speculative assumption because the possibility exists for a continuous wave forming, that runs along the face of the structure causing the signals to give false readings. Extensive analysis must be conducted before these assumptions can become conclusive. An additional check of the crest lengths was conducted utilizing the wave staff array located at the east end of the breakwater.

An observation of the storm produced pressures shows a definite but rather gradual drop in coherency as the distance increases. The same is also true for the wave array analysis. It should be noted that the high coherencies occur at the same peak density period of 2.5 seconds calculated from the auto-spectrum of the pressure transducers, the incident wave staff and wave array, adding confidence in the reliability of the data.

Plotting of coherency as a function of spacing was done for the storm data in which all coherencies were connected by lines. A downward trend in coherencies as spacing distance increased was observed. This is in direct agreement with Seltzer. Another plot was constructed plotting the average coherency against spacing distance. A spacing interval of 5 feet (1.5 M) was used and the results are as shown in figure 2. A smoother trend can be seen which is similar but not exact to plots created by Seltzer.

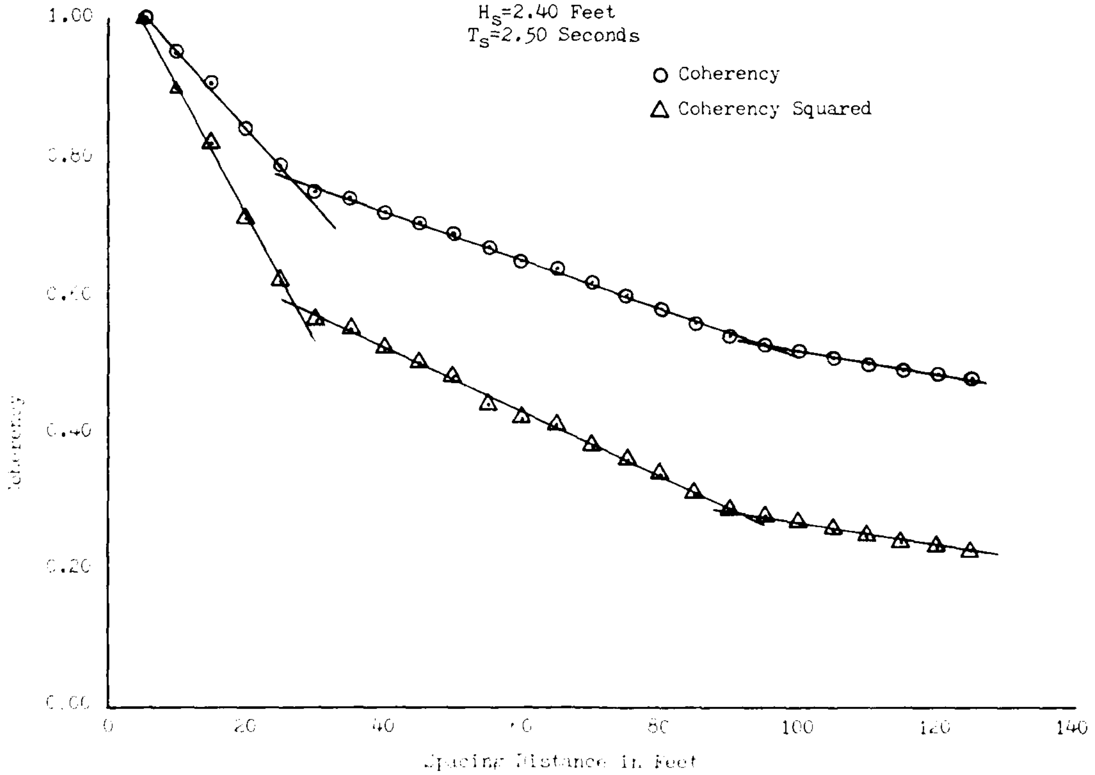

Figure 2. Average Coherency Versus Spacing Distance

It was assumed (following Seltzer) that a sharp drop in coherency would mark the end of a wave crest, so by drawing straight lines fitted to a series of points, sharp changes in slope would occur and their intersection would mark an approximate end of crest length. For this to have any meaning, only the data above .6 coherency was used. It should be noted that in addition to the average coherency plotted in figure 2, the squared coherency is also plotted, and lines drawn through the points also mark the effective crest length. As a result, the effective crest lengths L' are given as 27 and 27.5 feet, (8.2 and 8.4 M) respectively, from the average and squared average plots. Although highly speculative, there appears to be some agreement in the results. Analysis of the wave staff array coherencies also plotted shows the effective crest length of only 15 feet (4.6 M). This difference verifies the observation of Seltzer and others that the effective crest seen by the structure is different to that occurring in open sea. This may be due to phenomena such as reflection and breaking of waves against the structure.

To compare to Seltzers results, L'/L, which equals the ratio of effective crest length to wave length, was calculated using Scotts (1969) wave length to wave period relationship for short crested waves of $L = 3.70T^2$ and the above results. The following ratios were calculated for L = 23.1 feet (7.0 M); L'/L = 1.17 for L' = 27 feet (8.2 M); and L'/L = 1.19 for L' = 27.5 feet (8.4 M). These ratios are large compared to Seltzer's results of .29 to .72 but low compared with Weigel's results (9) of 2 to 3. As is the case in conducting a highly speculative analysis such as this, caution should be given to these results and a more comprehensive study should be conducted with better data before any conclusive material or design criteria can be developed.

General comparison of this report's results with the design of East Bay and Friday Harbor floating breakwaters will briefly be discussed. Both East Bay and Friday Harbor are Corps of Engineers design projects of similar construction with slight differences in anchor systems.

East Bay floating breakwater is 656 feet (200 M) in length consisting of three modules 218 feet (66.5 M) long by 16 feet (4.9 M) wide by 5 feet 3 inches (1.6 M) deep. The modules are post-tensioned, reinforced concrete boxes with foam fill identical to the prototype with the exception of preformed holes along each edge of the modules. These holes were for the timber anchor piling, allowing the breakwater to rise and fall with the tide while providing lateral support. Timber piles were selected because of the shallow water depths.

The design wave height of 2.7 (.8 M) feet and period of 2.9 seconds is close to the wave height and period of one time series analyzed, meaning the results in this report can be directly applied. The design values for moments and shears were conservative, as in the design of the prototype; however, the response of the East Bay breakwater may be different because of the timber anchor piles. The stiffness of the timber piles is more linear than the catenary anchor cables, resulting in more accurate structure design loads.

By observation a reduced design wave should have been used for the East Bay design. This would allow for even smaller design loads which are still conservative.

Friday Harbor floating breakwater totals 1,590 feet (485 M) in length consisting of four separate sections of different lengths and widths. The breakwater is constructed using 330- and 660-foot-long (100.6 and 201.6 M) by 21-foot-wide (6.4 M) by 6-foot-deep (1.83 M) modules and two 300-foot-long (91.5 M) by 16-foot-wide (4.9 M) by 5-foot 6-inch-deep (1.7 M) modules. The modules are post-tensioned, reinforced concrete boxes identical to the prototype, except for the depth and anchor spacing. The anchor system is similar in design to the prototype.

The design wave, having a height of 3.2 feet (1.0 M) and period of 3.2 seconds, was a conservative selection because of the unknown moments and shears the structure would see. As a result, a conservative static analysis was used to calculate design response values. Results in this report show that a factor of safety of about 10 exists at Friday Harbor. By using FLOATX output rather than static analysis, and by providing modest post-tensioning, a conservative but less overdesigned structure could have been developed.

Conclusions and Recommendations. A large amount of field data related to the wind and wave induced motions and structural response of a floating breakwater were collected. Only a very small portion of the amount collected was processed and analyzed for this report, but the information gained on the dynamic behavior of the floating breakwater has been valuable.

Although the prototype breakwater is short compared to other floating structures in service, the results are representative and applicable to the floating breakwater. Reasonable agreement was found with the comparison of actual structural responses to FLOATX output; enough agreement to say that the prototype experienced only rigid body motion. Caution should be used until further analysis of the data verifies the general trend discussed here.

The measured results reasonably agree with the predictions of FLOATX. In all cases, except for torsion, the FLOATX values were conservative. This means that floating structures can be designed with confidence using FLOATX. Although the prototype breakwater is shorter in relation to its depth than most floating structures in service, FLOATX is still able to predict the response of floating structures of rectangular cross section.

Rigid body motion dominated the response of the prototype, and in many cases the deformation and strains in the structure were so small as to be virtually unmeasurable. From this, the structural design of the breakwater can be based on minimum practical wall thicknesses, reinforcing, and modest pre- or post-tensioning. Based on inputting into FLOATX, the significant wave used in the design of the prototype, the breakwater appears to have been overdesigned by a factor of 4.

Some of the cross-spectral analyses helped to verify the reliability of the data recorded and data generated by myself. In most cases this cross-spectral analysis was so contaminated by noise, lack of zero values, gain settings, etc., that it was useless. Occasionally this analysis did show the dynamic response of the structure as unity or near unity between internal and external structural parameters when attacked by a random short crested sea state. Values of unity or near unity show a linear response exists, which means the breakwater is experiencing rigid body motion.

The cursory analysis of determining the effective crest length, although not by any means conclusive, shows the difficulty in trying to develop rational criteria for analyzing such a random occurring event. It is hoped that further analysis leading to the development of rational design criteria for use by practicing engineers will be conducted.

Comparisons with designs conducted after initiation of the prototype project show that the East Bay and Friday Harbor breakwaters are also overdesigned. This can lead to some conservative relatively basic design changes to criteria used currently by the Seattle District of the Corps of Engineers. The dimensions currently used should not be changed because of the good wave attenuation characteristics they provide.

The following recommendations for the design of floating breakwaters are considered conservative based on the results presented in this report. FLOATX provides reliable conservative response predictions for floating structures and should be used for their design. The maximum values output by FLOATX should be used.

The design of the breakwater should utilize pre- or post-tensioning so that tension never occurs in the concrete. This allows for: (1) protection against fatigue failure, (2) reduced potential for cracking due to high tensile stresses; and (3) reduced chance of failure by corrosion of reinforcing steel. A minimum amount of prestressing should be set by the designer to provide adequate protection against vessel impact, towing or launching of the breakwater, or extreme event occurrence.

Thicknesses of walls and slabs are generated by the minimum reinforcement cover required by American Concrete Institute, Building Code Requirements 318-83. Design of walls and slabs should be based on sound engineering judgment with some allowance for vessel or log impact loads.

The anchor system, including cables, stake piles, shackles, and chains can be reduced. Corrosion not design loads might then become the critical criterion. Increasing the anchor spacing could render the design loading critical; but then, a combination of corrosion and design forces should be accounted for. Another result of increasing the anchor spacing is that the response parameters of the structure would change; therefore, an economic balance point of optimum spacing and structure loading exists.

APPENDIX I - REFERENCES

1. Georgiadis, Constantinos, and Billy J. Hartz. 1982. A Computer Program for the Dynamic Analysis of Continuous Floating Structures in Short Crested Waves. C.W. Harris Hydraulics Laboratory Technical Report No. 74 University of Washington, Department of Civil Engineering.

2. Logcher, R.D., Conner, J.J., Jr., Nelson, M.F., Portland Cement Association, and Ohtmer, O. 1976. ICES STRUDL User Manual Vol. I, II, and III. Structures Division and Civil Engineering systems Laboratory. Department of Civil Engineering. Massachusetts Institute of Technology. Cambridge, Massachusetts.

3. Miller, Robert W., Derald R. Christensen, Ronald E. Nece, and Billy J. Hartz. 1984. "Rigid Body Motion of a Floating Breakwater: Seakeeping Predictions and Field Measurements." Water Resources Series Technical Report No. 84. University of Washington, Seattle, Washington.

4. Newland, D.E. 1975. An Introduction to Random Vibrations and Spectral Analysis. 1st Edition. Longman Group Limited. London.

5. Papoulis, A. 1984. Probability, Random Variables and Stochastic Processes. Second Edition. McGraw-Hill Book Company. New York, New York.

6. U.S. Army Coastal Engineering Research Center. 1977. Shore Protection Manual. Vol. I, II, and III. Department of the Army, Corps of Engineers, Third Edition.

7. U.S. Army Corps of Engineers. 1981. Floating Breakwater Prototype Test Program: Prototype Design Document. Department of the Army, Seattle District, Corps of Engineers.

8. Vugts, Jan Hendrik. 1968. "The Hydrodynamic Coefficients for Swaying, Heaving, and Rolling Cylinders in a Free Surface." Shipbuilding Laboratory Report No. 112 S. Technological University of Delft, Netherlands.

9. Weigel, Robert L. 1964. Oceanographical Engineering. Prentice Hall, Inc. New Jersey.

England

APPENDIX II - NOTATION

The following symbols are used in this paper:

A	Cross-Sectional Area
B	Width
C	Constant
C	Damping Matrix
C_D	Pressure Drag Coefficient
D	Draft
H_s	Significant Wave
$H_{1/3}$	Significant Wave
H_1	One-Percent Significant Wave
K	Stiffness Matrix
L	Length/Wave Length
L'	Effective Crest Length
M	Mass Matrix
M_a	Hydrodynamic Added Mass
MLLW	Mean Lower Low Water
$R(t)$	Exciting Wave Forcing Function
T	Wave Period
W	Natural Frequency
$\underline{X}$	Generalized Displacement Matrix
$\underline{\dot{X}}$	Generalized Velocity Matrix
$\underline{\ddot{X}}$	Generalized Acceleration Matrix
$X(t)$	Displacement at Time t
$\dot{X}(t)$	Velocity at Time t
$\ddot{X}(t)$	Acceleration at Time t
X	Percent of Critical Damping
ϕ^T	Transpose of Mode Shapes
σ	Standard Deviation
ρ	Water Density

CONSTRUCTION OPTIMIZATION THROUGH SHIPYARD FABRICATION

J. Michel Benoit*

1. ABSTRACT

The main purpose underlying industrialized prefabrication is minimization of contingencies affecting structural reliability and cost. The tremendous progress in engineering technology leading to sophisticated concepts and designs needs to be extended to the construction and fabrication stage with the same rigour and with reliable quality control procedures.

Safety and costs should be acceptable to society and owner. If it is often true that good safety is good economy, the reverse can lead to disaster.

Cost evaluation (present value) is to include maintenance and repair aspects, potential failures and malfunctions as well as final demolition and dismantling.

The basic idea of shipyard prefabrication is to make use of standard materials and repetitive procedures in a well controlled environment. These basic principles of industrialized production have led to high quality products meeting cost and schedule constraints.

2. THE PROTOTYPE SYNDROME

The idea of prefabrication and repetitiveness is most attractive to a construction manager eager to limit cost and contingencies while improving quality and production rates. While each major marine project or offshore installation is to meet very specific needs and standards in a very unique environment, the minimization of material cost would often lead to a unique prototype version. Though different from other related structures, a value engineering study of such a prototype structure often leads to the desirability of more redundancy and standardization on the basis of established techniques and well proven procedures.

The cost savings and high product reliability provided by shipyard prefabrication prompts the marine engineer to tailor structural concepts to such prefabrication. The occasional increase in material is largely compensated by the lower fabrication costs and by higher structural strength and redundancy.

---

* Principal Engineer,MKE, 180 Howard Street, San Francisco, CA 94105

While still unique in its global, overall configuration, such a marine structure can be composed exclusively of structural shipyard components.

3. STEEL VERSUS CONCRETE

Prefabrication on an industrialized level has largely favored steel because of its greater adaptability and workability. Cutting, welding, and modular assembly of steel substructures is a standard operation which can be performed anywhere. Modifications, repair procedures and non-destructive testing of steel components require no particular precautions. Furthermore, the reliability and steadiness of material properties for all high strength steel materials are unmatched.

However, industrialized prefabrication of concrete has its realm of application in the marine environment, and in the offshore field through its excellent corrosion resistance and through its good fatigue and impact behaviour when post-tensioned.

Indeed, fracture control is an overall approach to the construction of structures aimed at ensuring that the risk of failure by a crack-dominated mechanism is kept below an admissible level. Whereas concrete appears to be less prone to crack propagation because of the lower stress levels, both materials require thorough scrutinization throughout the structure's design life. The main items to consider are:

1) Selection of material type, grade, welding procedures and heat treatment.
2) Knowledge of resistance to dominant types of failure; fracture toughness, fatigue crack growth rates, corrosion fatigue, creep crack growth, etc.
3) Design stresses and configuration.
4) Environmental conditions.
5) Capability of non-destructive testing methods.
6) Knowledge of potential fabrication defects.
7) Frequency and sensitivity of in-service inspection.

The geometric tolerances on steel prefabrication are kept very tight as a consequence of automatic computer aided cutting, positioning, welding and block assembly procedures.

Structural concrete prefabrication on an industrialized basis has mainly focused on piling, girder and panel elements with limited possibilities for structural pre-assembly.

Concrete precasting yards of major structural components for marine structures have focused on specific projects located in a critical wave environment or characterized by particularly difficult logistical problems. Typical examples are the concrete gravity base structures constructed and outfitted in the sheltered fjords of Norway and Scotland, and subsequently towed and immersed at the production site in the North Sea.

Many major breakwater structures in Europe, North Africa and in the Great Lakes consist of huge matching prefabricated concrete (post-tensioned and reinforced) caissons which were constructed in a temporary drydock to be finally towed, immersed and ballasted at the site of the work. Base preparation requires a significant effort. Some concrete caissons with a displacement of up to 12,000 tons have been towed for over 600 miles from Messina, Italy across the Mediterranean to various sites in Libya and Tunisia.

A large number of ready-made piers and berths for oil tankers and bulk carriers have been installed throughout the world using self-elevating steel hull structures. These hull structures are typical of shipyard prefabrication.

4. FABRICATION AND SERVICE FACTORS IN SHIPYARD CONSTRUCTION

The ultimate carrying capacity and structural reliability of a structure is conditioned by the quality standards to which the structure has been designed, fabricated, assembled and installed. Irrespective of the degree of sophistication used in the engineering design phase and of the tight quality control covering fabrication and installation, it is a fact of life that minor structural imperfections cannot be avoided. Though shipyard prefabrication tends to reduce their amplitude and frequency, the Committee on International Ship Structures has undertaken the task of compiling statistical data from ships and offshore structures under construction or in service, obtaining meaningful information on damages, tracing the origin of damage to factors such as wrong design, construction defects or inadequate material properties, assessing accurately the extent of damage and the actual conditions under which such damage occured.

The economic consequences of such damages have been considered in recognition of the fact that damages and repairs resulting therefrom do not only present technical interest, but are also related to the profitable operation of the facility.

An average crack growth rate of the order of 4 inch per year for oil tankers with 3 to 22 years of regular service appears to be the rule. No definite trend has been found between propagation rate and age of ship.

The assessment of damage distribution and causative faults such as plate misalignment, joint discontinuities, different stiffener arrangements, residual welding stresses and distortions as a function of the welding procedures, number of passes and welding parameters has led to the recommendation of "preferred standard details". The emphasis on performance evaluation of structural details results from the recognition that most of the minor defects of the structure initiate at the detail design of members such as bracket connections, welded cross joints, cut-outs, etc.

These statistical data obtained from real-life surveys have led all major shipyards to adjust their in-house standards, procedures and quality control methods to integrate this gain in experience.

To established acceptable probabilities of failure, a correlation of the results from the system with service experience is essential. Classification Societies are the only bodies which, having a large amount of information on damages in service, could reasonably define such probabilities and identify areas where strict control should be exercised. To this effect, Classification Societies operate Technical Record Data bases which contain all relevant information on damages to ship structures reported to the society. Combination of these records has led to the general rules and regulations covering design and fabrication of vessels and offshore structures. Incorporation of these valuable recommendations and guidelines into design and fabrication is a major asset of the shipping and offshore industry.

5. FRACTURE CONTROL CONCEPT

Fracture mechanics provides a connection between mechanical analysis and macroscopic material toughess properties. The three main objectives are:

1) Determination of crack parameters by applying continuous solid mechanics to elements containing cracks or flaws.
2) Study and determination of the macroscopic toughness properties of the materials.
3) Fracture or crack growth criteria which are relationships between crack parameters and toughness properties.

Such fracture control plan aims at avoiding failure by fracture over the design life of the structure. It includes consideration of load and environmental conditions, structural configurations, material properties selection and quality control, fabrication processes, inspection and maintenance.

The basic approach for fracture control is the same for marine structures, aircraft structures, bridges, highrises or transmission towers. However, the design parameters, tolerance levels, and quality control levels are quite different. Indeed, while marine and aircraft structures are essentially subject to fatigue and dynamic impact loading at low temperatures where brittle failure is of concern, most other structures are designed and fabricated to cope with high static loads and low cycle fatigue.

The National Materials Advisory Board of the National Research Council has issued a comprehensive publication on the application of fracture mechanics technology for crack control in marine structures. EPRI, AWS and NRC have issued in-depth studies addressing crack initiation and propagation in various steel materials, weldments, tubular joints and welded connections for a wide temperature range and for diverse stress block spectra.

Implementation of a stringent fracture control plan at the level of design, fabrication, maintenance and repair throughout the service life of the structure is a well established fact in aviation, shipping, offshore and nuclear industries.

6. DESIGN FOR FABRICATION

While satisfying the basic design criteria, for fundamental safety and reliability, the design engineer can improve these factors as well as the general economy of the project by tailoring concept and details to fit well-proven shipyard procedures and standards and by allowing for easy maintenance and repair methods.

The fallacy of identifying weight with cost needs to be dispelled by underscoring the importance of standardization, repetitivity, simplicity and redundancy.

The main technical, organizational and management requirements that must be fulfilled can be summarized as follows:

1) Design for production ease.
2) Optimize cost by adjusting sizes and detail design arrangements.

3) Specify production processes best fit for structural performance and reliability.
4) Make provisions for steady interface between design and production with continuous value-engineering approach to shop drawings, fabrication procedures and quality control.

6.1 Design for Production

Efforts are to be made to conceive and design structures to be more compatible with the facilities and procedures of typical shipyards. It is convenient to distinguish three levels at which design impacts production optimization:

A) Global Level

- Overall Shapes: flat plates and single curvature shell elements are much more economical than doubly curved shells.
- Substructuring: block assembly procedure allows paralled construction of structural components. These substructures shall be limited in size and weight and should have simple boundaries.
- Repetitivity: use of standard units and modules in order to maximize repetitive operations and to avoid unnecessary cutting and welding ensuring thus continuity and simplicity of construction.

B) Secondary Level

- Panel Stiffening: single or two-directional stiffening arrangement?
- Plate Type: flat for corrugated plates?
- Framing/Bulkheads: choice between transverse or longitudinal frame arrangements or stiffened plate bulkheads.

C) Detailed Level

- Sections & Plates: Standardization of section and plate sizes in function of availability.

° Welding:	minimize welding by use of thicker plates and heavier sections: trade-off between material and labor costs.
° Connections:	use proven details recommended for performance, reliability and ease of fabrication, hence economy.

6.2 Cost Optimization

Formal cost optimization techniques to develop more economic designs are easiest at the secondary and at the detailed level where labor, material, handling and tooling costs can be evaluated more accurately. A "minimum cost" design configuration changes to a certain extent with the economic context as well as with the shipyard equipment and standards.

However, large variances are not likely within a certain range of the design parameters because of the fairly universal standardization of shipyard fabrication methods.

The very few research studies aimed at global cost optimization through shipyard fabrication generally confirm that:

- there is always an economical trade-off between weight and cost;
- least-cost designs involve thicker plating and fewer stiffeners and frame;
- unit cost updates are essential;
- practical constraints of fabrication have to be identified and incorporated in the analysis: need for continuity, design of connections, depth, weight and overall size limitations, etc.

6.3 Impact of Fabrication Methods on Structural Capability

Identification of the various ways in which fabrication processes effects the reliability and performance of marine structures has led to steadily improved design standards and procedures. The surveys performed worldwide by shipyards, classification societies and research organization follow essentially the same pattern:

- collect reliable statistical data on defects and damages in service;

- establish clearer relations between defects and subsequent performance and reliability;
- relate defects to constructional procedures;
- deduce a rational system of tolerance specifications and quality control.

Since structural joints and connections are most prone to defects and imperfections -- stress concentrations, residual welding stresses, slag inclusions, embrittlement, misalignment, distortions, welding defects, etc. -- through human and production factors, it follows that the overall weights and costs of marine structures are penalized by unreliability at joints. Hence, deliberate over-design of joints and connections might increase the fabrication cost only slightly while guaranteeing a better structural behaviour and minimizing potential maintenance and repair costs.

It can be seen that design, fabrication, and long term serviceability are tightly linked in any cost-reliability optimization study.

6.4 Information Management

The effective optimization of reliability and cost through shipyard prefabrication can be implemented only under the provision of thorough knowledge of shipyard standards, procedures and logistics. The main factors affecting design for fabrication optimization are:

- the flow of information covering production practices, preferences and costs; constraints on size, lift and dimensions; established standards on tolerances, procedures and details.

- the organization of design, drawings and production functions to foster overall interaction and stronger liaison, perhaps through a production engineering department charged with implementing design for fabrication optimization.

- longer lead times allowing for particular changes and adjustments.

- estimating procedures able to reflect the benefits of industrialized prefabrication optimization in leading to more competitive prices at the tendering stage.

6.5 Recommendation

Optimization of structural reliability and global economy can only be achieved through broad knowledge of fabrication standards, methods and equipment generally used in the shipyard industry.

The offshore activities have developed an increasing awareness of shipyard prefabrication methods. Classification societies in particular start encouraging interrelations between marine engineers and shipyards.

Further communication and interfacing between design and production is essential at all levels in order to incorporate the latest developments in material characteristics, fabrication procedures, quality control methods and maintenance and repair operations.

Cost sensitivity studies should be performed at the onset of the final design process in order to establish the governing parameters affecting global cost. This still allows timely design changes leading to updated cost and quality optimization.

Though cost and reliability parameters might change geographically and in time, it is obvious that the main design parameters affecting production still remain the same because of the great standardization of materials, fabrication methods and because of the computer aided mechanization.

7. SELF INSTALLING MARINE FACILITIES

An interesting case history of fabrication-compliant design is provided by the large number of prefabricated self-installing "De-Long" type barges used as piers, berthing facilities and working platforms.

These marine structures comprise three distinct features:

1) standard large diameter (71 inch O.D) steel caissons;
2) a large multicellular hull structure;
3) a twin stage jacking and gripping system.

Though each of these three items can be considered as a standard "of-the-shelf" type product, the final, assembled structure is fairly unique through its general arrangement, sizing, environmental and site constraints.

The use of 71 inch O.D. circular cylindrical piles or caissons for foundation purposes provides tremendous soil adaptability under provision of sufficient pile length. Redundancy "at will" offered by the large number of piles further allows easy preloading and automatic in-situ pile testing possibilities.

The large multicellular hull structure whose design and fabrication is necessarily certified by a Certification Agency provides an ideal working platform with a tremendous carrying capacity. The deep hull wells through which the 71 inch piles are sliding provide ample restraint in sidesway motion during jacking as well as after pile weld-off operations.

The lifting system which comprises twelve elevating jacks and two sets of circumferential holding grippers allows for a 15 foot per hour average elevation rate with a lifting capacity of 500 short tons.

This system permits complete shipyard fabrication, outfitting and testing. Tow and installation of these ready-made structures can be performed without resorting to an exterior logistical support system.

Typical examples of ready-made marine facilities of this type are:

- Colombia - Cerrejon Commodities Pier: 100' x 900' - (3 units)
- Saudi Arabia - Ras Tanoura oil tanker berthing facility:
  1.1 mile long installation comprising 4 double berth platforms in 90 ft. deep water
- Indonesia - Balikpapan timber loading pier - 70' x 750' - (3 units)
- Abu Dhabi - Umm Shaif and Zakum Oil Production Platforms - 45 units
- Holland - Scheveningen pier terminal casino.

The idea of shipyard fabrication and outfitting has been carried quite further by considering barge mounted facilities such as power plants, desalination plants, hospitals and petrochemical industrial facilities. Needless to conclude that design, fabrication and outfitting are very tightly intertwined and that it becomes imperative to promote awareness for prefabrication optimization at the design stage in the largest sense.

REFERENCES

1. I.S.S.C. 1979, Reports of Committee III-3: "Fabrication and Service Factors" and of Committee V-1: " Design Philosophy, Criteria and Procedure.

2. Flint, A.R. and Baker, M.J.: "Rationalization of Safety and Servicability Factors in Structural Codes: CIRIA/UEG Report UR9, Oct. 1977.

3. Mowatt, G.A.: "LR, SAFETY Systems Manual - Structural Safety and Reliability", Development Unit Report No. 220, Lloyd's Register of Shipping, 1977.

4. Lind, N.C.: "Reliability based on Structural Codes Optimization Theory and Practical Calibration", in [12], 1977.

5. Caldwell, J.B.: "Design for Production", WEGEMT Graduate School on Advanced Ship Design Techniques, Newcastle 1978.

6. Evans, J.H.: "Overall Optimization Criteria", Chapter 24. Ship Structural Design Concepts. Cornell Press, 1975.

7. Ganschiniets, D.: " Production-kindly construction in large shipbuilding", Schiff und Hafen, Vol. 22, 1970.

8. Degenkolw, F.: "Method Planning in the Fabrication of Steel Hulls", Symposium on Structural Design and Fabrication. Welding Institute, London 1975.

9. Marsh, A.L.: "The Constraints Imposed on Design by Shipbuilding Production Technology", Symposium on Structural Design and Fabrication. Welding Institute, London, 1975.

10. Loire, R.: "Les ouvrages auto-eleves dans les travaux maritimes", Construction, February, 1977.

11. Smagghe, J. and Loire, R.: "Le Verdon: Travaux executes en un temps record grace a l' utilisation d' une plate-forme autoelevatrice", Travaux, December, 1970.

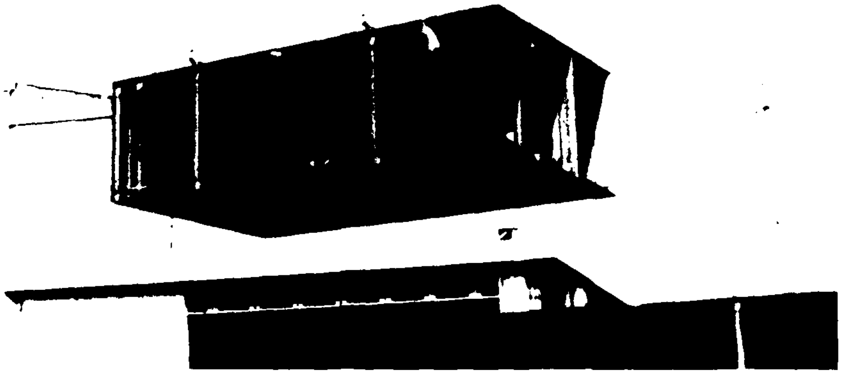

Block Prefabrication

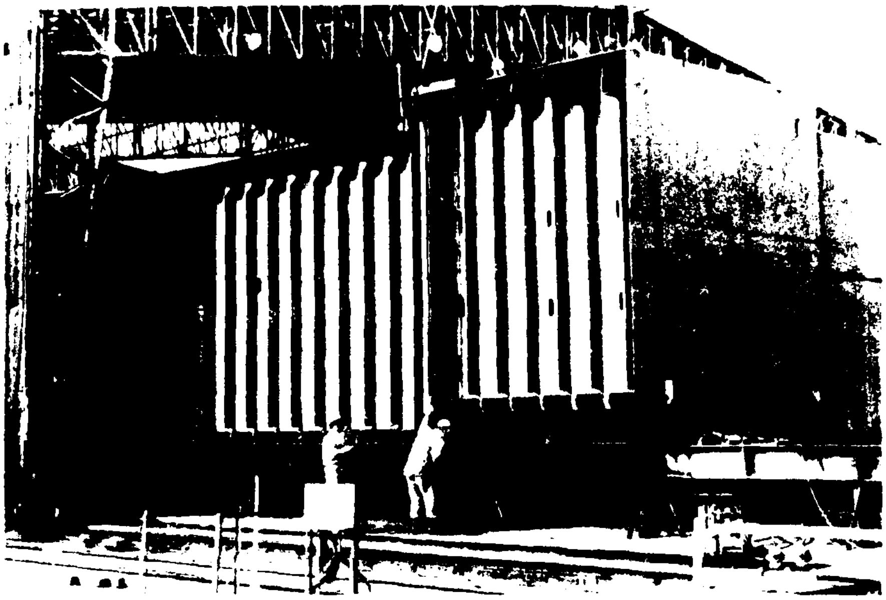

Block Assembly in Drydock

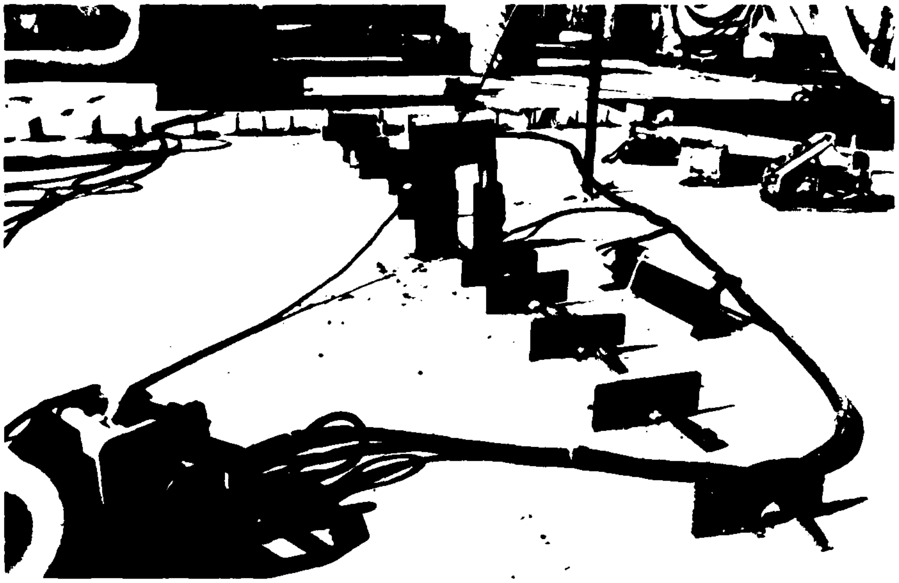

Assembly Welds

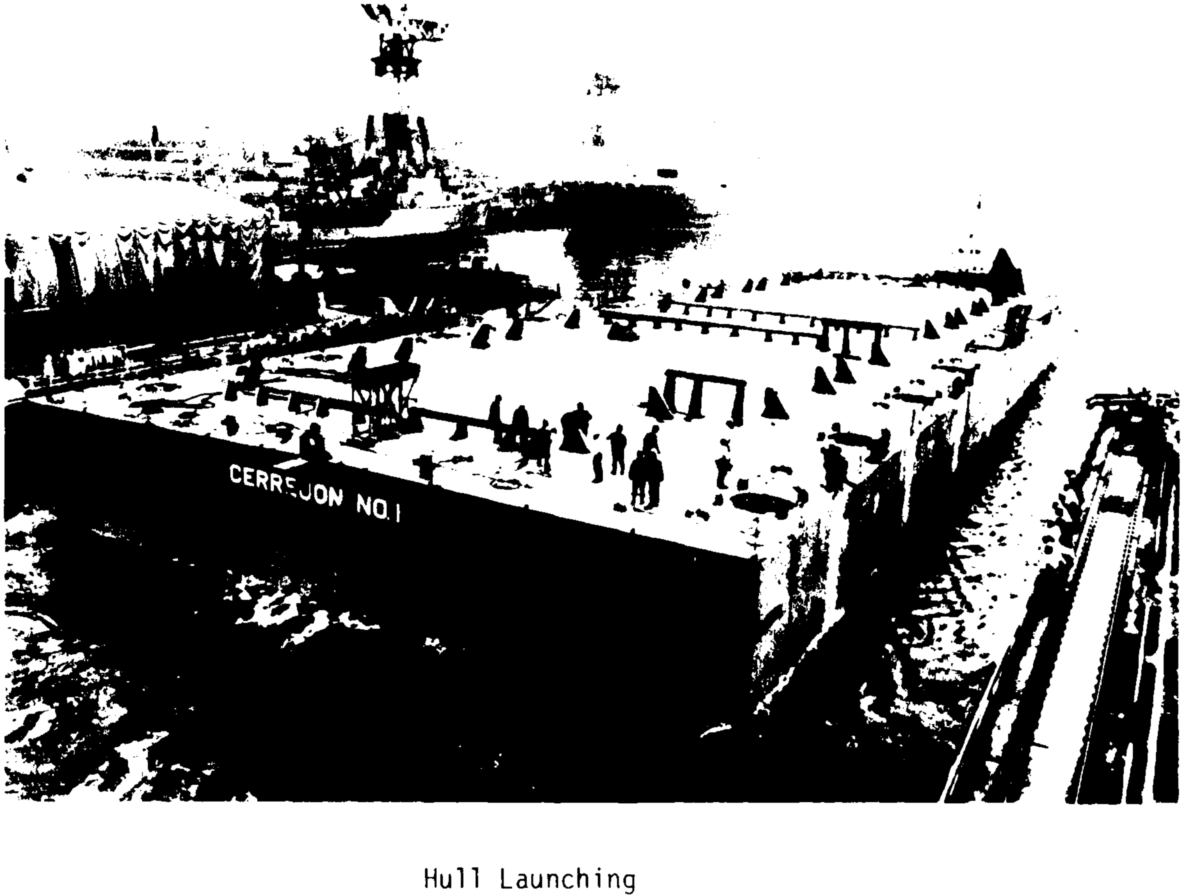
CERREJON NO.1

Hull Launching
Cerrejon Coal Project (Colombia-1984)

Pier elevation and installation
(Cerrejon-1984)

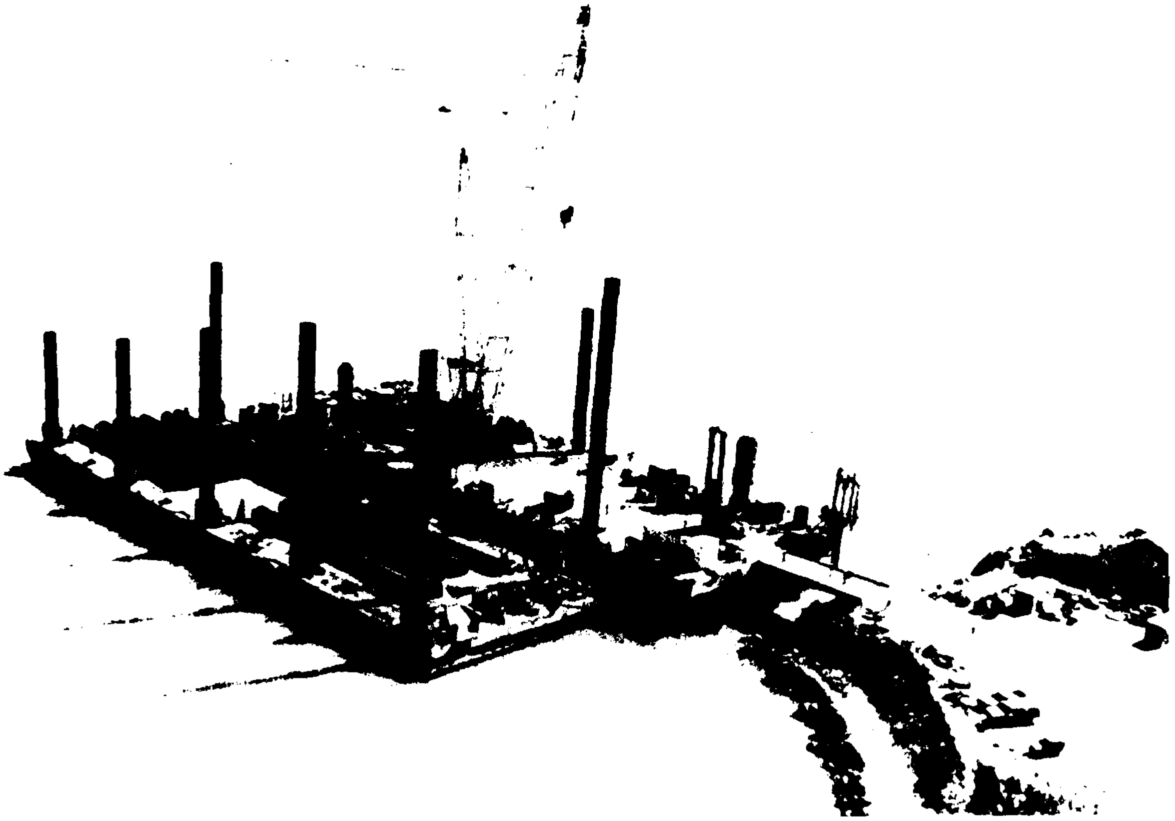

Arrival of second pier hull section
(Cerrejon-1984)

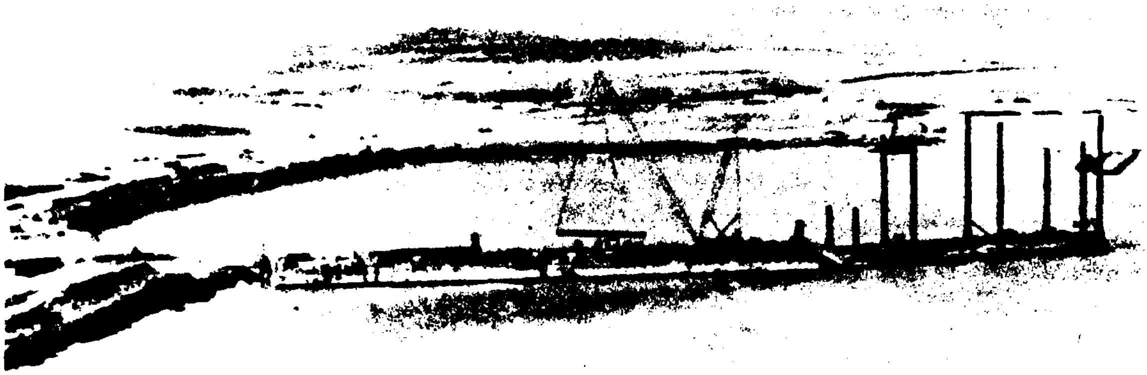

Positioning of third pier section
(Cerrejon-1984)

Specifying Materials for Coastal Concrete Structures

Harold Davis[1] and John Rutherford[2]

This paper describes the various types of concrete and reinforcing steel specified for the new Monterey Bay Aquarium and for the rehabilitation of an existing seawall at Hopkins Marine Laboratory. The discussion emphasizes proper material handling and special construction techniques required to obtain sound, durable, corrosion-resistant construction.

Introduction

The Monterey Bay Aquarium opened its doors to the public for the first time on October 20, 1984. The $40 million dollar concrete and timber structure straddles the boundary between Monterey and Pacific Grove, California and extends into the subtidal zone of Monterey Bay. The structure is exposed to a wide range of marine wave forces and marine corrosion conditions. A careful study of the effects of marine conditions on the old Hovden Cannery, first constructed in 1915, yielded valuable information to both designers and constructors of the facility.

Lessons learned during design and construction of the Aquarium were valuable in executing the structural rehabilitation of a badly damaged seawall at Hopkins Marine Station, adjacent to the Aquarium project.

Site Conditions

Fig. 1 shows the marine and geologic conditions which influenced design of both projects. A deep wave spectra study (Thornton, 1979) showed that the sites are sheltered from open ocean waves from the south and north. Only waves from the WNW can deliver significant energy to the project areas. Major active faults near the site include the San Andreas, Zayante and San Gregorio. Numerous smaller faults paralleling the San Gregorio Fault lie shoreward of the San Gregorio. The Monterey Canyon Fault extends seaward from the vicinity of Moss Landing. The onshore and offshore bedrock is granitic (quartz monzonite) covered with a shallow depth of sand extending seaward from a point about 215 m (700 ft) outboard of the Mean Tide Line. A short distance north of the sites the bedrock is shale, covered in some areas with sand several hundred feet deep. Littoral drift in the immediate area is not significant and the sand depth in the small pocket beach northwest of the site varies seasonally less than 1 meter (3 ft) on the average. Records of tsunamis in Monterey Harbor indicate only minor effects from tsunamis caused by earthquakes along the Alaskan coast.

---

[1] Vice President, Rutherford and Chekene, San Francisco, CA 94107
[2] Chairman, Rutherford and Chekene, San Francisco, CA 94107

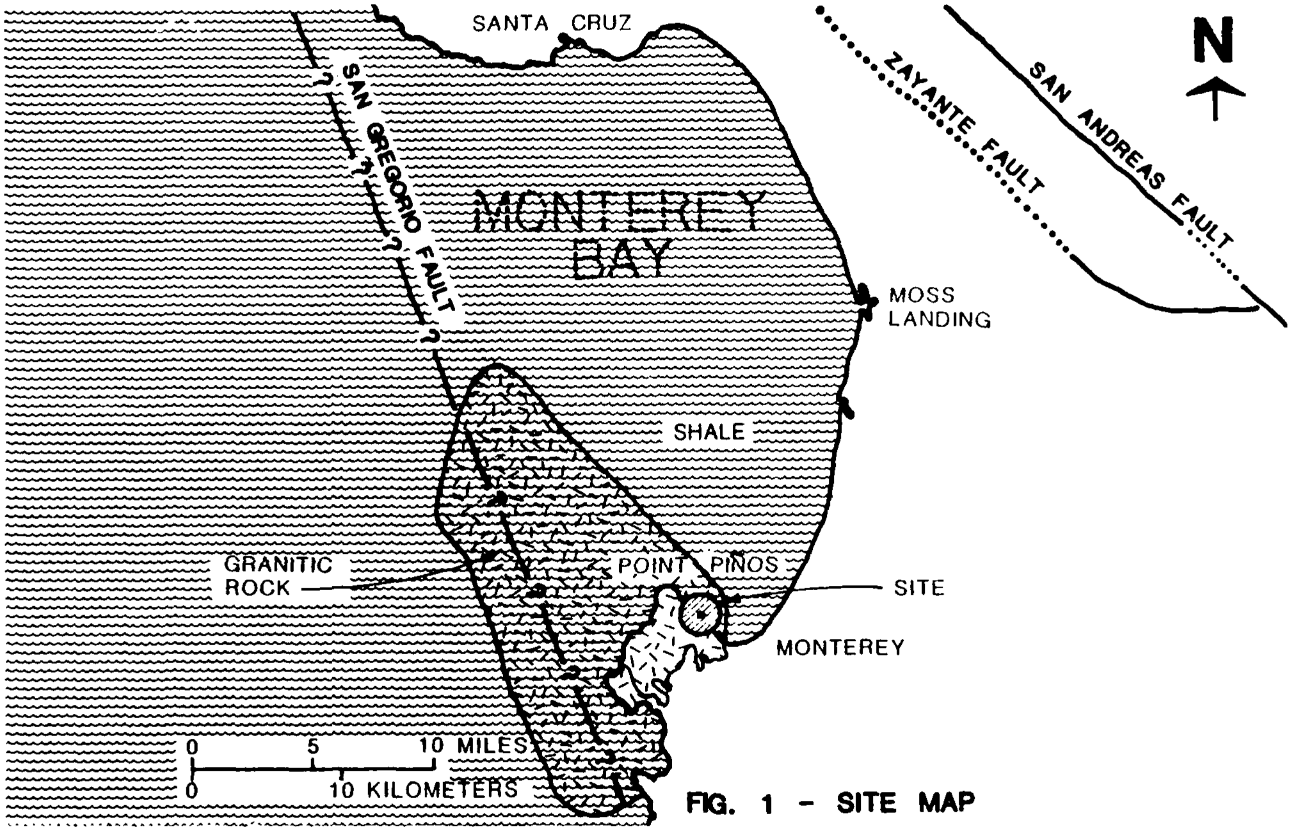
SANTA CRUZ
ZAYANTE FAULT
SAN ANDREAS FAULT
N
SAN GREGORIO FAULT
?
MONTEREY BAY
MOSS LANDING
SHALE
GRANITIC ROCK
POINT PINOS
SITE
MONTEREY
0
5
10 MILES
0
10 KILOMETERS

FIG. 1 - SITE MAP

Storm Wave Damage

Greatest ocean wave damage in the Monterey area apparently occurred on April 29, 1915 and on February 2, 1960. During the latter event, seawater smashed through the third story window of a hotel along Cannery Row near the site. Reported storm wave damage in general has consisted of street flooding along Cannery Row and Ocean View Avenue and broken windows and first floor flooding of establishments along the outboard side of Cannery Row.

A geologic hazard investigation (Curtis, 1978) disclosed small faults near the site and later pier drilling for onshore foundations yielded evidence of a fault within the site. There is no evidence for activity along these faults in recent times. The San Gregorio Fault, the King City Fault and the San Andreas Fault are extensive and active. These faults, although 10 km (6 mi) or more from the sites, govern earthquake resistant design.

Design Criteria

The Monterey Bay Aquarium incorporates both an overwater deck and a seawall. The new shore protection at Hopkins Marine Laboratory includes both rock slope protection and repair of an existing concrete wall. The criteria listed below governed design of shore protection for both projects.

1. Design wave: 100 year return period, 7 m (22 ft), height at 6 m (20 ft) contour, 16-second period, approaching from WNW.

2. Design tsunami run-up: 100 year return period, +3 m (9 ft).

3. Earthquake: Zone 4, Uniform Building Code, 1979 Edition.

Monterey Bay Aquarium

The Monterey Bay Aquarium (Fig. 2) is a three-story reinforced concrete and heavy timber structure with a partial basement constructed within the beach, tidal and subtidal zones of Point Alones on the site of the old Hovden Cannery. The facility houses exhibits of Monterey Bay marine life in three large tanks and numerous smaller tanks holding a total volume of over 2,800,000 l (750,000 gal) of seawater. A seawater system circulates 130 l/s (2050 gpm) through the exhibits, drawing water through a double-piped intake extending 296 m (970 ft) to an intake filter screen at a depth of 17 m (55 ft) below MLLW. The concrete must withstand a wide range of marine exposure conditions, ranging from atmospheric corrosion onshore to continuous submergence for precast concrete intake anchors.

When the project was first conceived, the proposed site was still occupied by the rapidly disintegrating structures of the historic Hovden Cannery. The Cannery was built in several stages, beginning in 1915, and its wood and concrete structures had been subjected for many years to the same marine exposure as the proposed Aquarium. The design team spent several weeks photographing, measuring, and studying the wood and reinforced concrete elements of the old cannery, hoping to learn lessons from the past. Among many observations useful for the design of the aquarium concrete structures were the following:

1. The condition of concrete structures varied widely. Some concrete elements in the tidal zone, subject to intermittent wave forces and abrasion, were in excellent condition. Other elements, such as the reinforced concrete suspended slabs which were exposed only to saltwater spills from the canning process, had collapsed completely.

2. All exposed ferrous metals, including galvanized fittings, were severely corroded. No stainless steel fittings were found.

3. Concrete elements containing reinforcing bars with at least 7.5 cm (3 in) of cover with few exceptions showed little sign of cracking, spalling or distress other than surface abrasion regardless of the severity of marine conditions.

4. Concrete elements where reinforcing cover was less than 2.5 cm (1 in) were usually severely cracked and spalled, with moderate to severe corrosion of the reinforcing. Large portions of the suspended concrete slab extending over the beach and tidal zone had collapsed.

5. Dowels extending from existing concrete structures to provide for possible future additions were almost completely destroyed.

6. Wood forms left in place on several tidal zone concrete columns and footings appeared to be effective abrasion protection.

7. A wave deflector constructed on the outboard wall of the cannery pumphouse was effective in preventing storm waves from entering a large window immediately above.

8. Foundation elements extending to sound rock were intact. Elements of an existing seawall resting on sand or even on in-situ weathered rock were frequently cracked and displaced.

9. Unreinforced concrete anchor blocks and footings in the subtidal zone were usually in excellent condition.

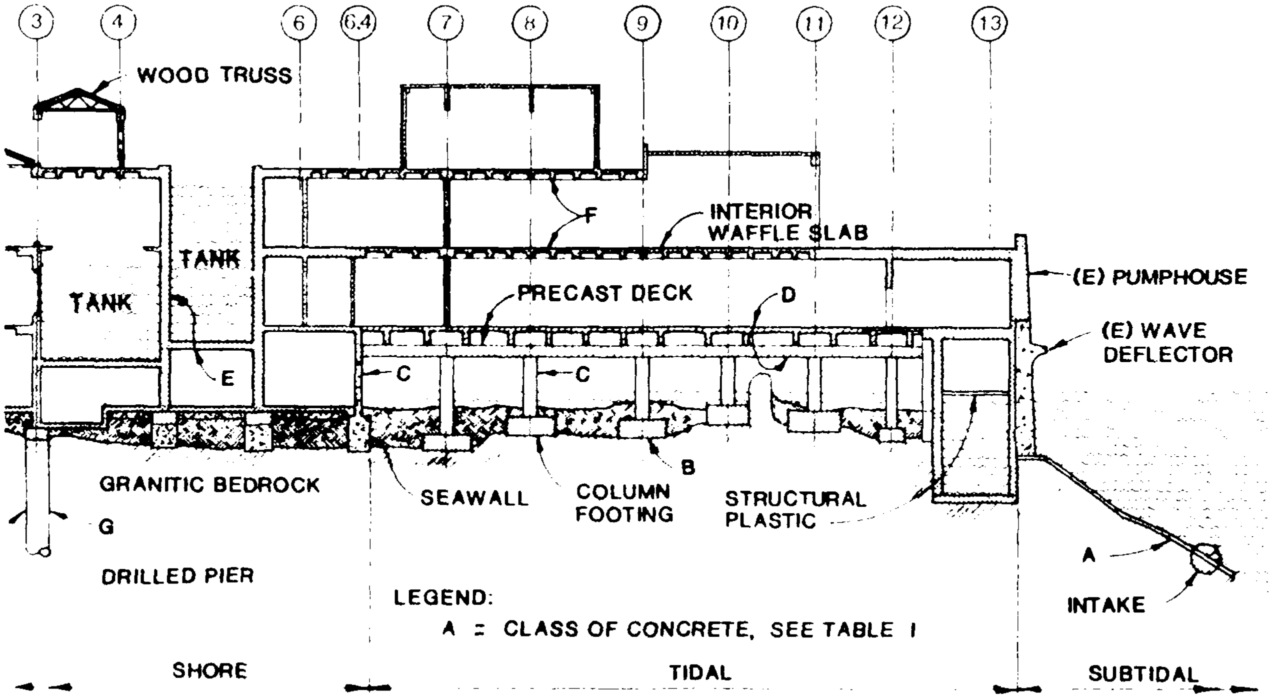
3
4
6
6.4
7
8
9
10
11
12
13
WOOD TRUSS
TANK
TANK
F
INTERIOR WAFFLE SLAB
PRECAST DECK
D
(E) PUMPHOUSE
(E) WAVE DEFLECTOR
E
C
C
B
GRANITIC BEDROCK
SEAWALL
COLUMN FOOTING
STRUCTURAL PLASTIC
G
DRILLED PIER
A
INTAKE
LEGEND:
A = CLASS OF CONCRETE, SEE TABLE I
SHORE
TIDAL
SUBTIDAL

FIG. 2 - AQUARIUM CROSS SECTION

Relying in part on information gained from examination of the Hovden Cannery and other structures along Cannery Row, the Aquarium designers specified a range of concrete mixes, varied to meet the demands of marine exposure conditions and functional requirements. Fig. 2 indicates general locations of classes of concrete mixes and Table 1 illustrates the general classes of concrete mix designs. The classes are simplified to show the most significant design parameters. The contract documents specified additional classes of concrete to cover variations in aggregate size and other constituents.

Table 1 - Concrete Classes

Class	Exposure Condition	Strength	Rebar	Fly Ash	Shrinkage Limit	Where Used
A	Submerged	27.6 MPa (4000psi)	Uncoated	Yes	0.045	Precast Intake Anchors
B	Submerged, Intertidal	20.7 MPa (3000psi)	Coated	No	No	Column Footings
C	Intertidal	27.6 MPa (4000psi)	Coated	Yes	0.045	Seawall, Columns
D	Wave Splash, Spills of Salt Water	27.6 MPa (4000psi)	Coated	Yes	0.045	Precast Deck Elements
E	Submerged	41.3 MPa (6000psi)	Coated	Yes	0.045	Concrete Exhibit Tanks
F	Spills of Salt Water	27.6 MPa (4000psi)	Top Bars Coated	No	0.040	Interior Floors
G	Fresh Water, Soil	20.7 MPa (3000psi)	Uncoated	No	No	Onshore Drilled Piers

Project specifications included the following provisions for increasing concrete resistance to marine corrosion:

1. Reinforcing type. Grade 40 and grade 60 billet-steel bars (ASTM A615) were used throughout the project, even in precast concrete beams and girders. No prestressing was used. Small-diameter bars with closer spacing were used in preference to widely-spaced large bars to control concrete cracking. Tank wall intersections were detailed to limit rotation and width of cracks.

2. Epoxy-coated reinforcing. At the time of design, epoxy coating for reinforcing was relatively new, with a short history of use in the midwestern and eastern United States for highways and bridge decks. The Monterey Bay Aquarium was the first west coast project to use substantial tonnage of epoxy-coated reinforcing. As shown in Table 1, coating was specified for elements where direct seawater exposure was possible. Special handling of coated reinforcing was specified, including padded slings, plastic bundling ties, cribbing for storage, and strongbacks for lifting bundles to prevent sagging abrasion. Welding was limited, with field-coating required over all damaged surfaces.

3. Reinforcing accessories. Plastic coated steel wire was used for epoxy-coated reinforcing bar ties and for bar supports. Type 316L stainless steel bolts or fibre-reinforced plastic studs were used for exposed anchors embedded in concrete.

4. Cement. Type II (Santa Cruz) cement conforming to ASTM C150 was used for all concrete. This cement had been used for concrete piles at a nearby wharf in Monterey Harbor and yielded a concrete significantly more durable than similar concrete piles using other types of cement.

5. Fly ash. Fly ash conforming to ASTM C618, Type F (Pozzolanic Northwest) was used in concrete subjected to direct saltwater exposure. Fly ash replaced about 15 percent of the cement used in these mixes.

6. Water-reducing admixtures. All concrete in Classes B through F contained varying amounts of liquid admixtures to reduce the amount of water required for mixing and placement.

7. Reinforcing cover. Concrete cover for reinforcing bars was varied according to exposure conditions, ranging from 15 cm (6 in) minimum clearance for reinforcing in footings within the tidal zone to standard clearances for reinforcing at protected interior concrete surfaces. Table 2 presents a general summary of clearances used.

8. Footing forms. Project specifications called for individual footing caissons for all underwater footings rather than construction of a cofferdam around the perimeter of the entire tidal building area. Aside from protecting marine life this permitted use of square precast concrete caisson forms with 8 cm (3 in) thick walls placed at each subtidal cast-in-place concrete footing. These were left in place after footing concrete was cast, providing extra protection for the concrete footings.

9. Column forms. Columns in the intertidal zone were formed using 0.5 cm (3/16 in) thick fiber-reinforced plastic duct material. Specifications required that these column forms be left in place to provide extra protection for concrete surfaces.

Table 2 - Reinforcing Cover

Exposure Condition	Minimum Cover	Structural Element
Intermittent submergence	15 cm (6 in)	Footings in tidal zone
Continuous submergence	7.5 cm (3 in)	Intake Anchorage blocks
Intermittent submergence	10 cm (4 in)	Columns in tidal zone
Wave spray	7.5 cm (3 in)	Bottom of deck over tidal zone
Seawater spills and storm wave run-up	5 cm (2 in)	Top of deck over tidal zone
Waterproofed surfaces (interior of tank)	10 cm (4 in)	Concrete exhibit tanks

The existing concrete seawall at the Aquarium site was in poor condition and could not be economically repaired. A new seawall (Fig. 3) was constructed as the initial phase of project development. Construction scheduling required that the wall be completed to less than full height, then backfilled before casting the slab-on-grade deck on the shoreward side of the wall. The wall was designed to withstand hydraulic and wave force pressures on the seaward side and backfill pressure on the shore face under both cantilever and simple span support conditions. An exploratory trench dug at low tide along the wall alignment revealed diverse foundation conditions, ranging from exposed bedrock to large voids filled with weak soils. The contractor was required to excavate the voids and was given the option of extending the footing concrete to the bottom of the void or filling the void with lean concrete prior to casting the structural concrete. Where the mass of lean concrete was sufficient to prevent overturning after backfill was placed, no anchors to bedrock were required. Where the structural concrete was placed directly on exposed sound rock, two rows of anchors drilled into bedrock developed resistance to earth and seawater pressures. The wall was then cast and backfilled to Elevation 3.4 m (11.0 ft) NGVD and remained as a cantilever element for several months during drilling of the onshore pier foundations. During this period the epoxy-coated reinforcing dowels extending from the top of the wall were exposed to wave splash and minor abrasion. After cleaning, prior to casting the topmost 1.8 m (6 ft) of wall, the epoxy coating was still generally sound, with a few minor areas of deterioration. These areas were field-coated with a compatible epoxy compound.

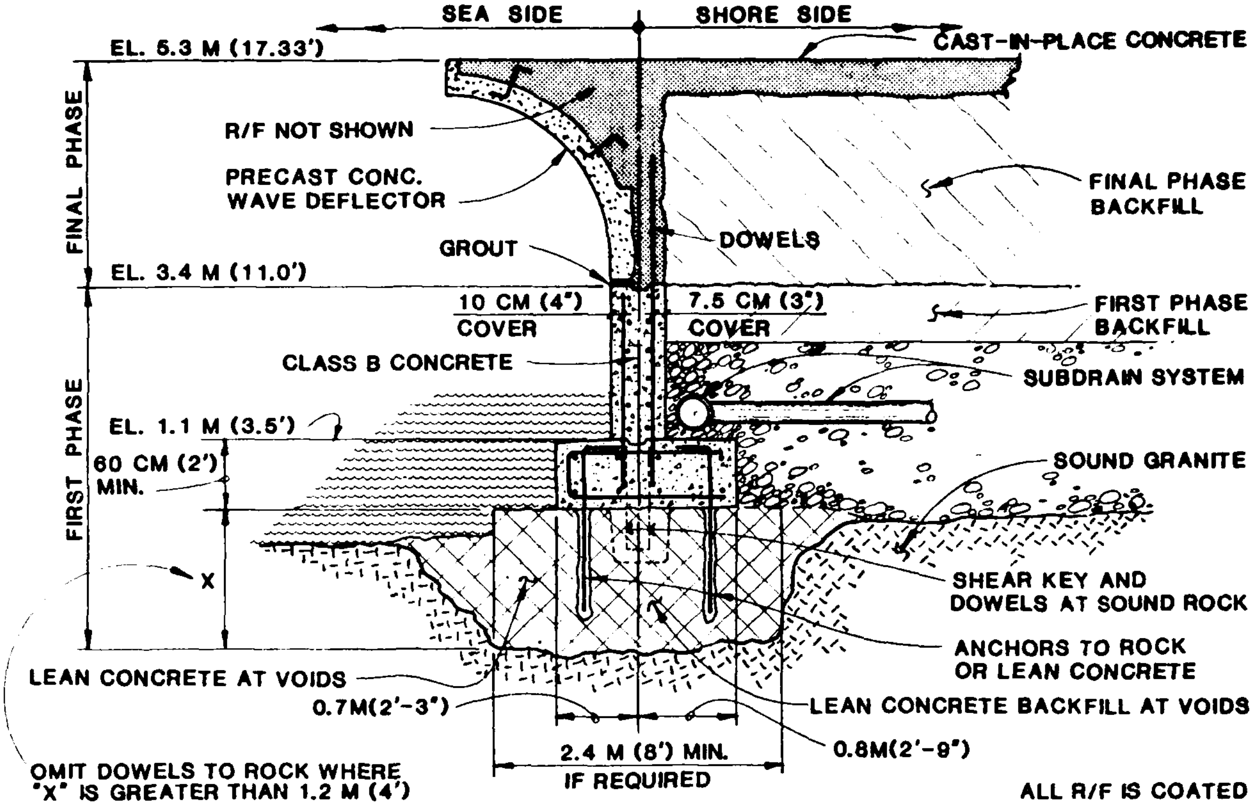
SEA SIDE
SHORE SIDE
EL. 5.3 M (17.33')
CAST-IN-PLACE CONCRETE
FINAL PHASE
R/F NOT SHOWN
PRECAST CONC.
WAVE DEFLECTOR
FINAL PHASE
BACKFILL
GROUT
DOWELS
EL. 3.4 M (11.0')
10 CM (4")
COVER
7.5 CM (3")
COVER
FIRST PHASE
BACKFILL
CLASS B CONCRETE
SUBDRAIN SYSTEM
FIRST PHASE
EL. 1.1 M (3.5')
60 CM (2')
MIN.
SOUND GRANITE
X
SHEAR KEY AND
DOWELS AT SOUND ROCK
ANCHORS TO ROCK
OR LEAN CONCRETE
LEAN CONCRETE AT VOIDS
0.7M(2'-3")
LEAN CONCRETE BACKFILL AT VOIDS
0.8M(2'-9")
2.4 M (8') MIN.
IF REQUIRED
OMIT DOWELS TO ROCK WHERE
"X" IS GREATER THAN 1.2 M (4')
ALL R/F IS COATED

FIG. 3 - SECTION OF SEAWALL

Where the seawall was not covered by concrete deck extending outboard of the wall, a precast concrete wave deflector with a profile similar to that used on the existing pumphouse was installed to prevent wave damage to the windows and deck overhead. This was anchored to the cast-in-place concrete placed to complete the wall to elevation 5.3 m (17 ft 4 in). Prior to casting the slab on grade, the wall was backfilled, with the top supported by the outboard concrete decking.

Hopkins Marine Station Seawall Repair

This small project is of interest primarily for use of shotcrete concrete on epoxy-coated reinforcing. The seawall fronts a small pocket beach northwest of the Monterey Bay Aquarium and the 30 m (100 ft) section along a proposed pump station site was close to collapse. The Station's budget did not permit wall replacement. Rehabilitation costs were estimated and proved affordable.

Study of old photographs of the area indicated that the wall was constructed in 2 stages. Before 1915 the shore consisted of a shallow, gently sloping sand beach overlying granitic rock of highly irregular profile. Sometime after 1915 a low gravity wall 60 cm (2 ft) thick of concrete construction was cast, resting on bedrock. The area was then backfilled with beach sand and debris. Several years later a 25 cm (10 in) thick concrete wall with onshore triangular concrete buttresses at approximately 6 m (20 ft) centers was added. The top section apparently rested on the base with no dowels between upper and lower sections. The lower section cracked in several places and the upper section was occasionally overtopped by storm waves which removed sand backfill from behind the wall and eventually cracked the unsupported portions of the wall by pounding against the seaward face. At the time of our examination the wall had settled almost 30 cm (12 in) vertically and was displaced outward about 20 cm (8 in) at the center. Two alternate designs were prepared to provide shore protection:

> Alternate A. A facing of 2 ton rocks placed against the face of the existing wall and sloping down at a slope of 1 vertical to 3 horizontal to a toe excavated to bedrock.
>
> Alternate B. (Fig. 4) A new reinforced concrete facing placed against the seaward face of the existing wall and supported by tiebacks to concrete deadmen on shore.

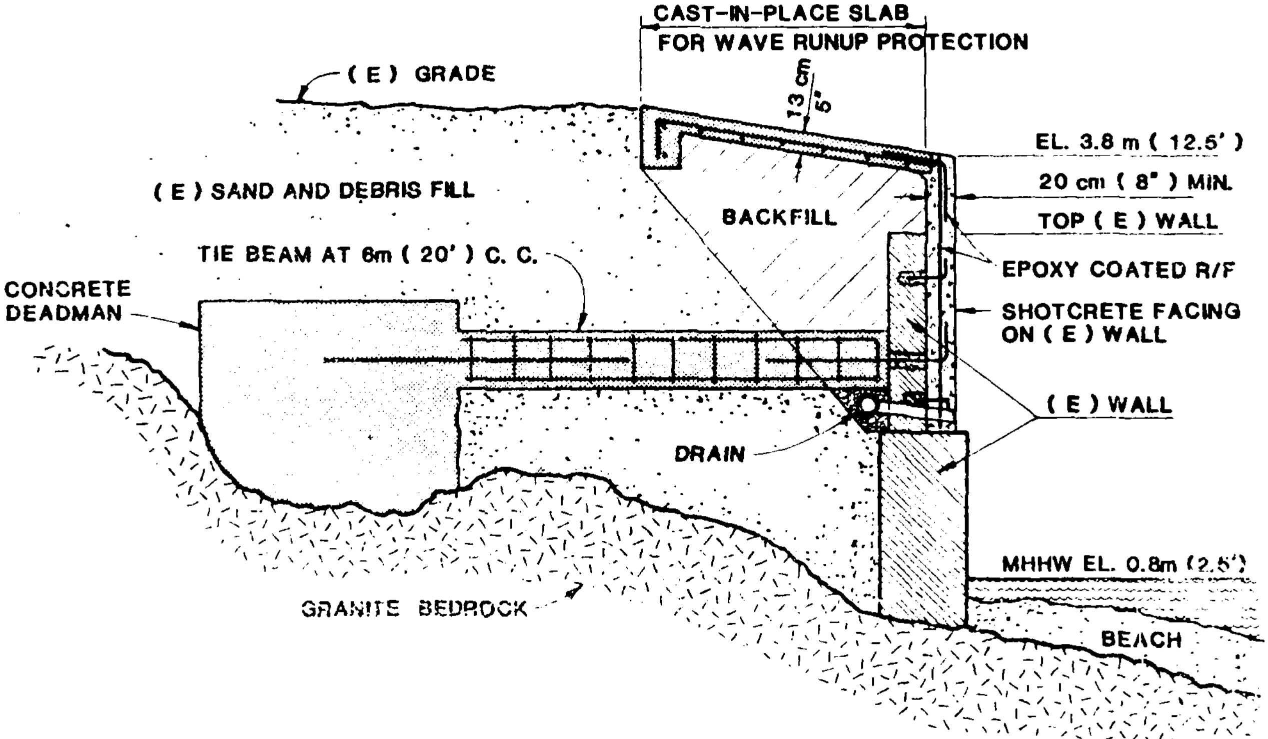
CAST-IN-PLACE SLAB
FOR WAVE RUNUP PROTECTION
(E) GRADE
13 cm
5"
EL. 3.8 m (12.5')
20 cm (8") MIN.
TOP (E) WALL
(E) SAND AND DEBRIS FILL
BACKFILL
TIE BEAM AT 6m (20') C. C.
EPOXY COATED R/F
CONCRETE DEADMAN
SHOTCRETE FACING ON (E) WALL
(E) WALL
DRAIN
MHHW EL. 0.8m (2.5')
BEACH
GRANITE BEDROCK

FIG. 4 - EXISTING SEAWALL REPAIR

Alternate B (Fig. 4) was bid lower than the rock facing alternate, although the latter alternate was adopted to protect a short stretch of low bluff beyond the end of the existing wall. The contractor bid a shotcrete option for the vertical wall facing. Shotcrete consisting of Type II cement and a 10 mm (3/8 in) maximum size aggregate was placed at a nozzle pressure of 3.1×10^5 Pa (45 psi) and the epoxy coating of the reinforcing was carefully inspected for possible damage due to abrasion. No damage was observed.

Construction Problems

Contractors on both projects found that the use of coated reinforcing steel required careful handling and more than normal vigilance to prevent damage. These precautions soon became routine and both projects progressed smoothly after initial problems were solved. Maintenance of the tightly specified minimum cover for reinforcing was sometimes difficult, requiring extra supports for high lifts of wall concrete. The use of waterstops at seawater tank construction joints proved particularly troublesome for proper reinforcing placement and almost all water seepage observed after the tanks were filled and tested occurred at these joints. In addition, the use of plastic coated tie wire meant more labor effort to get effective clamping of bar intersections. For this reason, smaller size bars consistent with structural design requirements were required.

Conclusions

The use of special concrete mixes and coated reinforcing bars for coastal structures increase the construction cost and require careful handling procedures. Examination of existing coastal structures using similar provisions for concrete and/or reinforcing indicate that these structures are more durable and require less maintenance than projects built to lesser standards. Experience with the design and rehabilitation of two coastal projects suggest the following precautions:

1. Fly ash. The contractor had no difficulty placing and finishing concrete containing fly ash. Where reconsolidation by vibration is desirable, fly ash mixes proved better than conventional mixes. Careful control of concrete batch inspection is required and design drawings must clearly indicate exactly where fly ash concrete is to be used.

2. Epoxy-coated reinforcing specifications. ASTM A775 for epoxy coating on reinforcing bars does not cover field procedures necessary to prevent coating damage. Specifications must include these procedures. CRSI Engineering Data Report Number 19 contains a list of suggested provisions for handling and placing epoxy-coated reinforcing bars.

3. Design drawings. Structures containing both coated and uncoated reinforcing bars present a difficult problem in defining where coated reinforcing should be used. Where most of the reinforcing is coated, a safe procedure is to label all uncoated reinforcing with a symbol and add two general notes:

   A. Except where noted otherwise, coat all reinforcing bars with epoxy.

   B. Use epoxy-coated bars for all dowels extending from elements containing epoxy-coated reinforcing bars into elements containing reinforcing bars noted as uncoated.

4. Construction scheduling. Epoxy coating deteriorates rather rapidly when subjected to both abrasion and seawater exposure. Specify a limit to elapsed time between bar placement and placement of concrete. Where coated dowels could be subject to long exposure, provide for dowel holes cast in place or drilled at the time of placement. Coated dowels can then be placed at a later time, using epoxy grout or resin capsule anchorage systems.

5. Shotcrete. Although shotcrete placement can be used successfully with epoxy-coated reinforcing bars, aggregate size and nozzle pressure must be limited and carefully controlled during placement to prevent abrasion.

6. Joint cleaning. Use high-pressure water jets rather than sandblasting to clean construction joints containing exposed epoxy-coated dowels.

7. Field bending. Pull-out tests of epoxy-coated bars grouted into site rock established the ability of epoxy coating to resist substantial bar strain without apparent damage. Field bending of bars partially embedded in concrete should be avoided except under direct supervision of the Engineer.

Acknowledgements

The Monterey Bay Aquarium is owned by the Monterey Bay Aquarium Foundation, established by Lucile and David Packard. The project was conceived by marine biologists Steve Webster, Charles Baxter and Nancy and Robin Burnett. Julie Packard is Aquarium director and Linda Rhodes was staff project manager during construction. Esherick Homsey Dodge and Davis were project architects and Syska and Hennessy were electrical and mechanical engineers. Rutherford and Chekene performed geotechnical, civil, structural and primary seawater system design. Rudolph and Sletten constructed the project.

Rutherford and Chekene designed the Hopkins Marine Station shore protection and associated seawater system. Power-Anderson constructed both the shore protection and seawater system.

Appendix - References

1. Curtis, Garniss H., "Geologic Hazard Report for the Monterey Bay Aquarium", unpublished, May, 1979.

2. Thornton, E.B., "Wave Design Criteria and Related Environmental Impacts for the Proposed Monterey Bay Aquarium", unpublished, October, 1979.

The Use of Steel Fiber Reinforced Concrete For Casting of Large Dolosse

Richard A. Gutschow,* M. ASCE

Introduction

The use of steel fiber reinforced concrete (SFRC) has passed from purely experimental laboratory scale applications into field applications involving worldwide placement of large volumes annually. Since 1972, the South Pacific Division of the Corps of Engineers has been casting dolosse with SFRC. Most recently 1,000 were cast at Humboldt Bay, California and over 500 will be cast during 1986 at Crescent City Harbor, California. The following presents the methods used to evaluate the effectiveness of the SFRC in casting a 42 ton (38,100 Kg.) dolos (singular of dolosse). The most desirable steel fiber characteristics are discussed and the results of laboratory tests on SFRC, using currently available steel fibers, are also described.

Prototype and Experimental Investigations

Model Studies conducted by the Corps of Engineers, Waterways Experiment Station, Vicksburg, Mississippi, found that the most effective solution in providing protection against the Northern California sea environment was the use of dolosse. During the latter part of the 1971-72 casting (approximatelv 2,500 conventionally reinforced dolosse), a small number of dolosse were made experimentally using SFRC. Full scale destructive tests were employed as well as laboratroy tests. One test was accomplished by placing the horizontal legs of two dolosse flat on a slab. A rigid steel tension collar was placed around each end of the legs, and then a load was applied between the dolosse with a hydraulic jack until a fracture and ultimate failure occurred. This measured the relative strengths of the units. The other test measured relative durability by dropping the dolosse. Coursey (1973) describes the program and its results.

The destructive test results and the service of the SFRC dolosse have shown a significant improvement in the quality (strength and durability) of the units over those conventionally reinforced and nonreinforced. Since the cost of using SFRC and the conventional deformed steel bars are nearly identical, it then became most practical to use SFRC in the casting of dolosse.

---

*Chief of Materials and Investigation Section, Los Angeles District, U.S. Army Corps of Engineers.

Mechanical Properties of SFRC

The field tests and performance of the steel fiber reinforced concrete dolosse have indicated that their high flexural strength and resistance to impact or dynamic loads are superior properties. SFRC also plays a supplementary role in resisting material disintegration and inhibiting cracks.

Toughness is another property provided by the use of SFRC. It has an energy absorbing quality and is measured during flexural strength tests; upon occurrence of the "first crack," the parameter is evaluated. Toughness is defined by ACI (1978) as an area under a load deflection curve. The toughness index is a function of that area and both properties may help in predicting relative performance where post-cracking energy absorption or resistance to failure after cracking is important. However, using toughness and a toughness modulus as criteria for performance of SFRC dolosse becomes difficult for these massive structures. The ASTM C1018-84, Standard Test Method for Flexural toughness of Fiber-Reinforced Concrete (Using Beam with Third-Point Loading), (1985), provides guidance for the evaluation of these parameters. Barr and Mohamad Noor (1985) propose an alternative definition of the toughness index. With the variation of interpretation at hand, it was decided to conduct laboratory tests on SFRC beams, using various steel fibers available, and compare the results. The results would be used as criteria for owner-supplied mix designs since the tests are not amenable to field construction quality assurance programs.

Laboratory Investigation

During 1985, a laboratory testing program was conducted by the Corps of Engineers, South Pacific Division Laboratory. The testing involved mixing various quantities and types of steel fibers into a standard concrete mix and casting the concrete into beam molds for flexural testing. The purpose of the program was to satisfy the following objectives:

- To determine the performance characteristics of the various fibers during mixing.
- To determine the influences of the quantity of fibers on the flexural properties of the concrete.
- To compare the energy absorbing characteristics of the hardened concrete using the various fibers.
- To establish a baseline method of conducting mix design studies using contractor submitted materials.
- To provide a basis for specifying criteria for fibers.

For the concrete mix, coarse and fine aggregates consisted of subrounded to rounded alluvial material composed of serpentinite and metavolcanics. Both crushed and naturally screened coarse aggregates were used and met gradation requirements for size

No. 67 aggregate (ASTM C-33) having a maximum nominal size of 1-inch (25 mm). Type II low-alkali cement was used for the various mixes along with a water-reducing admixture.

Four types of fibers were used for the testing. Two types were deformed with one having a hooked end with a circular cross-section and the other having a crimped length with a crescent shaped cross-section. The remaining 2 fibers were straight with a circular cross-section and rectangular cross-section. All of the fibers were made from a low carbon steel with a minimum tensile strength of 50 ksi (345 MPa). The straight fiber with the circular cross-section was coated with brass.

Fiber quantities of 90 and 120 pounds were batched into single cubic yard mixes of concrete to give final proportions of 89.4 and 118.9 lbs/yd^3 (53 and 71 Kg/m^3) respectively. Table 1 lists the mix designations and the steel fiber properties. The laboratory concrete mix proportions used in the testing program are given in table 2.

The mixing for the fiber reinforced concrete was performed in accordance to the ASTM C-192. The aggregates and water were first added to the mixer, followed by the cement and admixtures. The fibers were added to the concrete in the last 2 minutes of the total required mixing time of 8 minutes with the exception of the collated 2-inch (51 mm) hooked fibers. These long fibers were initially batched with the same mix times as the other fibers, but the fibers did not break apart and disperse within the concrete. An additional 2 minutes of mix time was then added for these fibers with no change in results. Then, presoaking in water was attempted to weaken the glue bond and to help the mixing action break apart the fibers, with no improvement in the results.

In order to minimize any preferential alignment that may occur with the longer fibers the fresh concrete was placed into 6 x 6 x 38-inch (152 x 132 x 965 mm) molds. Also the beams produced were of the largest practical size for tests representative of large structures such as the dolosse. Five beams were cast for each designated mix. During the casting of each mix, slump, air content, and unit weight were measured. The average slump for the fiber reinforced concrete was 1-1/2 inches (38 mm) with a range of 1 to 2 inches (25 to 51 mm) whereas the control mix without fibers had a slump of 3 inches (76 mm). Even though a high range water reducing admixture was used to increase the workability, handling of the concrete was difficult, especially for the longer fibers. Placing the concrete in the molds required extensive vibration in order to assure proper compaction. The air content value averaged 3 percent by volume for the various mixes and unit weight measurements averaged 156.8 pounds per cubic foot (2510 kg/m^3) with fibers. Attempts were made to perform ASTM test method C995-83, "Time of Flow of Fiber-Reinforced Concrete Through Inverted Slump Cone," however the fibers had a tendency to plug the small opening of the inverted cone.

Flexural tests were performed according to ASTM C-78 at 3, 14, and 28 days. Each beam was tested twice by loading half the beam span between the apparatus beam supports, and a load-deflection curve was electronically plotted for 5 of the 10 flexural tests.

The toughness index is an indication of energy absorption after initial cracking, where the test values obtained indicate the ability of the fiber reinforced concrete to remain together after cracking. Toughness indices are calculated from the plotted load-deflection curves according to ASTM C-1018, using the area under the curve at which the first crack is deemed to have occurred. This area is then divided into the area under the load-curve up to the point of deflection at some multiple of the deflection at first crack. The I_5 index which corresponds with the area that is 3.0 times the deflection at the first crack, is the minimum value for which the C-1018 test employs. Based on the 1972 destructive testing of the dolosse, the deflection values for the I_5 index was apparently not reached, since the legs of the dolosse had fallen off just shortly after the ultimate load. The area under the curve corresponding to 1.5 times the first crack deflection was then selected to obtain toughness index data that would represent a closer approximation to the failure of the dolosse. The index using this area was labeled as $I_{1.5}$, and both indices of $I_{1.5}$ and I_5 were calculated for comparison.

Laboratory Test Results

The results of the flexural tests indicated an average increase in flexural strength of 7.2 percent over the unreinforced concrete (control mix) strength of 940 psi (6.48 to 7.34 MPa) at 28 days. The average 28 day strength for the beams with steel fiber was 1008 psi (6.95 MPa) with a range of 950 to 1065 psi (6.55 to 7.34 MPa) that corresponds to the G90 and F90 mixes, respectively. Flexural strengths generally increased with the greater quantities of deformed and straight-circular fibers, but decreased slightly with the increase of rectanglular straight fibers. The longer fiber lengths did not appear to make a significant difference in the flexural strengths. Since the long collated fibers (mixes D90 and D120), were found to remain collated in the hardened concrete beams, slightly higher flexural strengths may be expected for uncollated fibers of the same length. Results of the flexural testing is shown in table 3.

The results of the toughness index calculations showed all the fiber mixes to have comparable values with the $I_{1.5}$ index and some variation with the I_5 index. The average $I_{1.5}$ value was 1.99 with a range from 1.95 to 2.06. These values indicate that the fibers essentially absorb the same proportion of energy up to the deflection that was just past the point of the ultimate load or that point assumed to be the failure of the dolosse. The average I_5 value was 4.22 with a range of 3.44 to 4.90. The straight rectangular fiber mixes had the lowest average of I_5 values.

Unlike other fiber mixes tested in this investigation, the concrete beams having straight rectangular fibers appeared to rapidly lose their ability to absorb energy after reaching the ultimate load. The other beams, including those with straight circular fibers, continued to deflect and absorb energy well after the ultimate load was applied. With the applied load taken to 0.075-inch (2 mm) deflection, the load deflection curves indicated that beams with the longer deformed fibers can absorb substantially more energy than the other fibers after first crack. The calculated toughness indices are shown in table 3.

Examination of the beams after the breaks revealed exposed fibers protruding from the break surface. The fibers did not break in tension, but had pulled out of the concrete. The collated fibers in mixes D90 and D120 were still glued together and had not dispersed evenly through the beams. The break surface also revealed some bond failure between the larger rounded aggregates and the cement paste.

CONCLUSIONS AND RECOMMENDATIONS. Results of the field and laboratory tests offer the following conclusions and recommendations relative to SFRC mixes in casting of large dolosse.

In order to maintain the workability of the fibrous concrete mix the coarse aggregate should contain a 1-inch (25 mm) maximum nominal size screening. To minimize aggregate bond failure, at least 30 percent of the coarse aggregate is recommended to consist of crushed angular material. A maximum sand-aggregate ratio of 50 percent is adequate for the workability of the concrete while giving satisfactory results.

A water cement ratio of less than 0.45 is recommended. To provide improved workability with the mix containing fibers and a low water-cement ratio, a high range water reducing admixture should be used in the concrete mix. Where conditions warrant, air-entrainment may also be used.

The 2-inch collated lengths fibers were not able to disperse in the concrete mix after adding an additional 2 minutes of mix time, in spite of presoaking the fibers overnight. Although presoaking appeared to soften the glue, the fibers remained collated and corrosion had begun on the surface of the fibers. As a result of these findings, the use of collated fibers should be used with caution.

The tensile strength of the steel fibers had no apparent influence on the test results. The cement bond to the fibers failed before the fibers reached their maximum tensile strengths, causing the fibers to pull out of the concrete matrix.

The flexural strength test results did not indicate any significant advantage by using long fibers over short fibers. While the workability of the concrete was greatly reduced with the addition of steel fibers, the handling of long fiber mixes was found to be much more difficult during placement into the beam molds. In order to minimize problems during the quality control program, a recommended range in fiber length should be from 0.75 to 1.25 inches (19 to 32 mm). A corresponding aspect ratio (ℓ/d) between 24 and 65 would be a suitable requirement for the fibers in order to minimize clumping during mixing.

For supplemental guidance on mixing, placing, and curing, refer to ACI Committee 544 (1984).

Table 1. Mix Designations and Steel Fiber Properties.

Mix Desig.[1]	Fiber Description	Fiber Length Inches(mm)	Tensile Strength ksi (MPa)	Aspect Ratio	Fiber Count per Pound(kg)
A90	Deformed	1 (25)	125(862)	24-33	2300
A120	crimped				(5070)
B90	half round	2 (51)		49-63	1700
B120	wire				(3750)
C90	Hooked end	1 (25)	175(1207)	50	9900
C120	smooth				(21820)
C90	wire	2 (51)		100	6000
D120					(13230)
E90	Straight	3/4(19)	50(345)	45	21600
E120	smooth				(47620)
F90	rectangular	1 (25)		60	16200
F120	cross section				(35710)
G90	Straight	3/4(19)	135(930)	62.5	18100
	smooth				(39900)
G120	drawn brass				
	coated				

---

[1] The labeled mix designations indicate the use of 90 and 120 lb/yd^3 (53 and 71 kg/m^3) of steel fibers.

Table 2. Laboratory Concrete Mix Propertions.

Ingredient	Unit	Weight
Type II cement	lb/yd^3(kg/m^3)	635(377)
Fine aggregate	lb/yd^3(kg/m^3)	1602(950)
Coarse aggregate	lb/yd^3(kg/m^3)	1073(637)
Coarse aggregate, crushed	lb/yd^3(kg/m^3)	553(328)
Water	lb/yd^3(kg/m^3)	267(158)
Steel Fibers	lb/yd^3(kg/m^3)	90-120(53-71)

Water-cement ratio ≈ 0.42

AD-A168 715 PROCEEDINGS OF WEST COAST REGIONAL COASTAL DESIGN 4/5
CONFERENCE HELD ON 7-8 NOVEMBER 1985 AT OAKLAND
CALIFORNIA(U) CORPS OF ENGINEERS SAN FRANCISCO CALIF
UNCLASSIFIED SOUTH PACIFIC DIV APR 86 F/G 13/2 NL

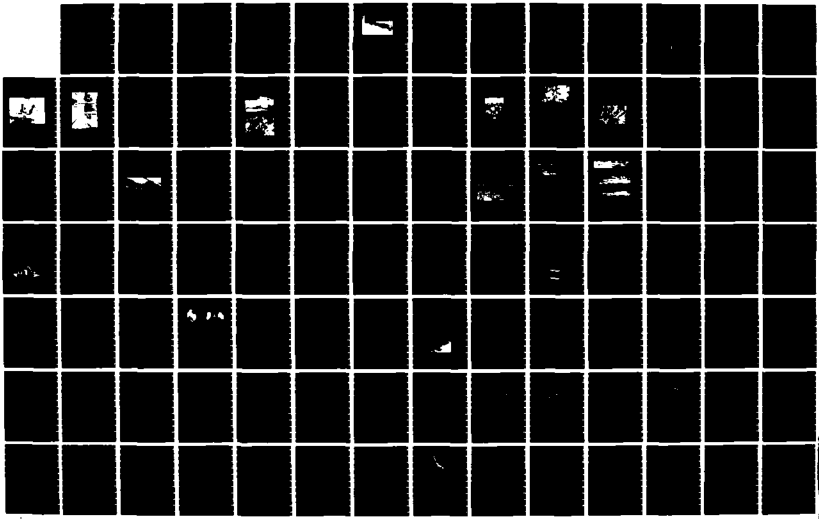

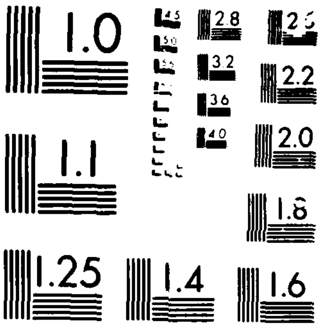
1.0
2.8
2.5
3.2
2.2
3.6
4.0
2.0
1.1
1.8
1.25
1.4
1.6

Table 3. Laboratory Flexural Beam Test Results.

Mix Identification	Flexural Strength psi (MPa) 3-day	14-day	28-day	Toughness Index $I_{1.5}$	I_5
A90	640(4.41)	890(6.14)	955(6.58)	1.99	3.94
A120	670(4.62)	910(6.27)	1000(6.89)	1.99	4.10
B90	675(4.65)	940(6.48)	990(6.82)	2.01	4.54
B120	690(4.76)	925(6.38)	990(6.82)	2.04	4.90
C90	610(4.20)	885(6.10)	980(6.76)	2.00	4.23
C120	590(4.07)	885(6.10)	1000(6.89)	1.98	4.39
D90	590(4.07)	860(5.93)	985(6.79)	1.97	4.15
D120	600(4.14)	900(6.21)	1005(6.93)	2.06	4.70
E90	665(4.59)	955(6.58)	1060(7.31)	1.97	3.82
E120	705(4.86)	975(5.72)	1050(7.23)	1.95	3.44
F90	695(4.79)	970(6.69)	1065(7.34)	1.99	3.94
F120	745(5.13)	990(6.83)	1060(7.31)	1.97	3.73
G90	670(4.62)	850(5.86)	950(6.55)	2.01	4.68
G120	680(4.69)	895(6.17)	1030(7.10)	1.95	4.36
Control Mix	670(4.62)	815(5.62)	940(6.48)	---	---

Appendix - References.

1. ACI Committee 544, "Measurement of Properties of Fiber Reinforced Concrete," (ACI 544.2R-78), American Concrete Institute, Detroit, 1978, 7 pp.

2. ACI Committee 544, "Guide for Specifying, Mixing, Placing, and Finishing Steel Fiber Reinforced Concrete," (ACI 544.3R-84), American Concrete Institute, Detroit, 1984, 9 pp.

3. Barr, B. and Mohamad Noor, M.R., "The Toughness Index of Steel Fiber Reinforced Concrete," Journal of the American Concrete Institute, ACI, Vol 82, No. 5, Sept.-Oct. 1985, pp 622-629.

4. Coursey, Greer E., "New Shape in Shore Protection," Civil Engineering, ASCE, Vol 43, No. 12, Dec. 1973, pp. 68-71.

5. "Standard Test Method for Flexural Toughness of Fiber-Reinforced Concrete (Using Beam with Third-Point Loading)", Standard C1018-84, Annual Book of ASTM Standards, Vol 04.02, American Society for Testing and Materials, Philadelphia, Pa., 1985.

KEY WORDS: dolos; dolosse; flexural strength; laboratory tests; steel fibers; steel fiber reinforced concrete (SFRC); toughness; toughness index

ABSTRACT:

The use of steel fiber reinforced concrete (SFRC) has passed from purely experimental laboratory scale applications into field applications involving worldwide placement of large volumes annually. Since 1972, the South Pacific Division of the Corps of Engineers has been casting dolosse with SFRC. Most recently 1,000 were cast at Humboldt Bay, California and over 500 will be cast during 1986 at Cresecent City Harbor, California. Presented are the methods used to evaluate the effectiveness of the SFRC in casting a 42 ton (38,100 Kg) dolos (singular of dolosse). The most desirable steel fiber characteristics are discussed and the results of laboratory tests of SFRC, using currently available steel fibers, are also described.

PROTOTYPE MEASUREMENT OF THE STRUCTURAL RESPONSE OF DOLOS ARMOR UNITS

Mr. Thomas R. Kendall[1]

Mr. Gary L. Howell[2]

Mr. Thomas A. Denes[3]

ABSTRACT

At present, a design procedure is not available to the coastal engineer for the prediction of structural strength requirements for dolos armor units. As units have increased in size, structural failures have become more frequent. A program has been initiated by the Corps of Engineers to measure the structural stresses, strains, and forces on dolosse in a high energy prototype environment. As part of the rehabilitation of the outer breakwater at Crescent City, California, twenty new dolosse will be instrumented. Due to the general lack of prototype information on the behavior of armor units, an international workshop held to review the state of the art in structural investigations of armor units concluded that collection of such prototype data was a necessary first step in the development of a structural design methodology.

1. Introduction

In the early 1970's, the U. S. Army Corps of Engineers, San Francisco District pioneered the use of large dolos armor units in the United States. The north and south jetties at Humboldt, California were armored with two layers of 42 ton dolosse around the head sections as part of their rehabilitation in 1971-1972. In 1974, 40 ton dolosse were placed on the Crescent City, California outer breakwater (Figure 1) as part of its rehabilitation (Magoon, et al., 1974). The economic advantages of the dolos unit were well known at that time, as was the hydraulic stability characteristics of dolosse under wave attack. However, District engineers were concerned about the limited knowledge of dolos strength characteristics, and related requirements on dolos construction, such as whether steel reinforcing would be required.

---

[1] Coastal Engineer, San Francisco District, U. S. Army Corps of Engineers

[2] Research Hydraulic Engineer, U. S. Army Engineer Waterways Experiment Station, Coastal Engineering Research Center

[3] Civil Engineer, San Francisco District, U. S. Army Corps of Engineers

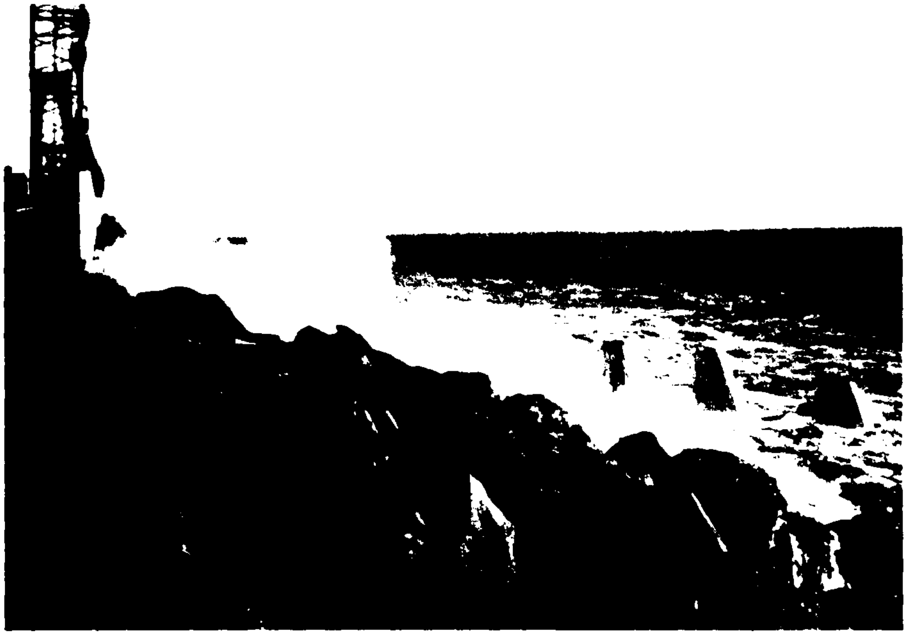

FIGURE 1: PLACING DOLOSSE AT CRESCENT CITY, 1974

Because of these concerns and experiences during the casting and construction of the dolosse at Humboldt, some experimentation and investigations were performed (Coursey, 1973; Barab and Hanson, 1974). Structural strength of dolosse was investigated by jacking and drop tests. Unreinforced dolosse, conventionally reinforced dolosse, and dolosse reinforced with various concentrations of metal fibers were evaluated. Material properties testing of the concrete with and without metal fibers was also performed. The general conclusion was that although fiber reinforcing did not result in large increases in the strength of dolos units, the fibers helped hold the units together after fracture.

Since reinforcing dolosse can significantly increase the manufacturing cost of units, the structural strength requirements for a given armor unit design has remained a controversial question in breakwater engineering. The dolosse placed at Crescent City in 1974 were unreinforced. Corps wide experience with breakage of units has not shown a consistent pattern tracable to the level of reinforcing used because of the interplay of design factors, hydraulic stability, and construction quality control (Markle and Davidson, 1984). However, it is apparent, after over ten years of experience with dolos breakwaters, that the percentage of broken units has been notably high for some breakwaters . The late 1970's and early 1980's have seen the catastrophic failure of several foreign breakwaters using large dolos armor units. Structural failure of dolos units has been suggested as a contributing cause in these failures, focusing renewed attention on the lack of a structural design or analysis procedure.

The limited progress in developing a design methodology can be attributed to the difficulty of the problem and to the lack of any real prototype data to develop and verify modeling techniques capable of addressing the structural problem. All past attempts to use both physical and numerical modeling techniques have resulted in limited progress because of the lack of prototype scale data (Burcharth, 1980).

In 1983, the San Francisco District was again faced with the requirement to rehabilitate the Crescent City breakwater and Humboldt jetties. It was recognized that the rehabilitation also presented the opportunity to use the casting and placement of new dolosse to implement a program to obtain measurements of the forces and stresses on dolosse in the prototype. Representatives of the San Francisco and Los Angeles Districts, and South Pacific Division of the Corps approached the Waterways Experiment Station (WES), Coastal Engineering Research Center (CERC) to initiate feasibility studies of various alternatives for instrumenting dolosse and developing a data acquisition system capable of functioning in the breakwater under storm conditions. Of the two possibilities for the prototype study, Crescent City was selected over Humboldt because of its more even bathymetry and milder wave conditions. In eary 1984, a formal proposal was developed by WES as a joint effort of CERC and the WES Structures Laboratory including both the Structural Mechanics Division and the Concrete Technology Division. The proposal was accepted by the Office, Chief of Engineers (OCE) and a Test Working Group was formed to manage the study with representatives from OCE, the Districts, South Pacific Division, and WES laboratory elements.

2. Program Objectives

The breakwater at Crescent City, provides a unique opportunity to study the structural response of large dolosse in the prototype. New 42 ton dolosse will be cast and placed on top of and adjacent to the existing dolosse. The wave climate at Crescent City is sufficiently severe each year to guarantee waves which will cause measurable motion and impact loading of the dolosse. Figure 2 shows the layout of the breakwater. The main leg is approximately 3700 feet in length and the easterly extention (dogleg) is approximately 1,000 feet long. The dolos section is comprised of 246 unreinforced dolosse distributed along the last 230 feet of the main stem. Since their placement as part of the breakwater rehabilitation in 1974, up to seventy units have been reported to be broken (Edmisten, 1982). At least 22 of these breakages can be attributed to the casting and placement operations (Markle and Davidson, 1984).

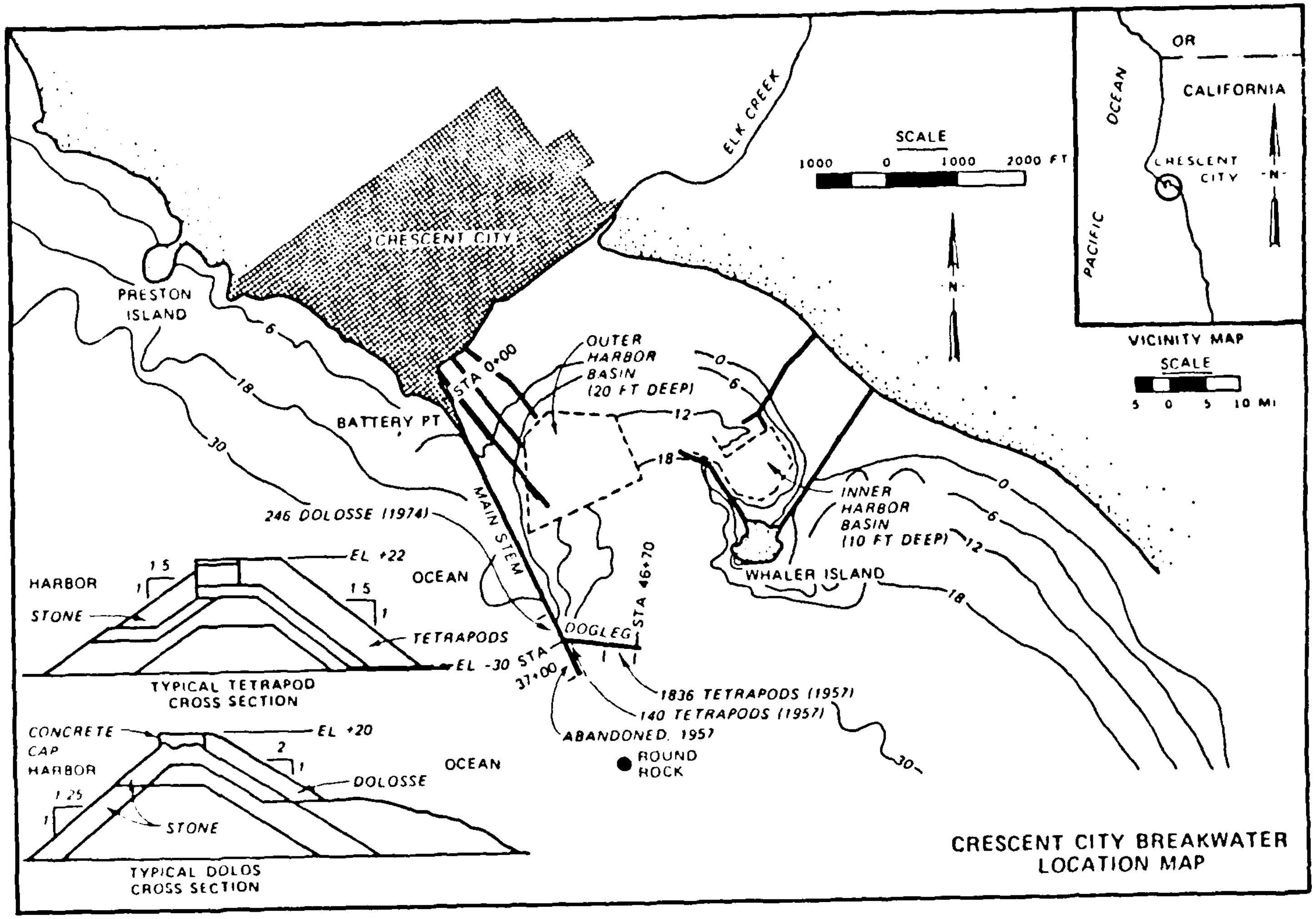
CRESCENT CITY BREAKWATER LOCATION MAP
OR
OCEAN
CALIFORNIA
PACIFIC
CRESCENT CITY
N
VICINITY MAP
SCALE
5 0 5 10 MI
SCALE
1000 0 1000 2000 FT
N
ELK CREEK
CRESCENT CITY
PRESTON ISLAND
BATTERY PT
STA 0+00
OUTER HARBOR BASIN (20 FT DEEP)
INNER HARBOR BASIN (10 FT DEEP)
WHALER ISLAND
MAIN STEM
DOGLEG
STA 46+70
STA 37+00
246 DOLOSSE (1974)
1836 TETRAPODS (1957)
140 TETRAPODS (1957)
ABANDONED, 1957
ROUND ROCK
OCEAN
0
6
12
18
30
HARBOR
STONE
EL +22
1.5
1
TETRAPODS
EL -30
TYPICAL TETRAPOD CROSS SECTION
CONCRETE CAP
HARBOR
EL +20
2
1.25
DOLOSSE
STONE
TYPICAL DOLOS CROSS SECTION

FIGURE 2: CRESCENT CITY BREAKWATER (From Markle and Davidson, 1984)

Markle and Davidson also report that most of the broken dolosse have remained in their original positions although gradual settlement has been observed over the years. In November 1984, however, a slip failure occurred after which nearly all the dolosse in a narrow band near the middle of the dolos section were broken. Even so, both the extent and the cause of breakage remains controversial.

The primary objective of the study at Crescent City is to provide high quality field measurements which may be used to calibrate and validate numerical models of the structural response of dolos armor units in a given breakwater and wave environment. It is anticipated that experience gained from the dolos case may provide insight into related analysis of other types of concrete armor units. The evaluation of the stresses will be performed with finite element numerical modeling of the structural shape of the dolos using field measurements to define the loading and boundary conditions. Likewise, models of dolos motion due to wave forcing will be evaluated with prototype data from both offshore and breakwater measurements. The results of these analyses, when validated by prototype data, could lead to a simplified structural design procedure based on wave conditions similar to that available for breakwater stability.

3. Dolos Workshop

Because of the unique interdisciplinary nature of the dolos structural problem, and the fact that the Crescent City experiment might be the only opportunity in the near future to acquire prototype data of this type, the Test Working Group decided to hold a research workshop before plans for the study were completely finalized. The Workshop on Measurement and Analysis of Structural Response in Concrete Armor Units was convened by CERC in Vicksburg, Mississippi, on 23 and 24 January 1985. Twenty-three scientists and engineers from six foreign countries and the United States participated in the workshop. This group of distinguished researchers, representing academic, government, and private sector interests, possessed a broad background of knowledge and a diversity of experiences. Case histories from breakwater designs around the world were presented and discussed with respect to engineering lessons learned (Wood, et al., 1985).

In the final afternoon session of this workshop a set of recommendations was developed for the Crescent City study. These recommendations were:

a. It is important to define the incident wave conditions completely.

b. It is necessary to obtain excellent bathymetry near the structure.

c. It is important to maintain good photographic records of the dolos prototype tests.

d. It is necessary to evaluate impact, pulsating, and static stresses in the dolos armor units.

e. It is necessary to perform drop tests to destruction on instrumented and non-instrumented dolosse.

Consensus of the participants was that the overall design of the prototype measurement program was good and need not be modified. There was an overall enthusiasm for this study and many of the participants expressed interest in continued involvement with the results from this experimental program.

4. Description of the Field Measurements

Prototype data from Crescent City will be derived from twenty special dolos armor units instrumented with internal strain gage assemblies. The strain gages will be configured to measure the moments and the torque about one shank-fluke interface. Coincident with the strain measurements, the velocity of motion of six of the dolosse will be measured with six degrees of freedom. Velocity data may be used to determine impact energy for correlation with sea state and resulting stress. Figure 3 shows a sketch of how the internal instrumentation is arranged inside the dolos. The strain gages are mounted on rebar rosettes at the shank-fluke interface and the accelerometers and data acquisition electronics are located in the cylinder cast in the trunk midsection.

Offshore directional wave measurements will be made as well as scalar wave measurements near the breakwater. Hydrodynamic pressures within the core material, along the face of the cap, and within the dolos matrix will be measured. A description of the measurement plan was presented at the 41st Meeting of the Coastal Engineering Research Board (Domurat and Howell, 1984).

Measurement Strategy and Interpretation

As a result of recommendations by the Dolos Workshop, data acquisition procedures for the field measurements have been expanded to assure the description of stresses and strains on the time scale of wave periods as well as impact stresses and static stresses. Following the convention of Burcharth (1984), total stress will be considered as the summation of static stress, pulsating stresses, and impact stresses. Pulsating stresses are those defined to be on the same time scale as wave periods, whereas impact stresses are on the time scale of the fundamental vibration modes of the dolos. Prototype data will be analyzed so as to create a statistical distribution of each component of stress as a function of sea state. Such an analysis would result in an empirical description of the hypothetical curve suggested by Burcharth (Figure 4).

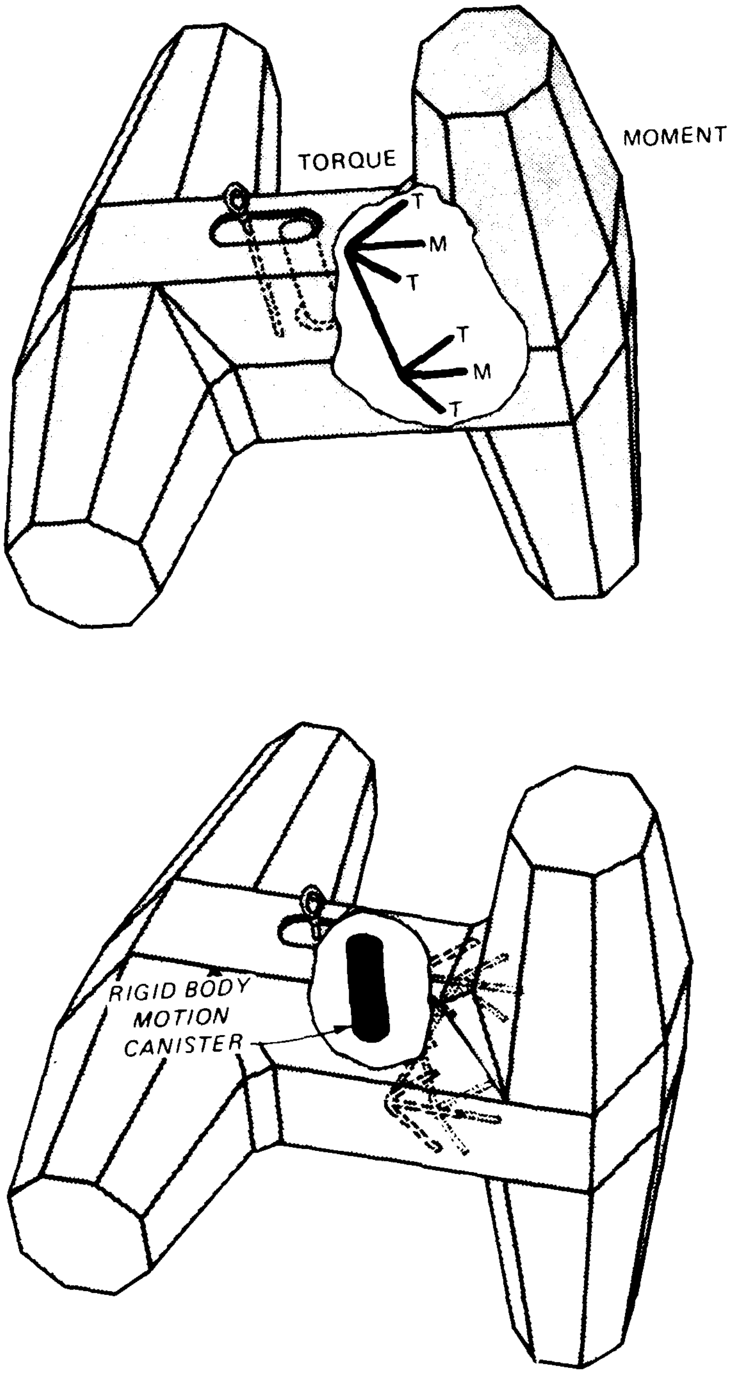
TORQUE
MOMENT
T
M
T
T
M
T
RIGID BODY
MOTION
CANISTER

FIGURE 3: INSTRUMENTATION OF DOLOS (From Wood, et al., 1985)

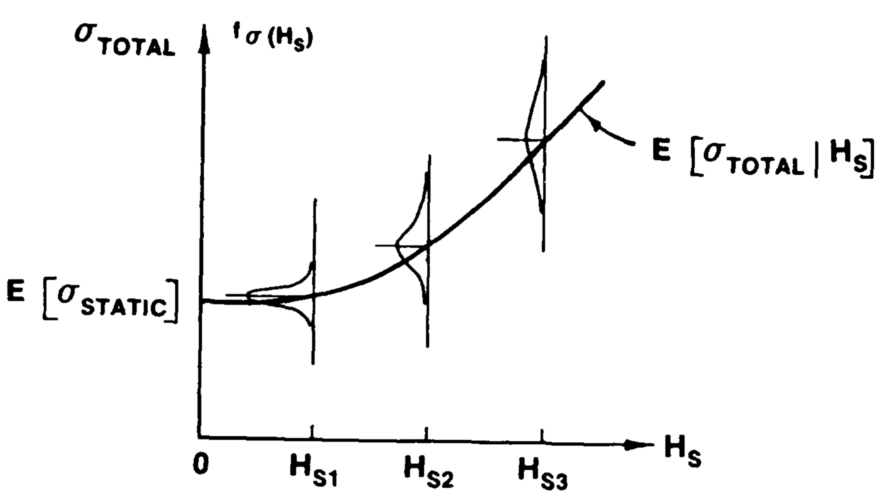

FIGURE 4: QUALITATIVE ILLUSTRATION OF DEPENDENCE OF STRESS (σ) ON WAVE HEIGHT (H) (From Burcharth, 1984)

Placement of Instrumented Dolos

During the initial phase of the study several placement plans have been proposed, evaluated, and reviewed. Final candidate strategies were discussed in detail at the Dolos Workshop. A consensus has emerged favoring a placement strategy which would group all instrumented dolosse together in a single matrix. The strategy is based on the requirement to identify the surrounding boundary conditions of each instrumented dolos as well as the need to have a statistically significant number of measurements from dolosse exposed to the same, or nearly the same, wave environment. Although the importance of spatial sampling of conditions affecting dolosse at other points on the breakwater is recognized, it is felt that the difficulty of determining and comparing wave conditions along the breakwater will make comparison of results from widely separated dolosse difficult. Similar considerations of the importance of characterizing the incident wave conditions led to the decision to place the instrumented dolos matrix near the middle of the trunk section armored with dolosse. The exact position has been selected based on considerations of cable protection and installation. The instrumented section is a four by five matrix with the six accelerometer dolosse placed on top and in the center. The matrix is centered at the mean water line.

Dolos Cable Protection

During the Fall of 1984, a test of proposed cable protection systems for the instrumented dolosse was conducted at Crescent City. The primary system tested was modified anchor chain. Chain sizes of up to three inches in diameter, weighing from 70 to 80 pounds per foot, were used. The primary purpose of the chain assemblies was to form an anchor system for the dolos signal cable coming up the breakwater to the cap. Different methods of attaching the cable to the chain were implemented including holes, clamps and bindings. Additionally, a single armored cable was deployed without chain.

After subsequent inspections it was determined that the chain assemblies did not move during mild to moderate wave conditions. Attempts to inspect chain motion during severe wave conditions were unsuccessful. However, indications from other inspections indicate little, if any movement, due to wave action. The armored cable did show cyclic motion during moderate conditions, indicating that cable fatigue failures of unanchored armored cable would occur. None of the methods employed to attach the cables to the chain proved to be entirely satisfactory. The methods using holes in the chain caused too much stress to the cable due to the multiple sharp blends. The straight run of cable along the chain was the most satisfactory, except that the attachment methods either failed or were too time consuming to install.

An additional lesson learned from the test was the possibility of potential damage to the cable during installation due to the ability of the chain to bend at a sharp angle, thus forcing the cable below its minimum bend radius.

Based on the results of the test it was decided to use a modified anchor chain as the cable protection. The chain will be modified such that the cable may be attached along the chain without bends, and at the same time the modification will restrict the bend radius of the chain to a 24 inch minimum. A development and evaluation program performed at WES has been completed and the resulting chain modification is shown in Figure 5. When applied to the chain, the sleeve limits the bending of the chain as shown in Figure 6, while also providing a protective channel for the cable. Tests using the modification indicate that the cable is easily installed in the protection system and is not pinched or damaged by any of the possible motions of the assembly.

5. Conclusion

The Crescent City Dolos prototype study represents a unique effort to solve an important and difficult problem in coastal engineering. A strong cooperative relationship has been established between District engineers responsible for breakwater design and construction, and research engineers who need data from prototype scale breakwater armor units. This cooperation has allowed the collection of research data which would otherwise be cost prohibitive. The results of the study will be used to develop a structural design methodology for dolos armor units, providing a tool to designers which has been needed but unavailable. The ability to analyze and design dolos units to meet strength requirements will result in decreased cost and risk in breakwater construction and maintenance.

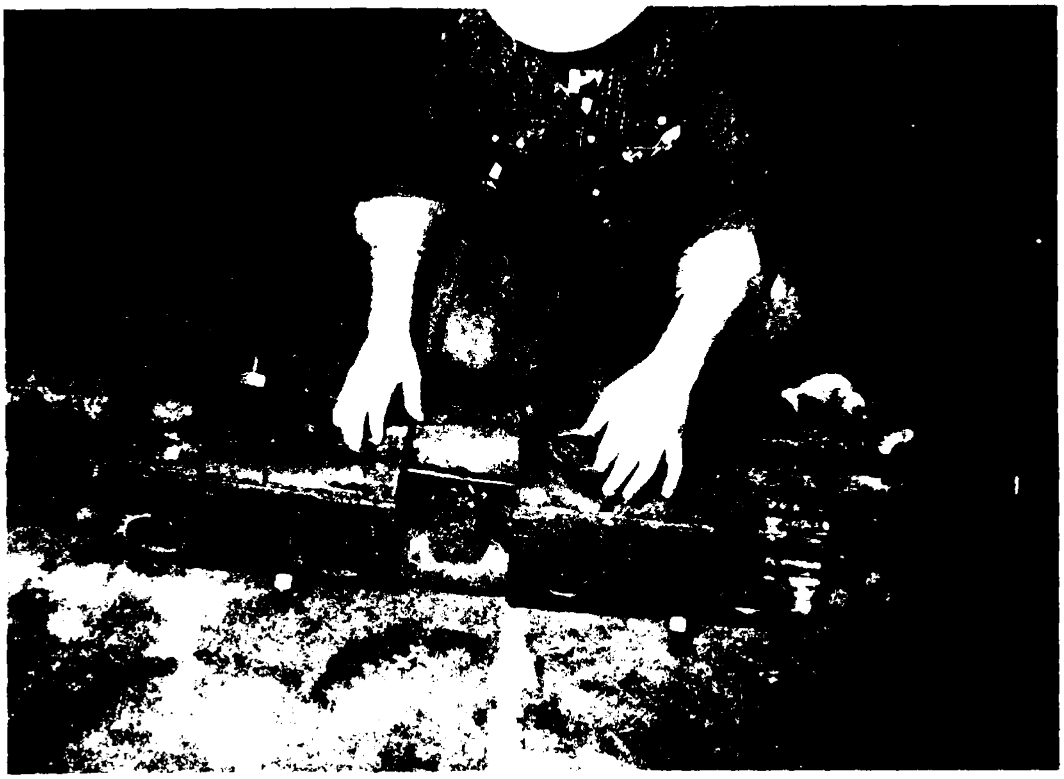

FIGURE 5: MODIFIED ANCHOR CHAIN PROTECTING DOLOS SIGNAL CABLE

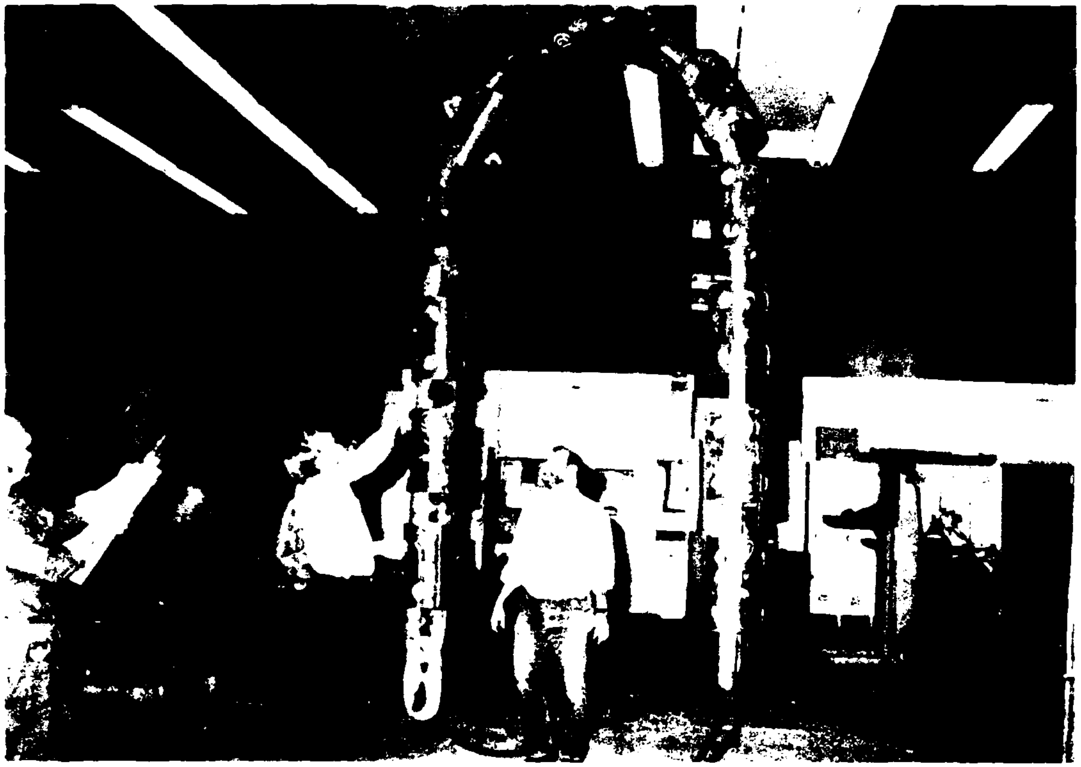

FIGURE 6: LIMITED BENDING RADIUS
OF ANCHOR CHAIN SYSTEM

References

BARAB, S. and D. Hanson. 1984. "Investigation of Fiber Reinforced Breakwater Armour Units," Fiber Reinforced Concrete, Publication SP-44, American Concrete Institute, Detroit, MI, pp. 415-434.

BURCHARTH, H. F. 1980. "Full Scale Trials of Dolosse to Destruction," Coastal Engineering, 1980 Proceedings, Vol. II, Chapter 118, pp. 1928-1947.

BURCHARTH, H. F. 1984. "Fatigue in Breakwater Armour Units," Sohngardsholmsvej 57, DK-900, Aalborg Universitets Center, Aalborg, Demark.

COURSEY, G. E. 1973. "New Shape in Shore Protection," Civil Engineering, American Society of Civil Engineers, December 1973, pp. 68-71.

DOMURAT, G. W. and G. L. HOWELL. 1984. "Measurements of Forces in Dolos Armour Units," Proceedings of the 41st Meeting of the Coastal Engineering Research Board, Seattle, Washington, Coastal Engineering Research Center, U. S. Army Engineer Waterways Experiment Station, Vicksburg, MS. pp. 70-80.

EDMISTEN, J. R. 1982. "Crescent City Harbor, California - 20 August 1982 Inspection of Outer Breakwater Dolos Section," Memorandum for Record, 28 September 1982, U. S. Army Engineer Division, South Pacific, San Francisco, CA.

MAGOON, O. T., R. L. SLOAN, and G. L. FOOTE. 1974. "Damages to Coastal Structures," Coastal Engineering. Proceedings 14th Coastal Engineering Conference, June 24-28, 1974, Vol. 3, American Society of Civil Engineers. pp. 1655-1676.

MARKLE, D. G. and D. D. DAVIDSON. 1984. "Breakage of Concrete Armour Units; Survey of Existing Corps Structures," Miscellaneous Paper CERC-84-2, U. S. Army Engineer Waterways Experiment Station, Vicksburg, MS.

WOOD, W. L., G. L. HOWELL, and R. A. COLE. 1985. "Crescent City Dolos Project," Proceedings of the 43rd Meeting of the Coastal Engineering Research Board, Vicksburg, MS, Coastal Engineering Rearch Center, U. S. Army Engineer Waterways Experiment Station, pp. 114-136.

Degradation Of Rock Used In Erosion Control

Robert O. Van Atta*

ABSTRACT

The susceptibility of basaltic rock to degrade in service in rip-rapping or as road base aggregate is a world-wide problem. Research has shown that the major cause of degradation of basaltic rock is the presence of swelling clays. The results of standard durability testing, e.g. Los Angeles abrasion, sand equivalent, sulfate soundness, and so forth, depend almost entirely upon the mechanical strength of the rock and do not, generally, reveal the presence of swelling clay. Petrographic testing involving staining to reveal the presence of clay and X-ray diffractometry to identify swelling clay offers a solution to this problem of more accurate determination of rock durability.

Introduction

It is important that rock used in erosion control structures, in addition to having suitable density, be of durable quality. Along the central and northern Oregon coast, basaltic rock is the most commonly used material, as it is in many other places. Basalt aggregate is also widely used for road construction and concrete. This paper will deal with some causes of degradation and with durability testing of basaltic rock, although other rock types may be subject to degradation by the same causes and the same durability testing can be applied to them.

Siletz Spit and Salishan Property and Other Examples

In 1972 and 1973 severe winter storms coinciding with high spring tides caused extensive beach erosion along the central and northern Oregon coastline. The first efforts to control wave erosion by rip-rapping with basaltic rock were generally unsuccessful. This was due in part to degradation of the rock. In the Siletz Bay area, where there was extensive damage to homes (Figure 1), including total destruction in some cases, basalt from the Siletz River Volcanics formation was used, owing to its availability closeby. Much of this rock is submarine in origin, erupted on the sea floor some 45 million years ago. Swelling clay minerals are almost ubiquitous secondary alteration products in the basalt, together with chalcedony ("agate"), zeolites and calcium

---

* Department of Geology, Portland State University, Portland, OR 97207

carbonate in the form of calcite. In rip-rap used on the inside of the spit swelling clay was a major cause of extensive degradation to fine gravel and sand-size particles, although the rock also lacks mechanical strength because of numerous fractures and probably would not pass standard durability tests for this reason alone.

Figure 1 A. Salishan property damage, Siletz Spit, Lincoln County, Oregon.

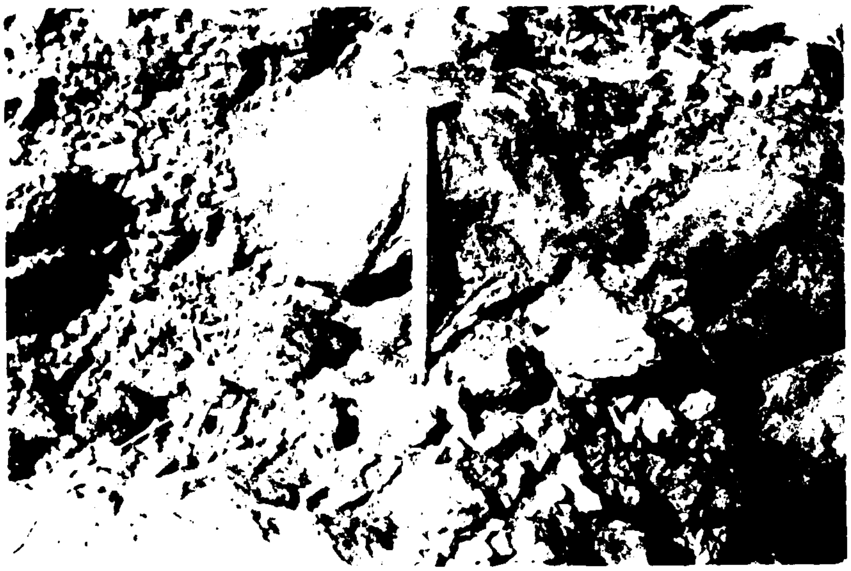

Figure 1 B. Degraded Siletz River Volcanics used as rip-rap, Siletz Spit, inside beside Siletz River channel.

In Ventura County, California, a rhyolitic volcanic agglomerate (breccia) was taken from the Hawley Quarry. Six and eight-foot diameter boulders were used for harbor construction in the Ventura county Small Boat Harbor at Silver Strand. Clasts within the matrix of these boulders became highly weathered and eroded out and cracks developed in the matrix, leading to the further degradation of the rock (Smith, 1967).

Degradation of Basalt

In the case of basaltic rock, degradation continues to be a major problem, despite decades of development of standard durability tests. Some basaltic rocks which will pass standard testing (for example, Washington degradation, L. A. abrasion, sulphate soundness, sand equivalent tests) will, nevertheless, show signs of failure in service. In the case of basalt used for aggregate in road construction, there are notable examples of failures, such as the Upper Nestucca River Access Road, Tillamook County, Oregon, where 22 miles of road showed signs of failure after only 7 months of service, due to degradation of the base course.

The problem of degradation of basalt is worldwide (Scott, 1955; Day, 1962; Hosking and Tubey, 1969; Black and Sameshima, 1979; Orr, 1979, Cole and Sandy, 1980) and has led to international conferences on the subject, such as that held in May, 1984, at Nice, France.

What is the cause of degradation of basaltic rock? This type of rock includes those rocks which are characterized by primary ferromagnesian and calc-alkaline feldspar minerals, together with iron and titanium oxides and, sometimes, glass. The ferromagnesian and feldspar minerals and the glass are especially susceptible to hydrothermal alteration during the cooling and crystallization of molten rock (deuteric alteration). Furthermore, these minerals are quite unstable under weathering conditions, especially glass and olivine, one of the ferromagnesian minerals.

Secondary minerals formed during hydrothermal or deuteric alteration of basaltic rock include various clay minerals, zeolites, calcium carbonate, other carbonate minerals, iddingsite, hydrated iron oxide minerals and quartz in various forms.

Swelling Clay

Of the secondary minerals, swelling clay is widely acknowledged as the major cause of degradation of these basaltic igneous rocks (Minor, 1960; Day, 1962; Nyoeger, 1964; Hosking and Tubey, 1969; Van Atta and Ludowise, 1976; Orr, 1979; Black and Sameshima, 1979). Most frequently, swelling clay minerals do not affect the mechanical strength of the rock very much unless very large (more than 45 or 50) percentages are present. Therefore, results of standard tests often do not correlate well with service performance of basaltic rocks (Figure 2). The other secondary minerals may or may not affect the mechanical strength of the rock, depending, again, upon amount and textural distribution of a given mineral in the rock.

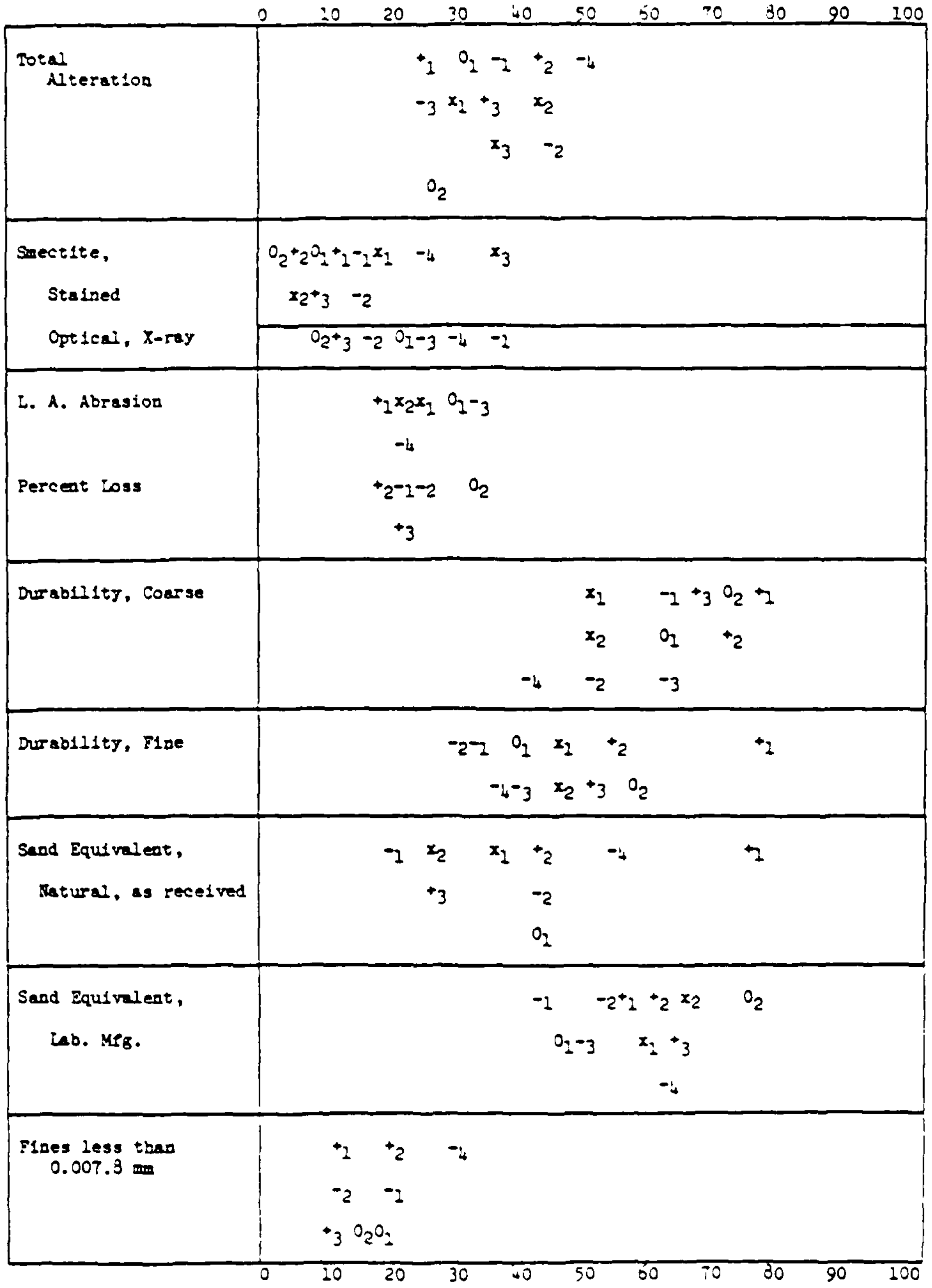

Figure 2 Performance of basalt from 12 sources compared with durability test results. Service ranking of rock shown by: +, good; O, marginal; -, poor; X, no service. Note that only for, "Durability, fine", did service ranking correlate well with test results. (Van Atta and Ludowise, 1976).

Swelling clays include smectite minerals, such as montmorillonite, and various mixed-layer clays, such as mica/smectite, chlorite/smectite, illite/smectite and so forth. Swelling clays are believed to cause degradation of rock when they take up water molecules between layers in the clay mineral crystal structure, with resultant expansion. The amount of water taken up and the degree of expansion, depends upon the magnitude of interlayer charge, the number and kinds of interlayer cations, the conditions of humidity and the nature of solutions available to the clay (Brindley, 1981).

In the smectite group of clays, the interlayer cations include, for example, sodium (Na) or calcium (Ca). The smectite clay montmorillonite may have either Na+ or Ca++ interlayer cations. Ca-montmorillonite may expand from 9.6 Angstroms layer spacing when fully hydrated, while Na-montmorillonite may continue to expand with water until a gel is formed (Brindley, 1981), Blake (1967) reports that swelling pressure exerted by a 30 percent montmorillonite clay paste in 0.001 Molar NaCl can be as much as 5x10 dynes cm^{-2} or 700 lb. in^{-2}. The swelling property of Na-montmorillonite, is, of course, the basis for the utility of bentonite (weathered volcanic ash) employed in sealers for porous materials, such as masonry.

In experimental work dealing with dimensional stability of cut rock prisms (15 mm square and 150 mm long) Shayan and Ritchie (1985) found that in 69 to 70 cycles [soaking the rock prisms one week in saline solutions (0.15 M NaCl and 0.15 M KCl) and drying for one week] considerable shrinkage and expansion took place in a basaltic rock with a high percentage of swelling clay while basalt with a lower percentage of clay did not show as much movement.

Table 1. Movement of rock prisms (%), cycled from a fog room (23°C) to a drying room at the specified temperature. (After Shayan and Ritchie, 1985)

Rock	First cycle			total movement at nth cycle		No. of cycles (n)	% swelling clay
	Expansion on wetting	Shrinkage on drying at		Fog/23°C	Fog/50°C		
		23°C	50°C				
Green basalt	0.025	0.003	0.016	0.024	0.034	69	25
Grey basalt	0.013	0.001	0.004	0.013	0.015	69	8
Blackstone	0.070	0.003	0.017	0.092	0.334	70	40

Although the exact mechanism by which degradation of various rocks takes place has not been verified experimentally, it is believed that fractures (macro and micro) in a rock bearing swelling clay allow ingress of water which is adsorbed by the clay, causing sufficient pressure by expansion to further develop microfracturing which in turn allows more water to enter and be adsorbed by the clay and so forth (Van Atta and Ludowise, 1976).

Testing of Basalt for Durability

It has been known for more than 50 years that basaltic rocks pose special problems in durability testing but it has only been since the 1970s that petrographic (microscopic and X-ray) testing and special "accelerated soundness" testing (ethylene glycol, DMSO soaking and so forth) has been seriously employed (West and others, 1971; Lay, 1981; Miles, 1972; Fielding and Macarrone, 1982; Van Atta and Ludowise, 1976, Cole and Sandy, 1980). Tests such as these are not standardized, however, but are used to supplement standard tests.

It has also been pointed out that careful field study in the search for suitable source rock is an essential first step in assessing the durability potential of basaltic rocks (Van Atta and Ludowise, 1976). Basaltic rock which has been formed as submarine lava flows or breccias almost certainly contains swelling clay as a hydrothermal alteration product because of reaction with seawater. Similarly, subaerial basaltic flows which have entered stream valleys or shallow bodies of fresh water will include hydrothermally altered lower portions. (Figure 3).

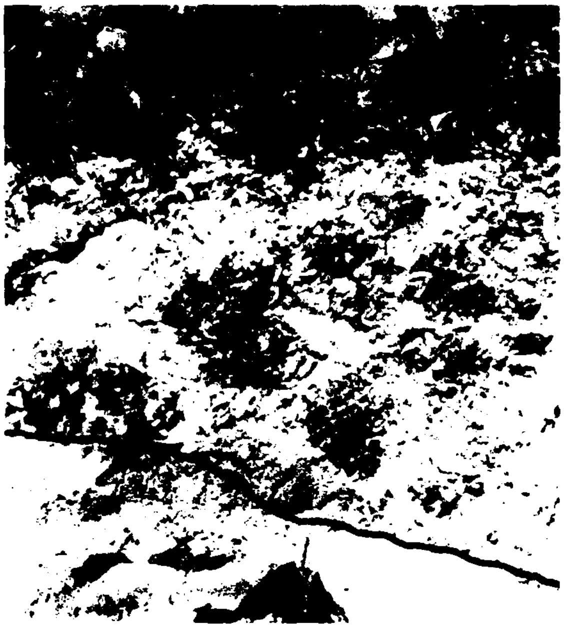

Figure 3 A. Hydrothermally altered basalt in alluvial channel, Geelong, Victoria, Australia. Note highly altered rock at base of flow (outlined), in contact with sediments.

Basaltic lava flows which are emplaced subaerially with little if any contact with water can generally be expected to contain much less swelling clay.

Interestingly, basaltic rock which originates as an intrusion, such as gabbro or diabase sills and dikes, may or may not contain deleterious secondary minerals such as swelling clay. If the intrusive magma contained considerable water and other volatiles, chilling of the margins of the cooling and crystallizing rock mass may have trapped fluids and vapors inside and extensive deuteric alteration by "stewing" of the internal part of the intrusion may have taken place.

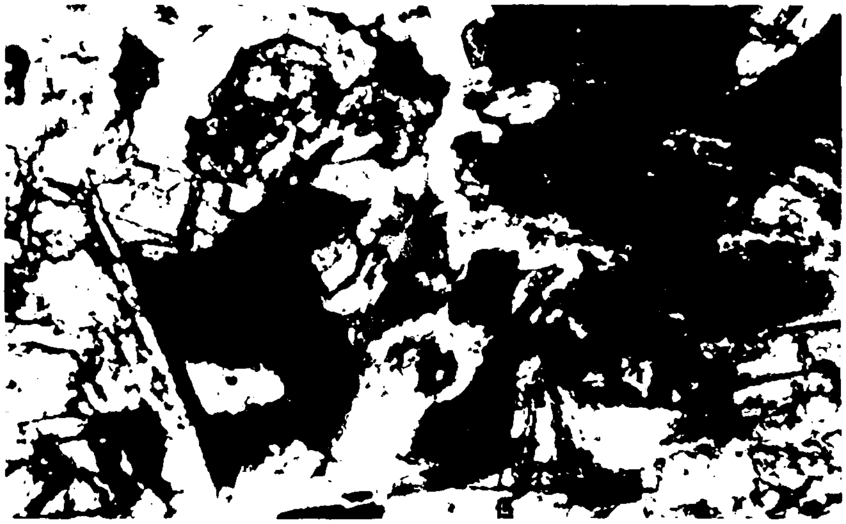

Figure 3 B. Photomicrograph. Swelling clay (in dark areas and fractures in feldspar) in hydrothermally altered basalt, Geelong, Victoria, Australia; a more deleterious textural distribution.

Petrographic Testing

Petrographic testing of basaltic rocks is essential if durability of these troublesome materials is to be accurately assessed. Although the need for petrographic study had been implied in earlier publications, it remained for West and others (1971) and Van Atta and Ludowise, (1976) to make published recommendations that microscope and X-ray study of rock to determine the amount and textural distribution of swelling clay minerals was always necessary in order to assess the durability potential of basaltic rocks. Other rock types are less likely to contain swelling clays but, nevertheless, they too, should be routinely examined petrographically. Swelling clays can be a serious problem in other volcanic rocks, such as dacite.

Cole and Sandy (1980) devised a secondary mineral rating (Rsm) for basaltic aggregate durability based on petrographic testing, which quantified the factor of textural distribution of secondary minerals. This can be expressed as:

$$Rsm = [\Sigma (P.M)]\ Tr$$

Where P = percentage of the secondary mineral in the rock
M = a stability rating for a particular mineral
Tr = a textural or mineral distribution rating for secondary alteration in the rock

In the stability rating, minerals such as calcite ($CaCO_3$) and non-swelling clay, such as kaolinite or chlorite, are given a low value. Swelling clays, such as swelling chlorite or smectite are given higher values. Cole and Sandy tentatively suggested that rocks with a secondary mineral rating of 140 and less will prove to be durable while rocks with Rsm values greater than 140 will prove unsound. The Rsm value of 140 corresponds to a [illegible] degradation factor of about 40 and a secondary mineral content of 30 percent.

In petrographic testing it is not possible to surely identify swelling clays with the mocroscope alone. X-ray diffraction, however, provides a rapid and reliable method of identification. With X-ray diffraction there is, however, no simple, reliable method of accurate quantitative determination of clay mineral species present in a rock. By the use of organic stains the amount of clay can be more surely determined either in powdered rock or by point counting in thin sections of rock. It is thus possible to combine microscope determination of the amount of clay with X-ray identification of the clay mineral species and thereby, indirectly, measure the amount of deleterious clay present in the rock. Such a method has been recently proposed by Cole, Lancucki and Shayan (1984) as a means of verifying quarry potential. In the determination of the amount of clay present in thin sections of rock by use of the petrographic microscope, staining to reveal the presence and textural distribution affords an excellent and simple technique. Two different textural distributions of clay, one of which is more deleterious than the other, are shown in Figures 3B and 4.

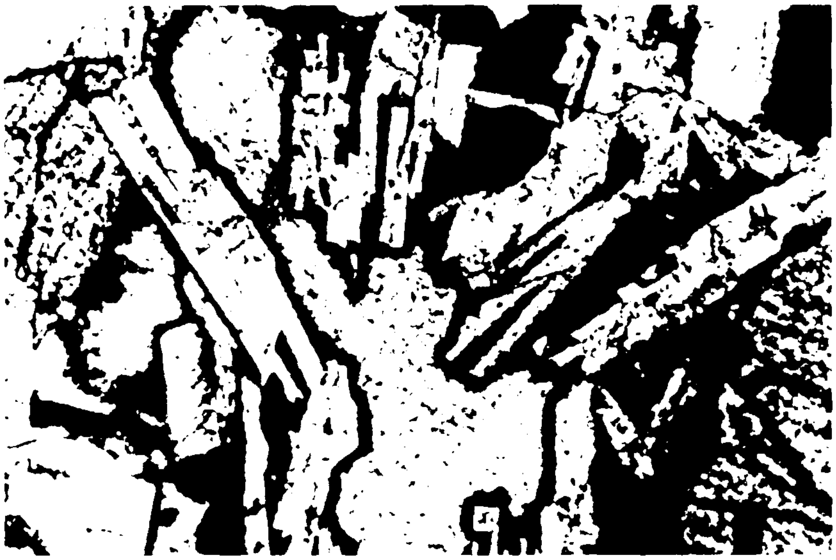

Figure 4 A. Less deleterious textural distribution of clay. Clay (black) surrounds some grains, little in fractures. (Photomicrograph.)

Organic Stains for Clay Mineral Determination

Reactions between organic compounds and clays, which produce color changes in the compound, have been studied for at least 50 years. Theng (1974) has reviewed the subject of colored clay-organic reactions. One of the most thorough studies of clay-organic reactions involving color changes was undertaken in the American Petroleum Institute Project, API 49 (Mielenz and others, 1950). In this study, it was found that many organic substances will be adsorbed by clays, either in a natural condition or pretreated (usually with an acid, like HCl) with an accompanying color change which may be specific for a given species of clay mineral. Clay with a high cation exchange capacity (CEC), such as smectites, may cause a pronounced color change. Some organic compounds are merely adsorbed or absorbed by the clay without any color change. The change in color by clays treated with organic staining agents is believed to be caused by either redox reactions, generally because of iron in the clay, or because of an acid-base type of reaction (Hendricks and Alexander, 1949; Hauser and Leggett, 1940; Furukawa and Brindley, 1973).

Many of the organic reagents tested in the API Project undergo color changes in clays which are very similar to colors of common non-clay secondary minerals found in rocks, such as yellow-brown, orange-brown, red-brown (goethite, lepidocrocite, hematite). In other cases the colors produced are very similar to those found in some of the common ferromagnesian primary minerals, such as yellow-green, greenish-yellow, greenish-brown or green. Because so many of the organic staining agents undergo color changes with clay which are so very similar to natural colors of non-clay secondary minerals, very few of them can be easily used for quantitative determination of clays in thin sections of basaltic rock. This is especially true in the case of smectite (Van Atta, 1983).

Methylene Blue

The organic staining agents methylene blue and benzidine are especially useful for quantitative determination of deleterious clay minerals in thin sections of rocks because they show a blue or blue-green color change. There are no common blue primary or secondary minerals found in rocks. Methylene blue absorption, (MBA) can also be used as a measure of total surface area of clay, which reflects the amount and nature of clay which is present in a rock (Cole and Sandy, 1980). The MBA test is now widely used to determine the amount of clay present in rocks. For this purpose, the rock being tested is pulverized (Sameshima and Black, 1979: Jones, 1964; Cole and Sandy, 1980; Hills and Pettifer, 1985). It does not appear, however, that this testing procedure is much used in the USA.

Methylene blue works quite well in staining clay in thin sections of rock. The staining can be done very rapidly (a minute or so) and the dye also clearly reveals the textural distribution of clay. However, clay minerals in general are stained blue or blue-green by absorption of methylene blue. In this respect, it is not specific for the most deleterious clays of the swelling type; any of the clay minerals present may be stained. Furthermore, since the test solution is blue, fractures and porous areas in a thin section of rock may absorb methylene blue. Absorption of methylene blue in microfractures can be advantageous, however, because determination of the amount of microfracturing allows an estimate of shrinkage potential of a rock, which may prove to be a deleterious property. With experience, one may quite easily distinguish between the blue-green color produced in clay and the blue caused by absorption in other areas.

Benzidine

Benzidine, a cyclic aromatic hydrocarbon, undergoes a redox reaction whereby it is changed to its monvalent cation (Figure 5) which is blue. Solomon and others (1968) made an extensive study of the mechanism of the benzidine blue reaction. They found that transition metals, such as iron in the trivalent state at clay layer surfaces or aluminum at edge sites can oxidize benzidine to form a semiquinone which is blue. The electron transfer is most pronounced at planer surfaces with ferric iron.

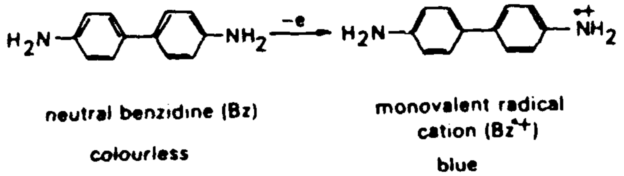

Figure 5. (Theng, 1981)

The benzidine blue reaction is most intense (produces the deepest blue color) with iron-bearing smectite which has been oxidized in a 10% solution of ammonium persulfate prior to testing. Van Atta and Ludowise (1976) used benzidine to stain thin sections of basaltic rock in order to determine the quantity and textural distribution of smectitic clay.

Since benzidine is, however, a known carcinogen (Weiss, 1980; Christensen and Luginbyhl, 1975), it is not possible to obtain it in the USA. Its manufacture has been stopped for more than ten years.

There are obvious advantages to the use of benzidine for the detection of deleterious clay. Chiefly, it is specific smectite and probably swelling chlorite and its use with thin sections of rock reveals the textural distribution of these deleterious clays. Additionally, since an aqueous solution of benzidine is colorless, absorption of the test solution in fractures and porous areas of a thin section is not detectable. A comparative study of the effectiveness of benzidine and methylene blue for the determination of amounts of swelling clay present in thin section of rocks shows that the two staining methods are both useful, since they compliment each other (Shayan and Van Atta, in preparation).

Procedures for use of methylene blue and benzidine staining in basaltic rocks are available from the author. If benzidine is available, good definition of clay mineral content and textural distribution as well as definition of smectite and, possibly, swelling chlorite, may be had by staining one half of a thin section of rock with methylene blue and the other half with benzidine. Care should be taken to subject just one half to each of the stains, oxidizing only the half to be stained with benzidine and avoiding overlap of stained halves.

Conclusion

The principal cause of degradation of basaltic rock used in erosion control or as aggregate in road construction or concrete is the presence of swelling clays. Swelling clays are especially common in basaltic rocks, although other rock types, especially some volcanic rocks and sandstones, may also contain swelling clays. Such rocks will commonly pass standard durability tests. Therefore, petrographic testing by examination of thin sections of rock and X-ray determination of species of clay minerals present must be done as a routine durability testing procedure. Methylene blue can be used to allow determination of the percentage of clay in the rock and its textural distribution. Benzidine, if available, can be used to reveal the presence of swelling clays, such as smectite and swelling chlorite.

References

Black, P.M. and Sameshima, T., 1979, An assessment of basalt and andesite road-aggregate resources in the Auckland District: New Zealand Roading Symp., p. A4-1, A404.

Blake, C.D., ed. 1967, Fundamentals of Modern Agriculture: Sidney, NSW, Sidney Univ. Press, 497p.

Brindley, G.W., 1981, Structures and chemical composition of clay minerals in Longstaffe, F.J. (ed.), Short course in clays for the resource geologist: Mineralogical Assoc. of Canada, Short Course Handbook, vol. 7, May.

Christensen, H.E. and Luginbyhl, T.T. (editors), 1975, Suspected carcinogens: a subfile of NIOSH toxic substances list: U.S. Dept. of Health, Education and Welfare, DHEW (NIOSH) Public. no. 75-188.

Cole, W.F., Lancucki, C.J. and Shayan, A., 1985, Verifying quarry potential: Austral. Road. Res. Board Proc., vol. 12, part 2, p. 93-102.

Cole, W.F. and Sandy, M.J., 1980, A proposed secondary mineral rating for basalt road aggregate durability: Austral. Road Res., v. 10, no. 3, p. 27-37.

Day, H.L., 1962, A progress report on studies of degrading basalt aggregate bases: Hwy. Res. Brd., Bull. 344, p. 8-16.

Fielding, B.J. and Macarrone, S., 1982, Accelerated soundness tests for altered basalts: Austr. Road Res. Board Proc., p. 129-144.

Furukawa, T. and Brindley, G.W., 1973, Adsorption and oxidation of benzidine and aniline by montmonillonite and hectorite: Clays and clay mineralogy; v. 21, p. 279-288.

Hauser, E.A. and Leggett, M.B., 1940, Color reactions between clays and amines: Jour. Am. Chem. Soc., v. 62, p. 1811-1814.

Hendricks, S.B. and Alexander, L.T., 1940, A qualitative color test for the montmorillonite type of clay minerals: Jour. Am. Soc. AGRON., v. 32, p. 455-458.

Hills, J.F. and Pettifer, G.S., 1985, The clay mineral content of various rock types compared with methylene blue value: Jour. Chem. Tech. and Biotechnol., v. 35, p. 168-180.

Hosking, J.R. and Tubey, L.W., 1969, Research on low-grade and unsound aggregates: Road Res. Lab. (U.K.), Lab. Rep. LR 293.

Jones, F.O., New, fast and accurate test measurement of bentonite in drilling mud: Oil and Gas Jour., v. 1, p. 76-78.

Lay, M.G., 1981, Source book for Australian roads, Kierang Sharp, ed.: Austral. Road Res. Board, 501 p.

Meilenz, R.C., King, M.E. and Schlieltz, N.D., 1950, Staining tests in Section 6, Analytical data on reference clay minerals: Am. Petrol. Inst. Proj. 49, Clay Mineral Standards, Prelim. Report no. 7, p. 135-160.

Miles, D.K., 1972, Accelerated soundness test for aggregate: Utah State Hwy. Dept., Materials and Tests Div., State Study no. 500-917, 81 p.

Minor, C.E., 1960, Degradation of mineral aggregates: ASTM Spec. Tech. Publ. no. 277, p. 109-121.

Nyoeger, E., 1964, Petrological investigation into the secondary minerals of an older basalt flow north of Melbourne: Austral. Road Res. Brd., vol. 2, p. 1-10.

Orr, C.M., 1979, Rapid weathering delerites: The Civil Engineer in So. Africa, vol. 21, p. 161-167.

Scott, L.E., 1955, Secondary minerals in rock as a cause of pavement and base failure: Hwy. Res. Brd. Proc., vol. 34, p. 412-417.

Shayan, A. and Ritchie, D.J., 1985, Influence of sodium and potassium cations on the dimensional stability of rock prisms: Durability of Building Materials, vol. 3, p. 365-378 (Elsevier, Amsterdam).

Shayan, A. and Van Atta, R.O., Comparison of methylene blue and benzidine stains for the detection of smectite clays in aggregate: (in preparation).

Smith, D.D., 1967, Final report on secondary mineral alteration of aggregate base and subbase: State of Calif., Div. of Highways, Materials Research Dept., Res. Rpt. no. M & R 632425, Jan.

Solomon, D.H., Loft, G.C. and Swift, A., 1968, Reactions catalysed by minerals - IV: The mechanism of the benzidine blue reaction: Clay Minerals, v. 7, p. 389-397.

Theng, B.K.G., 1974, Mechanisms of formation of colored clay-organic complexes, A Review: Clays and Clay Minerals, v. 19, p. 383-390.

_____, 1981, Clay-activated organic reaction in Van Alphen, H., and Veniale, F., Int. Olay Conf. Prod.: Devel. in Sed. 35, p. 197-238.

Van Atta, R.O. and Ludowise, H., 1976, Microscopic and X-ray examination of rock for durability testing: Fed. Hwy. Admin. Report FHWA-RD-77-36, 90 p.

Van Atta, R.O., 1983, Investigation of non-hazardous stains for detection of smectite clays in rocks: Final Report, FHWA Project 7/82-3/83, unpubl.

Weiss, G. (editor), 1980, Hazardous chemicals data book: Park Ridge, N.J., Noyes Data Corp.

West, T.R., Johnson, R.B. and Smith, N.M., 1971, Tests for evaluating degradation of base course aggregates: Nat'l. Corp. Hwy. Res. Prog. Report 98, 92 p.

EROSION CONTROL ON A PORTION OF THE SILETZ RIVER SANDSPIT

Lester E. Fultz, P.E., P.L.S.

Abstract:

This Paper is a "then" and "now" description of a portion of the Siletz River Sandspit on the Central Oregon Coast which suffered very heavy erosion in the winter of 1973. The "then" phase includes a description of the extent of the erosion and a description of the engineering and construction activities used to correct the erosion. The "now" phase describes the same area of the Sandspit as it is today. The Siletz River Sandspit was developed for single family residential use in the SALISHAN development. All homesites were leased rather than sold in the conventional manner. Considerable financial burdens in the erosion created problems to both the Developer and the Lessees. The author of this Paper believes that the descriptions clearly illustrate how human beigs can counteract the destrustive forces of the Pacific Ocean.

The "then" phase considerations:

Background

The Siletz River Sandspit began eroding in the fall of 1972. The erosion worsened as the winter season progressed to the point where the worst erosion occurred early in 1973. The erosion came as a shock to the Developer of the Sandspit and the large number of persons who had leased homesites from the Developer for residential use.

The author of this Paper owned and operated a private engineering and land surveying practice in Lincoln City, Oregon, located across the Siletz River Bay from the subject area. The population of the area is limited and the author operated the only office of his kind in the immediate area. The proximity of the author's office to the Siletz River Sandspit created a situation in which the author and his office were soon involved.

In the subject erosion instance, a local contractor who had contracted with a group of property Owners to re-claim and

---

* The author is an independent professional engineer and a professional land surveyor, semi-retired and residing on ocean front property in Neskowin, Oregon.

protect their property from future erosion. This subject portion of the Siletz River Sandspit consisted of Homesites 220, 221, 222, 222-A, 223, 224, 225, 226, 226-A, 227 & 228. Although these homesites are about two (2) miles from the end of the Sandspit, they were in the area which suffered the most erosion. The severity of the erosion is illustrated by the fact that the erosion had penetrated to within twenty (20) feet of Salishan Drive, the only roadway to existing single family residences north of the subject area. This group of homesites included and un-finished residence (Homesite 226-A) which had washed into the Pacific Ocean before our entrance in to the topographic survey.

Topographic Information:

The amount of the erosion in the subject area of the Sandspit is difficult to describe. A picture makes an explanation much simpler. In this case a portion of an aerial photograph taken by the Oregon State Highway Department in April, 1973 is used to demonstrate the erosion.

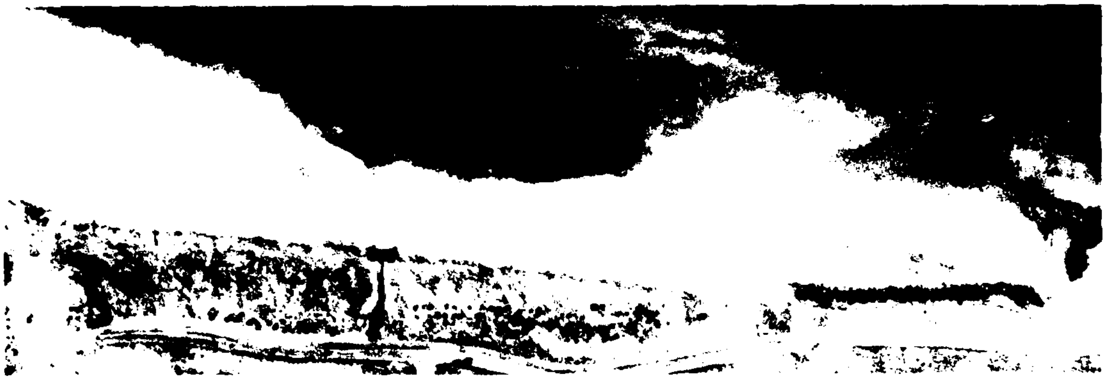

1973 Flight

There are certain items which this photograph illustrates. One of these is the extent of the erosion. Another is the obvious erosion forces exerted on teh residence shown at the northerly end of the subject area. The large rock that was hauled in and end dumped to protect the house and the land in the subject area is visible in the photograph. That rock was only for temporary correction of the erosion and was later moved into its final position westerly or toward the Pacific Ocean. The photograph clearly shows the narrowness of the Sandspit and Salishan Drive.

The topographich survey was initiated from the northerly end of the subject area. The northerly end is on the reader's right in the photograph. Two base lines were used, one along Salishan Drive on the east or bottom of the picture, the other on the beach 150 feet westerly. This base line on the beach worked very well because of the heavy erosion adjacent to Salishan Drive.

A cross-section was made at 100-foot intervals after an initial section of 0+50. Three of the cross-sections have been selected to graphically illustrate the extent of the erosion.

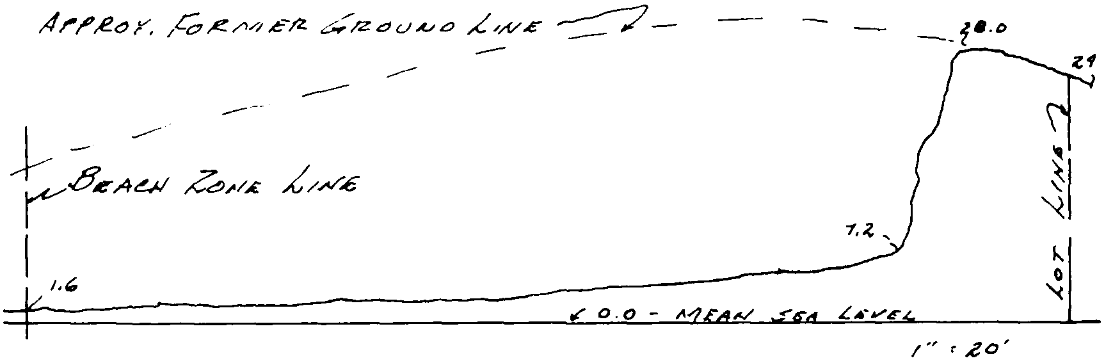
APPROX. FORMER GROUND LINE
28.0
24
BEACH ZONE LINE
7.2
1.6
0.0 - MEAN SEA LEVEL
LOT LINE
1" = 20'

Station 1+50

This cross-section is approximately on the centerline of Homesite 228, and illustrates the erosion at the most severely eroded portion of the subject area. The viewer will notice the notation, "Beach Zone Line". This denotes the location of the arbitray Zone Line established by the 1969 Oregon Beach Bill. That act gives the public an un-limited right for recreational use all of the land between the Zone Line and the mean high water line of the Pacific Ocean. The Beach Bill also requires a permit for any activity other than recreational westerly of the Zone Line. The Oregon Parks and Recreation Division is the agency responsible for issuance of these permits.

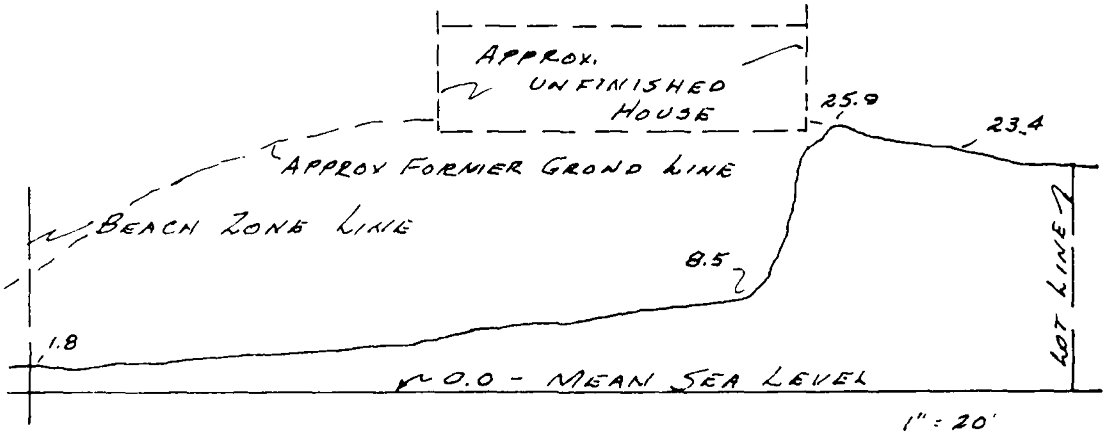
APPROX. UNFINISHED HOUSE
25.9
23.4
APPROX FORMER GROND LINE
BEACH ZONE LINE
8.5
1.8
0.0 - MEAN SEA LEVEL
LOT LINE
1" = 20'

Station 3+50

This cross-section is on the approximate centerline of Homesite 226-A from which the un-finished house washed into the Pacific Ocean. One can easily see the extent of the erosion which caused the problem. The approximate location of the residence on the homesite has been added to this section to help a reader understand the position of the house with relationship to the beach. One can see that the residence was very vulnerable to the erosive actions of storm tides. One can also notice that no ocean front protection had been provided for the residence prior to construction. This homesite was *not* unique because until the erosion began in the fall of 1972 none of the homesites of the Siletz River Sandspit had ocean front protection constructed prior to the erection of the residence.

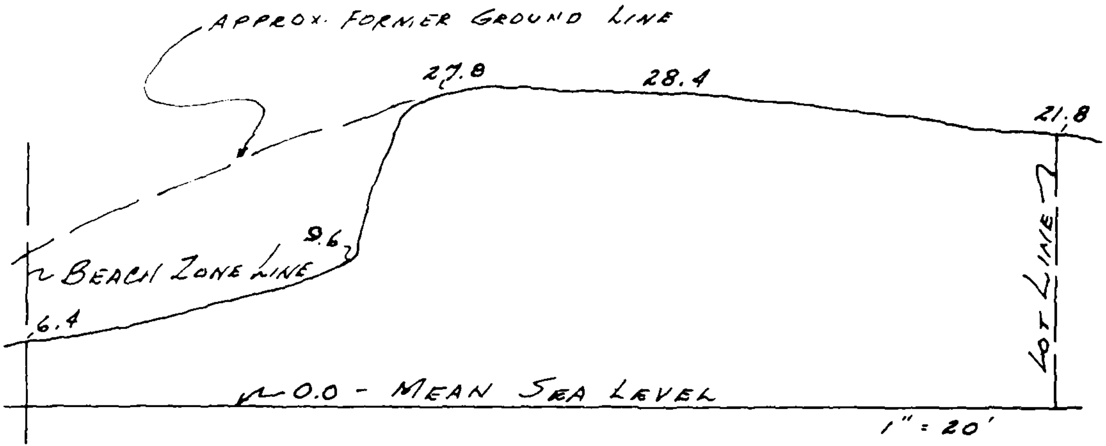

Station 7+50

This cross-section illustrates the condition on the approximate lot line of Homesites 222-A and 223. The erosion is much less that at Stations 1+50 and 3+50. It appears that the erosion was less at this point becouse of the ocean front structure constructed for the homesite south of Homesite 220.

The foregoing discussion has explained the conditions from which the "then" problem originated. The following paragraphs will explain with illustrations the engineering and construction activities involved in correcting the erosion problem in the subject area. The explanations and illustrations also include the author's method of designing ocean front structures that time has proven to be very effective against the Pacific Ocean's worst erosion conditions.

There are certain pertinent facts that the author wishes to give the reader which, though not necessarily unique to the Central Oregon Coast, must be taken into account when designing a good ocean front structure. These facts are:

1. The tide differential is much higher on the northwest coastline compared to most areas of the United States. This range is twelve (12) feet on the tide table. This figure is confusing to those who are not familiar with ocean tide tables. The zero (0.0) on ocean tide tables is based on a mean elevation for mean lower low water. This tide level is about [illegible] feet below mean sea level on the Central Oregon Coast.

2. The Pacific Ocean does not live up to its name. It is anything but a mild body of water. The storm tides will create water levels double the elevations on the tide tables. Because the Pacific Ocean Coastline is such a ferocious environment, the engineering techniques must be modified to design an ocean front structure that will sustain the forces exerted on it by the Pacific Ocean.

3. The un-favorable environment creates different construction problems. The construction of a good ocean front structure is virtually impossible in the fall of the year when the tides become high unless sufficient work was accomplished on the toe of the structure before the unfavorable tides set in. This means that very careful planning is required to produce an economical structure.

Erosion Correction:

The amount of the erosion created serious design problems. One of these problems is illustrated in the cross-sections shown in preceding paragraphs which visually emphasizes the amount of material taken from the homesites. Another problem is constructing a permanent barrier to futher erosion. The subject example of erosion is much more severe than normal but the engineering of an appropriate structure is no different from the normal procedure used by the author.

A cross-section is used to illustrate the design of the ocean front structure for the subject area. This cross-section is also typical of the design principles employed by the author in all designs for ocean front structures on the Pacific Ocean Coast in Oregon. Accordingly, the explanation which accompanies the cross-section will apply to the subject eroded area and to all designs for ocean front protection structures.

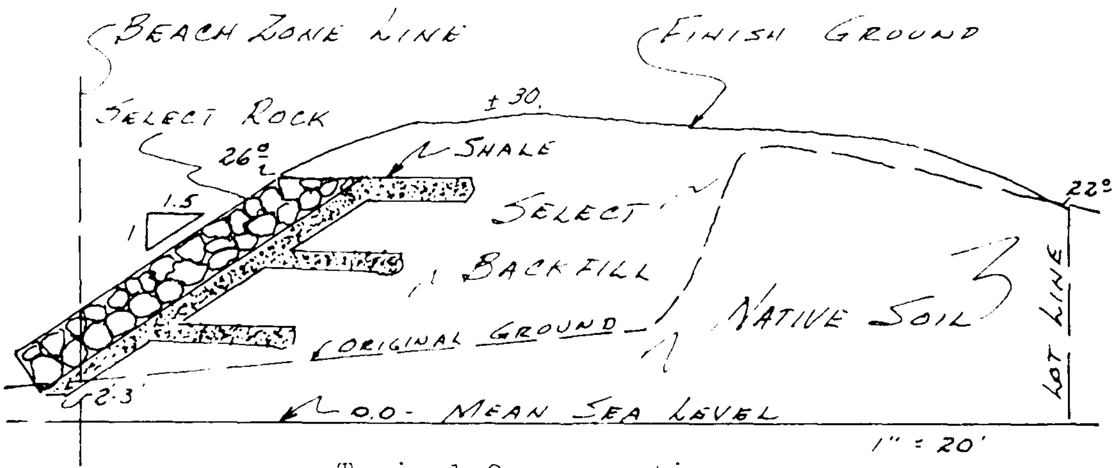

Typical Cross-section

Explanation of Typical Cross-section:

The typical cross-section is a general representation of the usual condition in sand areas on the Central Oregon Coast. It is not typical of semi-rock banks, silt-sand and stone banks. The elevation of the existing ground can vary widely also. This typical cross-section shows an elevation of 6.0 feet above mean sea level but this can vary up to 12 to 15 feet above mean sea level. It can also be much lower as the author has experienced elevations several feet below mean sea level. The shale material shown in horizontal layers on the landward side of the structure represents roadways that may be constructed to assist in the construction of the ocean front structure. These roadways may not be required in a different ocean front environment. The location of the Zone Line will also vary. In some instances completely out of the picture toward the ocean, other times very much further toward the land side. The amount of select backfill will also vary accordinging to the situation, as well as the depth of the backfill.

Specific Comments on the Typical Cross-section:

1. The depth of a toe trench for the oceanward portion of the structure is very important. The depth of the toe trench determines how well an ocean front structure performs. The author's experience on similar structures has definitely shown that the toe trench should be placed as low as possible. On the Siletz River Sandspit, the successful structures toe trenchs are placed at an elevation of about 2.0 feet above mean sea level. The toe trenches would have been constructed lower but this was the elevation of standing water.

   The author has observed ocean front protective structures for which the toe trench elevation ranges from 5 to 10 feet above mean sea level. Needless to explain that these structures quickly failed as the toe was undercut allowing the large rocks to assume a natural angle of repose of about 1.5 on 1.0.

2. Another important item in a successful ocean front protection structure is the treatment of the native material adjacent to the ocean front structure. In the case of fine material like sand or other types of material easily affected by water or moisture. it is imperative that a filter material be installed between the structure rock and the native material. The author has shown a shale balnket on the typical cross-section as this material is plentiful and economical on the Central Oregon Coast. This material works very well because it is pervious to water yet prevents the fine materials from passing through the shale material.

The filter layer can be other material than the shale shown in the typical cross-section. There has been much progress in the development of "geotextiles and certain contractors have used them successfully. The author believes that the geotextiles will eventually be used for the filter blanket shown.

The three horizontal layers of shale material are shown as roadway access to assist in the construction of the structure. This system works well in a sand environment but may not be necessary at all, especially in the case where the structure is completely constructed from the ocean side.

3. The rock shown in the typical cross-section is an important ingredient in a successful structure. The rock is shown because this material is plentiful on the Central Oregon Coast. The author realizes that satisfactory rock is not economically available in many areas of the United States. The author recognizes that there are other materials that have been used successfully.

   The selected rock should not be "dumped" into place. The author has seen structures constructed by this method fail in a short time. Rather, the select rock should be "placed" into position. The author is familiar with the rock jetties at the estuaries of several rivers in Oregon and has followed the progress that the contractors on these jetties have made in the use of large cranes to position the rocks into place. The same technique must be used on ocean front structures exposed to strong ocean storms. The "keying" of the rock accomplished by individual placement of each rock is vitally important in preventing rock movement and fallout.

   The best results have been obtained by the contractors on the Central Oregon Coast by carefully selecting the rock for the structure so that the largest rock are placed at the toe. The cranes that have been used in the author's experience have generally been in the 3/4-yard to 1.5-yard range. These machines can handle up to 8-ton rock. However, even though the large rock are best at the toe, this does not mean that smaller rock should not be placed in the toe. The author has seen some fine structures in which a good mix of large rock and smaller rock have been used to accomplish the best "keying" results.

   The elevation to which the structure is constructed is usually a matter of judgement by Owner and contractor. The author prefers a finish elevation of about 25 feet above mean sea level on the Central

Oregon Coast for exposed sandy beach areas. This elevation can be lower for rocky banks and less severe environments. Naturally, if the finish elevation of the structure is less, then the select backfill fill can also be less.

Transition Period from "Then" to "Now":

The twelve years from the "then" period to the "now" period saw some profound changes in the subject area. There was no residential construction on the Siletz River Sandspit from 1973 to 1977 because the County Building Department refused to issue building permits because of the erosion. In 1977, the County Commissioners issued an Order stating that if a registered engineer would sign an affidavit stating that, "the subject homesite had been protected against all reasonable ocean action", a building permit would be issued. This Order provided for residential growth on the Siletz River Sandspit.

Again the author will reiterate a previous statement regarding the use of pictures to save words. In this case, the Oregon State Highway Department had aerial pictures taken of the Siletz River Sandspit similar to the photograph on Pzge 2 of this Paper. A similar portion of the 1976 and 1984 flights are shown below with comments.

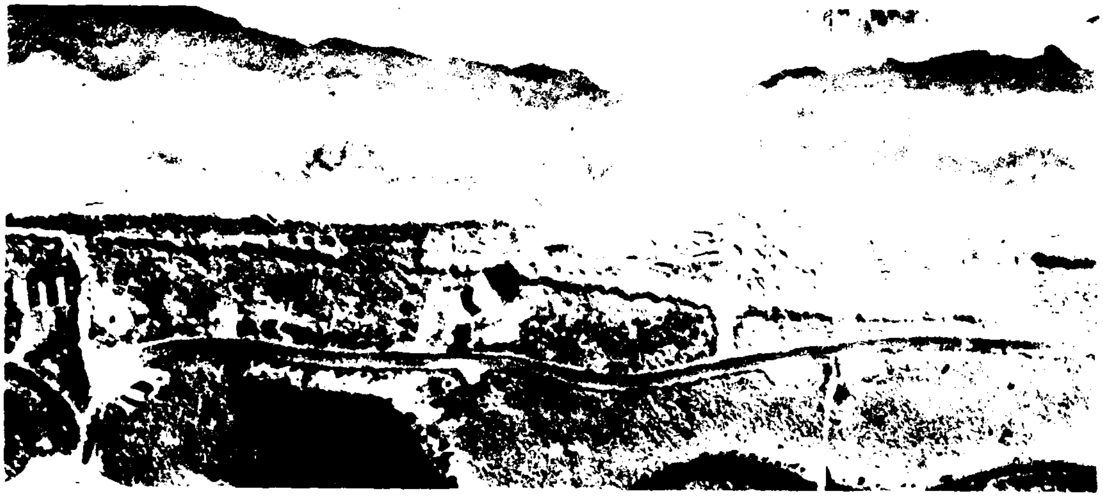

1976 Flight

This photograph still shows the 1973 erosion line. It also shows a residence constructed slightly to the left of the center of the photograph. The photograph also illustrates a sequence of construction of the structure as the structure appears to be complete from the residence to the left or south. A line of rock is visible from the residence to the right or to the north but the final elevation has not been completed since drift logs are visible to the right of the center of the photograph. Note the dune grass easterly of the structure to the left of the residence.

1984 Flight

This photograph shows seven residences in the subject area [illegible]. Note that there is no rock visible in the photograph. One should also note that the drift logs are a long distance onto the beach when compared with the 1976 flight photograph.

The aerial photographs illustrate the faith the homesite owners have in the ocean front protection structure. The record of construction confirms this faith. It is:

1. Homesite No. 223 ---------- October 1976
2. Homesite No. 229 ---------- October 1978
3. Homesite No. 222-A -------- June 1979
4. Homesite No. 226-A -------- October 1979
5. Homesite No. 221 ---------- September 1980
6. Homesite No. 227 ---------- June 1981
7. Homesite No. 226 ---------- October 1981
8. Homesite No. 220 ---------- March 1985

The "New" Flight:

The author made some current photographs of the existing conditions on September 26, 1985. The author also re-surveyed the [illegible] topographic survey to illustrate the changes in the land in the subject area. This information follows in [illegible] paragraphs.

[illegible]

View Toward Southwest

View Toward Northwest

View Of Oceanfront

These photographs illustrate the extent of the development of the subject area as of today. Note the pleasant build-up of dune grass and natural vegetation.

Three cross-sections have also been provided to show the "now" condition. These cross-sections are identified as before with the stationing running from the north erly direction. An interesting feature of these "now" cross-sections is the amount of material on the land compared to the previous cross-sections of the "then" phase.

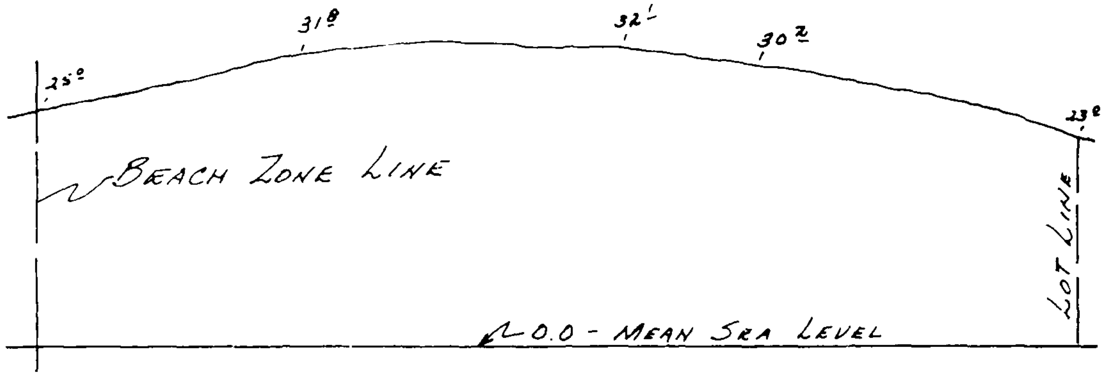
25⁰
31⁸
32¹
30²
23⁰
BEACH ZONE LINE
LOT LINE
0.0 - MEAN SEA LEVEL

Station 1+00

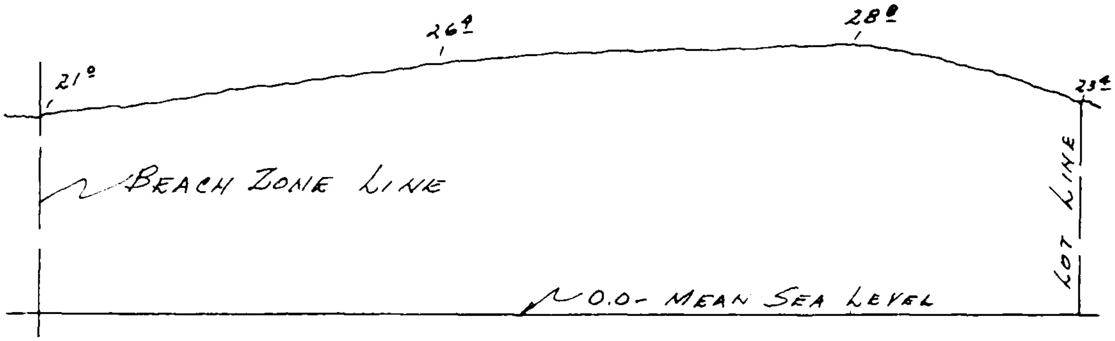
21⁰
26⁴
28⁰
23⁴
BEACH ZONE LINE
LOT LINE
0.0- MEAN SEA LEVEL

Station 3+75

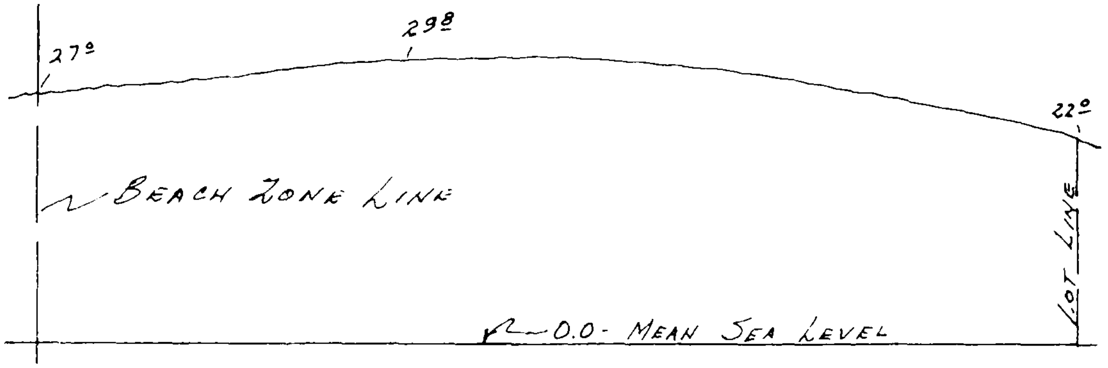
27⁰
29⁸
22⁰
BEACH ZONE LINE
LOT LINE
0.0- MEAN SEA LEVEL

Station 7+50

A comparison of the above sections with the cross-sections shown on Pages 3 and 4 of this Paper demonstrates the large amount of material that was transported into the area plus the accumulation of material (sand) from the beach itself.

The author has made some calculations of the quantity difference. These calculations show that approximately 10,000 cubic yards of material has been accumulated in the cross-sections made at the points of most erosion. This is a substantial financial increase to the homesites value.

Summary:

The erosion of the Siletz River Sandspit on the Central Oregon Coast created much attention as the wire services gave the event world wide publicity. There were well educated persons who predicted successive and increasing severe problems on the Sandspit. One prediction by a university professor was that the Sandspit was a lost area because there was no way Man could fight Nature.

The fact that successful efforts were made to reclaim this and other portions of the Siletz River Sandspit does demonstrate that Man can overcome severe obstacles. The fact that this severely eroded area of the Sandspit has been developed with many expensive residences is mute testimony to the courage and depth of faith of the Owners belief that the erosion problem has been overcome. The writer agrees that the Sandspit will have an erosion problem in the event of a massive tidal wave or other similar natural catastrophe but in such an event there will be many other areas that will be adversely affected also.

The author wishes to reiterate the last sentence of the Abstract of this Paper on Page 1. That is that the erosion events on the Siletz River Sandspit and the corrective action taken clearly demonstrate that Man can improve on Nature.

The erosion events described in this Paper on the Central Oregon Coast are only a small portion of similar erosion events on this country's river, lake and ocean frontage. When one considers the thousands of miles of similar frontage in the world, it is logical to conclude that there will be many erosion problems in the future. A Regional Coastal Design Conference such as the one for which this Paper has been prepared is a great step toward preparing for future problems.

Respectfully submitted,

Lester E. Fultz

Lester E. Fultz, P.E., P.L.S.

REGISTERED PROFESSIONAL ENGINEER
4821
OREGON
MAY 13, 1960
LESTER E. FULTZ
Lester E. Fultz

REGISTERED
PROFESSIONAL
LAND SURVEYOR
Lester E. Fultz
OREGON
LESTER E. FULTZ
1425

GOLDEN GATE BRIDGE PIER SHIP COLLISION STUDY

Wayne O. MacDonell[1] and Bo M. Jensen[2]

ABSTRACT

The southern tower of the Golden Gate Bridge is about 1,100 feet from shore in 60 to 90 feet of water. This paper describes a study to assess both the present structural condition of the pier and fender, and the adequacy of the pier and fender to resist ship impacts. Shipping traffic and navigational procedures were investigated to determine probable vessel impact conditions. Possible ship impact effects are described, and strengthening methods are presented.

1. INTRODUCTION

The number of significant ship collisions with bridge piers throughout the world has increased in recent years, due to growth in shipping traffic and size of ships. The number of ships navigating the Golden Gate since completion of the Golden Gate Bridge in 1937 has decreased approximately 50%. However, these passenger, cargo and tanker vessels have increased tenfold in size when compared with earlier ships.

The southern tower of the Golden Gate Bridge is about 1,100 feet from shore in 60 to 90 feet of water, on serpentine rock. The pier includes an external concrete fender used temporarily as a cofferdam during

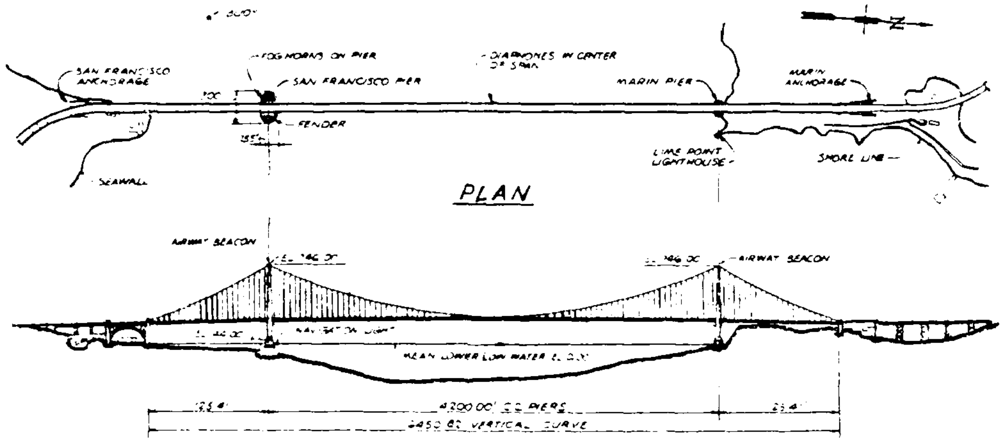
N
FOG HORNS ON PIER
DIAPHONES IN CENTER OF SPAN
SAN FRANCISCO ANCHORAGE
SAN FRANCISCO PIER
MARIN PIER
MARIN ANCHORAGE
FENDER
SEAWALL
LIME POINT LIGHTHOUSE
SHORE LINE
PLAN
AIRWAY BEACON
AIRWAY BEACON
NAVIGATION LIGHT
MEAN LOWER LOW WATER
4200.00' C.C. PIERS
VERTICAL CURVE

ELEVATION

GOLDEN GATE BRIDGE

---

[1] Senior Engineering Manager, Earl and Wright, One Market Plaza, San Francisco, California 94105

[2] Business Development Manager, Earl and Wright, San Francisco, California 94105

construction and permanently as protection against ship impact. This paper presents results of an investigation by Earl and Wright for the Golden Gate Bridge, Highway and Transportation District, of the adequacy of the fender and pier to resist ship impact.

2. SOUTH PIER CONSTRUCTION AND PRESENT CONDITION

A search was made for documentation pertinent to the south pier and fender design and construction, to help clarify, and add new information concerning the design and construction. Drawings, the Chief Engineer's Report, Construction Specifications, other design reports, test records, photographs, and inspection reports were all reviewed.

Complete "As Built" engineering drawings did not exist prior to this study. Many of the actual existing details were shown, however, on the Contractors drawings. Due to the extensive changes made during the construction in 1933 and 1934, the original details were altered, but the engineering drawings were not revised to reflect the changes. A complete set of "As Built" drawings was prepared during this study.

The pier and fender was inspected. A report of a 1982 underwater inspection and accompanying videotapes were reviewed in detail to evaluate the surface condition of the concrete.

Many of the joints viewed were spalled. These joints may have been in this condition for many years, even since the original construction. The original photographs showed the use of chicken wire inside the base formwork to retain the tremie concrete where gaps in the forms existed at the bottom of the formwork. This procedure for retaining the concrete could have allowed the concrete mortar to wash out during the pour, leaving only aggregate at these joints. Spalling could easily have occurred at these locations. It was undoubtedly difficult to properly seal the cofferdam formwork along the base as well as along some of the vertical joints. Washing out of the concrete mortar could have occurred in other vertical joints in a similar manner.

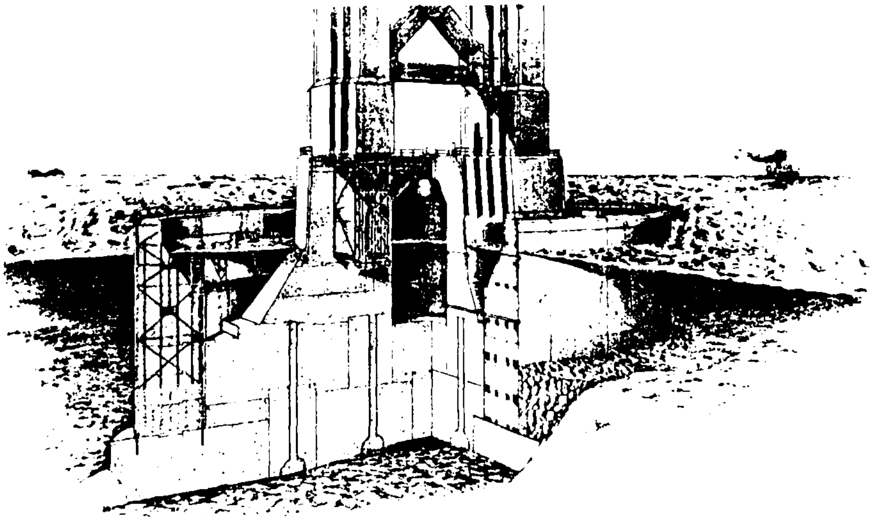

PIER AND FENDER ISOMETRIC SECTION

The above-water portions of the fender and pier were visually inspected in the 1982 work. This inspection covered 100% of the surface from the top of the fender or pier down to the water at elev. +4 ft ±.

Four revisions were made to the original configuration during construction. The fourth revision was the final or "As Built" version. The original version and the four revisions are shown below (Ref. 1). Key changes were:

First Revision:	The fender key was excavated down into the serpentine base rock to solve concern about possibility that the fender could slide.
Second Revision:	The pier foundation area was increased by including the fender in the pier foundation.
Third Revision:	The idea of men working under pressure in the caisson was abandoned. Rather, tremie concrete would be placed up to elev. -64 ft. Shafts with domed ends resting on the base rock were positioned in the pier concrete to allow inspection and testing of the rock after tremie concrete was placed.
Fourth Revision: (Final Version)	The fender was designed as a cofferdam for dewatering the interior of the fender area. Dewatering was made possible by raising the tremie concrete level to elev. -35 ft.

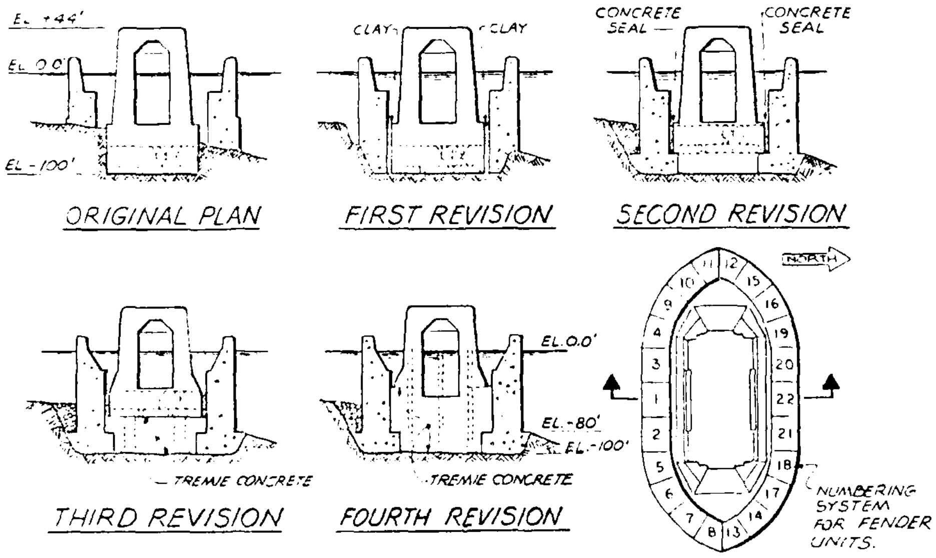
EL +44'
EL 0.0'
EL -100'
CLAY
CLAY
CONCRETE SEAL
CONCRETE SEAL
TREMIE CONCRETE
TREMIE CONCRETE
EL 0.0'
EL -80'
EL -100'
NORTH
1
2
3
4
5
6
7
8
9
10
11
12
13
14
15
16
17
18
19
20
21
22
NUMBERING SYSTEM FOR FENDER UNITS.

ORIGINAL PLAN FIRST REVISION SECOND REVISION

THIRD REVISION FOURTH REVISION

PROGRESSIVE DEVELOPMENT OF FENDER AND PIER CONSTRUCTION

PLAN

The final version of the pier and fender was far superior to the original. Positive keying action in the base rock gave more shear capacity and resistance to sliding than placing the fender directly on top of the base rock. Also, combining the pier and fender foundations increased the total foundation area from 16,000 sq ft to 37,800 sq ft.

This increase in area decreased the foundation pressure from 354 psi to 150 psi. Finally, the ability of the fender to resist ship impact was increased dramatically due to the revised foundation details and interior lateral support provided by bringing the pier foundation concrete up to elev. -35 ft.

3. SHIPPING TRAFFIC

It is necessary to know the vessel traffic pattern through the Golden Gate to assess the likelihood of vessels hitting the San Francisco pier. The channel is sufficiently deep and wide to allow separate inbound and outbound lanes. Inbound traffic moves on the south side of the channel, adjacent to the San Francisco pier. Vessels leaving the bay sail in the north channel regardless of the current direction and therefore are not near the south pier.

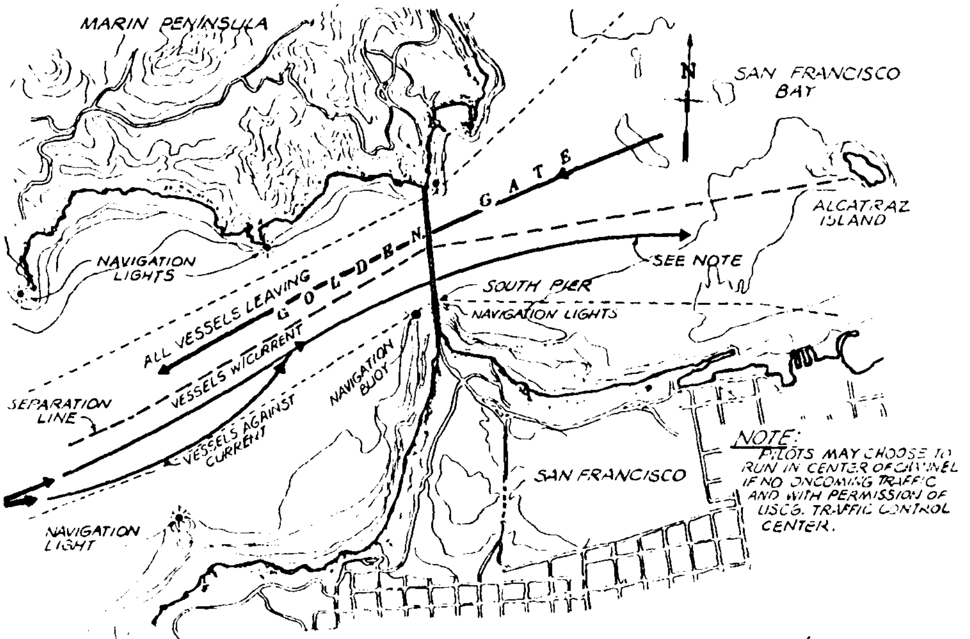

MARIN PENINSULA
N
SAN FRANCISCO BAY
GOLDEN GATE
ALCATRAZ ISLAND
NAVIGATION LIGHTS
SEE NOTE
SOUTH PIER
NAVIGATION LIGHTS
ALL VESSELS LEAVING
VESSELS W/CURRENT
NAVIGATION BUOY
SEPARATION LINE
VESSELS AGAINST CURRENT
SAN FRANCISCO
NAVIGATION LIGHT

NOTE: PILOTS MAY CHOOSE TO RUN IN CENTER OF CHANNEL IF NO ONCOMING TRAFFIC AND WITH PERMISSION OF USCG. TRAFFIC CONTROL CENTER.

TRAFFIC PATTERN FOR VESSELS ENTERING & LEAVING SAN FRANCISCO BAY

To maintain good steering control, most ships maintain a minimum speed of 5 knots. The usual speed is closer to 10 knots, especially with oil tankers. Therefore, the usual maximum tanker speed of vessels entering the Golden Gate is approximately 15 knots with the current, or as low as 3 knots against the current. One containership recently entered at 27 knots on an incoming tide, with no opposing traffic and a clear view ahead. The total speed was a combination of speed through the water of about 24 knots plus the current speed of 3 knots.

The maximum draft of ships normally allowed in San Francisco Bay is 50 ft (Corps of Engineers data shows 1 to 3 ships of 52 to 53 ft per year). This maximum draft limitation is because the entrance channel through the San Francisco Bar is maintained at about 55 ft and some areas inside the bay are even shallower. This depth is relative to MLLW. Higher tides increase the channel depth. Another effect on draft is vessel "squat," where the vessel is drawn down to additional depth by the venturi effect of the water under the ship. A ship of almost rectangular cross section (like a tanker) traveling at 16 knots could squat 10 ft in shallow water. Since this effect is speed-dependent, very large tankers with little bottom clearance must proceed slowly through shallow channels. Because of draft limitations, supertankers cannot enter San Francisco Bay.

When fog limits visibility, the practice calls for a "controllable" speed in which the vessel can stop in half of its length. Therefore, when visibility is zero, the entrance is closed. However, fog may be light in some areas and heavy a mile ahead. Once committed to enter or exit the main ship channel, a ship must continue. Stopping or turning back in fog conditions is more dangerous than slowly proceeding. There are two fog horns on the south pier to warn ships away. At the center of the bridge span, over the center of the channel, two diaphones indicate the center of the channel when fog limits visibility.

When the bridge was completed in 1937, bells and fog horns were the guidance system. Radar came later, during World War II. Unfortunately, structures such as the bridge leave a long radar "shadow" on the radarscope which may hide other objects within the "shadow." In 1971 two oil tankers collided in heavy fog approximately 0.2 miles west of the bridge. The shadow effect contributed to this accident. The vessels knew of each other's presence initially, but were not communicating on the same radio channel and lost each other in the radar shadow. Since 1971 the Coast Guard has maintained a control center for two sensitive radar systems at the top of Yerba Buena Island, to monitor shipping inside the bay. Radar on Point Bonita west of the bridge provides information from outside the bay. A total of 4 screens are monitored 24 hours a day. Almost all merchant vessels now participate in the Coast Guard's vessel traffic service. Each merchant vessel on the radar screen is identified and confirmed by radio contact. Ships are advised when they are out of the traffic lanes, and warned of nearby ships.

Ship size and frequency of passage data were used to determine the vessels for impact calculations and the probability of occurrence. This data was obtained from the U.S. Army Corps of Engineers, the U.S. Coast Guard and the Marine Exchange. Only cargo vessels and tankers were investigated. A maximum variation of 3.5% in traffic count occurs between the three sources. The COE data fell between the other two sources, and was used for this study, with the added benefit that the data included drafts of vessels entering the bay. The frequency of vessels entering the bay and their corresponding draft was determined for the period 1976-81.

The maximum as well as the most frequent cargo vessels and tankers entering the bay are as follows:

Vessel Type	DWT (Long Tons)	Displacement (Long Tons)	Draft (Feet)
Maximum: Cargo	60,000	71,500	41
Tanker	150,000	180,000	53
Most Frequent: Cargo	10,500	12,000	25
Tanker	27,000	32,000	32

4. COLLISION PROBABILITY

Risk models have been developed for existing bridges (Refs. 2 and 3) and have been suggested for the design of new bridges (Refs. 2 and 4). The risk model used for this study is approximate and is intended only to evaluate the order of magnitude of the total risk to the bridge. The probability of a collision "P" is the product of the causation probability "Pc", and the geometrical probability "P_g" (P = Pc x Pg).

The causation probability Pc assumes that a given fraction of the ships passing the bridge will be out of control due to human and mechanical failure. The value of this probability has been evaluated (Ref. 5) for other situations. A causation probability of 2×10^{-4} was chosen for this study. That is, there is a 1 in 5,000 chance that a ship will be out of normal control.

The probability of a ship colliding with the south pier depends on two significant factors: whether the vessel is heading into or out of the bay, and the prevailing current direction. Vessels entering with the current generally sail straight through the middle of the channel, near mid-span, and would normally be carried straight through under the bridge rather than toward the south pier in event of mechanical failure. Vessels entering against the current generally approach from a more southerly direction more in line with the pier. However, the current pattern tends to push a vessel toward the center of the channel rather than toward the pier. A large vessel would not normally sail faster than 5 knots against the current; thus a vessel without power would stop by the current in about one-half mile . Vessels within one-half mile of the pier have already moved toward the middle of the shipping lane. Therefore it is unlikely that, even with mechanical failure, a vessel would strike the pier.

Of the ships out of control, only those ships that could eventually collide with the bridge constitute a real risk. This probability of hitting the bridge is called the geometric probability, Pg. It is possible to calculate the geometrical probability of a collision by a ship out of control on the basis of the location and geometry of the pier and the size of the ship. Different geometric probabilities are calculated for inbound and outbound vessels due to their different potential proximities to the south pier. A "geometric probability" for impact was calculated as 0.025 for inbound and and 0.0075 for outbound vessels. That is, there is a 1 in 40 chance that an out-of-control inboard vessel could collide with the pier, and a 1 in 133 chance that an outbound out-of-control vessel could strike the pier. Therefore, the probability of an inbound vessel hitting the south pier was calculated as 5×10^{-6} or 1 in 200,000 ($P = 2 \times 10^{-4} \times 0.025$) and and for an outbound vessel 1.5×10^{-6} or 1 in 660,000.

Based on the frequency of passage data, 2777 cargo vessels and 1136 tankers enter the bay each year. Therefore, it can be expected that during 100 years approximately 277,000 cargo vessels and 114,000 tankers will enter the bay. It is assumed that an identical number will leave the bay. Consequently, there is a probability of (277,000/200,000 + 277,000/660,000 =) 2 cargo vessels, and (114,000/200,000 +114,000/660,000 =) 1 tanker colliding with the pier during 100 years.

5. FENDER/PIER STRUCTURAL ADEQUACY

Three fender impact load cases were investigated. The first is at the western end of the pier. This condition would be the result of a ship navigating perpendicular to the bridge span (its normal direction) and colliding head-on with the pier. The second position considers a vessel striking perpendicular to the northwest face. The third position is on the north side at 30° to the fender face. These positions were chosen to evaluate impact along both the fender's stronger east/west and weaker north/south axes, and to provide an accurate evaluation of fender adequacy against ship collision that could result from actual traffic patterns.

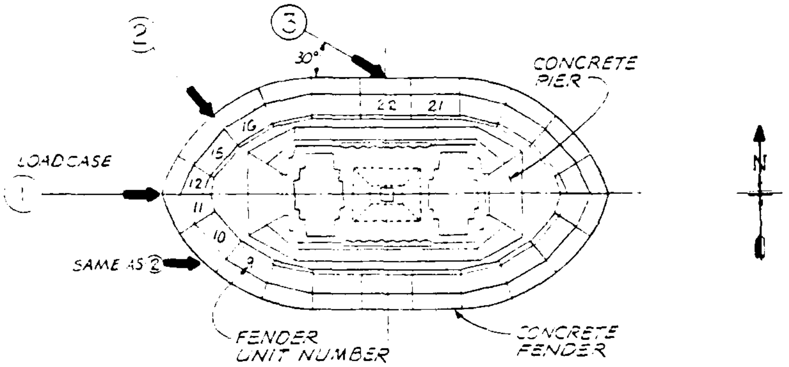

FENDER IMPACT LOADCASES

Two design vessels, the most likely and the extreme vessels were identified for checking the pier. The most frequent vessels were judged to be the most likely to hit the fender and were therefore used as a design vessel. The fender was checked for the most frequent tanker (32,000 LT displacement). The extreme vessel is the maximum anticipated vessel to navigate the Golden Gate over the next 100 years. The extreme vessel is calculated from the present-day maximum vessel (tanker) by increasing the maximum vessel size and speed to allow for possible future changes. The study assumed for the next 100 years an unchanged number of ships, 10% increase in speed, and 25% increase in displacement. The relationship between shipping data and design vessels is:

SHIPPING DATA	DESIGN VESSEL
Maximum Displacement	Extreme
Most Frequent	Most Likely

The impact force created by a right-angle collision of a ship against a stiff pier has been studied by Woison (Ref. 6). From these tests it was concluded that the average impact force is approximately constant during collision. The impact force increases at the beginning of the impact for approximately 0.1 - 0.2 seconds to a maximum value, Pm, approximately double the average impact force, Pavg. The maximum impact force, Pm, for an impact against a stiff pier is calculated as follows: $Pm \approx \sqrt{198}\, DWT \pm 50\%$ and $Pavg = Pm/2$

Where DWT = vessel deadweight in long tons
Pm = maximum impact force in kips
Pavg = average impact force in kips

No experiments were conducted for broadside impact, which was assumed to be equal to a bow impact force. The vessels and impact forces used are:

		VESSEL	
VESSEL TYPE	IMPACT FORCE (KIPS)	DISPL. (LT)	DRAFT (FT)
EXTREME	126,000	225,000	53 (est.)
MOST FREQUENT TANKER	48,500	32,000	32

The kinetic energy of a ship varies with the displacement of the ship and the square of its velocity. $E = \frac{1}{2}\, Cm\, MV^2$

where E = kinetic energy (K-FT)
Cm = factor for additional hydrodynamic mass
M = Ship's mass $\left(\frac{K\text{-}Sec^2}{Ft}\right)$
V = Ship's speed (ft/sec)

The coefficient Cm for hydrodynamic mass varies with the vessel's orientation. Accepted values are 1.1 for bow or stern impact and 1.4 for broadside impact (Ref. 7).

In head-on collisions, all of the kinetic energy of the ship must be expended. The collision energy ΔE to be transformed in a glancing blow into another energy form has been proposed by Saul and Stevenson (Ref. 8) to be $\Delta E = \eta E$. Where η is the fraction of the initial ship's energy to be absorbed by the ship and/or pier. This relationship was used.

Impact energies for the design vessels are shown below:

Vessel Type	Maximum Displacement (LT)	Max. Speed (Knots)
Maximum Cargo Vessel	71,500	15
Maximum Tanker	180,000	15
Extreme Vessel	225,000	16.5
Most Frequent Cargo	12,000	15
Most Frequent Tanker	32 000	15

The resulting impact energies are as follows:

Vessel Type	Impact Energy (K-Ft x 1000) Bow/Stern Impact Load Condition* 1 & 2	3
Extreme Vessel	6678	1670
Most Frequent Tanker	785	196

Concrete and reinforcing steel properties used for this study are as follows:

Concrete: Ultimate compressive strength (F'c) = 4000 psi. This value was used as all original test records indicate strengths greater than 4000 psi. A visual examination of concrete core samples taken in the fender following the strength calculations indicated that the concrete is in good condition. A reinforcing bar was encountered at a depth of 10 inches in one tremie concrete core. No visible corrosion was noted. It appears that good bond between the reinforcing steel and concrete was achieved. Allowable stresses for the design vessel condition were based on the American Concrete Institute Building Code Allowable stresses for extreme vessel impact condition were based on ultimate concrete capacity.

Steel: Reinforcing steel yield strength (Fy) = 40,000 psi. This value is based on the original test records.

The fender was investigated for three impact load cases:

Impact Condition 1 - Unit 11/12

Unit 11/12 forms the monolithic unit on the west end of the fender. The fender at this location is most able to resist applied load through arching action. A two-dimensional finite element analysis was done. The concrete was not allowed to take tension. Unit 11/12 can resist a 48,400 kip impact force from a 31,900 LT displacement vessel. It will therefore resist the most frequent tanker impact force. It is possible however, that local failure of the concrete fender will occur.

Impact Condition 2 - Unit 15/16

The fender in this area has some arching action though not as significant as the west end unit 11/12. A two-dimensional finite element analysis was done, as on Unit 11/12, to determine the amount of arching action and resulting forces imposed on the adjacent units. Unit

15/16 can resist a 24,200 kip impact force from an 8000 LT displacement vessel, approximately 50% of the most frequent tanker impact force. The fender strength is limited by the supporting ability of the adjacent units. Shear across the construction joints and thrust from the arching action exceed the supporting ability of unit 11/12. Impact from vessels larger than 8000 LT will tend to dislodge the two monolithic units to the south. The unit hit (15/16) might be forced against the bridge pier.

Impact Condition 3 - Unit 21/22

This unit is essentially flat, and therefore has little or no arching action. It was assumed the unit is supported both vertically as a cantilever and horizontally as a beam. Support for the horizontal action is provided by the shear keys at the construction joints to the adjacent units and by the bottom of the moat at elev. -35 ft. The impact vessel strikes at a 30° angle. This angle reduces the force imposed perpendicular to the unit to 50% of the straight-on or perpendicular collision. The unit is also subject to a force parallel to the unit equal to 17% of the perpendicular collision. Unit 21/22 can resist an impact force of 40,600 kips from a 22,400 LT displacement vessel. This resistance is slightly less than the most frequent tanker. No energy dissipation was assumed due to vessel rotation. Higher impact forces overstress the shear keys to the adjacent units and cause instability of the unit as a cantilever. One possible mode of failure is shown below.

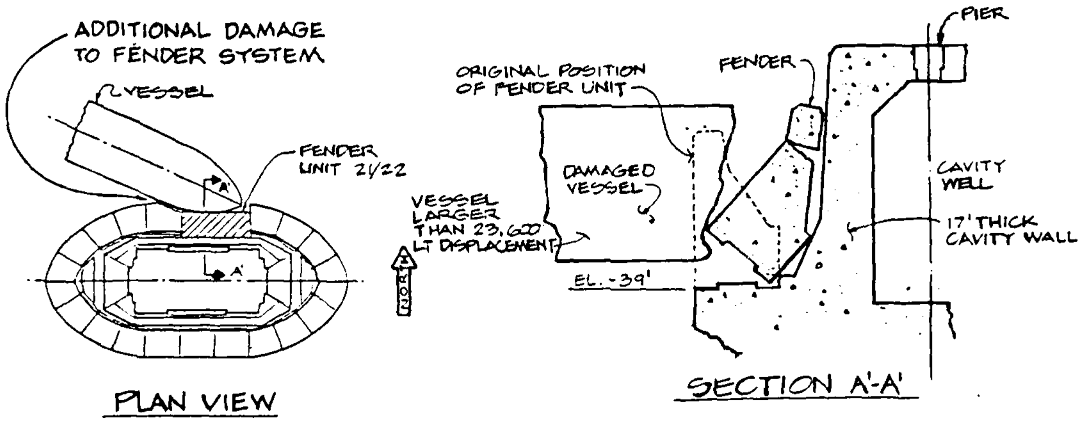
ADDITIONAL DAMAGE TO FENDER SYSTEM
℄ VESSEL
FENDER UNIT 21/22
A'
A'
NORTH
VESSEL LARGER THAN 23,600 LT DISPLACEMENT
ORIGINAL POSITION OF FENDER UNIT
DAMAGED VESSEL
FENDER
PIER
CAVITY WELL
17' THICK CAVITY WALL
EL. -39'

PLAN VIEW

SECTION A'-A'

POSSIBLE FAILURE OF UNIT 21/22

The fender surrounding the pier protects against direct impact on the pier itself. This protection may not be completely effective due to the limited structural capacity of the fendering system. The combined fender and pier is adequate to protect the bridge from the most frequent and extreme vessel impacts. Foundation stresses produced by an extreme event are acceptable. It is possible for an impact on the north side to overstress the pier cavity wall. However, the pier should be capable of supporting the bridge tower in this damaged condition.

Impact Condition	Fender Capacity by Vessel Size		
	DWT (LT)	DISPL (LT)	Impact Force (Kips)
1	26,600	31,900	48,400
2	6,700	8,000	24,000
3	18,700	22,400	40,600

6. IMPROVEMENTS TO FURTHER SAFEGUARD PIER

The south pier fender does provide ship protection, and was designed with considerable foresight. However, vessels have increased in both weight and speed over the last 50 years. Ways of increasing the protection of the pier fall into two categories: structural strengthening of the fender, and protection of the fender against impact by not allowing vessels to hit the fender.

General rehabilitation would involve dewatering of the moat to allow a detailed survey of the concrete in the dry condition on the interior of the fender. Sediment in the moat would be removed. Cracks and holes in the concrete could be repaired at that time.

Strengthening would require construction of a new concrete beam along the inside face of the fender on the flat northern side, and filling the west arched end with sand (shown below). The beam would be designed to withstand the extreme ship impact by spanning between new 2 ft thick supporting walls located on each side of the pier's 17 ft thick cavity wall. Ship impact (all vessels) on the western end of the fender would be resisted by the combined action of the fender and sand backfill.

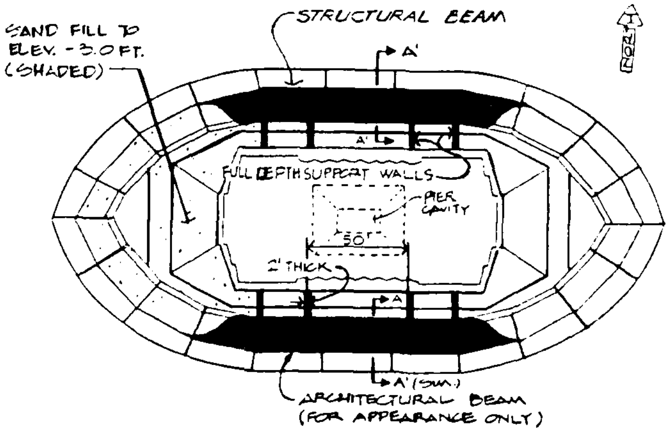

PLAN

FENDER STRENGTHENING

Bridge piers in general have been protected by piles around the pier, clusters of piles, dolphins, or artificial islands. The use of piles or dolphins of a reasonable size at the south pier would not provide the strength or energy absorbing capability required.

A conceptual study was made of an artificial island, which is submerged with the top of berm at elev. -18 ft. to allow for clear passage of small craft around the pier. The island would extend out from the pier horizontally for 75 ft and then slope down at a 3:1 slope (horizontal:vertical) to elev. -55 ft. The remainder would slope down at 2:1. Based on the preliminary studies, an island of this size could stop both the design vessel and extreme vessel approaching the pier at 15 knots. There are several disadvantages to an artificial island in the Golden Gate such as reducing the shipping lane width, changing the current patterns and wave action. Mariners may also object to the island as an unseen hazard.

It is possible to construct a new concrete fender surrounding and dowelled to the existing fender wall. The new fender would be approximately 20 ft wide. The resulting wall would provide enough resistance against ship collisions. For the south and east sides a simpler new fender could be added to create architectural symmetry with the north and west sides.

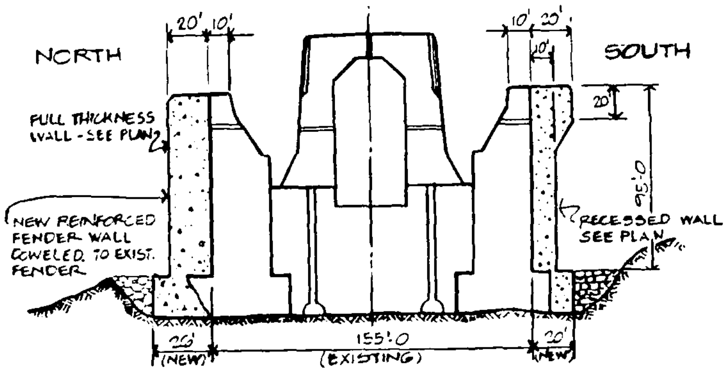

CROSS SECTION

FENDER STRENGTHENING - NEW FENDER

Cost estimates were prepared for the various improvement schemes. These estimates were intended to provide only an order of magnitude for alternative comparison purposes.

Improvement Methods	Estimated Cost
General Rehabilitation	$ 1,318,000
Structural Strengthening	$ 4,642,000
Protection Against Impact (Submerged Artificial Island)	$12,200,000
New Fender	$45,000,000

7. CONCLUSIONS

Several alternative courses of action were presented.

Alternate A) Leave the Pier/Fender in its Present Condition

It is very unlikely that a vessel will hit the pier; no collisions have occured since the bridge opened in 1937. Precautions include using bar pilots, radar, and ship-to-ship and ship-to-shore communications. Also, tidal current patterns tend to drive vessels away from the south pier.

The fender at the west end of the pier, most likely to be hit, can resist the most likely tanker. Vessels larger than 31,900 LT could damage the fender, but structural effects on the pier and bridge may not be significant. The northwest face can resist only an 8,000 LT vessel, smaller than both design vessels. Impacts here could subject the fender and pier to significant forces and produce local concrete failure, but the pier would probably resist the load. The north face, probably least likely to be hit, can resist a 22,400 LT vessel, about three-quarters of the most likely tanker's displacement. Ship impact on this side could force the fender against the pier cavity wall.

Alternate B) Strengthen Existing Fender

The fender could be strengthened for impacts on the west end and north side. The north side strengthening would require removal of silt in the moat, replacing it with sand and installation of a concrete beam and supporting walls.

Alternate C) Submerged Island

An artificial rock island along the west and north side of the fender would stop ships before they could reach the fender. This system has both functional and cost disadvantages and was not recommended, but was included for cost comparison only.

Alternate D) New Fender

A new fender constructed around the existing fender could resist the extreme impact force. This approach would involve significant cost and construction effort, and also was included only for cost comparison.

8. STRENGTHENING

The Golden Gate Bridge, Highway and Transportation District has included Alternate B, general rehabilitation and structural strengthening of the fender in their five year plan as recommended by Earl and Wright. The general rehabilitation will include dewatering the moat, disposing of the moat sediments, and inspecting/repairing fender and pier cracks. Structural strengthening will include new concrete beams on the north and south forces of the fender, supporting walls on the north face and sand fill in the west end of the moat.

9. REFERENCES

1. Strauss, Joseph B., The Golden Gate Bridge (Report of the Chief Engineer to the District - September 1937)

2. Rasmussen, B.H. "Design Assumptions and Influence on Design of Bridge," ibid, pp. 233-246

3. Jensen, A.D. and Sorensen, E.A. "Ship Collision and the Faro Bridges," ibid., Preliminary Report, pp 457-458.

4. "Ship Collision with Bridges - The nature of Accidents, their Prevention and Mitigation," Marine Board - National Research Council, National Academy Press, Wash, D.C. 1983.

5. Macduff, T. "The Probability of Vessel Collisions," Ocean Industry, Sept. 1974.

6. Woison, G. "Conclusions from Collision Examinations for Nuclear Merchant Ships in the FRG," Symposium on the Safety of Nuclear Ships, Proceedings 5-9 Dec 1977 Hamburg, pp 137-147.

7. Det norske Veritas, Technical Note TNA 202 Ship Collisions.

8. Saul, R. and Swenson, H. "Means of Reducing the Consequences of Ship Collisions with Bridges and Offshore Structures," Ship Collisions with Bridges and Offshore Structures - Introductory Report, IABSE Colloquim, Copenhagan, Denmark 1983, pp 165-178.

9. American Concrete institute, Building Code Requirements for Reinforced Concrete (ACI 318-77)

WEST COST REGIONAL COASTAL DESIGN CONFERENCE

Golden Gate Bridge Pier Ship Collision Study Presentation

BIOGRAPHICAL SUMMARIES

WAYNE O. MacDONELL, P.E.
Senior Engineering Manager
Earl and Wright

Mr. MacDonell has 34 years' experience in civil/structural engineering design and construction engineering for bridges, marine terminals, offshore platforms, marine vessels and other structures. His recent responsibilities include project management for the upending system of British Petroleum's Magnus North Sea platform, the world's heaviest self-floating steel structure, and replacement of an aging timber trestle at Shell Oil's Martinez Refinery on San Francisco Bay. Before joining Earl and Wright in 1962, he worked for several years for the State Division of San Francisco Bay Toll Crossings. He is a registered civil engineer, and earned his BSCE at U.C. Berkeley.

BO M. JENSEN, P.E
Business Development Manager
Earl and Wright

Mr. Jensen's 17 years of structural analysis and design experience covers bridges, buildings, and offshore structures including arctic units. His credentials include responsibility for design of North Sea offshore platforms and their components on assignment in London from 1979 to 1982. He managed a Copenhagen joint venture company from 1982 to 1983, and in 1985 became Business Development Manager in San Francisco. A registered structural and civil engineer, he holds a M.S. in structural engineering from U.C. Berkeley and a BSCE from U.C. Davis.

DANIEL E. MOHN, P.E.
Chief Engineer
Golden Gate Bridge, Highway and Transportation District

Mr. Mohn joined the State of California's Bridge Department in 1955, and with breaks to work for private firms spent some 15 years with the agency on such assignments as the San Mateo-Hayward and San Diego-Coronado Bridges, which pioneered the use of orthotropic design and modular fabrication and construction technology for steel bridges in the U.S. He worked on rehabilitation of the Golden Gate Bridge in 1973, and in 1982 was named Chief Engineer, responsible for design, construction, rehabilitation and maintenance of the Bridge and other district facilities. He earned his BSCE at U.S. Berkeley and is a registered civil engineer.

THE ANALYSIS AND DESIGN OF CONCRETE ARMOUR UNITS

INTRODUCTION

The analysis and design of an armour layer for a rubble mound breakwater that uses concrete armour units must consider both hydraulic stability and the structural integrity of the armour units.

Hydraulic stability is assessed using a physical model in which the model breakwater is subjected to simulated design wave conditions. In this summary an instrumentation scheme for measuring the loads on the armour units in the same physical model is described.

A procedure is outlined whereby the structural integrity of the concrete armour units is assessed. In addition, the information required to design reinforcement for the unit using standard engineering procedures is obtained.

OBJECTIVE

The objective of the instrumentation scheme and procedure that is described in this summary is to determine the armour unit load levels and to provide design recommendations based on these results.

APPROACH

A physical model of the breakwater is built and an instrumented armour unit is placed at various locations within the armour layer. The model breakwater is then subjected to the design wave conditions and the magnitude, duration, nature and rate of loading are determined.

R.D. Scott, Queen's University, Kingston, Ontario, Canada.
D.J. Turcke, Queen's University, Kingston, Ontario, Canada.
W.F. Baird, W.F. Baird & Associates, Ottawa, Ontario, Canada.

INITIAL STUDIES

Initially, model armour units were constructed of an appropriate material such that strain gauges mounted on the surface would detect the induced load levels. This was a viable approach; however, there was a need to increase the sensitivity of the instrumentation in order to work at geometric scales commonly used for assessing the hydraulic stability of the armour layer.

CURRENT STUDIES

A new and unique instrumentation scheme has been developed which significantly increases the sensitivity of the instrumented unit. The device consists of a strain gauged thin-walled aluminum tube inserted in an armour unit.

This technique is now being used to undertake analytical studies of breakwaters from which design recommendation and design procedures can be identified.

Each instrumented unit is extensively calibrated by applying known loads before placement in the armour layer and after testing.

SAMPLE ANALYSIS AND RESULTS

A sample analysis was undertaken using a 1:40 model of a breakwater with 30 tonne dolos units on a 1:2 slope. The structure was subjected to regular waves with a height of 32 feet and a period of 11 seconds.

The instrumented unit was placed at various locations above, at, and below the still water level in both the top and bottom layers of the armour. Moments and torques were then measured and each experiment repeated three times.

The instrumentation measures the moments and torques at the mid-point of the dolos shank. Using these results, a finite element analysis was undertaken to identify the regions of high stress within the dolos. These results showed that a stress intensity factor of between 2 and 3 for locations at the fluke-shank interface could be expected.

The data describing the moments and torques can be usefully displayed using an interaction diagram.

This diagram provides a clear graphical illustration of the interplay between moments and torques with respect to several design considerations such as concrete strength, and unreinforced and reinforced sections.

CONCLUSIONS

The sample analysis showed that some of the 30 tonne unreinforced units located in the vicinity of the still water level had failed under these wave conditions. However, with the introduction of minimum reinforcing steel the moment resistance of the unit can be significantly increased. Consequently, this reinforced unit would be an acceptable design.

Other conclusions that can be drawn from these results are as follows:

- the most severe loading cases occurred in the vicinity of the still water level and in the upper layer of the armour units,
- the response profile, characterized by the magnitude, duration, nature and rate of loading, was dependent on the location in the breakwater.

In these particular tests a few dolos units rocked a small amount under wave action. No severe rocking or displacement of armour units was observed. Therefore from the standpoint of hydraulic stability these wave conditions did not represent the design conditions.

APPLICATION TO DESIGN

The procedure has a proven application to the assessment and design of concrete armour units. The analysis technique is not unique to the dolos unit; it can be adapted to provide information on the loads on most types of concrete units.

INTERACTION FAILURE CURVES FOR 30 t DOLOS AND REGULAR WAVES H=32 ft.

(THESE WAVES PRODUCED MINOR ROCKING OF A FEW DOLOS UNITS, NO UNITS WERE DISPLACED FROM THE ARMOR LAYER)

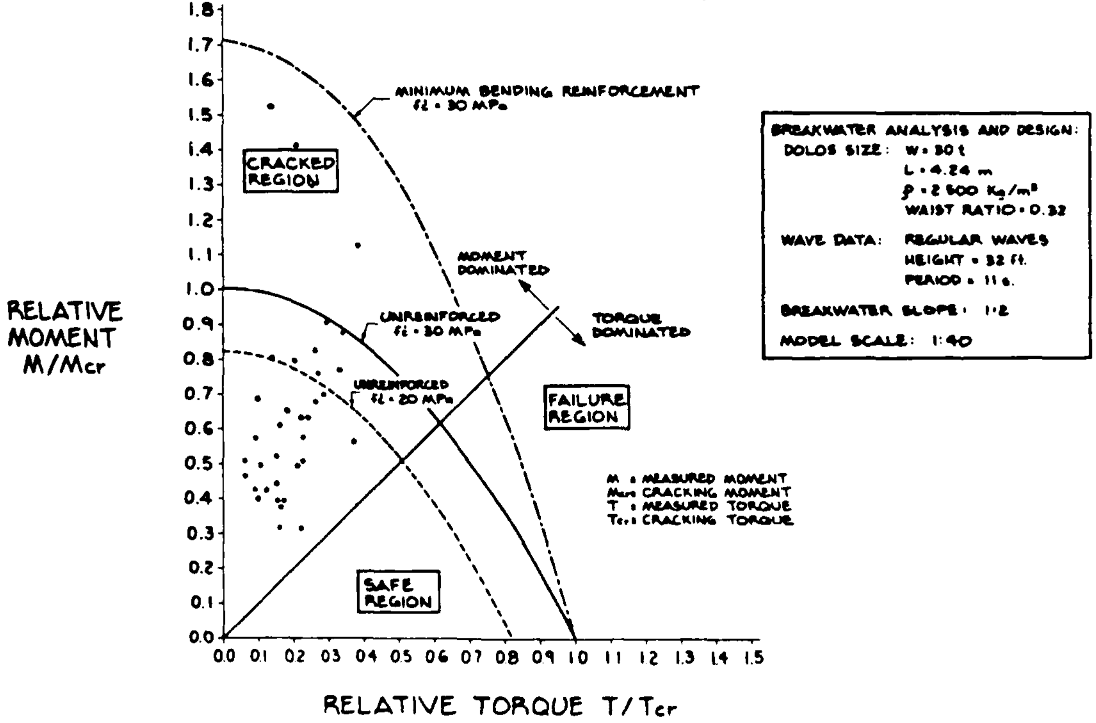

RESULTS FROM A PROTOTYPE FLOATING BREAKWATER TEST PROGRAM

ERIC NELSON, 1/ LAURIE BRODERICK, 2/

Introduction. In February 1981, the Corps of Engineers initiated a 3-1/2-year prototype test program to provide design guidance for floating breakwater applications in semiprotected coastal waters, lakes, and reservoirs. The test was designed not only to obtain field information on construction methods and materials, connector systems, and maintenance problems, but also to measure wave transmission characteristics, anchor loads, and structural response. Program planning, engineering, and design work were completed in September 1981, and the construction and placement of a 150-foot-long by 16-foot-wide concrete breakwater and a 100-foot-long by 45-foot-wide tire breakwater was completed in August 1982. Monitoring and data collection were concluded in January 1984. The Corps of Engineers' Office of the Chief of Engineers (OCE) had overall responsibility for program management. Guidance regarding site selection, breakwater design, and monitoring was provided by the Floating Breakwater Prototype Test Working Group comprised of representatives from OCE (Research and Development Office, Hydraulics and Hydrology Division, and Engineering Division); the Waterways Experiment Station (WES) (Coastal Engineering Research Center (CERC), and Structures Laboratory); the North Pacific Division; and the Seattle District. In addition, staff from the University of Washington's Department of Civil Engineering provided consultation during the test program. Analysis of the collected data was done by the CERC. The Seattle District had primary responsibility for carrying out all other major facets of the program.

The breakwater test site was in Puget Sound off West Point at Seattle, Washington. The site was in an exposed location, assuring that, within the period available for testing, wave conditions would approximate design waves normally associated with sites considered suitable for floating breakwaters. Water depth at the site varied between 40 and 50 feet at mean lower low water (MLLW), and bottom materials consisted of gravel and sand. The diurnal tide range at the site is 11.3 feet and the extreme range is 19.4 feet.

The prototype structures that were built and monitored were of two types: a concrete box design (figure 1) and a pipe-tire design (figure 2). The 150-foot-long concrete breakwater was composed of

1/Hydraulic Engineer, U.S. Army Engineer District, Seattle, Washington.
2/Hydraulic Engineer, U.S. Army Engineer District, Portland, Oregon.

two 75-foot-long units, each 16 feet wide and 5 feet deep (draft of 3.5 feet). The pipe-tire breakwater was composed of nine 16-inch-diameter steel pipes and 1,650 truck tires fastened together with conveyor belting to form a structure that was 45 feet wide and 100 feet long.

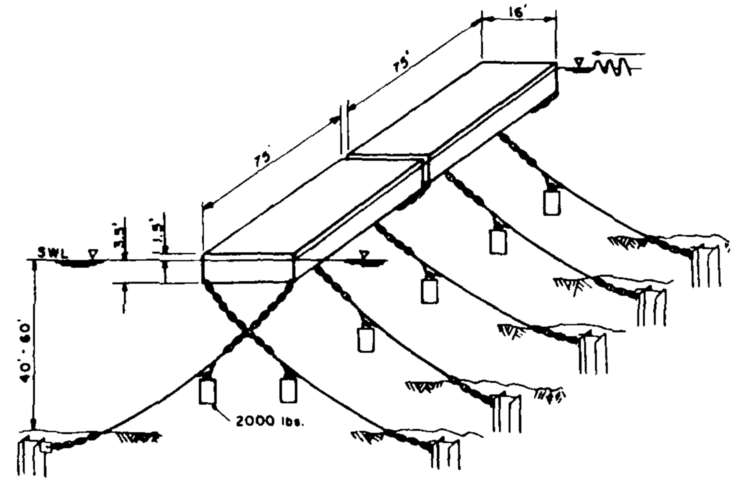

FIGURE 1. CONCRETE BREAKWATER (NOT TO SCALE)

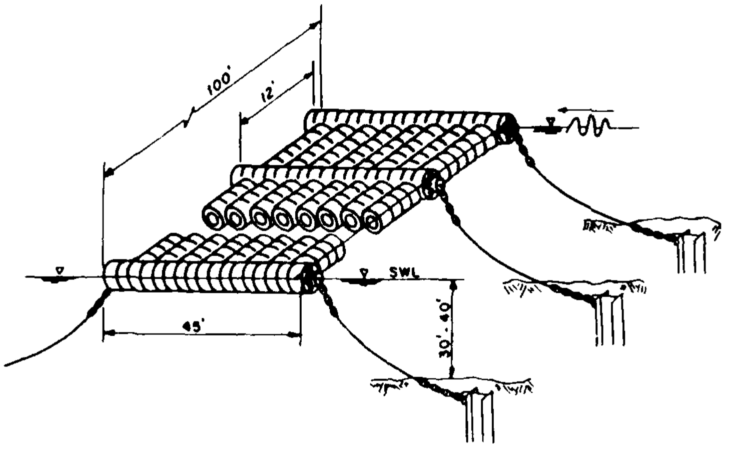

FIGURE 2. PIPE-TIRE BREAKWATER (NOT TO SCALE)

Concrete Breakwater Construction. The two 75-foot-long concrete breakwater units were constructed in Bellingham, Washington, 90 miles from the test site. Work on these units began with the erection of exterior plate steel forms. Three-eighths-inch-diameter welded wire fabric was then placed on the sides, ends, and bottom of the forms, with the top left open to allow placement of styrofoam blocks during the concrete placement process. All small pieces of reinforcing steel were epoxy coated and the welded wire parts were galvanized for corrosion protection. Prior to casting, 16 rebar strain gages were fastened into the deck, sides, bottom, and corners as part of the monitoring system. The concrete placement for each float began at 5 a.m.; by sunrise the 4-3/4-inch-thick bottom had been completed. The styrofoam blocks that served as the interior forms were then dropped into place. After the sides of the floats had been placed to within 1 foot of the deck surface, the deck reinforcing steel was laid, and the final concrete placement was begun. Placing and finishing of the deck completed the casting process in a total of 9 hours. Test samples of concrete were taken throughout the placement. The concrete weight varied between 131 and 134 pounds per cubic foot, with an average 7-day strength of 4,000 to 5,000 p.s.i. and a 28-day strength of 5,000 to 6,000 p.s.i. (Light weight concrete was specified to reduce the structure weight and increase the breakwater's freeboard). After the concrete had cured for 7 days, the ten 1/2-inch diameter strands in each of the six post-tensioning tendons were tensioned to 25,000 pounds, for a total of 250,000 pounds in each tendon.

When the 140-ton units were lifted from the casting area and lowered into the waterway, the longitudinal strain gages in the lower center edges of the B float were monitored. A maximum strain of 1,700 microstrains was recorded, indicating that loads were about two-thirds of the yield strength of the reinforcing steel. After both units were launched, they were joined end-to-end with two flexible connectors and towed approximately 90 miles south to the West Point test site.

Pipe-Tire Breakwater Construction. The pipe-tire breakwater was assembled one bay at a time on a construction platform located adjacent to a waterway. As each 12-foot by 45-foot bay was completed, it was moved into the waterway. Construction of the breakwater closely followed the sequence described by Harms (reference 1). The matrix of 1,650 truck tires was bound by loops of 5-1/2-inch-wide, 3-ply conveyor belting. A special tool fabricated from a car jack was used to tighten the belting before the loop ends were joined together with five 1/2-inch-diameter by 2-inch-long nylon bolts. The ends of the bolt threads were melted with a welding torch to prevent the nuts from working off the bolts. After 12 rows of 11 tires had been fastened together, the breakwater was ready to have a 16-inch-diameter, styrofoam filled pipe inserted into the beamwise row. The completed bay was dragged into the adjacent waterway by using an overhead crane and a small tugboat. This process was repeated for each of the eight bays (nine pipes). After construction procedures had been perfected, assembly time for each bay was approximately 8 hours for two men. Inserting the pipe, and moving the completed bay off the assembly platform required an additional two men and took approximately 4 hours. Construction time was considerably reduced by the use of heavy equipment and the special tools fabricated by the contractor.

Anchoring. The concrete breakwater was anchored in place by ten, 30 foot-long steel H-piles (HP 14 by 102) embedded their full length. The five anchor lines on each side of the breakwater were spaced about 35 feet apart. A bridle assembly near the surface joined the two units to a common anchor line at the center of the breakwater. Anchor lines consisted of 1-3/8-inch-diameter galvanized bridge rope with 15 to 25 feet of 1-1/4-inch stud link chain at each end. Anchor line lengths were sized to provide a scope no steeper than 1 vertical to 4.5 horizontal under maximum high tide conditions. Initial anchor line tensions were 5,000 ± 1,000 pounds. A 2,000-pound concrete clump weight was attached to the bridge rope 44 feet from the upper end of each anchor line. The purpose of this design was to produce a more even anchor line tension over the full range of tides and thereby to reduce the horizontal excursions of the breakwater, particularly at lower tide elevations. Positioning of the four corner H-pile anchors to a 5 degree inward angle was designed to provide resistance to longitudinal displacement of the breakwater. Four months prior to the termination of the field test, the clump weights were removed. During this 4-month period, the effects of this clump weight removal on float motions, anchor forces, and wave attenuation were monitored.

The pipe-tire breakwater was anchored about 30 feet from the end of the concrete breakwater with ten 20-foot-long steel H-piles (HP 12 by 53). Anchor lines consisting of 1-1/4-inch-diameter, three strand, nylon rope with 10 feet of 3/4-inch stud link chain at each end were attached to both ends of each pipe. This design resulted in an anchor line spacing of 12 feet. The scope for these anchor lines was no steeper than 1 vertical to 4 horizontal under maximum high tide conditions. The center and end H-piles had one anchor line each, while the remaining four anchor piles were attached to three anchor lines apiece. The four end pilings were offset at an outward angle to counteract the opposing longitudinal component of force from the adjacent anchor lines.

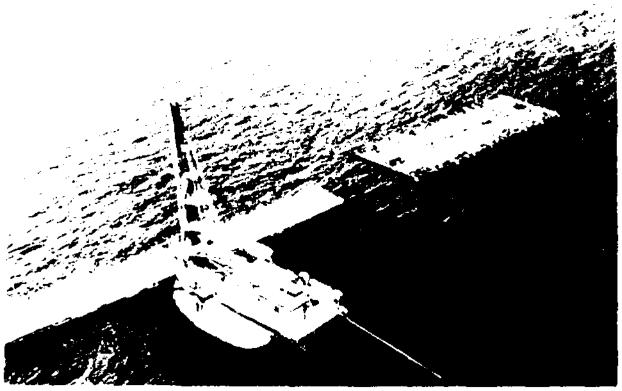

PHOTO 1. FINAL ANCHORING OF BREAKWATERS AT TEST SITE

Observations of Performance and Durability. The prototype breakwater test site at West Point was selected because of its exposure to wind waves. This choice proved to be more than adequate for providing the desired wave conditions. During the 18-month test period, more than 20 storms moved through Puget Sound. One storm brought winds in excess of 60 knots and generated waves over 4 feet high. Most often, storm winds were in the 20- to 40-knot range with wave heights between 2 and 3.5 feet. Access to the breakwater was difficult when winds exceeded 10 knots; 15-knot winds made working conditions potentially hazardous.

Visual comparisons of incident and transmitted wave height indicated that, under all observed wave conditions, the pipe-tire and the concrete breakwaters provided an adequate and very similar degree of wave protection for both wind waves and boat wakes. Readily apparent was the fact that the concrete breakwater reflected the wave energy, but the pipe-tire breakwater dissipated it through viscous damping. As a result of wave reflection, the windward side of the concrete breakwater was always noticeably rougher than the windward side of the pipe-tire breakwater.

Overtopping of the concrete breakwater by ship wakes and wind waves was quite pronounced. Sheet flow 6 inches deep was common. As a result, a lush crop of algae thrived on the deck of the structure, making the surface treacherously slippery. The actual freeboard of the concrete breakwaters was about 13 inches, 4 to 5 inches less than anticipated in the original design. The reduced freeboard undoubtedly contributed to the amount of overtopping.

The relatively high initial tension in the anchor lines of the concrete breakwater (5,000 pounds with the 2,000-pound clump weights attached and 1,500 pounds without the clump weights) appeared to minimize the lateral travel of the floats even during low tides and fast tidal current flows (2 knots). Lateral displacements were estimated to be less than 2 feet even when the clump weights were removed.

Lateral displacement of the pipe-tire breakwater did not appear excessive (about 15 feet), but tidal currents running at a 45-degree angle to the anchor lines tended to carry the pipe-tire breakwater in a longitudinal direction to the end of the concrete breakwater, a distance of about 30 feet.

Water leakage into the hollow end compartments of the concrete breakwater was a serious problem early in the test. Primary leak points were the "watertight" access hatches and the 2-inch-diameter post-tensioning bolt holes that were used when making the rigid conections between the two floats. Because calculations indicated that the breakwater could sink if the end compartments filled, emergency pumping operations were carried out on several occasions. Eventually, reworking the hatch covers and filling the bolt holes with sealant reduced the leakage rate to manageable levels.

One of the major goals of the test program was to investigate various methods of connecting (or fendering) the two 140-ton floats. Four different connection methods were tested: two types of flexible connectors, complete disconnection (with fendering), and rigidly bolting the units together. Both the fendering and the rigid connection were successful. None of the flexible connector designs survived their test period undamaged, although considerable progress was made toward a viable flexible connection design.

Advantage was taken of calm periods to make repairs and to conduct additional tests. Four boat wake tests and an anchor line stiffness (pull) test were conducted at various times in the program. For two of the boat wake tests, 41-foot Coast Guard cutters were used to generate waves. The other two tests used large (75 foot and 110 foot) tugboats. Boat generated waves were in the 2- to 3-foot range. For the anchor stiffness test, a 4,000-horsepower tugboat was used to pull on the breakwater with varying loads, while surveying instruments measured displacements, and load cells in the anchor lines monitored anchor forces. This test was conducted to obtain simultaneous measurements of breakwater lateral displacement and the resisting anchor force, which are properties of the anchor system that affect overall float motions and internal loads.

Upon completion of the field test, diver inspections of the anchor lines and the concrete floats were made. No significant damage, wear, or cracking was found on the floats. The galvanized steel bridge ropes were visibly corroded, and the shackles used to attach the clump weights to the anchor lines were worn; but, otherwise, the anchor line hardware, including the chain, was found to be in excellent condition.
(Because of the relativley short duration of the test, no corrosion protection system was used on the anchor lines).

For nearly a year, the pipe-tire breakwater proved to be remarkably durable. Except for minor repairs to the keeper pipes, it withstood the winter storms of 1982 without any maintenance. But in June 1983, almost a year to the day after the pipe-tire breakwater was installed, the first problem of any consequence developed. After a minor storm, routine inspection revealed that one of the longitudinal pipes had broken. A closer scrutiny revealed that the 45-foot pipe had been fabricated from a 40-foot section and a 5-foot section. A poor weld between the two sections had finally failed because of a combination of corrosion and fatigue, allowing the two pipe sections to pull out of the tires. One month later, when a second pipe failed in exactly the same manner, a decision was made to terminate testing of the pipe-tire breakwater. The pipe-tire breakwater anchor lines were inspected during the removal process. No major problems were found in the nylon anchor lines or connecting hardware. After the breakwater was removed, it was surplused and eventually reinstalled at a private marina in southern Puget Sound. Monitoring of the long-term durability of this unit is planned.

While the Prototype Test Program was underway, two projects using floating breakwaters were designed and constructed by the Seattle District, Corps of Engineers. In 1983, a 600-foot-long breakwater was constructed for the 800 boat East Bay Marina at Olympia, Washington. A year later, another floating breakwater, 1,600 feet long, was anchored at Friday Harbor, Washington. As originally planned, the prototype test breakwater was refurbished and incorporated into the Friday Harbor Project. Throughout the test program, information obtained from the construction and operation of the prototype breakwater was used to refine the East Bay and Friday Harbor designs. Preliminary prototype test data were used to confirm float sizes. Construction specifications were broadened to allow the use of either lightweight or standard weight concrete, with appropriate adjustments in float draft. Details of the East Bay connector system were changed to reduce maintenance, and the Friday Harbor fender system is a direct spinoff of the one developed during the prototype testing.

Data Collection. The monitoring program for the prototype test was conducted by the Civil Engineering Department of the University of Washington under contract with the U.S. Army Corps of Engineers. The purpose of the monitoring program was to collect data that would serve as a basis for establishing and evaluating the fundamental behavior of the two breakwater types under study. The University designed a system to measure and record pertinent environmental and structural variables that are involved in the design and mathematical modelling of the test breakwaters and similar structures. The parameters that were measured included incident and transmitted waves, wind speed and direction, anchor line forces, stresses in the concrete units, relative float motion, rotational and linear accelerations, pressure distribution on the concrete breakwater, water and air temperatures, and tidal current data.

"Off the shelf" transducers for measuring many of the parameters were not available. A major effort was required to design and fabricate anchor force load cells, wave measuring spar buoys, a relative motion sensor, pressure sensor housings, and embedment strain gages. By the end of the monitoring program, approximately 60 transducers had been installed in and around the breakwater. Over 3 miles of underwater electrical cable was required to feed signals to the onboard data acquisition system that was housed on the concrete breakwater. Using large lead-acid batteries for power, the system was completely self contained. In addition to the input transducers, the system included a microprocessor controlled data logger and special purpose signal conditioning electronics, which were designed and built by the University. The data acquisition system was programmed to sample selected transducers for 1 minute on an hourly basis. When either wind speed, current speed, anchor force, or significant wave height exceeded a preset threshold value, an 8-minute record of all transducers was made at a sampling rate of 4 hertz. The microprocessor was capable of a limited amount of data processing, including calculations of maximum, minimum, mean, and standard deviation of selected parameters. After each data tape was retrieved from the breakwater, it was processed at the University. Selected statistics and data plots were analyzed to determine whether all critical components of the data acquisition system were operating properly. When problems were detected, repairs were made as soon as the breakwater was safely accessible. Keeping this complicated and extensive system operational in such a hostile environment proved to be a challenging enterprise. Salt water flooded instrumentation, waves and tidal currents broke transducers and tore out electrical leads, and logs, fish nets, and other debris caused damage continuously. Despite these difficulties in the 18 months of data collection, 121 data tapes were recorded, representing approximately one-quarter billion measurements. After initial processing at the University, the data were transferred to the Coastal Engineering Research Center for detailed analysis.

Data Analysis. Detailed analysis of the data was initiated in June 1984, with the major effort being directed toward the transmission and anchor force characteristics of the breakwaters. These two parameters had the highest priority because they were considered to be key factors in the effort to optimize the cost effectiveness of floating breakwater design. Other parameters such as the internal concrete strains and wave pressures were checked to insure the reliability of the data but detailed analysis was deferred.

Figures 3 and 4 present the wave transmission characteristics and anchor line forces for the concrete breakwater. Results for the three configurations of the concrete breakwater (rigidly connected with clump weights, rigidly connected without clump weights, and flexibly connected without clump weights), are represented by different symbols. For all three configurations the wave transmission coefficients (transmitted height/incident height) plotted in figure 3 are centered around a value of 0.40. This value was near the expected level of performance, and indicates that this size breakwater would provide adequate protection for waves up to approximately 3 feet in height. The peak forces measured in the concrete breakwater's anchor lines are shown in figure 4. The anchor line forces increase only slightly, with increasing wave height and average approximately 40 pounds per lineal foot of breakwater (in addition to the initial tension). The various configurations of the concrete breakwater seemed to have little effect on the peak anchor force. Figures 5 and 6 present the wave transmission characteristics and the anchor line forces for the pipe tire breakwater. The average wave transmission coefficient of 0.42 is close to the expected value for the wave heights tested (see figure 5). The peak anchor loads for the tire breakwater shown in figure 6, average approximately 75 pounds per lineal foot. Again, as for the concrete breakwater, the peak anchor load does not vary significantly over the range of wave heights measured during the test.

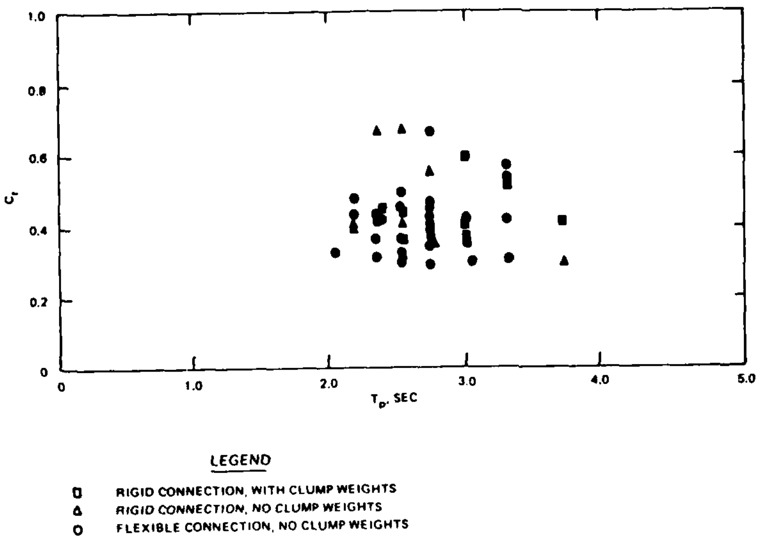

FIGURE 3. TRANSMISSION COEFFICIENT, C_t, VERSUS WAVE PERIOD, T_p; CONCRETE BREAKWATER.

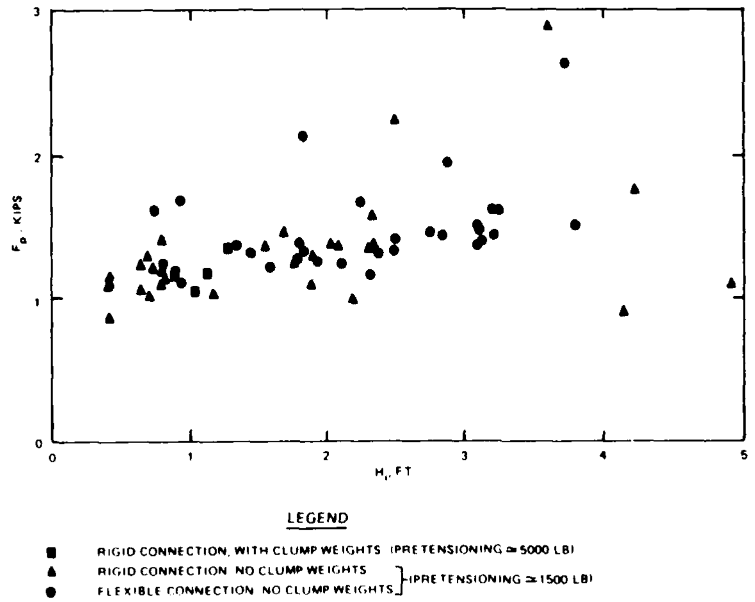

FIGURE 4. PEAK ANCHOR LINE FORCE, F_p, VERSUS INCIDENT WAVE HEIGHT, H_i; CONCRETE BREAKWATER.

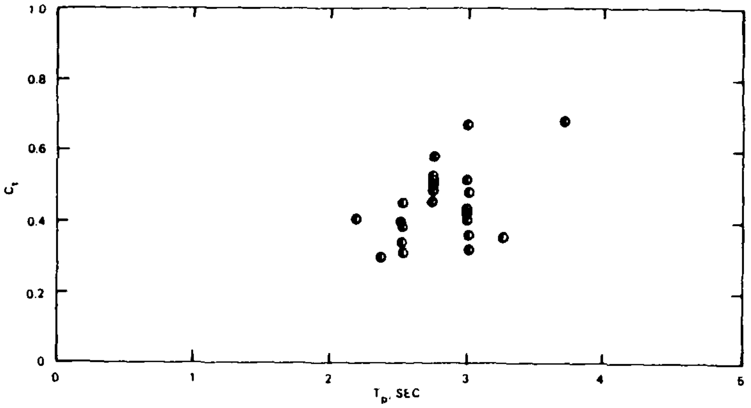

FIGURE 5. TRANSMISSION COEFFICIENT, C_t, VERSUS WAVE PERIOD, T_p; PIPE-TIRE BREAKWATER.

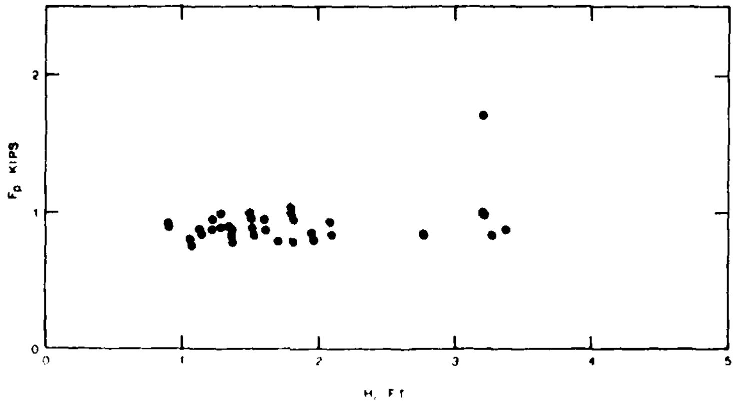

FIGURE 6. PEAK ANCHOR LINE FORCE, F_p, VERSUS INCIDENT WAVE HEIGHT, H_i; PIPE-TIRE BREAKWATER.

The variation of transmission coefficient with wave period, typical of most laboratory tests, does not appear in the prototype measurements. At the West Point test site the generation of large wave heights and periods was limited by the relatively short fetches, and the breakwaters were not subjected to wave conditions that would produce high transmission coefficients. At the lower end of the scale, wave and boat wake "chop" up to one foot high occurred frequently even on the leeward side of the breakwater. This background noise resulted in relatively high transmission coefficients for smaller wave heights regardless of how well the breakwater was attenuating the incident waves. These site specific characteristics resulted in a concentration of wave attenuation measurements around 0.40. Selection of the concrete breakwater size was based on 2-dimensional model tests which indicated a transmission coefficient of 0.40 could be expected for a range of wave periods for 2.0 to 3.5 seconds. Prototype performance appears to follow closely the model test results, at least for this relatively narrow range of wave periods. While the test site periods were limited, they do represent the most important range for floating breakwater applications in semi-protected waters.

The measured wave loads on the concrete breakwater anchor lines were about one-half of the predicted loads, but the predicted loads on the pipe-tire breakwater were similar to measured values for wave heights less than 2 feet. The anchor line forces, plotted in figures 4 and 6, do not show the anticipated increase with increasing wave height. This lack of sensitivity to wave height changes may result from a combination of factors. Anchor force predictions for the concrete breakwater did not account for viscous losses. These losses increase when larger waves break over the breakwater, and when the breakwater motion becomes more extreme. The anchor system for the pipe-tire breakwater was much more compliant that those used in a previous prototype test or in model tests, and wave impact loads probably were absorbed more readily by the prototype-test anchor lines than by those used previously. Finally, the random nature of the wind waves at the test site complicates the correllation of the prototype test results with monochromatic model test data.

Conclusions and Recommendations. The following conclusions and recommendations are based on Prototype Test results, and on field experience gained during the test and during the concurrent construction of two Corps floating breakwater projects in Puget Sound.

(1) Wind generated wave heights measured at the test site compared favorably with the predicted values.

(2) Measured values of wave transmission for both the concrete and the pipe-tire breakwater were similar to the predicted values. Both breakwaters provide satisfactory protection (transmitted wave of 1 foot or less) for waves up to 3 feet high.

(3) For the concrete breakwater, measured values of anchor forces were about 50 percent of the predicted loads if the long-period sway component of the predicted value is ignored. The prototype test anchor force records do not show the obvious long-period component that was present in previous anchor line force measurements. The apparent lack of this long-period force may be due to the relatively high initial tension and rapidly increasing anchor stiffness that was characteristic of the prototype test anchor system.

(4) For the pipe-tire breakwater the measured values of anchor forces were similar to the predicted loads for incident wave heights less than 2 feet. Differences between the model test anchor system and the prototype anchor system make any detailed comparison difficult.

(5) Measurements from the strain gages embedded in the concrete breakwater indicated that bending moments were less than 50 percent of the predicted values. The highest strain was measured during the launching process. Loads encountered during launching and towing may govern structural requirements.

(6) Of the methods tested for connecting (or fendering) the concrete floats, both the complete disconnection with fendering, and the rigid connection were successful. None of the flexible connector designs survived their test period undamaged.

(7) Most of the urethane foam flotation in the crowns of the tires of the pipe-tire breakwater remained securely intact and in place throughout the test. The durability of the foam was enhanced by the physical protection provided by the very stiff sidewalls of the truck tires. If more flexible automobile tires were used, the foam probably would be more vulnerable to damage. In 1 year, the average foam weight increased 250 percent due to the absorption of water. This absorption combined with underfilling of tires during the original construction could have led eventually to buoyancy problems. The long-term water absorption rate of foam flotation remains a concern, and should be taken into account when flotation requirements are being calculated. The pipe-tire breakwater original design flotation requirement of 75 pounds positive buoyancy for tires, other than those on the beamwise pipes, probably is not overly conservative for long-term use.

(8) The keeper pipes on the pipe-tire breakwater should be redesigned. If a single 4-inch-diameter by 40-inch-long keeper pipe were welded in place, the expensive 4-way cross coupler and 2-inch I.D. pipes, which were vulnerable to corrosion and loosening, could be eliminated. Also, designers should consider the potential for corrosion of all small metal parts, such as cotter keys.

(9) Although a number of the bolted connections had one or two broken bolts, none of the connections failed. Binding the tires of the pipe-tire breakwater with loops of conveyor belting and fastening the loops together with nylon bolts appear to produce a strong durable structure.

(10) The 16-inch-diameter pipe for the pipe-tire breakwater should be used in standard lengths to avoid welding. If welding is required, all welds should be carefully inspected.

(11) Construction cost of the prototype tests 150-foot-long concrete breakwater was approximately $2,600 per lineal foot (1981). In 1983, construction of a 1,600-foot-long breakwater of similar design (anchored in a similar depth) cost $1,200 per lineal foot indicating a considerable cost per foot reduction when the breakwater length was increased ten fold.

(12) Construction cost of the prototype tests 100-foot by 45-foot pipe-tire breakwater was $1,600 per lineal foot (1981) including anchors. Uncertainties in availability of used truck tires and in construction methods resulted in this relatively high cost.

REFERENCES

1. Harms, V. W., Westerink, J. J., Sorensen, R. M., and McTamany, J. E., "Wave Tranmission and Mooring-Force Characteristics of Pipe-Tire Floating Breakwaters," Technical Paper No. T.P. 82-4, U.S. Army, Engineer Waterways Experiment Station, Coastal Engineering Research Center, Vicksburg, Mississippi, 1982.

2. Nelson, E. E., L. L. Broderick, Floating Breakwater Prototype Test Program, Draft Technical Report, Waterways Experiment Station, Vicksburg, MS, 39180, publish 1986.

CONVERSION FACTORS, U.S. CUSTOMARY TO METRIC (SI) UNITS OF MEASUREMENT

Multiply	By	To Obtain
feet	0.3048	meters
miles (U.S. Statute)	1.6093	kilometers
pounds (mass)	0.4536	kilograms
tons (2000 lb mass)	907.1847	kilograms
pounds per cubic feet	16.0185	kilograms per cubic meter

Summary of Panel Discussion

STRUCTURES AND MATERIALS

Chairman: Orville T. Magoon
American Shore and Beach Preservation Association

Panelists: David Hawley, Hawley International
Irwindale, California
Thomas Richardson, US Army Corps of Engineers
Waterways Experiment Station (WES), Vicksburg, Mississippi
George C. Fotinos, Ben C. Gerwick, Inc.
San Francisco, California
Donald Treadwell, Geomatrix Consultants
San Francisco, California

Introduction

A number of difficult problems face planners and designers in the coastal zone. However, the conference clearly demonstrated that by combining the talents of the disciplines concerned with the coastline a number of solutions can be found. In this session on structures and materials, we heard nine excellent presentations and viewed a poster presentation on a variety of topics, ranging from numerical modeling of the behavior of a floating breakwater to an assessment of the possible effects of a ship colliding with the Golden Gate Bridge.

Most of these papers emphasized solution-oriented approaches. Two technical topics were especially well represented by coordinated papers. The first paper deals with a study of floating breakwaters performed by the US Army Corps of Engineers, North Pacific Division, using theory and experimental field verification to advance the state of design for such structures. The subject of the second paper deals with the structural integrity of individual concrete armor units used in rubble-mound structures, and it was treated in similar depth. Highlights of papers presented are given below.

Floating Breakwaters

The papers on floating breakwater focus on the problems of determining structure and mooring design forces as well as performance and analysis. Senaka Ratnayake discussed computer-assisted modeling as a viable alternative to costly physical model studies, and George C. England reported on the results of full-scale physical model studies on two types of floating breakwaters.

Marine Construction

Two aspect of marine construction are highlighted in a paper by J. Michel Benoit and one by Harold Davis and John Rutherford. Discussing the benefits of shipyard fabrication, Benoit states that this type of production has led to high quality products by making maximum use of standard materials and repetitive procedures in a well controlled environment. Davis and Rutherford emphasize the need for proper material handling and special construction techniques in order to obtain sound, corrosion-resistant concrete structures in the marine environment. Their paper describes the various types of concrete and reinforcing specified for the new Monterey Bay Aquarium.

Dolos Armor Units

The use of steel fiber reinforcement in large concrete dolosse is presented by Richard A. Gutschow. Of particular interest is the recent experience with such units at Humboldt Bay and Crescent City, California. A program to measure the structural stresses, strains, and forces on dolosse in a high-energy prototype environment is described by Thomas R. Kendall, Gary L. Howell, and Thomas A. Denes. Twenty new 42-ton dolosse are to be instrumented and placed as part of the rehabilitation of the outer breakwater at Crescent City. The poster display by W. F. Baird et al. concerns the design of concrete armor units. Baird presented a procedure to design reinforcement for concrete armor units and to assess the structural integrity of a concrete armor unit.

Erosion Control

The paper by Robert O. Van Atta deals with the degradation of rock (stone) used in coastal erosion control. Drawing on his experience along the central and northern Oregon coast, the author emphasizes durability testing of basaltic rock. Erosion control on a portion of the Siletz River sandspit in

Oregon is described by L. E. Fultz using a "before" and "after" approach. The author emphasizes the need for careful placement of armor rock during construction.

Collision Study

The paper by Wayne O. MacDonell, Bo M. Jensen, and Daniel E. Mohn describes a study to assess both the present structural condition of the pier and fender of the southern tower of the Golden Gate Bridge and their adequacy to resist ship impacts. Possible ship impact effects are described, and strengthening methods are presented.

Orville T. Magoon
Chairman, Structures and
Materials Session

Empirical Prediction of Wind-Generated Gravity Waves

Jung-Tai Lin*, M. ASCE

ABSTRACT: By applying two closure approximations that the wind-wave momentum per unit area per unit weight of the water is characterized by the wind frictional velocity and the dominant wave frequency and that the effective wave drag is proportional to the wind stress exerted on the water surface, the wind-wave momentum equation was solved analytically. The analytical results compare well with experimental data obtained from the laboratory and the field.

Introduction

In the analysis of coastal processes, wave information is one of the critical elements. Prediction of wind-generated gravity waves would provide the necessary information for navigational safety, off-shore and coastal structure design, shoreline protection, oil slick dispersion and ocean wave energy conversion.

For predicting the growth of wind-generated gravity waves, Sverdrup and Munk (29) and Bretschneider (2) analytically solved the fetch equation and the duration equation by using the closure approximation that related the wave steepness to the wave age [see Kinsman (10)]. On the other hand, Mitsuyasu (19) experimentally provided empirical formulas, based on his laboratory and field data, and the field data by Burling (3). In his paper, Mitsuyasu also presented the SMB prediction formulas which appeared to fit the field data reasonably well but not the laboratory data. After reviewing these previous studies in the prediction of wind-wave growth, it becomes clear that further analysis is needed to establish better prediction of wind-waves over a wider range of fetches.

Wind-Wave Momentum

For predicting wave growth, Stewart (28) suggested the wind-wave momentum equation

$$\frac{dM}{dt} = \tau_w \quad \ldots\ldots\ldots\ldots\ldots\ldots\ldots\ldots\ldots\ldots\ldots\ldots\ldots\ldots (1)$$

where M is the wind-wave momentum per unit area, t is the time, and τ_w is the effective wind-wave drag applicable for the wave growth. For irrotational surface waves, M is related to the wave energy per unit area, E, by $M = E/C$ [Phillips (24)], where C is the wave speed. In the case of wind-generated gravity waves, the average wave energy per unit area is expressed by $E = \rho_w g\overline{\eta^2}$, [Barber and Tucker (1)], where ρ_w is the density of the water, g is the gravitational acceleration, $\overline{\eta^2}$ is the mean square of the water surface displacement, η deviated from the mean water surface. If C is approximately represented by the phase speed of the dominant wind wave, C_o, then, the wind-wave momentum per unit area per unit weight of water is expressed as $M/\rho_w g = \overline{\eta^2}/C_o$.

---

*President, United Industries Corporation, 12835 Bell-Red Rd., #120, Bellevue, Wa. 98005, Tel: (206) 453-8995

In order to solve Eq. 1, two closure approximations are required; one is for the wind-wave momentum and the other for the effective wave drag. The first closure approximation is stated as: the wind-wave momentum per unit area per unit weight of the water is characterized by the wind frictional velocity $u_\star$, and the dominant wave frequency n_o. By dimensional reasoning, we have established the following relationship:

$$\frac{\overline{\eta^2}}{C_o} = A_1 \frac{u_\star}{n_o^2} \text{...}(2)$$

where A_1 is a non-dimensional coefficient having a numerical value that could vary with the depth of water due to the effects of shoaling and bottom friction on the wave development. In this paper, we will consider wind waves in deep water, i.e., the water depth is greater than half of the dominant wave length, and expect that A_1 would be a numerical constant. For wind waves in deep water, the phase velocity of the dominant wave C_o is related to the dominant wave frequency by

$$C_o = \frac{g}{n_o} \text{...}(3)$$

and, thus, Eq. 2 is arranged as $\overline{\eta^2}\, n_o^3/u_\star g = A_1$, which is consistent with the rearranged three-halves power law, $\overline{\eta^2}\, n_o^3/U_{10} g$ = const. proposed by Toba (1972). Further, the relationship expressed in Eq. 2 can be used to derive the relationship between the wave steepness H_o/λ_o, and the wave age $g/u_\star n_o$ as below.

$$\frac{H_o}{\lambda_o} = \frac{\sqrt{2A_1}}{\pi} \left(\frac{u_\star n_o}{g}\right)^{\frac{1}{2}} \text{...}(4)$$

using $H_o^2 = 8\overline{\eta^2}$ and $\lambda_o = 2\pi g/n_o^2$. Eq. 4 is consistent with the empirical relationship, $H_o/\lambda_o \sim (C_o/U_{10})^{-\frac{1}{2}}$ suggested by Toba (1972).

Before proceeding further with our analysis, it is important to verify Eq. 2 using the experimental data of wind waves obtained in the laboratory and the field. In Fig. 1, we present the wave momentum per unit area per unit weight of the water, $\overline{\eta^2}/C_o$, plotted against $u_\star/n_o^2$ for wind waves in deep water. These experimental data were obtained under a wide range of wind and wave conditions and in different areas around the world: in the ocean off-shore from Maui, Hawaii by Cox and Munk (4); in a reservoir by Burling (3); in the open Atlantic Ocean by Moskowitz (20); in an open ocean by Longuet-Higgins, et al. (16); in the Hakata Bay by Mitsuyasu (17); in the West Atlantic by Ross, et al. (25); in the Lake Kasumigaura by Taira (30); in the Spanish Banks, Vancouver, Canada by Dobson (5) and by Elliott (7); in Hurricane Camille by Patterson (23); in Hurricane Ava and a North Sea storm by Ross and Cardone (26); in the North Sea by Hasselmann, et al.(9) and by

Von Müller (21); in the East China Sea by Mitsuyasu, et al. (19); in Lake Ontario by Donelan [(6) available from Kitaigorodskii, et al. (11)]; and in four different wind-wave tanks by Mitsuyasu (17), by Wu (33), by Ou (22), and by Liu and Lin (14). When reducing field data presented in Fig. 1, there were cases for which the wind frictional velocity was not directly available. For these cases, we estimated the wind frictional velocity based on the anemometer speed, U_{10}, using the empirical formulas provided by Wu (32) $u_* = \sqrt{C_d} U_{10}$, where $C_d = 0.0026$ for $U_{10} > 15$ m/sec, $C_d = 0.0005 \sqrt{U_{10}}$ for $1 < U_{10} < 15$ m/sec.

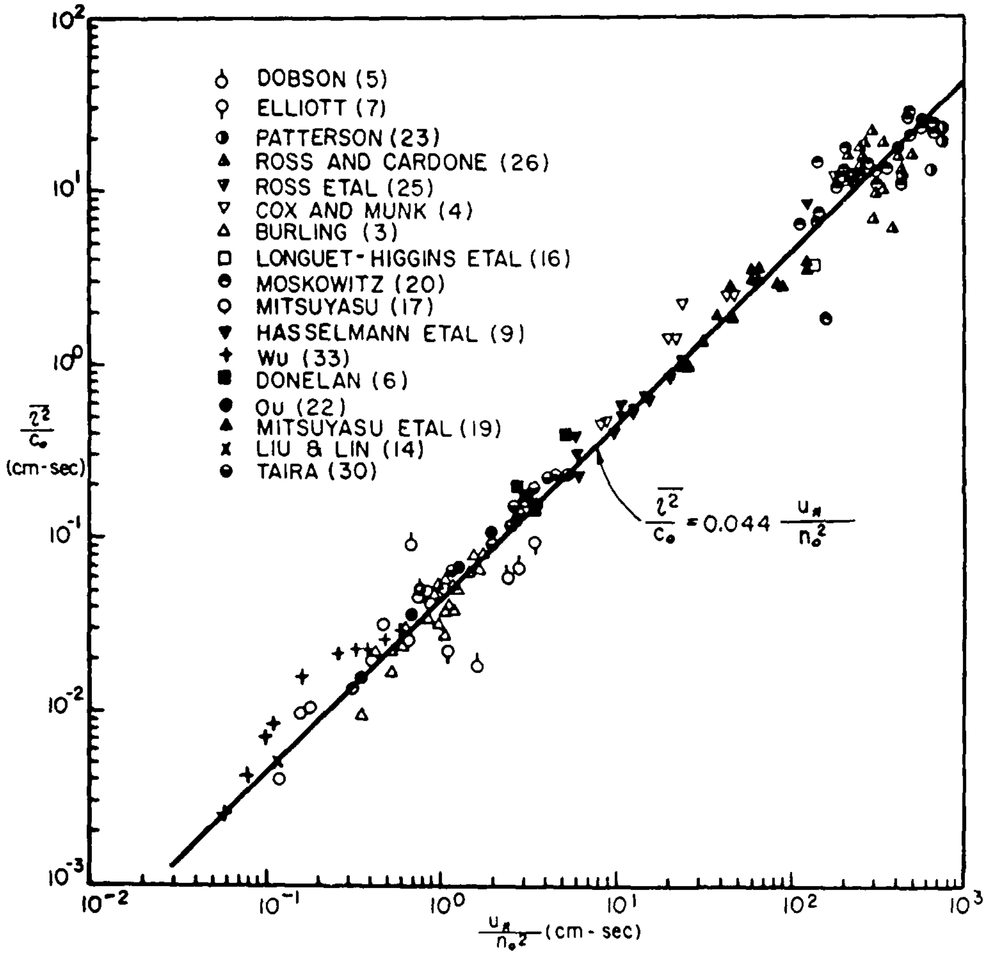

Fig. 1 Wind-wave momentum per unit area per unit weight, $\overline{\eta^2}/C_o$ vs u_*/n_o^2

As shown in Fig. 1, the values of $\overline{\eta^2}/C_o$ and u_*/n_o^2 both cover a wide range of more than four decades on a log-log graph. A solid line is drawn in Fig. 1 to correlate these data and it can be approximated by

$$\frac{\overline{\eta^2}}{C_o} = 0.044 \frac{u_*}{n_o^2} \quad \text{for } 0.06 < \frac{u_*}{n_o^2} < 1000 \text{..............................} (5)$$

Hence, the value of the non-dimensional coefficient A_1 expressed in Eq. 2 is determined to be 0.044. In Fig. 2, we replotted these wave data by H_o/λ_o vs $u_* n_o/g$, and the experimental data are fitted well with the empirical formula

$$\frac{H_o}{\lambda_o} = 0.094 \left(\frac{u_* n_o}{g}\right)^{\frac{1}{2}} \quad \ldots\ldots\ldots\ldots\ldots\ldots\ldots\ldots\ldots\ldots (6)$$

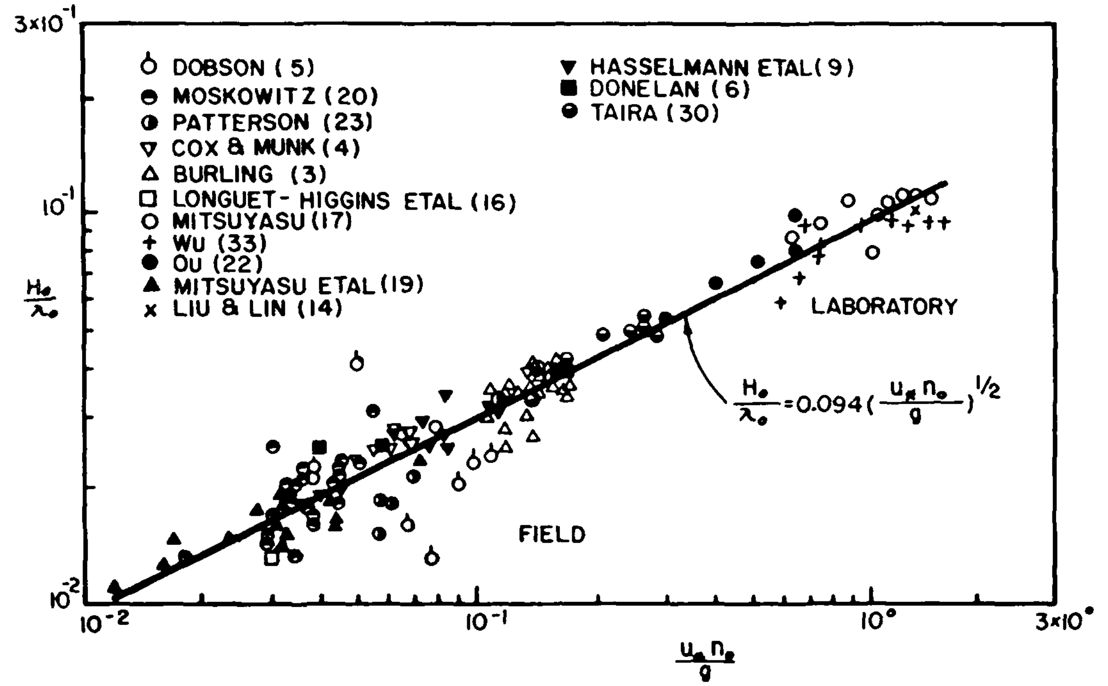

Fig. 2 Wave steepness, H_o/λ_o vs non-dimensional wave frequency $u_* n_o/g$

Wave Growth with Fetch

For steady wind waves, the partial derivative with respect to the time $\partial/\partial t = 0$, and Eq. 1 is rewritten as

$$C_g \frac{dM}{dF} = \tau_w \quad \ldots\ldots\ldots\ldots\ldots\ldots\ldots\ldots\ldots\ldots (7)$$

where F is the fetch, and C_g is the dominant wave group speed which is equal to $C_o/2$ for wind waves in deep water. By substituting Eqs. 2 and 3 into Eq. 7, we have derived the equation expressing the growth of wind waves with fetch,

$$\frac{\rho_w g^2}{2n_o} \frac{d}{dF} \left(\frac{A_1 u_*}{n_o^2}\right) = \tau_w \quad \ldots\ldots\ldots\ldots\ldots\ldots\ldots\ldots\ldots\ldots (8)$$

In order to solve Eq. 8, another closure approximation is required for expressing the effective wave drag τ_w, and it is stated as: The effective wave drag τ_w is proportional to the wind stress exerted on the water surface. By dimensional reasoning, we have established the following relationship:

$$\tau_w = A_2 \rho_a u_*^2 \quad \ldots\ldots\ldots\ldots\ldots\ldots\ldots\ldots\ldots\ldots (9)$$

where A_2 is a non-dimensional coefficient. Substituting Eq. 9 into Eq. 8 and assuming that at zero fetch, the dominant wave period is zero; that coefficients A_1 and A_2 are numerical constants; and that u_*, ρ_a, and ρ_w are independent of the fetch, one may solve Eq. 8 as below:

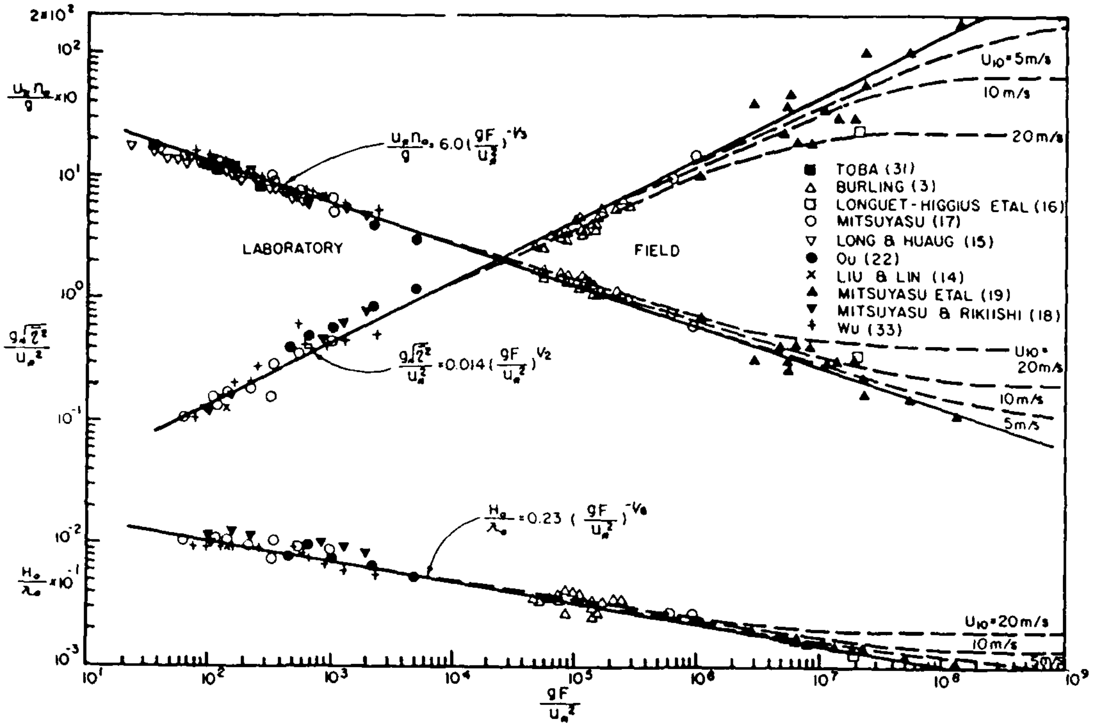

Fig. 3 Comparison of the analytical results of Eqs. 10 and 11 with experimental data for $A_1 = 0.044$, $A_2 = 0.057$, and $\rho_a/\rho_w = 0.0012$

$$\frac{u_* n_o}{g} = \left(\frac{3 A_2 \rho_a}{A_1 \rho_w}\right)^{-1/3} \left(\frac{gF}{u_*^2}\right)^{-1/3} \quad \text{..............................}(10)$$

By combining Eq. 10 with Eq. 2, the following is obtained:

$$\frac{g\sqrt{\bar{\eta}^2}}{u_*^2} = \left(\frac{3 A_2 \rho_a}{\rho_w}\right)^{\frac{1}{2}} \left(\frac{gF}{u_*^2}\right)^{\frac{1}{2}} \quad \text{..................................}(11)$$

To verify the analytical solutions expressed in Eqs. 10 and 11, we present the experimental data available from the laboratories and the field in Fig. 3. Two solid lines are drawn in the figure to represent Eqs. 10 and 11 with $A_1 = 0.044$, $A_2 = 0.057$ and $\rho_a/\rho_w = 0.0012$. Eqs. 10 and 11 appear to fit the experimental data very well for $60 < gF/u_*^2 < 10^6$. At large fetches $gF/u_*^2 > 10^6$, the data points appear to deviate from the respective Eqs. 10 and 11. Furthermore, previous experiments observed that at large fetches, wind-waves would grow to an asymptotic state. To account for these observations, we would further refine the closure approximation of the effective wave drag to be:

$$\tau_w = A_3 \rho_a u_* (U_c - C_o) \quad \text{..}(12)$$

where U_c is the characteristic wind speed responsible for the momentum transfer between the wind and the waves and A_3 is non-dimensional coefficient. Eq. 12 would show that the wave growth would approach an asymptotic state when the dominant wave speed would approach U_c at large fetches, and *the effective wave drag would be significantly* reduced.

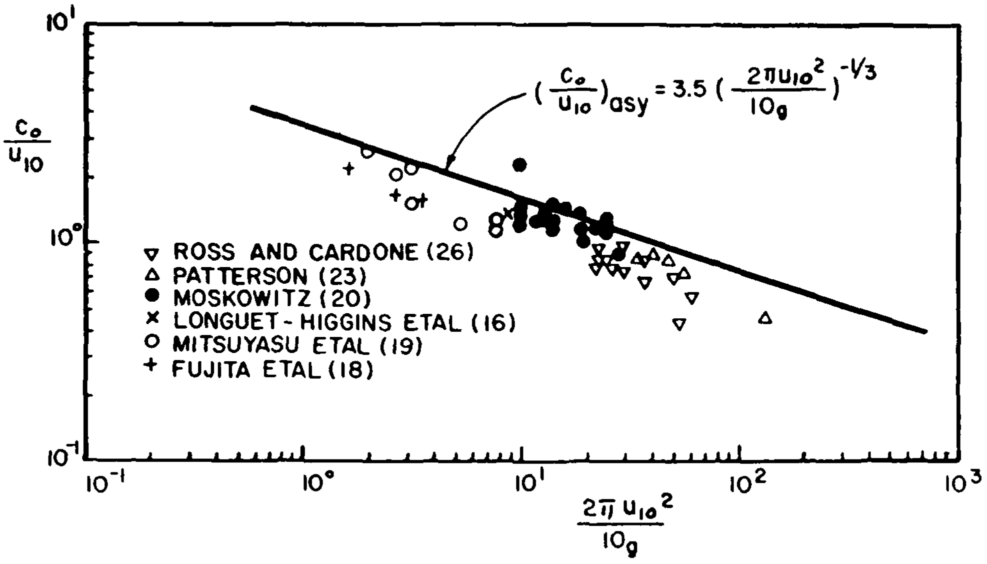

Fig. 4 C_o/U_{10} veried with wind speed U_{10}

For understanding the asymptotic behaviour of the wind waves at large fetches, we examined the wind wave data obtained in the open ocean by Longuet-Higgins, et al. (16), Moskowitz (20), Ross and Cardone (26), Mitsuyasu (19), and Fujita, et al. (8). In Fig. 4, we plotted C_o/U_{10} vs $2\pi U_{10}^2/10g$; here U_{10} is in m/sec and g is in m/sec^2. Further, we assume that the asymptotic development of wind waves may be represented by the envelope applied to the data presented in Fig. 4. For the present analysis, the envelope may be approximated by

$$(\frac{C_o}{U_{10}})_{asy} = A_4(\frac{2\pi U_{10}^2}{10g})^{-1/3} \quad \ldots\ldots (13)$$

where A_4 is a non-dimensional coefficient. Since at large fetches, U_c should approach C_o, Eq. 13 would further suggest that we may obtain an empirical equation for U_c expressed as below:

$$U_c = A_4 U_{10}\,(\frac{2\pi U_{10}^2}{10g})^{-1/3} \quad \ldots\ldots (14)$$

Next, we would assume that at short fetches, $C_o \ll U_c$ and Eq. 11 should become as Eq. 9. Thus, Eq. 12 is rewritten as

$$\tau_w = A_2 A_5 \rho_a u_* (\frac{u_*}{A_5} - C_o) \quad \ldots\ldots (15)$$

where $A_5 = (\sqrt{C_d}/A_4)\,(2\,U_{10}^2/10g)^{1/3}$. By substituting Eq. 15 into Eq. 8, we have obtained a fetch equation

$$\left(\frac{g}{u_* n_o}\right)^2 \frac{d(g/u_* n_o)}{d(gF/u_*^2)} = \frac{A_2 A_5}{A_1}\,\frac{\rho_a}{\rho_w}\left(\frac{1}{A_5} - \frac{g}{u_* n_o}\right) \text{........................} (16)$$

Under the assumed boundary condition that $g/u_* n_o = 0$ at $gF/u_*^2 = 0$, Eq. 16 has the solution expressed as below:

$$-\frac{g}{u_* n_o} - \frac{A_5}{2}\left(\frac{g}{u_* n_o}\right)^2 - \frac{1}{A_5}\ln\left(1 - A_5\frac{g}{u_* n_o}\right) = \frac{A_2 A_5^2}{A_1}\,\frac{\rho_a}{\rho_w}\,\frac{gF}{u_*^2} \text{.............} (17)$$

At short fetches, $A_5 g/u_* n_o \ll 1$, and one may prove readily that Eq. 17 would become Eq. 10. At large fetches, Eq. 17 provides the asymptotic value of $u_* n_o/g$ as

$$\left(\frac{u_* n_o}{g}\right)_{asy} = \frac{\sqrt{C_d}}{A_4}\left(\frac{2\pi U_{10}^2}{10g}\right)^{1/3} \text{..} (18)$$

In Fig. 3, we present the analytical result of Eq. 17 in broken lines for $A_1 = 0.044$, $A_2 = 0.057$, $A_4 = 3.5$, and $\rho_a/\rho_w = 0.0012$ and for three anemometer speeds $U_{10} = 20$, 10, and 5 m/sec. By using Eq. 5, and 17, we can obtain the growth of the rms wave height. In Fig. 3 $g\sqrt{\overline{\eta^2}}/u_*^2$ is plotted vs gF/u_*^2 for those three anemometer speeds.

Wave Growth with Duration

Next we attempted to solve the wind-wave growth with duration as expressed in Eq. 1. By inserting Eqs. 2, and 15 into Eq. 1, a non-dimensionalized duration equation is derived as

$$\frac{d}{d(tg/u_*)}\left(\frac{g}{u_* n_o}\right)^2 = \frac{A_2 A_5}{A_1}\,\frac{\rho_a}{\rho_w}\left(\frac{1}{A_5} - \frac{g}{u_* n_o}\right) \text{......................} (19)$$

Assuming that $g/u_* n_o = 0$ at $tg/u_* = 0$; that A_1, A_2, and A_4 are numerical constants and that u_*, ρ_a, and ρ_w are independent of time, one can solve Eq. 19 as below:

$$-\frac{2g}{u_* n_o} - \frac{2}{A_5}\ln\left(1 - \frac{A_5 g}{u_* n_o}\right) = \frac{\rho_a}{\rho_w}\,\frac{A_2 A_5}{A_1}\,\frac{gt}{u_*} \text{........................} (20)$$

At small durations, i.e., $A_5 g/u_* n_o \ll 1$, Eq. 20 is simplifed as

$$\frac{g}{u_* n_o} = \left(\frac{\rho_a A_2}{\rho_w A_1}\right)^{\frac{1}{2}} \left(\frac{gt}{u_*}\right)^{\frac{1}{2}} \qquad (21)$$

and, by combining Eqs. 21 and 2, the wind-wave rms height growth with duration becomes:

$$\frac{g\sqrt{\overline{\eta^2}}}{u_*^2} = \left(\frac{\rho_a A_2}{\rho_w A_1^{1/3}}\right)^{3/4} \left(\frac{gt}{u_*}\right)^{3/4} \qquad (22)$$

It is worth pointing out that Eq. 22 contains both non-dimensional coefficients A_1 and A_2, while Eq. 11 includes A_2 only. Thus, the value of A_2 can readily be determined by correlating the data of wind-wave rms height with the fetch using Eq. 11.

Based on the analysis for the wind-wave growth with fetch, we have determined that $A_1 = 0.044$, $A_2 = 0.057$, and $A_4 = 3.5$. Using these nondimensional coefficients and $\rho_a/\rho_w = 0.0012$, we have derived the wind-wave growth with duration at small durations,

$$\frac{u_* n_o}{g} = 25.4 \left(\frac{gt}{u_*}\right)^{-\frac{1}{2}} \qquad (23)$$

$$\frac{g\sqrt{\overline{\eta^2}}}{u_*^2} = 0.0016 \left(\frac{gt}{u_*}\right)^{3/4} \qquad (24)$$

Two solid lines are drawn in Fig. 5 to represent Eqs. 23 and 24. For comparison, we have plotted the experimental data obtained in the Lake Kasumigaura by Taira (30) and in a wind-wave tank by Mitsuyasu and Rikiishi (18). The field data compares well with the analytical results expressed in Eqs. 23 and 24, but the laboratory data deviates from these results. The following is our explanation for the discrepancy.

The transient measurement of wind-wave growth with duration should, by definition, be conducted by following the waves at the dominant wave group speed; however, this kind of measurement is difficult to perform. Instead, the transient measurement has been conveniently conducted at a fixed station to record the variation of wave growth with time. Mathematically, the transient measurement would in essence assume that $d/dt = \partial/\partial t$ by neglecting the partial derivative with fetch, or $\partial/\partial F = 0$. This assumption may be valid when the origin of the wave generation is far away from the observation station, and it may conveniently be satisfied in the field. For example, in Taira's experiment, the observation station was about 12 km downwind from the shoreline of the Lake Kasumigaura.

Effective Wind Wave Drag

According to Eq. 15, the effective wind-wave drag coefficient is defined as

$$C_w = \frac{\tau_w}{\rho_a u_*^2} = A_2 \left\{1 - A_5 \frac{g}{u_* n_o}\right\} \qquad (25)$$

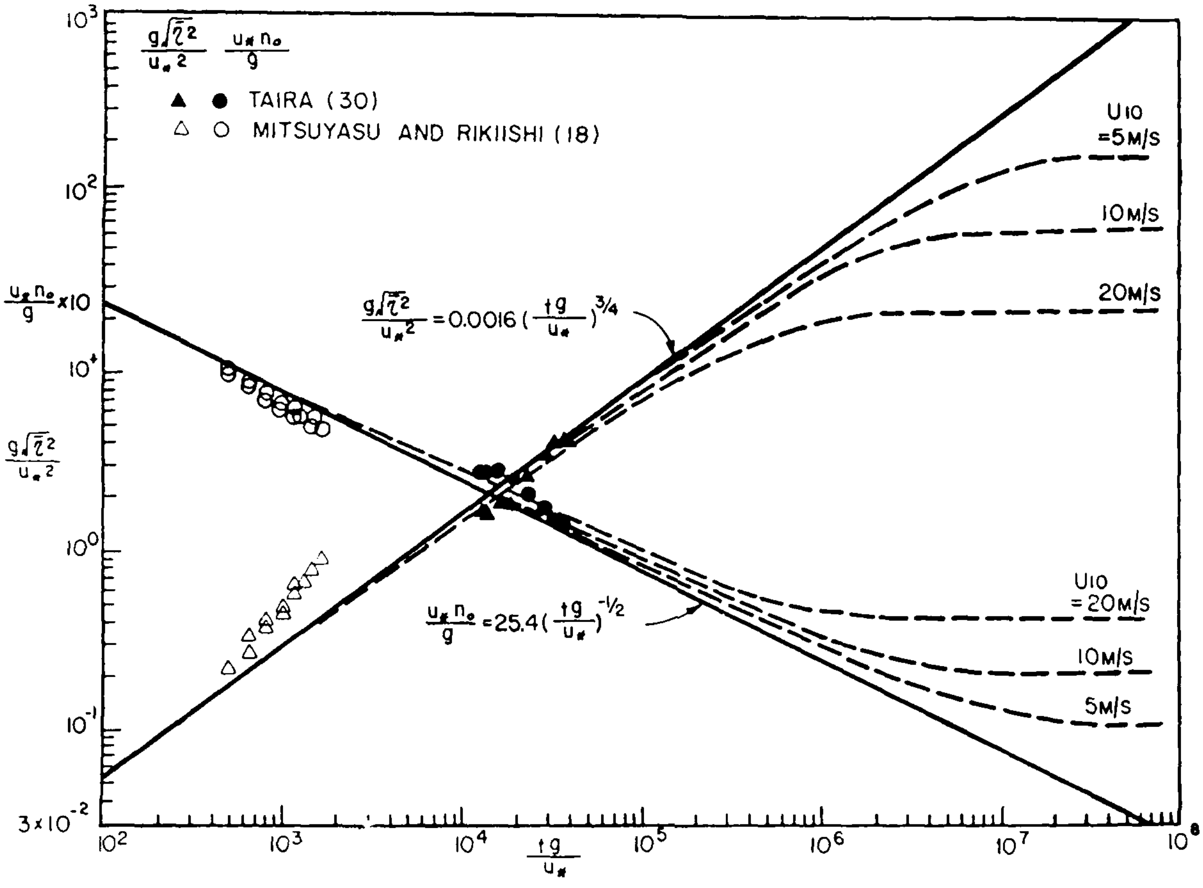

Fig. 5 Comparison of the analytical results of Eqs. 21 and 22 with experimental data for $A_1 = 0.044$, $A_2 = 0.057$, and $\rho_a/\rho_w = 0.0012$

In Fig. 6, we have plotted the effective wind-wave drag coefficient C_w vs $g/u_* n_o$ for three anemometer speeds at U_{10} = 20, 10, and 5 m/sec. When $g/u_* n_o << 1$ for short fetches or durations, the value of C_w has an asymptotic value of 0.057. As $g/u_* n_o$ increases for a given U_{10}, the value of C_w decreases to zero at the asymptotic value of $g/u_* n_o$. Taira (1972) conducted field experiments to measure the value of C_w and his data are presented in Fig. 6 for comparison with Eq. 25. The value of C_w was estimated to be less than 0.1 by Phillips (24) based on his analysis of wind-wave spectrum, 0.2 by Stewart (28), 0.1 by Starr (27) and 0.06 ~ 0.07 by Korvin-Kroukovsky (12).

From measurements in two separate wind-wave tanks, Wu (33) and Lin and Gad-el-Hak (13) observed that about half of the wind stress is transferred to the water turbulent boundary layer directly underneath the water surface (the surface layer). According to the present analysis based on the closure approximations expressed in Eqs. 2 and 15, the effective wind-wave drag responsible for the wind-wave growth is only about 6 percent of the wind

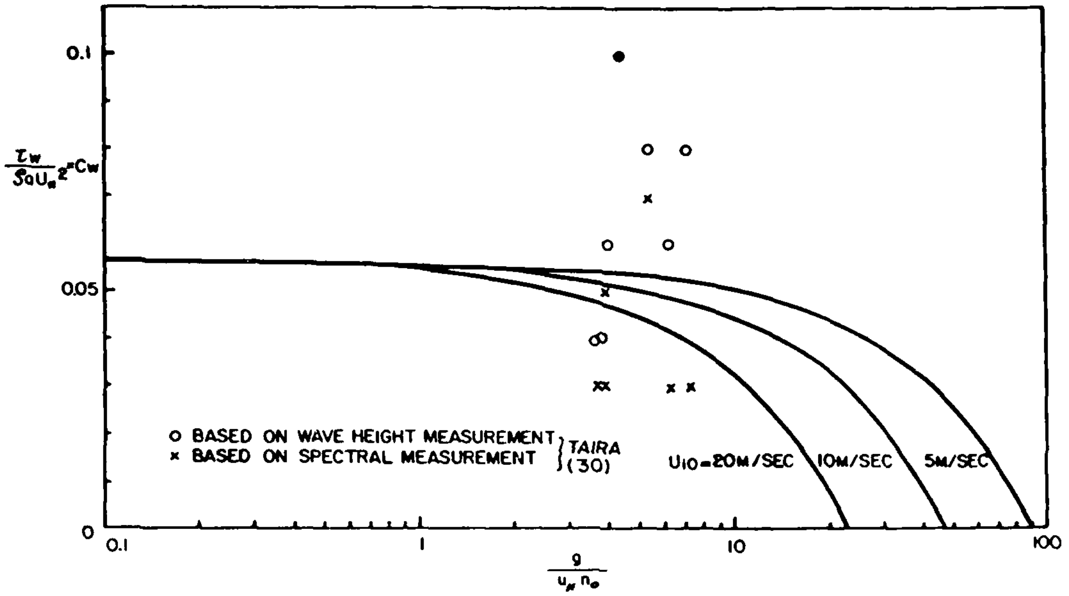

Fig. 6 Effective wind-wave drag coefficient C_w vs the wave age $g/u_* n_o$

stress for small fetches or durations and becomes even smaller for larger fetches or durations. If the measurement results obtained in the laboratory by Wu, and by Lin and Gad-el-Hak are applicable to the field, i.e., about half of the wind stress is transferred to the surface layer and if the effective wind-wave drag coefficient is limited to about 6 percent of the wind stress, then about 44 percent of the wind stress would transfer through the surface layer possibly by the wave breaking process, and contribute to the underlying currents of the ocean below the surface layer.

Discussion

When establishing the empirical equation of the characteristic wind speed U_c which is responsible for the momentum transfer between the wind and the waves, we have relied on the experimental data plotted in Fig. 4 to suggest Eq. 14 with $A_4 = 3.5$. The data plotted in Fig. 4 is by no means exhaustive. Additional field data plotted in Fig. 4 could suggest a different value of the coefficient A_4 or even a different formulation of Eq. 14. Research is therefore urged to obtain additional field data to further define U_c.

In deriving the analytical results expressed in Eqs. 10, 17, and 20, we assumed that u_*, ρ_a, and ρ_w would not vary with the fetch or the duration. When the wave field developed over a large fetch or a long duration, then, one may solve Eq. 7 or 1 together with the two closure approximations expressed in Eqs. 2 and 15 by using the finite difference method with the specified values of u_*, ρ_a, and ρ_w over the fetch or the duration.

Acknowledgement

This paper was prepared under an IR&D funding available from the Ocean Wave Energy Conversion Program of United Industries Corporation.

APPENDIX I - Reference

1. Barber, N. F. and Tucker, M. J., "Wind Waves", The Sea ,ed. by M. N. Hill, Vol. 1: Physical Oceanography, Interscience, New York, 1966, pp. 664 - 669.
2. Bretschneider, C. L., Revisions in Wave Forecasting: Deep and Shallow Water", Proc. 6th Conf. on Coastal Engineering, ASCE, Council on Wave Research, 1958.
3. Burling, R. W., "The Spectrum of Wave at Short Fetches", Dtsch. Hydrogr. Z., Vol. 12, 1959, pp. 45-64, pp. 96-117.
4. Cox, C. and Munk, W., "Measurement of the Roughness of the Sea Surface from Photographs of the Sun's Glitter", J. Opt. Soc. Amer., Vol. 44. No. 11, 1954, pp. 838-850.
5. Dobson, F. W., "Measurements of Atmospheric Pressure on Wind-Generated Sea Waves", J. Fluid Mech., Vol. 48, 1971, p. 91.
6. Donelan, M.A., "Whitecaps and Momentum Transfer", Turbulent Fluxes through the Sea Surface, Wave Dynamics and Prediction, Favre, A. and Hasselmann, K., eds., Plenum Press, 1978, pp. 273 - 287.
7. Elliott, J.A., "Microscale Pressure Fluctuation Near Waves being Generated by the Wind", J. Fluid Mech., Vol. 54, 1972, p. 427.
8. Fujita, T., Nemato, S., Tekeuchi, K. and Tosha, M, "Vertical Profile of Wind Speed over the Open Sea", J. Meteoro. Soc., Japan, Vol. 61, 1983, pp. 100-109.
9. Hasselmann, K., Ross, D. B., Von Müller, P., and Sell, W., "A Parametric Wave Prediction Model", J. Phys. Oceano., Vol. 6, 1976, pp. 200-228.
10. Kinsman, B., Wind Waves, Prentice Hall, Inc., Englewood Cliffs, N.J., 1965.
11. Kitaigorodskii, S. A., Donelan, M.A., Lumley, J.L. and Terray, E.A., "Wave Turbulent Interactions in the Upper Ocean. Part II Statistical Characteristics of Wave and Turbulent Components of the Random Velocity Field in the Marine Surface Layer", J. Phys. Oceano, Vol. 13, 1983, pp. 1988-1999.
12. Korvin-Kroukovsky, B.V., "Balance of Energies in the Development of Sea-Waves: Semiemperical Evaluation", Dept. Hydrograph. Z., Vol. 18, 1965, pp. 145-160.
13. Lin, J. T. and Gad-el-Hak, M., "Turbulent Current Measurements in a Wind-Wave Tank", J. Geophy. Res., Vol. 89, 1984, pp. 627-636.
14. Liu, H. T. and Lin, J. T., "On Spectrum of High-Frequency Wind Waves", J. Fluid Mech., Vol. 123, 1982, pp. 165 - 185.
15. Long, S. R. and Huang, N. E., "On the Variation of Growth of Wave Slope Spectra in the Capillary - Gravity Range with Increasing Wind", J. Fluid Mech., Vol 77, 1976, pp. 209-228.
16. Longuet-Higgins, M. S., Cartwright, D.E. and Smith, N.O., "Observations of the Directional Spectrum of Sea Waves using the Motions of a Floating Buoy", Ocean Wave Spectra, Englewood Cliffs, N.J., Prentice-Hall Inc., 1963, pp. 111 - 136.
17. Mitsuyasu, H., "On the Growth of the Spectrum of Wind-Generated Waves (I)", Reports of Research Institute for Applied Mechanics, XVI, Vol. 55, Kyushu Univ., Japan, 1968.

18. Mitsuyasu, H., and Rikiishi, K., "The Growth of Duration Limited Wind Waves", J. Fluid Mech.,Vol. 85, 1978, pp. 705-730.

19. Mitsuyasu, H., Tasai, F., Sukara, T., Mizuno, S., Ohkusu, M., Honde, T., and Rikiiski, K., "Observation of the Power Spectrum of Ocean Waves Using a Clover Leaf Buoy", J. Phys. Oceanogr., Vol. 10, 1980, pp. 286-296.

20. Moskowitz, L., "Estimates of the Power Specra for Fully Developed Seas for Wind Speeds of 20 to 40 knots", Tech. Report for U.S. Navy Oceanographic Office under Contract N62306-1042, 1963.

21. Von Müller, P., Parameterization of One-Dimensional Wind waves Spectra and their Dependence on the State of Development, Max-Planck-Institute for Meteorology, University of Hamburg, West Germany, 1976.

22. Ou, S. H., "The Equilibrium Range in Frequency Spectra of the Wind-Generated Gravity Waves", Proc. 4th Conference on Ocean Engineering in Republic of China, Taiwan, ROC, Sept., 1980, pp. 217 - 227.

23. Patterson, M. M., Oceanographic Data from Hurricane Camille, Shell Co. Report, 1974.

24. Phillips, O. M., The Dynamics of the Upper Ocean, Cambridge, 1966.

25. Ross, D.B. and Cardone, V.J., and Conaway, J. W., "Laser and Microwave Observations of Sea-Surface Conditions for Fetch-Limited 17 to 25 m/s Winds", IEEE Trans Geosci. Electronics, GE-8, 1970, pp. 326.

26. Ross, D.B. and Cardone, V.J., "Observations of Oceanic White Caps and Their Relation to Remote Measurements of Surface Wind Speed", J. Geophys. Res., Vol. 79, 1974, pp. 444-452.

27. Starr, V.P., "A Momentum Integral for Surface Waves in Deep Water", J. Marine Res., Vol. 24, 1947, pp. 141-178.

28. Stewart, R. W., "The Wave Drag of Wind Over Water", J. Fluid Mech, Vol. 10, 1961, pp. 189-194.

29. Sverdrup, H. U. and Munk, W. H., "Wind, Sea and Swell: Theory of Relations for Forecasting", U.S. Navy Hydrographic Office Publ. No. 601, 1947, 44 pp.

30. Taira, K., "A Field Study of the Development of Wind Wave", J. Oceano. Soc., Japan, Vol. 28, 1972, pp. 187-202.

31. Toba, Y., "Local Balance in the Air-Sea Boundary Processes, I. on the Growth Process of Wind Waves", J. Oceano. Soc. Japan, Vol. 28, 1972, pp. 109-121.

32. Wu, J., "Wind Stress and Surface Roughness at Air-Sea Interface", J. Geophy. Res., Vol. 74, 1969, pp. 444-455.

33. Wu, J., "Wind Induced Drift Currents", J. Fluid Mech, Vol. 68, 1975, pp. 49-70.

Extending Wave Station Measurements to Intermediate Locations by Wave Transformation Models

Omar Shemdin*

Paper unavailable at time of publication.

---

* Ocean Research and Engineering, La Canada, California.

Coast of California Storm and Tidal Waves Study: Preliminary Observations from the San Diego Region Directional Wave Data Network and Beach Profile Program

Thomas J. Dolan[1]
A.M., ASCE

Abstract

The Coast of California Storm and Tidal Waves Study (CCSTWS) implemented a comprehensive regional coastal zone monitoring program in 1983. This program focuses on the San Diego Region of the southern California shoreline from Dana Point to the Mexican Border. Two major components of this program are a directional wave data network comprised of five nearshore wave arrays and an offshore buoy, and semi-annual beach and nearshore bathymetric surveys. Preliminary analysis of the directional wave data indicates that the wave network provides sufficient resolution to detect long period southern and northern swell events from individual storms. Complete analysis of the entire synoptic 18 month wave data set should provide the first long-term empirical estimation of the effects of island sheltering on southern California's nearshore wave climate. The initial three beach profile surveys suggest that the southern California coastline undergoes a typical seasonal transformation from a summer to a winter profile, however, many anomalies were observed which may reflect local conditions. Data collected as part of CCSTWS will provide a baseline data set for the southern California littoral zone on which to base future engineering and planning studies and decisions.

Introduction

Coastal erosion problems, whether a result of man or nature, can not be examined in isolation. The budget of sediment in the littoral zone is controlled by a dynamic system of processes operating over broad spatial and temporal scales. Short-term, site-specific studies often do not provide sufficient data with which to assess the impact of proposed coastal structures or modifications to the upcoast and downcoast shoreline. In order to provide a sound basis for future U.S. Army Corps of Engineers planning studies and long range coastal planning, the Coast of California Storm and Tidal Waves Study (CCSTWS) was initiated by the Los Angeles District in 1982 with funds appropriated by the

---

[1] Project Manager, U.S. Army Corps of Engineers, Los Angeles District, Coastal Resources Branch, SPLPD-CS, P.O. Box 2711, Los Angeles, CA 90053

House Energy and Water Development Appropriations Committee in its bill, Report No. 97-177, 97th Congress, July 14, 1981.

The primary purpose of CCSTWS is to provide coastal data and information to planners and decision-makers so that more informed decisions can be made regarding the restoration and maintenance of the 1,100 mile California coastline. The study's objectives include the quantification of regional sediment budgets (sediment sources, sinks and transport characteristics), quantification of past shoreline changes, and the application of techniques which can assess, on a regional scale, future shoreline changes (13, 14). In 1983 work began in the San Diego Region, an 80 mile costal reach encompassing the shoreline between Dana Point and the Mexican Border (Figs. 1, 2). Work activities include field data collection, historical research and literature review. The key study feature in this region is the operation of a coastal zone monitoring program which provides concurrent collection of critical coastal processes data. This monitoring program consists of the following elements:

-Wave data collection, including five directional wave arrays and one offshore directional wave buoy

-Semi-annual beach and nearshore bathymetric surveys at 50 stations

-Sediment sample analysis of cliff, beach and nearshore sediment

-River sediment disharge data collection at six stations

-Semi-annual aerial color photography

-Submarine canyon transport study

This paper deals exclusively with preliminary observations based upon the data collected by the directional wave data network and the beach profile program. The reader should consult the reference list for CCSTWS publications which discuss the other elements of the regional monitoring program (14 ,15).

Study Area

Approximately 63 miles of the 80 mile length of the San Diego Region's shoreline are developed. The remaining 17 miles of coastline, along the U.S. Marine Corps Base at Camp Pendleton, remain in an almost natural state (1). Beaches in the region are generally backed by cliffs which are broken by numerous rivers, streams, and lagoons. Beaches are composed of a variety of sediments ranging from fine sand to cobble depending on the native

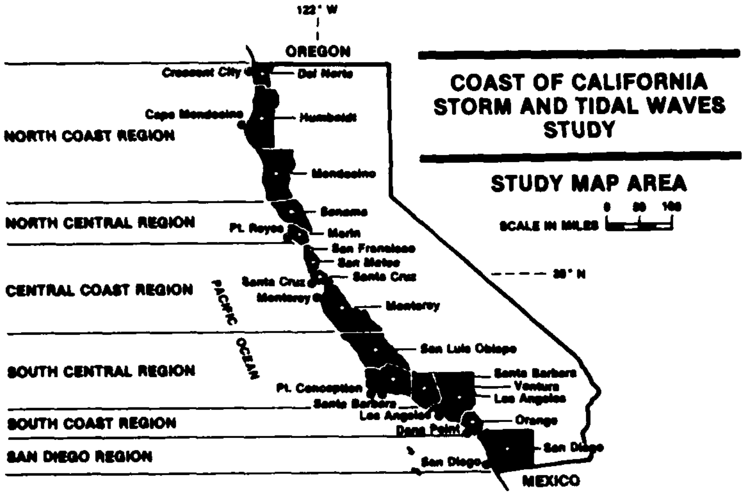
122° W
OREGON
COAST OF CALIFORNIA
STORM AND TIDAL WAVES
STUDY
STUDY MAP AREA
0 50 100
SCALE IN MILES
36° N
NORTH COAST REGION
NORTH CENTRAL REGION
CENTRAL COAST REGION
SOUTH CENTRAL REGION
SOUTH COAST REGION
SAN DIEGO REGION
PACIFIC OCEAN
Crescent City
Del Norte
Cape Mendocino
Humboldt
Mendocino
Sonoma
Pt. Reyes
Marin
San Francisco
San Mateo
Santa Cruz
Santa Cruz
Monterey
Monterey
San Luis Obispo
Pt. Conception
Santa Barbara
Santa Barbara
Ventura
Los Angeles
Los Angeles
Orange
Dana Point
San Diego
San Diego
MEXICO

Fig 1. CCSTWS Study Area Map

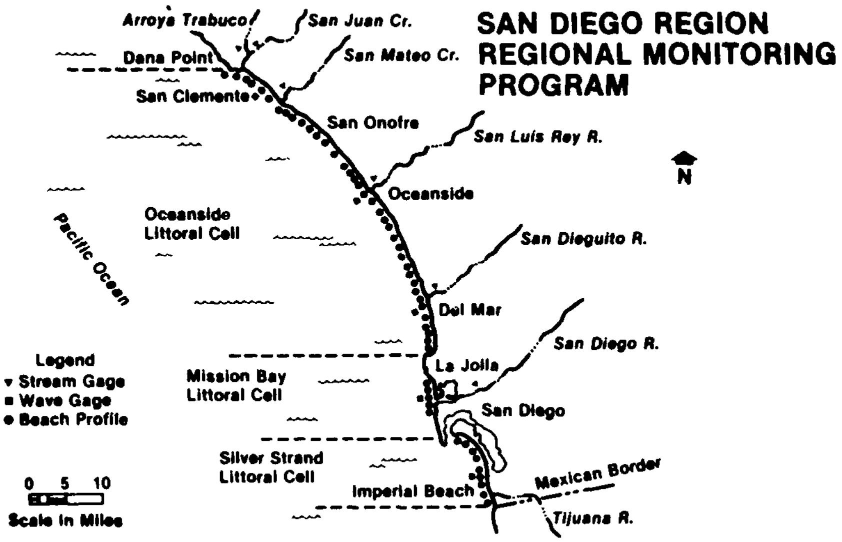
SAN DIEGO REGION
REGIONAL MONITORING
PROGRAM
N
Arroyo Trabuco
San Juan Cr.
San Mateo Cr.
Dana Point
San Clemente
San Onofre
San Luis Rey R.
Oceanside
Oceanside
Littoral Cell
Pacific Ocean
San Dieguito R.
Del Mar
San Diego R.
La Jolla
San Diego
Mission Bay
Littoral Cell
Silver Strand
Littoral Cell
Imperial Beach
Mexican Border
Tijuana R.
Legend
▾ Stream Gage
■ Wave Gage
● Beach Profile
0 5 10
Scale in Miles

Fig 2. San Diego Region Littoral Cells and Locations of Primary Elements of Regional Coastal Zone Monitoring Program.

source material and the erosional state of the beach. Rock outcroppings are sometimes found nearshore paralleling the beach. Littoral cells in the San Diego Region are relatively well defined by the presence of rock headlands or points which act as littoral barriers that tend to contain and segment littoral sediments. Figure 2 identifies the three major littoral cells composing the region: Oceanside, Mission Bay and Silver Strand. Areas which have experienced severe coastal erosion include Capistrano Beach (near San Clemente), Oceanside, Carlsbad, and Imperial Beach.

The nearshore wave climate is strongly influenced by the geography of the southern California bight, that area south of Pt. Conception. Point Conception and the Channel Islands provide a degree of sheltering from storm generated waves. Only waves with approach angles falling within the gaps or "windows" between the islands can directly impinge upon the coast, otherwise the wave energy is partially or fully blocked by the islands. Unblocked wave energy and direction can also be dramatically influenced by the process of refraction around the offshore islands and banks. Waves affecting southern California originate from any one, or a combination, of four sources (6). During the northern hemisphere winter extratropical low pressure systems originating in the Gulf of Alaska move in a easterly direction and can generate significant swells which approach southern California from the northwest quadrant. The storms typically track north of Pt. Conception but during the El Nino years of 1982-1983 the storm tracks were shifted south, permitting large waves to approach the coast directly from the west and those waves were not appreciably blocked by the Channel Islands. During the northern hemisphere summer (the southern hemisphere's winter) southern California can receive wave energy from two distinct southern sources. Waves approaching from the south-southwest sector are common when tropical storms which form over the Mexican Baja peninsula move out to sea in a westerly direction. Less common, but still significant, are the long period southern swells from the southwest quadrant which originate from intense lows in the southern hemisphere and can propagate over 6000 miles before landfall. In addition to these three storm sources of wave energy, local winds within the Channel Island chain are important in producing local, short period waves (i.e., sea).

Wave Data Collection

The CCSTWS wave data collection program has three primary objectives: (1) document nearshore wave climate and potential longshore transport, (2) collect sufficient directional wave data to develop empirical estimators of nearshore wave energy given the wave climate in a deep ocean non-sheltered location, and (3) provide data with which to test numerical wave transformation models which incorporate the dominant physical processes which control the propagation of wave energy through the island chain, i.e., island blocking, refraction, and diffraction.

Nearshore wave data is provided by a set of five nearshore wave arrays or "slope arrays" located at Imperial Beach, Mission Bay, Del Mar, Oceanside, and San Clemente (Fig. 3). The arrays were sited at these specific locations in the San Diego Region in order to gain information about the spatial variability of wave energy (9). The arrays feature four pressure transducers, each mounted on the end of steel members in a cross configuration measuring 6 m on a side. The arrays are located in approximately 10 m of water. Seventeen minutes of data (1024 data points) are transmitted by phone line to a Prime mini-computer at the Scripps Institution of Oceanography in La Jolla every 6 hours for analysis (11). Four sensor arrays were chosen because analysis of the four pressure signals provides the sea surface slope components from which the longshore component of momentum flux (Sxy) can be calculated. The momentum flux estimates then provide a basis on which to calculate wave direction and potential longshore sediment transport. The papers by Seymour and Higgins (3, 10) should be consulted for a complete description of the slope array data analysis methodology. This nearshore wave data program is cooperatively funded by the U.S. Army Waterways Experiment Station, CCSTWS, and the Los Angeles District. The system is operated and maintained by the Scripps Institution of Oceanography.

Deepwater, offshore directional wave data is provided by a National Oceanic and Atmospheric Administration (NOAA) 10 m diameter discus hull buoy. The buoy was deployed for an 18 month period from April 1984 to October 1985. Its location at 32.8 N and 119.5 W placed it in the Tanner Basin in a depth of approximately 1390 m (Fig. 3). This location placed it approximately 200 km west of San Diego and seaward of the Channel Islands, where it was open to unsheltered swells and seas approaching from any angle between the northwest and the south. The buoy was instrumented with a heave-pitch-roll wave data analysis system; a 17 minute record was analyzed every hour and the results transmitted via GOES satellite to the NOAA Data Buoy Center in Mississippi. Data products include wind velocity, wave energy spectra, and principal wave direction. Directional spectra are determined by the classical method of Longuet-Higgins et. al. (4). The paper by Steele et. al. (12) should be consulted for full details of the analysis procedures.

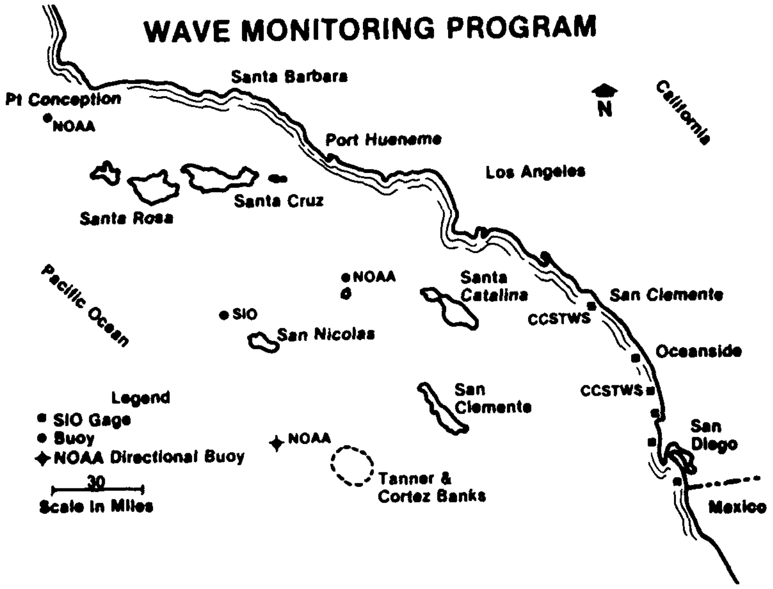
WAVE MONITORING PROGRAM
Pt Conception
NOAA
Santa Barbara
Port Hueneme
Los Angeles
N
California
Santa Rosa
Santa Cruz
Pacific Ocean
NOAA
SIO
Santa Catalina
San Nicolas
CCSTWS
San Clemente
Oceanside
CCSTWS
San Clemente
San Diego
Legend
■ SIO Gage
● Buoy
✦ NOAA Directional Buoy
30
Scale in Miles
NOAA
Tanner & Cortez Banks
Mexico

Fig 3. San Diego Region Wave Data Network.

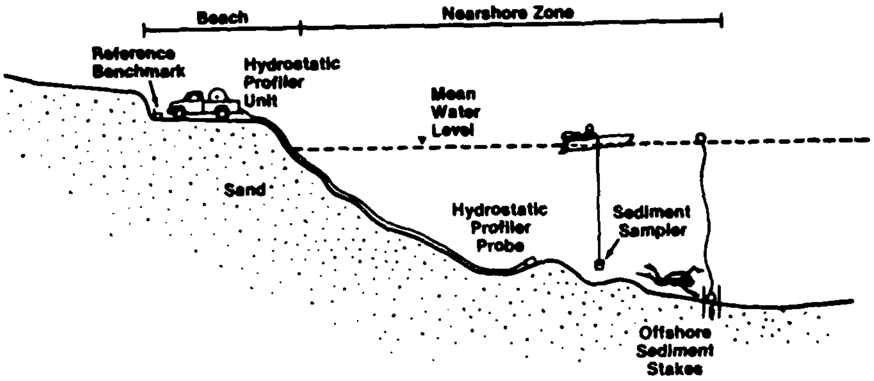
Beach
Nearshore Zone
Reference Benchmark
Hydrostatic Profiler Unit
Mean Water Level
Sand
Hydrostatic Profiler Probe
Sediment Sampler
Offshore Sediment Stakes

Fig. 4. Beach Profile Program: Hydrostatic Profiler System, Sediment Collection and Offshore Rods.

Beach and Nearshore Bathymetric Data Collection

The primary objective of the beach profile program is to characterize, on a regional scale, the seasonal fluctuations in the beach profile and nearshore bathymetry over a four year period. This time history of the beach profile will provide essential information regarding the offshore/onshore movement of littoral sediment, the changes in sand volume and the movement of the mean water line.

The beach and nearshore bathymetry program consists of surveys at 50 sites established at 1 to 2 mile intervals along the sandy coastline of the San Diego Region (see Fig. 2). The surveys are scheduled twice a year, during the late summer and early autumn (September and October) and following the winter storm season (April-May). The Scripps Institution of Oceanography conducted the initial three surveys discussed in this paper using a hydrostatic profiler system (16). The system features a closed water-filled tube, approximately 600 m long, which is towed offshore by a small boat (Fig. 4). The tube is fitted with pressure transducers at either end. The elevation difference between the ends of the cable results in a pressure difference which is recorded as the cable is winched back towards the shore. This pressure difference is directly related to the elevation difference (by the hydrostatic pressure relationship) between the two ends of the tube. The pressure and offshore distance data is recorded on a data cassette which is returned to the lab for editing and analysis. All measurements are referenced to a benchmark permanently established on the beach. The vertial accuracy of the profiler is approximately ±10 cm. Beach profile measurements were limited to a depth of about -6 m (mean lower low water) because of the length and bulk of the cable. In addition, offshore sedimentation reference rods were established at depths of -6, -10, and -15 m in order to measure sand level changes of less than 2 cm in water depths greater than the operational depth of the hydrostatic profiler system. The reference rods are monitored by divers who measure the distance of the sand bed from the top of the rod.

Preliminary Observations

Wave Data. Tropical storm activity in the eastern Pacific Ocean off the Baja peninsula was at a high level during the summer and early autumn of 1985. Twenty-four tropical storms were recorded, and most of these storms tracked west or northwest sending swells with periods of 10 to 14 seconds to southern California. The CCSTWS wave data network was in full operation during this period and the arrival of these southern tropical storm swells was documented. One example of this synoptic data record will be discussed below.

On 1 July 1985 Hurricane Delores was located approximately 1000 miles south of San Diego (Fig. 5). The storm had sustained winds of 60 mph and was moving in a northwest direction. The energy density spectrum recorded at the Tanner Basin buoy on 2 July 1985 is shown in Figure 6. The spectrum displays two distinct peaks, a dominant peak at about 11 s (0.09 hz) and a secondary peak at about 6 s (0.16 hz). The upper panel displays the mean wave direction at each frequency and clearly shows a discontinuity in direction. The long period spike is associated with a wave direction of approximately 180 degrees (true south) and represents the swells generated by the hurricane. (All wave angles are in relation to true north and represent the angle from which the wave is approaching. Therefore, 180 degrees represents wave fronts approaching directly from the south.) The secondary peak exhibits a wave direction of approximately 320 degrees or almost directly in line with the wind direction of 315 degrees. The directional data clearly suggests that the shorter period wave energy represents a transitional local sea/swell condition at the buoy.

The concurrent nearshore energy spectra recorded at Imperial Beach, Oceanside, and San Clemente is shown in Figure 7. The upper panel of each diagram also shows wave direction but the information shown in those panels requires a different interpretation. The slope arrays are located in about 10 m water depth and, therefore, wave refraction causes the wave to approach the shore almost normally (i.e., the wave front is almost parallel to the beach) by the time the wave passes over the slope array. However, there is still a component of the original deep water wave direction present and this is detected by comparing the calculated wave direction against the orientation of the shore normal. Wave directions less than the shore normal direction represent a southern deep water wave direction, and directions greater than the shore normal angle represent a northern deep water direction. This rationale assumes straight and parallel contours offshore of the slope arrays; this assumption is grossly valid in the vicinity of the arrays.

The nearshore energy spectra (Fig. 7) demonstrate that each slope array site was open to the hurricane swell. All three arrays recorded the distinct energy spike at 11 s that was also recorded by the buoy. The southern direction of the swell was also detected and is represented by the fact that wave direction angles in the vicinity of the energy peak were less than the shore normal angle at each site. The Imperial Beach spectrum (Fig. 7a) exhibits a reduced energy peak compared to Oceanside and San Clemente (Figs. 7b,c). Both Oceanside and San Clemente are oriented more towards the south (shore normals of 235 and 237 deg., respectively) compared to Imperial Beach (283 deg.) Southern swells would undergo a greater degree of refraction at

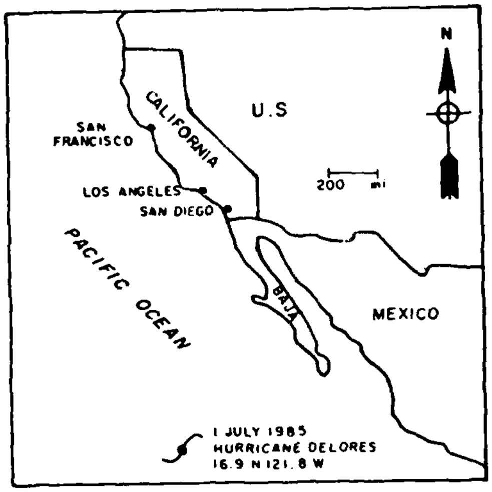
N
U.S
CALIFORNIA
SAN FRANCISCO
200 mi
LOS ANGELES
SAN DIEGO
PACIFIC OCEAN
BAJA
MEXICO
1 JULY 1985
HURRICANE DELORES
16.9 N 121.8 W

Fig. 5. Location of Hurricane Delores on 1 July 1985.

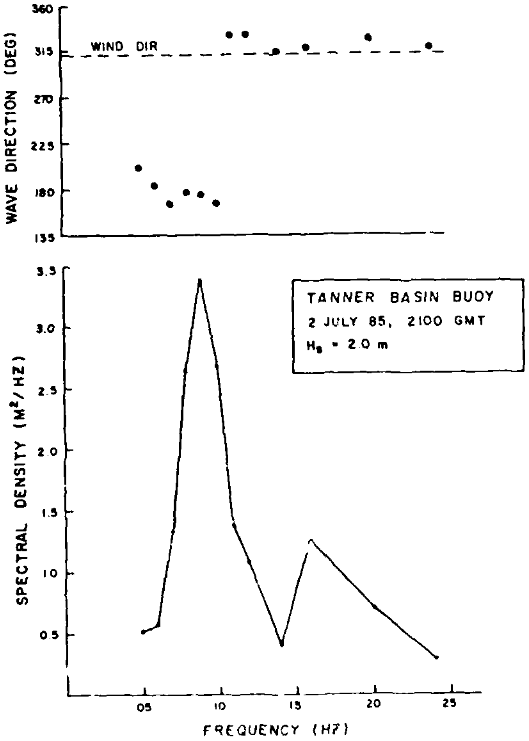

Fig. 6. Tanner Basin Buoy Energy Density Spectrum and Wave Direction for 2 July 1985.

AD-A168 715 PROCEEDINGS OF WEST COAST REGIONAL COASTAL DESIGN 5/5
CONFERENCE HELD ON 7-8 NOVEMBER 1985 AT OAKLAND
CALIFORNIA(U) CORPS OF ENGINEERS SAN FRANCISCO CALIF
UNCLASSIFIED SOUTH PACIFIC DIV APR 86 F/G 13/2 NL

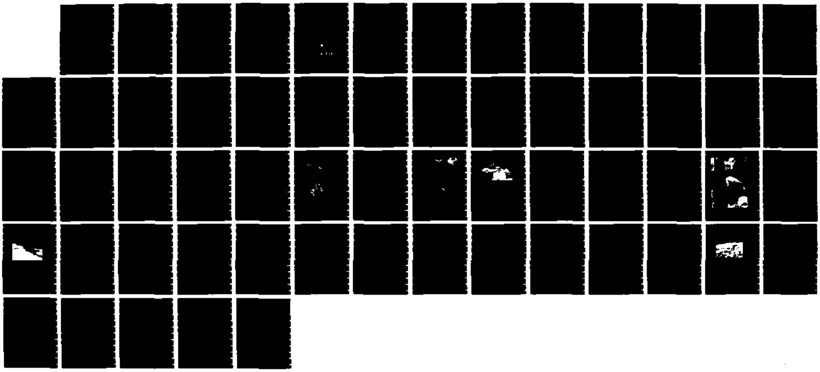

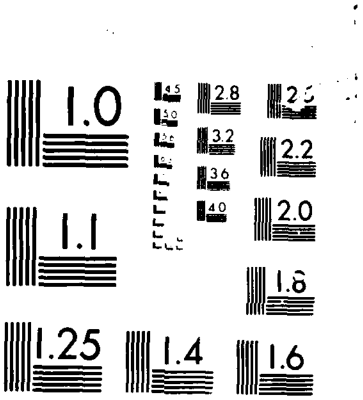
1.0
1.1
1.25
1.4
1.6
1.8
2.0
2.2
2.8
3.2
3.6
4.0
4.5
5.0

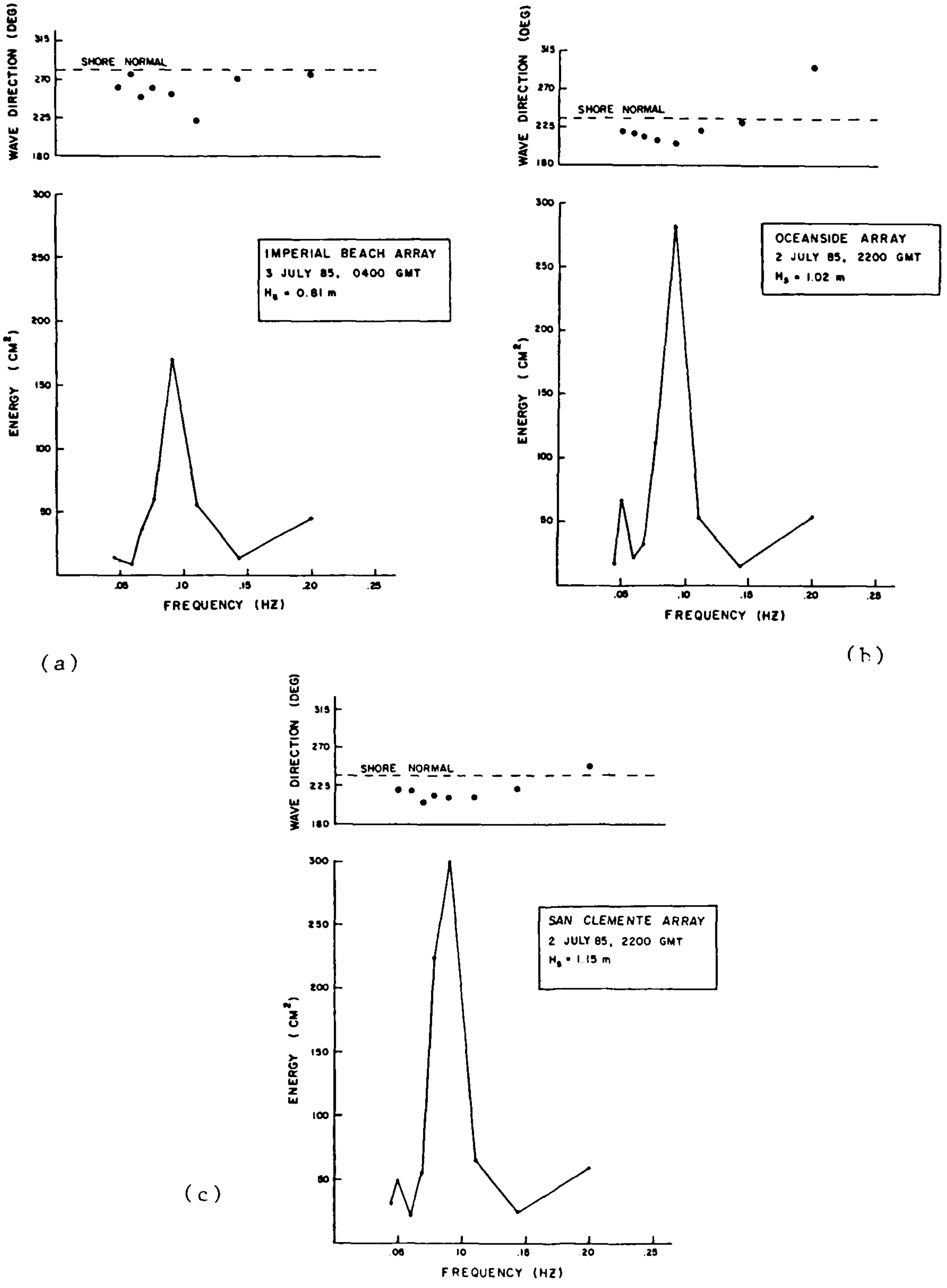

(a)

(b)

(c)

Fig. 7. Slope Array Energy Spectra and Wave Direction for 2-3 July 1985: (a) Imperial Beach, (b) Oceanside and (c) San Clemente.

Imperial Beach and wave energy would be reduced compared to the more southerly facing beaches. The southerly beach orientation at Oceanside and San Clemente may also explain the small southern secondary peak evident at 20 s (0.05 hz) which is not evident in the Imperial Beach spectrum. The rise in energy at the high frequency end of each of the spectra probably represents a local, low energy sea condition generated by a northwest wind.

One example of the effect of island sheltering on the nearshore wave climate is shown in Figure 8. The energy spectrum at the Tanner Basin buoy on 9 May 1984 (Fig. 8a) indicates a broad dominant peak (or peaks) in the vicinity of 6.5 s (0.15 hz), and a secondary peak near 17 s (0.06 hz). The dominant peak is associated with a northwest wind direction of about 315 degrees, while the secondary peak exhibits a southern direction of about 180 degrees. The corresponding spectrum at the Oceanside array (Fig. 8b) only exhibits a distinct southern swell peak at 20 s. It does not display any of the offshore sea/swell energy at frequencies greater than 0.10 hz. This lack of higher frequency wave energy indicates the effects of island sheltering. For a wave direction of about 315 degrees Oceanside is in the wave shadow of the Channel Islands and Pt. Conception, and because of the relatively short period of the energy (6.5 s) refraction of the wave rays around the islands and offshore banks would be minimal and, therefore, contribute little energy to Oceanside near 0.15 hz.

In addition to the directional energy spectra provided by the CCSTWS wave data network, the slope array data is also being analyzed for point estimates of potential longshore sediment transport based on the Sxy results. Figure 9 illustrates potential transport for 1984 at the Oceanside array. It will be noted that although there is an annual cumulative net transport to the south, there is daily transport reversal, which is particularly evident during the summer months (June, July, August, September). This reversal represents a fundamental shift in nearshore wave direction at Oceanside during the summer (5). Typically, during the winter and early spring, swells are generated by storms north of Pt. Conception and these waves cause a southerly longshore transport. During the summer (late spring and autumn represent transition periods) waves approach primarily from the south, generated by tropical and southern hemisphere storms. Figure 9, and previous annual data sets reported by Castel and Seymour (2), represent the first purely empirical evidence supporting this "classical" explanation of longshore transport patterns at Oceanside.

Beach Profile Data. Three beach and nearshore bathymetric surveys have been conducted: 1983 post-summer, 1984 post-winter and 1984 post-summer. Figure 10 shows the excursion of the MLLW

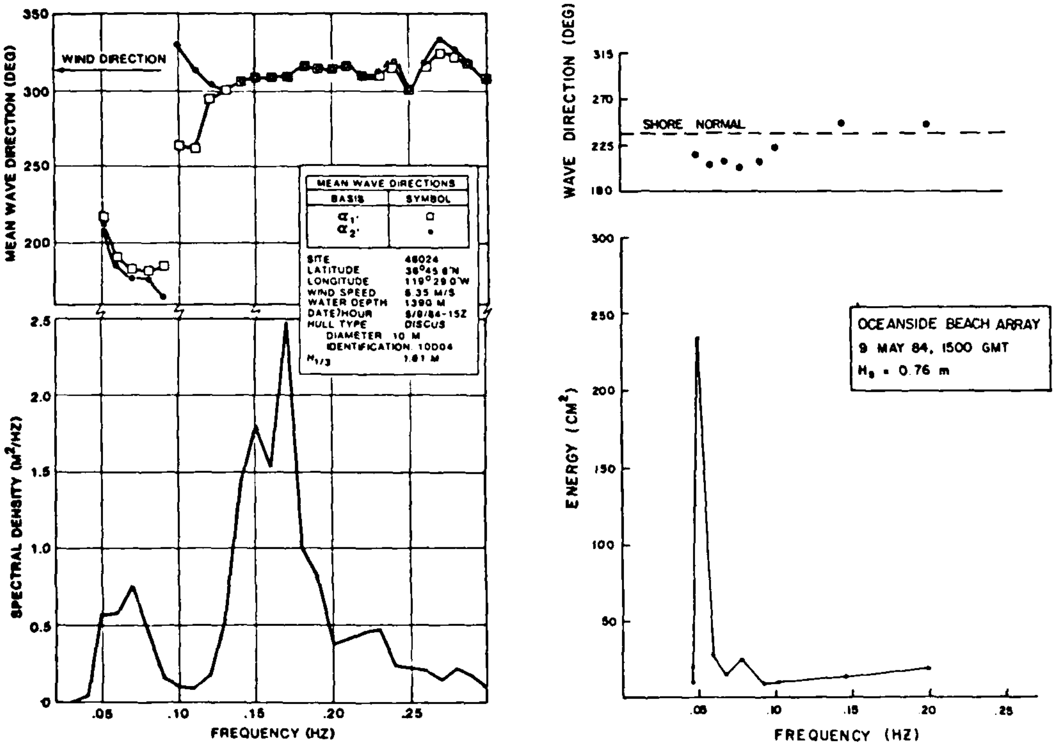

(a)

(b)

Fig. 8. Energy Spectra and Wave Direction for 9 May 1984: (a) Tanner Basin Buoy (Steele et. al. 1985), and (b) Oceanside Slope Array.

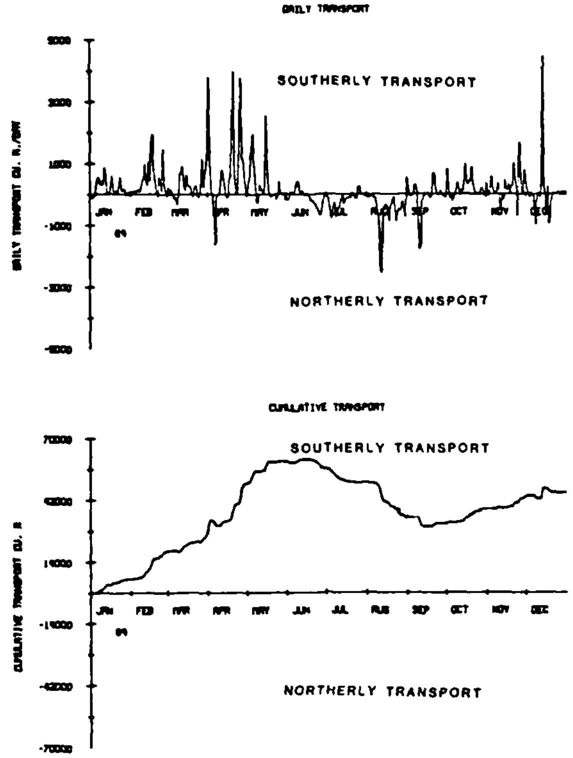

Fig. 9. Potential Daily and Cumulative Longshore Sediment Transport at Oceanside for 1984.

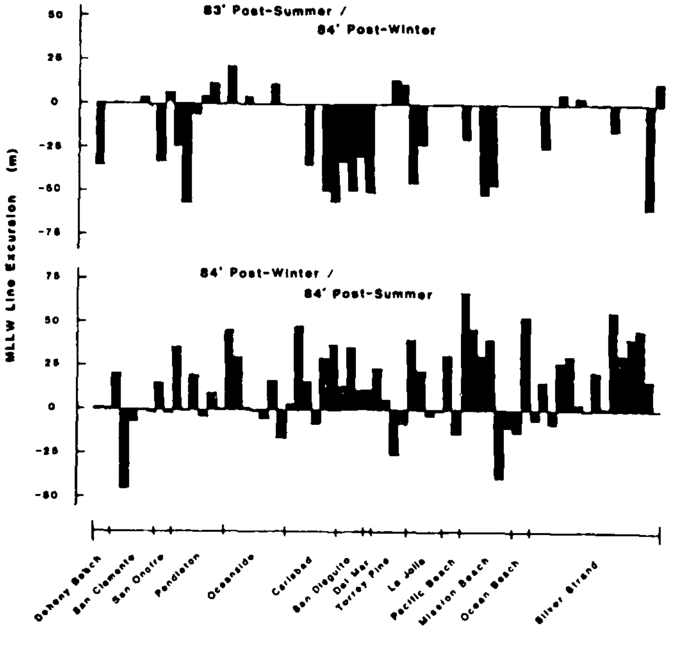

Fig. 10. Excursion of Mean Lower Low Water (MLLW) Line Between Beach Profile Surveys.

line between two pairs of surveys. Many of the profiles exhibit a seasonal excursion range which exceeds 50 m. This figure also clearly shows that the beach face undergoes a seasonal transformation from a summer to a winter profile, widening during the summer and contracting during the winter. Some anomalous behaviour is also evident and this may reflect the dominance of certain local conditions. Figure 11 indicates that although there were relatively large positive and negative volume changes on the profile lines over the course of a summer, the net change on a majority of the lines was relatively small (less than 50 cubic meters). This data possibly suggests that offshore transport balances onshore transport for many of the lines, and that for those profiles exhibiting large net changes a combination of longshore and onshore/offshore transport dynamics needs to be investigated.

Preliminary results from the offshore sedimentation reference rod surveys is shown in Figure 12. Little or no change in sand height was detected at the -10 and -15 m water depths. The only significant changes occurred at the -6 m depth where the largest measured change was -28 cm. This data suggests that the depth of closure or the limit of active sediment movement has been near the -6 m depth for the time period from December 1983 to January 1985.

Qualitative comparisons with 1982-1983 beach profiles suggest that the sandy beaches in southern California have recovered from the severe erosion which occurred during the 1982-1983 winter storms. No major storms have occurred since March 1983 and the data presented here suggest that the beaches are generally in a state of dynamic equilibrium. The mild wave climate during the past three years may also explain why the offshore limit of active sediment transport appears to have been confined to depths less than the -6 m contour.

Future Investigations

Island Sheltering. Pawka and Guza (7, 9) used a linear wave refraction and island blocking model to investigate the influence of island sheltering on the southern California nearshore wave climate, and noted the sensitivity of nearshore wave energy to small changes in deep ocean wave direction. Their results suggest that nearshore wave energy can change by an order of magnitude with an offshore wave direction change of less than 5 degrees. Pawka (8) documented this variability in nearshore directional wave spectra due to island sheltering using a high resolution linear array at Torrey Pines. Semi-quantitative estimates of island sheltering effects have also been prepared to support specific coastal engineering projects (6). However, the directional wave spectra presented here suggest that the directional resolution of the CCSTWS wave data network may be

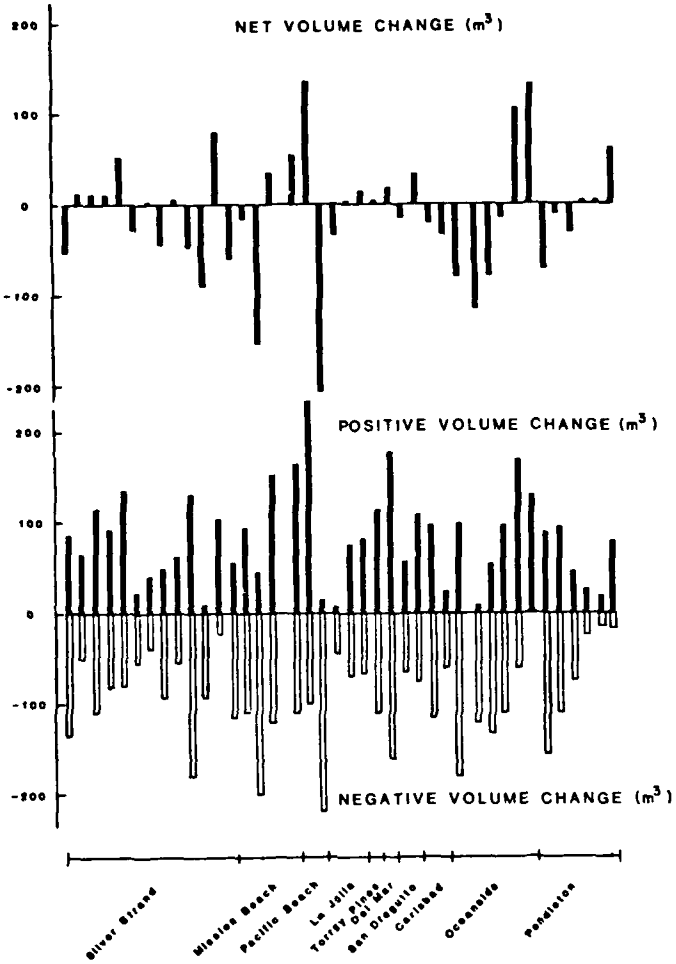

Fig. 11. Beach Profile Volume Changes Between 1984 Post-Winter and 1984 Post-Summer Surveys.

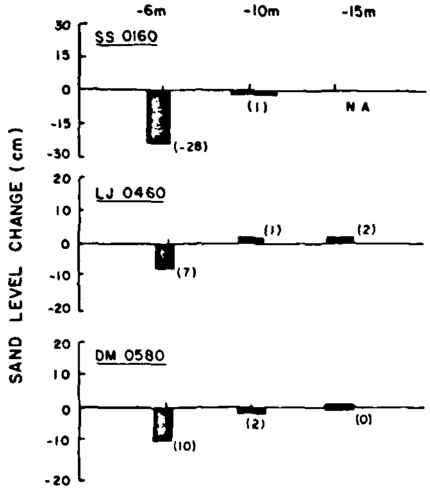

Fig. 12. Changes in Sand Level Height Between Dec. 1983 and Jan. 1985 at Silver Strand, La Jolla and Del Mar Offshore Sedimentation Reference Rod Sites.

sufficient to support the first long-term empirical estimation of the effects of island sheltering on southern California's nearshore wave climate. Future investigations will focus on analyzing the complete, synoptic 18 month data set in order to determine the nearshore wave energy response to changes in offshore wave direction and frequency.

Beach Profile Dynamics Additional historical beach profile data will be added to our survey data base in order to ascertain any longer-term changes in the beach and nearshore bathymetry. There also will be an attempt to correlate gross profile changes with the recorded wave climate. In addition a new survey technique utilizing a sea sled and a land based laser survey station will serve to double the maximum operating depth from -6 m to -12 m (15). This additional capability will provide more accurate detection of offshore sand volume changes. Supplemental offshore sediment reference rods will also be established at -13.5, -15.5 and -18.5 m. These modifications to the survey program will also prove beneficial if southern California experiences a major storm event during the next 2 years.

References

1. California Department of Navigation and Ocean Development, "Assessment and Atlas of Shoreline Erosion Along the California Coast," State of California, Resources Agency, Sacramento, Calif. 1977.

2. Castel, D. and Seymour, R.J., "Longshore Sand Transport Report, February 1978 through December 1981." University of Calif., San Diego, Scripps Institution of Oceanography, La Jolla, 1982.

3. Higgins, A.L., Seymour, R.J. and Pawka, S.S., "A Compact Representation of Ocean Wave Directionality," Applied Ocean Research, Vol. 3, No. 3, 1981, pp. 105-112.

4. Longuet-Higgins, M.S., Cartwright, D.F., and Smith, N.D., "Observations of the Directional Spectrum of Sea Waves Using the Motions of a Floating Buoy," in Ocean Wave Spectra, Prentice-Hall, Englewood Cliffs, New Jersey, 1963.

5. Marine Advisors, "Design Waves for Proposed Small Craft Harbor at Oceanside, California," U.S. Army Corps of Engineers, Los Angeles District, Calif., 1960.

6. Marine Advisors, "A Statistical Survey of Ocean Wave Characteristics in Southern California Waters," U.S. Army Corps of Engineers, Los Angeles District, Calif., January 1961.

7. Pawka, S.S., "Wave Directional Characteristics on a Partially Sheltered Coast," Ph. D. Dissertation, Univ. of Calif., San Diego, La Jolla, 1982.

8. Pawka, S.S., "Island Shadows in Wave Directional Spectra," Journal of Geophysical Research, Vol. 88, No. C4, March 1983, pp. 2579-2591.

9. Pawka, S.S. and Guza, R.T., "Coast of California Waves Study - Site Selection," U.S. Army Corps of Engineers, Los Angeles District, California, 1983.

10. Seymour, R.J., and Higgins, A.L., "Continuous Estimation of Longshore Sand Transport," Proceedings of Coastal Zone 78, ASCE, Vol. III, New York, 1978, pp. 2308 - 2318.

11. Seymour, R.J., Session, M.H. and Castel, D., "Automated Remote Recording and Analysis of Coastal Data," Journal of Waterways, Port, Coastal and Ocean Engineering Division, ASCE, Vol, III, No. 2, March 1985, pp. 388-400.

12. Steele, K.E., Lau, J.C., and Hsu, Y.L., "Theory and Application of Calibration Techniques for an NDBC Directional Wave Measurements Bouy," Journal of Oceanic Engineering, IEEE, 1985 (in press).

13. U.S. Army Corps of Engineers, Los Angeles District, "Coast of California Storm and Tidal Waves Study: Plan of Study," Los Angeles, Calif., 1983.

14. U.S. Army Corps of Engineers, Los Angeles District, "Coast of California Storm and Tidal Waves Study: Annual Report 1983," Ref. No. CCSTWS 84-1, Los Angeles, Calif., 1984.

15. U.S. Army Corps of Engineers, Los Angeles District, "Coast of California Storm and Tidal Waves Study: Annual Report 1984," Ref. No. CCSTWS 85-1, Los Angeles, Calif., 1985.

16. U.S. Army Corps of Engineers, Los Angeles District, "Coast of California Storm and Tidal Waves Study: Nearshore Bathymetric Survey Report, No. 1," Ref. No. CCSTWS 84-2, Los Angeles, Calif., 1984.

Flushing of Entrance Channel for Coastal Lagoons: Mathematical Simulation

Howard H. Chang*

Paper unavailable at time of publication.

---

* San Diego State University, San Diego, California.

COASTAL EROSION ALONG SOUTHERN MONTEREY BAY

E. B. Thornton[1], M. ASCE, A. J. Sklavidis[2], W. Lima Blanco[3],
D.M. Burych[1], S. P. Tucker[1], D. Puccini[4]

The permanent beach erosion in Southern Monterey Bay is episodic, occurring infrequently when high tide coincides with stormy weather, which allows wave action to erode the base of the cliffs. A model is developed to predict cliff erosion based on the hypothesis that erosion only occurs when the water level due to combined tides, wave set-up and run-up exceeds the toe of the cliff elevation. The erosion model was calibrated using a spectral wave climatology, predicted tides, and aerial photographs covering an 18 year period. Refraction of the wave energy is responsible for the variability of erosion rates along the shore. The bathymetry of Monterey Bay is such that the refracted wave energy and observed erosion are greatest in the Fort Ord area decreasing to the south. The model gives a reasonable prediction of the spatial variation of the mean recession rates.

Introduction

Monterey Bay, California's second largest, is semi-circular and opens to the west. The bay is 12 miles wide in an east-west direction and 25 miles long in a north-south direction. The outer limits of the bay floor correspond to the edge of the continental shelf. Southern Monterey Bay cliffs consist of coarse sand, making them highly susceptible to erosion from wave action and surface runoff.

In the southern Monterey Bay, the primary sources of sand are the Salinas River discharge, cliff erosion and alongshore sand transport by waves and currents, while the sand is lost to the deep ocean, onto land, and to sand mining. The difference between losses and gains determines whether there will be beach erosion or accretion. Sediment budget studies conducted by Dorman (1968) and Arnal et. al. (1973) concluded that there is a net loss of sand, and therefore, a continuous erosion of Southern Monterey Bay beaches.

Erosion rates have been estimated for a number of beaches by measuring the recession of the beach over time. The recession was measured by comparing historical aerial photographs (starting as far back as 1939) and bottom charts (from 1356). Beach erosion is the permanent loss of coastal land. The erosion is best measured by the recession of either the top or the toe of the coastal bluff. Topographic elevations, such as mean high water line (MHWL), are also used to define the coastline; but because the location of MHWL shows

1. Naval Postgraduate School, Monterey CA 93943

2. Hydrographic Services, Athens BST 902, Greece

3. Direccion de Hidrografia y Navegacion, Observatorio Cajigal-La
Planicie-Urb 23 de Enero, Caracas, Venezuela

4. Fleet Numerical Oceanographic Center, Monterey, CA 93943

considerable seasonal variations, defining the coastline in this manner generally results in inconsistent or noisy erosion rates. The erosion rates show considerable variation, with a general increase in rate from the vicinity of Monterey Harbor to a maximum around Fort Ord. The increasing erosion rate is directly attributable to the increased exposure to storm waves towards Fort Ord. The variation in wave intensity is due to the effects of wave refraction caused by the variable bottom topography of Monterey Bay, and the Monterey Bay submarine canyon in particular.

The objective of this paper is to predict coastal changes due to storms on a recessive shoreline. It is hypothesized that erosion is episodic and occurs during simultaneous occurrences of high tides and storm waves; thus, it is proposed that cliff erosion can be calculated, provided that local tide elevation, wave height, and a function relating storm energy and erosion are known.

Erosion rates were obtained using photogrammetry. Several of the previous erosion studies utilized imprecise photo comparison techniques leading to erratic and questionable results. Precise photogrammetric techniques used here and associated errors are described. The waves were calculated using a 20 year directional wave spectrum climatology. Deep water spectra were refracted to shallow water locations. The tides were predicted hourly. Model predictions of beach erosion based on waves and tides are compared with the measured erosion rates.

Erosion Rates Measured Using Photogrammetry

The recession of a shoreline due to erosion can be measured using aerial photographs. The coast of Southern Monterey Bay has been photographed at an average interval of about five years since 1939. However, in the last decade the photographic interval has been shorter, about every three years, and most recently yearly, which allows a determination of erosion rates and a picture of coastal change.

Four sites were selected for measuring cliff erosion in this study referred to as Fort Ord, Sand Company, Phillips Petroleum, and Beach lab (see Fig. 1). The general criteria for choosing the study areas were that a cliff be adjacent to the shoreline, the location be close to a development which had been affected by erosion, and the area be previously studied so that earlier findings could be compared with the proposed model. The distribution of the chosen areas gives a clear representation of the erosion rates from Monterey Harbor to just north of Fort Ord.

Several measurement points along the beach profile, such as high tide line, toe of the cliff, and top of the cliff, were considered (see Figure 2). It was desired to choose a point that would be sharply defined in aerial photographs and indicative of permanent change (erosion). The beach profile at a water line datum, such as MLLW or MHHW, is highly variable due to seasonal cross-shore transport. The toe of the cliff is not always well defined due to slumping of cliff material, causing displacement of the base of the cliff. Also, in several aerial photographs the bottoms of the cliffs were not clearly defined due to the shadow of the cliff.

The sharp representation of the top of the cliff in aerial photographs offers a clear and identifiable point of reference, and the change in the location of the top of the cliff is a measure of permanent erosion. Seventy percent of the coast of Southern Monterey Bay is adjacent to cliffs having an average height of 30 ft. The erosion of cliff tops is due to slumping caused by erosion at the base of the cliff. Therefore, long-term erosion was inferred by measuring the locations of the cliff tops.

A photo is a perspective or central projection, in which all points are projected onto the reference plane through one point called the perspective center. A photo is only orthographic in the ideal case when the film and ground lie in parallel planes; therefore, direct measurements from a single photo may cause error (Moffitt and Mikhail, 1980). Because the study of coastal erosion requires very accurate shoreline determination, photogrammetric errors must be considered. The most important errors inherent in photographs are, in order of importance, the scale variation, relief displacement, and tilt. The distances between selected reference points were surveyed in the field to determine the scale of the photo. To achieve the greatest accuracy, special attention was given to the selection of reference points. Objects with sharp, well defined images on the photographs were selected as close as possible to the area being studied to minimize errors due to scale variation or tilt.

Ground relief causes displacements of images on a photograph. This displacment is known as relief displacement and is defined as the displacement of images radially inward or outward with respect to the photographic model, depending on whether the ground objects are below, or above the datum (Slama, 1980). Errors due to relief displacement were minimized by calculating the elevation of the measured points and correcting their locations using a stereo model. The tilt error was minimized by only using photographs in which the scale variations for the stereo model were less than 5 percent, i.e., selecting photos taken with small camera tilt.

The cliff top contours for years 1946, 1956, 1966, 1976, 1978, and 1984 were measured for the four beach sections. Shoreline recession and erosion rates were determined from the cliff contours. Recession rates along the shoreline are not uniform. The cliff top contours indicate variability along the shoreline in the recession (see for example Fig. 3) It is assumed that the average erosion rate for each area is more representative than the erosion rates at any single point in the study area. Thus, the cliff top was averaged over at least 800-2000 feet alongshore. The average recession rate for each study area were computed from the rates of change at a number of points along the shoreline to reduce the random measurement errors. The standard deviation was also calculated, providing a measure of the variability of the erosion rate over the measured shoreline. The average volumetric erosion rate was calculated by multiplying the average cliff top recession with the average cliff elevation.

The erosion rates are summarized in Table 1. The average erosion rate is a minimum in the southern part and increases northward, with a maximum average erosion rate of 7.3 ft/yr (2.2 m/yr) at the northern Fort Ord region. No significant discrepancies were found between the results of the present study and those of earlier studies. For the southern part of the Beach Lab region Jones (1983) found the recession rate to be 1.1 ft/yr (0.33 m/yr). The difference between recession rates of the present study and Jones' is +0.8 ft/yr (0.24 m/yr). The recession of the cliff toe at the Phillips Property was previously studied by Thompson (1981); he found a recession rate of 1.8 ft/yr (0.54 m/yr), while we found 2.8 ft/yr. An earlier study of the Sand Dune region was performed by Moffitt (1968), who observed a recession rate of 6.9 ft/yr (2.1 m/yr). The difference between the erosion rate he found and ours is 0.6 ft/yr (0.18 m/yr). The Fort Ord region was studied previously by Jones (1983). The erosion rates he found do not appear to be consistent with ours, but they show (as we do) that the northern part has eroded more rapidly than the southern part.

Table 1. Measured Recession Rates (ft/yr)

LOCATION	1966-76	1976-78	1978-83	1966-83
Ft. Ord	3.6	11.1	12.3	6.8
S. Dune	0.9	1.7	1.8	1.2
P.P. Property	1.4	4.6	2.3	2.0
B. Lab	0.5	0.6	0.9	0.6

With only a few exceptions the cliff tops always recessed shoreward between photographs. This is contrary to the findings of earlier investigators (Thompson, Moffitt, Jones). The earlier studies indicated accretion occurred along sections of the shoreline in some time intervals. This is not surprising since they measured the position of the toe of the cliff or of the waterline, which we found to be unreliable. Thompson measured the toe of the cliff, which would indicate accretion in the case when the cliff slumps down. He did not remove errors caused by relief displacement or use a highly accurate photogrammetric instrument (mirror stereoscope). Moffitt measured the variation of the shoreline using as reference the position of the waterline. He corrected the location of the waterline for the tidal fluctuation, but did not take into consideration the seasonal variation and the meteorological effects in sea level variation. Jones measured only a few points (one to three points) for each region using a mirror stereoscope without removing the effects of relief.

Wave Climatology, Wave Set-up, Run-up and Tides

A 21-year (1964-1985) wave climatology for Monterey Bay was calculated using deep water wave spectra obtained from the U.S. Navy Fleet Numerical Oceanography Center. The spectra were generated using the spectral ocean wave model (SOWM) every 6 hours for the twenty year period. The hindcasts are for the Northern Hemisphere oceans only and do not include swell that has propagated from the Southern Hemisphere; the winds of the Southern Hemisphere were not known with sufficient accuracy to permit hindcasts (Pierson, 1982). The SOWM has been verified (see for example Lazanoff and Stevenson, 1975; and Pierson, 1982) and shown to give reasonable estimates of wave spectra. The deep water wave spectra were calculated at the nearest grid points to Monterey Bay at 36.1 N; 123.8 W were used for the wave analysis. The waves are transformed by refraction and shoaling as they propagate from deep to shallow water. Assuming conservation of energy flux and long crested waves, the wave spectrum in shallow water (subscript h) is related to the deep water wave spectrum (subscript o) by

$$E_h(f,\theta) = K_r^2(f,\theta)\, K_s^2(f)\, E_o(f,\theta_o)\, J \qquad (1)$$

where f is the wave frequency, θ, the wave direction, K_r is the refraction coefficient, K_s is the shoaling coefficient and J is the Jacobian of the transformation.

Wave refraction diagrams were calculated for 5 directions in 30-degree increments from 185.5 to 335.5 azimuth and 12 periods (7.5 to 25.7 s). Waves having periods shorter than 7.5 seconds were not considered. Such short period-waves are locally generated in deep water, and experience indicates they are not representative of the short-period, locally-generated waves at the coast. The wave refraction analyses showed the four sites studied to be protected from open waves from the south and north; only waves from the WNW to WSW can deliver significant energy. The study showed that, due to wave refraction, the open ocean waves approach shore within a narrow range of angles. A value of K_r greater than one results in an amplification of wave energy whereas K_r less than one results in a decrease in energy. Examination of the refraction coefficient tables shows that the coefficients are mostly less than one and in general are greater at Fort Ord and decrease to the south. Amplification does occur for some wave components from the west at Fort Ord; winter storms are often from the west. Amplification occurs for some wave components from the WNW (305.5) at Sand Dune and Phillips Property, but the components for other directions are significantly reduced due to refraction. No amplification of components occurs at the Beach Lab.

Since the spread of angles of the shallow water wave spectra is small, it is convenient to collapse the shallow water wave spectra into one-dimensional wave spectra as a function of frequency only.

$$E_h(f) = \sum_{\theta} E_h(f,\theta)\ \Delta\theta \qquad (2)$$

The significant wave height (the average of the highest one-third of the waves) is a commonly used wave statistic. H_s is calculated as a function of the total energy of the spectrum.

$$H_s = 4\left(\sum_{f} E_h(f)\ \Delta f\right)^{1/2} \qquad (3)$$

The modal period is the period of the spectral peak and is representative of the average period of the waves. The significant wave height and modal period are used in the analysis.

Wave set-up is the increase in mean sea level in the shoreward direction across the surf zone due to the shoreward transport of momentum by waves. The wave set-up was measured on a mild sloping beach by Guza and Thornton (1981) and found proportional to the deep water wave height. Holman and Sallenger (1983) extended the measurements for steeper beaches and a much wider range of wave heights. They found similar results but with some correlation with tidal stage. For high tide conditions, the set-up is given by

$$S_s = 0.14\ H_{s,o} \qquad (4)$$

where $H_{s,o}$ is the significant wave height in deep water.

Wave run-up refers to the rush of water from broken waves up the beach and is measured by the vertical elevation reached above the still-water level. Coincident arrival with high tide may cause increased erosion of the shoreline. The magnitude of the vertical run-up can be determined by the characteristics of the waves, by the refractive effects of the bottom topography and by the configuration of the beach. Guza and Thornton (1981) found that in their measurements on mild beaches the vertical extent of run-up, R_v, was proportional to the deep water wave height. Again, Holman and Sallenger (1983) extended the range of measurements and suggest for high tide conditions

$$R_v=0.88\ H_{s,o} \qquad (5)$$

The set-up and run-up formulations were incorporated in a simple erosion model described next.

As the sea rises and falls with the tide, different elevations of the beach become subject to the action of the sea. The rise and fall of the sea due to tides is regular and predictable. Hourly tidal predictions were calculated using 20 tidal constituents based on 13 years of tide measurements at Monterey.

Some additional, usually minor, short term factors that may influence the coastal sea level are: changes in atmospheric pressure over the ocean surface, changes in average density of the sea water column due to temperature and salinity changes, and wind set-up or set-down against the coast due to storms (Bretschneider, 1980). A correction or adjustment of the high water line location to account for wind tides is not possible because of the lack of local wind data.

Predictive Beach Erosion Model

A simple model is proposed here based on the hypothesis that erosion occurs infrequently when the total water elevation, S, exceeds the toe of the cliff elevation T. Each time that the total water level, S, is greater than the toe elevation, erosion can occur in the cliff (see Figure 4). The cliff recession is assumed to be given by

$$R = K \frac{(S-T)}{\tan\beta} \qquad (6)$$

where R is the magnitude of the horizontal recession, β is the slope of the beach. The slope for each region was calculated using the slope between the 0 and 2 fathom isobath contours. The average top and toe elevations of the cliff were found by leveling in the study areas. The proportionality factor K in (6) accounts for differences in material and other (unknown) factors.

The total water elevation S, is calculated by

$$S = S_t + S_s + R_v \qquad (7)$$

where S_t accounts for the tide height above MLLW, predicted by harmonic analysis, the wave set-up, S_s is given by (4) and the vertical extent of wave run-up, R_v is given by (5). The wave set-up and run-up formulas are parameterized on the significant deep water wave height, $H_{s,o}$. An effective deep water wave height was calculated by taking the shallow water wave height calculated in 4 meters back out into deep water assuming conservation of energy flux without accounting for refraction

$$H_{s,o} = H_{s,4M} \left(\frac{1}{K_s(f_p)}\right) \qquad (8)$$

where f_p is the peak frequency in the shallow water wave spectrum. The maximum water elevation due to tides and waves was predicted hourly for the intervals between photographs, and the predicted recession using (6) was summed. The predicted recession rates were obtained by application of the model using a proportionality coefficient $K = 0.000096$.

The average measured and predicted recession rates for the entire comparison interval 1966-1983 are compared in Figure 5. The model predicts maximum erosion at Fort Ord decreasing south, but predicts less erosion at Sand Dune than at Phillips Petroleum. The high measured recession rate relative to the predicted rate at the Sand Dune area suggests an anomalously high recession rate. The higher than expected recession rate may be associated with the sand mining off the beach at this location.

Conclusion

The primary objective of this study is to develop and evaluate a model for the prediction of coastal erosion rates in Southern Monterey Bay. A sequence of six aerial photographs taken during the interval 1946-1984 were used to measure coastal erosion. It was demonstrated that the aerial photographs provide a suitable means to determine coastal changes. Previous studies had not used accepted photogrammetric techniques to compensate for scale variation, relief displacement and plane tilt. Careful analysis was applied here to minimize errors. Scale variations between photographs were estimated by determining the average scale of each photograph from horizontal ground points. Errors due to relief displacement were minimized by measuring the X-parallax of each point.

It was shown that the top of the cliff offers a consistent measurement point for erosion studies. It was found that the erosion along the coast of Southern Monterey Bay is progressive --there is no accretion. The average cliff top recession rate is a minimum in the southern part of the bay and increases northward, with a maximum average erosion rate of 7.3 ft/yr (2.2 m/yr) at Fort Ord.

A simple predictive model was proposed based on the hypothesis that the permanent beach erosion in Southern Monterey Bay is episodic, occurring infrequently when high tides coincide with stormy weather, which allows wave action to erode the toe of the cliffs. The tides were predicted using harmonic analysis. The wave heights were calculated in shallow water by refracting deep water directional wave spectra provided by Fleet Numerical Oceanography Center (FNOC). Erosion occurs when the total water elevation exceeds the toe of the cliff elevation. The total water elevation is the combination of tides plus set-up and run-up, which are proportional to the wave height. The model was calibrated against the measured recession rates for the years 1966-1983 when the wave data are available. The model reasonably predicts the spatial variation of the recession rates, indicating maximum erosion at Fort Ord and decreasing to the south.

Acknowledgements

We would like to thank the University of California at Santa Cruz and the San Francisco Division and Los Angeles Division of the U.S. Army Corps of Engineers for providing aerial photographs, and the U.S. Geological Survey in Menlo Park for reproducing some of the aerial photographs.

References

Arnal, R.E., Dittmer, E., and Shumaker, E., "Sand transport studies in Monterey Bay, California, 73-571, Moss Landing Marine Laboratory, 1973

Bretschneider, D.E., "Sea Level Variations at Monterey, California," M.S. Thesis, Naval Postgraduate School, Monterey, March 1980.

Dorman, C.E., "Southern Monterey Bay Littoral Cell a Preliminary Sediment Report," Master of Science Thesis, Naval Postgraduate School, 234 pp, 1968.

Guza, R.T., and Thornton, E.B., "Wave Set-up on a Natural Beach," J. Geophysical Research, 86 (C5) 4133-4137, 1981.

Holman, R.A., and Sallenger, A.H., "Setup and Swash on a Natural Beach," J. Geophysical Research, 90 (C1), 945-953, 1985.

Jones, G.B., "Coastal Erosion at Selected Points on Southern Monterey Bay," Senior Thesis, University of California, Santa Cruz, July 1983.

Lazanoff, S.M., and Stevenson, N.M., "A Twenty Year Northern Hemisphere Wave Climatology," in Favre, A. and K. Hasselman (1978): Editors. Turbulent Fluxes Through the Sea Surface, Wave Dynamics and Prediction, Plenum Press, 677 pp., 1978.

Moffitt, F.H., "History of Shoreline Growth from Analysis of Aerial Photographs," Technical Report HEL-2-21, 1968.

Moffitt, F.H., and E.M. Mikhail, Photogrammetry, 3d ed., Harper and Row, 1980.

Pierson, W.J., "The Spectral Ocean Wave Model (SOWM), A Northern Hemisphere Computer Model for Specifying and Forecasting Ocean Wave Spectra," David W. Taylor Naval Ship Research and Development Center Report, 191 pp, 1982.

Slama, C.C., (Editor-in-Chief), Manual of Photogrammetry, 4th ed., American Society of Photogrammetry, 1980.

Thompson, W.C., "Report on Coast Erosion and Run-up on Phillips Petroleum Property", prepared for Ponderosa Homes, Santa Clara, December 1981.

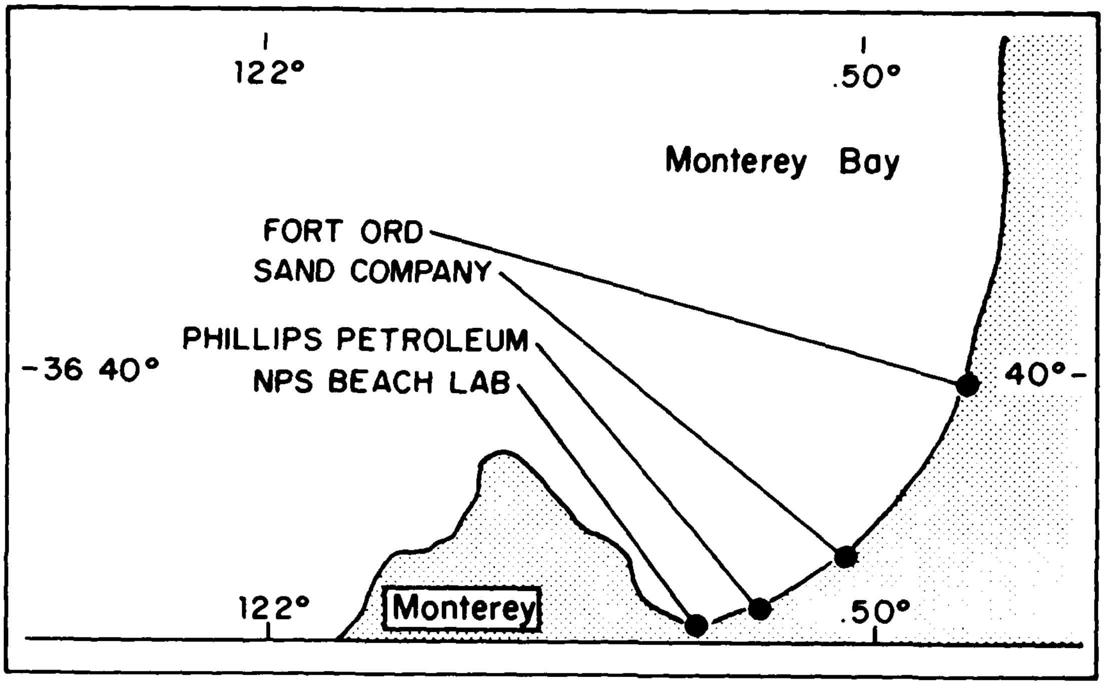
122°
.50°
Monterey Bay
FORT ORD
SAND COMPANY
PHILLIPS PETROLEUM
NPS BEACH LAB
-36 40°
40°-
122°
Monterey
.50°

Figure 1 Selected Areas of Study

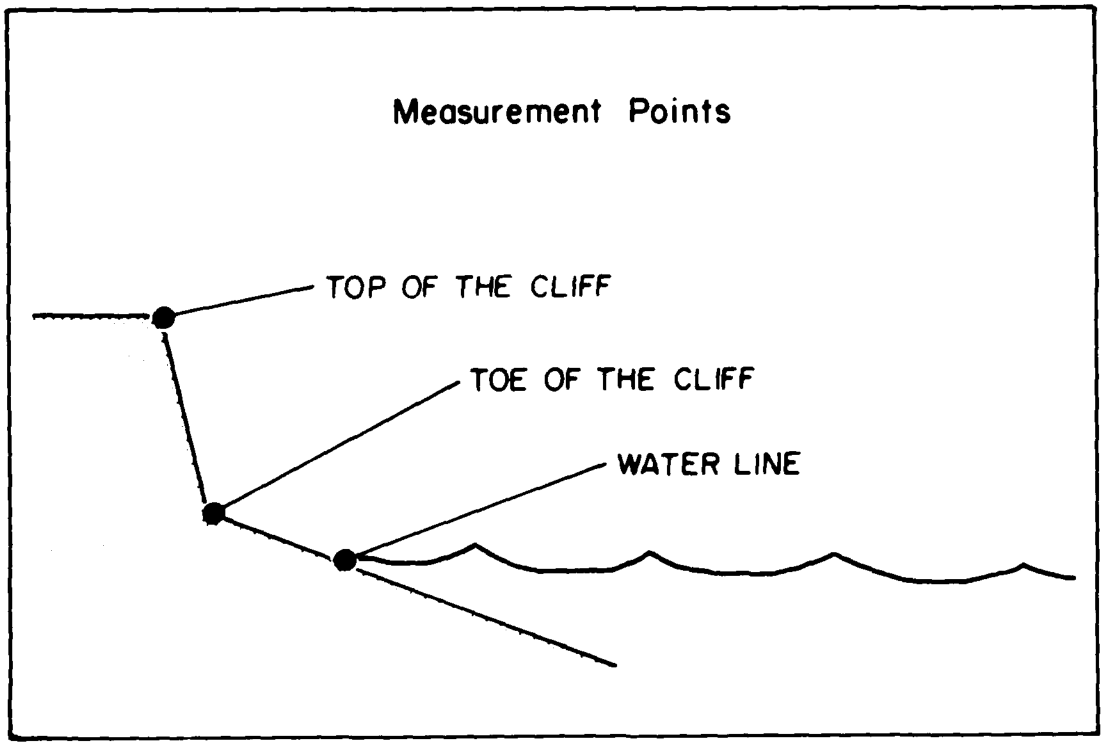
Measurement Points
TOP OF THE CLIFF
TOE OF THE CLIFF
WATER LINE

Figure 2 Selected Measurement Points

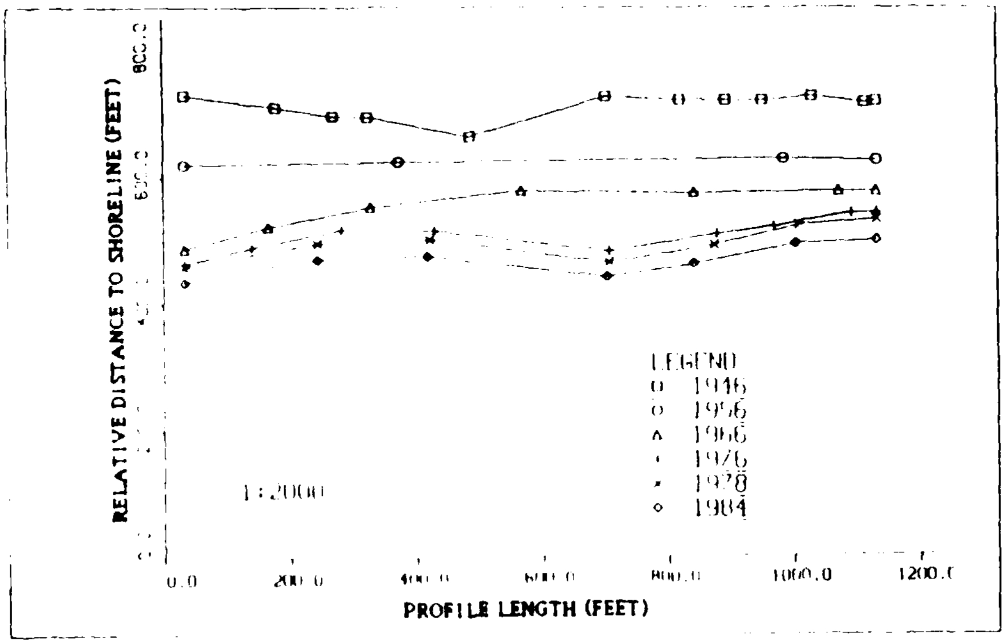

Figure 3 Sand Dune (South)

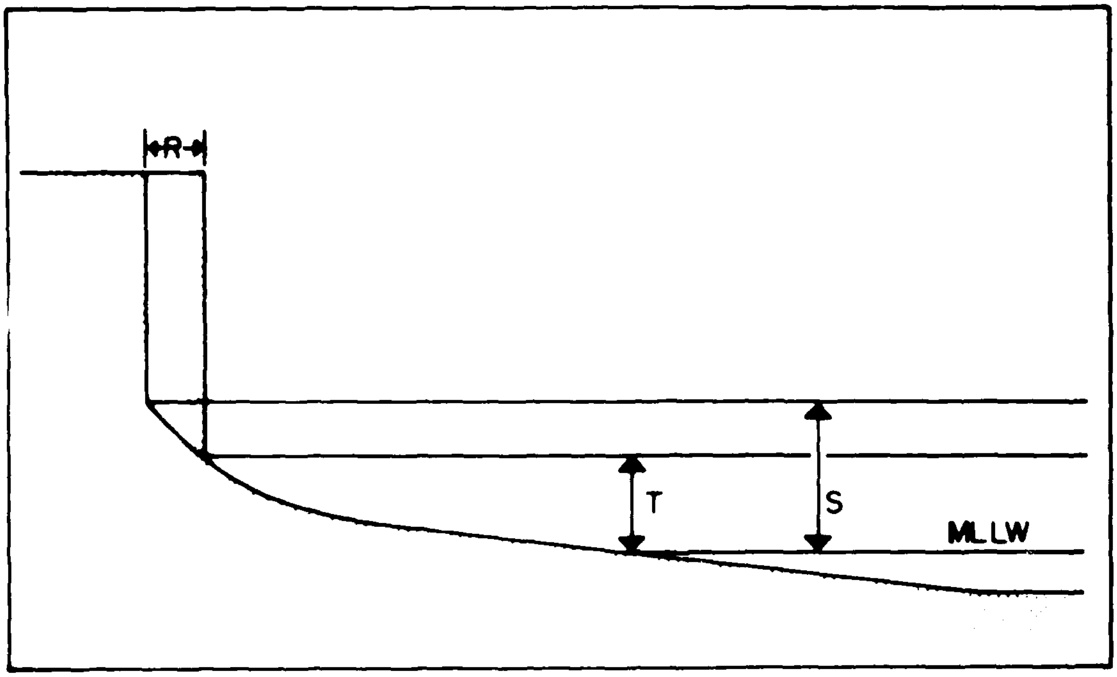

Figure 4 Characteristics of the response Model

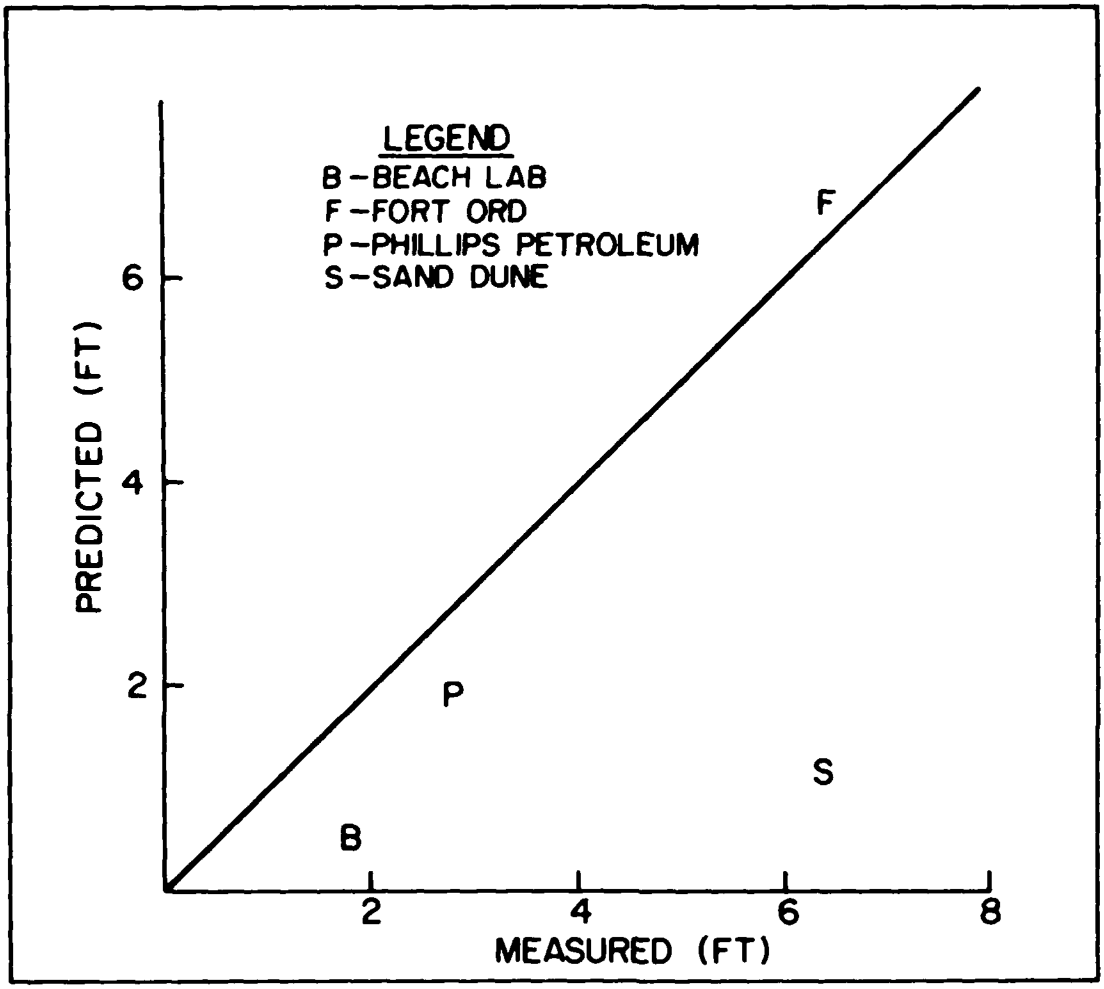

Figure 5. Measured vs. Predicted Recession Rates (1966-83)

Net Shore-drift Along the Pacific Coast of Washington State

Maurice L. Schwartz*, James Mahala*, and Hiram S. Bronson. III**

Introduction

We have previously reported on the geomorphology of the Pacific coast of the State of Washington (Terich and Schwartz, 1981) and on net shore-drift study techniques in Puget Sound (Jacobsen and Schwartz, 1981). In this report, we return to the Pacific coast to delineate the compartmentalization of drift cells and the direction of net shore-drift along the shore from the mouth of the Columbia River, on the south, to Cape Flattery, on the north.

While shore drift in the southern portion of this sector has been investigated to some extent (Phipps and Smith, 1978; Plopper, 1978), data of this nature on the entire coast has not been published before. Throughout the study, our approach has been based essentially upon long-term geomorphic and sedimentologic indicators (Jacobsen and Schwartz, 1981).

Methods

Short-term studies of net shore-drift are prone to errors. Investigations employing tracers or sediment traps over a few months time are only recording drift for that period; while drift determina ions based upon wave hindcasting and the construction of wave orthogonals are subject to the vagaries of judgement and calculations of the investigator. Serious mistakes can be made by utilizing these methods without adequate field verification of the geomorphology and sedimentology of the coastal stretch under consideration.

There is a growing body of literature (Engstrom, 1978; Hunter et al, 1979; Self, 1977; Sunamura, 1972) that outlines the advantages of geomorphic and sedimentologic indicators in determining net shore-drift directions. We have organized and expanded upon these methods, to develop a more systematic approach in the field (Morelock et al, 1985). The techniques outlined here have been employed to good advantage in investigations conducted on the marine shores of nine counties in Washington State (Schwartz and Blankenship, 1984; Schwartz and Chrzastowski, 1984; Schwartz and Harp, 1984; Schwartz and Hatfield, 1984; Schwartz and Taggart, 1984), on the north coast of Puerto Rico (Morelock et al, 1985), and most recently along the Padre

*Dept. of Geology, Western Washington University, Bellingham, WA 98225
**Huxley College, Western Washington University, Bellingham, WA 98225

Island, Mexico coastal sector (Schwartz and Anderson, 1985).

These indicators are: sediment accumulation and erosion at groins and other obstacles; spit development; headland-bay or log-spiral beaches; direction of stream diversion; beach width and height; sediment-size gradation; changing bluff or cliff morphology along the coast; uniquely identifiable sediment; and nearshore bar development and orientation. Usually, within a drift cell, a few of these indicators may be found, thus together corroborating the direction of net shore-drift.

Waves and fetch also come into consideration. The predominant waves in this area are from the southwest and west-by-southwest, and attain considerable height. For example, Corps of Engineers design wave data shows that off of Grays Harbor (Fig. 1) westerly significant waves have a height of 9.14 m and 12 sec. period (Corps of Engineers, 1973). Regional cyclones, however, may develop northwesterly waves. As a result, net shore-drift is mainly to the north along the Pacific coast of Washington; but local reversals occur: a) in the wave shadow of headlands, b) where the orientation of the coast differs considerably from the overall trend, c) at inlets where ebb-flow deposits cause refraction over shoals, and 4) where waves are refracted around islands or stacks near the coast.

In the following discussion, the Pacific coast of Washington is divided into three sectors (Fig. 1), from south to north, for the sake of graphic presentation. These sectors are based on geomorphic subdivisions outlined in an earlier report (Terich and Schwartz, 1981) on this coastal region: I Southern Sector - sandy beaches backed by beach ridges (Fig. 2); II Central Sector - sandy beaches in front of sedimentary-rock cliffs (Fig. 3); III Northern Sector - some sandy, but mostly gravelly beaches backed by cliffs composed of igneous rocks (Fig. 4).

Discussion

Net shore-drift in the most southerly drift cell within the study area is to the south, toward the North Jetty of the Columbia River. This is a rather short distance; and there is an equally short sector of sediment transport to the north towards Cape Disappointment. From Cape Disappointment, net shore-drift continues to the north, uninterrupted, for approximately 40 km along Long Beach Peninsula, to the end of the recurved spit at Ledbetter Point on the south side of the Willapa Bay inlet.

Along the inner north side of the Willapa Bay inlet, net shore-drift is to the east-southeast into the bay. On the outer coast, there is a drift cell which begins at Cape Shoalwater and ends at the South Jetty at Point Chehalis on the south side of the inlet to Grays Harbor, with drift to the north.

On the north side of the inlet to Grays Harbor, there is net shore drift to the south, ending at the North Jetty at Point Brown. Where net shore-drift begins again to the north, there is the start of a long drift cell (approximately 57 km); extending past the mouths of the Copalis and Moclips rivers to terminate at Point Grenville.

The next sector of net shore-drift is to the north, from Point Grenville to the mouth of the Quinalt River at Cape Elizabeth. From Cape Elizabeth net shore-drift is to the north, terminating at Pratt Cliff; then again to the north, past the mouth of the Queets River, to the Hoh River mouth.

From this point to the region of Cape Flattery, the coast consists of many headlands, and pocket beaches, with offshore stacks-arches; thus creating numerous short drift cells, with drift mainly to the north or south.

There is a short sector of net shore-drift, to the north, from the mouth of the Hoh River towards Hoh Head; then, in succession, four more short sectors, in the same direction, to Taylor Point. North of Taylor Point, along a stretch known locally as Third Beach, net shore drift seems to be seasonably to the south.

Approaching La Push net shore-drift on Second, and then First Beach, is to the north. Another southerly reversal to the overall trend, has formed a spit developed to the south across the mouth of the Quileute River.

North of this spit, there are five short, discrete sectors of northerly net shore-drift; the northernmost four being bracketed by headlands. The next drift cell, upcoast, consists of a short reversal to the south.

Along the coast west of Ozette Lake there are four more sectors of northerly net shore-drift, the last terminating at Sands Point. North of Sands Point, there is a short southerly net shore-drift cell, but between that drift cell and the Tskawahyah Island tombolo there are two separate northerly sectors of drift. In the lee of the tombolo, net shore-drift is to the south.

From here, a short and then a somewhat longer drift cell, both with drift to the north, extend up the coast to Point of the Arches. On the north side of Point of the Arches, there is located the last sector of southerly net shore-drift. At the north end of this pocket beach, and in an adjacent one to the north, there are two more drift cells with net shore-drift, in both, directed toward the north.

There is no net shore-drift along the outer coast of Cape Flattery due to the almost pervasive presence of plunging sea-cliffs or bare, rocky wave-cut platforms.

Summary

Utilizing long-term geomorphic and sedimentologic net shore-drift indicators, as described in more detail in an earlier journal (Jacobsen and Schwartz, 1981) we have mapped the drift cells and direction of net shore-drift along the Pacific coast of Washington State.

In the Southern and Central sectors (Fig. 2 and 3), net shore-drift is predominantly to the north. Diverging from this, there is drift to the east-southeast on the north side of the Willapa Bay inlet due to the orientation of the coastal sector there, and relatively short southerly reversals just north of the Columbia River mouth and the Grays Harbor inlet due to wave refraction around submerged shoal deposits (Hayes, 1979; Nummedal, 1983). In the Northern Sector (Fig. 4), most of the numerous drift cells (28) have net shore-drift to the north (22); but six net shore-drift directions are to the south, either because of wind-shadow effects or wave refraction around stacks and arches.

Knowledge of many coastal sectors of the world would be greatly enhanced by similar mapping projects.

Acknowledgments

We offer our sincere thanks to the Washington State Department of Ecology for the funding which made this investigation possible, and to Joy Dabney for drafting the map figures.

References

Corps of Engineers, 1973, West coast deepwater port facilities study: North and South Pacific Divisions, U.S. Army Corps of Engineers, Portland and San Francisco, various pagination.

Engstrom, W.N., 1978, The physical stability of the Lake Tahoe shoreline: Shore and Beach, v. 45, p. 9-13.

Hayes, M.O., 1979, Barrier island morphology as a function of tidal and wave regime, in S.P. Leatherman, ed., Barrier Islands from the Gulf of St. Lawrence to the Gulf of Mexico: Academic Press, p. 1-27.

Hunter, R.E., Sallenger, A.H., and Dupre, W.R., 1979, Methods and descriptions of maps showing the direction of longshore sediment transport along the Alaskan Bering seacoasts: U.S.. Geological Survey Miscellaneous Field Studies Map MF-1049, 7 p., 5 plates.

Jacobsen, E. E., and Schwartz, M. L., 1981, The use of geomorphic indicators to determine the direction of net shore-drift: Shore and Beach, v. 49, p. 38-43.

Morelock, J., Schwartz, M. L., Hernandez-Avila, M., and Hatfield, D. M., 1985, Net shore-drift on the north coast of Puerto Rico: Shore and Beach, in press.

Nummedal, D., 1983, Barrier islands, in P. D. Komar, ed., CRC Handbook of coastal processes and erosion: CRC Press, Boca Raton, Florida, p. 77-121.

Phipps, J. B., and Smith, J. M., 1978, Coastal accretion and erosion in southwest Washington: Dept. of Ecology, Olympia, Washington, 76 p.

Plopper, C. S., 1978, Hydraulic sorting and longshore transport of beach sand, Pacific coast of Washington: Syrcuse University, Syracuse, N. Y., unpublished PhD thesis, 156 p.

Schwartz, M. L., and Anderson, B., 1985, Coastal geomorphology of Padre Island, Mexico: Shore and Beach, in press.

Schwartz, M. L., and Blankenship, D. G., 1984, Mason County coastal zone atlas net shore-drift: Washington State Department of Ecology, Olympia, Washington, 55 p. & maps.

Schwartz, M. L., and Chrzatowski, M. J., 1984, King County coastal zone atlas net shore-drift: Washington State Department of Ecology, Olympia, Washington, 34 p. & maps.

Schwartz, M. L., and Harp, B. D., 1984, Pierce County costal zone atlas net shore-drift: Washington State Department of Ecology, Olympia, Washington, 57 p. & maps.

Schwartz, M. L., and Hatfield, D. M, 1984, Thurston County coastal zone atlas net shore-drift: Washington State Department of Ecology, Olympia, Washington, 30 p. & maps.

Schwartz, M. L, and Taggart, B. E., 1984, Kitsap County coastal atlas net shore-drift: Washington State Department of Ecology, Olympia, Washington, 43 p. & maps.

Self, R. P., 1977, Longshore variation in beach sands, Nautla area, Veracruz, Mexico: Journal of Sedimentary Petrology, v. 47, p. 1437-1443.

Sunamura, T., 1972, Improved method for inferring the direction of littoral drift from grain size properties of beach sands: Annual Report of the Engineering Research Institute, Faculty of Engineering, Tokyo, v. 31, p. 61-68.

Terich, T. A., and Schwartz, M. L., 1981, A geomorphic classification of Washington State's Pacific coast: Shore and Beach, v. 49, p. 21-27.

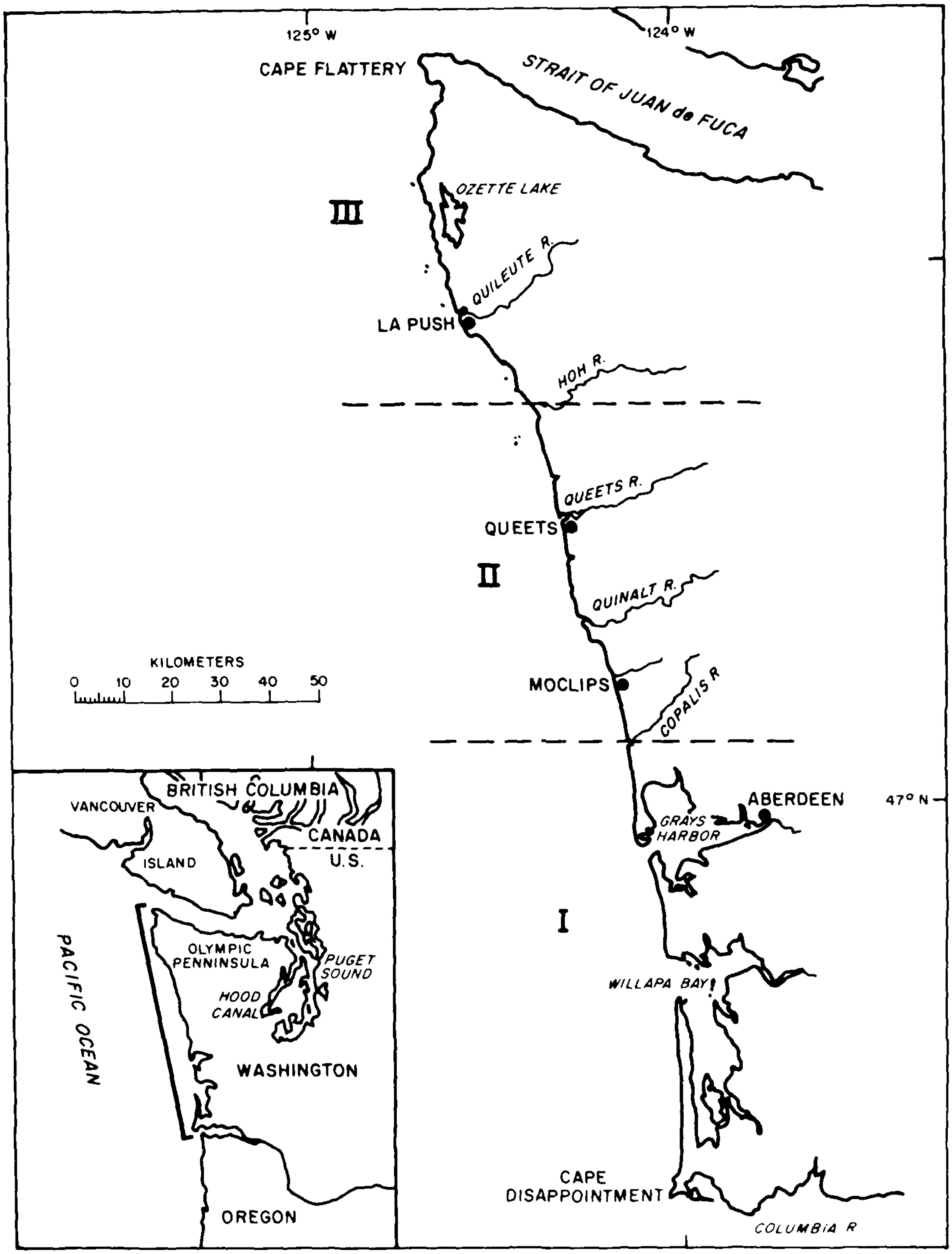
125° W
124° W
CAPE FLATTERY
STRAIT OF JUAN de FUCA
OZETTE LAKE
III
QUILEUTE R.
LA PUSH
HOH R.
QUEETS R.
QUEETS
II
QUINALT R.
KILOMETERS
0 10 20 30 40 50
MOCLIPS
COPALIS R
ABERDEEN
47° N
GRAYS HARBOR
I
WILLAPA BAY
CAPE DISAPPOINTMENT
COLUMBIA R
BRITISH COLUMBIA
VANCOUVER
ISLAND
CANADA
U.S.
PACIFIC OCEAN
OLYMPIC PENNINSULA
PUGET SOUND
HOOD CANAL
WASHINGTON
OREGON

Figure I. Location map of the Pacific coast of Washington State.

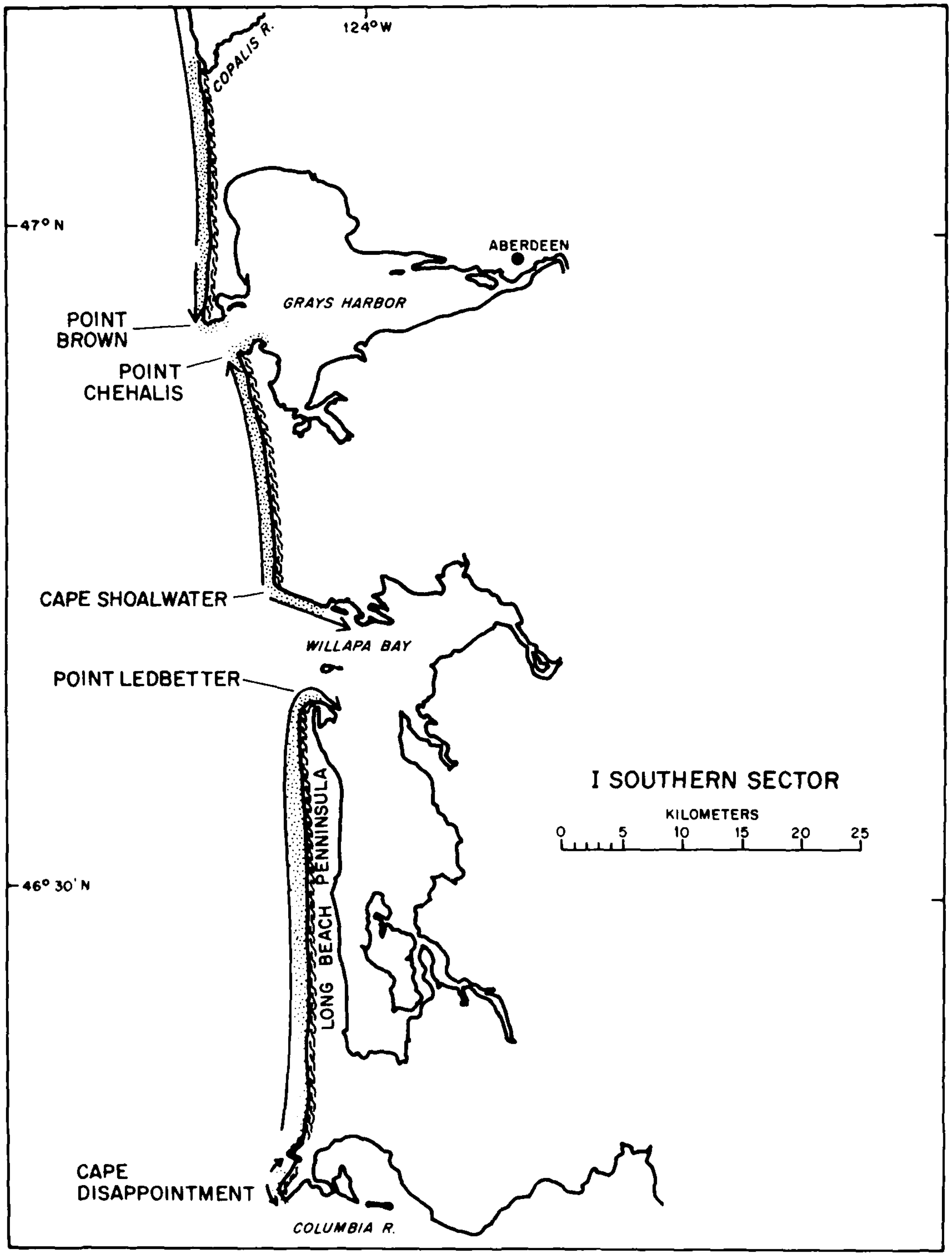
124°W
COPALIS R.
47° N
ABERDEEN
GRAYS HARBOR
POINT BROWN
POINT CHEHALIS
CAPE SHOALWATER
WILLAPA BAY
POINT LEDBETTER
LONG BEACH PENNINSULA
I SOUTHERN SECTOR
KILOMETERS
0
5
10
15
20
25
46° 30' N
CAPE DISAPPOINTMENT
COLUMBIA R.

Figure 2. Net shore-drift along the southern sector (1) of the Pacific coast of Washington State.

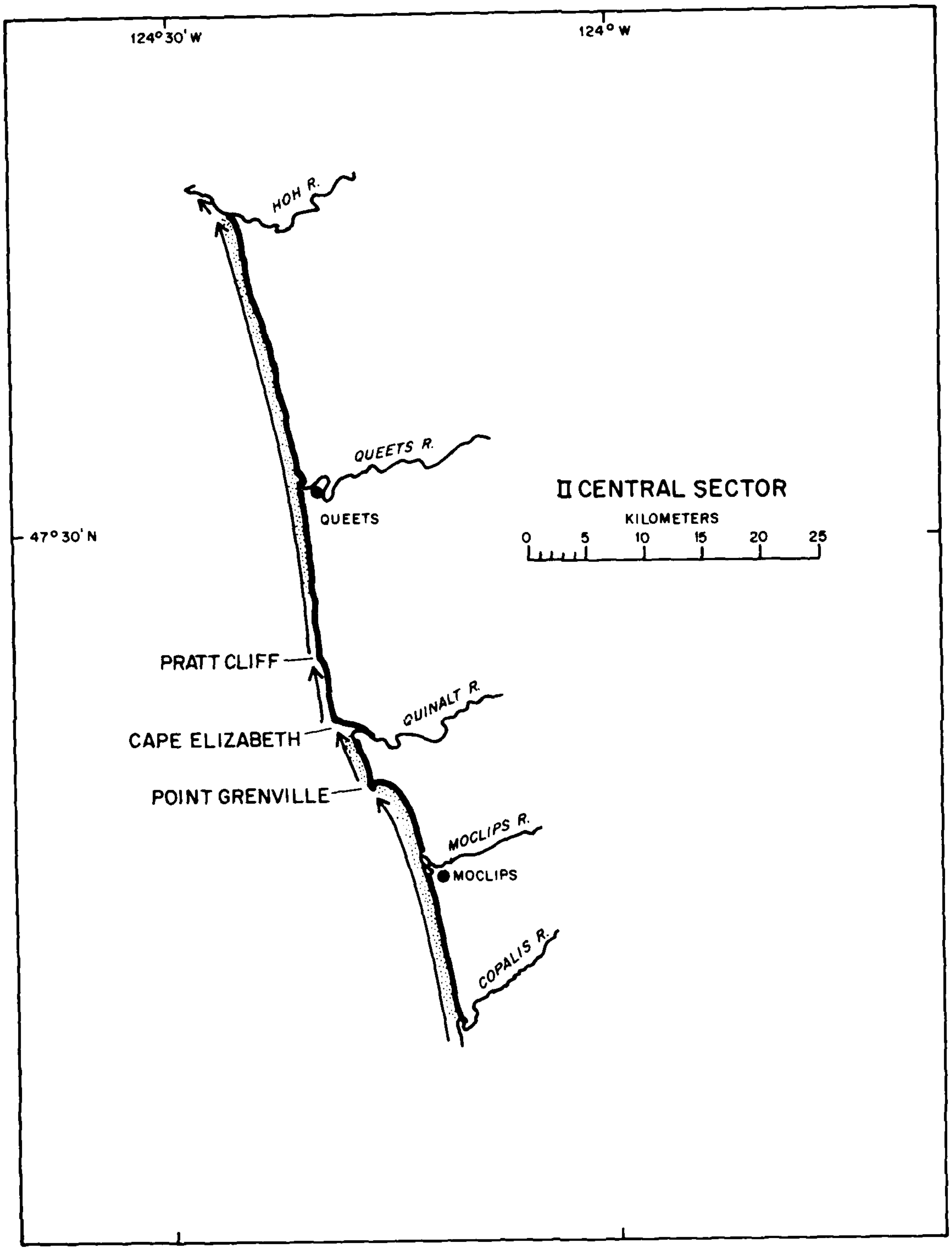
124°30' W
124° W
47°30' N
HOH R.
QUEETS R.
QUEETS
II CENTRAL SECTOR
KILOMETERS
0
5
10
15
20
25
PRATT CLIFF
QUINALT R.
CAPE ELIZABETH
POINT GRENVILLE
MOCLIPS R.
MOCLIPS
COPALIS R.

Figure 3. Net shore-drift along the central sector (II) of the Pacific coast of Washington State.

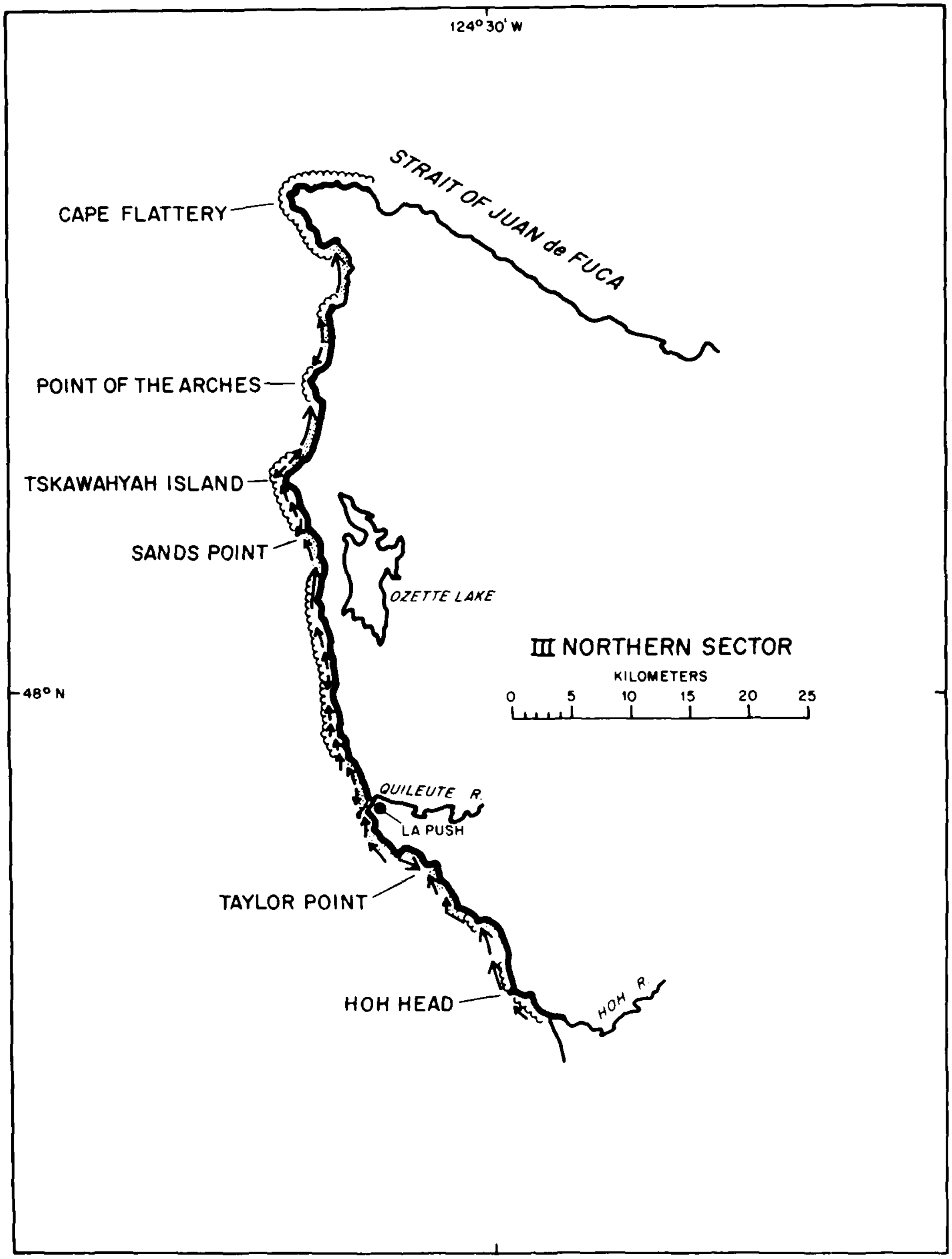
124°30' W
STRAIT OF JUAN de FUCA
CAPE FLATTERY
POINT OF THE ARCHES
TSKAWAHYAH ISLAND
SANDS POINT
OZETTE LAKE
III NORTHERN SECTOR
KILOMETERS
0
5
10
15
20
25
48° N
QUILEUTE R.
LA PUSH
TAYLOR POINT
HOH HEAD
HOH R.

Figure 4. Net shore-drift along the northern sector (III) of the Pacific coast of Washington State.

THE SEVERE EROSION OF CAPE SHOALWATER, WASHINGTON

Thomas Terich* and Terence Levenseller**

ABSTRACT

Cape Shoalwater on the southwest Pacific coast of Washington State has been eroding at rates in excess of 30 meters per year since the turn of the century. It is the most active coastal erosion site along the Pacific coast of the United States. The region receives a plentiful supply of littoral sediments and the neighboring coastlines are advancing. Study reveals the erosion is resulting from the long-term northward migration of the tidal channel towards the Cape leading to very rapid shoreline retreat. There is some evidence of a slowing erosion rate due to the development of a secondary channel opening to the south of the main channel.

Introduction

The contemporary shoreline of Washington State's southern coast began to take shape with the postglacial stabilization of sea level approximately 4000 to 5000 years B.P. At that time great quantities of sediment were delivered to the coast by the Columbia River draining eastern Washington and the Chehalis River which for the period of time was the only major meltwater outlet for the ice-filled Puget Lowland (McKee, 1972). The sediments were worked by littoral and eolian processes into the coastal configurations observed today. One of the most prominent features is Long Beach Peninsula, a spit 43 km long (27 miles) trending north from the Columbia River (Figure 1).

The northward growth of the spit progressed until only a relatively narrow channel connected the sheltered waters of Willapa Bay with the Pacific Ocean. Concurrently a smaller, less prominent south trending spit, Cape Shoalwater, also grew into the mouth of the channel from the north. As the converging spits grew toward one another, the channel narrowed and tidal velocities increased.

The two spits probably evolved through several periods of advance and retreat. The most recent maximum approach of the two spits was just after the turn of this century. A sequential development of relict beach ridges on both the Long Beach Peninsula and Cape Shoalwater confirm their convergent development (U.S. Army Corps of Engineers, 1967).

*Associate Professor, Department of Geography and Regional Planning, Western Washington University

**Master of Science Candidate, Department of Geography and Regional Planning, Western Washington University

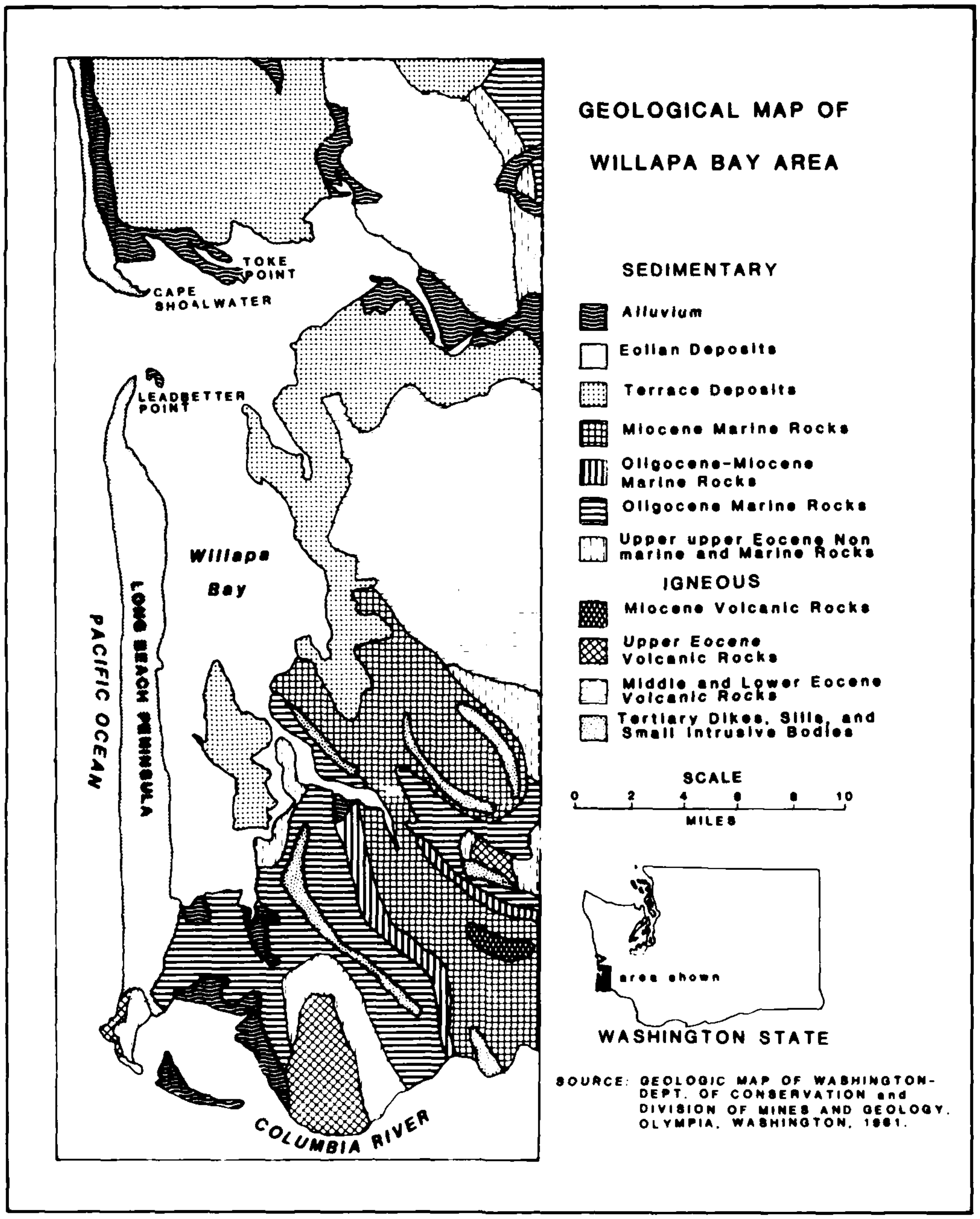
GEOLOGICAL MAP OF WILLAPA BAY AREA
SEDIMENTARY
Alluvium
Eolian Deposits
Terrace Deposits
Miocene Marine Rocks
Oligocene-Miocene Marine Rocks
Oligocene Marine Rocks
Upper upper Eocene Non marine and Marine Rocks
IGNEOUS
Miocene Volcanic Rocks
Upper Eocene Volcanic Rocks
Middle and Lower Eocene Volcanic Rocks
Tertiary Dikes, Sills, and Small Intrusive Bodies
SCALE
0 2 4 6 8 10
MILES
area shown
WASHINGTON STATE
TOKE POINT
CAPE SHOALWATER
LEADBETTER POINT
Willapa Bay
LONG BEACH PENINSULA
PACIFIC OCEAN
COLUMBIA RIVER
SOURCE: GEOLOGIC MAP OF WASHINGTON-DEPT. OF CONSERVATION and DIVISION OF MINES AND GEOLOGY, OLYMPIA, WASHINGTON, 1961.

Figure 1. Location and regional geology of Willapa Bay and Cape Shoalwater.

Until recently there was some controversy among coastal researchers regarding the net movement of littoral sediments along this part of the coast. The development of converging spits at Willapa Bay and Gray's Harbor, approximately 32 km (20 miles) to the north, have helped to fuel the controversy. Twenhofel (1943) was among the first of the researchers to argue for a net northward sediment transport based on the predominent northward growth of Long Beach Peninsula and southerly storm waves that frequent the coast. Cooper (1958) acknowledged the importance of the southerly storm waves, but maintained that the more gentle prevailing northwesterly swells were more effective movers of beach sediment. He promoted a net southerly sediment transport along the Washington coast. Ballard (1964) investigated the energy component of waves striking the shores of the Pacific Northwest. His studies showed a distinct seasonality of the wave regime. During summer, waves are predominantly from the northwest causing longshore currents and sediment transport to the south. In winter the directions are reversed, however; winter storm waves are of significantly high energy. These higher energy storm waves drive strong northerly longshore currents and carry large volumes of littoral sediments. The result is a seasonal reversal of sediment transport, however, with a net dominant northerly flow. Studies of the longshore energy flux conducted by the U.S. Army Corps of Engineers (1967) also showed a predominant net northerly littoral transport. Sedimentological studies by Venkatarathnam and McMannis (1973) and more recently Plopper (1978) provide additional evidence for a net northerly sediment transport along this part of the coast. Plopper investigated the hydraulic sorting and mineralogical characteristics of littoral sediments along the entire Washington coast. He found both the mineralogy and sorting characteristics to complement Ballard's wave energy studies. The relative sizes of the two opposing spits projecting into the Willapa Channel provides further empirical support for these findings. Recently Schwartz et al. (1985) have confirmed a net northerly flow of beach sediment along this part of the Washington coast with one short divergent segment from Cape Shoalwater southeasterly into Willapa Bay.

Erosion History

Cape Shoalwater has had a very long continuous erosion history. U.S. Coast and Geodetic Survey Charts dating back to the turn of the century provide evidence of the shoreline changes. One of the earliest known charts for the area, published in 1911, shows Cape Shoalwater with topographic, triangulation and hydrography surveys dating from 1871 to 1891 (Figure 2a). The Cape is shown as a pronounced south trending spit projecting southeasterly into Willapa Channel. The configuration of the shoreline appears relatively smooth, giving no indication of erosional retreat. At the time of the survey, the navigable channel was approximately 1.5 kilometers wide with maximum depths to 26 meters (85 ft.).

The Willapa Bay Lighthouse is shown in a photograph circa 1900 (Figure 3). At that time, it was located approximately 2 kilometers inland from the north shore of the channel entrance to Willapa Bay. In the following years the shoreline rapidly retreated northward forcing the relocation of the lighthouse in the late 1930s.

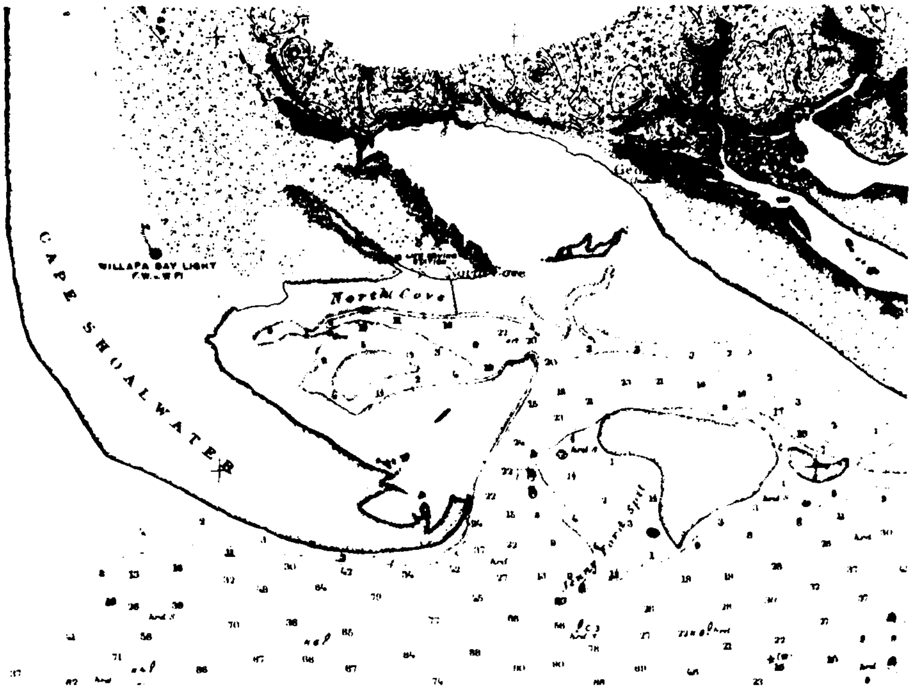
CAPE SHOALWATER
WILLAPA BAY LIGHT
North Cove

Figure 2a. U.S. Coast and Geodetic Survey chart published in 1911 with survey data to 1891.

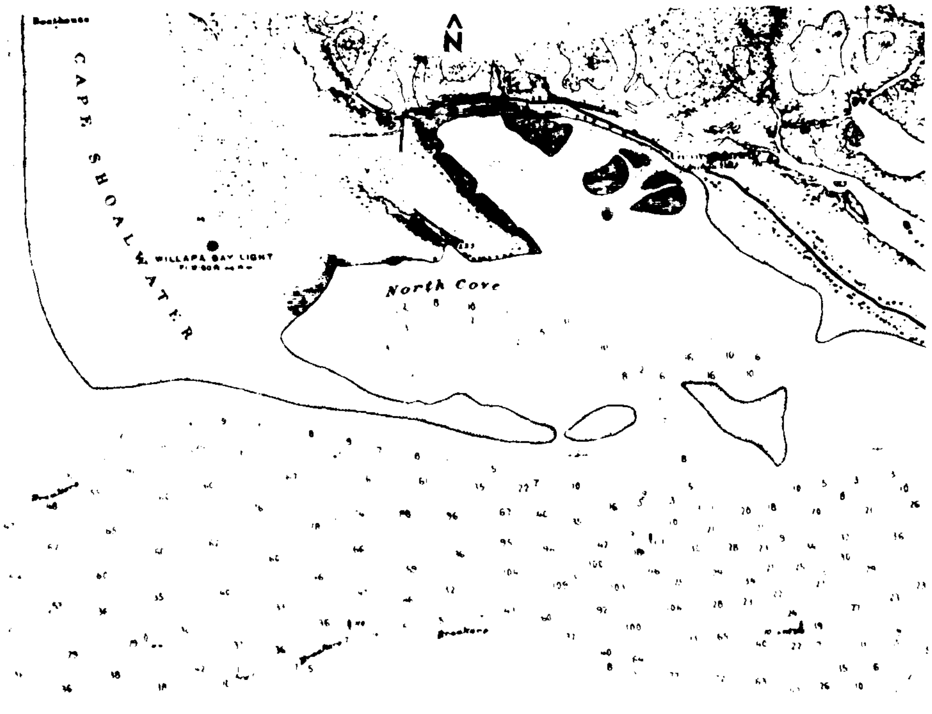
Boathouse
N
CAPE SHOALWATER
WILLAPA BAY LIGHT
North Cove
Breakers

Figure 2b. U.S. Coast and Geodetic Survey chart published in 1912 with survey data to 1911.

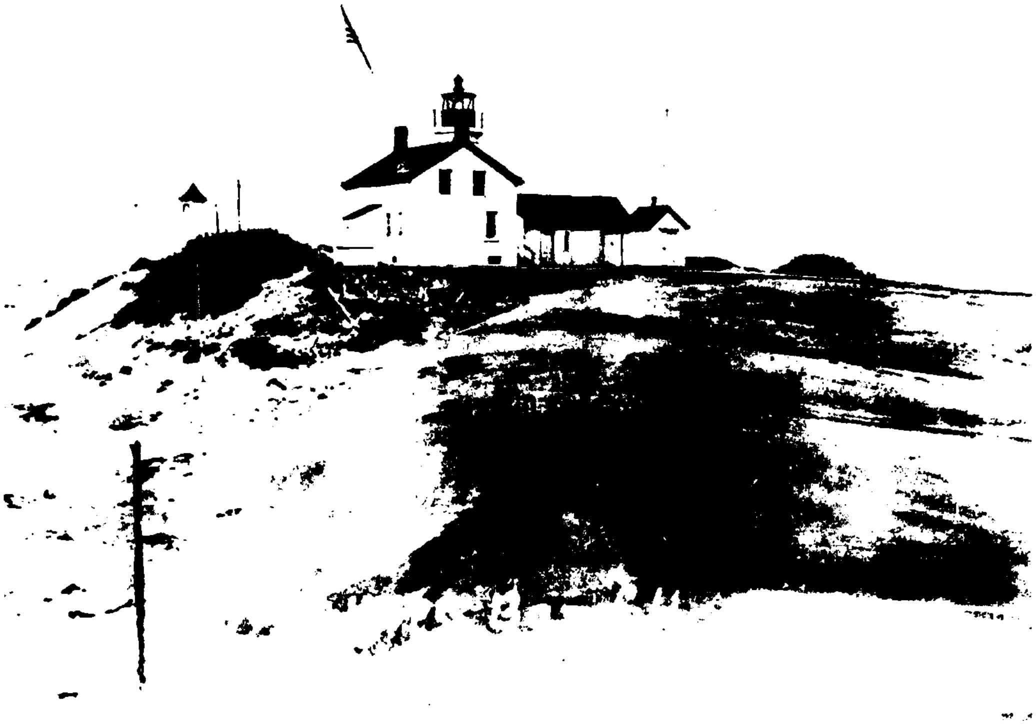

Figure 3. Circa 1900 photograph of the Willapa Bay Lighthouse (courtesy of William Jacobsen).

In 1912 another Coast and Geodetic Survey chart was published updating survey data to 1911. This chart clearly shows erosion of the Cape (Figure 2b). Thus, erosion must have begun sometime between 1891 and 1911. Comparative measurements of these two early charts reveal a total shoreline retreat of approximately 760 meters (2500 ft.). Assuming an average annual recession rate of 45 m/yr. (150 ft./yr.), erosion would have had to commence in the mid 1890s. Four years later, the 1916 chart shows the southern projection of the spit to be completely missing. The shoreline along the Cape no longer gently curved to the southeast into the channel but turned abruptly to the east. Concurrently the large shoal north from Ledbetter Point appeared to have grown significantly in size. Charts subsequent to 1928 showed relatively minor shoreline configuration changes, but the overall recession of the shoreline proceeded.

In 1955, the U.S. Army Corps of Engineers was authorized by the Public Works Committee of the U.S. Senate to begin investigating the effects of erosion on the navigation channel across the outer bar and erosion control measures at Cape Shoalwater. In 1956 the committee concluded its study recommending against an immediate engineering solution to the erosion problem. They concluded that further study was necessary to determine the most feasible solution to the serious erosion and navigation problems and that prospective benefits were insufficient to justify the cost of rectifying the problems (U.S. Army Corps of Engineers, 1956).

Additional study was initiated in January 1966 at the request of the Washington State Department of Conservation. The study was conducted by civil engineering and oceanography professors from the University of Washington along with staff from the U.S. Army Corps of Engineers. The committee was known as the "Erosion Advisory Committee." Their studies showed the long-term erosion rate to average 42 m/yr. (140 ft./yr.). Some periods of very little erosion were followed by accelerated erosion rates of up to 75 m/yr. (250 ft./yr.). During the times of active erosion, it was estimated that 20 hectares (50 acres) of land were lost annually.

The committee concluded that the erosion is a symptom of a much larger problem, namely the progressive northward migration of the main channel entrance to Willapa Bay. As the channel moves toward Cape Shoalwater, southerly storm waves break close to shore easily eroding the beach. The eroded materials are then carried into the bay or out to sea by tidal currents. The committee estimated mean maximum tidal flow through the channel to be 53,000 m^2/sec (400,000 c.f.s.), roughly equal to the flow of the lower Mississippi River. An attempt to halt the channel migration was therefore compared to similar projects along the Mississippi River. A concrete or asphalt mattress revetment, a design to stabilize similar channel migrations along the Mississippi was estimated to cost a minimum $2,000,000.

Several other alternatives to slowing the erosion were explored, among them were jetty construction, pile diking and groin emplacement. No short-term measures seemed feasible to the committee. Any long-term solutions were very costly. The committee also explored a nonstructural alternative. Diversion of the main channel to a shorter more efficient route might halt its northern migration. A smaller secondary channel near Ledbetter Point could be dredged, encouraging tidal currents to flow through it, thus reducing the volume of flow through the main channel. There was concern whether the shorter channel, once dredged, would widen and deepen naturally. Furthermore, there was no assurance that this newer channel would itself remain in a stable location.

The committee concluded there were no interim or temporary engineering solutions that were economically justifiable. They recommended that any funds dedicated to alleviating the erosion would perhaps be better spent purchasing the threatened land in the path of the erosion rather than attempting to resist the erosion itself.

Erosion Rates

There is no other place along the Pacific Coast of the United States that has had such a rapid and sustained erosion history as Cape Shoalwater. The U.S. Army Corps of Engineers have monitored the erosion using charts and field surveys. These data show an average annual erosion rate of 37.8 m/yr. (126.0 ft./yr.) from 1890 to 1965 (Figure 4). During this 75-year erosion history, the shoreline has retreated a total of 3750 m (12,500 ft.).

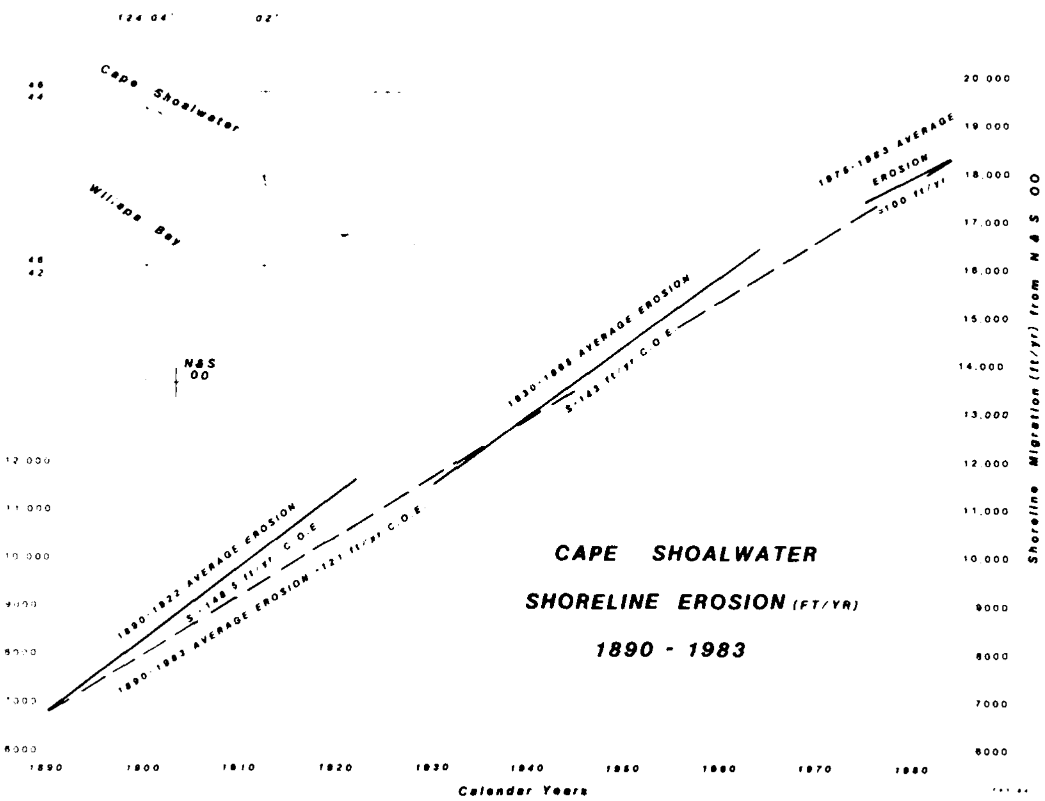

Figure 4. Erosion rates 1890 to 1983. Data 1890 to 1965 by U.S. Army Corps of Engineers, Seattle District. 1975 to 1983 erosion rates measured by author from N.O.S. charts.

There was some concern that channel dredging, which began in 1930, might have contributed to, or accelerated, the erosion of the Cape. Average annual erosion rates prior to channel dredging (1890-1922) were compared with subsequent years (1930-1965) when dredging was done yearly, some during World War II. Shoreline measurements between 1890 and 1922 yielded an average annual erosion rate of 44.5 m/yr. (148.5 ft./yr.). Measurements taken during the period of annual dredging from 1930 to 1965 showed an average annual erosion rate of 42.9 m/yr. (143 ft./yr.). There clearly was no significant difference between the erosion rates for the two periods indicating that the channel dredging has no apparent effect on the erosion of Cape Shoalwater.

The erosion data for the 75-year period from 1890 to 1965 clearly showed a trend of sustained erosion. There was no evidence indicating that the erosion would slow or stop. In 1967, the U.S. Army Corps of Engineers projected the sequential retreat of the shoreline at Cape Shoalwater through 1994 (Figure 5). They concluded that the erosion would continue unabated through the low dune areas to the west, but slow to the east where uplands composed of more resistant terrace deposits are located. The projections show slightly greater accelerated erosion than has actually occurred. The 1985 shoreline configuration is farther south by nearly 100 meters than projected.

Of great concern in the late 1960s and early 1970s was the inevitable breaching of the State Highway 105 (Figure 6). In 1971 the State of Washington prepared a new alignment 1 km north along the base of the uplands. By the mid 1970s the old highway was being undermined and was soon completely severed (Figure 7). At this same time controversy also emerged about the fate of an old pioneer cemetery adjacent to the eroding highway. Some suggested leaving it to erode away, as moving it would be too costly. Others pleaded for relocation of the cemetery. Several prominent public officials were brought into the issue, including the Governor of the State (Seattle Times, April 18, 1976). Despite the cost, the cemetery was moved and sited adjacent to the new alignment of the state highway.

In order to update the erosion rates as determined by the U.S. Army Corps of Engineers since 1965 (Figure 4), the location of the Cape Shoalwater shoreline was measured from National Ocean Survey charts for 1975, 1980 and 1984 by the author. The comparative measurements for the nine-year period yielded an average annual erosion rate of 30 m/yr. (100 ft./yr.). This rate is lower than the 37.8 m/yr. (126.0 ft./yr.) annual erosion rate from 1890 to 1965. The lower rate might reflect some measurement inaccuracies that are inherent with map measurements or indicate actual slowing of the erosion rate. There is some additional evidence supporting a slowing of the erosion rate. Over the last several years the Pacific County Assessor's Office has plotted the approximate high water mark as shown on aerial photos to section maps scaled at 1 inch to 400 feet. The high water lines were not plotted with cartographic precision, yet comparative measurements taken several points along the lines plotted between 1976 and 1981 yield average annual shoreline recession rate of nearly 30 m/yr. This erosion rate is very close to the 30 m/yr. average erosion rate between 1975 and 1984 as measured from National Ocean Survey charts.

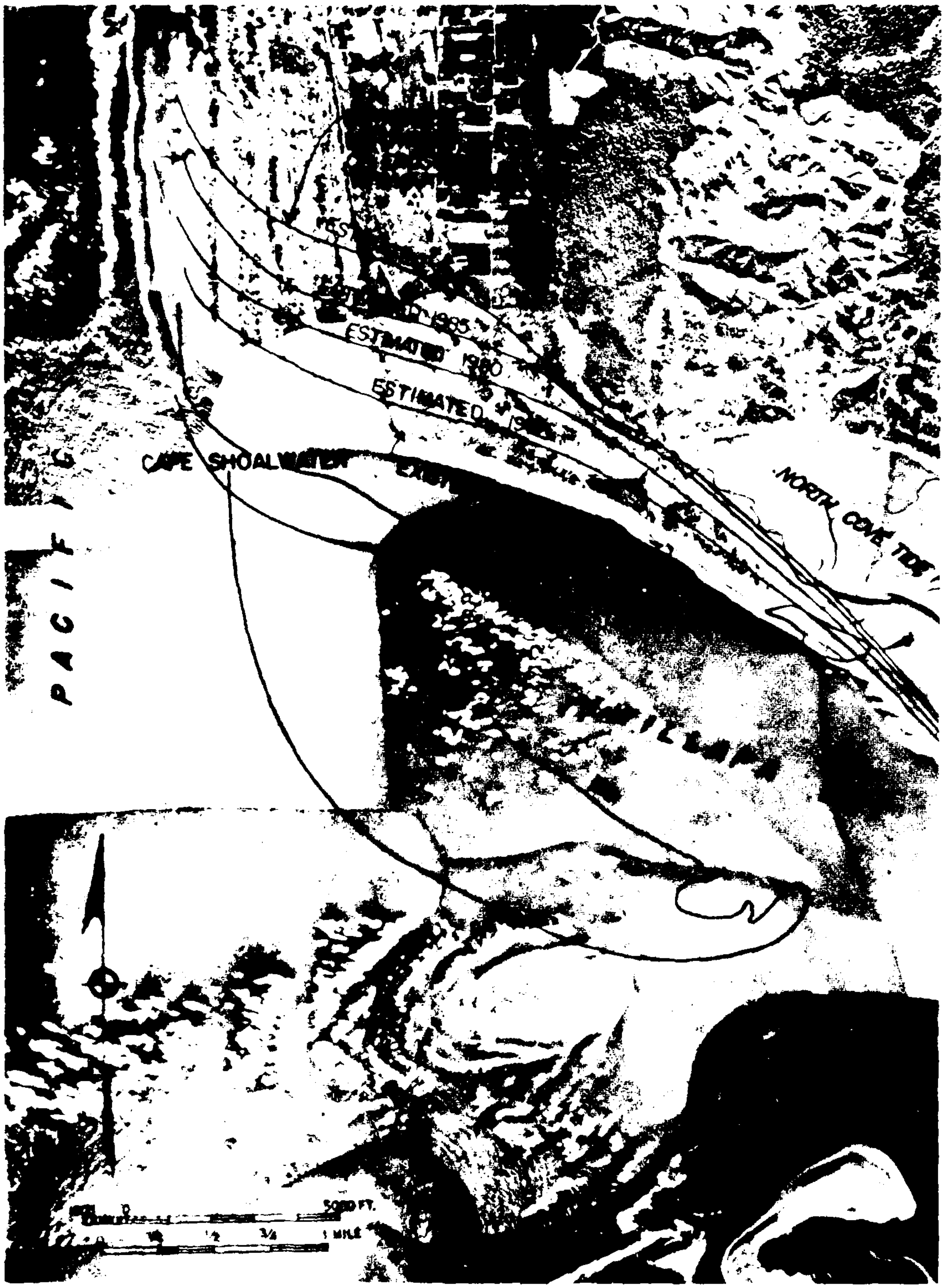
PACIF
CAPE SHOALWATER
EXIST
ESTIMATED 1985
ESTIMATED 1980
ESTIMATED
NORTH COVE TIDE
5000 FT.
0
1/4
1/2
3/4
1 MILE

Figure 5. Cape Shoalwater shoreline configurations from 1891 with estimated limit to 1994 (U.S. Army Corps of Engineers, Seattle District).

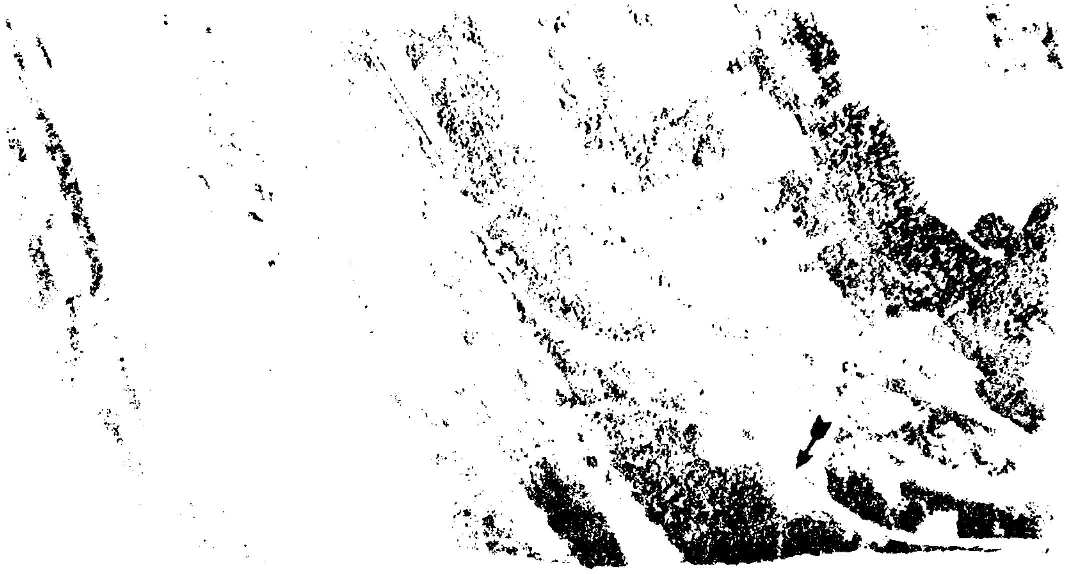

∧
N

1974

Figure 6. Aerial photography of Cape Shoalwater taken in 1974. Black arrow indicates the location of the old coast highway threatened by erosion. The new highway alignment is under construction to the north.

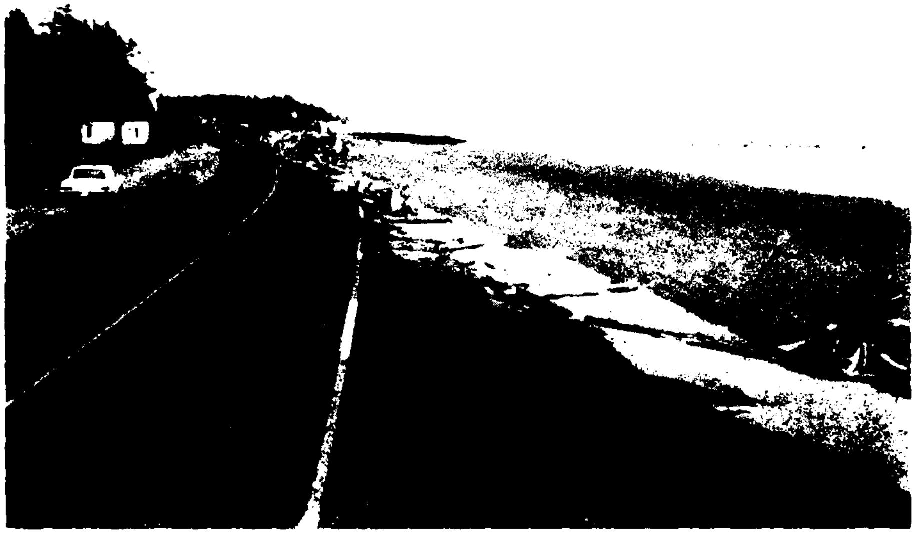

Figure 7. A 1976 view to the east of the old coastal highway eroding away.

Causes of the Erosion

The persistent, severe erosion of Cape Shoalwater presents a perplexing problem. The severity of erosion suggests the area is starved of sediment and that a lack of sediment is primarily responsible for the erosion. There is, however, no evidence of sediment starvation in the area. On the contrary, Phipps and Smith (1978) have shown this coastal region to have an abundance of littoral sediment. The sediment supply has resulted in many decades of net shoreline accretion to the Long Beach Peninsula exceeding 6 m/yr. (20 ft./yr.). The shoreline north of Cape Shoalwater has also accreted westerly at rates ranging from 1.2 to 3.9 m/yr. (4.0 to 13 ft./yr.). Thus, a lack of regional sediment supply is not the cause of the erosion.

It is possible that the abundant sediment supply might actually be contributing to the erosion of Cape Shoalwater. As prevailing longshore currents transport sediment to the north along the Long Beach Peninsula, the wide Willapa Channel is encountered. Tidal currents flowing transverse to the prevailing longshore transport significantly alter the littoral transport regime (Plopper, 1978). This leads to the growth of large shoals and sand bars within the channel. As the shoals grow and migrate, they continually force the tidal channel to the north closer to Cape Shoalwater. Storm waves breaking close to the shore in concert with the scouring action of the northward migrating channel result in the active erosion of the Cape. Cross sections of the channel show a steady, uninterrupted northward migration of the primary channel since 1891 (Figure 8). The average rate of northward movements over the 92-year record is approximately 33 m/yr. (110 ft./yr.). This rate is very close to the 36 m/yr. (121 ft./yr.) average erosion rate for Cape Shoalwater from 1890 to 1983.

The erosional retreat of Cape Shoalwater has not been matched by a northerly growth of the Long Beach Peninsula. Historical comparisons of Ledbetter Point at the north end of the Long Beach Peninsula show periods of advance and retreat with no significant northward growth (Phipps and Smith, 1978). The long period of erosion has, however, significantly widened the channel entrance. In 1873 the straight line distance between Ledbetter Point and the south shore of Cape Shoalwater was approximately 4.75 km (2.96 miles). In 1983 that same distance was 9.75 km (6.09 miles), 5 km (3.12 miles) wider. Extensive shoals have grown in the channel since the turn of the century. There is evidence that the channel shoals are also periodically nourished by sediments north from Cape Shoalwater. A pattern of bar development and migration is observed from a sequence of Coast and Geodetic Survey charts (Figure 9). A bar, resembling the embryonic image of the former spit that occupied this nearby site in the 1980s was shown west of Cape Shoalwater. Between 1956 and 1959 it grew in a southwesterly direction. The tidal channel breached the bar and the severed portion migrated to the south and east between the years 1960 and 1967 eventually welding onto the main shoal in the channel. There is evidence that this might be cyclic phenomenon and is contributing, along with littoral sediments from the south, to the overall growth of shoals in the channel (U.S. Army Corps of Engineers, 1967). As the

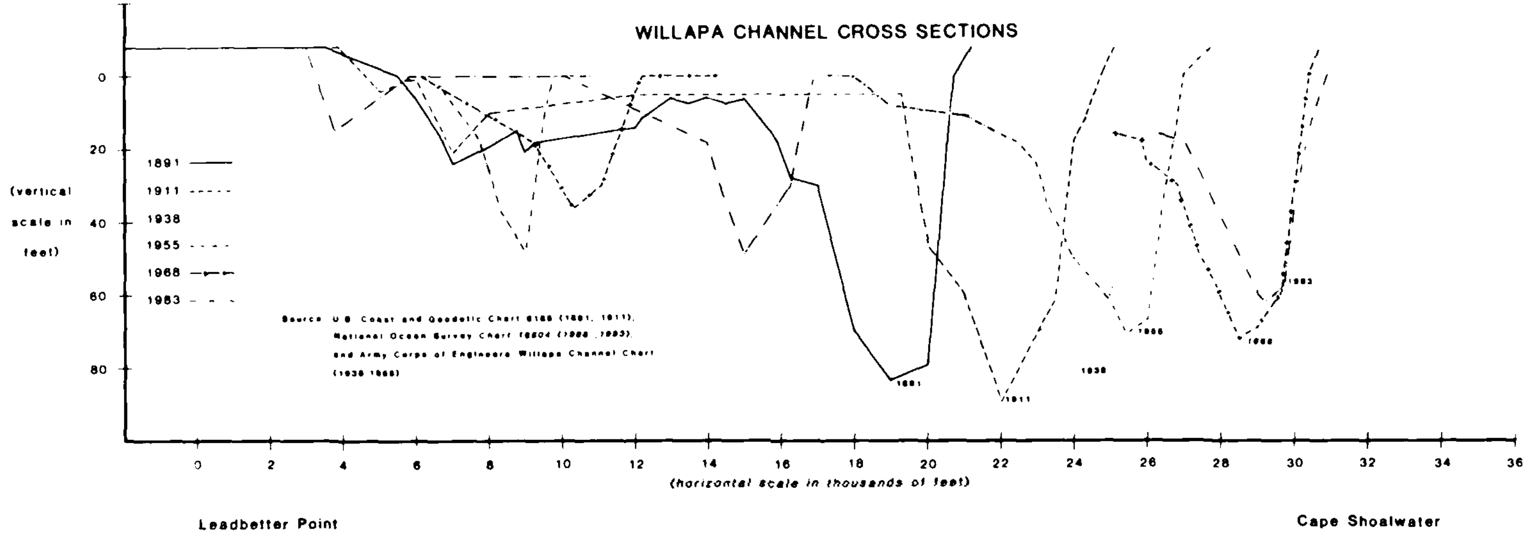

Source U.S. Coast and Geodetic Chart 6185 (1891, 1911), National Ocean Survey Chart 18504 (1968, 1983), and Army Corps of Engineers Willapa Channel Chart (1938-1955)

Figure 8. The progressive migration of the Willapa Channel thalweg toward Cape Shoalwater.

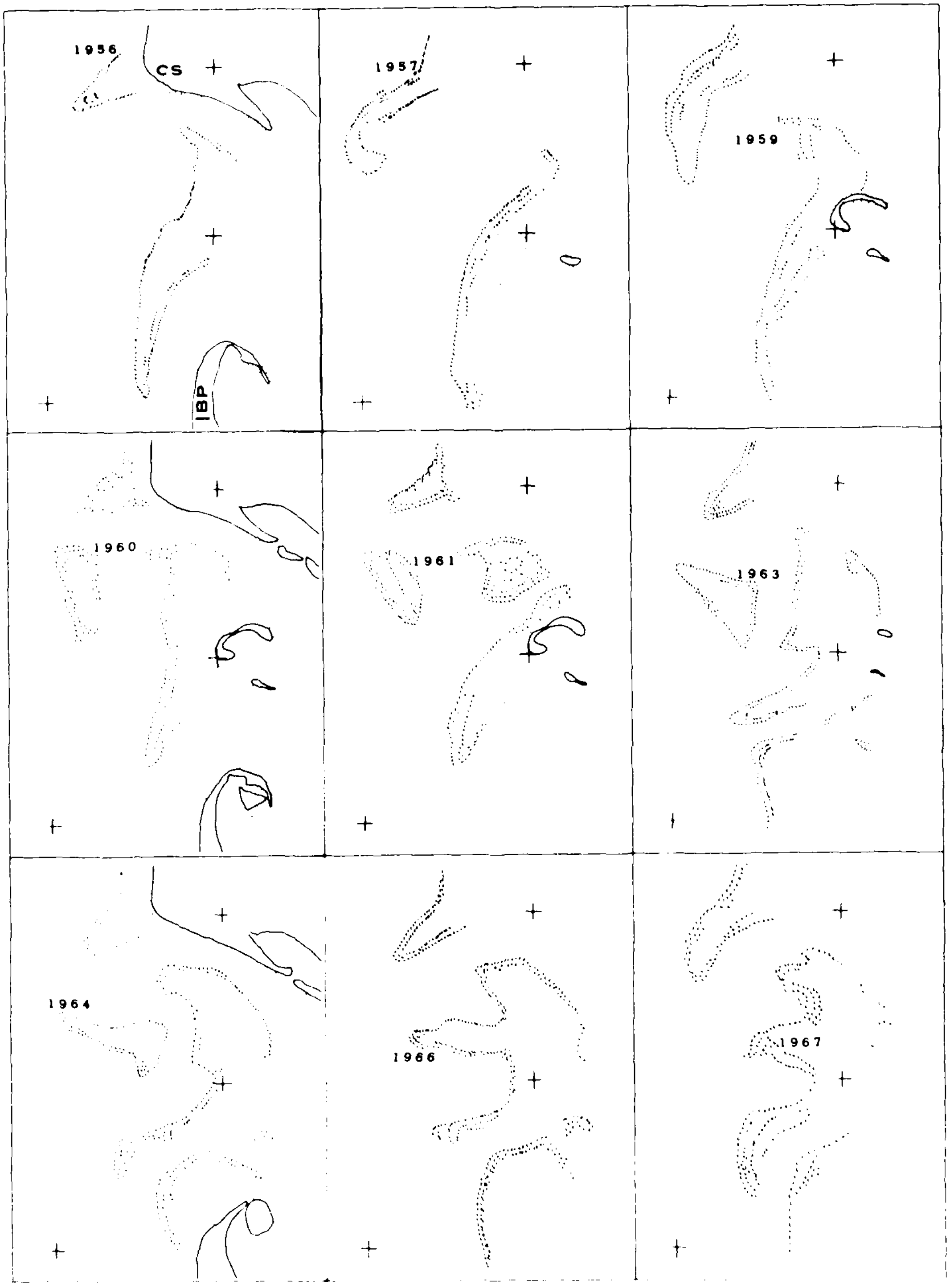
1956
CS
IBP
1957
1959
1960
1961
1963
1964
1966
1967

Figure 9. Migration of an embryonic spit south from Cape Shoalwater 1956-1959, then east to eventually join the Willapa Channel shoals 1960-1967 (C.S. = Cape Shoalwater; L.B.P. = Long Beach Peninsula).

shoals grow in size, they force the tidal channel to the north, closer to the Cape Shoalwater, perpetuating the erosion.

Conclusion

Cape Shoalwater has been eroding faster and for a longer time than any other site along the Pacific Coast of the United States. The problem has received little attention beyond the immediate region. Up to now most of the eroded land has been rural, endangering or destroying relatively few man-made structures. Should the erosion continue as predicted, it will soon advance upon a developed subdivision of small cottages. As this occurs there will undoubtedly be some greater attention focussed on the area.

There is little doubt that the erosion of Cape Shoalwater is due to the northward migration of the Willapa Channel. The abundance of littoral sediments in the region and the net northerly longshore current are forcing the channel thalweg to the north against the cape. The greatest source of these channel sediments is from the south; however, there is evidence of some cyclic contribution of bar sediments from the north as well.

Recent measurements indicate that the erosion rate is slowing. There are several possible reasons. One of the less obvious is the relatively recent development of Ledbetter Channel, a new secondary channel just north of Ledbetter Point at the north end of the Long Beach Peninsula. Navigation charts show that over the last several years, it has become deeper and longer. By 1983 it had developed into an unobstructed channel penetrating through the shoals out to the sea. Its hydraulic efficiency might increase to a point where it significantly reduces the volume and velocity of flow through the main channel. This could result in the slowing of the erosion to Cape Shoalwater.

By any relative measure, even a slowing of the erosion rate to 30 m/yr. (100 ft./yr.) is still very active erosion. A housing subdivision is endangered and the new highway, moved to the north in 1977, is once again being threatened. The severe retreat of the shoreline over the last 90 years indicates there is little evidence for any significant change in the erosion rate of Cape Shoalwater in the near future.

Acknowledgements

The authors gratefully acknowledge the friendly assistance of A. David Schuldt and Eric Nelson, U.S. Army Corps of Engineers, Seattle District; the manuscript reviews of Dr. Richard Smith and Dr. Maurice Schwartz; and the skilled graphics provided by Eugene Hoerauf, Department of Geography and Regional Planning, Western Washington University.

References

1. Andrews, R.S., 1965. Modern Sediments of Willapa Bay, Washington: A Coastal Plain Estuary. M.S. thesis, Dept. of Geology, University of Washington, 52 p.

2. Ballard, R.L., 1964. Distribution of Beach Sediment near the Columbia River. University of Washington Dept. of Oceanography Technical Report No. 98, 82 p.

3. Cooper, W.S., 1958. Coastal Sand Dunes of Oregon and Washington. Geological Society of American Memoir 72, 189 p.

4. Erosion Advisory Committee, 1966. Considerations for the Temporary Arresting of the Erosion at Cape Shoalwater, Washington. Unpublished report to Washington State Dept. of Conservation, 9 p.

5. McKee, Bates, 1972. Cascadia, New York. McGraw-Hill, 394 p.

6. Plopper, C.S., 1978. Hydraulic Sorting and Longshore Transport of Beach Sand, Pacific Coast of Washington. Unpublished Ph.D. Dissertation, Dept. of Geology, Syracuse University, 185 p.

7. Phipps, J.B. and J.M. Smith, 1978. Coastal Accretion and Erosion in Southwest Washington. State of Washington, Dept. of Ecology Report 78-12, 75 p.

8. Schwartz, Maurice, et al., 1985. Net Shore Drift along the Pacific Coast of Washington State. Shore and Beach, Vol. 53, No. 3, pp. 21-25.

9. Seattle Times, April 18, 1976, "Cementary Slowly Washing Away."

10. Twenhofel, W.H., 1943. Origin of the Black Sands of Southwest Oregon. Oregon Dept. of Geology and Mineral Industries, Bulletin 24, 25 p.

11. U.S.Army Corps of Engineers, 1956. Report of Public Hearing on Willapa River and Harbor Washington. Seattle District, 37 p.

12. U.S. Army Corps of Engineers, 1967. Available Data Pertinent to Willapa Bay and Grays Harbor. Seattle District unpublished report, 37 p.

13. U.S. Army Corps of Engineers, 1967. Willapa Bay, Washington. Committee on Tidal Hydraulics. Vicksburg, Mississippi, 17 p.

14. U.S. Army Corps of Engineers, 1968. Feasibility Study: Navigation and Beach Erosion, Willapa River and Harbor and Naselle River, Washington. Seattle District, 92 p.

15. U.S. Army Corps of Engineers, 1971. Navigation and Beach Erosion: Willapa River and Harbor and Nascelle River, Washington. Seattle District, 25 p.

16. U.S. Army Corps of Engineers, 1971. Inventory Report Columbia-North Pacific Region: Washington and Oregon. North Pacific Divison, 79 p.

17. U.S. Army Corps of Engineers, 1975. Grays Harbor and Chehalis River Navigation Project: Operation and Maintenance. Seattle District, 86 p.

KEY WORDS

Erosion, Cape Shoalwater, Washington State, Pacific Coast, Willapa Bay

Performance of Beach Nourishment Projects in Varying Wave Climates

Norman K. Skjelbreia and Eric E. Nelson*

Paper unavailable at time of publication.

---

* US Army Corps of Engineers, Seattle District.

Coastal Erosion in the California State Park System

Syd Willard*

Abstract

The California Department of Parks and Recreation is responsible for managing over 210 lineal miles of California's magnificent coastline. The Department's coastal units extend from Border Field State Park in San Diego County on the international border to Pelican State Beach, near the California-Oregon state line. DPR has struggled to balance preservation of natural systems, preservation of important historical and archeological resources, and provision of a variety of recreational opportunities for the visiting public. Despite inherent conflicts of our multiple objectives, the Department of Parks and Recreation is developing a workable approach to preservation, management, and development of our coastal units. Management options are selected during the General Plan process, according to the natural, cultural, and physical characteristics of each area.

Significant storms occurred in 1978, 1980, 1982, and 1983, resulting in extensive damage to facilities and losses of beach sand. A new coastal erosion policy was adopted in 1984, which helped to determine the best approach to take for a given situation -- protection of facilities or benign "work with nature".

We have found that in certain cases, if we have the luxury of time to wait for the natural cycles to operate, if we control the human-induced erosion and revegetate denuded dunes and bluffs with native species, we can regain a sandy, esthetic, and popular beach rather than live with a steep, narrow, cobble beach, or even worse, no beach at all.

Introduction

The California Department of Parks and Recreation (DPR) is responsible for managing over 210 lineal miles of California's 1,100-mile coastline. The Department's coastal units extend from Border Field State Park on the Mexico-California border to Pelican State Beach near the California-Oregon state line. The classification of the various beach units determines the philosophical and operational parameters of each property. Most coastal units are classified as State Beach, with State Park, State Reserve, State Recreation Area, State Historic Park, and State Vehicular Recreation Area making up the remainder of the classifications.

---

* Staff Geologist, California Department of Parks and Recreation, P.O. Box 2390, Sacramento, CA 95811.

The Public Resources Code defines State Beaches as "consisting of areas with frontage on the ocean. . .designed to provide swimming, boating, fishing, or other beach oriented recreational activities." Furthermore, improvements undertaken in State Beaches are to consider compatibility of design with the surrounding scenic and environmental characteristics. Areas which contain ecological, geological, scenic, or cultural resources of significant value are to be preserved within State Parks, State Reserves, or Natural or Cultural Preserves for present and future generations.

An additional classification is State Seashore, which consists of "relatively spacious coastline areas with frontage on the ocean, . . .possessing outstanding scenic or natural character and significant recreational, historical, archeological, or geological values." The purpose of State Seashores is to preserve those values and to make possible the enjoyment of the coastline and related recreational activities consistent with the preservation of those values.

As a resource-oriented department, DPR has struggled to balance the preservation and perpetuation of coastal properties with providing recreational facilities and opportunities for the visiting public. Demands for camping, picnicking, sanitary restrooms, parking on or near the beach, convenient and safe access, and recreation support facilities are not necessarily compatible with the Department's objectives for preservation and protection of fragile and significant natural and cultural resources. Despite the inherent conflicts of its multiple objectives, DPR is developing a workable approach to preservation, management, and development of coastal units. A recent departmental policy (following the extensive damage from the storms of 1983) has helped to establish long-term management and development objectives. In addition, increased funding for restoration of natural systems including dune and bluff stabilization has provided the wherewithal to accomplish some much-needed restorative work in rapidly eroding or degrading areas.

Storm Damage

The storms of 1978, 1980, 1982, and 1983 resulted in extensive damage to public as well as private properties. Not surprisingly, State Park System lands were not spared. Beach-level campgrounds, emergency beach access roads, parking lots, restrooms, stairways, piers, and other support facilities have been damaged, rebuilt, and damaged again. In addition to loss of facilities, loss of land base, cultural and archeological resources, and reduced recreational and esthetic appeal has occurred. In many cases, the only direct cost associated with storm damage is staff and equipment time to remove debris (logs, rocks, seaweed, construction materials) from the beach and/or parking lot. In these cases, no permanent storm damage occurs -- due in part at least to proper planning and siting of facilities. In other cases, permanent (structural) loss occurs, but usually the damaged facility is a coastal-dependent one in an acknowledged high-risk area. DPR tries to avoid hazards and to minimize the risk to facilities, but realizes that sometimes certain developments are limited to high-risk areas (i.e., piers, stairways to beach).

The cost of maintaining these coastal-dependent facilities is admittedly high. The following DPR dollar amounts are those costs associated with storm debris removal, emergency facility protection measures (riprap, sandbags), demolition of damaged facilities, and reconstruction of some (but not all) facilities along the coast:

1978	1980	1982	1983*
$594,000	$1,862,000	$135,000	$2,198,000

In 1978, almost half of the storm damage expenditures were for a single project — the pier at San Buenaventura State Beach. In 1980, 1982, and 1983, Seacliff State Beach dominated the storm damage expenditures (1980 - $1,630,786, 1982 - $75,770, 1983 - $899,723*).

The experience of repeated significant storm damage in various coastal units has resulted in the re-evaluation of development in areas known to be subject to ocean wave erosion and seacliff retreat. Comparative analyses are performed during resource inventory and general planning phases of development. Maps are produced which identify those areas which are suitable for various types of development, and those areas which should remain undeveloped, due to natural or cultural resource values or to vulnerability to natural hazards, such as coastal erosion and seacliff retreat.

Coastal Unit Erosion Problems and Solutions

Many coastal units of the State Park System share similar erosion problems. Runoff from inland developments is often diverted from natural drainage courses, collected by culverts, and channeled over the clifftops to the beach. Because of increased inland development and decreased surface area available for percolation, runoff increases and erosion around the (often undersized) culverts results. Interception of inland runoff parallel to the coast and diversion back into natural drainage courses and lagoons helps to control catastrophic cliff failure around storm drains. DPR is attempting to implement this strategy along several San Diego coast units in cooperation with the City of Carlsbad.

Protective devices for structures (riprap, seawalls) can result in several negative effects, even if the device successfully performs in protecting the structure. Erosion on either side of the protected area will continue, ultimately resulting in a peninsula, or projecting headland. The protected structure is then subject to greater wave energy. The protective device often occupies premium beach space, affecting lateral access and recreation on the beach. Avoidance is the simplest solution to this problem. Use of moveable facilities in high-hazard areas, and pulling them back out of erosion's way, is the preferred approach, when facilities (lifeguard towers, restrooms, concession buildings) are necessary.

---

* Damage survey report estimates, not actual expenditures.

Concentrated recreational use in vegetated dunes and uplands can result in loss of cover and increased erosion. Play activities (tunneling in the cliffs and shortcuts to the beach) can also result in major vegetative losses and increased erosion. DPR is actively addressing the problems of overuse and uncontrolled use by employing a variety of "low-tech", labor-intensive erosion control techniques such as straw "planting" in dunes, revegetating coastal terraces in active dunes with native plant species, identifying formal access routes, and fencing off revegetated areas in hazardous locations.

Young beach enthusiasts shun stairway in favor of shortcut down the bluff, promoting additional bluff erosion. Note unsightly riprap in foreground and non-native iceplant on left.

Coastal Erosion Policy

In the fall of 1982, a photographic record was initiated for the coastal units of San Diego County, in support of the preparation of a General Plan for nine state park units. Black and white photographs and color slides documented a period of extreme coastal erosion, sand loss, and seacliff retreat. Field mapping and aerial photography analysis further documented areas of rapid seacliff retreat, sea cave development, and geologically unstable areas (shear zones, jointed bedrock, clay layers, and landslides). These records served as the basis for resource and development policies for the General Plans which were approved by the California State Park and Recreation Commission in November 1983.

Resource policies were developed regarding bluff setback zones, use of portable or expendable facilities in areas subject to direct wave attack, prohibition of bluff fortifications, use of non-irrigated native vegetation for erosion control, preparation of drainage plans to direct storm runoff parallel to the cliffs and into natural drainage courses, sand replenishment, and beach-level and seacliff monitoring. Since these policies only dealt with San Diego Coast units, the departmental policy on coastal erosion was drafted to provide overall guidance and direction for all coastal units.

In short, the intent of the policy is to avoid construction of new permanent facilities in areas subject to coastal erosion, and to promote the use of expendable or moveable facilities where the expected useful life is limited due to the location in erosion-prone areas. The policy was approved by Director Wm. S. Briner October 24, 1984:

COASTAL EROSION

INTRODUCTION

Coastal erosion, seacliff retreat, and littoral sand movement are ongoing natural processes along the California coastline. Rates of coastal erosion vary from fractions of an inch per year to 50 to 60 feet in a year. Sections of the California coastline have eroded several city blocks eastward in the last 100 years. Coastal erosion is episodic, site-specific, and directly related to meteorological changes, as well as structural and geological characteristics. Of the approximately 1,810 miles of coastline, 1,500 miles are subject to significant erosion and 80 miles are critically eroding (with threatened facilities). The remainder of the coastline is subject to significant erosive factors intermittently, depending on weather and storm trends.

Ocean-wave erosion and seacliff retreat are responsible for creating invaluable scenic and esthetic resources by carving out graceful coves, rocky headlands, and steep ocean cliffs. Even the popular sandy beaches are the result of erosive factors. The dynamic processes of ocean-wave erosion and seacliff retreat are problems only when facilities are in jeopardy or when public safety is threatened.

POLICY

THE DEPARTMENT OF PARKS AND RECREATION SHALL AVOID CONSTRUCTION OF NEW STRUCTURES AND COASTAL FACILITIES IN AREAS SUBJECT TO OCEAN-WAVE EROSION, SEACLIFF RETREAT, AND UNSTABLE CLIFFS, UNLESS SPECIFIC DETERMINATIONS HAVE BEEN MADE THAT THE RISK OF LOSS OF THE FACILITY IS CLEARLY OFFSET BY THE INVESTMENT AND NEED FOR THE FACILITY. MEASURES SHALL BE TAKEN TO MINIMIZE HUMAN-INDUCED EROSION BY REDUCING: CONCENTRATED SURFACE RUNOFF FROM USE AREAS, ELEVATED GROUNDWATER LEVELS FROM IRRIGATION AND URBANIZATION, AND SURFACE DISTURBANCE OF BLUFFTOP SOILS. IN RECOGNITION OF CALIFORNIA'S ACTIVELY ERODING COASTLINE, NEW STRUCTURES AND FACILITIES LOCATED IN AREAS KNOWN TO BE SUBJECT TO OCEAN-WAVE EROSION, SEACLIFF RETREAT, OR UNSTABLE BLUFFS SHALL BE EXPENDABLE OR MOVEABLE. STRUCTURAL PROTECTION AND REPROTECTION OF DEVELOPMENTS SHALL BE ALLOWED ONLY WHEN THE COST OF PROTECTION IS COMMENSURATE WITH THE VALUE (PHYSICAL AND INTRINSIC) OF THE DEVELOPMENT TO BE PROTECTED, AND WHEN IT CAN BE SHOWN THAT THE PROTECTION WILL NOT NEGATIVELY AFFECT THE BEACH OR THE NEAR-SHORE ENVIRONMENT.

Conclusion

DPR's objectives for coastal resource management and development are necessarily different from private developers, businesses, or homeowners on the coast. We are often limited in our options for facilities by our narrow land base, as well as resource constraints. We must provide for present use, while assuring perpetual use and enjoyment. DPR has gained valuable insights into the magnitude and time scale of coastal erosion since 1978. We have modified our development approach as conditions have changed. We have learned from our successes and failures and from the successes and failures of others. We have attempted to avoid development in areas of coastal erosion. We have rejected the wholesale fortification of bluffs and beaches in favor of portable or expendable facilities, wherever feasible. We choose areas to be fortified and protected very carefully, so as not to exacerbate the erosion problem and further detract from the natural scene that draws millions to the shore each year. Application of the specific resource policies that are developed for General Plans, as well as DPR's coastal erosion policy, will help to assure the continued operation and management of State Park System units as special places for present and future generations to enjoy and experience.

Summary of Panel Discussion

COASTAL PROCESSES

Chairman: Ronald M. Noble, American Society of Civil Engineers/
Coastal Engineering Research Center
Noble Coastal & Harbor Engineering
Tiburon California

Panelists: James Houston, US Army Corps of Engineers
Waterways Experiment Station (WES), Vicksburg, Mississippi
Choule Sonu, Tekmarine, Inc.
Sierra Madre, California
Reinhard Flick, California Department of
Boating and Waterways, La Jolla, California
Robert L. Wiegel, University of California, Berkeley

The coastal processes session included a wide range of papers presented by specialists in coastal engineering, marine geology, river hydraulics, geography, and research. However, all papers included one common denominator: identification of the predominant wave climate and its effect on sediment transport and shoreline erosion. This report of the coastal processes session will present my conclusions based on the talks presented in this session. However, I will not discuss my comments pertaining to each individual paper presented, as this was done at the conference by our four panelists: James Houston, Choule Sonu, Reinhard Flick, and Robert Wiegel. Instead, I will summarize the papers presented.

The morning session consisted of presentations by Jung-Tai Lin, "Empirical Prediction of Wind-Generated Gravity Waves"; Omar H. Shemdin, "Extending Wave Station Measurements to Intermediate Locations by Wave Transformation Models"; and Thomas J. Dolan, "Coast of California Storm and Tidal Waves Study: A Regional Coastal Zone Monitoring Program." Lin's talk dealt with the empirical prediction of wind-generated waves by analytically solving the wind-wave momentum equation and comparing the results with laboratory and field experimental data. Shemdin discussed the status of his many years of numerical modeling in extending measured wave data to intermediate locations with special emphasis on directional spectral, while Dolan reviewed the US Army Corps of Engineers' (Corps') ongoing program of measuring wave data and beach profiles along southern California.

The midmorning session consisted of presentations by Howard H. Chang, "Flushing of Entrance Channel for Coastal Lagoons: Mathematical Simulation"; Edward B. Thornton, "Coastal Erosion Along Southern Monterey Bay"; and Maurice L. Schwartz, "Net Shore-Drift Along the Pacific Coast of Washington State." Chang presented his numerical modeling techniques to describe the river hydraulic flushing characteristics as they encounter the open ocean tides and waves. Thornton discussed a simple predictive model for evaluating coastal erosion rates along southern Monterey Bay using wave, tide, and beach data, while Schwartz mapped drift cells and direction of net shore drift along Washington State's coastline utilizing geomorphic and sedimentologic net shore drift indicators.

The afternoon session consisted of presentations by Thomas Terich, "The Severe Erosion of Cape Shoalwater, Washington"; Dave Schuldt, "Performance of Beach Nourishment Projects in Varying Wave Climates"; and Syd Willard, "Coastal Erosion in the California State Park System." Terich presented a case history of severe erosion which revealed that erosion is resulting from the long-term northward migration of the tidal channel toward Cape Shoalwater allowing southerly storm waves close access to easily erodible dunes. Schuldt presented several case histories of Corps beach nourishment and shore protection projects along the Washington coastline, while Syd Willard discussed several cases of coastal erosion and their solutions within California's State Park system.

As a consulting engineer working in the coastal environment, I consider these presentations on coastal modeling and monitoring, as well as the case studies, to be very useful to the engineer in assessing design waves, sediment transport, and shoreline erosion on various projects. Since most consulting projects are allotted neither the time nor the budget to perform long-term investigations, the results presented at this conference and other similar conferences and technical proceedings are very valuable to support the efforts of the consulting engineer.

It is essential to continue these coastal research projects and case studies in order to further our understanding in such areas as:

(1) Defining the wave directional spectral.

(2) Defining wave-sediment interaction.

(3) Developing better modeling techniques.

(4) Developing more refined field monitoring techniques.

(5) Identifying surface, groundwater, and soil effects on coastal erosion.

It is difficult to accurately predict changes in the offshore and onshore sand levels and to define the complete wave directional spectral; however, these conditions are very significant in most coastal projects. In conclusion, these specialty conferences are very important to those of us working in the coastal environment in order to keep abreast of the latest coastal investigations, their data, and their findings. It is also essential that efforts be continued to distribute the generated coastal data to those professionals who can make use of this information.

Ronald M. Noble
Chairman, Coastal Processes Session

END

DTIC

8-86